USGS
science for a changing world

Future Wave and Wind Projections for United States and United States-Affiliated Pacific Islands

Open-File Report 2015–1001

U.S. Department of the Interior
U.S. Geological Survey

Cover image:
Aerial photograph of waves breaking on the fringing reef off Ennuebing Island, Kwajalein Atoll, Republic of the Marshall Islands

USGS
science for a changing world

Future Wave and Wind Projections for United States and United States-Affiliated Pacific Islands

By Curt D. Storlazzi, James B. Shope, Li H. Erikson, Christie A. Hegermiller, and Patrick L. Barnard

Open-File Report 2015-1001

U.S. Department of the Interior
U.S. Geological Survey

U.S. Department of the Interior

SALLY JEWELL, Secretary

U.S. Geological Survey

Suzette M. Kimball, Acting Director

U.S. Geological Survey, Reston, Virginia: 2015

Suggested citation:
Storlazzi, C.D., Shope, J.B., Erikson, L.H., Hegermiller, C.A., and Barnard, P.L., 2015, Future wave and wind projections for United States and United States-affiliated Pacific Islands: U.S. Geological Survey Open-File Report 2015–1001, 426 p., *http://dx.doi.org/10.3133/ofr20151001*.

ISSN 2331–1258 (online)

Contents

Tables

Figures

Appendixes

Appendix A. Wave Height, Wave Period, and Wave Direction Statistics

Appendix B. Wind Speed and Wind Direction Statistics

Appendix C. Monthly Trends in Wave Heights

Appendix D. Monthly Trends in Wind Speeds

Abbreviations

AORI	Atmosphere and Ocean Research Institute, University of Tokyo
BCC	Beijing Climate Center, China
CDF	cumulative density function
CMIP	Coupled Model Inter-Comparison Project
D_p	mean wave direction
DBDB2	Digital Bathymetric Data Base
DJF	December to February time period
DOD	U.S. Department of Defense
DOI	U.S. Department of the Interior
GCM	global climate model
GFDL	Geophysical Fluid Dynamics Laboratory, NOAA
GIS	geographic information system
GPD	generalized Pareto distribution
GSHHS	Global Self-consistent Hierarchical High-resolution Geography Database
H_s	significant wave height
INMCM	Institute of Numerical Mathematics (Russia) climate model
JAMSTEC	Japan Agency for Marine-Earth Science and Technology
JJA	June to August time period
MAE	mean absolute error
MAM	March to May time period
MIROC	Model for Interdisciplinary Research on Climate
NDBC	National Data Buoy Center
NGDC	National Geophysical Data Center
NIES	National Institute for Environmental Studies, Japan
NRL	Naval Research Laboratory

nVar	normalized variance
NWW3	a near-global domain for the wave model
R_v	return value
RCP	representative concentration pathways
SON	September to November time period
SRES	Special Report on Emission Scenarios
SWAN	Simulating WAves Nearshore, a wave model
T_p	peak wave period
U_a	wind speed
U_θ	wind direction
WTP	western tropical Pacific
WW3	WAVEWATCH–III wave model

Future Wave and Wind Projections for United States and United States-Affiliated Pacific Islands

By Curt D. Storlazzi[1], James B. Shope[2], Li H. Erikson[1], Christie A. Hegermiller[2], and Patrick L. Barnard[1]

Abstract

Changes in future wave climates in the tropical Pacific Ocean from global climate change are not well understood. Spatially and temporally varying waves dominate coastal morphology and ecosystem structure of the islands throughout the tropical Pacific. Waves also impact coastal infrastructure, natural and cultural resources, and coastal-related economic activities of the islands. Wave heights, periods, and directions were forecast through the year 2100 using wind parameter outputs from four atmosphere-ocean global climate models from the Coupled Model Inter-Comparison Project, Phase 5, for Representative Concentration Pathways (RCP) scenarios 4.5 and 8.5 that correspond to moderately mitigated and unmitigated greenhouse gas emissions, respectively. Wind fields from the global climate models were used to drive a global WAVEWATCH-III wave model and generate hourly time-series of bulk wave parameters for 25 islands in the mid to western tropical Pacific for the years 1976–2005 (historical), 2026–2045 (mid-century projection), and 2085–2100 (end-of-century projection). Although the results show some spatial heterogeneity, overall the December-February extreme significant wave heights, defined as the mean of the top 5 percent of significant wave height time-series data modeled within a specific period, increase from present to mid-century and then decrease toward the end of the century; June-August extreme wave heights increase throughout the century within the Central region of the study area; and September-November wave heights decrease strongly throughout the 21st century, displaying the largest and most widespread decreases of any season. Peak wave periods increase east of the International Date Line during the December-February and June-August seasons under RCP4.5. Under the RCP8.5 scenario, wave periods decrease west of the International Date Line during December-February but increase in the eastern half of the study area. Otherwise, wave periods decrease throughout the study area during other seasons. Extreme wave directions in equatorial Micronesia during June-August undergo an approximate 30° clockwise rotation from primarily west to northwest. September-November RCP4.5 extreme mean wave directions rotate counterclockwise by approximately 30 to 45° in equatorial Micronesia; September-November RCP8.5 extreme mean wave directions within equatorial Micronesia rotate

[1]U.S. Geological Survey.
[2]University of California at Santa Cruz.

clockwise by approximately 20 to 30°. Extreme wind speeds decreased within both scenarios, with the largest decreases occurring in the September-November season. Extreme wind directions under RCP4.5 rotated clockwise by more than 60° in equatorial Micronesia during the September-November season and by approximately 30° during June-August. RCP8.5 extreme wind directions rotated counterclockwise during September-November within the same region by 30 to 50° and clockwise by 30 to 40° at one island. The spatial patterns and trends are similar between the two different greenhouse gas emission scenarios, with the magnitude and extent of the trends generally greater for the higher (RCP8.5) scenario.

Introduction

The oceanographic processes that disturb coasts and insular shelves include the actions of surface waves, internal waves, and currents (tidal, density, wave-driven, wind-driven, and geostrophic). The Pacific Ocean can generate extremely large ocean surface waves, and the resulting near-bed wave-orbital velocities on insular shelves are generally much larger than velocities due to currents and internal waves (see, for example, Storlazzi and Reid, 2010). Although a few studies have investigated the wave climate in Hawaii (for example, Vitousek and Fletcher, 2008; Hoeke and others, 2011), there is little information on the wind and wave climate for most of the western Pacific Ocean because of a lack of observational platforms (such as National Data Buoy Center buoys). Whereas scientific understanding of the dominant processes controlling coastal morphology and coastal and marine ecosystem structure on islands has improved over the past decade, our understanding of the linkages between these factors and variations in the wave climate across the Pacific and U.S.-managed assets is limited.

Furthermore, the influence of global climate change on wind and wave conditions is not well understood. Stationary statistical approaches (such as return values) have typically been used to predict future extreme and mean wind and wave conditions, but with the changing climate this may not be a valid approach. Although some nonstationary statistical approaches (for example, nonstationary generalized extreme values) may sufficiently capture the variations and changes, recent work seems to point in the direction that the current climate alone cannot be used to estimate future conditions. It has been shown that calculated return values from different decades are not compatible with each other in the North Pacific (for example, Caires and others, 2006) and that under different climate scenarios for the 21st century, the rate of projected future wave height changes is not constant and depends on variations in the greenhouse-gas forcings (see, for example, Wang and Swail, 2006). Applying downscaling methods, such as making causal relations between winds and sea-level pressures with wave heights, may be appropriate for areas of the Atlantic and other smaller water bodies, but for the Pacific Ocean, where swell of periods in excess of 15 seconds generated by very distant storms is of concern, it is more difficult to make such empirical relations. An alternative option is then to obtain wave conditions through analytical or numerical wave models forced with projected climate conditions from global climate models (GCMs).

Some work has been done to estimate future wave conditions in the Pacific using wave models and projected winds from GCMs (for example, Cayan and others, 2008; Mori and others, 2010; Hemer and others, 2013). However, the data are sparse and not freely available for trend- and region-specific analysis. Furthermore, the recent and continued update of GCM outputs warranted the development of a new mean and extreme wave climatology for U.S. assets in the Pacific Basin. This climatology is important because wave- and wind-driven processes drive inundation (for example, Stockdon and others, 2006) that results in coastal erosion and damage to infrastructure and fresh-water supplies (for example, in the Federated States of Micronesia in 2008; Fletcher and Richmond, 2010) and can damage natural resources and kill U.S.-Federally protected species (for example, in the Northwestern Hawaiian Islands in January and February 2011; unpublished data). Such impacts may only be exacerbated in the future with projected trends in sea-level rise (for example, Storlazzi and others, 2011). Furthermore, numerical modeling efforts have shown how wave energy constrains marine species' distribution in the Pacific Ocean (for example, Storlazzi and others, 2005). Information on potential changes in wind and wave climate under future global climate change scenarios is therefore crucial to understanding not only the sustainability of existing infrastructure, natural, and cultural resources, but also planning for future investments in infrastructure and the viability of coastal-related economic activities such as fishing and tourism.

Project Objectives

The goal of this effort was to provide hourly data and statistical measures (mean and mean of top 5 percent values) of wave height, wave period, wave direction, wind speed, and wind direction for Department of the Interior (DOI)- and Department of Defense (DOD)-managed assets in the Pacific Ocean for the historical (1976–2005) time period and future time periods (out to the year 2100). The goal was accomplished by forcing the WAVEWATCH-III numerical wave model with winds computed by global climate models (GCMs) for two climate scenarios, Representative Concentration Pathways (RCP) RCP4.5 and RCP8.5 (see section on "Methods" for further descriptions). Resulting model data are summarized with wave and wind statistics at 25 islands (table 1) comprising U.S. National Parks, National Wildlife Refuges, U.S. National Monuments, areas managed by the U.S. Office of Insular Affairs, and U.S. Department of Defense facilities.

The data presented herein provide information required for adaptive conservation planning by providing a better understanding of potential climate change impacts. This effort investigated trends and variability, on an island and archipelago scale, of geophysical variables that are expected to respond to global-scale forcing. Furthermore, the data generated by this effort are expected to be crucial in projecting future transient sea level extremes on coasts and small islands, because winds and waves are the key processes driving extreme water levels and inundation.

Study Area

Wave and wind statistics were generated for 25 locations across the western tropical Pacific (WTP) at a number of United States territories and U.S.-affiliated islands (fig. 1). The modeled area encompasses a number of varying regions subject to varying climates. The trade winds dominate in the region, blowing from the east. However, despite the main winds being the trades, the stronger winds, and thus the larger waves, result from storm systems within the region. The northeast quadrant of the study area receives strong winds and large waves from higher latitude storms during the boreal winter (Semedo and others, 2011). Winds in the rest of the eastern half of the study area remain dominated by the trade winds, though larger swell waves are likely due to storms from the South Pacific and Southern Ocean. The western half of the study area's extreme winds and waves are dominated by typhoons, which are generated in the center of the region and proceed to the west, and by extratropical cyclones from the North Pacific (Mori and others, 2010). Therefore, islands such as Guam receive larger, more destructive waves because it is subject to larger typhoons. However, this study focused primarily on swell waves from extratropical regions and how they may change in the future. These swell waves, while likely smaller than typhoon-generated waves, still pose a hazard to the western Pacific islands throughout the 21st century.

Methods

Global Climate Model Input Data

A dynamical downscaling (Wang and others, 2009) approach was used to generate recent and future wave climates for the study areas by using updated climate scenarios and models as input for the numerical wave model WAVEWATCH-III (WW3; Tolman, 2009). For the purpose of assessing recent past and projected wave climates, a suite of atmosphere-ocean coupled GCM simulations of near-surface (10-m height) wind fields were chosen on the basis of the availability of (1) "historical" runs for evaluation of how realistic the models are in simulating the recent past, (2) projections out to the year 2100, (3) GCM simulations completed by spring 2012, and (4) frequency of synoptic (nonaveraged) outputs (3-hr interval). Based on these requirements, the following set of experiments from four modeling centers were chosen: (a) Beijing Climate Center, Meteorological Administration, China, model BCC-CSM1.1; (b) Institute for Numerical Mathematics, Russia, model INM-CM4; (c) Model for Interdisciplinary Research on Climate—AOEI, NIES, JAMSTEC, Japan, model MIROC5; and (d) Geophysical Fluid Dynamics Laboratory, United States, GFDL-ESM2M. These GCM model outputs were generated in support of the Coupled Model Inter-Comparison Project, Phase 5 (CMIP5; World Climate Research Programme, 2013). GCM model resolutions are described in table 2. CMIP5 was proposed, conceived, and developed by the climate modeling community with the intent of providing a framework for coordinated climate change experiments conducted at various institutions around the globe (Taylor and others, 2009). Although hundreds of model simulations are available as part of this effort, this work focused on a few select simulations, as described above.

Future emission scenarios differed slightly from past CMIP work, in which SRES scenarios (named after their publication "Special Report on Emission Scenarios") provided six alternative scenarios based on narrative storylines (for example, van Vuuren and others, 2011). The "new" scenarios or so-called "representative concentration pathways" (RCPs) are labeled according to the approximate target radiative forcing at year 2100 (for example, RCP4.5 identifies a concentration pathway that approximately results in a radiative forcing of 4.5 watts per square meter (W/m^2) by year 2100 relative to preindustrial conditions). In this study, GCM results from two climate scenarios were used, one representing a medium mitigation (RCP4.5; Thomson and others, 2011) and one a high-emissions scenario of 8.5 W/m^2 by year 2100 (RCP8.5; Riahi and others, 2010). Projections for scenarios RCP4.5 and RCP8.5 are available for two separate time periods in the 21st century: years 2026–2045 and 2085–2100, as prescribed by the CMIP5 modeling framework. The historical (1976–2005) simulations were used to assess model skill and determine the magnitude of change in the future scenarios.

WAVEWATCH-III Wave Modeling

To reduce uncertainty in model variability, wind speed and direction from the four different GCMs were used as boundary conditions to the third-generation physics-based WAVEWATCH-III (WW3, ver. 3.14, Tolman, 2009) numerical wave model. WW3 solves the random phase spectral action density balance equation for wave number-direction spectra. The implicit assumption of this equation is that properties of the medium (water depth and current) as well as the wave field itself vary on time and space scales that are much larger than the variation scales of a single wave. The model was implemented over a near-global domain (NWW3, latitude 80°S to 80°N) at a 1° x 1.25° spatial resolution. Bathymetry and shoreline positions were populated with the Naval Research Laboratory's (NRL) Digital Bathymetric Data Base (DBDB2) version 3.0 (National Research Laboratory, 2013) and the National Geophysical Data Center's (NGDC) Global Self-consistent Hierarchical High-resolution Geography Database (GSHHS) version 2.2.2 (National Geophysical Data Center, 2013), respectively. Wave spectra were computed at a directional resolution of 15° and using 25 frequency bands ranging nonlinearly from 0.04 to 0.50 Hz. Parameterizations of physical processes (source terms) include wave growth and decay due to the actions of wind, nonlinear resonant interactions, dissipation, bottom friction, surf-breaking (for example, depth-induced breaking) and scattering due to wave-bottom interactions.

Map files of wave heights, periods, and directions and wind speeds and directions were saved on a daily basis, while time series of wind and wave parameters at deep-water observation (output) points in the model were saved on a 3-hourly and hourly basis, respectively. WW3 was run at a global resolution scale to capture the Pacific Ocean in a computationally efficient manner (table 1). A few output points (coincident with NDBC measurement buoys) were used for model/measurement comparisons; comparisons were done in a probabilistic sense (for example, cumulative density functions), not in a time-series sense, as the goal was to understand the overall climate and not the details of potential future modeled storm events, which were not possible

without major downscaling of winds. The deep-water output points are intended to serve as points for analysis of wave climate trends, which can then be used as inputs to nearshore wave models (for example, Deltares' SWAN) investigating impacts to infrastructure, natural, and cultural resources.

Wave Parameter Statistics

Modeled output data comprised (1) significant wave height (H_s), peak wave period (T_p), and mean wave direction (D_p) values saved at hourly intervals and (2) wind speed (U_a) and wind direction (U_θ) values saved at 3-hour intervals. H_s is defined as 4 times the standard deviation of the wave displacement time series during a modeled time period, which approximates the mean of the top third of measured wave heights within that period, with units in meters (m). T_p is defined as the wave period with the largest energy within a modeled timestep, with units of seconds (s). U_a units are in meters per second (m/s). D_p and U_θ values are defined within this report as the direction in degrees clockwise from North (°) in which the waves and winds are travelling. Outputs from each GCM-driven WW3 model run were combined into a multimodel ensemble. An ensemble of models has been shown to more accurately represent observed data than any one model for dynamic GCMs and regional climate models (RCMs) with similar parameters (Donat and others, 2010).

Averages and variances (or standard deviations) for monthly and seasonal extreme H_s (σ^2_{Hs}), T_p (σ^2_{Tp}), D_p (σ_{Dp}), U_a (σ^2_{Ua}), and U_θ ($\sigma_{U\theta}$) values were calculated for hindcast, mid-century, and end-century periods, with averages for each RCP emission scenario being calculated for the latter two periods. Angular standard deviation values were calculated for wave directional data because the standard deviation values produced were more easily interpretable compared to variances, which, when calculated, produced an extremely large range to visualize, as the angular standard deviation values were often more than 10°, resulting in variances that ranged from 100 to more than 1,000 variance being the square of the standard deviation. Variance values for other variables were more comparable with one another. The process was repeated for extreme H_s scenarios, which use the variables relating to the the mean of the top 5 percent of H_s or U_a time-series values modeled within each modeled time period. For example, extreme H_s values are calculated as the mean of the top 5 percent of H_s values within a time period, whereas extreme T_p values are defined as the mean of the T_p values associated with the top 5 percent of H_s values within a given time period. Changes in bulk parameters were derived by subtracting hindcast means from forecast averages. The climate variables for the December-February (DJF), March-May (MAM), June-August (JJA), and September–November (SON) seasons were mapped using the ArcGIS geographic information systems software developed by the Environmental Systems Research Institute with the expectation that the largest or most important changes in H_s would occur during those seasons. For example, H_s during the northern hemisphere winter in Hawaii is typically larger than during other seasons (Vitousek and Fletcher, 2008). Therefore, changes in

these wave heights may have a stronger impact on overtopping and erosional events as witnessed throughout the tropical Pacific Ocean in 2009 (Hoeke and others. 2013).

Return values (R_v) for each modeled point for H_s and U_a were generated for 2-, 5-, 10-, 20-, 50-, and 100-year events for the hindcast, RCP4.5 projections, and RCP8.5 projections following the methods of Caires and Sterl (2005) and Caires and others (2006). The ensemble H_s and U_a data were declustered so that the largest events were selected, but consecutive exceedances of individual storms were not selected. Individual events were declustered to be at least 3 days apart, to ensure that each selected large wave or wind event was from a separate storm. The largest declustered 150 events (30 years of 5 events per year on average) from the hindcast ensemble and declustered 100 events (20 years of 5 events per year on average) from each forecast ensemble were fitted to a generalized Pareto distribution (GPD), which can be used approximate H_s and U_a extrema. The GPD method is a peak-over-threshold method. In each calculation, the threshold value selected was the minimum value of the selected declustered extreme modeled events. Once fitted, the R_v trend is extrapolated from the 20 or 30 years of data modeled to a 100-year event. Therefore, it is possible to estimate an R_v for a 100-year event without 100 years of data, contrary to more traditional methods. The 95-percent confidence intervals of R_v values were also calculated at each point.

Model Skill

Ensemble model hindcasts (1976–2005) were compared to buoy measurements from the National Data Buoy Center (NDBC) platforms in the Hawaiian Island Chain for the same period to evaluate how well the model approximated observed climate trends (National Data Buoy Center, 2013). The Pacific Ocean historical buoy dataset is largely scattered; until recently, only a small areal extent of the ocean basin was buoyed. Only the Hawaiian Island Chain has observation platforms with sufficiently long datasets that corresponded to selected island locations of Molokai, Kauai, and the Big Island; these are NDBC stations 51001, 51002, 51003, and 51004 (fig. 2). The selected buoys collected deep-water wave and meteorological measurements at hourly intervals. This dataset, however, was limited to H_s, T_p, U_a, and U_θ, with D_p not recorded. The WAVEWATCH-III model resolution limited the spatial overlap of output points and buoy locations. Therefore, model output points were compared to historical buoy measurements instead of comparing virtual buoy output to physical buoys. The model resolution of 1.25° latitude and 1.00° longitude limited the ability to place an output point coincident to physical buoy locations.

Model performance was assessed by the mean absolute error (MAE) and normalized variance (nVar) calculated from hindcasted and observed values of H_s. The MAE is a good indication of model accuracy when model and observed values are at approximately the same scale (Hyndman and Koehler, 2006). The MAE is given by:

$$MAE = \frac{1}{N}\sum_{i=1}^{N}|obs_i - mod_i|$$

where obs_i = the observed value at the i^{th} value and mod_i = the modeled value at the i^{th} value.

The MAE was calculated probabilistically from the empirical cumulative density functions (CDFs) of the seasonal and annual ensemble model and observed datasets after the CDFs were interpolated to the same number of points within cumulative frequency space. That is, the CDFs were interpolated to the same number of points in terms of the y-axis. This interpolation enabled functions to be input into the MAE equation, which required both inputs to be the same length, and preserved the curves' positioning along the H_s (x-axis) and the x-axis distance between the two curves. The MAE formula then returned a mean of the distance in terms of H_s (x-axis) position calculated at each interpolated y-axis point in the function. The MAE was calculated for each season (DJF, MAM, JJA, and SON) by computing the H_s CDF curves for each season within the historical and model data after isolating the season time-series within each dataset. The result was that individual seasons could be compared for accuracy. Much of the large-wave activity in the tropical Pacific is due to DJF storms at higher latitudes. By comparing seasons, the wave activity of a season that was typically more responsible for larger waves could be evaluated for accuracy, despite another season (such as JJA, which typically delivered less wave energy to the islands) possibly being more inaccurate. The entire time-series of both historical and model hindcast data were also compared and the resultant CDF comparisons were plotted (figs. 3–5). The MAE values of the complete time-series was also calculated and labeled as "Yearly" in tables 3–8. The nVar is the ratio of modeled to observed variance where a value of 1 indicates the variances are identical and is given by:

$$nVar = \frac{\gamma_{mod}^2}{\gamma_{obs}^2}$$

where γ_{mod}^2 = the variance of the model dataset and γ_{obs}^2 = the variance of the observed dataset.

Results

Model Skill

The individual models compared favorably to the NDBC datasets based on the shape of CDFs alone (figs. 3–5). However, there was much variation between models, resulting in a wider spread of potential approximations for the data, most notably in the tails of each distribution. The ensemble hindcast dataset showed relatively small error values when compared to the observed dataset for the Hawaiian sites (tables 3–5). The Molokai point approximates all four stations around Hawaii well, with the largest yearly MAE value across all stations being 0.22 m (table 3, fig. 3). The point it best approximates, however, is station 51001 in the northwest sector of the islands, with both DJF and yearly errors lower than 0.14 m. Similarly, the nVar of this station

tends to be closer to 1, which indicates that the ensemble and observed variances in the data are similar.

A similar trend is found for the Big Island dataset (table 4) with Stations 51004 and 51002, which are spatially closer to the modeled point, showing smallest annual MAE values across all stations of 0.08 m and 0.06 m, respectively (fig. 4). Station 51003 also approximated the Big Island dataset; it has a very small DJF MAE and reveals a smaller nVar and standard deviation (Std). The Kauai point best represented station 51001 with an annual MAE of 0.18 m (table 5, fig. 5). This point did not approximate the remaining points as well compared to the other modeled points, likely because of the effect of the islands on wave propagation at stations 51003, 51002, and 51004 that is unresolved in the coarse-resolution GCMs. The yearly-normalized variance ratio was 1.01, indicating that variances at these modeled point were captured well.

In summary, the ensemble hindcast H_s dataset approximated the NDBC buoy stations well. Generally, the modeled points represented the stations closest to their positions, but each served as a good representation for each station when compared to the complete observed dataset. The points collectively reflected the broad Hawaiian wave climate for the hindcast period, indicating that while individual trends are captured well, the larger wave trends of the Hawaiian chain are also captured within the model. Deviations from the observed dataset in figures 3–5 reflected the position of the modeled points relative to the island. For example, the modeled Molokai point over-predicted the waves present at 51004, which was expected because the station is to the southeast of the Big Island, which serves to block many of the larger waves that come from the northwest during the boreal winter.

Tables 6–8 show the MAE, Std, and nVar for the top 5 percent of H_s. As expected, the extreme H_s showed a larger model deviation from the observed values. The annual MAE for all points was approximately 0.40 to 0.60 m, indicating that the models did not represent the extremes as closely as the entire observed dataset. Additionally, the MAE for each station did not necessarily represent the nearest modeled point. For example, the modeled Kauai did not best approximate Station 51001 for all seasons, producing a value of 0.58 m, but showed similar annual error for stations 51003 and 51004, 0.52–0.54 m (table 8). However, for the boreal winter season, when wave heights in the area are largest, the modeled points displayed small error approximating the nearest stations, with Kauai having an error of 0.08 m compared to Station 51001, for example. Additionally, the nVar for each location indicated that the variance in the dataset was also not as well reflected in the observed dataset, with the observed values often varying more than modeled values. The processes that govern the formation of extreme wave events are difficult to capture, and it is therefore more likely that there were a greater number of variations that altered observed wave trends that the model was not able to emulate.

The modeled points in Hawaii represented the historical datasets well, often having a yearly MAE of less than 0.20 m. However, the deviation of modeled extreme H_s events demonstrates that the models do not necessarily predict extrema as accurately. The larger

deviation in extreme H_s was expected, and although the error was larger, the modeled points still represented the Hawaiian Islands' wave climates well. The accuracy of the remainder of the modeled points for the hindcast period could not be ascertained because of a lack of complete datasets in the remainder of the study area. However, given the accuracy of the Hawaiian points, it is more likely that the model ensembles of other locations simulated the hindcasted period accurately as well.

Regional Results

The results for each of the model points are listed in appendixes A–B and their monthly trends are displayed in appendixes C–D. The modeled points were grouped into one of six regions based on proximity and apparent similarity of wave climate trends within the "Results" and "Discussion" sections to more easily describe basinwide trends. These areas are the Western, Marianas, Central, Northeast, Eastern Equatorial, and Southern regions. The Western region contains the islands of Palau and Yap. The Marianas region comprises Asuncion, Saipan, and Guam. The Central region is the largest, with Chuuk, Kosrae, Enewetak, Bikini, Pohnpei, Wake, and Majuro. The Northeast region contains the Big Island of Hawaii, Molokai, Kauai, Midway, Johnston Atoll, and the Northwest Hawaiian Islands points. The Eastern Equatorial region contains Palmyra, Kingman Reef, Howland, and Jarvis. Finally, the Southern region encompasses two locations: American Samoa and Rose Atoll.

Wave Climate Parameter Changes

The Western Region

Mid-Century: 2026–2045

RCP8.4

Mean

The average DJF and SON H_s of the Western region decreased by 0.10 to 0.20 m (fig. 6, fig. 9). MAM and JJA mean H_s values did not change significantly (fig. 7, fig. 8). σ_{Hs}^2 values did not change significantly.

Mean T_p, associated σ_{Tp}^2 values, and D_p values did not change significantly within the region (figs. 38–41, figs. 70–73).

Top 5 Percent

DJF mean H_s values dropped by 0.20 to 0.30 m (fig. 10). MAM values did not change significantly, while JJA values decreased by 0.10 to 0.20 m (fig. 11, fig. 12). The largest decrease

was during the SON season, where values decreased by >0.30 m (fig. 13). Extreme σ_{Hs}^2 did not change significantly.

Mean T_p values decreased at Palau during the DJF and SON seasons by 0.25 to 0.50 s (fig. 42, fig. 45). JJA values similarly decreased by 0.25 to 0.50 s (fig. 43). MAM T_p means did not change significantly, nor did σ_{Tp}^2 values during any season (fig. 44). DJF and MAM mean D_p values rotated clockwise by 5 to 10° at Palau (figs. 74–75). JJA mean D_p values rotated counterclockwise by 10 to 20° (fig. 76). SON σ_{Dp} values increased by >15.0° and mean D_p values rotated counterclockwise by 20 to 30° (fig. 77).

RCP8.5

Mean

The region displayed a decrease of 0.10-0.20 m during the DJF and SON seasons (fig. 14, fig. 17). Mean H_s did not change significantly in the remaining seasons (figs. 15–16). σ_{Hs}^2 did not change significantly.

Mean T_p and associated σ_{Tp}^2 values did not change significantly within the region (figs. 46–49). σ_{Dp} values did not change significantly throughout all seasons, and mean wave directions rotated clockwise by 5 to 10° during the JJA season (figs. 78–81).

Top 5 Percent

Extreme mean H_s values decreased by 0.10 to 0.30 m for the DJF season and decreased by >0.30 m during the SON season (fig. 18, fig. 21). Extreme values for the remaining seasons did not change significantly (figs. 19–20). Extreme σ_{Hs}^2 values did not change significantly.

T_p means decreased by 0.25 to 0.50 s at Palau during the DJF and JJA seasons (fig. 50, fig. 52). SON T_p means also decreased by 0.25 to 0.50 s (fig. 53). MAM T_p means did not change significantly, nor did σ_{Tp}^2 in any season (fig. 51). DJF σ_{Dp} values increased by 5.0 to 10.0° at Palau and decreased by the same amount at Yap (fig. 82). D_p rotated clockwise by 5-10°. The D_p values rotated clockwise by 5-10° during the MAM season (fig. 83). JJA σ_{Dp} values decreased by 10.0 to 15.0°, and D_p rotated by 5-15° counterclockwise (fig. 84). SON σ_{Dp} values increased by 5.0-10.0° at Yap (fig. 85).

End-Century: 2081–2100

RCP4.5

Mean

The mean H_s values of the DJF and SON seasons decreased by 0.10 to 0.20 cm (fig. 22, fig. 25). Mean values did not change significantly during the other seasons (figs. 23–24). σ_{Hs}^2 values did not change significantly.

Mean T_p and associated σ_{Tp}^2 values did not change significantly within the region (figs. 54–57). The D_p of Palau rotated clockwise by 5 to 10° during the JJA season but otherwise did not change throughout the region during other seasons (figs. 86–89). σ_{Dp} values increased at Yap by 5.0 to 10.0° during the SON season but did not change significantly during other seasons.

Top 5 Percent

The DJF extreme mean values decreased by 0.20 to 0.30 m (fig. 26). MAM and SON extreme values decreased by a smaller range of 0.10 to 0.20 m (fig. 27, fig. 29). Values did not change significantly during the boreal summer months (fig. 28). Extreme σ_{Hs}^2 values did not change significantly.

The extreme JJA T_p mean decreased by 0.25 to 0.50 s at Yap (fig. 60). T_p means did not change significantly during the remaining seasons and σ_{Tp}^2 values did not significantly change throughout all seasons (figs. 58–59, fig. 61). DJF σ_{Dp} values decreased by 5.0 to 10.0° at Palau and increased by 5.0 to 10.0° at Yap (fig. 90). Palau's D_p rotated clockwise by 5 to 10°. D_p at Palau rotated by 10 to 20° counterclockwise during the JJA season (fig. 92). σ_{Dp} values increased by >15.0° within the region during the SON season and mean directions rotated 20-30° counterclockwise at Palau and 100-110° counterclockwise at Yap (fig. 93). MAM D_p values did not change significantly (fig. 91).

RCP8.5

Mean

The region's DJF mean H_s values decreased by 0.20 to 0.30 m, while the MAM values dropped by a smaller, 0.10 to 0.20 m (figs. 30–31). The SON season values decreased by a mix of small and larger values, ranging from 0.10 to 0.30 m (fig. 33). The JJA values did not change significantly (fig. 32). σ_{Hs}^2 values decreased by 0.20 to 0.40 during the SON season. Values did not change during other seasons.

Mean T_p values decreased by 0.25 to 0.50 s during both the MAM and SON seasons (fig. 63, fig. 65). T_p means did not decrease during the remaining seasons (fig. 62, fig. 64). σ_{Tp}^2 did not change throughout all seasons. D_p values rotated clockwise by 5 to 10° during the JJA and SON seasons (figs. 96–97). D_p values did not change significantly during the DJF and MAM seasons (figs. 94–95). σ_{Dp} values did not change significantly throughout all seasons.

Top 5 Percent

Extreme H_s values decreased by 0.10 to >0.30 m for the DJF season (fig. 34). MAM values decreased by 0.20 to >0.30 m, and JJA values decreased by 0.10 to 0.20 m (figs. 35–36). The SON values had the strongest decrease in the region with each point decreasing by >0.30 m (fig. 37). Extreme σ_{Hs}^2 values did not change significantly from hindcast values.

Mean T_p values decreased by 0.25 to 0.50 s during the DJF, MAM, and SON seasons (figs. 66–67, fig. 69). JJA T_p values did not change significantly (fig. 68). σ_{Tp}^2 did not change significantly throughout all seasons. Palau's D_p rotated by 5-10° clockwise during the DJF season (fig. 98). MAM σ_{Dp} values decreased by 5.0 to 10.0°, and D_p rotated clockwise by 5 to 10° (fig. 99). JJA σ_{Dp} values decreased by the same amount, but directions rotated 15-20° counterclockwise (fig. 100). SON σ_{Dp} values increased by 10-15°, and directions rotated 30 to 40° counterclockwise at Palau and 80 to 90° clockwise at Yap (fig. 101).

Marianas Region

Mid-Century: 2026–2045

RCP4.5

Mean

MAM and SON values decreased by 0.10 to 0.20 m (fig. 7, fig. 9). The boreal summer and winter means did not change significantly from hindcast data (fig. 6, fig. 8). σ_{Hs}^2 values did not change significantly.

Mean T_p, associated σ_{Tp}^2 values, and D_p values did not change significantly within the region (figs. 38–41, figs. 70–73).

Top 5 Percent

Extreme wave heights increased by 0.10 to 0.20 m in Asuncion for the DJF season (fig. 10). Conversely, MAM extreme H_s means decreased by 0.10 to 0.20 m (fig. 11). JJA values decreased by more than 0.30 m, but in SON, the values decreased by >0.30 m at each point (figs.

12–13). JJA σ_{Hs}^2 values decreased by 0.20 to 0.40. SON σ_{Hs}^2 values increased at Asuncion by 0.20 to 0.40.

Mean T_p values decreased by 0.25 to 0.50 s during the DJF season at Asuncion and during JJA at Guam (fig. 42, fig. 44). The mean T_p values did not significantly change during other seasons (fig. 43, fig. 45). σ_{Tp}^2 did not significantly change during all seasons. The D_p of Asuncion rotated clockwise by 5 to 10° during DJF (fig. 74). MAM σ_{Dp} values decreased by 5.0 to 10.0° (fig. 75). JJA σ_{Dp} values increased by 10.0 to 15.0°, and SON values increased by 10.0 to >15.0° (figs. 76–77).

RCP8.5

Mean

Mean SON H_s values at each point decreased by 0.10 to 0.20 m, while the means for the remaining seasons did not change significantly (figs. 14–17). σ_{Hs}^2 values did not change significantly.

Mean T_p and associated σ_{Tp}^2 values did not change significantly within the region (figs. 46–49). Saipan's σ_{Dp} increased by 5.0 to 10.0° during the SON season (fig. 81). σ_{Dp} values did not change significantly throughout the remaining seasons, and directions did not change noticeably throughout all seasons (figs. 78–80).

Top 5 Percent

Extreme H_s values increased by 0.10 to 0.20 m during the MAM and JJA seasons (figs. 19–20). The SON values decreased by 0.10 to 0.20 m (fig. 21). The boreal winter season did not change significantly (fig. 18). σ_{Hs}^2 values increased during the SON season by 0.20 to 0.40 at Saipan and by >0.40 at Asuncion.

Mean T_p values decreased by 0.25 to 0.50 at Asuncion during DJF and at Guam during SON (fig. 50, fig. 53). T_p values did not significantly change during the remaining seasons (figs. 51–52). σ_{Tp}^2 did not significantly change during all seasons. D_p at Asuncion rotated 10 to 20° clockwise during the DJF season (fig. 82). σ_{Dp} values decreased by 5.0 to 15.0° over the region during MAM (fig. 83). The JJA σ_{Dp} value at Guam decreased by 5.0 to10.0° and D_p rotated 20-30° clockwise at Asuncion and 5 to 10° at Saipan (fig. 84). SON σ_{Dp} values increased by 10.0 to >15.0° and directions rotated clockwise by 5 to 20° (fig. 85).

End-Century: 2081–2100

RCP4.5

Mean

SON means decreased by 0.10 to 0.20 m (fig. 25). The means of the remaining seasons did not significantly deviate from hindcast values (figs. 22–24). σ_{Hs}^2 values did not change within the modeled region.

Mean T_p and associated σ_{Tp}^2 values did not change significantly within the region (figs. 54–57). The σ_{Dp} value decreased at Guam by 5.0 to 10.0° during the SON season (fig. 89). σ_{Dp} values did not change significantly during other seasons (figs. 86–88). D_p at each point did not change noticeably.

Top 5 Percent

MAM and JJA extreme H_s means decreased by 0.20 to 0.30 m (figs. 27–28). The SON mean decreased by more than 0.30 m from the hindcast mean (fig. 29). The DJF mean did not change significantly form the hindcast mean (fig. 26). MAM σ_{Hs}^2 values decreased by 0.20 to 0.40, except at the Guam point, which decreased by >0.40. Values did not change significantly during the remaining seasons.

T_p means decreased by 0.25 to 0.50 s during the DJF season (fig. 58). T_p means did not change significantly during other seasons (figs. 59–61). σ_{Tp}^2 did not change significantly throughout all seasons. The DJF D_p of Asuncion rotated 5 to 10° clockwise (fig. 90). MAM σ_{Dp} values decreased by 5.0 to 15.0° throughout the region and directions rotated by 5 to 10° counterclockwise as Asuncion (fig. 91). JJA σ_{Dp} values increased by 5.0 to 1.0°, and D_p values at Saipan and Guam rotated clockwise by 5 to 10° (fig. 92). SON σ_{Dp} valued increased by 5.0 to 15.0° throughout the region, and D_p values at Saipan and Guam rotated counterclockwise by 5 to 10° (fig. 93).

RCP8.5

Mean

DJF and MAM means decreased by 0.10 to 0.20 m (figs. 30–31). SON values decreased by a wider range of 0.10 to 0.30 m (fig. 33). The JJA season mean did not change significantly (fig. 32). σ_{Hs}^2 values did not change significantly.

Mean T_p values decreased by 0.25 to 0.50 s during the DJF, MAM, and SON seasons (figs. 62–63, fig. 65). JJA T_p means didn't change significantly (fig. 64). σ_{Tp}^2 did not change significantly throughout all seasons. σ_{Dp} values increased during the SON season by 5.0 to 1.0° (fig. 97). σ_{Dp} values did not change significantly during other seasons and directions did not change noticeably (figs. 94–96).

Top 5 Percent

DJF extreme H_s means decreased by 0.10 to 0.30 m, while JJA values decreased by 0.10 to 0.20 m (fig. 34, fig. 36). Both MAM and SON means decreased by more than 0.30 m (fig. 35, fig. 37). DJF σ_{Hs}^2 values increased by 0.20 to 0.40 at Guam. MAM values decreased by 0.20 to 0.40, with values decreasing by >0.40 at Guam. JJA σ_{Hs}^2 values increased by 0.20 to 0.40 at Guam and decreased by the same amount at Asuncion. SON values did not change significantly.

DJF T_p means decreased over a wide range. T_p mean decreased by 0.25 to 0.50 s at Guam, 0.50 to 0.75 s at Saipan, and >0.75 s at Asuncion (fig. 66). MAM and SON T_p means decreased by 0.25 to 0.50 s (fig. 67, fig. 69). JJA mean T_p values did not change significantly (fig. 68). σ_{Tp}^2 did not change significantly throughout all seasons. The D_p of Asuncion rotated 10 to 20° clockwise during the DJF season and 5 to 10° clockwise during the JJA season (fig. 98, fig. 100). σ_{Dp} values decreased by 5.0 to 15.0 during MAM (fig. 99). SON σ_{Dp} values increased by 5.0 to 15.0 across the region and directions rotated 10 to 20° clockwise (fig. 101).

Central Region

Mid-Century: 2026–2045

RCP4.5

Mean

The SON mean H_s value decreased by 0.10 to 0.20 m within the center of the island cluster (fig. 9). The mean values from other seasons did not change significantly (figs. 6–8). σ_{Hs}^2 values did not change significantly.

Mean T_p and associated σ_{Tp}^2 values did not change significantly within the region (figs. 38–41). The D_p of Majuro and Pohnpei rotated by 5 to 10° clockwise and of Kosrae by 10 to 20° clockwise during the SON season (fig. 73). The D_p of all points did not change significantly during remaining seasons, and σ_{Dp} values did not significantly change across all seasons (figs. 70–72).

Top 5 Percent

The region experienced decreases in extreme mean wave heights during most seasons. The DJF mean decreased by 0.20 to 0.30 m, and the MAM season decreased by a smaller 0.10 to 0.20 m (figs. 10–11). The SON mean extreme H_s decreased by more than 0.30 cm (fig. 13). There was no significant change in the JJA means (fig. 12). Extreme σ_{Hs}^2 values did not change significantly from hindcast values.

The MAM mean T_p value at Kosrae decreased by 0.25 to 0.50 s (fig. 43). The JJA and SON T_p mean at Chuuk decreased by 0.25 to 0.50 s. additionally, the σ_{Tp}^2 during SON at Kwajalein increased by 1.5 to 3.0 (figs. 44–45). T_p means did not change significantly during the DJF season and σ_{Tp}^2 values did not significantly change during the remaining seasons (fig. 42). DJF σ_{Dp} values increased by >15.0° but lowered to 5.0 to 15.0° closer to the Equator and the D_p of Wake rotated counterclockwise by 5 to 10° (fig. 74). The D_p at Kosrae rotated 5 to 10° clockwise and the regions σ_{Dp} values decreased by 5.0 to >15.0°, with the largest decrease at Kosrae, during the MAM season (fig. 75). σ_{Dp} values decreased by 5.0 to 10.0° during the JJA season (fig. 76). Directions rotated 10 to 20° counterclockwise in the southwest half of the region and 5 to 10° clockwise in the northeast half. SON σ_{Dp} values decreased by 10.0 to > 15.0 in the northwest half of the region (fig. 77). The D_p rotated 40 to 50° clockwise at Kosrae and 5 to 10° counterclockwise at Kwajalein.

RCP8.5

Mean

The SON mean H_s decreased by 0.10-0.20 m (fig. 17). The remaining seasons' mean did not change significantly (figs. 14–16). σ_{Hs}^2 values did not change significantly.

Mean T_p and associated σ_{Tp}^2 values did not change significantly within the region (figs. 46–49). D_p at Kosrae and Pohnpei rotated clockwise by 5 to 10° during SON and σ_{Dp} values did not change significantly throughout all seasons (figs. 78–81).

Top 5 Percent

DJF extreme H_s means decreased by 0.10 to 0.20 at the Enewetak, Wake, and Bikini points (fig. 18). Conversely, the JJA means at Enewetak, Bikini, and Kosrae increased by 0.10 to 0.20 m (fig. 20). Extreme H_s means for the SON season decreased by 0.20 to more than 0.30 m across the entire region (fig. 21). The boreal spring season averages did not change significantly

(fig. 19). Extreme σ_{Hs}^2 values increased by 0.20 to 0.40 at the Wake, Enewetak, and Bikini points. Values did not significantly change in other seasons.

The T_p mean at Kosrae increased by 0.50 to 0.75 s during the DJF season (fig. 50). T_p means during MAM decreased by 0.25 to 0.50 s at Pohnpei and Kosrae (fig. 51). Mean T_p values did not change significantly during other seasons (figs. 52–53). σ_{Tp}^2 did not significantly change during all seasons. DJF σ_{Dp} values increased by 5.0 to 10.0° at Kosrae, Chuuk, Pohnpei, and Wake (fig. 82). The MAM σ_{Dp} value at Chuuk decreased by 10.0 to 15.0°, and directions at Kosrae and Pohnpei rotated clockwise by 5 to 10° (fig. 83). JJA σ_{Dp} values decreased by 5.0 to 15.0° in the west half of the region, and islands' directions rotated 5 to 10° clockwise at Majuro, Enewetak, Bikini, and Wake (fig. 84). Kosrae's D_p in the rotated by 20 to 30° clockwise and the σ_{Dp} value at Wake increased by 10.0 to 15.0°. The σ_{Dp} values increased by 5.0 to 15.0° throughout. The SON D_p values of Kosrae, Pohnpei, and Kwajalein rotated counterclockwise by 10 to 20° and at Majuro by 5 to 10° (fig. 85).

End-Century: 2081–2100

RCP4.5

Mean

The DJF mean H_s values decreased by 0.10 to 0.20 m across the entire region, and the SON values decreased by the same amount but only in the western half of the region (fig. 22, fig. 25). The remaining seasons did not display significant changes form hindcast means (figs. 23–24). σ_{Hs}^2 values did not change significantly.

Mean T_p and associated σ_{Tp}^2 values did not change significantly within the region (figs. 54–57). The SON σ_{Dp} value at Enewetak increased by 5.0 to 1.0°, and the D_p of Kosrae rotated 5 to 10° clockwise (fig. 89). Directions and σ_{Dp} values did not change significantly through the other seasons (figs. 86–88).

Top 5 Percent

DJF, MAM, and SON extreme means decrease by 0.10 to 0.30 m, with the larger decreases occurring at the western points in the former two seasons and at the central islands in the latter (figs. 26–27, fig. 29). JJA means increase by 0.10 to greater than 0.30 m, with the largest deviations from hindcast means occurring at Enewetak and Bikini (fig. 28). MAM σ_{Hs}^2 values decreased by 0.20 to 0.40 at the Enewetak point. JJA values increased by 0.20 to 0.40 at Enewetak, Bikini, and Wake. Values did not significantly change during other seasons.

The T_p mean decreased by 0.25 to 0.50 s at Pohnpei during the MAM season (fig. 59). T_p means increased during the JJA season at Enewetak, Bikini, and Wake by 0.25 to 0.50 s (fig. 60). Means did not change significantly during other seasons (fig. 58, fig. 61). σ_{Tp}^2 did not change significantly throughout all seasons. DJF σ_{Dp} values increased by 5.0 to 15.0° at Chuuk, Pohnpei, and Kosrae and the D_p of Wake rotated 5 to 10° counterclockwise (fig. 90). MAM σ_{Dp} values decreased by 5.0 to 15.0°, and directions rotated clockwise by 5 to 10° at Chuuk, Kosrae, and Wake (fig. 91). JJA trends were split by west and east within the region (fig. 92). The west half of the area displayed a decrease of σ_{Dp} values by 5.0 to >15.0°, and directions rotated clockwise by 5 to 30°. The eastern half had an increase of σ_{Dp} values by 5.0 to >15.0° and directions rotated clockwise by 30 to 60°. The SON seasons displayed an increase of σ_{Dp} values by 5.0 to >15.0°, and directions shifted counterclockwise by 20 to 30° at Chuuk, 50 to 60° at Pohnpei, 80 to 90° at Kosrae, and 10 to 20° at Kwajalein (fig. 93).

RCP8.5

Mean

Mean DJF values decreased by 0.10 to 0.20 m (fig. 30). SON values decreased by a larger 0.10 to 0.30 m (fig. 33). The remaining seasons' means did not change significantly (figs. 31–32). SON σ_{Hs}^2 values decreased by 0.20 to 0.40 at Bikini, but values did not change significantly during other seasons.

Mean T_p values decreased by 0.25 to 0.50 s at Bikini through the DJF season and at Kosrae during JJA (fig. 62, fig. 64). T_p means decreased through the entire region by 0.25 to 0.50 s during the SON season (fig. 65). There were no significant changes in T_p means during MAM (fig. 63). Additionally, σ_{Tp}^2 values did not significantly change throughout all seasons. MAM σ_{Dp} values decreased by 5.0 to 10.0° at Chuuk (fig. 95). SON σ_{Dp} values decreased by 5.0 to 10.0° at Kosrae and directions rotated 5 to 10° clockwise at Kwajalein, Majuro, and Chuuk, and by 10 to 20° at Kosrae and Pohnpei (fig. 97). No significant changes were observed during other seasons (fig. 94, fig. 96).

Top 5 Percent

DJF means decreased by 0.10 to 0.30 m over the region (fig. 34). MAM mean values decreased over a wide range, from 0.10 to more than 0.30 m (fig. 35). JJA values increased from 0.10 to more than 0.30 m, with the largest increases occurring at Enewetak and Bikini (fig. 36). The strongest change was during the SON season, where the majority of the region's values decreased by >0.30 m (fig. 37). σ_{Hs}^2 values decreased by 0.20 to 0.40 at Wake during the DJF season. Values decreased by the same amount at Enewetak and Bikini during the MAM season.

JJA values decreased by >0.40 at Enewetak, Bikini, and Wake. SON valued increased by 0.20 to 0.40 at Enewetak and Wake.

DJF T_p means decreased by 0.25 to 0.50 s within the region, while the σ_{Tp}^2 at Kwajalein increased by 1.5 to 3.0 (fig. 66). σ_{Tp}^2 values did not significantly change in the other seasons. MAM T_p means decreased by 0.25 to 0.50 s except at Chuuk and Pohnpei, where values decreased by 0.50 to 0.75 s (fig. 67). JJA T_p means decreased at Chuuk by 0.25 to 0.50 s and increased by the same amount at Wake (fig. 68). SON T_p means decreased by 0.25 to 0.50 s, except at Chuuk, where the decrease was 0.50 to 0.75 s (fig. 69). The D_p of Wake during DJF rotated counterclockwise by 5 to 10° (fig. 98). MAM σ_{Dp} values decreased by 5.0 to 15.0° at Chuuk, Majuro, and Kwajalien (fig. 99). The D_p of Chuuk, Kosrae, and Pohnpei rotated clockwise by 5 to 10°. The JJA σ_{Dp} values decreased at Enewetak by 5.0 to 10.0° and its direction rotated clockwise by 30 to 40° (fig. 100). The other islands' directions in the western half of the region rotated 5 to 20° counterclockwise. The east half of the region's σ_{Dp} values increased by 5.0 to >15.0° and directions rotated 5 to 20° clockwise, and 20 to 30° at Wake and Bikini. SON σ_{Dp} values increased by 5.0 to >15.0° and directions rotated clockwise by 5 to 20° at Enewetak and Pohnpei, by 20 to 30° at Chuuk, and by 40 to 50° at Kosrae (fig. 101). There were no significant changes during the DJF season.

Northeast Region

Mid-Century: 2026–2045

RCP4.5

Mean

The mean H_s values of the Northeast region did not change significantly throughout all seasons (figs. 6–9). σ_{Hs}^2 values did not significantly change from hindcast values.

Mean T_p and associated σ_{Tp}^2 values did not change significantly within the region (figs. 38–41). The D_p of Midway rotated clockwise by 5 to 10° during the SON season (fig. 73). Other D_p and associated σ_{Dp} values did not change significantly throughout all seasons (figs. 70–72).

Top 5 Percent

The main Hawaiian Island points' extreme mean H_s decreased by 0.10 to 0.20 m during the JJA season (fig. 12). The values of the remaining seasons did not change significantly (figs. 10–11, fig. 13). SON extreme σ_{Hs}^2 values decreased by 0.20 to 0.40 at Midway and by >0.40 at the Northwest Hawaiian Islands point. Values did not change significantly during the other seasons.

DJF T_p mean values increased by 0.25 to 0.50 s at Kauai and Johnston Atoll (fig. 42). The Big Island T_p mean increased by 0.50 to 0.75 s. The MAM T_p mean of Kauai increased by 0.25 to 0.50 s and its σ_{Tp}^2 increased by 1.5 to 3.0 (fig. 43). JJA means remain unchanged but the σ_{Tp}^2 of Kauai increased by 1.5 to 3.0 (fig. 44). SON values did not significantly change (fig. 45). σ_{Tp}^2 values during the boreal winter and fall seasons did not change significantly. The DJF D_p of the Big Island and Johnston Atoll rotated counterclockwise by 5 to 10° (fig. 74). The MAM D_p of Kauai rotated counterclockwise by 5 to 10° (fig. 75). The JJA σ_{Dp} value at Johnston Atoll increased by 10.0 to 15.0°, and the D_p at the Northwest Hawaiian Islands rotated clockwise by 5 to 10° (fig. 76). SON σ_{Dp} values increased in the western half of the region by 5.0 to 10.0°, and wave directions in the Northwest Hawaiian Islands and Midway rotated 5 to 20° clockwise (fig. 77). The D_p of Kauai rotated clockwise by 5 to 10°.

RCP8.5

Mean

Mean valued decreased by 0.10 to 0.20 m during the SON season throughout the region (fig. 17). There were no significant changes observed in other seasons (figs. 14–16). σ_{Hs}^2 values did not change significantly.

Mean T_p values increased at Kauai during the JJA season and the Big Island point during SON by 0.25 to 0.50 s (figs. 48–49). Means did not change significantly during other seasons (figs. 46–47). σ_{Tp}^2 values did not significantly change throughout all seasons. MAM D_p rotated by 5 to 10° counterclockwise at the Northwest Hawaiian Islands point and by 10 to 20° at the Midway point (fig. 79). Midway's σ_{Dp} increased by 5.0 to 10.0° during the JJA season (fig. 80). Midway's D_p rotated clockwise by 5 to 10° during the SON season (fig. 81). DJF D_p values did not change significantly (fig. 78).

Top 5 Percent

Extreme values over most seasons decreased at all points within the region. DJF values decreased by 0.10 to 0.30 m at all points except the Big Island of Hawaii point, which increased by 0.10 to 0.20 m (fig. 18). MAM means decreased by 0.10 to 0.20 m at the Big Island of Hawaii point, but the remainder of the study area did not change significantly (fig. 19). The JJA and SON seasons' means decreased irregularly over the region by 0.10 to 0.20 m (figs. 20–21). Extreme σ_{Hs}^2 values did not change significantly.

Mean T_p increased at Johnston Atoll and Kauai during DJF by 0.25 to 0.50 (fig. 50). The Big Island point's T_p mean increased by 0.50 to 0.75 s, and its σ_{Tp}^2 decreased by 1.5 to 3.0. The JJA σ_{Tp}^2 of Kauai increased by 1.5 to 3.0 and the SON mean T_p values of Kauai increased by 0.25

to 0.50 s (figs. 52–53). The MAM season had not significant changes (fig. 51). DJF σ_{Dp} values increased by 5.0 to 10.0° except at the Big island point, which decreased by the 5.0 to 10.0° (fig. 82). Johnston Atoll Molokai's D_p rotated 10 to 20° clockwise. Kauai's D_p rotated clockwise by 5 to 10°. The MAM σ_{Dp} of Midway decreased by 5.0 to 10.0° and the Northwest Hawaiian Islands, Kauai, and Molokai points' mean D_p values rotated counterclockwise by 5 to 20° (fig. 83). JJA σ_{Dp} values increased by 5.0 to 15.0° across the region and Northwest Hawaiian Islands, and Midway's mean D_p rotated clockwise by 5 to 10° (fig. 84). The SON σ_{Dp} value of Kauai decreased by 5.0 to 10.0°, and the mean D_p of the Northwest Hawaiian Islands rotated clockwise by 10 to 20° (fig. 85). Midway's D_p rotated counterclockwise by 20 to 30°.

End-Century: 2081–2100

RCP4.5

Mean

The Midway and Northwest Hawaii points' H_s means decreased by 0.10 to 0.20 m from hindcast means during the SON season, but the remainder of the region during this season did not change significantly (figs. 22–25). Additionally, the means of these points did not deviate significantly from hindcast means during other seasons. σ_{Hs}^2 values did not change significantly.

Mean T_p values increased by 0.25 to 0.50 s at Molokai and the Big Island points during MAM and at Molokai and Kauai during JJA (figs. 55–56). T_p means didn't change significantly during other seasons, and σ_{Tp}^2 values did not significantly change throughout all seasons (fig. 54, fig. 57). The mean MAM D_p at Midway, Kauai, Molokai, and the Northwest Hawaiian Islands rotated counterclockwise by 5 to 20° (fig. 87). D_p means at Midway and the Northwest Hawaiian Islands rotated clockwise by 5 to 20°. D_p values did not change significantly during the remaining seasons (fig. 86, figs. 88–89).

Top 5 Percent

The top 5 percent of mean H_s values decreased during the SON season by 0.10 to 0.30 m (fig. 29). The extreme H_s means did not change significantly for other seasons (figs. 26–28). JJA σ_{Hs}^2 values increased by >0.40 within the region except at the Northwest Hawaiian Islands and Kauai points, which increased by 0.20 to 0.40. H_s values did not change significantly during other seasons.

Mean T_p values increased by 0.25 to 0.50 s at Johnston Atoll, Kauai, and Molokai during the DJF season (fig. 58). MAM T_p means increased by 0.25 to 0.50 s at Kauai and Johnston Atoll, and the Big Island's T_p mean increased by 0.50 to 0.75 s (fig. 59). JJA means increased by 0.25 to

0.50 s, except at Kauai, which increased by 0.50 to 0.75 s (fig. 60). σ_{Tp}^2 at the Big Island increased by 1.5 to 3.0 and at Kauai by >3.0. SON means decreased by 0.25 to 0.50 s at Johnston Atoll, Kauai, and Molokai (fig. 61). DJF σ_{Dp} values increased by 5.0 to 10.0° at Midway and the Northwest Hawaiian Islands. Johnston Atoll's D_p rotated counterclockwise by 5 to 10° (fig. 90). The MAM mean D_p at Kauai and Molokai rotated counterclockwise by 5 to 20° (fig. 91). JJA σ_{Dp} values increased by 5.0 to >15.0°, and mean D_p rotated clockwise at all islands except Johnston Atoll by 5 to 20° (fig. 92). Similarly, the mean D_p of Kauai, Johnston Atoll, Midway, and the Northwest Hawaiian Islands rotated 5 to 20° clockwise during the SON season (fig. 93). σ_{Dp} values increased by 5.0 to 10.0° throughout the region.

RCP8.5

Mean

DJF, MAM, and JJA mean H_s values decreased by 0.10 to 0.20 m over the region (figs. 30–32). SON H_s means decreased by a larger range of 0.10 to 0.30 m (fig. 33). SON extreme σ_{Hs}^2 values decreased by 0.20 to 0.40 at Midway. H_s values did not change significantly during the remaining seasons.

JJA T_p means increased by 0.25 to 0.50 s at the Big Island and Northwest Hawaiian Islands points and by 0.502 to 0.75 at the Molokai and Kauai points (fig. 64). σ_{Tp}^2 increased by 1.5 to 3.0 at the Big Island and Northwest Hawaiian Islands points. σ_{Tp}^2 increased by >3.0 at Molokai and Kauai. The SON Big Island T_p mean increased by 0.25 to 0.50 s (fig. 65). σ_{Tp}^2 values increased by 1.5 to 3.0 at the Kauai and the Big Island points. T_p means and associated σ_{Tp}^2 values did not change significantly during other seasons (figs. 62–63). The MAM and JJA mean D_p values of Midway rotated 5 to 10° counterclockwise and clockwise, respectively (figs. 95–96). The SON mean D_p at the Northwest Hawaiian Islands and Midway rotated clockwise by 10 to 20° and at Kauai and Johnston Atoll by 5 to 10° (fig. 97). The D_p values of the DJF season did not significantly change (fig. 94).

Top 5 Percent

Extreme DJF H_s means decreased by 0.10 to >0.30 m, with the largest decrease occurring at the Midway point (fig. 34). MAM H_s values decreased by 0.10 to 0.30 m (fig. 35). The Northwest Hawaii, Midway, and Johnston Atoll points decreased by 0.20 to >0.30 m. The whole region decreased by the same amount during the SON season (fig. 37). Extreme σ_{Hs}^2 values increased by 0.20 to 0.40 at the Big Island of Hawaii point during the DJF period. JJA values increased by 0.20 to 0.40 except at Midway, which increased by >0.40 (fig. 36).

DJF extreme T_p means increased by 0.25 to 0.50 s (fig. 66). MAM means increased by 0.25 to 0.50 s at Johnston Atoll, 0.50 to 0.75 s at Kauai, and >0.75 s at Molokai (fig. 67). JJA mean T_p values increased by 0.25 to 0.50 s, except at Molokai, which increased by 0.50 to 0.75 s (fig. 68). σ_{Tp}^2 values increased by 1.5 to 3.0, but Molokai and Kauai's σ_{Tp}^2 valuess increased by >3.0. Mean SON T_p values decreased by 0.50 to 0.75 s, except at Johnston Atoll, which decreased by 0.25 to 0.50 s (fig. 69). DJF σ_{Dp} values increased by 5.0 to 10.0°, and the D_p values of Kauai and Molokai rotated clockwise by 5 to 10° (fig. 98). MAM σ_{Dp} values increased by 5.0 to 10.0° at Johnston Atoll and the Big Island, while values decreased by 5.0 to 10.0° at Midway and Kauai (fig. 99). Mean D_p at the Northwest Hawaiian Islands, Kauai, and Molokai rotated counterclockwise by 5 to 30°. JJA σ_{Dp} values decreased by 5.0 to 10.0°, except at Midway, which decreased by 10.0 to 15.0° (fig. 100). The D_p values of the Big Island, the Northwest Hawaiian Islands, and Midway points rotated clockwise by 5 to 20°. SON σ_{Dp} values decreased by 5.0 to 10.0° at the Big Island point, and D_p at Kauai, Midway, and the Northwest Hawaiian Islands rotated clockwise by 10 to 30° (fig. 101).

Eastern Equatorial Region

Mid-Century: 2026–2045

RCP4.5

Mean

There was no significant change in mean H_s values from hindcast means over all seasons (figs. 6–9). σ_{Hs}^2 values did not change significantly.

Mean T_p and associated σ_{Tp}^2 values did not change significantly within the region (figs. 38–41). The D_p of Jarvis rotated counterclockwise by 5 to 10° during the JJA season (fig. 72). The D_p of all islands within the region rotated clockwise by 5 to 10° during the SON season (fig. 73). σ_{Dp} values did not change significantly throughout all seasons (figs. 70–71).

Top 5 Percent

Extreme mean H_s values decreased by 0.10 to 0.20 m at the Howland point during the DJF season, but the other points remain essentially unchanged (fig. 10). MAM means at Palmyra and Kingman Reef increased by 0.10 to 0.20 m, while the remaining points were unchanged (fig. 11). Means decreased by 0.20 to 0.30 m during the SON season (fig. 13). The JJA season means did not change significantly from hindcast means (fig. 12). Extreme σ_{Hs}^2 values decreased by 0.20 to 0.40 during the SON season.

DJF extreme T_p means increased by 0.25 to 0.50 s at Palmyra and Kingman Reef, and Howland's mean values increased by 0.50 to 0.75 s (fig. 42). MAM and JJA mean T_p values increased at Jarvis by 0.25 to 0.50 s (figs. 43–44). SON T_p means increased by a larger 0.50 to 0.75 s range (fig. 45). σ_{Tp}^2 values did not significantly change throughout all seasons. The MAM and JJA σ_{Dp} value at Howland decreased by 5.0 to 10.0° and the D_p of the latter season rotated 5 to 10° counterclockwise (figs. 75–76). The SON σ_{Dp} value at Jarvis decreased by 5.0 to 10.0°; it and Howland's D_p rotated clockwise by 10 to 20° and Palmyra and Kingman Reef's D_p rotated counterclockwise by 5 to 10° (fig. 77). The DJF D_p values did not change significantly (fig. 74).

RCP8.5

Mean

Mean H_s values did not deviate significantly from hindcast means during this period (figs. 14–17). σ_{Hs}^2 values did not change significantly throughout the region.

Mean T_p and associated σ_{Tp}^2 values did not change significantly within the region (figs. 46–49). The SON mean D_p values rotated 5 to 10° clockwise within the region but did not significantly change throughout other seasons (fig. 81). σ_{Dp} values did not change significantly (figs. 78–80).

Top 5 Percent

Palmyra and Kingman Reef extreme SON H_s means decreased by >0.30 m compared to hindcast mean values, while the rest of the region did not change (figs. 18–21). Additionally, means did not change significantly during the other seasons. SON σ_{Hs}^2 values decreased by 0.20 to 0.40, but remain unchanged throughout all other seasons.

Mean T_p values increased during the DJF season at the Palmyra and Kingman Reef points by 0.25 to 0.50 s (fig. 50). Howland's mean T_p decreased by 0.25 to 0.50 s during the MAM season, whereas Palmyra and Kingman Reef's values decreased by 0.50 to 0.75 s (fig. 51). The σ_{Tp}^2 at Palmyra and Kingman Reef decreased by 1.5 to 3.0. The SON season's mean T_p values increased by 0.25 to 0.50 s throughout the region (fig. 53). The σ_{Tp}^2 during this season at Palmyra and Kingman Reef increased by 1.5 to 3.0. JJA T_p values did not change significantly (fig. 52). MAM σ_{Dp} values decreased by 5.0 to 10.0° and the D_p of Jarvis rotated counterclockwise by 5 to 10° (fig. 83). SON σ_{Dp} values increased by 5.0 to 10.0°, except at Jarvis, where it's σ_{Dp} decreased by 10.0 to 15.0 and the D_p of all islands rotated 5 to 30° clockwise (fig. 85). The D_p values of the remaining seasons did not change significantly (fig. 84, fig. 82).

End-Century: 2081–2100

RCP4.5

Mean

Mean end-century H_s values and associated σ_{Hs}^2 values did not change significantly across all seasons (figs. 22–25).

Mean T_p and associated σ_{Tp}^2 values did not change significantly within the region (figs. 54–57). The mean D_p of Jarvis rotated counterclockwise by 5 to 10° during MAM (fig. 87). SON D_p values rotated clockwise by 5 to 10° across all islands (fig. 89). σ_{Dp} values did not change significantly throughout all seasons (fig. 86, fig. 88).

Top 5 Percent

Extreme H_s means decreased by 0.10 to 0.20 m during the SON season (fig. 29). H_s means did not change significantly during other seasons (figs. 26–28). Extreme σ_{Hs}^2 values did not change significantly.

DJF T_p means increased by 0.25 to 0.50s at the Palmyra and Kingman Reef points and decreased by the same amount during the MAM season (figs. 58–59). The mean T_p increased at Jarvis by 0.25 to 0.50 and the σ_{Tp}^2 values increased at Palmyra and Kingman Reef by 1.5 to 3.0 during the JJA season (fig. 60). Not significant T_p changes were observed during the SON season, and no significant σ_{Tp}^2 changes were observed in other seasons (fig. 61). The σ_{Dp} value at Jarvis increased by 5.0 to 1.0° during the DJF season (fig. 90). MAM displayed an increase of 5.0 to 10.0° in the σ_{Dp} of Jarvis as well as a 30 to 40 degree counterclockwise shift of the island's D_p (fig. 91). JJA σ_{Dp} values increased by 5.0 to 10.0 throughout the region and the mean D_p of Jarvis rotated clockwise by 5 to 10° (fig. 92). The σ_{Dp} of Jarvis increased by 5.0 to 10.0°; it and Howland's D_p rotated clockwise by 5 to 20° during the SON season (fig. 93).

RCP8.5

Mean

The DJF H_s means decreased by 0.10 to 0.20 m (fig. 30). Similarly, the Palmyra and Kingman Reef points decreased by 0.10 to 0.20 m for the SON season (fig. 33). The region's means did not change significantly during the other modeled seasons (figs. 31–32). σ_{Hs}^2 values did not change significantly.

The SON σ_{Tp}^2 value at Jarvis increased by 1.5 to 3.0 (fig. 65). However, significant σ_{Tp}^2 changes were not observed in the remaining seasons, and T_p values did not change significantly across all seasons (figs. 62–64). The SON σ_{Dp} values decreased at Howland and Jarvis by 5.0 to 10.0°, and the D_p values throughout the region rotated clockwise by 10 to 20° (fig. 97). D_p values did not change significantly during other seasons (figs. 94–96).

Top 5 Percent

Extreme DJF mean H_s values decreased by 0.10 to 0.30 m within the region (fig. 34). MAM H_s means decreased by 0.10 to 0.20 m, and SON H_s values decreased by 0.20 to >0.30 m (fig. 35, fig. 37). The means of the JJA season did not change significantly (fig. 36). σ_{Hs}^2 values decreased by 0.20 to 0.40 during the SON season. Values did not significantly change from hindcast values in the other seasons.

DJF T_p values increased by 0.25 to 0.50 s, except Palmyra and Kingman Reef, which increased by 0.50 to 0.75 s (fig. 66). Palmyra and Kingman Reef's mean T_p values decreased by 0.25 to 0.50 s and Howland's decreased by 0.50 to 0.75 s during the MAM season (fig. 67). JJA's mean T_p values decreased by 0.25 to 0.50 s at Howland, but increased by the same amount at Jarvis (fig. 68). Additionally, σ_{Tp}^2 values at Palmyra and Kingman reef increased by 1.5 to 3.0 during this season. The SON season trends were similar to the JJA trends, but Howland had a stronger mean T_p decrease of 0.50 to 0.75 s (fig. 69). The DJF σ_{Dp} value at Jarvis decreased by 5.0 to 10.0° (fig. 98). JJA σ_{Dp} values increased by 5.0 to 10.0° within the region (fig. 100). The D_p of Jarvis rotated counterclockwise by 5 to 10° during the MAM season (fig. 99). σ_{Dp} values increased by 5.0 to 15.0° at Kingman Reef, Palmyra, and Howland, and the σ_{Dp} at Jarvis decreased by 10.0 to 15.0° during SON (fig. 101). D_p at Jarvis and Howland rotated clockwise by 20 to 40°.

Southern Region

Mid-Century: 2026–2045

RCP4.5

Mean

There were no significant changes in the Southern islands' mean H_s values during the throughout all seasons (figs. 6–9). σ_{Hs}^2 values did not significantly change.

T_p means did not change significantly across all seasons within the region (figs. 38–41). σ_{Tp}^2 values did not change significantly across all seasons. D_p and σ_{Dp} values did not change significantly throughout all seasons (figs. 70–73).

Top 5 Percent

The mean of the top 5 percent of H_s values decreased at the American Samoa and the Rose point by 0.20 to 0.30 m during the DJF season (fig. 10). SON H_s values increased by 0.10 to 0.20 m at both islands within the region (fig. 13). Extreme σ_{Hs}^2 values decreased by 0.20 to 0.40 at the American Samoa point during the DJF season. Values did not change significantly throughout the remaining seasons (fig. 11–12).

Mean T_p values increased within the region by 0.25 to 0.50 s during the DJF period (fig. 42). The σ_{Tp}^2 at both islands increased by 1.5 to 3.0 during the same season. The mean T_p values during other seasons did not change significantly (figs. 43–45). The SON American Samoa point's σ_{Tp}^2 decreased by 1.5 to 3.0. The DJF σ_{Dp} at American Samoa decreased by 5.0 to 10.0° (fig. 74). The MAM D_p of Rose and American Samoa rotated clockwise by 5 to 10° (fig. 75). D_p values during the JJA and SON did not change significantly (figs. 76–77).

RCP8.5

Mean

There was not a significant change in mean H_s values from hindcast means over all seasons (figs. 14–17). σ_{Hs}^2 values did not change significantly.

Mean T_p values did not change significantly (figs. 46–49). σ_{Tp}^2 values did not change significantly across all seasons. The DJF D_p Rose rotated by 5 to 10° clockwise (fig. 78). D_p and σ_{Dp} values did not change significantly during other seasons (figs. 79–81).

Top 5 Percent

Extreme mean H_s values increased by 0.10 to 0.20 m at the American Samoa point and 0.20 to 0.30 m at the Rose Atoll point for the DJF period (fig. 18). During the SON season, the region's mean H_s values increased by 0.10 to 0.20 m (fig. 21). JJA mean H_s values increased at Rose by 0.10 to 0.20 m (fig. 20). DJF σ_{Hs}^2 values decreased by 0.20 to 0.40 at the American Samoa point. Extreme H_s values did not significantly change during the MAM or JJA seasons (fig. 19).

Mean T_p values increased at Rose by 0.25 to 0.50 s during the DJF season (fig. 50). During the same season, the region's σ_{Tp}^2 decreased by 1.5 to 3.0 at Rose and by >3.0 at American Samoa. MAM T_p means decreased by 0.25 to 0.50 s (fig. 51). The SON mean T_p increased by 0.25

to 0.50 s (fig. 53). The JJA T_p means did not change significantly (fig. 52). Rose and American Samoa's DJF D_p rotated clockwise by 10 to 20° at Rose and by 20 to 30° at American Samoa (fig. 82). D_p and σ_{Dp} values did not change significantly during other seasons (figs. 83–85).

End-Century: 2081–2100

RCP4.5

Mean

There was no significant change from hindcast mean H_s values across all seasons (figs. 22–25). σ_{Hs}^2 values did not change significantly.

The mean T_p and σ_{Tp}^2values did not change significantly throughout all seasons (figs. 54–57). D_p and σ_{Dp} values did not change significantly throughout all seasons (figs. 86–89).

Top 5 Percent

Extreme MAM and SON H_s means increased by 0.10 to 0.20 m (fig. 27, fig. 29). DJF and JJA means did not change significantly (fig. 26, fig. 28). DJF extreme σ_{Hs}^2 values decreased at American Samoa by >0.40 and extreme MAM σ_{Hs}^2 values increased by 0.20 to 0.40.

The DJF σ_{Tp}^2 at American Samoa decreased by 1.5 to 3.0 (fig. 58). The SON mean T_p values did not change significantly (fig. 61). The MAM and JJA mean T_p values did not change significantly (figs. 59–60). During the DJF season, both points' D_p rotated by 10 to 20° clockwise (fig. 90). The σ_{Dp} value at Rose decreased by 5.0 to 10.0°. Values did not change significantly during other seasons (figs. 91–93).

RCP8.5

Mean

There was no significant change from hindcast mean H_s values across all seasons at American Samoa and Rose Atoll (figs. 30–33).

Mean T_p values did not change significantly across all seasons (figs. 62-65). σ_{Tp}^2 values did not change significantly throughout all seasons. The mean D_p in the southern islands rotated by 5 to 10° clockwise during the DJF season (fig. 94). SON σ_{Dp} values decreased by 5.0 to 10.0° (fig. 97). Values did not change significantly during MAM and JJA (figs. 95–96).

Top 5 Percent

Extreme mean H_s values increased by 0.10 to 0.20 at Rose Atoll during the DJF season (fig. 34). JJA H_s values increased by 0.10 to 0.20 m at Rose (fig. 36). Extreme mean values did not change significantly for the MAM and SON seasons (fig. 35, fig. 37). DJF σ_{Hs}^2 values decreased by 0.10 to 0.20 at American Samoa. σ_{Hs}^2 values did not change significantly during other seasons.

The SON mean T_p values increased by 0.25 to 0.50 s (fig. 69). T_p values did not change significantly during other seasons (figs. 66–68). MAM σ_{Dp} values increased by 5.0 to 15.0° (fig. 99). The SON σ_{Dp} values decreased by 5.0 to 10.0° and Rose's and its D_p rotated 5 to 10° clockwise (fig. 101). Values did not change significantly during DJF and JJA (fig. 98, fig. 100).

Wind Climate Parameter Changes

Western Region

Mid-Century: 2026–2045

RCP4.5

Mean

The mean U_a of the Western region decreased by 0.25 to 0.50 m/s during the DJF season (fig. 102). Mean wind speeds did not change significantly during the other three seasons (figs. 103–105). σ_{Ua}^2 decreased at the Yap point by 0.75 to 1.50 during the SON season. σ_{Ua}^2 values did not change significantly during other seasons.

MAM $\sigma_{U\theta}$ values decreased by 5.0 to 10.0° (fig. 135). Yap's U_θ values rotated counterclockwise during the JJA season and clockwise during the SON season by 5 to 10° (figs. 136–137). DJF values did not significantly change during other seasons (fig. 134).

Top 5 percent

The means of top 5 percent of wind speeds did not change significantly except at the Yap point during the DJF season, which decreased by 0.25 to 0.50 m/s (figs. 106–109). Extreme σ_{Ua}^2 increased by 0.75 to 1.50 at Palau during the SON season. σ_{Ua}^2 values did not change significantly during the other seasons.

DJF $\sigma_{U\theta}$ values increased by 5.0 to 10.0° (fig. 138). JJA $\sigma_{U\theta}$ values increased by 5.0 to 10.0° and Palau's U_θ rotated counterclockwise by 5 to 10° (fig. 140). MAM $\sigma_{U\theta}$ values decreased

by 5.0 to 10.0° (fig. 139). SON $\sigma_{U\theta}$ values increased by 5.0 to 10.0° (fig. 141). During this season, Palau's U_θ rotated by 5 to 10° counterclockwise and Yap's U_θ rotated by 20 to 30° counterclockwise.

RCP8.5

Mean

Mean wind speeds decreased by 0.25 to 0.50 m/s during the DJF season (fig. 110). Mean values did not change significantly during the remaining seasons (figs. 111–113). σ_{Ua}^2 decreased during the SON season at Yap. σ_{Ua}^2 values did not change significantly during other seasons

MAM $U\theta$ $\sigma_{U\theta}$ values decreased by 5.0 to 10.0 (fig. 143). JJA U_θ values rotated clockwise at Palau by 5 to 10°. SON mean wave directions rotated 5 to 20° clockwise (fig. 144). Values did not change significantly during other seasons (fig. 142, fig. 145).

Top 5 percent

DJF extreme wind speed means decreased by 0.25 to 0.50 m/s (fig. 114). SON means decreased by 0.50 to 0.75 m/s (fig. 117). The remaining seasons displayed no significant changes (figs. 115–116). Extreme σ_{Ua}^2 values did not change in the region throughout all seasons.

The DJF $\sigma_{U\theta}$ value at Palau increased by 5.0 to 10.0° and U_θ through the region rotated 10 to 20° clockwise (fig. 146). $\sigma_{U\theta}$ values decreased by 5.0 to 15.0° during the JJA season (fig. 148). SON $\sigma_{U\theta}$ values decreased by 5.0 to 10.0° (fig. 149). The MAM season's values did not change significantly (fig. 147).

End-Century: 2081–2100

RCP4.5

Mean

There were no significant changes in U_a means observed during all seasons (figs. 118–121). SON σ_{Ua}^2 values decreased by 0.75 to 1.50 at all points. σ_{Ua}^2 values did not change significantly during the remaining seasons.

Yap's U_θ rotated counterclockwise by 5 to 10° during JJA (fig. 152). U_θ s rotated by 10 to 20° clockwise during the SON, but values did not change significantly during other seasons (figs. 150–151, fig. 153).

Top 5 percent

The DJF and SON extreme wind speeds decreased by 0.25 to 0.50 m/s (fig. 122, fig. 125). Other seasons showed no significant change in wind speeds (figs. 123–124). Extreme σ_{Ua}^2 values did not significantly change within the region.

SON $\sigma_{U\theta}$ values decreased by 10.0 to 15.0° (fig. 157). Direction values did not significantly change during other seasons (figs. 154–156).

RCP8.5

Mean

Mean wind speeds decreased by 0.50 to 0.75 m/s during the DJF season but increased by 0.25 to 0.50 m/s during the JJA season (fig. 126, fig. 128). The remaining seasons displayed no significant change in mean wind speeds (fig. 127, fig. 129). MAM σ_{Ua}^2 decreased by 0.75 to 1.50 at Yap. SON σ_{Ua}^2 values decreased by 0.75 to 1.50 throughout the region.

The JJA U_θ of Yap rotated by 10 to 20° counterclockwise (fig. 160). $\sigma_{U\theta}$ values decreased by 5.0 to 10.0° during the MAM and SON seasons (fig. 159, fig. 161). The U_θ of Yap rotated 10 to 20° clockwise during the SON seasons. DJF values did not change significantly (fig. 158).

Top 5 percent

DJF and SON mean wind speed values decreased by 0.50 to 0.75 m/s (fig. 130, fig. 133). MAM values decreased by 0.25 to 0.50 m/s (fig. 131). The JJA season values did not change significantly (fig. 132). JJA σ_{Ua}^2 increased at Yap by 0.75 to 1.50. SON σ_{Ua}^2 values increased by 0.75 to 1.50 at both islands within the region. U_a values did not change significantly during the other seasons.

DJF $\sigma_{U\theta}$ values increased by 5.0 to 10.0° and mean wave directions rotated by 5 to 10° clockwise at Palau (fig. 162). Similarly, the JJA U_θ of Yap rotated by 10 to 20° counterclockwise (fig. 164). MAM $\sigma_{U\theta}$ values decreased by 5.0 to 10.0° as did SON values (fig. 163, fig. 165). The U_θ of Palau rotated counterclockwise by 5 to 10° during the JJA season. SON U_θ rotated counterclockwise by 5 to 20°.

Marianas Region

Mid-Century: 2026–2045

RCP4.5

Mean

Mean wind speeds decreased by 0.25 to 0.50 m/s in the Marianas region during the SON season, but values did not change significantly during the other seasons (figs. 102–105). JJA σ_{Ua}^2 decreased by 0.75 to 1.50 at Asuncion. Guam σ_{Ua}^2 values decreased by the same amount during the SON season.

SON $\sigma_{U\theta}$ values increase by 5.0 to 10.0° (fig. 137). U_θ values did not significantly change during other seasons (figs. 134–136).

Top 5 percent

JJA extreme U_a means decreased by 0.25 to 0.50 m/s at Saipan and Guam, with speeds decreasing my >0.75 m/s at the Asuncion point (fig. 108). Similarly, SON values decreased by 0.25 to 0.50 m/s at Saipan and Asuncion but decreased by >0.75 m/s at Guam (fig. 109). The DJF and MAM means did not change significantly (figs. 106–107). MAM extreme σ_{Ua}^2 decreased by 0.75 to 1.50 at Guam. JJA σ_{Ua}^2 values decreased by 0.75 to 1.50 at Asuncion.

The JJA $\sigma_{U\theta}$ value increased by 10.0 to 15.0° at Saipan and rotated counterclockwise by 5 to 10° at the Saipan and Guam points (fig. 140). $\sigma_{U\theta}$ values decreased by 5.0 to 10.0° during MAM and increased by 5.0 to 10.0° during SON (fig. 139, fig. 141). The U_θ of Guam rotated clockwise by 10 to 20° during the SON season. DJF direction values did not change significantly (fig. 138).

RCP8.5

Mean

Mean U_a values decreased by 0.25 to 0.50 m/s during the MAM and SON seasons (fig. 111, fig. 113). The remaining seasons' mean values did not change significantly (fig. 110, fig. 112). σ_{Ua}^2 decreased by 0.75 to 1.50 at Guam during the SON season.

$\sigma_{U\theta}$ values decreased at the Guam point by 5.0 to 10.0° during the JJA season and increased by 5.0 to 15.0° during the SON season (figs. 144–145). $\sigma_{U\theta}$ values did not change significantly during other seasons (figs. 142–143).

Top 5 percent

MAM mean extreme U_a values decreased by 0.25 to 0.50 m/s (fig. 115). JJA changes were mixed. U_a mean increased at the Saipan point by 0.25 to 0.50 m/s and decreased at the Asuncion point by the same amount (fig. 116). SON values decreased by 0.25 to 0.75 m/s, with the largest

change occurring at the Guam point (fig. 117). DJF values did not change significantly (fig. 114). MAM σ_{Ua}^2 values decreased by 0.75 to 1.50, except at Guam, where the σ_{Ua}^2 decreased by >1.50. SON σ_{Ua}^2 values increased by 0.75 to 1.50 at Saipan and by >1.50 at Asuncion.

JJA $\sigma_{U\theta}$ values decreased at Guam by 10.0 to 15.0° and increased at Asuncion by 5.0 to 10.0° (fig. 148). Saipan and Asuncion's U_θ rotated clockwise by 10 to 20°. MAM $\sigma_{U\theta}$ valued decreased by 5.0 to 10.0° (fig. 147). SON $\sigma_{U\theta}$ values increased by 10.0 to >15.0° and U_θ s rotated clockwise by 5 to 30°, with the larger deviation from hindcast means occurring at Guam (fig. 149). DJF direction values did not change significantly (fig. 146).

End-Century: 2081–2100

RCP4.5

Mean

Mean U_a values decreased by 0.25 to 0.50 m/s during the SON season but did not change significantly during the remaining seasons (figs. 118–121). σ_{Ua}^2 decreased by 0.75 to 1.50 at Asuncion during the JJA season. SON σ_{Ua}^2 values decreased by 0.75 to 1.50 at all islands.

The JJA $\sigma_{U\theta}$ value at Guam decreased by 5.0 to 10.0° (fig. 152). SON $\sigma_{U\theta}$ values increased by 5.0 to 10.0° (fig. 153). $\sigma_{U\theta}$ values did not change significantly during other seasons (figs. 150–151).

Top 5 percent

MAM extreme U_a means decreased by 0.25 to 0.50 m/s (fig. 123). JJA values decreased by 0.25 to >0.75 m/s, with the largest change occurring at Asuncion (fig. 124). SON values decreased by 0.50 to >0.75 m/s (fig. 125). No significant change in extreme U_a means occurred during the DJF season (fig. 122). MAM σ_{Ua}^2 values decreased by 0.75 to 1.50 at Saipan and >1.50 at Guam. Values did not change significantly during other seasons.

MAM $\sigma_{U\theta}$ values decreased by 5.0 to 15.0° (fig. 155). Saipan's $\sigma_{U\theta}$ value increased by 10.0 to 15.0° and it and Guam's U_θ s rotated clockwise by 10 to 20° during the JJA season (fig. 156). The SON $\sigma_{U\theta}$ at Guam increased by 10.0 to 15.0° and its U_θ rotated clockwise by 10 to 20° (fig. 157). DJF direction values did not change significantly (fig. 154).

RCP8.5

Mean

Mean U_a values decreased during the DJF and SON seasons (fig. 126, fig. 129). No significant changes were observed during the other seasons (figs. 127–128). σ_{Ua}^2 values decreased by 0.75 to 1.50 during the MAM and SON seasons. The JJA σ_{Ua}^2 at Asuncion decreased by 0.75 to 1.50. σ_{Ua}^2 values did not change significantly during the DJF season.

JJA $\sigma_{U\theta}$ values decreased by 5.0 to 10.0°, and SON $\sigma_{U\theta}$ values increased by 5.0 to 10.0° (fig. 160). U_θ values did not significantly change during other seasons (figs. 158–159, fig. 161).

Top 5 percent

MAM U_a values decreased by 0.50 to >0.75 m/s while JJA values decreased by a smaller 0.25 to 0.50 m/s (figs. 131–132). SON values decreased by 0.25 to 0.75 m/s, with the largest change occurring at the Guam point (fig. 133). DJF values did not change significantly (fig. 130). The σ_{Ua}^2 of the Guam point increased by >1.50 during the DJF season. σ_{Ua}^2 values increased by a smaller amount of 0.75 to 1.50 during the JJA and SON seasons for the Guam and Asuncion points, respectively. MAM values decreased by 0.75 to 1.50, except at Guam where the σ_{Ua}^2 decreased by >1.50.

The DJF $\sigma_{U\theta}$ at Asuncion decrease by 5.0 to 10.0° (fig. 162). MAM $\sigma_{U\theta}$ values decreased by 5.0 to 15.0° (fig. 163). U_θ s during JJA rotated by 5 to 20° clockwise within the region (fig. 164). SON $\sigma_{U\theta}$ values increased by 5.0 to 15.0°, and the U_θ of Guam rotated 10 to 20° clockwise (fig. 165).

Central Region

Mid-Century: 2026–2045

RCP4.5

Mean

SON mean U_a values decreased at the Enewetak, Bikini, and Kwajalein points by 0.25 to 0.50 m/s (fig. 105). There were no significant changes observed during the remaining seasons (figs. 102–104). SON σ_{Ua}^2 values decreased by 0.75 to 1.50 at Pohnpei and Kwajalein. σ_{Ua}^2 values did not change significantly throughout the other seasons.

MAM $\sigma_{U\theta}$ values decreased by 5.0 to 10.0° (fig. 135). The JJA value at Bikini decreased by 5.0 to 10.0° (fig. 136). The $U\theta$ values of Chuuk and Kwajalein rotated counterclockwise by 5 to 10°. $U\theta$ values did not significantly change in other seasons (fig. 134, fig. 137).

Top 5 percent

MAM U_a values decreased by 0.25 to 0.50 m/s at Enewetak and Bikini (fig. 107). Means increased by the same amount throughout the region during the JJA season (fig. 108). SON means decreased by 0.25 to >0.75 m/s, with the largest change occurring at Pohnpei (fig. 109). Mean U_a values did not change significantly during the DJF season (fig. 106). MAM σ_{Ua}^2 values decreased by 0.75 to 1.50 at Enewetak, Bikini, and Kosrae. Conversely, σ_{Ua}^2 values increased by 0.75 to 1.50 at Enewtok, Bikini, and Pohnpei during the SON season.

DJF $\sigma_{U\theta}$ values decreased by 5.0 to 10.0 at Pohnpei and Kosrae, but by 10.0 to 15.0 at Chuuk (fig. 138). MAM $\sigma_{U\theta}$ decreased by 5.0 to 15.0° through the region (fig. 139). JJA $\sigma_{U\theta}$ values increased at Pohnpei by 5.0 to 10.0° and decreased at Majuro by 5.0 to 10.0° (fig. 140). $\sigma_{U\theta}$ values through the region increased by 5.0 to 10.0° during the SON season, except at Chuuk and Kosrae where they decreased by 10.0 to >15.0° (fig. 141). The U_θ of Bikini and Enewetak rotated clockwise by 5 to 20° and counterclockwise at Kosrae by the same amount. The U_θ of Pohnpei and Chuuk rotated clockwise by 60 to 70°.

RCP8.5

Mean

U_a means decreased during the SON season at Enewetak, Bikini, and Kwajalein (fig. 113). Values did not change significantly during the remaining seasons (figs. 110–112). The MAM σ_{Ua}^2 decreased by 0.75 to 1.50 at Bikini. SON values decreased at Pohnpei and Kwajalein by 0.75 to 1.50.

$\sigma_{U\theta}$ values decreased during the MAM season at Chuuk and Pohnpei by 5.0 to 10.0° and at Enewetak and Bikini during JJA by the same amount (figs. 143–144). The U_θ s of Chuuk and Kwajalein rotated clockwise by 5 to 10° in the SON season, and values did not change significantly during DJF (fig. 142, fig. 145).

Top 5 percent

Extreme U_a values decreased in the eastern half of the region during the JJA season by 0.25 to 0.50 m/s (fig. 116). SON values decreased by the same amount, though the sites of decrease were sparse, not displaying any observable clustering (fig. 117). JJA σ_{Ua}^2 values increased by 0.75 to 1.50 at Kwajalein and >1.50 at Wake. The SON σ_{Ua}^2 at the Majuro point

decreased by 0.75 to 1.50. U_a values did not change significantly during other seasons (figs. 114–115).

DJF $\sigma_{U\theta}$ values at Chuuk and Pohnpei increased by 5.0 to 10.0° and decreased by 5.0 to 10.0° at Majuro (fig. 146). Chuuk's $\sigma_{U\theta}$ value during MAM decreased by 5.0 to 10.0° (fig. 147). JJA $\sigma_{U\theta}$ values decreased by 5.0 to 10.0° at Pohnpei and increased by the same amount at Wake and Kosrae (fig. 148). The U_θ of Pohnpei and Kosrae rotated clockwise by 20 to 30 and 40 to 50°, respectively. The U_θ of Chuuk, Wake, and Kwajalein rotated clockwise by 5 to 20°. SON $\sigma_{U\theta}$ values decreased at Chuuk by 5.0 to 10.0° and increased throughout the rest of the region by 5.0 to >15.0° (fig. 149). The U_θ at Chuuk and Pohnpei rotated by 40 to 60° clockwise and at Majuro and Kosrae by 10 to 20° clockwise.

End-Century: 2081–2100

RCP4.5

Mean

DJF means decreased by 0.25 to 0.50 m/s at Chuuk, Pohnpei, and Majuro (fig. 118). Similarly, values decreased by 0.25 to 0.50 at Enewetak, Bikini, and Kwajalein during the SON season (fig. 121). JJA U_a means increased by 0.25 to 0.50 m/s throughout the region (fig. 120). MAM values did not change significantly (fig. 119). The MAM σ_{Ua}^2 at Majuro decreased by 0.75 to 1.50 and the SON σ_{Ua}^2 at Kwajalein decreased by 0.75 to 1.50.

MAM $\sigma_{U\theta}$ values decreased by 5.0 to 10.0° at Chuuk, Pohnpei, and Kosrae (fig. 151). JJA $\sigma_{U\theta}$ values decreased by 5.0 to 10.0° at Bikini and Enewetak (fig. 152). SON $\sigma_{U\theta}$ values increased by 5.0 to 10.0° at Enewetak, Bikini, and Kwajalein (fig. 153). U_θ of Chuuk, Pohnpei, Majuro, and Kwajalein rotated clockwise by 5 to 10° during SON. DJF direction values did not change significantly (fig. 150).

Top 5 percent

Extreme U_a means decreased by 0.25 to 0.50 m/s during the DJF and SON seasons and specifically at the Chuuk, Pohnpei, and Kosrae points during the MAM season (figs. 122–123, fig. 125). There was an increase in JJA U_a values by 0.25 to 0.75 m/s across the region, with the largest changes displayed at Enewetak, Bikini, and Kosrae (fig. 124). σ_{Ua}^2 values decreased by 0.75 to 1.50 at Bikini and Kosrae during the MAM season. JJA values increased throughout the region by 0.75 to 1.50, except at Chuuk, where values decreased by 0.75 to 1.50. SON σ_{Ua}^2 values increased by 0.75 to 1.50 at Enewetak, Bikini, and Majuro. Values did not change significantly during the DJF season.

DJF $\sigma_{U\theta}$ values increased at Chuuk and Kosrae by 5.0 to 10.0° (fig. 154). MAM $\sigma_{U\theta}$ values decreased by 5.0 to >15.0 at Kosrae, Chuuk, Pohnpei, and Kwajalein (fig. 155). JJA $\sigma_{U\theta}$ values decreased by 5.0 to >15.0° at Majuro and Chuuk, but values increased by 5.0 to >15.0 at Wake, Kosrae, Enewtok, and Bikini (fig. 156). The U_θ of Chuuk, Bikini, and Kwajalein rotated clockwise by 5 to 20° and the directions of Majuro, Pohnpei, and Kosrae rotated by 20 to 40° clockwise. SON $\sigma_{U\theta}$ values decreased at Chuuk, Pohnpei, and Kosrae by >15.0°, but values increased by 10.0 to >15.0° at Enewetak, Bikini, Kwajalein, and Majuro (fig. 157). U_θ rotated clockwise by 70 to 90° at Chuuk and Pohnpei, 60 to 70° at Majuro, and 5 to 30° at Kosrae, Enewetak, Bikini, and Kwajalein.

RCP8.5

Mean

DJF U_a means decreased by 0.25 to 0.50 m/s, and SON means decreased by the same amount at Enewetak, Bikini, and Kwajalein (fig. 126, fig. 129). MAM means increased by 0.25 to 0.50 m/s at Pohnpei, Kwajalein, and Majuro (fig. 127). JJA values increased by 0.25 to 0.50 m/s across the entire region (fig. 128). The σ_{Ua}^2 decreased at the Majuro point by 0.75 to 1.50 during the DJF and MAM seasons. Similarly, the σ_{Ua}^2 at the Wake point decreased by 0.75 to 1.50 during the JJA season. σ_{Ua}^2 values decreased across the entire region by 0.75 to 1.50 during SON.

MAM $\sigma_{U\theta}$ values decreased by 5.0 to 10.0° at Chuuk, Pohnpei, and Majuro (fig. 159). JJA $\sigma_{U\theta}$ values decreased by 5.0 to 15.0°, and the mean directions of Chuuk, Kosrae, Majuro, and Pohnpei rotated counterclockwise by 5 to 10° (fig. 160). Wind direction values did not change significantly during the DJF and SON seasons (fig. 158, fig. 161).

Top 5 percent

The top 5 percent of U_a values decreased by 0.25 to 0.75 m/s during the DJF, MAM, and SON, with the largest boreal winter values in the center of the region and fall values at Pohnpei (figs. 130–131, fig. 133). Conversely, JJA U_a values increased by 0.25 to 0.75 m/s, with the largest increases occurring at Enewetak, Bikini, and Pohnpei (fig. 132). MAM extreme σ_{Ua}^2 at Bikini decreased by 0.75 to 1.50. JJA σ_{Ua}^2 values increased by 0.75 to 1.50 at Pohnpei and Kwajalein and by >1.50 at Enewetak, Bikini, and Wake. SON season σ_{Ua}^2 values increased by 0.75 to 1.50 at Pohnpei and by >1.50 at Enewetak, Bikini, and Chuuk.

MAM $\sigma_{U\theta}$ values decreased by 5.0 to 15.0° (fig. 163). JJA mean wave directions rotated 5 to 20° clockwise at Enewetak, Bikini, Wake, and Kwajalein, but rotated 5 to 10° counterclockwise at Majuro and Kosrae (fig. 164). SON $\sigma_{U\theta}$ values decreased by 1.0 to >15.0° at Chuuk, Pohnpei, and Kosrae (fig. 165). U_θ rotated 30 to 40° clockwise at Chuuk and 20 to 40° counterclockwise at

Pohnpei and Kosrae during the SON season. DJF direction values did not change significantly (fig. 162).

Northeast Region

Mid-Century: 2026–2045

RCP4.5

Mean

Mean U_a values did not change significantly across all seasons (figs. 102–105). The DJF σ_{Ua}^2 decreased at Johnston Atoll by 0.75 to 1.560.

The $\sigma_{U\theta}$ value at the Northwest Hawaiian Islands increased by 5.0 to 10.0° during the DJF season (fig. 134). Wind direction values did not change significantly during other seasons (figs. 135–137).

Top 5 percent

Extreme U_a means decreased by 0.25 to 0.50 m/s at the Northwest Hawaii and Midway points during the DJF season and at the main Hawaiian Islands points during the SON season (fig. 106, fig. 109). U_a values did not change significantly during the remaining seasons (figs. 107–108). The σ_{Ua}^2 of the Northwest Hawaiian point increased by 0.75 to 1.50 during the SON season.

The DJF U_θ of Midway rotated by 5 to 10° clockwise and its $\sigma_{U\theta}$ value increased by 5.0 to 10.0° (fig. 138). Midway's U_θ rotated 10 to 20° clockwise during the MAM season and by 5 to 10° clockwise during the SON season (fig. 139, fig. 141). Johnston Atoll's $\sigma_{U\theta}$ value increased by 5.0 to 10.0° during the JJA and SON seasons (fig. 140).

RCP8.5

Mean

U_a means decreased by 0.25 to 0.50 m/s at the Big Island of Hawaii point during SON (fig. 113). The other seasons' means did not change significantly (figs. 110–112). The σ_{Ua}^2 at the Northwest Hawaiian point decreased by 0.75 to 1.50 during the DJF season.

The DJF U_θ of the Northwest Hawaiian Islands rotated clockwise by 20 to 30° (fig. 142). Wind direction values did not change significantly during other seasons (figs. 143–145).

Top 5 percent

DJF changes were mixed. The U_a values at the Big Island point increased by 0.25 to 0.50 m/s, but the Northwest Hawaii and Midway means decreased by 0.25 to 0.50 m/s (fig. 114). JJA means decreased by 0.25 to 0.50 m/s at the main Hawaiian Islands points (fig. 116). SON means decreased by 0.25 to 0.50 m/s across the whole region (fig. 117). MAM means did not change significantly (fig. 115). σ_{Ua}^2 values within the region did not change significantly.

The DJF $\sigma_{U\theta}$ values increased by 5.0 to 10.0° at Midway and the Northwest Hawaiian Islands and decreased by 5.0 to 15.0° at Molokai, Kauai, and Johnston Atoll (fig. 146). The U_θ of Midway rotated clockwise by 5 to 10° at Midway during the MAM season (fig. 147). JJA $\sigma_{U\theta}$ values increased by 5.0 to 10.0° at the Big Island point (fig. 148). The $\sigma_{U\theta}$ values during SON decreased by 5.0 to 15.0° at Midway and the Northwest Hawaiian Islands and increased by 5.0 to 10.0° at Johnston Atoll (fig. 149).

End-Century: 2081–2100

RCP4.5

Mean

There were no significant changes in U_a means across all seasons. DJF σ_{Ua}^2 values decreased by 0.75 to 1.50 at Johnston Atoll, the Northwest Hawaiian Islands point, and Midway (fig. 118). SON σ_{Ua}^2 values decreased by 0.75 to 1.50 at the Northwest Hawaiian Islands and Midway points (fig. 121). U_a Values did not change significantly during the other seasons (figs. 119–120).

The $\sigma_{U\theta}$ of the Northwest Hawaiian Islands increased by 5.0 to 10.0°, and its U_θ rotated 5 to 10° clockwise during the DJF season (fig. 150). $\sigma_{U\theta}$ values decreased by 5.0 to 10.0° at Midway and the Northwest Hawaiian Islands during SON (fig. 153). Wind direction values did not change significantly during other seasons (figs. 151–152).

Top 5 percent

Extreme U_a means decreased by 0.25 to 0.75 m/s during the DJF season at the Northwest Hawaii, Midway, and Johnston Atoll points (fig. 122). The Molokai and Johnston Atoll's means decreased by 0.25 to 0.50 m/s during the MAM season (fig. 123). The JJA season means decreased at the Northwest Hawaii point by 0.25 to 0.50, and the SON season U_a values decreased by 0.25 to 0.50 m/s at the Northwest Hawaii and Midway points (figs. 124–125). JJA σ_{Ua}^2 values

increased by 0.75 to 1.50 at the Northwest Hawaii point and by >1.50 at the Big Island and Midway points.

The DJF $\sigma_{U\theta}$ values at Kauai and Molokai decreased by 5.0 to 10.0° (fig. 154). The U_θ at Midway during MAM rotated by 5 to 10° clockwise (fig. 155). $\sigma_{U\theta}$ values increased by 5.0 to 15.0° during JJA (fig. 156). SON wind directions $\sigma_{U\theta}$ values decreased by 5.0 to 15.0° at Midway and the Northwest Hawaiian Islands while the rest of the region's values increased by 5.0 to 10.0° (fig. 157).

RCP8.5

Mean

U_a means decreased by 0.25 to 0.50 m/s, except at the midway point, which decreased by 0.50 to 0.75 m/s during the DJF (fig. 126). JJA means decreased by 0.25 to 0.50 m/s (fig. 128). SON values at the Big Island of Hawaii decreased by 0.25 to 0.50 m/s (fig. 129). The MAM season means did not change significantly (fig. 127). σ_{Ua}^2 values decreased by 0.75 to 1.50 at Johnston Atoll and by >1.50 at the Northwest Hawaii and Midway points during the DJF season. JJA values decreased by 0.75 to 1.50 at Northwest Hawaii, Kauai, and Johnston Atoll. SON values decreased by 0.75 to 1.50 at Kauai and the Northwest Hawaii points, but decreased further by >1.50 at Johnston atoll. The MAM season's σ_{Ua}^2 values did not change significantly.

DJF $\sigma_{U\theta}$ values decreased by 5.0 to 10.0° at the Big Island, Kauai, and Johnston Atoll points, and the U_θ of the Northwest Hawaiian Islands rotated clockwise 10 to 20° (fig. 158). The SON $\sigma_{U\theta}$ values decreased by 5.0 to 15.0° at the Northwest Hawaiian Islands, Midway, and Kauai (fig. 161). Wind direction values did not change significantly during other seasons (figs. 159–160).

Top 5 percent

DJF extreme mean U_a values decreased by 0.50 to >0.75 m/s (fig. 130). MAM values decreased by 0.25 to 0.75 m/s (fig. 131). JJA means decreased over a wide range of 0.25 to >0.75 m/s (fig. 132). Extreme means decreased by 0.25 to 0.50 m/s at the Big Island of Hawaii point for the SON season (fig. 133). Kauai's σ_{Ua}^2 increased by 0.75 to 1.50 during the SON season.

DJF $\sigma_{U\theta}$ values increased by 5.0 to 10.0° at the Northwest Hawaiian Islands and decreased by >15.0° at Molokai and Kauai (fig. 162). MAM direction $\sigma_{U\theta}$ values at the Northwest Hawaiian Islands and Kauai decreased by 5.0 to 10.0°, and the U_θ of Midway rotated by 20 to 30° clockwise (fig. 163). SON $\sigma_{U\theta}$ values decreased by 5.0 to >15.0° at the Northwest Hawaiian Islands and Midway (fig. 165). Midway's U_θ rotated 5 to 10° clockwise. JJA wind direction values did not change significantly (fig. 164).

Eastern Equatorial Region

Mid-Century: 2026–2045

RCP4.5

Mean

MAM mean U_a values increased by 0.25 to 0.50 m/s at the Palmyra and Kingman Reef points (fig. 103). Means did not significantly change during the other seasons through the region (fig. 102, figs. 104–105).

The MAM $\sigma_{U\theta}$ of Jarvis increased by 5.0 to 10.0° (fig. 135). The U_θ of Kingman Reef rotated counterclockwise by 5 to 10° during JJA (fig. 136). Wind direction values did not change significantly during other seasons (fig. 134, fig. 137).

Top 5 percent

The Palmyra and Kingman Reef points' extreme mean U_a values increased by 0.25 to 0.50 m/s during the MAM and JJA seasons (figs. 107–108). The SON U_a values decreased by 0.25 to 0.50 m/s throughout the entire region (fig. 109). The DJF values did not change significantly (fig. 106). SON σ_{Ua}^2 values decreased by 0.75 to 1.50 across the entire region. However, σ_{Ua}^2 values did not significantly change during other seasons.

DJF $\sigma_{U\theta}$ values decreased by 5.0 to 15.0° at Howland, Palmyra (fig. 138). Jarvis and Howland's U_θ rotated clockwise by 5 to 20°. The MAM $\sigma_{U\theta}$ value at Jarvis increased by 5.0 to 10.0° (fig. 139). The JJA wind direction values decreased by 5.0 to 10.0° at Howland and Kingman Reef, with Palmyra and Kingman Reef's U_θ rotating counterclockwise by 10 to 20° (fig. 140). The $\sigma_{U\theta}$ values of Jarvis and Howland decreased by 10.0 to 15.0° during the SON season (fig. 141). Palmyra's U_θ rotated counterclockwise by 5 to 10°.

RCP8.5

Mean

Mean U_a values increased during the MAM season at the Palmyra and Kingman Reef points (fig. 111). Otherwise, means did not change significantly at other points or during the other seasons (fig. 110, figs. 112–113). σ_{Ua}^2 values did not change within the region.

MAM $\sigma_{U\theta}$ values at Palmyra and Kingman Reef decreased by 5.0 to 10.0° (fig. 143). The U_θ of Kingman Reef within the JJA season rotated counterclockwise by 5 to 10° (fig. 144). Wind direction values did not change significantly during other seasons (fig. 142, fig. 145).

Top 5 percent

Extreme U_a values decreased by 0.20 to 0.50 m/s at the Jarvis point during the MAM season, while the other islands remain relatively unchanged (fig. 115). The SON extreme U_a values decreased by 0.25 to 0.50 m/s, except for the Howland point, which did not change significantly (fig. 117). Similarly, there were not significant changes observed in the remaining seasons (fig. 114, fig. 116). SON σ_{Ua}^2 values decreased by 0.75 to 1.50. Values did not change significantly during the remaining seasons.

DJF $\sigma_{U\theta}$ values decreased at Howland and Palmyra by 5.0 to 10.0° (fig. 146). The MAM $\sigma_{U\theta}$ value at Howland decreased by 10.0 to 15.0° (fig. 147). The JJA $\sigma_{U\theta}$ values decreased by 5.0 to 15.0° at Howland, Palmyra, and Kingman Reef (fig. 148). The U_θ of Palmyra and Kingman Reef rotated counterclockwise by 10 to 20°. SON $\sigma_{U\theta}$ values decreased by >15.0° at Jarvis and increased by 5.0 to 10.0° at Kingman Reef (fig. 149). Kingman Reef's U_θ rotated counterclockwise by 10 to 20°.

End-Century: 2081–2100

RCP4.5

Mean

Mean U_a values increased by 0.25 to 0.50 m/s at the Palmyra and Kingman Reef points during the MAM season (fig. 119). The remaining seasons had not significant changes observed (fig. 118, figs. 120–121). σ_{Ua}^2 values did not change significantly within the region.

The MAM $\sigma_{U\theta}$ values at Palmyra and Kingman Reef decreased by 5.0 to 10.0° (fig. 151). Wind direction values did not change significantly during other seasons (figs. 150, 152–153).

Top 5 percent

Extreme U_a values increased by 0.25 to 0.50 m/s throughout the region during the JJA season (fig. 124). SON values decreased by 0.25 to 0.50 m/s at Jarvis, but did not change significantly at the other points (fig. 125). U_a values did not significantly change during the remaining seasons (figs. 122–123). Extreme σ_{Ua}^2 values did not change significantly within the region.

The U_θ within the region rotated counterclockwise by 5 to 10° during the DJF season (fig. 154). The MAM $\sigma_{U\theta}$ at Jarvis increased by 5.0 to 10.0°, and Howland's U_θ rotated counterclockwise by 5 to 10° (fig. 155). JJA U_θ of Palmyra and Kingman Reef rotated

counterclockwise by 10 to 20° (fig. 156). SON $\sigma_{U\theta}$ values increased by 5.0 to 15.0°, and the U_θ of Palmyra rotated counterclockwise by 5 to 10° (fig. 157).

RCP8.5

Mean

MAM U_a means increased by 0.50 to >0.75 m/s throughout the region (fig. 127). Means did not significantly deviate from hindcast means during other seasons (fig. 126, figs. 128–129). σ_{Ua}^2 values decreased by 0.75 to 1.50 at Palmyra and Kingman Reef during the MAM season.

The DJF $\sigma_{U\theta}$ values at Palmyra and Kingman Reef decreased by 5.0 to 10.0° (fig. 158). The MAM $\sigma_{U\theta}$ at Jarvis increased by 5.0 to 10.0°, and the U_θ of Palmyra rotated counterclockwise by 5 to 10° (fig. 159). JJA mean wave directions at Palmyra and Kingman Reef rotated counterclockwise by 5 to 20° (fig. 160). SON wind direction values did not change significantly (fig. 161).

Top 5 percent

DJF extreme U_a means decreased by 0.25 to 0.50 m/s (fig. 130). SON values also decreased by 0.25 to 0.50 m/s, except the Howland point remain unchanged (fig. 133). JJA values intensified throughout the study area by 0.25 to 0.50 m/s (fig. 132). MAM values did not change significantly (fig. 131). SON σ_{Ua}^2 values decreased by 0.75 to 1.50 across the region.

DJF $\sigma_{U\theta}$ values decreased at Howland and Palmyra by 5.0 to 15.0°, and the U_θ of Jarvis rotated counterclockwise by 5 to 10° (fig. 162). MAM $\sigma_{U\theta}$ values increased by 5.0 to 10.0° at Palmyra and Jarvis (fig. 163). JJA mean wave directions at Palmyra and Kingman Reef rotated counterclockwise by 10 to 30° and by 5 to 10° counterclockwise at Howland (fig. 164). SON $\sigma_{U\theta}$ values increased by 5.0 to 10.0° at Palmyra and Kingman Reef and decreased by 5.0 to 15.0° at Howland and Jarvis (fig. 165). Palmyra's U_θ rotated counterclockwise by 10 to 20°.

Southern Region

Mid-Century: 2026–2045

RCP4.5

Mean

Mean U_a values did not change significantly across all seasons within the region (figs. 102–105). σ_{Ua}^2 values did not change significantly within the region.

U_θ and associated $\sigma_{U\theta}$ values did not change significantly (figs. 134–137).

Top 5 percent

DJF and JJA extreme mean U_a values decreased by 0.25 to 0.50 m/s (fig. 106, fig. 108). Values did not change significantly in the MAM and SON seasons (fig. 107, fig. 109). Extreme σ_{Ua}^2 values did not change significantly within the region.

Mean wave directions of the DJF season rotated by 5 to 20° counterclockwise, and $\sigma_{U\theta}$ decreased by 5.0 to 10.0° (fig. 138). MAM $\sigma_{U\theta}$ values increased by 5.0 to 10.0°, and U_θ rotated clockwise by 5 to 10° (fig. 139). Wind direction values did not change significantly during the JJA and SON seasons (figs. 140–141).

RCP8.5

Mean

Mean U_a and associated σ_{Ua}^2 values did not change significantly within the region (figs. 110–113).

The U_θ of Rose rotated clockwise by 5 to 10° during the MAM season (fig. 143). U_θ and associated $\sigma_{U\theta}$ values during other seasons did not change significantly (fig. 142, figs. 144–145).

Top 5 percent

The means of the top 5 percent of U_a values did not change significantly. The MAM σ_{Ua}^2 of Rose increased by 0.75 to 1.50 (fig. 115). Values did not change significantly during the remaining seasons (fig. 114, figs. 116–117).

$\sigma_{U\theta}$ values decreased by 5.0 to 10.0° during the DJF and MAM seasons, and U_θ rotated clockwise by 10 to 20 and 5 to 10°, respectively (figs. 146–147). Wind direction values did not change significantly during other seasons (figs. 148–149).

End-Century: 2081–2100

RCP4.5

Mean

Mean U_a, associated σ_{Ua}^2 values, and wind direction values did not change significantly throughout the modeled region (figs. 118–121, figs. 150–153).

Top 5 percent

Extreme U_a means did not change significantly throughout the region. DJF σ_{Ua}^2 values decreased by >0.75 (fig. 122). MAM values increased by 0.75 to 1.50, but did not change significantly during the remaining seasons (figs. 123–125).

The DJF $\sigma_{U\theta}$ values decreased by 5.0 to 10.0°, and U_θ rotated clockwise by 20 to 30° (fig. 154). SON $\sigma_{U\theta}$ values increased by 5.0 to 10.0° (fig. 157). Wind direction values did not change significantly during the MAM and JJA seasons (figs. 155–156).

RCP8.5

Mean

Mean U_a and associated σ_{Ua}^2 values did not change significantly within the region (figs. 126–129).

DJF $\sigma_{U\theta}$ values decreased by 5.0 to 15.0°, and SON $\sigma_{U\theta}$ values decreased by 5.0 to 10.0° (fig. 158, fig. 161). The U_θ of Rose rotated clockwise by 5 to 10° during DJF. Wind direction values did not change significantly during the MAM and JJA seasons (figs. 159–160).

Top 5 percent

Extreme U_a means did not change significantly within the region. MAM σ_{Ua}^2 values increased by 0.75 to 1.50 within the region (fig. 131). σ_{Ua}^2 values did not significantly change during the other seasons (fig. 130, figs. 132–133).

DJF $\sigma_{U\theta}$ values decreased by 5.0 to 10.0°, and U_θ values rotated clockwise by 20 to 30° (fig. 162). The MAM $\sigma_{U\theta}$ of Rose decreased by 5.0 to 10.0°, and both islands' U_θ rotated 5 to 10° counterclockwise (fig. 163). SON $\sigma_{U\theta}$ values decreased by 5.0 to 10.0° (fig. 165). Wind direction values during the JJA season did not change significantly from hindcast values (fig. 164).

Discussion

This section will primarily focus on the trends found present in the top 5 percent of H_s values, because trends within unfiltered values were small to insignificant. Extreme H_s values will likely be more important within these regions for planning purposes and understanding the changing nature of wave hazards in the future. Thus, it is more practical and important that these extreme trends are well understood.

Spatial and Temporal H_s and U_a Trends

Significant Wave Heights

Mid-Century: 2026–2045

RCP4.5 mean H_s values decreased primarily west of latitude 180° within the study area. These changes were concentrated in the Central region during the DJF, MAM, and SON seasons. The largest decrease occurred during the JJA season within the Marianas region; however, the other main observed change was a small decrease in H_s values in the Hawaiian Islands.

As with the RCP4.5 scenario, the RCP8.5 mean H_s values decreased primarily west of 180°. However, the largest areas of decrease during the SON season were within the Western and Marianas regions. JJA values increased within the Central region, and there were decreases in the eastern half of the study area. Additionally, during seasons when the Northern Hemisphere points decreased in either intensity or breadth, the Southern region's mean H_s values increased.

These trends suggest that within both scenarios, wave heights are decreasing mainly in the western regions of the study area by 0.20 to 0.30 m. The RCP4.5 scenario seems to have larger decreasing trends at the mid-century compared to the 8.5 scenario. These trends suggest that the extratropical cyclones that cause large swell waves within the Pacific seemed to decrease in frequency, decrease in strength, or change their storm tracks. The strongest decrease trends within the Northern Hemisphere occurred during the DJF and SON seasons, but during these periods the Southern region's H_s values increased, particularly at American Samoa, where the H_s increased by >0.30 m.

End-Century: 2081–2100

The H_s trends throughout the end-century scenarios were similar to those of mid-century, but they were larger in aerial extent and intensity. Most of the changes occurred in the western half of the modeled area, with the majority happening in the Central and Marianas regions. The SON extreme H_s means of the RCP4.5 scenario decreased widely across the study area and had the largest decreases of any season. As opposed to the mid-century JJA season, there was an increase in H_s values within the Central region, with the largest increases at Enewetak.

The RCP8.5 trends were similar to the RCP4.5 trends but tended to be more widespread and stronger. The SON decreases were widespread, affecting every region except the Southern region. The mean H_s values of the majority of the points within the Northern Hemisphere decreased by more than 0.30 m, the strongest trend observed through all seasons and scenarios. JJA patterns exhibited a stronger increase in Central H_s values of 0.10 to more than 0.30 m, but the surrounding regions' values decreased by 0.10 to more than 0.30 m. DJF and MAM H_s values decreased primarily in the western half of the study area. Also, the Southern region islands' H_s generally increased, with American Samoa's usually being larger, in all but the MAM season. The

similarity between the two end-century scenarios was in contrast to the mid-century values where the trends were similar but the stronger decreases were present in the RCP4.5 scenario. Boreal fall values remained the largest changes observed throughout all seasons, with the DJF values being the next largest.

Mean Wind Speeds

Mid-Century: 2026–2045

RCP4.5 SON U_a values decreased by 0.25 to more than 0.75 m/s in the Eastern Equatorial region, the Marianas region, and the southern islands of the Central region. Conversely, southern Central region islands increased by 0.25 to 0.50 m/s, while the Marianas islands' U_a values decreased, as did the Southern and Northeast regions' values.

As with the RCP4.5 scenario, the RCP8.5 SON U_a values decreased at the points west of 180° near the equator, though the decreases were smaller in intensity, 0.25 to 0.75 m/s, and aerial extent. JJA U_a values increased by 0.25 to 0.50 m/s within the Central region, similar to those of RCP4.5, but the affected points were fewer, and the U_a decreases present within other regions were not as clearly defined. Changes in mid-century U_a values were more intense and widespread during the RCP4.5 scenario.

End-century: 2081–2100

RCP4.5 extreme U_a values decreased widely during the SON season west of 180°. The largest decrease was within the Marians region, >0.75 m/s in the southern two islands. Within the MAM season, U_a values decreased in the southern Central islands and the Marianas by 0.25 to 0.50 m/s. This trend followed the general decrease in SON values of the mid-century.

RCP8.5 SON U_a values decreased strongly throughout the study area, with decreases of more than 0.75 m/s in the far western islands and southern Central region and the western islands within the Northeast region. Similarly, MAM U_a values decreased throughout the study area, with the larger decreases of 0.50 to more than 0.75 m occurring north of 10°N. JJA values increased within the Central and Eastern Equatorial regions, by 0.25 to 0.75 m/s, and the Northeast's U_a values decreased, mimicking the end-century RCP8.5 JJA H_s values. DJF U_a values decreased throughout most regions, with the western Northeast points displaying the largest decreases.

Throughout all seasons, the end century U_a values exhibited mainly the same trends as the mid-century scenarios, but the trends were intensified by the end of the century. The mid-century RCP4.5 U_a changes were generally stronger and more widespread than the RCP8.5 changes. However, these trends reversed by the end of the century, where the RCP8.5 changes were generally stronger, more widespread, and well defined.

Spatial and Temporal T_p, D_p, and U_θ Trends

Peak Wave Periods

Mid-Century: 2026–2045

RCP4.5 T_p values increased in the eastern half of the study region by 0.25 to 0.75 s during the SON and DJF seasons. Values decreased by 0.25 to 0.50 s in the western islands that are close to the equator during the JJA season.

The RCP8.5 scenario T_p values decreased in the westernmost islands by 0.25 to 0.50 s during SON and by 0.25 to 0.75 s in the Central equatorial and Eastern Equatorial islands during the MAM season. However, there was a 0.25 to 0.75 s increase in the eastern half of the study area during the DJF season.

End Century: 2081–2100

RCP4.5 SON T_p values decreased by 0.25 to 0.50 s in the Northeast region. DJF and JJA values increased in the east half of the study region and the Central region.

The RCP8.5 SON season had widespread decreases across the Northern Hemisphere points. DJF values are split between the west and east half of the study area. Points west of 180° displayed decreasing T_p values, while the east had 0.25 to 0.50 s increases. MAM and JJA values increased in the Northeast region by 0.25 to >0.75 s. The end-century scenario represented an increase of some basic trends observed during the mid-century period.

As with the H_s values, RCP8.5, while showing similar or weaker trends in the mid-century period, displayed a stronger change during each season than the 4.5 scenario. By the end of the century, the 4.5 scenario displayed little deviation from hindcast values. The end-century trends of 4.5 are generally weak, such that there were no significant trends discernable. The sole trend observed in both scenarios was an increase in JJA T_p values in the Northeast region. The changes in mean T_p were small; therefore, the changes observed and their relation to wave generation areas or storm changes were tenuous.

Mean Wave Directions

Mid-Century: 2026–2045

RCP4.5 D_p changes were mainly relegated to regions west of 180°, with the majority of the changes occurring in the Central region. The σ_{Dp} values increased by 10.0 to more than 15.0° within the west and were accompanied with the largest observed directional shifts for the time period and scenario. There were 5.0 to 15.0° σ_{Dp} increases within the Central and Marianas regions during the DJF and JJA, respectively.

The majority of the RCP8.5 changes occurred during the SON season. σ_{Dp} values generally increased west of 180° and had the most widespread directional shifts, occurring primarily in the Marianas region and the Central region, closer to the equator. There was an east and west trend present during the JJA, where the Northeast σ_{Dp} values increased by 0.50 to 15.0 degree and the equatorial islands west of 180° decreased by 0.50 to 15.0°. The two scenarios differed primarily within the SON season. The RCP4.5 scenario showed a larger and more widespread increase of σ_{Dp} values and directional shifts within the west islands compared to the RCP8.5 scenario. Otherwise, the RCP8.5 showed more complex JJA patterns in σ_{Dp} values, reflecting changes in dominant JJA extreme wave generation.

End-Century: 2081–2100

The RCP4.5 SON σ_{Dp} values displayed a large increase west of 180° of generally more than 15.0°. This increase was accompanied by large counterclockwise shifts in the islands near the equator within these west regions. The JJA season's σ_{Dp} values increased in the east half of the study area and within the eastern islands of the Central region.

The RCP8.5 JJA σ_{Dp} values followed a similar pattern of increasing within the Northern hemisphere islands east of 165°, but the values generally increased by a weaker 0.50 to 10.0° compared to the stronger values observed in the RCP4.5 scenario. However, the Islands in the Central region displayed a clockwise D_p shift, though smaller than the RCP4.5 scenario; Enewetak remained the largest D_p shift and, similarly, its σ_{Dp} value decreased. MAM σ_{Dp} values generally decreased within the west half of the study area, similar to those of RCP4.5. The SON σ_{Dp} values in the western half of the study region increased, but the increases were weaker than in the RCP4.5 scenario.

The RCP4.5 end-century scenario displayed generally stronger SON and JJA trends in D_p values. Both JJA values seemed to indicate a weakening of the trade wind's influence on extreme D_p values within the central region. Enewetak appeared to go through a transition from being dominated by trade wind swell waves to Southern ocean swell waves, causing the reorientation of extreme wave directions towards the north. The increase of σ_{Dp} values indicated that the extreme wave heights during this season, probably more composed of trade wind swell during the hindcast period, have become subject to increased large swell from other regions. Similarly, the trade winds seem to become more dominant during the SON seasons, because in the Central region, directions rotated clockwise closer to the equator and within the Marianas region during RCP8.5, but they rotated counterclockwise during RCP4.5.

Mean Wind Directions

Mid-Century: 2026–2045

RCP4.5 SON $\sigma_{U\theta}$ values increased west of 180°, except for Chuuk and Kosrae, which decreased by 10.0 to more than 15.0°. MAM $\sigma_{U\theta}$ values decreased in the west half of the study area, but the other seasons did not show a significant trend.

RCP8.5 values showed larger changes in $\sigma_{U\theta}$ and direction values during the SON season than RCP4.5. Points west of 180° increased by 5.0 to more than 15.0°, and many points experienced significant clockwise rotations in U_θ. DJF $\sigma_{U\theta}$ values decreased throughout the eastern half of the study region by 5.0 to 10.0°.

End-Century: 2081–2100

The end-century RCP4.5 SON trends were much more complex than those present in the mid-century. The largest changes were still within the Central region. The $\sigma_{U\theta}$ of the southern islands within the region decreased by more than 15.0°, and their mean direction values rotated clockwise from the northwest to the northeast. The $\sigma_{U\theta}$ of the eastern islands within the Central region increased by more than 15.0°.

RCP8.5 SON trends change dramatically from mid-century values. The southern Central region islands rotated counterclockwise. MAM $\sigma_{U\theta}$ values decreased across the study area, though directions did not change significantly. There were not many significant deviations from hindcast values during other seasons. RCP8.5 end-century SON wind directions did not match the RCP4.5 scenario or represent an intensification of the trends displayed within RCP4.5. Instead, RCP4.5 end-century wind direction changes more closely resembled the changes present within the mid-century RCP8.5 scenario. Therefore, wind directions within the RCP8.5 scenario may have represented the end member of changes, whereby changes were much larger until the mid-century, but over a longer period, these U_θ values returned to approximately hindcast directions.

Implications

The end-century RCP8.5 scenario's trends appear to be an intensification of the trends of the RCP4.5 scenario, except for D_p and U_θ values. This pattern suggests that the intensification of the radiative forcing will result in similar, but stronger variable changes by 2100. H_s changes over the next century are forecasted to be a spectrum of large decreases across the tropical Pacific, with the strength of the decrease scaling with the intensity of the radiative forcing. This trend was broadly observed by Hemer and others (2013), who projected H_s values to decrease by 5 to 10 percent of hindcast values throughout the northern Pacific during the January-March and July-September periods by the end of the 21st century. However, Hemer and others (2013) did not address the SON season, therefore not describing the large decreases in H_s values forecasted in this study. The decrease in H_s values may be linked to a decrease in extratropical cyclone frequency, strength, or storm tracks. Ulbrich and others (2008), using an ensemble of models,

project storm tracks within the North Pacific to shift poleward, which would have a direct effect on the extreme swell waves produced. Changes in storm tracks would explain the large decrease of H_s values projected throughout most periods, except JJA, when North Pacific storm activity is reduced. It is unlikely that these changes are due to tropical cyclone or El Niño Southern Oscillation activity, as neither phenomenon is captured well within the selected global climate models (GCMs).

Wave periods are related to frequency as 1/frequency. Therefore, as wave periods increase, the frequency of the spectrum decreases. Lower frequency spectra indicate a greater distance between swell wave generation region and the affected area. The end-century RCP8.5 scenario displays a DJF difference between T_p trends for the west and east halves of the study area. These changes in T_p are similar to the trends observed by Hemer and others (2013) for January-March, where the eastern half of the study regions values increased and those in the west decreased. However, July-September values show a clear decrease, but within this study, JJA values do not suggest any significantly comparable trends. Eastern T_p values increase while western values decrease, possibly indicating that the DJF waves will be generated closer to the western half of the study area and farther from the eastern half. This trend assumes that DJF extreme waves throughout the study area are generated by extratropical storms in the North Pacific.

The RCP4.5 end-century scenario display generally stronger SON and JJA trends in D_p values but little to no change during the DJF season. The changes in wave directions that are present during JJA differ from the general directions presented by Hemer and others (2013) whereby the Central, Western, and Marianas regions' directions are predominantly oriented from south to north. This difference is likely due to the fact that these directions were the result of averaging the directions of the top 5 percent of wave heights. Both values seemed to indicate a weakening of the trade winds' influence on extreme D_p values within the Central region. Merrifield (2011) described historical increases in Pacific trade-wind intensity as tracking signatures of global warming trends, and inferred that this trend should persist into the future unless other processes began to override these tendencies. Therefore, it would be unlikely, as radiative forcing increased within both scenarios, for the trade winds themselves to weaken. Instead, it appears that changes in the Central region's wave directions were subject to strong, extratropical forcing.

Enewetak is projected to go through a transition from being dominated by trade-wind waves to Southern Ocean swell. The increase of $\sigma_{U\theta}$ values indicates that the extreme east-to-west-trending wave heights during the JJA season, possibly more composed of trade wind waves during the hindcast period, have become subject to increased large swell from other regions. During RCP8.5, it seemed that the trade-wind waves become more dominant, influencing Central islands, whereas during RCP4.5, Southern Hemisphere swell seems to dominate the Central equatorial islands. Under the assumption that the trend in trade wind intensity will continue to scale with increased radiative forcing, it would appear that a larger portion of extreme wave

heights will be generated by trade winds during the end-century RCP8.5 scenario, resulting in the stronger east-to-west shift in wave directions opposed to mid-century directions.

Overall, increases in wind speeds during the JJA season within the Central region corresponded with increases in wave heights within the region. However, the cause of the decreasing strength of U_a values throughout other seasons remains uncertain. Unlike other variables, end-century RCP8.5 directions more closely matched hindcast means. It is possible that over the short term or weaker radiative forcing, new processes may affect local wind conditions, exacerbated by the degree of climate change, but under extended forcing, previous trends will once again become dominate. However, this supposition will need to be studied further.

Conclusions

Extreme wave climates within the tropical Pacific Ocean were forecasted to change dramatically during the 2026–2045 and 2081–2100 periods. H_s trends predicted by both RCP4.5 and RCP8.5 show marked decreases in H_s magnitudes by the end of the 21st century. The end-century trends of the two scenarios were similar, with the magnitude and breadth of the H_s values within RCP8.5 generally being larger. This difference suggests that over the next century, the response of wave climate parameters within the tropical Pacific may be a spectrum of change, with the magnitude of the change dependent on the magnitude of the radiative forcing. T_p and U_a values respond similarly. The forecasted region to experience the most change is the Central region, where H_s values generally decrease dramatically and D_p values rotated often more than 40° within the southern portion of the region. Clearly these islands will be subject to new conditions that will need to be studied more and in greater depth. Additionally, past work has mainly focused on the boreal winter and summer seasons; however, it was found within this study that SON H_s values changed the most, suggesting that future studies would benefit from describing the MAM and SON seasons as well.

Acknowledgments

This work was carried out under the USGS's Pacific Coral Reef Project as part of an effort in the United States and its trust territories to better understand the affect of geologic and oceanographic processes on coral reef systems and the USGS's Climate Change Impacts to the U.S. Pacific and Arctic Coasts Project to understand the impact of climate change on U.S. and U.S.-affiliated island shorelines. This project was funded by the USGS's Coastal and Marine Geology Program and the Pacific Islands Climate Change Cooperative (PICCC). Sean Vitousek (USGS) and Patrick Limber (USGS) contributed numerous excellent suggestions and a timely review of our work. Peter Stauffer (USGS) provided the editorial review and Susan Cochran (USGS) performed all of the formatting and layout for this report. Use of trademark names does not imply USGS endorsement of products.

Additional Digital Information

For an online PDF version of this report, please see:

http://pubs.usgs.gov/of/2015/1001/

For more information on the U.S. Geological Survey's Pacific Coastal and Marine Science Center, please see:

http://walrus.wr.usgs.gov/

For more information on the U.S. Geological Survey's Pacific Coral Reef Project, please see:

http://coralreefs.wr.usgs.gov/

Direct Contact Information

Regarding this report

Curt D. Storlazzi (Project Chief): *cstorlazzi@usgs.gov*

References Cited

Caires, S., and Sterl, A., 2005, 100-year return value estimates for ocean wind speed and significant wave height from the ERA-40 data: Journal of Climate, v. 18, p. 1032–1048.

Caires, S., Swail, V.R., and Wang, X.L., 2006, Projections and analysis of extreme wave climate: Journal of Climate, v. 19, p. 5581–5605.

Cayan, D.R., Bromirski, P.D., Hayhoe, K., Tyree, M., Dettinger, M.D., and Flick, R.E., 2008, Climate change projections of sea level extremes along the California Coast: Climatic Change, v. 87, no. S1, p. S57–S73.

Donat, M.G., Leckebusch, G.C., Wild, S., and Ulbrich, U., 2010, Benefits and limitations of regional multi-model ensembles for storm loss estimations: Climate Research, v. 44, p. 211–225.

Fletcher, C.H., and Richmond, B.M., 2010, Climate change in the Federated States of Micronesia; Food and water security, climate risk management, and adaptive strategies: University of Hawaii Sea Grant Report TT–10–02, 32 p.

Hemer, M.A., Fan, Y., Mori, N., Semedo, A., and Wang X.L., 2013, Projected changes in wave climate from a multi-model ensemble: Nature Climate Change, v. 3, p. 471–476.

Hoeke, R.K., Storlazzi, C.D., and Ridd, P.V., 2011, Hydrodynamics of a bathymetrically complex fringing coral reef embayment—wave climate, in situ observations and wave prediction: Journal of Geophysical Research—Oceans, v. 116, C04018

Hoeke, R.K., McInnes, K.L., Kruger, J.C., McNaught, R.J., Hunter, J.R., and Smithers, S.G., 2013, Widespread inundation of Pacific islands triggered by distant-source wind-waves: Global and Planetary Change, v. 108, p. 128–138.

Hyndman, R.J., and Koehler, A.B., 2006, Another look at measures of forecast accuracy: Journal of Forecasting, v. 22, p. 679–688.

Merrifield, M.A., 2011, A shift in western tropical Pacific sea level trends during the 1990s: Journal of Climate, v. 24, p. 4126–4138.

Mori, N., Yasuda, T., Mase, H., Tom, T., and Oku, Y., 2010, Projection of extreme wave climate change under global warming: Hydrological Research Letters, v. 4, p. 15–19

National Data Buoy Center, 2013, Pacific Ocean historical buoy dataset: National Oceanic and Atmospheric Administration, accessed online at http://www.ndbc.noaa.gov/.

National Geophysical Data Center, 2013, Global self-consistent hierarchical high-resolution geography database version 2.2.2: National Geophysical Data Center online data, accessed online at http://www.ngdc.noaa.gov/mgg/shorelines/gshhs.html.

Naval Research Laboratory, 2013, Digital bathymetric database version 3.0: Naval Research Laboratory online data, accessed online at http://www7320.nrlssc.navy.mil/DBDB2_WWW/v3.0/NRLCOM_dbdb2.html.

Riahi, K., Krey, V., Rao, S., Chirkov, V., Fischer, G., Kolp, P., Kindermann, G., Nakicenovic, N., and Rafai, P., 2010, RCP-8.5; Exploring the consequence of high emission trajectories: Climatic Change, v. 109 no. 1–2, p. 33–57.

Semedo, A., Sušelj, K., Rutgersson, A., and Sterl, A., 2011, A global view on the wind sea and swell climate and variability from ERA-40: Journal of Climate, v. 24, p. 1461–1479.

Stockdon, H.F., Holman, R.A., Howd, P.A., and Sallenger, A.H., 2006, Empirical parameterization of setup, swash, and runup: Coastal Engineering, v. 53, p. 573–588.

Storlazzi, C.D., and Reid, J.A., 2010, The influence of ENSO cycles on wave-driven sea-floor sediment mobility along central California continental margin: Continental Shelf Research, v. 30, p. 1582–1599.

Storlazzi, C.D., Brown, E., Field, M.E., Rogers, K., and Jokiel, P.L., 2005, A model for wave control on coral breakage and species distribution in the Hawaiian Islands: Coral Reefs, v. 24, p. 43–55.

Storlazzi, C.D., Elias, E., Field, M.E., and Presto, M.K., 2011, Numerical modeling of the impact of sea-level rise on fringing coral reef hydrodynamics and sediment transport: Coral Reefs, v. 30, p. 23–38.

Taylor, K.E., Stouffer, R.J., and Meehl, G.A., 2009, A summary of the CMIP5 experiment design: Program for Climate Model Diagnosis and Intercomparison Report, 33 p., accessed online at http://cmip-pcmdi.llnl.gov/cmip5/docs/Taylor_CMIP5_design.pdf.

Thomson, A.M., Calvin, K.V., Smith, S.J., Kyle, G.P., Volke, A., Patel, P., Delgado-Arias, S., Bond-Lamberty, B., Wise, M.A., Clarke, L.E., and Edmonds, J.A., 2011, RCP4.5; a pathway for stabilization of radiative forcing by 2100: Climatic Change, v. 109, no. 1-2, p. 77–94.

Tolman, H.L., 2009, User manual and system documentation of WAVEWATCH III™ version 3.14: National Oceanic and Atmospheric Administration, National Weather Service, National Centers for Environmental Prediction Technical Note 276, 194 p.

Ulbrich, U., Pinto, J.G., Kupfer, H., Leckebusch, G.C., Spangehl, T., and Reyers, M., 2008, Changing Northern Hemisphere storm tracks in an ensemble of IPCC climate change simulations: Journal of Climate, v. 21, p. 1669–1679.

van Vuuren, D.P., Edmonds, J.A., Kainuma, M., Riahi, K., Thomson, A.M., Hibbard, K., Hurtt, G.C., Kram, T., Krey, V., Lamarque, J-F., Masui, T., Meinshausen, M., Nakicenovic, N., Smith, S.J., and Rose, S., 2011, The representative concentration pathways—an overview: Climatic Change, v. 109, p. 5–31.

Vitousek, S., and Fletcher, C.H., 2008, Maximum annually recurring wave heights in Hawaii: Pacific Science, v. 62, no. 4, p. 541–555.

World Climate Research Programme, 2013, CMIP5—Coupled Model Intercomparison Project Phase 5—overview: World Climate Research Programme, accessed online at http://cmip-pcmdi.llnl.gov/cmip5/.

Wang, X.L., and Swail, V.R., 2006, Climate change signal and uncertainty in projections of ocean wave height: Climate Dynamics, v. 26, p. 109–126.

Wang, X.L., Swail, V.R., and Cox, A., 2009, Dynamical versus statistical downscaling methods for ocean wave heights: International Journal of Climatology, v. 30, no. 3, p. 317–332, DOI: 10.1002/joc.1899.

Table 1. Table of names and locations of WAVEWATCH III model points within the mid-to-western tropical Pacific Ocean.

[Negative latitudes are degrees south; negative longitudes are degrees west]

Modeled location name	Latitude (ºN)	Longitude (ºE)
American Samoa	-14.25	-170.00
Kauai	22.00	-160.00
Big Island of Hawaii	19.00	-154.00
Midway	28.20	-177.40
Chuuk	7.40	151.85
Saipan	15.25	145.75
Asuncion	19.70	145.40
Kosrae	5.20	163.00
Palau	7.30	134.50
Pohnpei	6.75	158.00
Yap	9.50	138.10
Majuro	7.10	171.30
Enewetak	11.50	162.20
Bikini	11.60	165.40
Molokai	21.25	-157.00
Northwest Hawaiian Islands	25.75	-171.75
Guam	13.50	144.75
Kwajalein	8.75	167.75
Wake	19.25	166.75
Johnston Atoll	16.75	-169.50
Kingman Reef	6.50	-162.50
Palmyra Atoll	5.83	-162.08
Rose Atoll	-14.50	-168.25
Howland	0.75	-176.50
Jarvis	-0.50	-160.00

Table 2. List of Global Climate Models used, wave model used, and the model resolutions.

Global Climate Model	Resolution (longitude x latitude) in Degrees
BCC-CSM1.1	2.8 x 2.8
INM-CM4	2.0 x 1.5
MIROC5	1.4 x 1.4
GFDL-ESM2M	2.5 x 1.5
Global Wave Model	**Resolution (longitude x latitude) in Degrees**
WAVEWATCHIII	1.25 x 1.00

Table 3. Table showing comparisons between hindcast significant wave height data, in meters, at the Molokai point and historical significant wave height data from selected NDBC stations throughout the Hawaiian Islands by months.

[DJF=December-February, MAM=March-May, JJA=June-August, and SON=September-November; NDBC, National Data Buoy Center; statistics shown are mean absolute error (MAE), standard deviation (Std), and normalized variance (nVar)]

Time Period	NDBC 51001			NDBC 51002			NDBC 51003			NDBC 51004		
	MAE	Std	nVar	MAE	Std	nVar	MAE	Std	nVar	MAE	Std	nVar
DJF	0.14	0.17	0.68	0.40	0.15	1.46	0.44	0.14	1.40	0.39	0.18	1.55
MAM	0.08	0.09	0.81	0.12	0.05	1.22	0.07	0.08	1.24	0.13	0.08	1.38
JJA	0.10	0.08	1.40	0.15	0.04	1.23	0.15	0.14	1.79	0.12	0.07	1.42
SON	0.19	0.17	0.85	0.23	0.17	1.71	0.33	0.16	1.65	0.19	0.16	1.75
Yearly	0.10	0.12	0.81	0.15	0.16	1.65	0.22	0.15	1.51	0.16	0.16	1.73

Table 4. Table showing comparisons between hindcast significant wave height data, in meters, at the Big Island of Hawaii point and historical significant wave height data from selected NDBC stations throughout the Hawaiian Islands by months.

[DJF=December-February, MAM=March-May, JJA=June-August, and SON=September-November; NDBC, National Data Buoy Center; statistics shown are mean absolute error (MAE), standard deviation (Std), and normalized variance (nVar)]

Time Period	NDBC 51001			NDBC 51002			NDBC 51003			NDBC 51004		
	MAE	Std	nVar	MAE	Std	nVar	MAE	Std	nVar	MAE	Std	nVar
DJF	0.34	0.34	0.50	0.09	0.04	1.07	0.11	0.03	0.97	0.10	0.07	1.18
MAM	0.11	0.13	0.65	0.08	0.03	0.98	0.09	0.03	1.03	0.07	0.04	1.14
JJA	0.28	0.10	1.52	0.05	0.06	1.34	0.32	0.16	1.95	0.09	0.07	1.53
SON	0.18	0.12	0.83	0.22	0.17	1.68	0.33	0.17	1.63	0.19	0.16	1.73
Yearly	0.17	0.20	0.59	0.07	0.06	1.21	0.21	0.04	1.09	0.09	0.08	1.31

Table 5. Table showing comparisons between hindcast significant wave height data, in meters, at the Kauai point and historical significant wave height data from selected NDBC stations throughout the Hawaiian Islands by months.

[DJF=December-February, MAM=March-May, JJA=June-August, and SON=September-November; NDBC, National Data Buoy Center; statistics shown are mean absolute error (MAE), standard deviation (Std), and normalized variance (nVar)]

Time Period	NDBC 51001			NDBC 51002			NDBC 51003			NDBC 51004		
	MAE	Std	nVar	MAE	Std	nVar	MAE	Std	nVar	MAE	Std	nVar
DJF	0.22	0.05	0.92	0.63	0.30	1.95	0.67	0.29	1.88	0.61	0.32	2.05
MAM	0.05	0.03	1.00	0.12	0.11	1.52	0.18	0.17	1.52	0.16	0.17	1.72
JJA	0.18	0.13	1.72	0.10	0.07	1.53	0.22	0.19	2.17	0.11	0.07	1.71
SON	0.29	0.15	0.93	0.34	0.20	1.86	0.44	0.20	1.80	0.29	0.20	1.91
Yearly	0.18	0.07	1.01	0.26	0.28	2.05	0.36	0.25	1.88	0.26	0.27	2.13

Table 6. Table showing comparisons between hindcast top 5 percent of significant wave height data, in meters, at the Molokai point and historical significant wave height data from selected NDBC stations throughout the Hawaiian Islands by months.

[DJF=December-February, MAM=March-May, JJA=June-August, and SON=September-November; NDBC, National Data Buoy Center; statistics shown are mean absolute error (MAE), standard deviation (Std), and normalized variance (nVar)]

Time Period	NDBC 51001			NDBC 51002			NDBC 51003			NDBC 51004		
	MAE	Std	nVar	MAE	Std	nVar	MAE	Std	nVar	MAE	Std	nVar
DJF	0.67	0.24	0.51	0.76	0.18	2.02	0.74	0.16	1.52	0.76	0.09	1.28
MAM	0.37	0.06	0.82	0.12	0.03	1.02	0.28	0.09	0.85	0.33	0.07	0.44
JJA	0.35	0.27	3.71	0.06	0.05	1.29	0.51	0.13	1.52	0.08	0.09	0.81
SON	0.46	0.44	0.33	0.64	0.14	1.77	0.65	0.08	1.43	0.54	0.05	1.19
Yearly	0.49	0.03	1.06	0.49	0.02	1.06	0.46	0.04	1.07	0.44	0.02	1.03

Table 7. Table showing comparisons between hindcast top 5 percent of significant wave height data, in meters, at the Big Island of Hawaii point and historical significant wave height data from selected NDBC stations throughout the Hawaiian Islands by months.

[DJF=December-February, MAM=March-May, JJA=June-August, and SON=September-November; NDBC, National Data Buoy Center; statistics shown are mean absolute error (MAE), standard deviation (Std), and normalized variance (nVar)]

Time Period	NDBC 51001			NDBC 51002			NDBC 51003			NDBC 51004		
	MAE	Std	nVar	MAE	Std	nVar	MAE	Std	nVar	MAE	Std	nVar
DJF	1.36	0.39	0.31	0.12	0.08	1.26	0.04	0.04	0.93	0.15	0.05	0.69
MAM	0.52	0.12	0.61	0.03	0.02	0.96	0.17	0.05	0.68	0.20	0.05	0.37
JJA	0.56	0.22	3.51	0.22	0.10	1.36	0.72	0.10	1.31	0.30	0.08	0.71
SON	0.41	0.35	0.41	0.71	0.20	2.10	0.74	0.16	1.79	0.64	0.09	1.37
Yearly	0.42	0.03	1.07	0.44	0.05	1.14	0.39	0.03	1.06	0.38	0.04	1.12

Table 8. Table showing comparisons between hindcast top 5 percent of significant wave height data, in meters, at the Kauai point and historical significant wave height data from selected NDBC stations throughout the Hawaiian Islands by months.

[DJF=December-February, MAM=March-May, JJA=June-August, and SON=September-November; NDBC, National Data Buoy Center; statistics shown are mean absolute error (MAE), standard deviation (Std), and normalized variance (nVar)]

Time Period	NDBC 51001			NDBC 51002			NDBC 51003			NDBC 51004		
	MAE	Std	nVar	MAE	Std	nVar	MAE	Std	nVar	MAE	Std	nVar
DJF	0.08	0.07	0.78	1.39	0.33	3.10	1.39	0.28	2.29	1.39	0.22	1.90
MAM	0.05	0.02	1.07	0.44	0.08	1.38	0.58	0.14	1.10	0.66	0.12	0.54
JJA	0.53	0.28	4.14	0.23	0.08	1.39	0.67	0.15	1.74	0.23	0.03	0.84
SON	0.33	0.36	0.32	0.84	0.19	1.76	0.83	0.17	1.39	0.72	0.07	1.07
Yearly	0.59	0.02	1.05	0.59	0.03	1.05	0.54	0.02	1.05	0.52	0.02	1.02

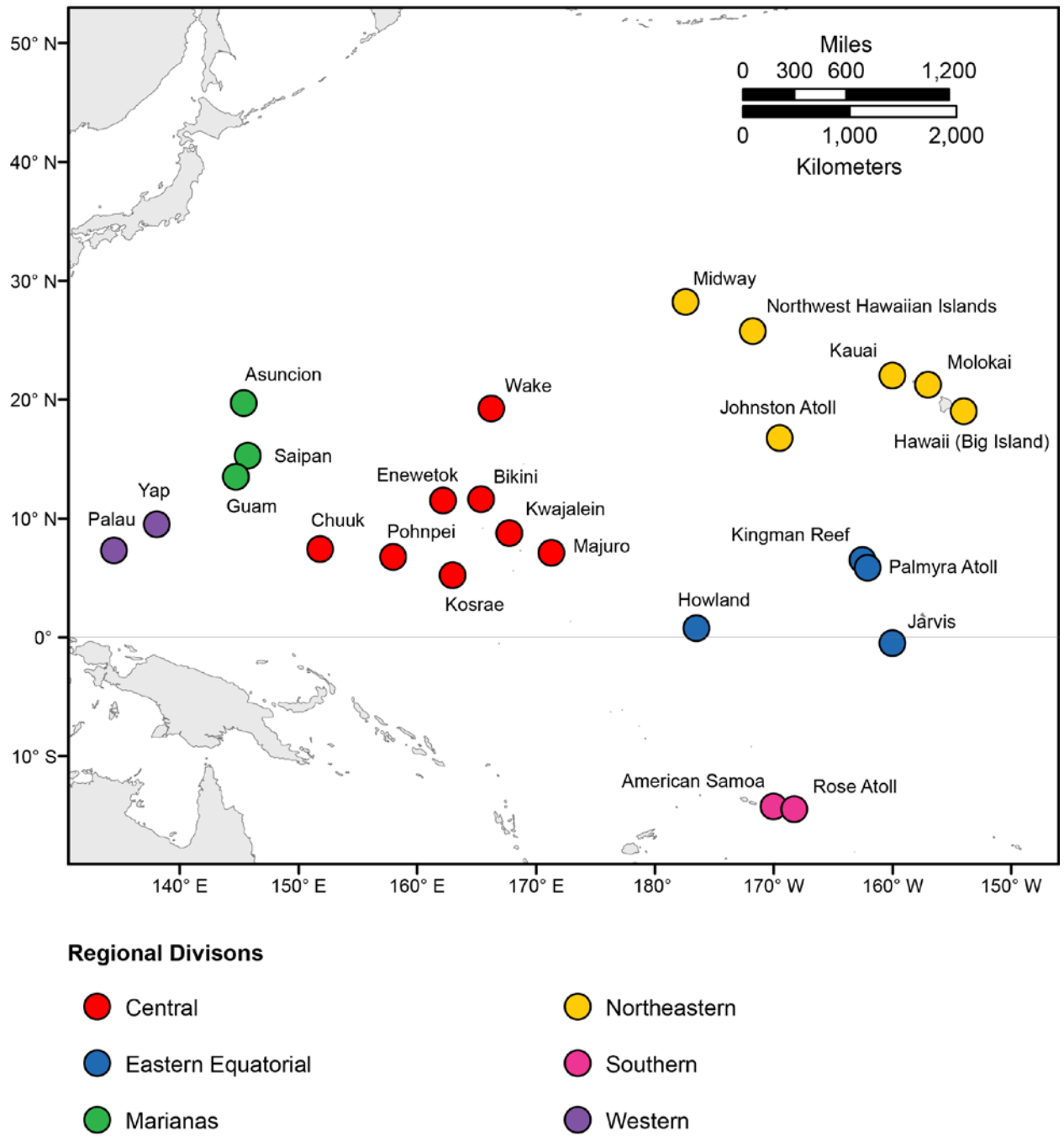

Figure 1. Map showing the locations of the 25 modeled points within the tropical Pacific Ocean used in this study.

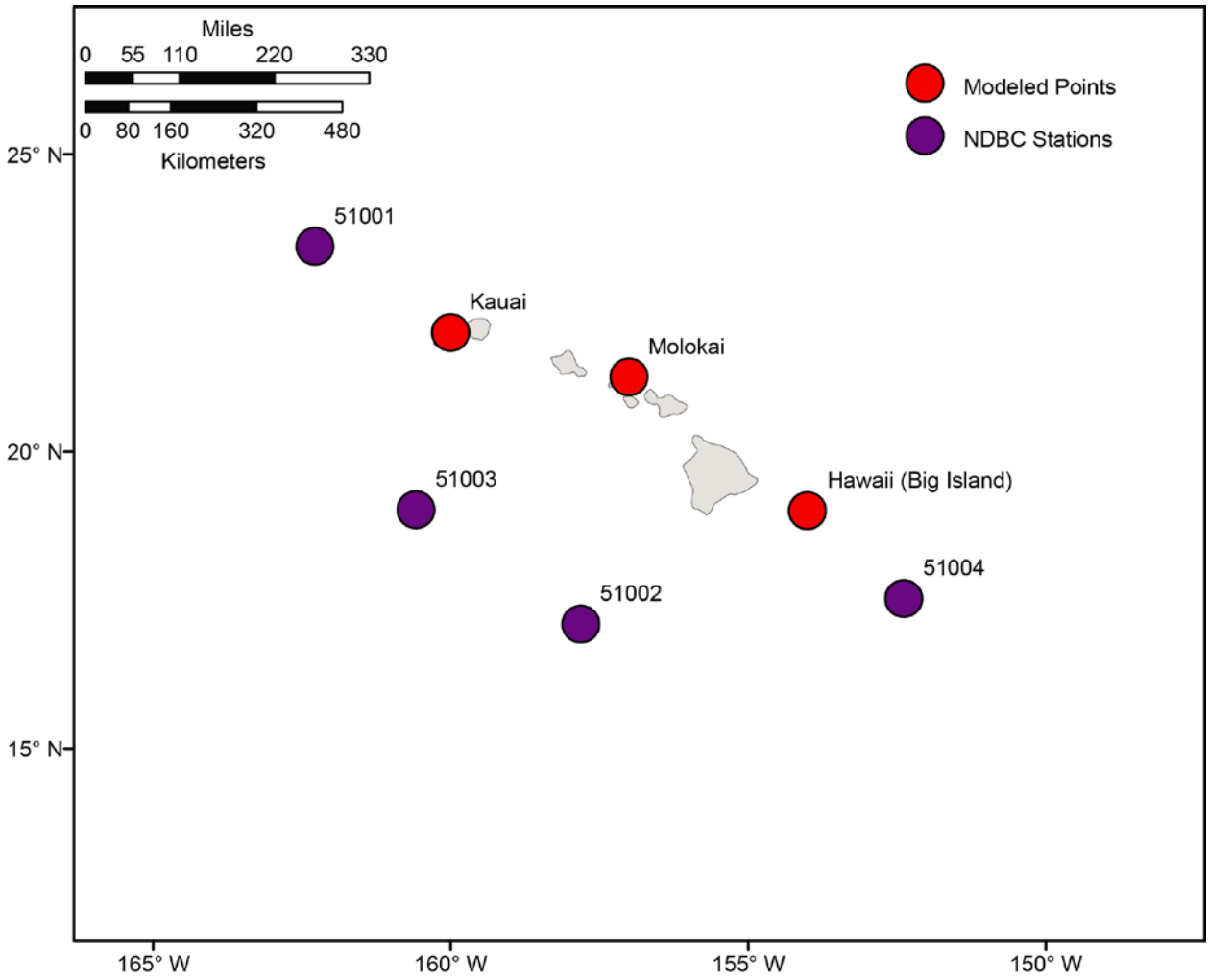

Figure 2. Map showing the locations of selected National Data Buoy Center stations, in purple, and modeled points, in red, within in the Hawaiian Island Chain.

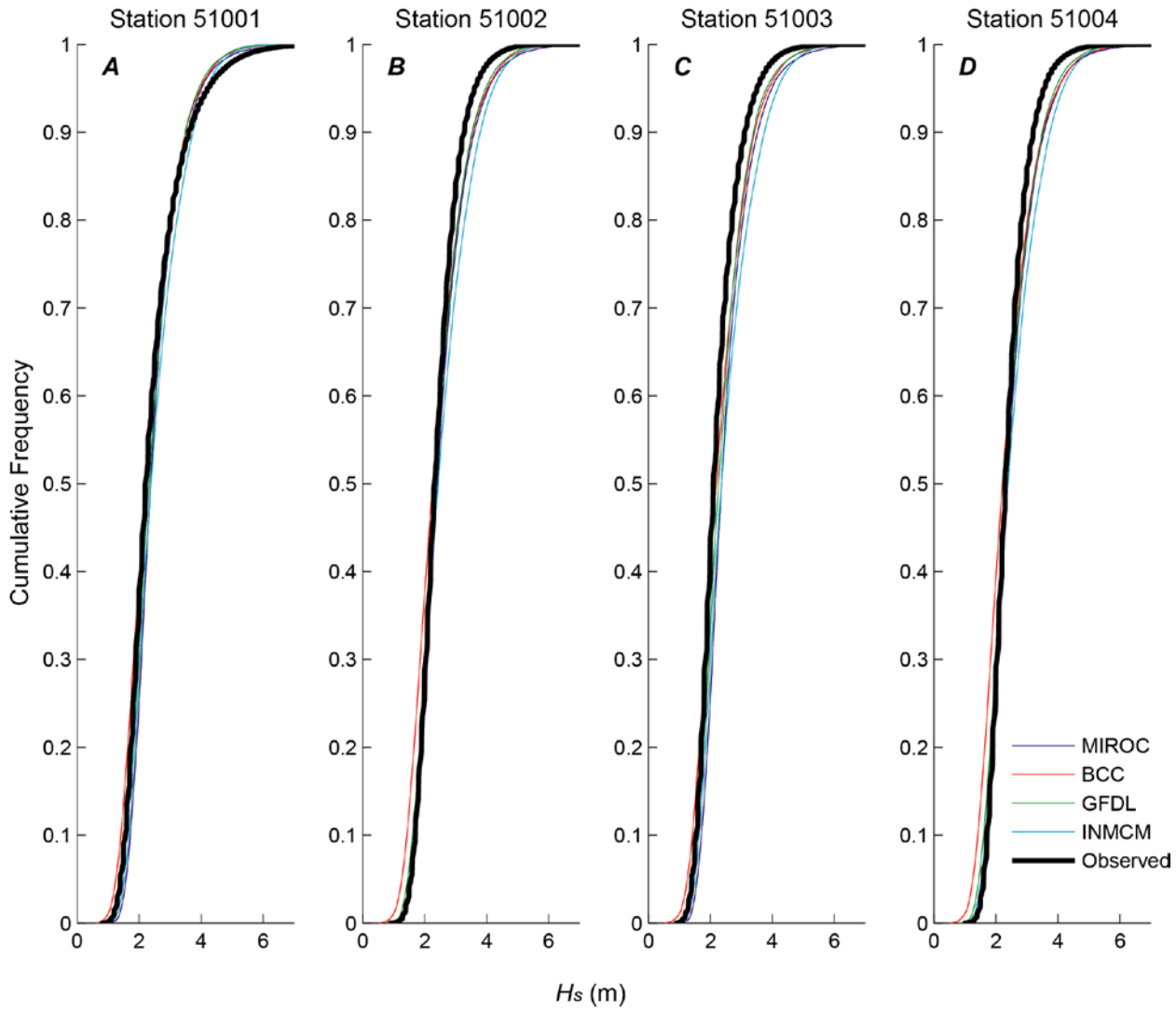

Figure 3. Plots showing comparisons of the empirical cumulative density functions of hindcasted (1986-2005) Molokai point significant wave heights (H_s) in meters, from each GCM-driven WW3 model run with the observed historical cumulative density function at each NDBC station. *A.* Comparison of station 51001 significant wave height cumulative density function with hindcasted Molokai WW3 generated cumulative density functions. *B.* Comparison of station 51002 significant wave height cumulative density function with hindcasted Molokai WW3 generated cumulative density functions. *C.* Comparison of station 51003 significant wave height cumulative density function with hindcasted Molokai WW3 generated cumulative density functions. *D.* Comparison of station 51004 significant wave height cumulative density function with hindcasted Molokai WW3 generated cumulative density functions.

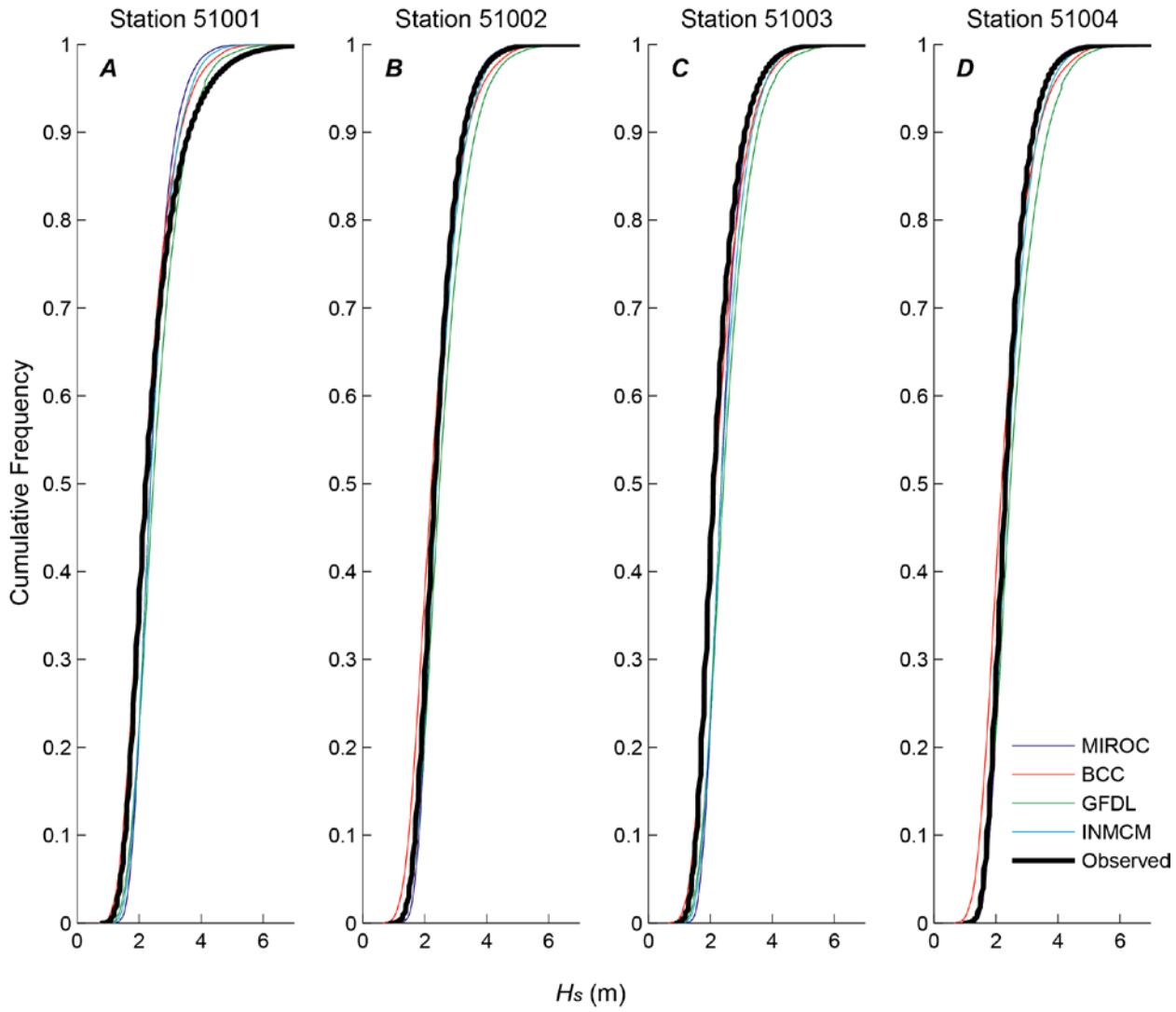

Figure 4. Plots showing comparisons of the empirical cumulative density functions of hindcasted (1986-2005) Big Island of Hawaii point significant wave heights (H_s) in meters from each GCM-driven WW3 model run with the observed historical cumulative density function at each NDBC station. *A*. Comparison of station 51001 significant wave height cumulative density function with hindcasted Big Island of Hawaii WW3 generated cumulative density functions. *B*. Comparison of station 51002 significant wave height cumulative density function with hindcasted Big Island of Hawaii WW3 generated cumulative density functions. *C*. Comparison of station 51003 significant wave height cumulative density function with hindcasted Big Island of Hawaii WW3 generated cumulative density functions. *D*. Comparison of station 51004 significant wave height cumulative density function with hindcasted Big Island of Hawaii WW3 generated cumulative density functions.

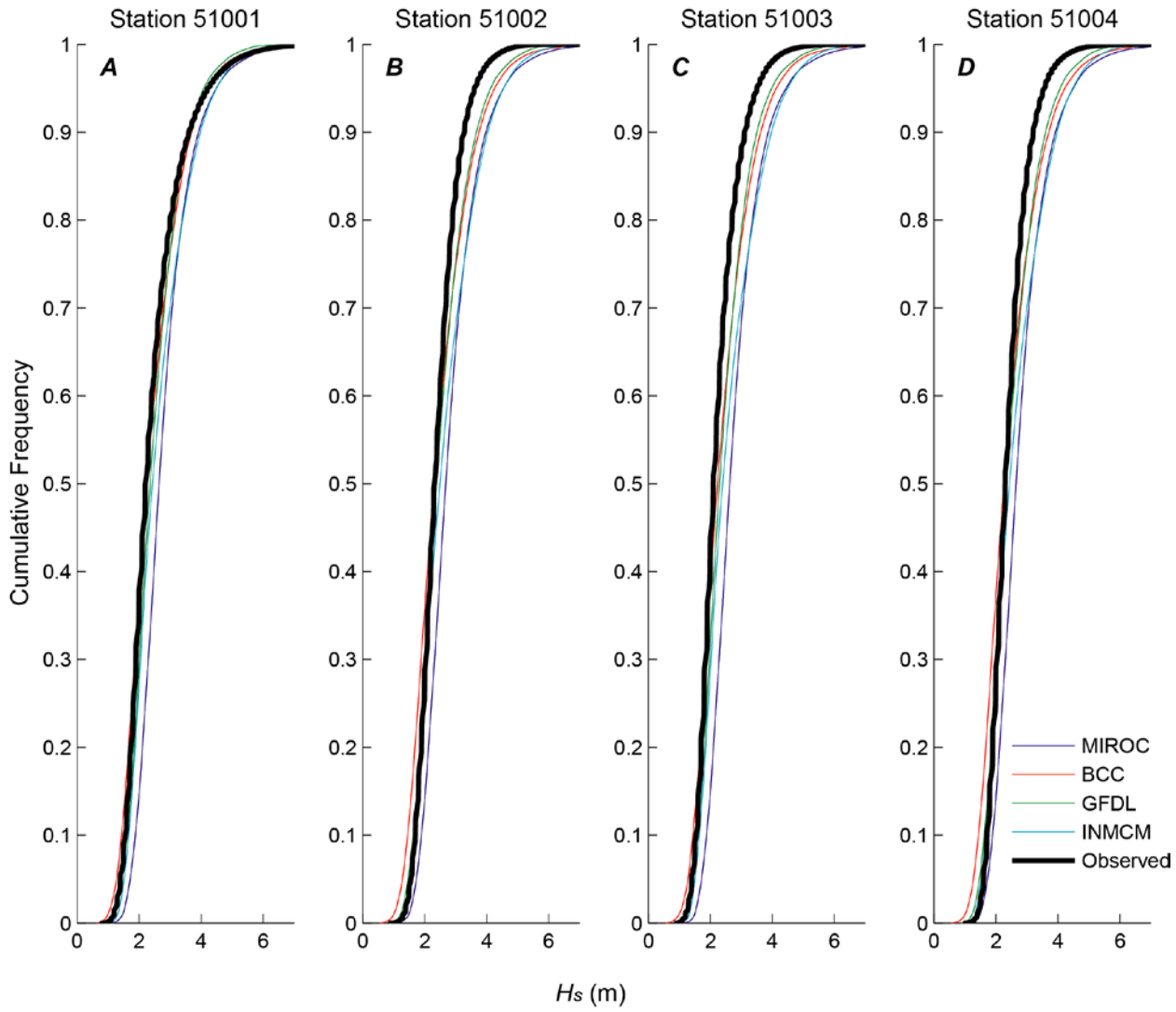

Figure 5. Plots showing comparisons of the empirical cumulative density functions of hindcasted (1986-2005) Kauai point significant wave heights (H_s) in meters from each GCM-driven WW3 model run with the observed historical cumulative density function at each NDBC station. *A*. Comparison of station 51001 significant wave height cumulative density function with hindcasted Kauai WW3 generated cumulative density functions. *B*. Comparison of station 51002 significant wave height cumulative density function with hindcasted Kauai WW3 generated cumulative density functions. *C*. Comparison of station 51003 significant wave height cumulative density function with hindcasted Kauai WW3 generated cumulative density functions. *D*. Comparison of station 51004 significant wave height cumulative density function with hindcasted Kauai WW3 generated cumulative density functions.

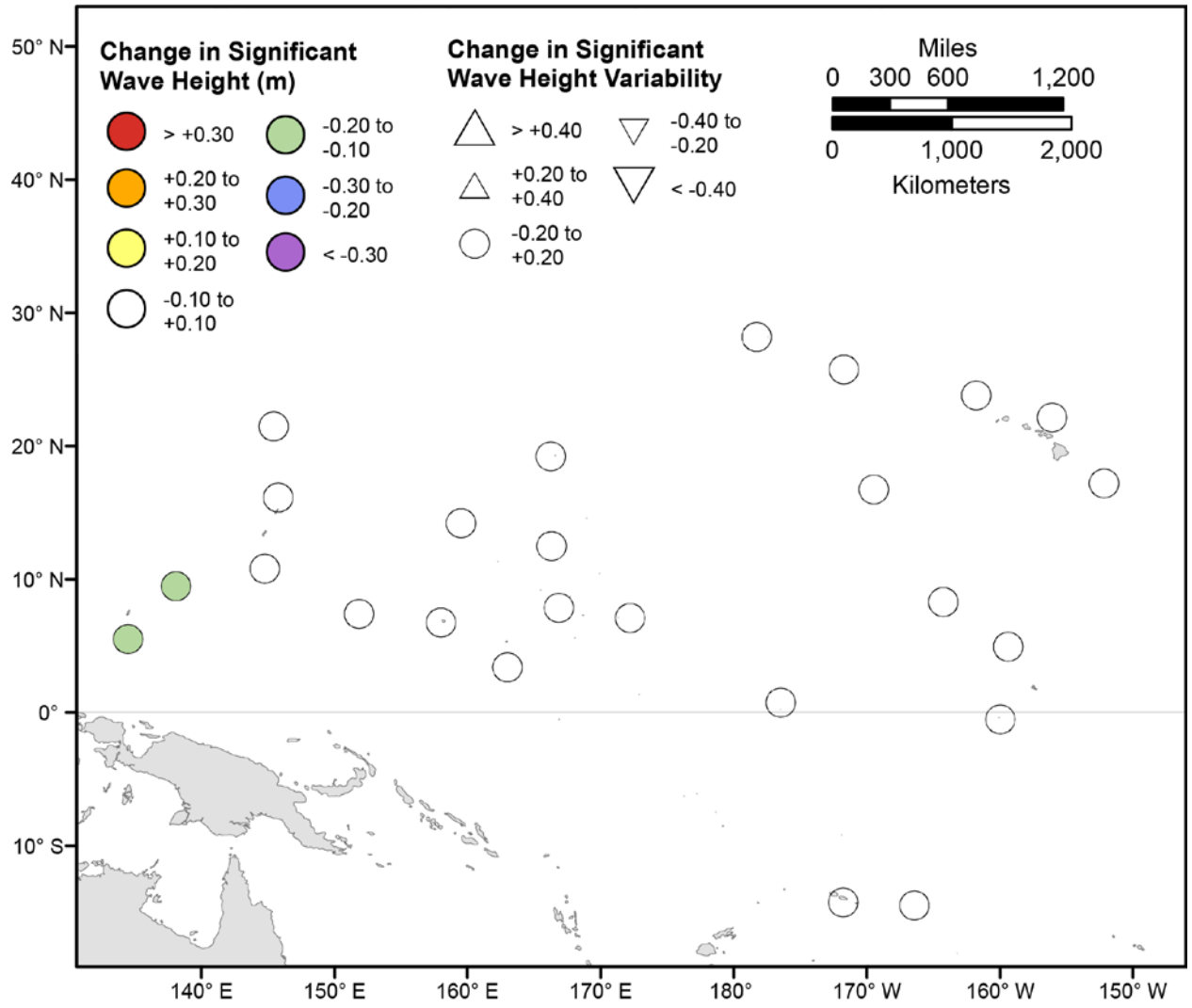

Figure 6. Map showing forecasted differences in mean significant wave height and variance in significant wave height for the years 2026–2045 from hindcasted values during the December-February season under the RCP4.5 future climatic scenario. The colors correspond to the magnitude of change in modeled mean significant wave heights during 2026–2045 from those hindcasted for 1976–2005. The shapes correspond to the magnitude of change in modeled variance in significant wave height during 2026–2045 from those hindcasted for 1976–2005. Units are in meters.

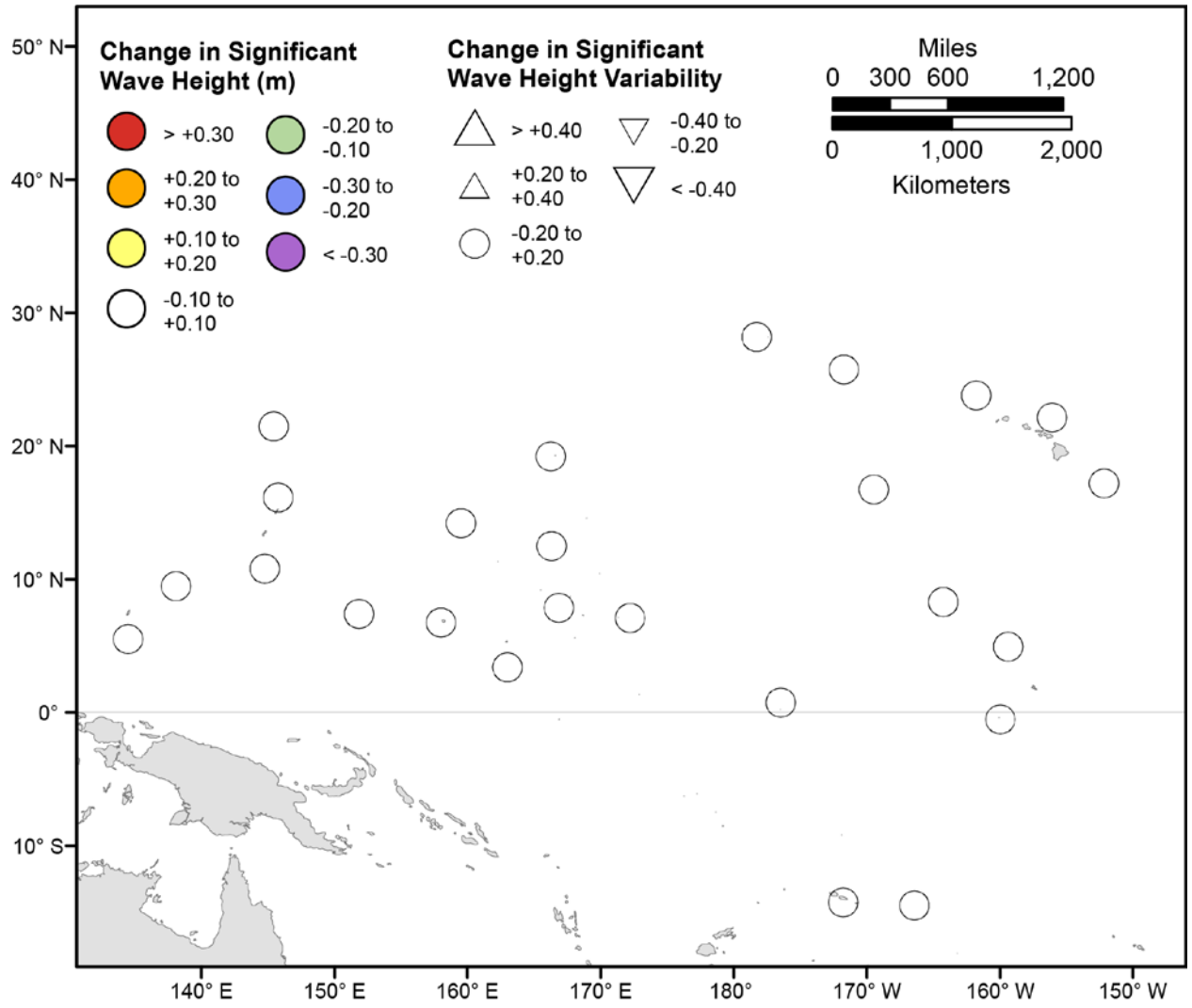

Figure 7. Map showing forecasted differences in mean significant wave height and variance in significant wave height for the years 2026–2045 from hindcasted values during the March-May season under the RCP4.5 future climatic scenario. The colors correspond to the magnitude of change in modeled mean significant wave heights during 2026–2045 from those hindcasted for 1976–2005. The shapes correspond to the magnitude of change in modeled variance in significant wave height during 2026–2045 from those hindcasted for 1976–2005. Units are in meters.

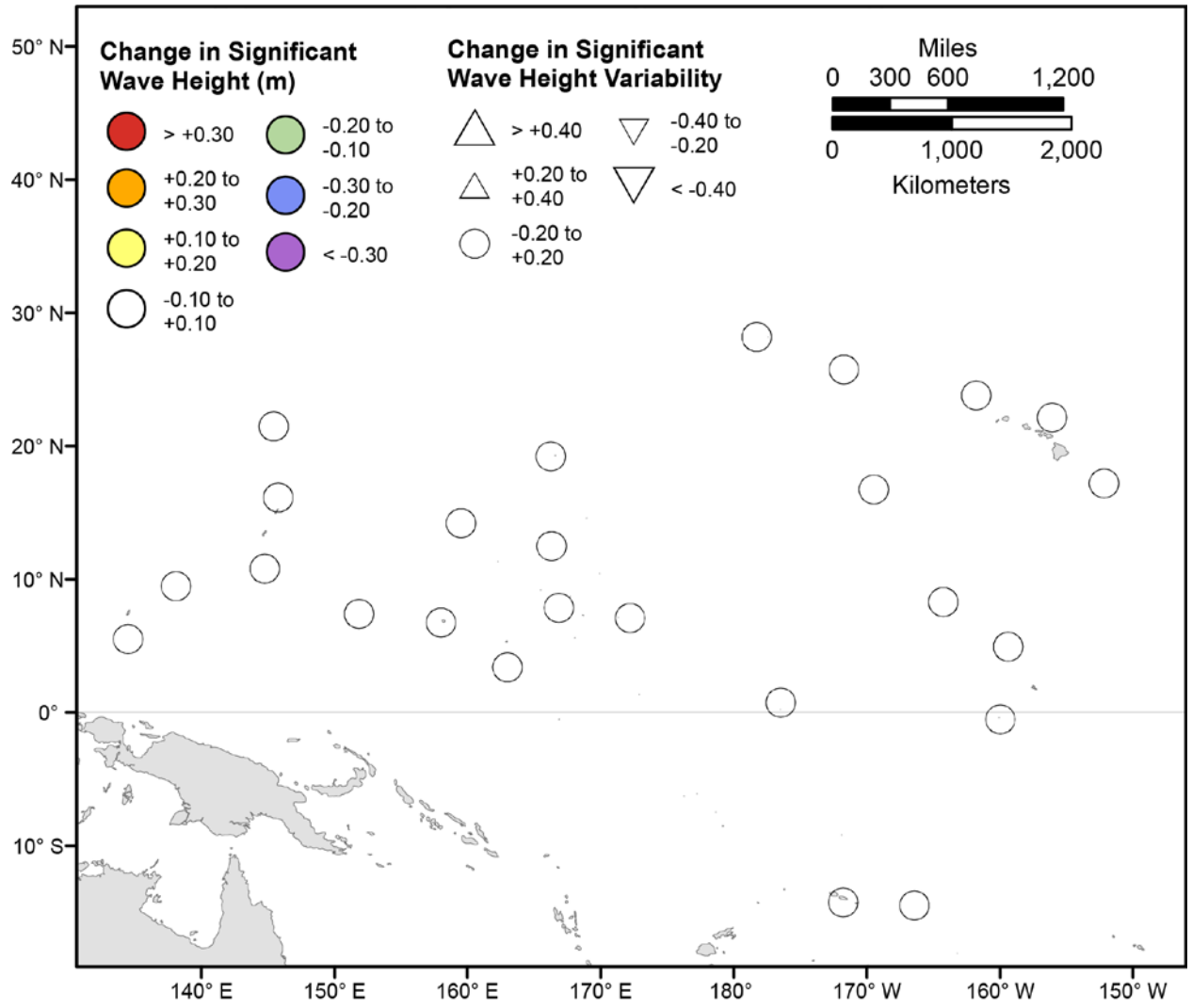

Figure 8. Map showing forecasted differences in mean significant wave height and variance in significant wave height for the years 2026–2045 from hindcasted values during the June-August season under the RCP4.5 future climatic scenario. The colors correspond to the magnitude of change in modeled mean significant wave heights during 2026–2045 from those hindcasted for 1976–2005. The shapes correspond to the magnitude of change in modeled variance in significant wave height during 2026–2045 from those hindcasted for 1976–2005. Units are in meters.

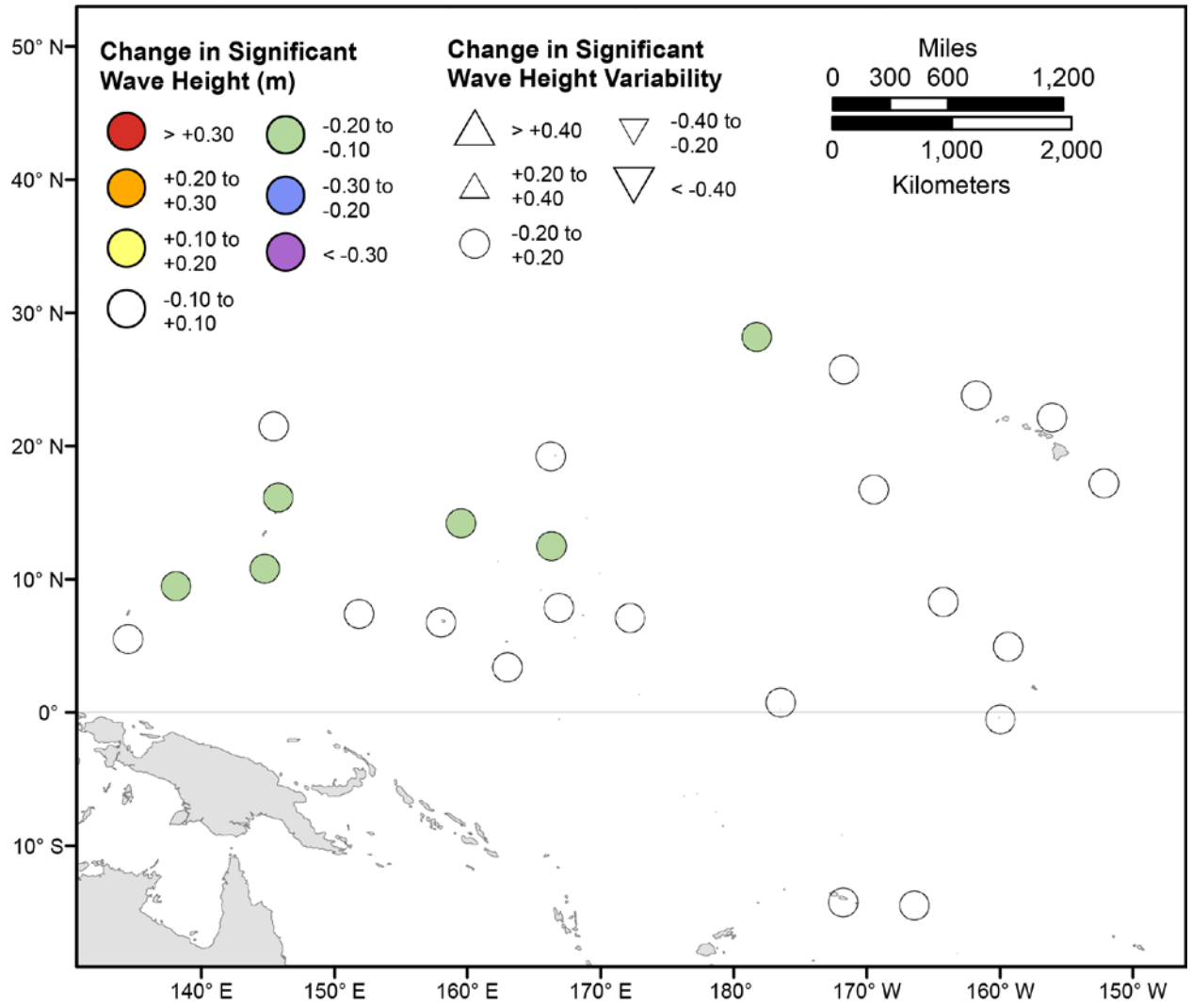

Figure 9. Map showing forecasted differences in mean significant wave height and variance in significant wave height for the years 2026–2045 from hindcasted values during the September-November season under the RCP4.5 future climatic scenario. The colors correspond to the magnitude of change in modeled mean significant wave heights during 2026–2045 from those hindcasted for 1976–2005. The shapes correspond to the magnitude of change in modeled variance in significant wave height during 2026–2045 from those hindcasted for 1976–2005. Units are in meters.

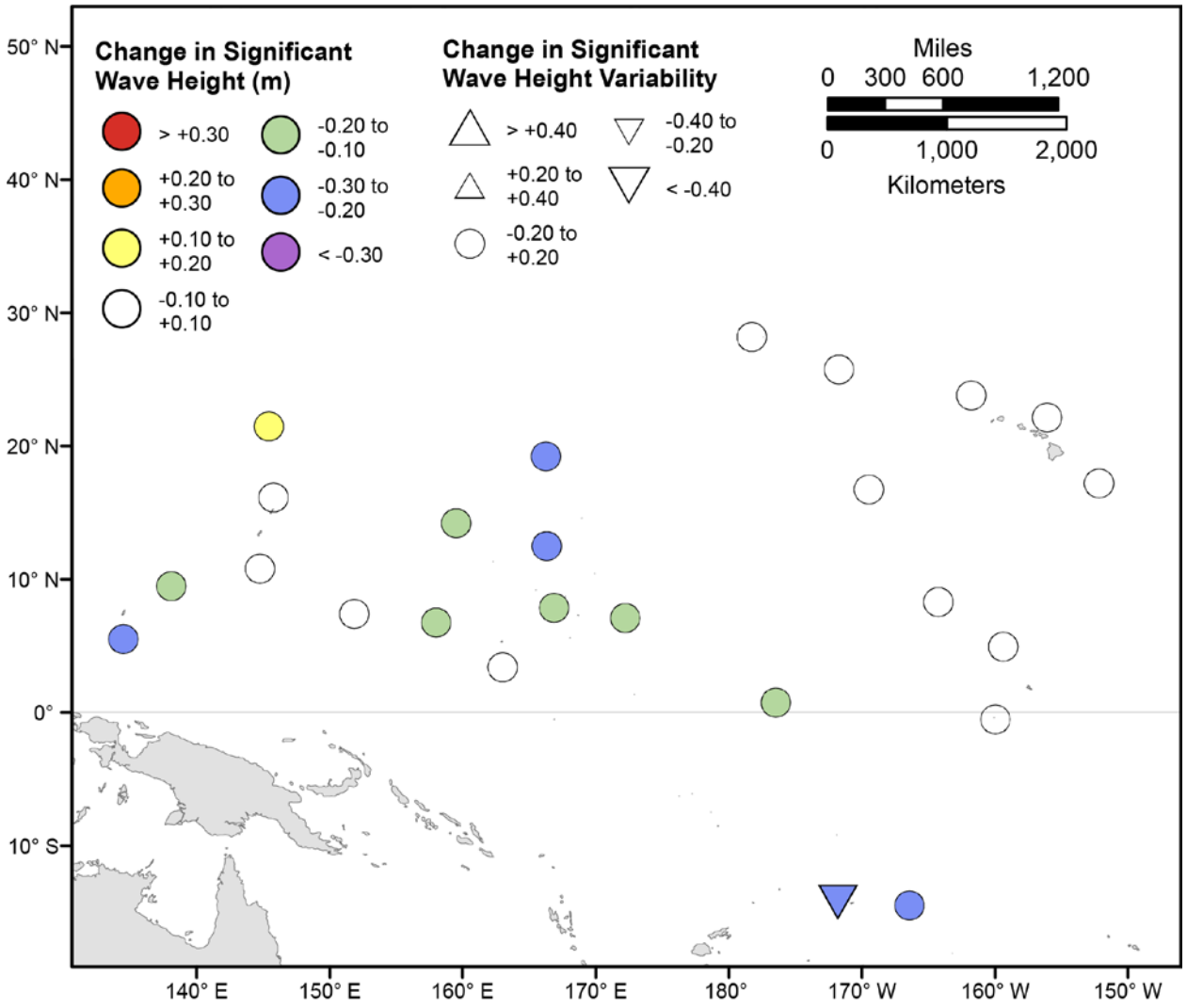

Figure 10. Map showing forecasted differences in the mean of the top 5 percent of significant wave heights and variance in the top 5 percent of significant wave heights for the years 2026–2045 from hindcasted values during the December-February season under the RCP4.5 future climatic scenario. The colors correspond to the magnitude of change in modeled mean significant wave heights during 2026–2045 from those hindcasted for 1976–2005. The shapes correspond to the magnitude of change in modeled variance in significant wave height during 2026–2045 from those hindcasted for 1976–2005. Units are in meters.

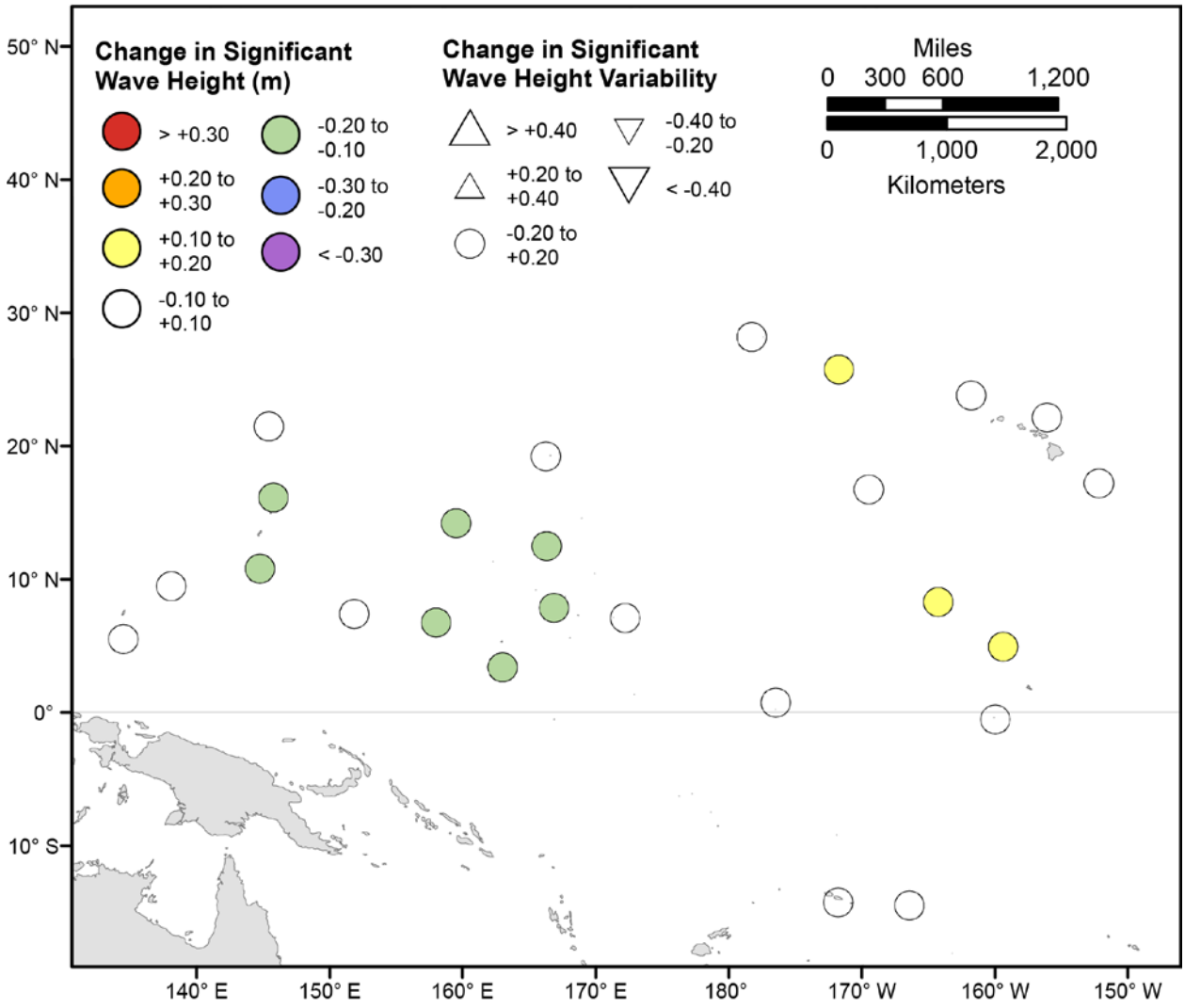

Figure 11. Map showing forecasted differences in the mean of the top 5 percent of significant wave heights and variance in the top 5 percent of significant wave heights for the years 2026–2045 from hindcasted values during the March-May season under the RCP4.5 future climatic scenario. The colors correspond to the magnitude of change in modeled mean significant wave heights during 2026–2045 from those hindcasted for 1976–2005. The shapes correspond to the magnitude of change in modeled variance in significant wave height during 2026–2045 from those hindcasted for 1976–2005. Units are in meters.

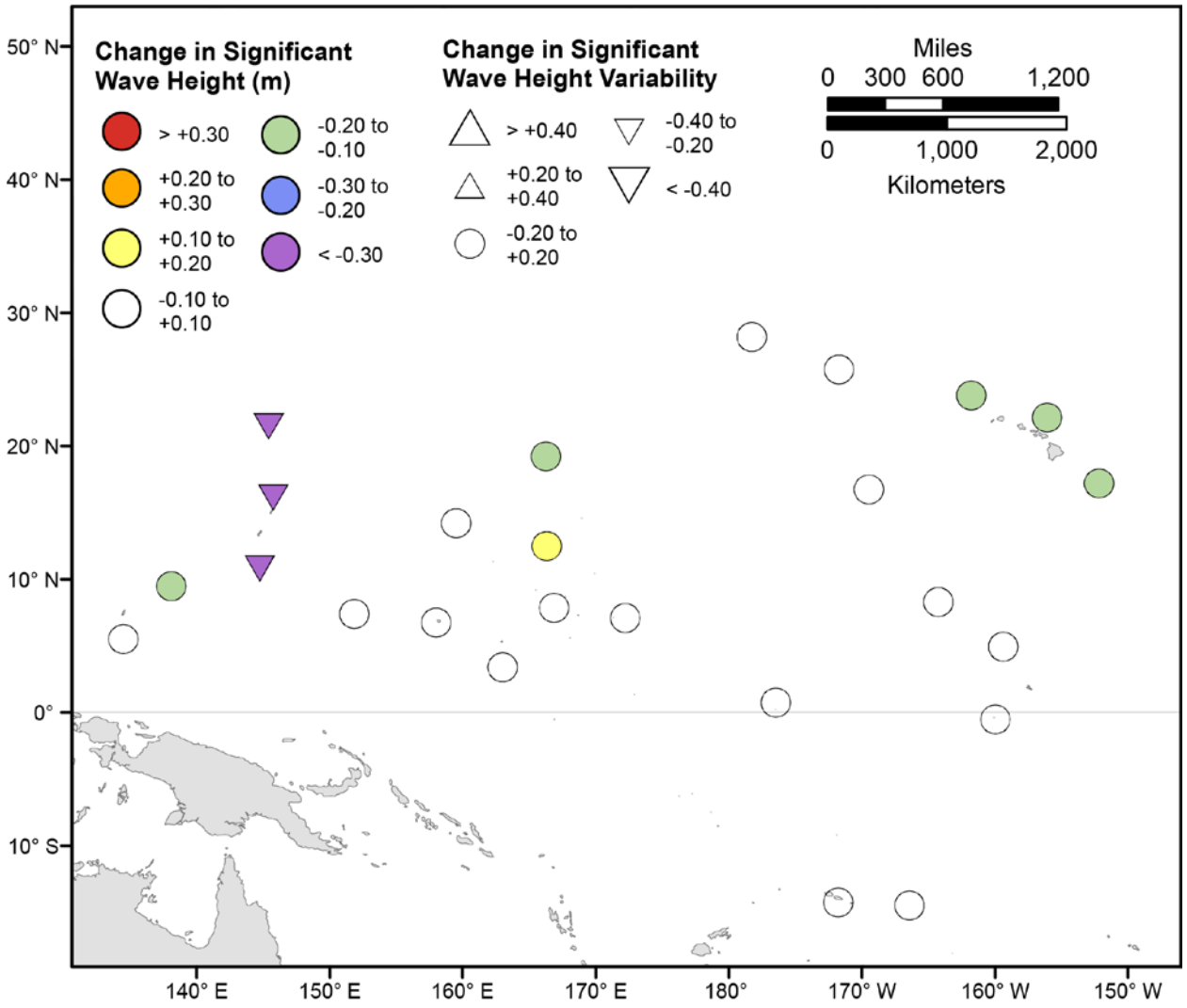

Figure 12. Map showing forecasted differences in the mean of the top 5 percent of significant wave heights and variance in the top 5 percent of significant wave heights for the years 2026–2045 from hindcasted values during the June-August season under the RCP4.5 future climatic scenario. The colors correspond to the magnitude of change in modeled mean significant wave heights during 2026–2045 from those hindcasted for 1976–2005. The shapes correspond to the magnitude of change in modeled variance in significant wave height during 2026–2045 from those hindcasted for 1976–2005. Units are in meters.

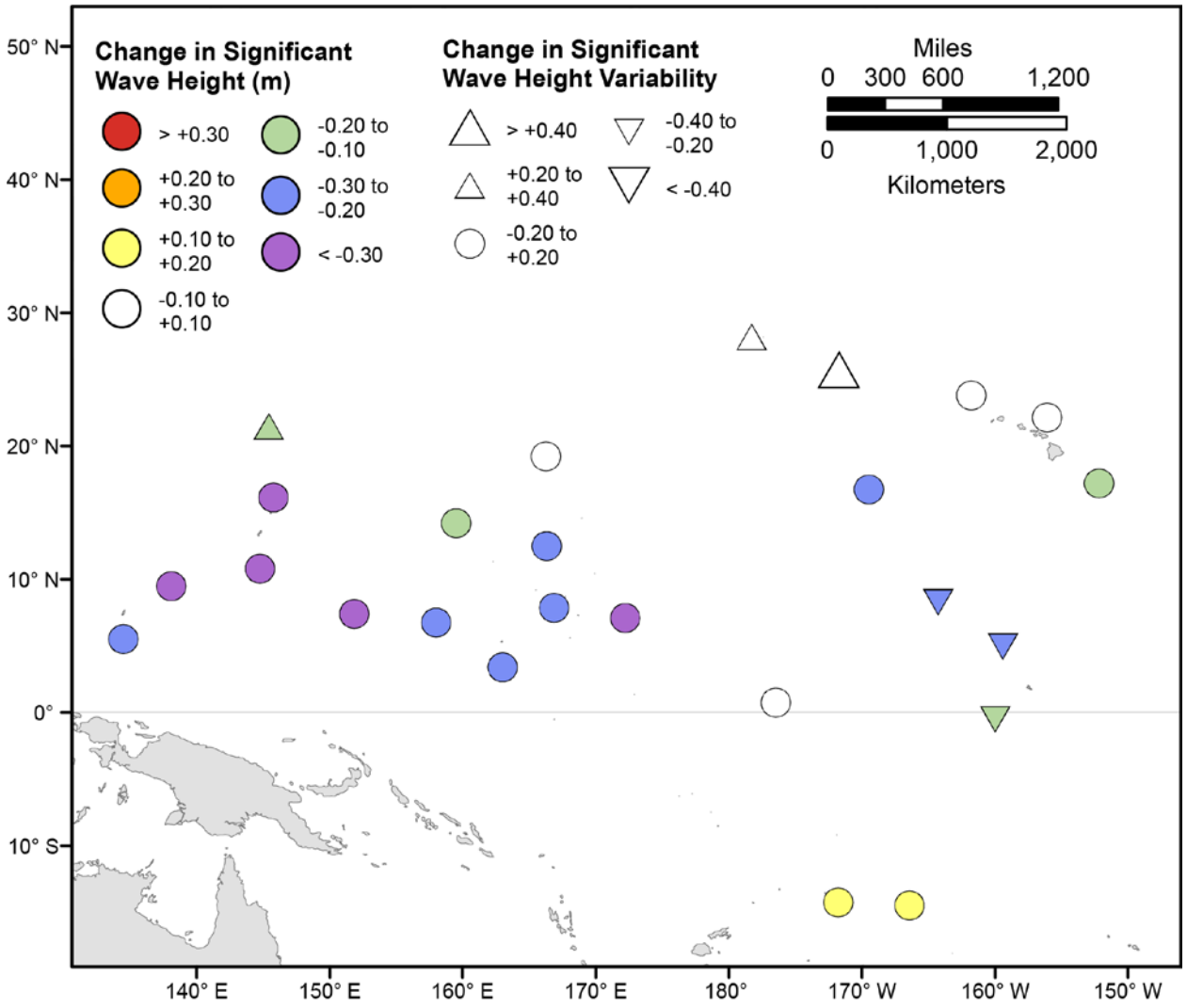

Figure 13. Map showing forecasted differences in the mean of the top 5 percent of significant wave heights and variance in the top 5 percent of significant wave heights for the years 2026–2045 from hindcasted values during the September-November season under the RCP4.5 future climatic scenario. The colors correspond to the magnitude of change in modeled mean significant wave heights during 2026–2045 from those hindcasted for 1976–2005. The shapes correspond to the magnitude of change in modeled variance in significant wave height during 2026–2045 from those hindcasted for 1976–2005. Units are in meters.

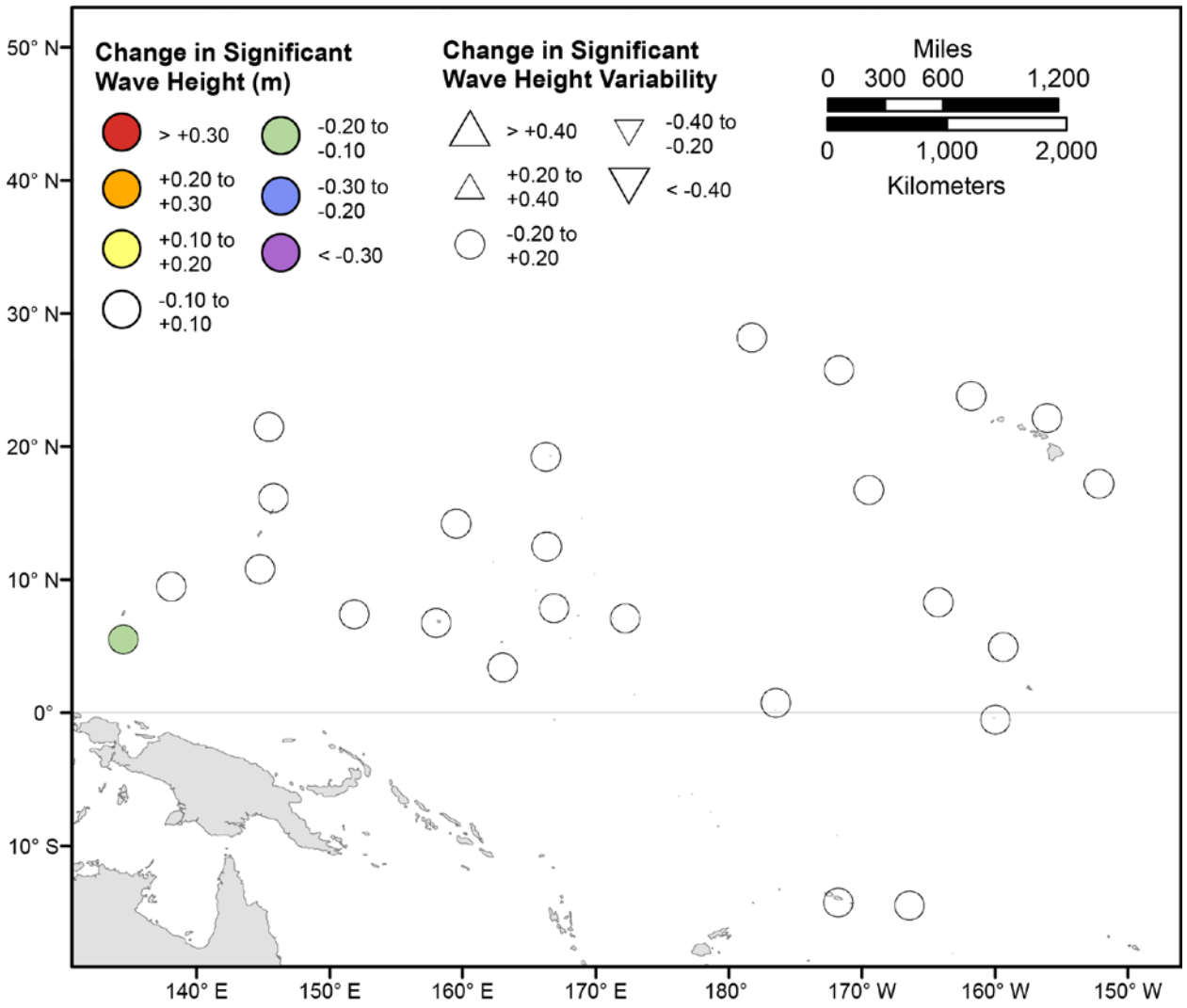

Figure 14. Map showing forecasted differences in mean significant wave height and variance in significant wave height for the years 2026–2045 from hindcasted values during the December-February season under the RCP8.5 future climatic scenario. The colors correspond to the magnitude of change in modeled mean significant wave heights during 2026–2045 from those hindcasted for 1976–2005. The shapes correspond to the magnitude of change in modeled variance in significant wave height during 2026–2045 from those hindcasted for 1976–2005. Units are in meters.

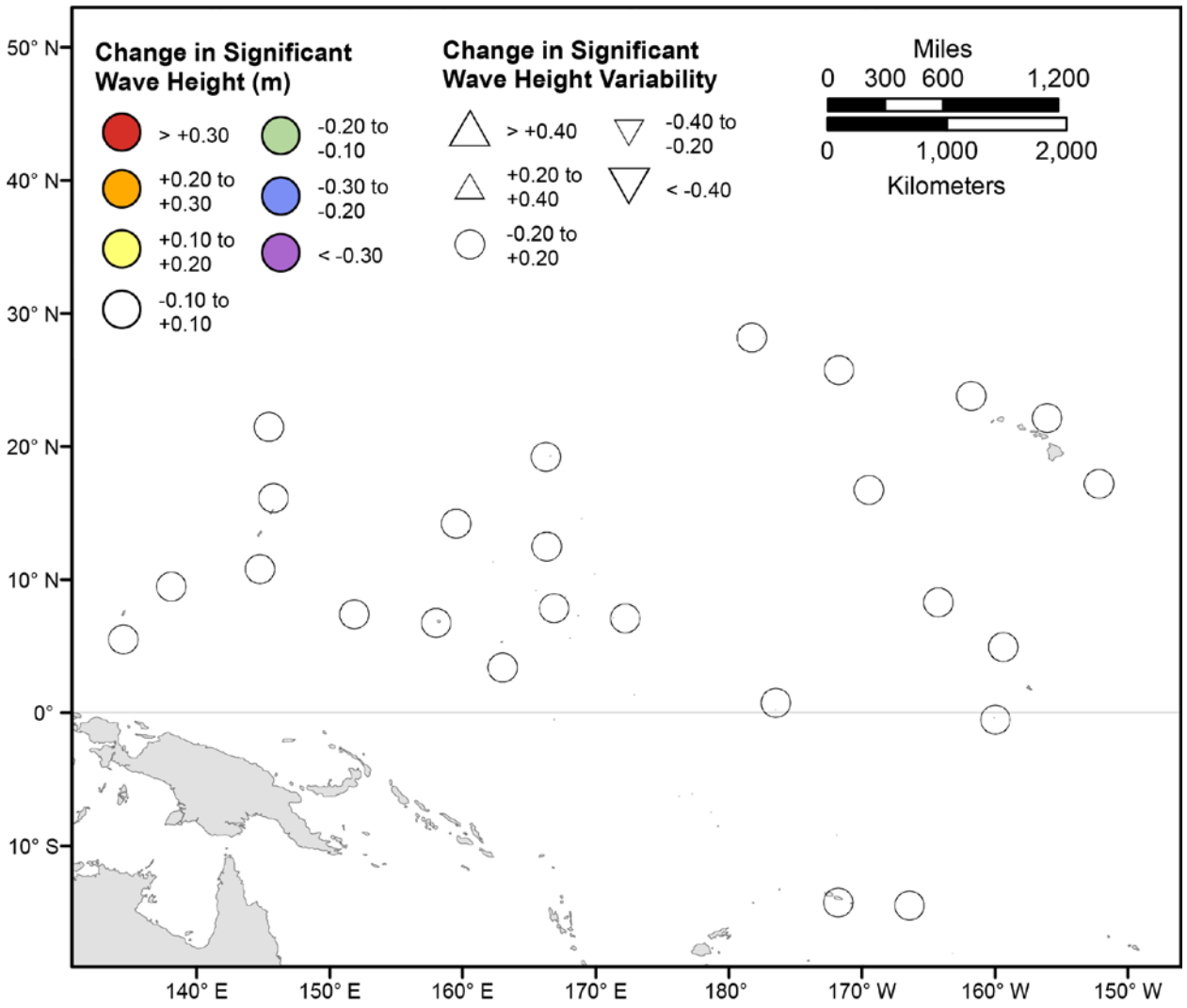

Figure 15. Map showing forecasted differences in mean significant wave height and variance in significant wave height for the years 2026–2045 from hindcasted values during the March-May season under the RCP8.5 future climatic scenario. The colors correspond to the magnitude of change in modeled mean significant wave heights during 2026–2045 from those hindcasted for 1976–2005. The shapes correspond to the magnitude of change in modeled variance in significant wave height during 2026–2045 from those hindcasted for 1976–2005. Units are in meters.

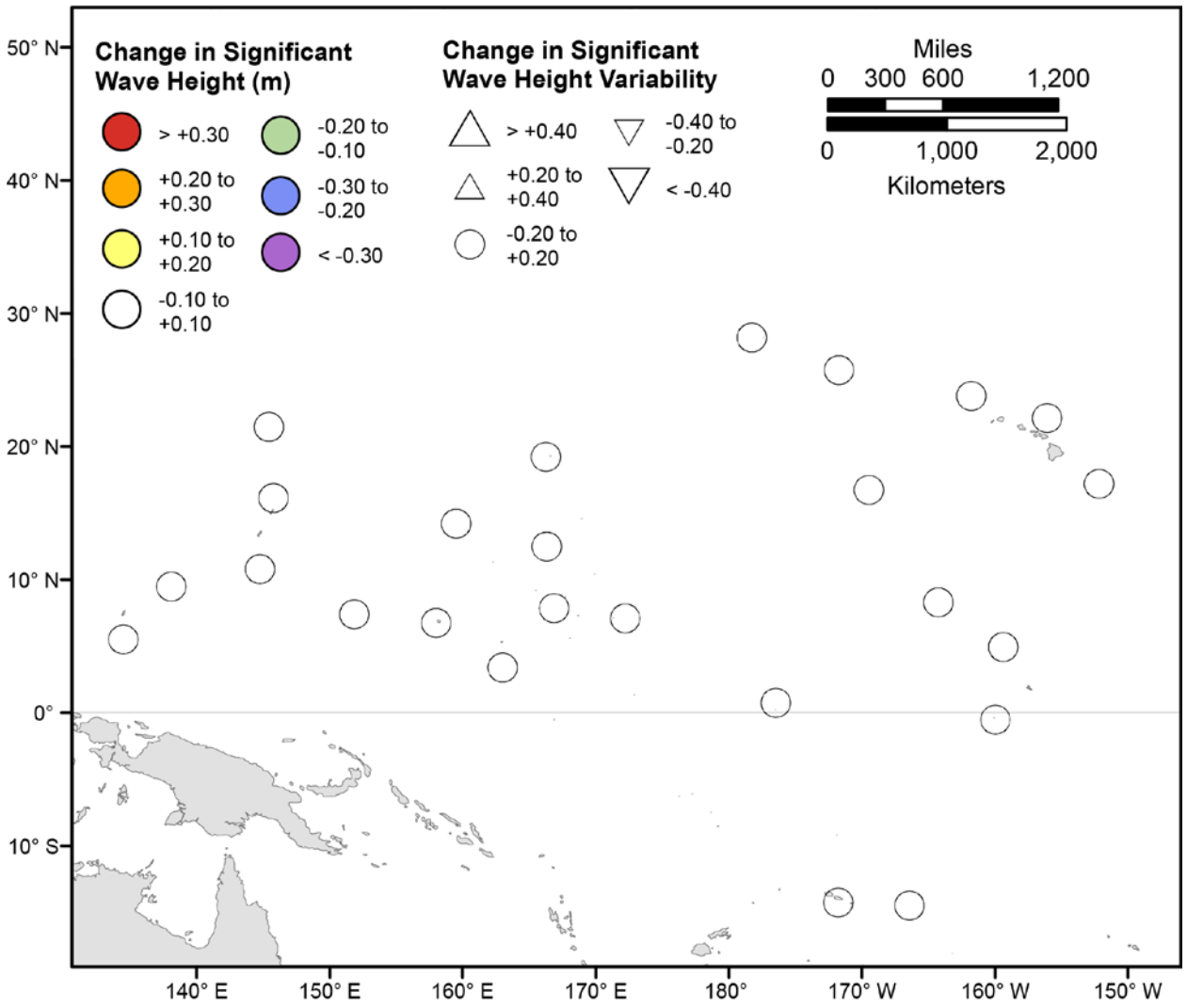

Figure 16. Map showing forecasted differences in mean significant wave height and variance in significant wave height for the years 2026–2045 from hindcasted values during the June-August season under the RCP8.5 future climatic scenario. The colors correspond to the magnitude of change in modeled mean significant wave heights during 2026–2045 from those hindcasted for 1976–2005. The shapes correspond to the magnitude of change in modeled variance in significant wave height during 2026–2045 from those hindcasted for 1976–2005. Units are in meters.

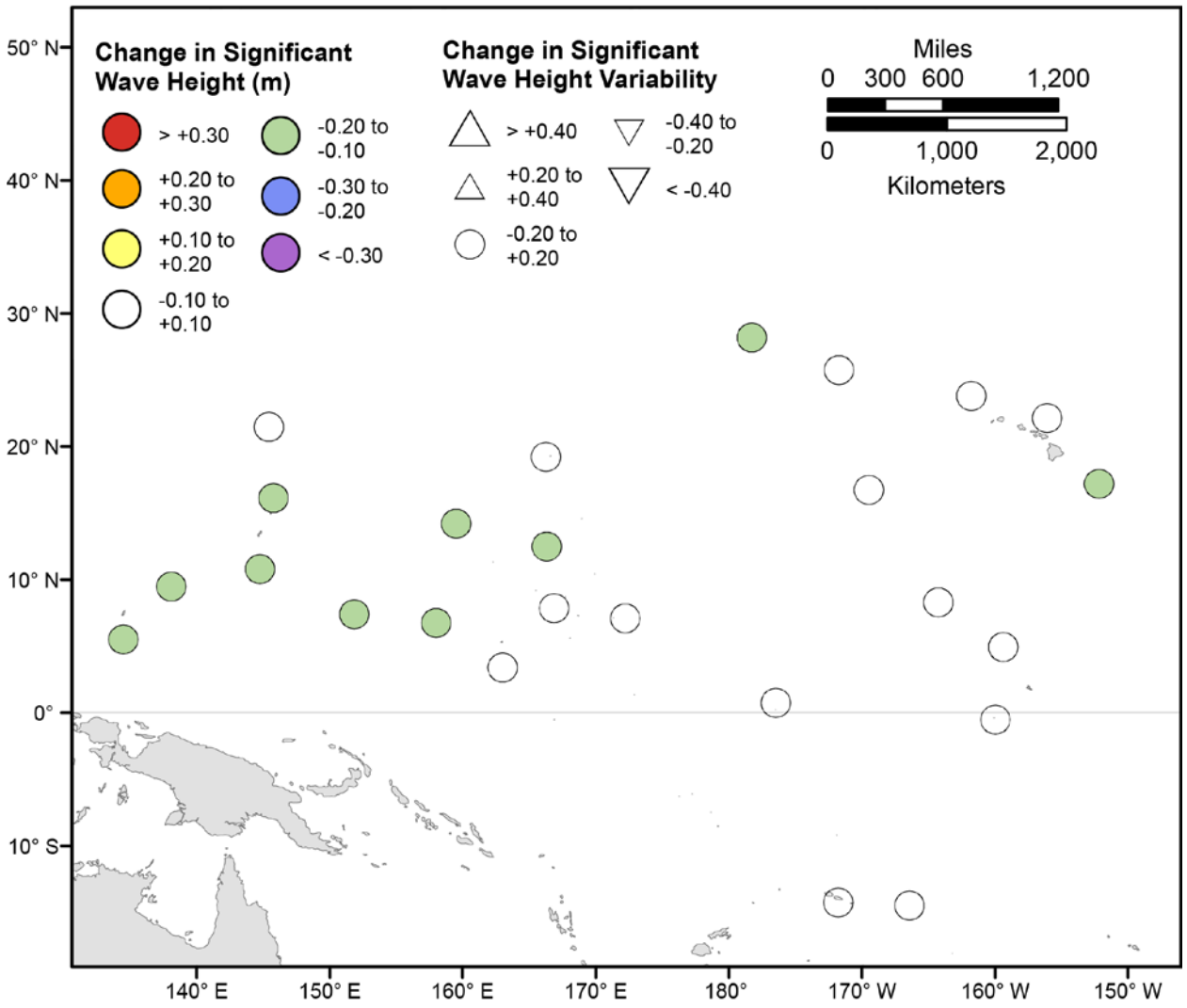

Figure 17. Map showing forecasted differences in mean significant wave height and variance in significant wave height for the years 2026–2045 from hindcasted values during the September-November season under the RCP8.5 future climatic scenario. The colors correspond to the magnitude of change in modeled mean significant wave heights during 2026–2045 from those hindcasted for 1976–2005. The shapes correspond to the magnitude of change in modeled variance in significant wave height during 2026–2045 from those hindcasted for 1976–2005. Units are in meters.

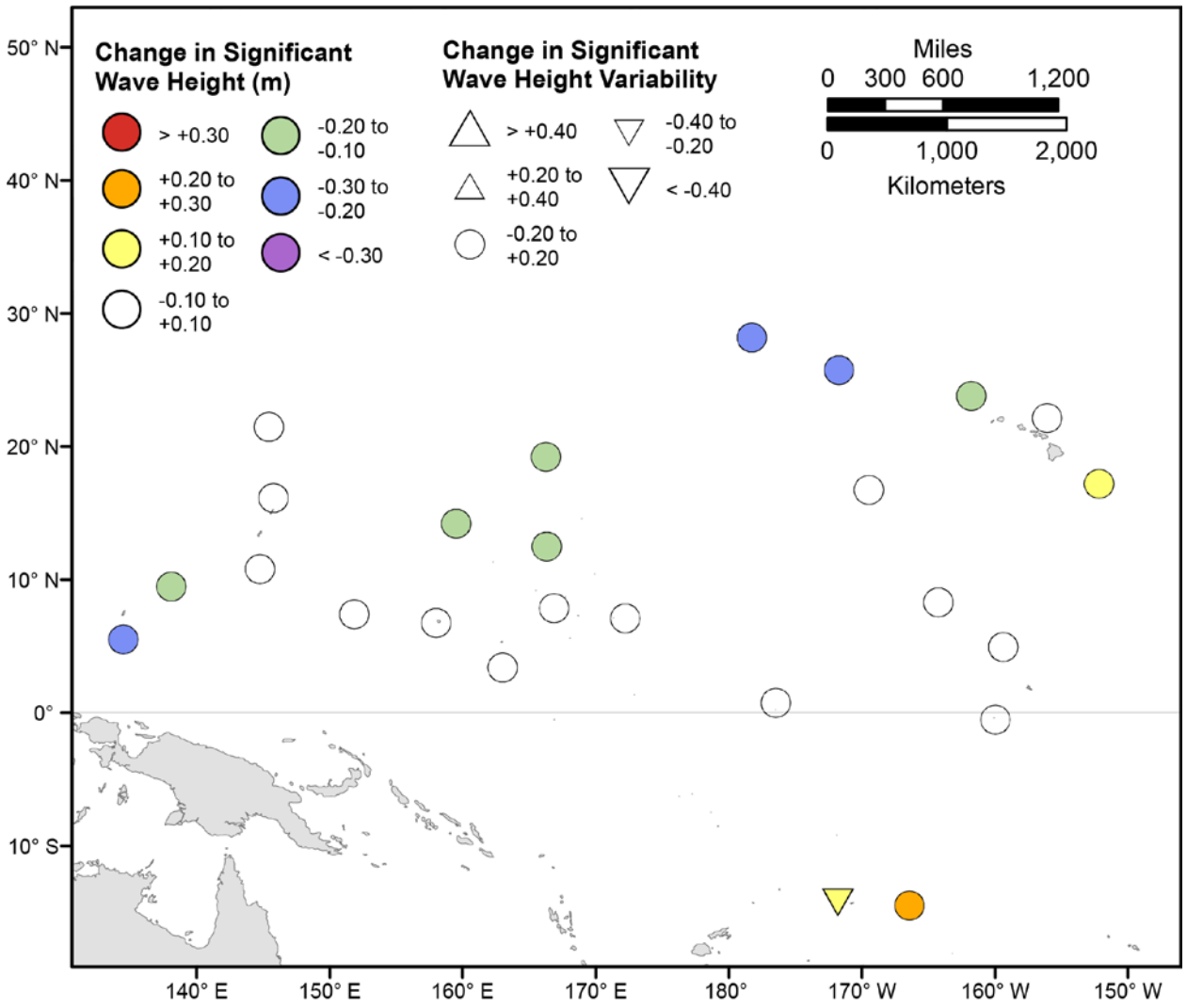

Figure 18. Map showing forecasted differences in the mean of the top 5 percent of significant wave heights and variance in the top 5 percent of significant wave heights for the years 2026–2045 from hindcasted values during the December-February season under the RCP8.5 future climatic scenario. The colors correspond to the magnitude of change in modeled mean significant wave heights during 2026–2045 from those hindcasted for 1976–2005. The shapes correspond to the magnitude of change in modeled variance in significant wave height during 2026–2045 from those hindcasted for 1976–2005. Units are in meters.

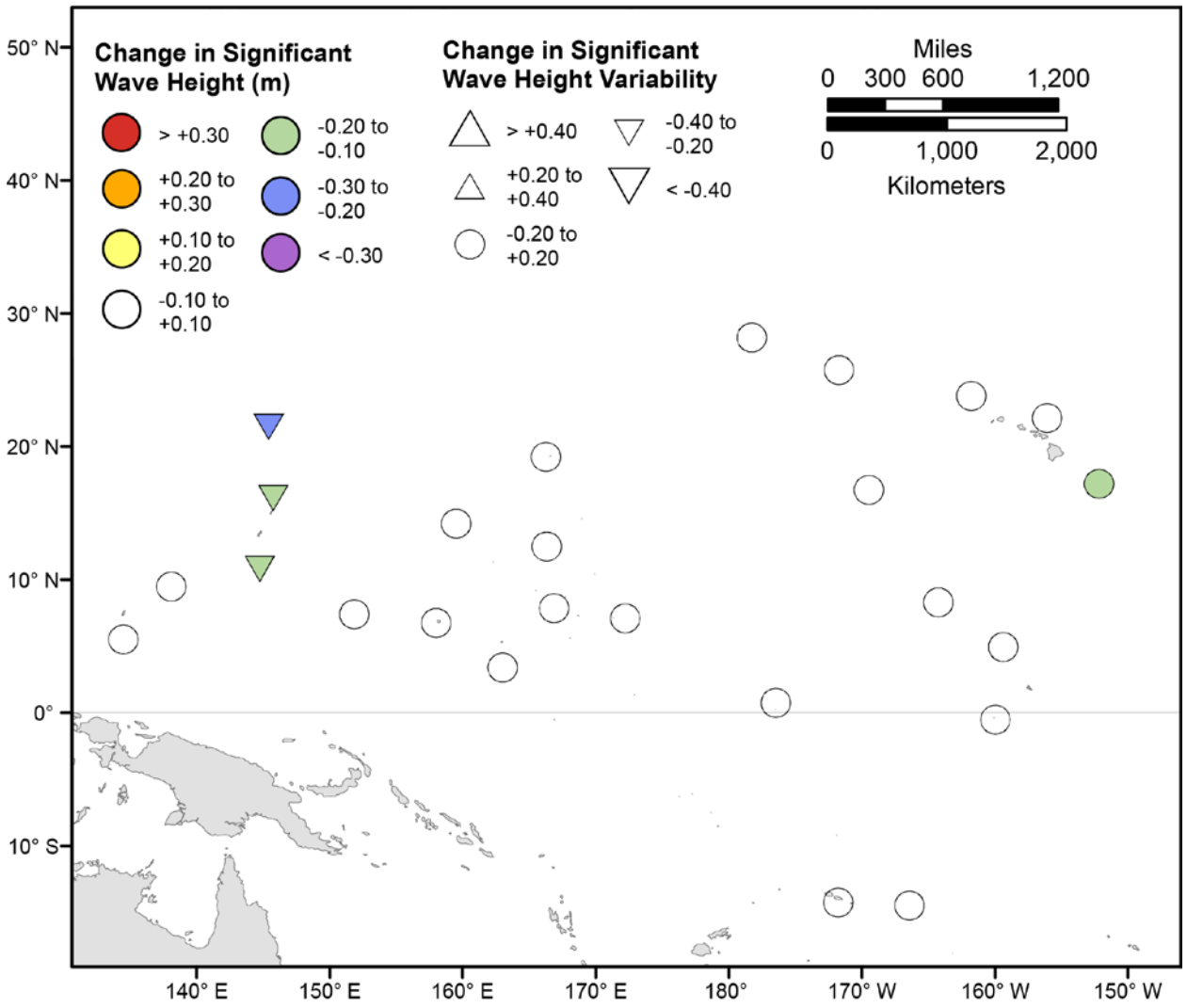

Figure 19. Map showing forecasted differences in the mean of the top 5 percent of significant wave heights and variance in the top 5 percent of significant wave heights for the years 2026–2045 from hindcasted values during the March-May season under the RCP8.5 future climatic scenario. The colors correspond to the magnitude of change in modeled mean significant wave heights during 2026–2045 from those hindcasted for 1976–2005. The shapes correspond to the magnitude of change in modeled variance in significant wave height during 2026–2045 from those hindcasted for 1976–2005. Units are in meters.

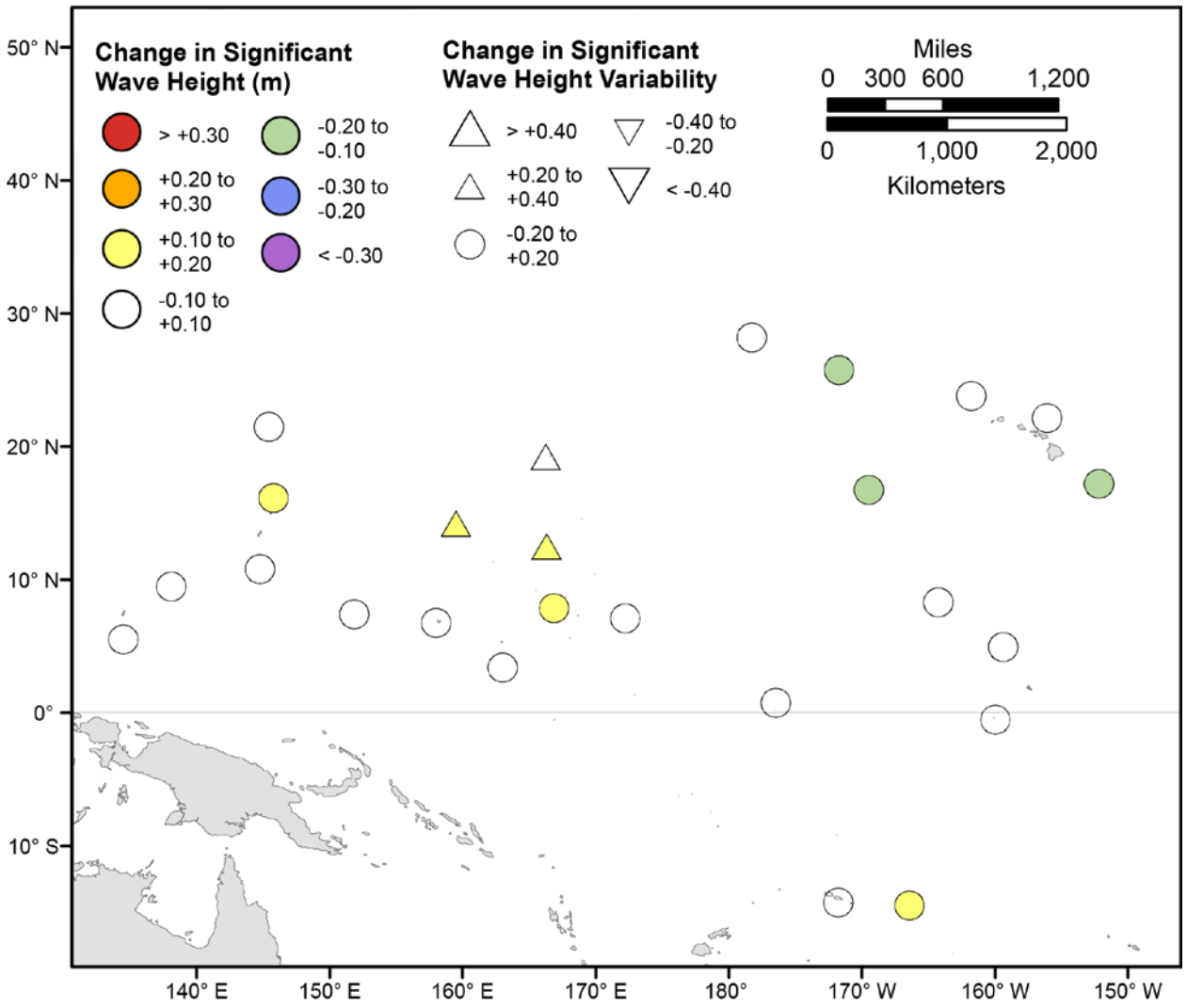

Figure 20. Map showing forecasted differences in the mean of the top 5 percent of significant wave heights and variance in the top 5 percent of significant wave heights for the years 2026–2045 from hindcasted values during the June-August season under the RCP8.5 future climatic scenario. The colors correspond to the magnitude of change in modeled mean significant wave heights during 2026–2045 from those hindcasted for 1976–2005. The shapes correspond to the magnitude of change in modeled variance in significant wave height during 2026–2045 from those hindcasted for 1976–2005. Units are in meters.

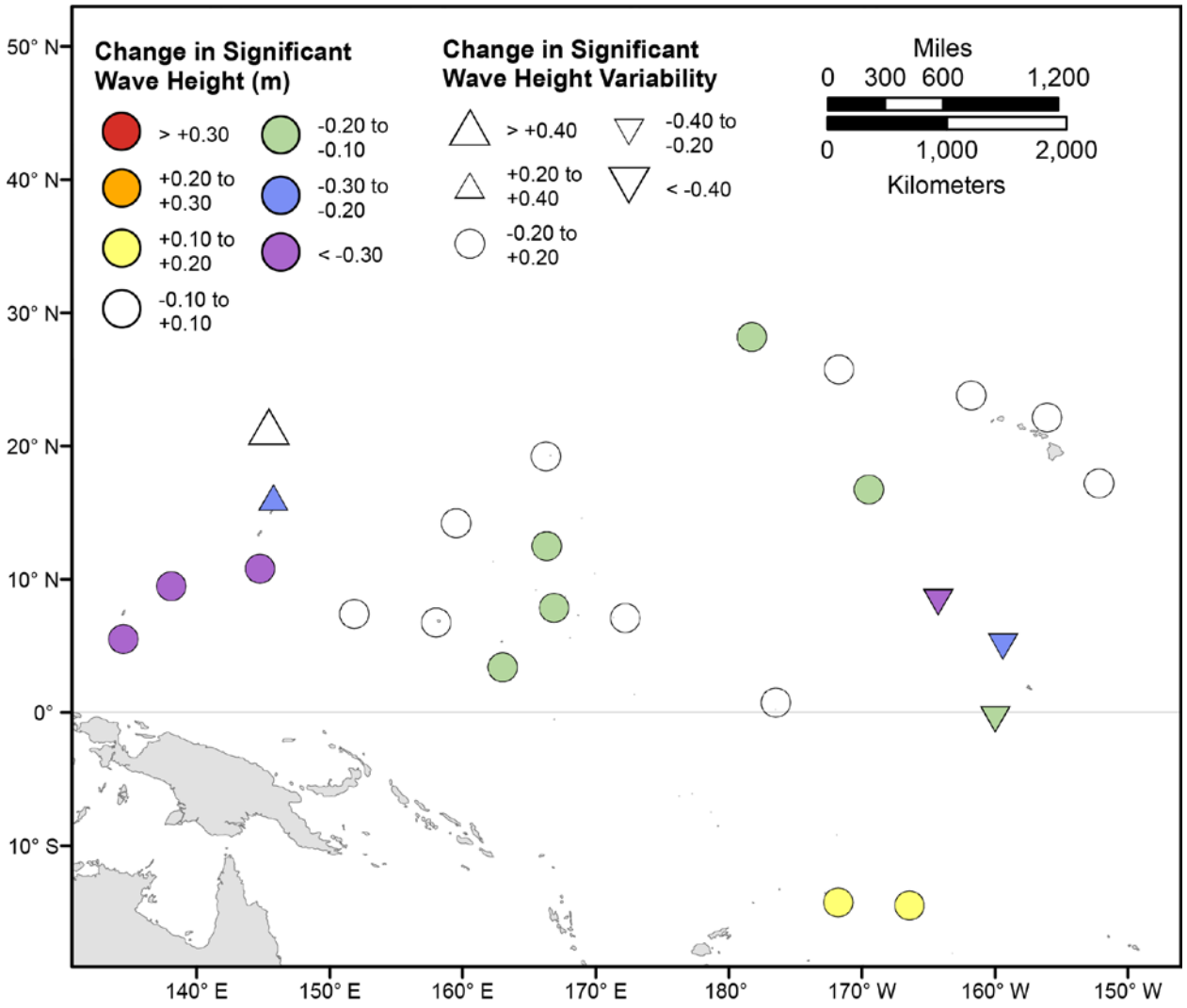

Figure 21. Map showing forecasted differences in the mean of the top 5 percent of significant wave heights and variance in the top 5 percent of significant wave heights for the years 2026–2045 from hindcasted values during the September-November season under the RCP8.5 future climatic scenario. The colors correspond to the magnitude of change in modeled mean significant wave heights during 2026–2045 from those hindcasted for 1976–2005. The shapes correspond to the magnitude of change in modeled variance in significant wave height during 2026–2045 from those hindcasted for 1976–2005. Units are in meters.

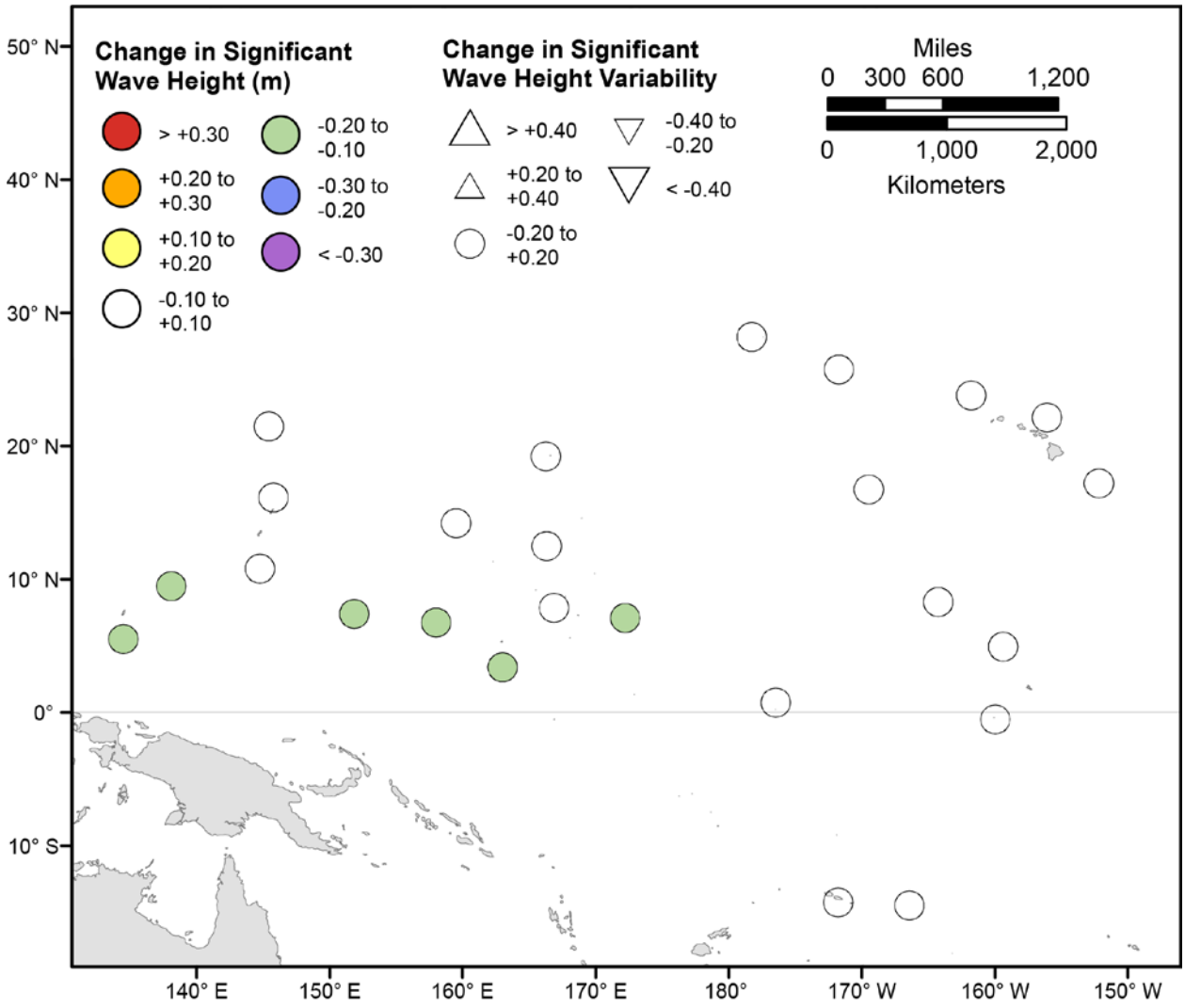

Figure 22. Map showing forecasted differences in mean significant wave height and variance in significant wave height for the years 2081–2100 from hindcasted values during the December-February season under the RCP4.5 future climatic scenario. The colors correspond to the magnitude of change in modeled mean significant wave heights during 2081–2100 from those hindcasted for 1976–2005. The shapes correspond to the magnitude of change in modeled variance in significant wave height during 2081–2100 from those hindcasted for 1976–2005. Units are in meters.

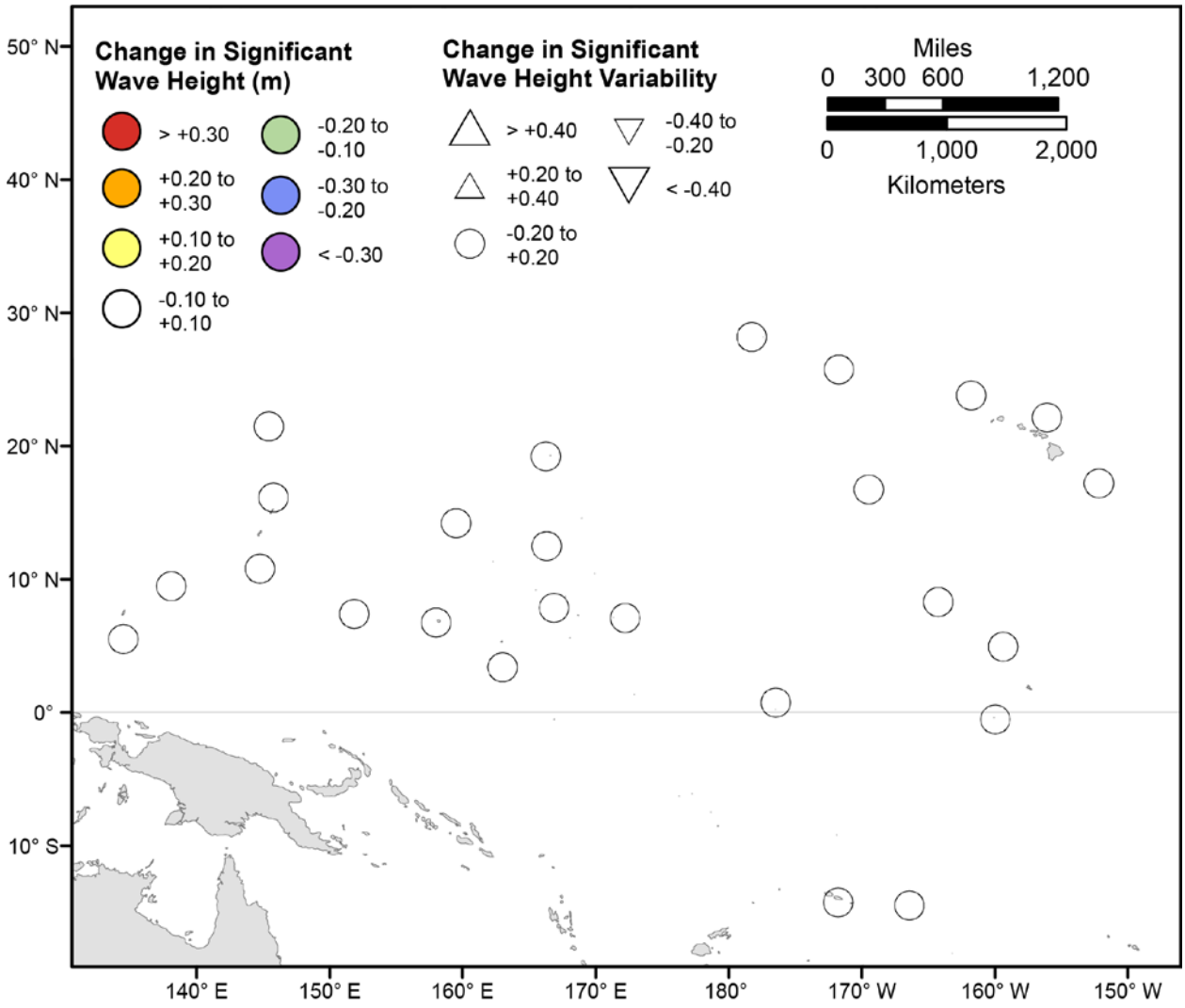

Figure 23. Map showing forecasted differences in mean significant wave height and variance in significant wave height for the years 2081–2100 from hindcasted values during the March-May season under the RCP4.5 future climatic scenario. The colors correspond to the magnitude of change in modeled mean significant wave heights during 2081–2100 from those hindcasted for 1976–2005. The shapes correspond to the magnitude of change in modeled variance in significant wave height during 2081–2100 from those hindcasted for 1976–2005. Units are in meters.

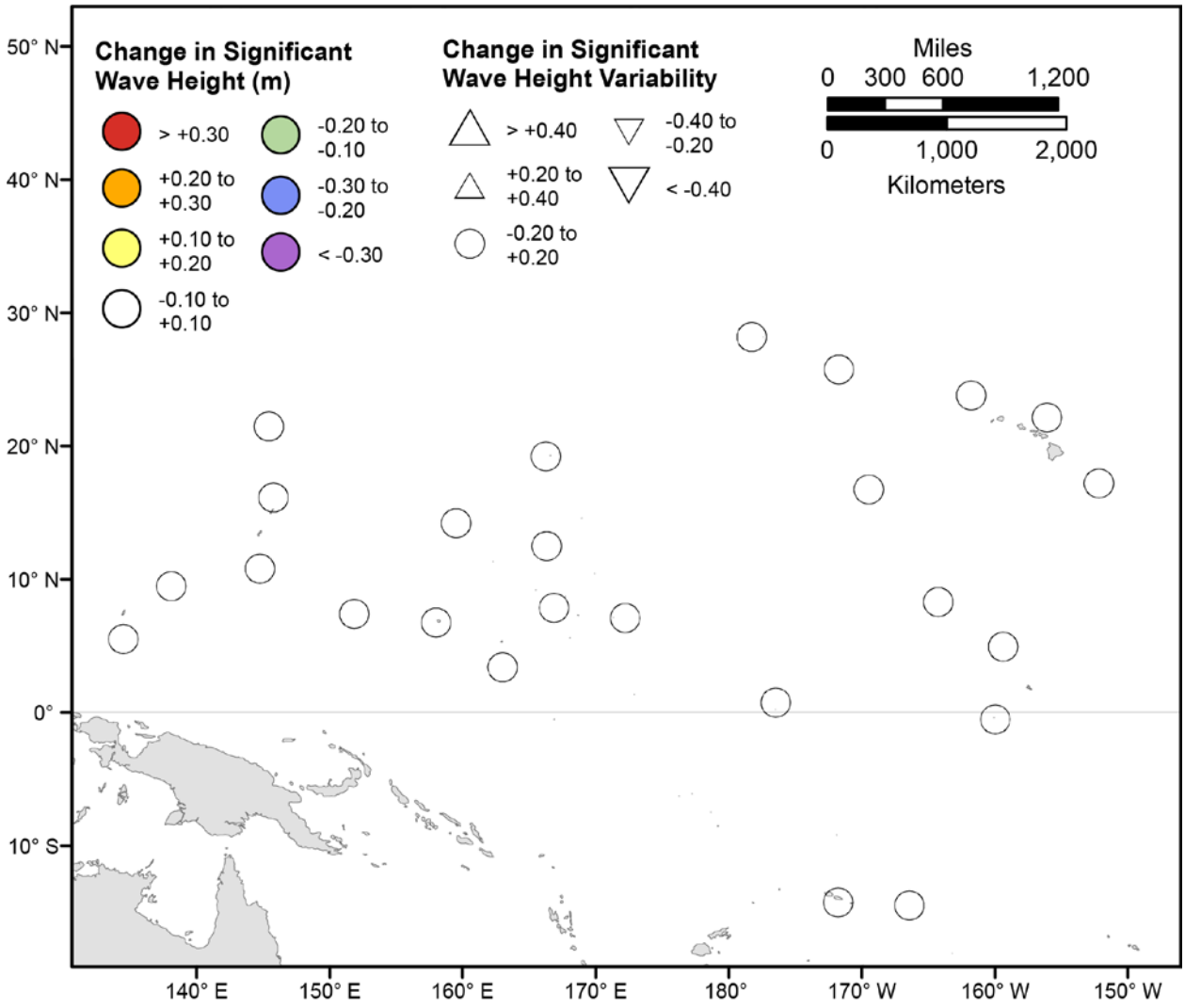

Figure 24. Map showing forecasted differences in mean significant wave height and variance in significant wave height for the years 2081–2100 from hindcasted values during the June-August season under the RCP4.5 future climatic scenario. The colors correspond to the magnitude of change in modeled mean significant wave heights during 2081–2100 from those hindcasted for 1976–2005. The shapes correspond to the magnitude of change in modeled variance in significant wave height during 2081–2100 from those hindcasted for 1976–2005. Units are in meters.

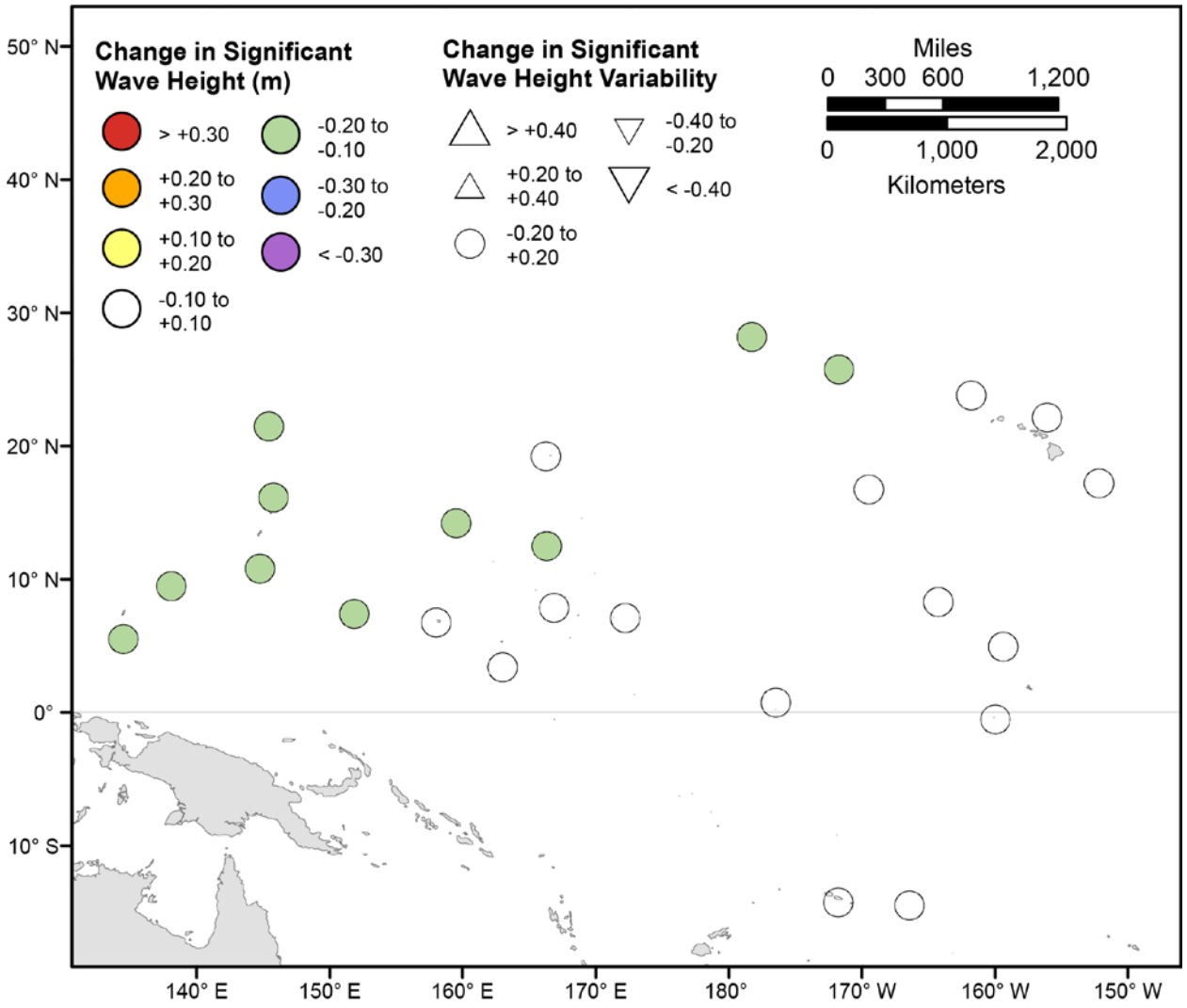

Figure 25. Map showing forecasted differences in mean significant wave height and variance in significant wave height for the years 2081–2100 from hindcasted values during the September-November season under the RCP4.5 future climatic scenario. The colors correspond to the magnitude of change in modeled mean significant wave heights during 2081–2100 from those hindcasted for 1976–2005. The shapes correspond to the magnitude of change in modeled variance in significant wave height during 2081–2100 from those hindcasted for 1976–2005. Units are in meters.

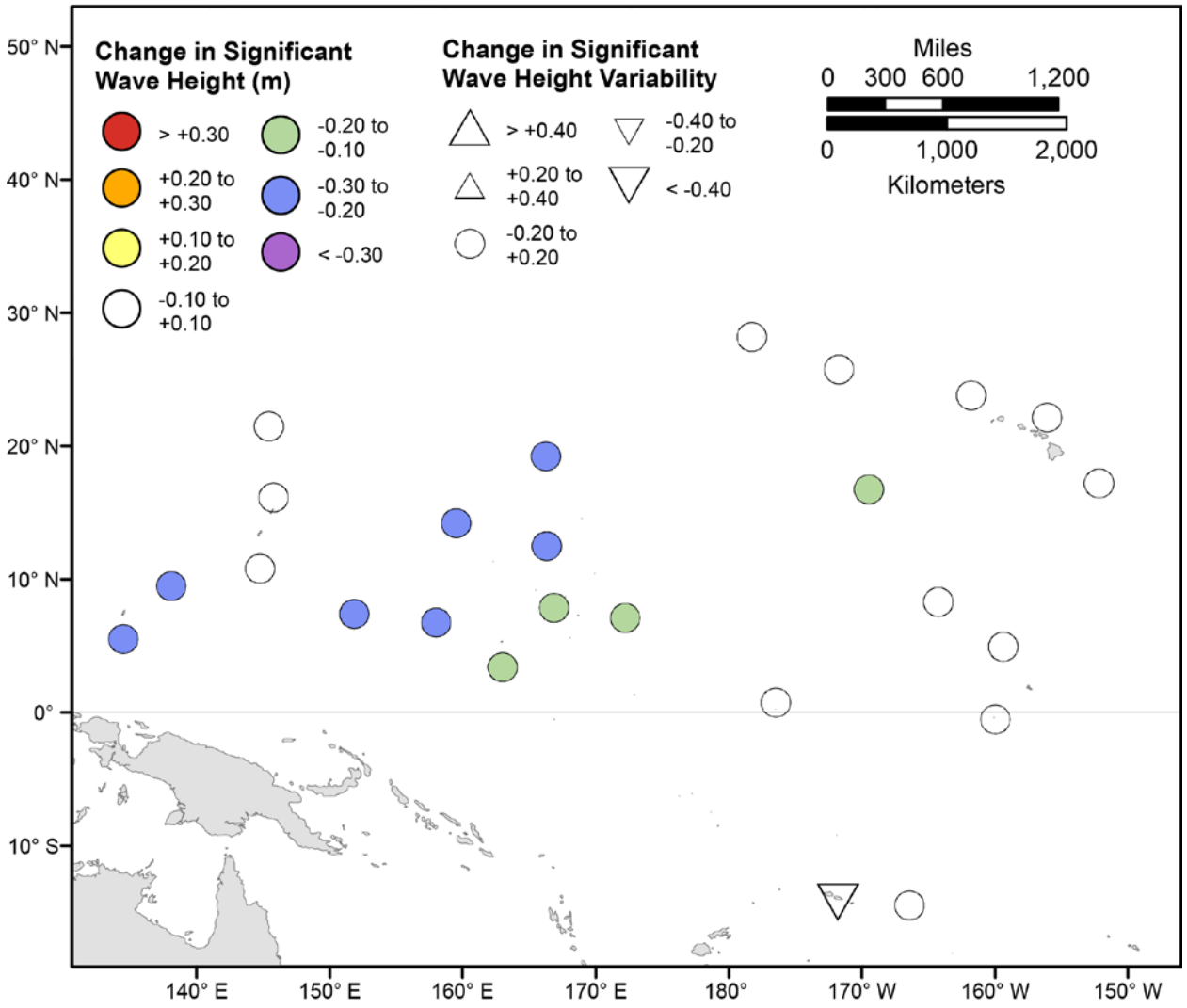

Figure 26. Map showing forecasted differences in the mean of the top 5 percent of significant wave heights and variance in the top 5 percent of significant wave heights for the years 2081–2100 from hindcasted values during the December-February season under the RCP4.5 future climatic scenario. The colors correspond to the magnitude of change in modeled mean significant wave heights during 2081–2100 from those hindcasted for 1976–2005. The shapes correspond to the magnitude of change in modeled variance in significant wave height during 2081–2100 from those hindcasted for 1976–2005. Units are in meters.

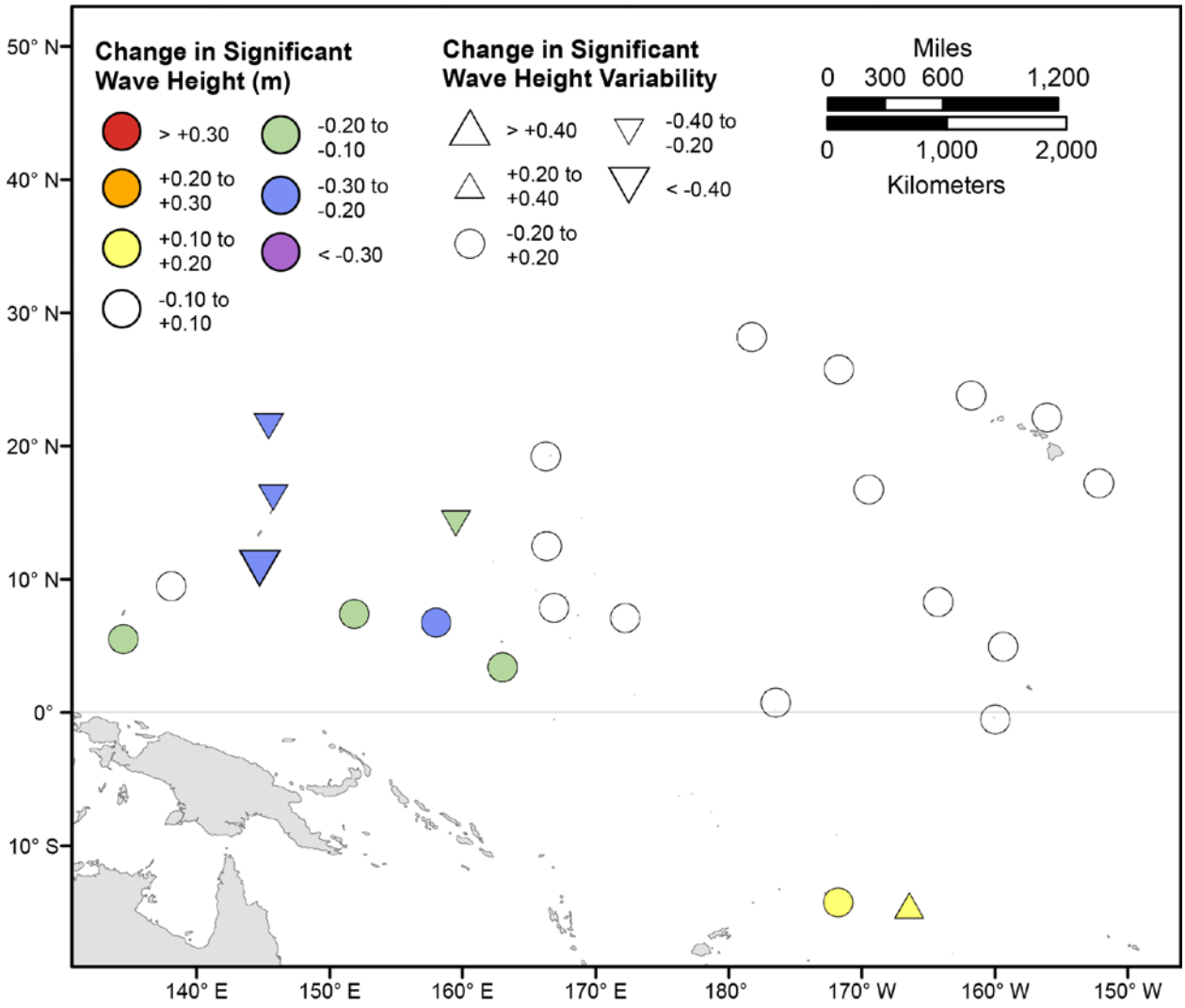

Figure 27. Map showing forecasted differences in the mean of the top 5 percent of significant wave heights and variance in the top 5 percent of significant wave heights for the years 2081–2100 from hindcasted values during the March-May season under the RCP4.5 future climatic scenario. The colors correspond to the magnitude of change in modeled mean significant wave heights during 2081–2100 from those hindcasted for 1976–2005. The shapes correspond to the magnitude of change in modeled variance in significant wave height during 2081–2100 from those hindcasted for 1976–2005. Units are in meters.

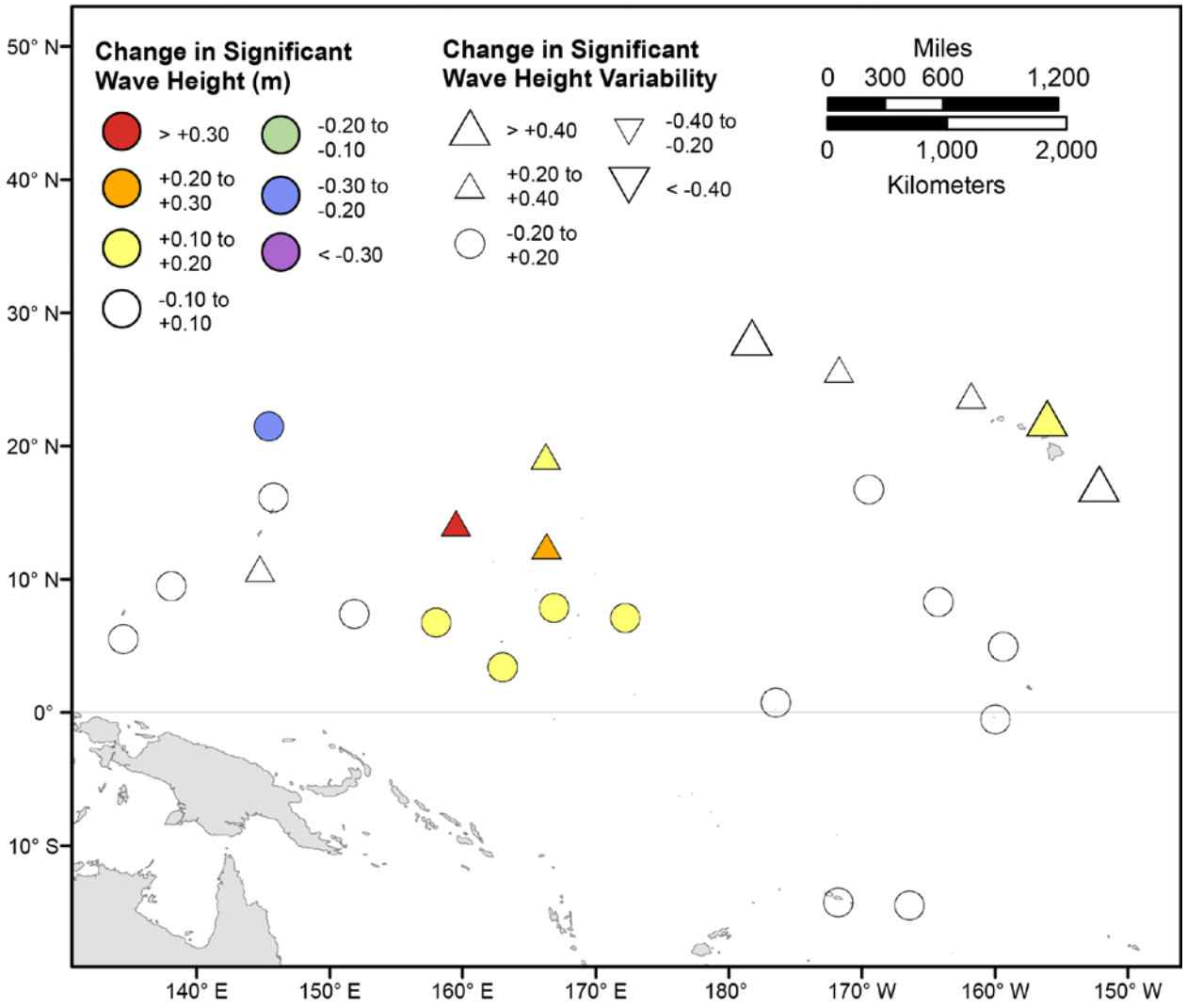

Figure 28. Map showing forecasted differences in the mean of the top 5 percent of significant wave heights and variance in the top 5 percent of significant wave heights for the years 2081–2100 from hindcasted values during the June-August season under the RCP4.5 future climatic scenario. The colors correspond to the magnitude of change in modeled mean significant wave heights during 2081–2100 from those hindcasted for 1976–2005. The shapes correspond to the magnitude of change in modeled variance in significant wave height during 2081–2100 from those hindcasted for 1976–2005. Units are in meters.

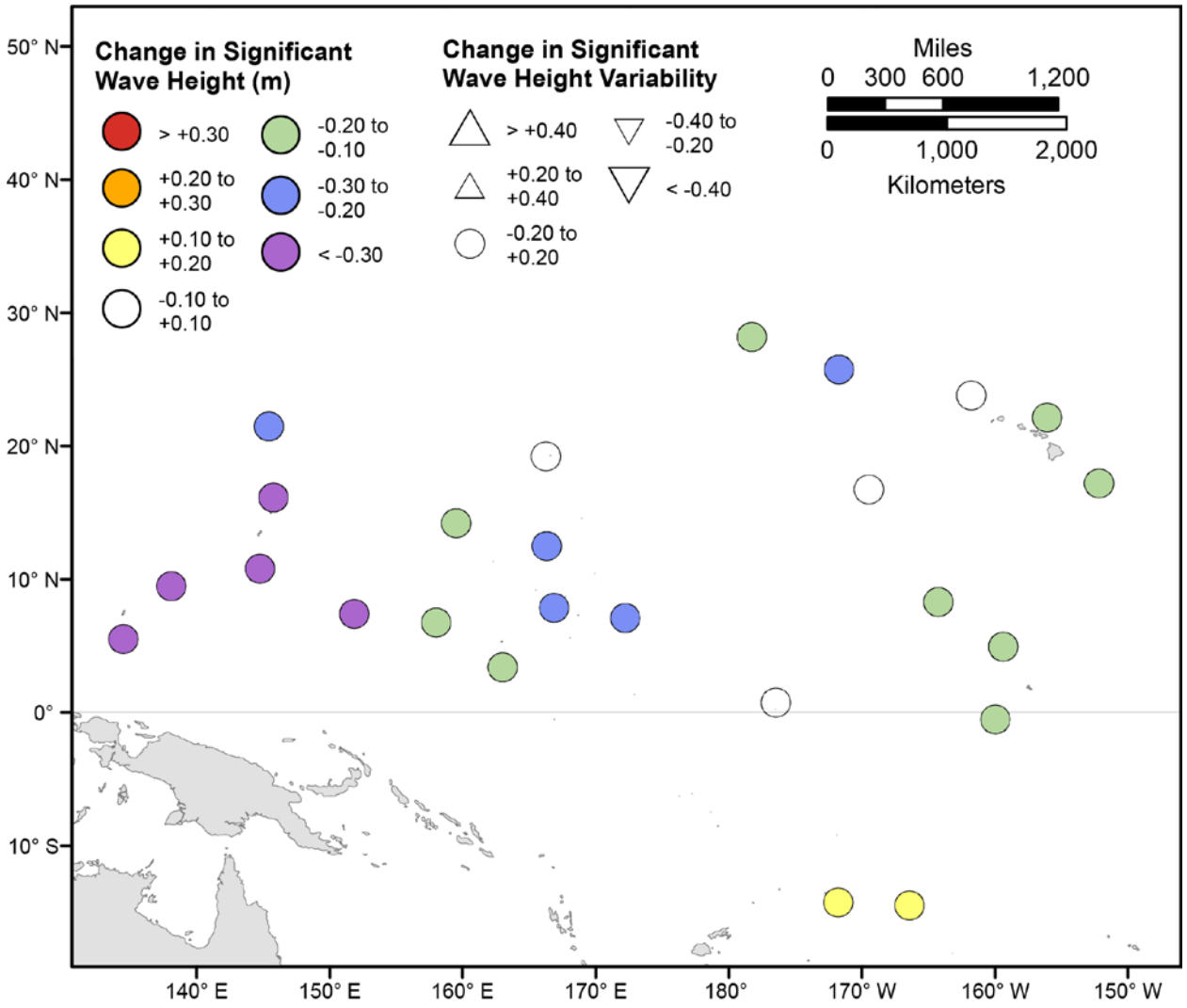

Figure 29. Map showing forecasted differences in the mean of the top 5 percent of significant wave heights and variance in the top 5 percent of significant wave heights for the years 2081–2100 from hindcasted values during the September-November season under the RCP4.5 future climatic scenario. The colors correspond to the magnitude of change in modeled mean significant wave heights during 2081–2100 from those hindcasted for 1976–2005. The shapes correspond to the magnitude of change in modeled variance in significant wave height during 2081–2100 from those hindcasted for 1976–2005. Units are in meters.

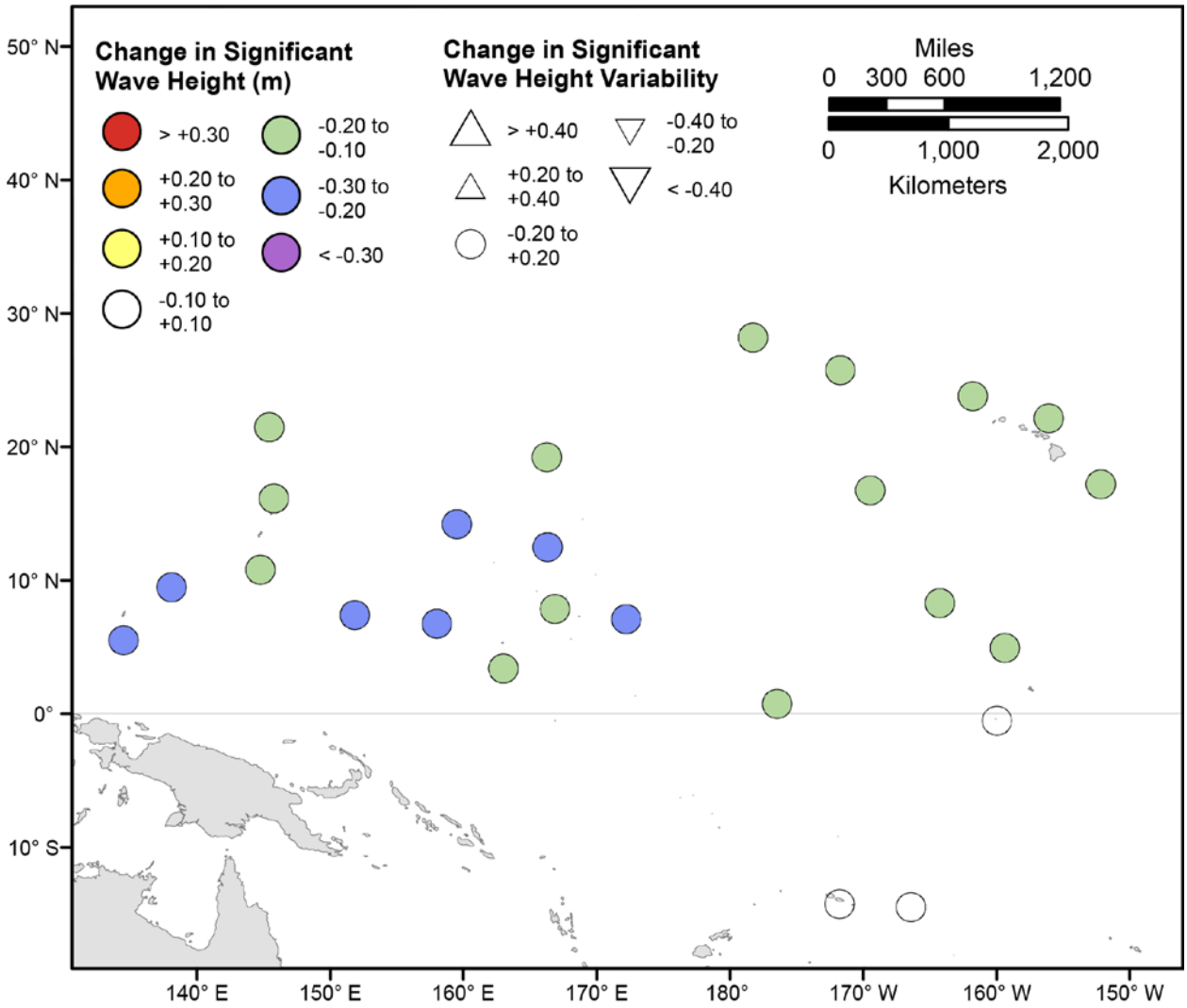

Figure 30. Map showing forecasted differences in mean significant wave height and variance in significant wave height for the years 2081–2100 from hindcasted values during the December-February season under the RCP8.5 future climatic scenario. The colors correspond to the magnitude of change in modeled mean significant wave heights during 2081–2100 from those hindcasted for 1976–2005. The shapes correspond to the magnitude of change in modeled variance in significant wave height during 2081–2100 from those hindcasted for 1976–2005. Units are in meters.

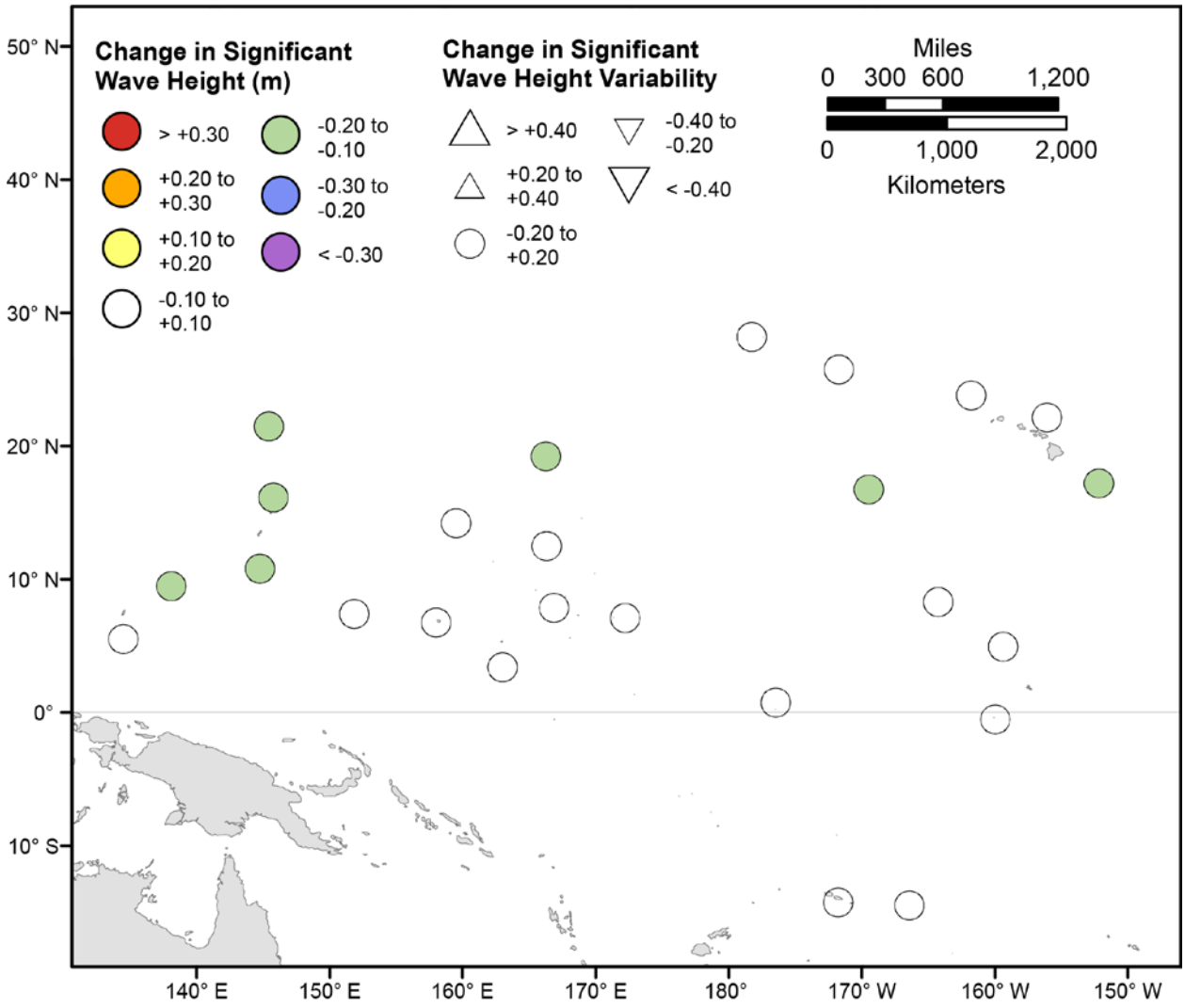

Figure 31. Map showing forecasted differences in mean significant wave height and variance in significant wave height for the years 2081–2100 from hindcasted values during the March-May season under the RCP8.5 future climatic scenario. The colors correspond to the magnitude of change in modeled mean significant wave heights during 2081–2100 from those hindcasted for 1976–2005. The shapes correspond to the magnitude of change in modeled variance in significant wave height during 2081–2100 from those hindcasted for 1976–2005. Units are in meters.

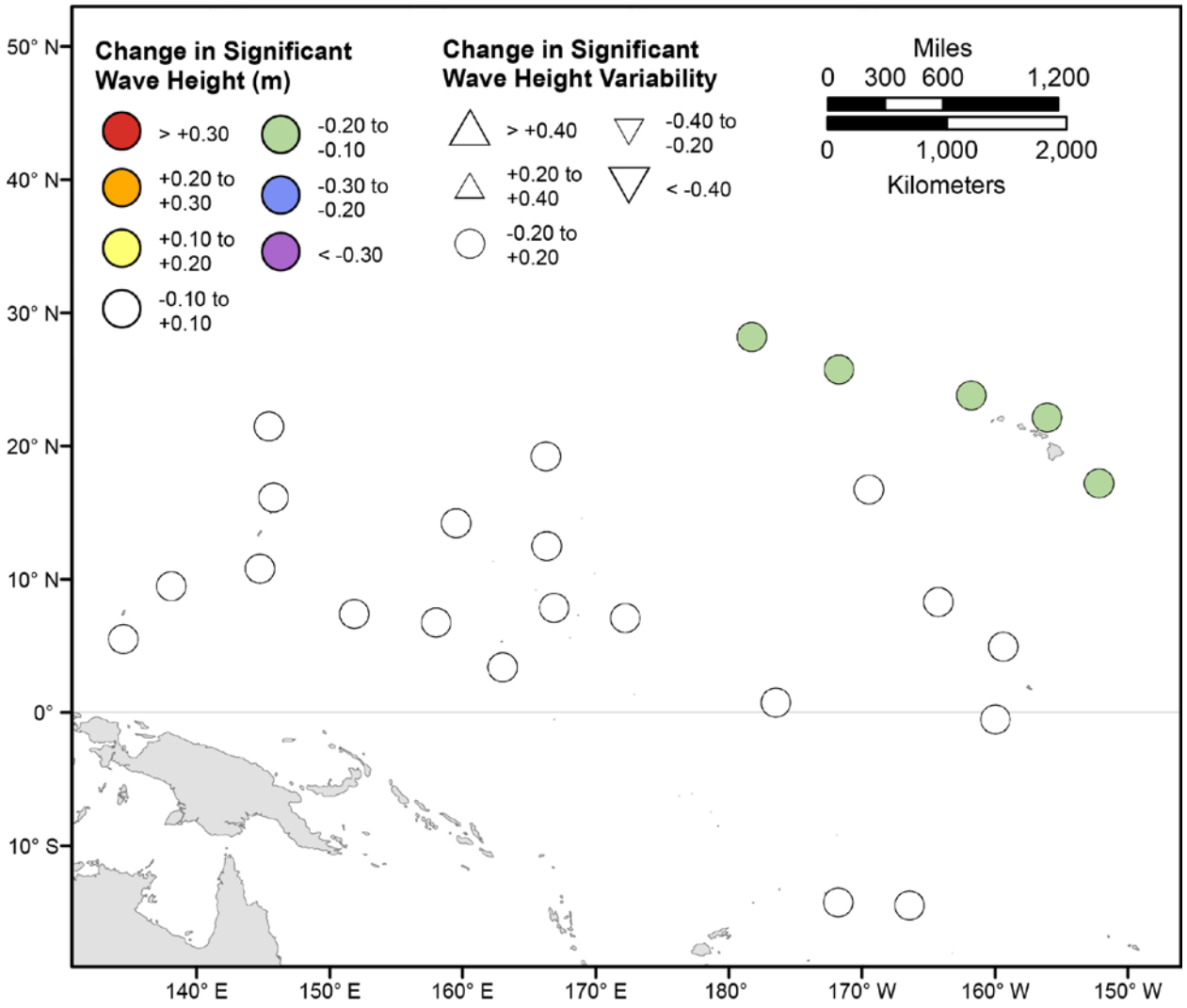

Figure 32. Map showing forecasted differences in mean significant wave height and variance in significant wave height for the years 2081–2100 from hindcasted values during the June-August season under the RCP8.5 future climatic scenario. The colors correspond to the magnitude of change in modeled mean significant wave heights during 2081–2100 from those hindcasted for 1976–2005. The shapes correspond to the magnitude of change in modeled variance in significant wave height during 2081–2100 from those hindcasted for 1976–2005. Units are in meters.

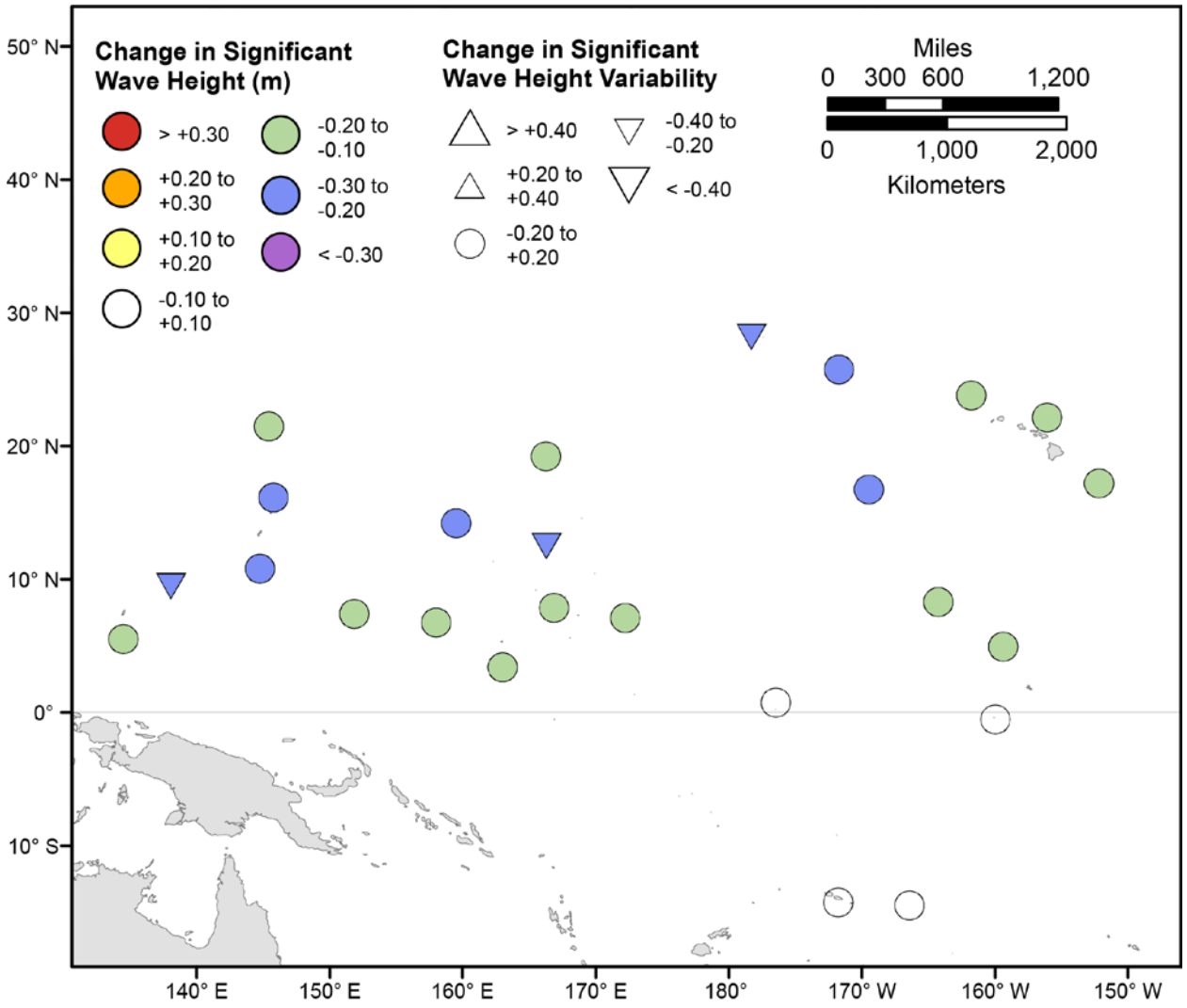

Figure 33. Map showing forecasted differences in mean significant wave height and variance in significant wave height for the years 2081–2100 from hindcasted values during the September-November season under the RCP8.5 future climatic scenario. The colors correspond to the magnitude of change in modeled mean significant wave heights during 2081–2100 from those hindcasted for 1976–2005. The shapes correspond to the magnitude of change in modeled variance in significant wave height during 2081–2100 from those hindcasted for 1976–2005. Units are in meters.

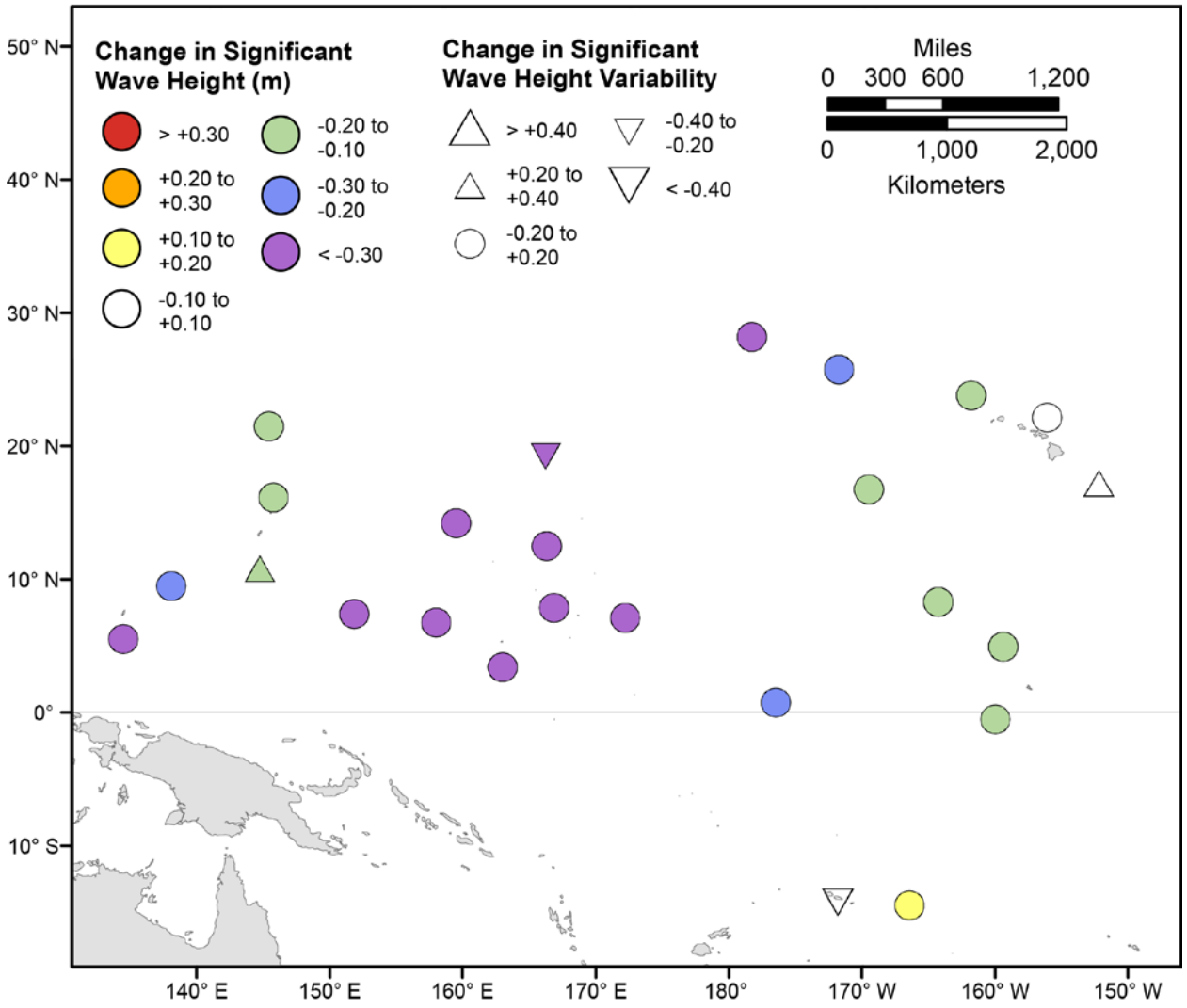

Figure 34. Map showing forecasted differences in the mean of the top 5 percent of significant wave heights and variance in the top 5 percent of significant wave heights for the years 2081–2100 from hindcasted values during the December-February season under the RCP8.5 future climatic scenario. The colors correspond to the magnitude of change in modeled mean significant wave heights during 2081–2100 from those hindcasted for 1976–2005. The shapes correspond to the magnitude of change in modeled variance in significant wave height during 2081–2100 from those hindcasted for 1976–2005. Units are in meters.

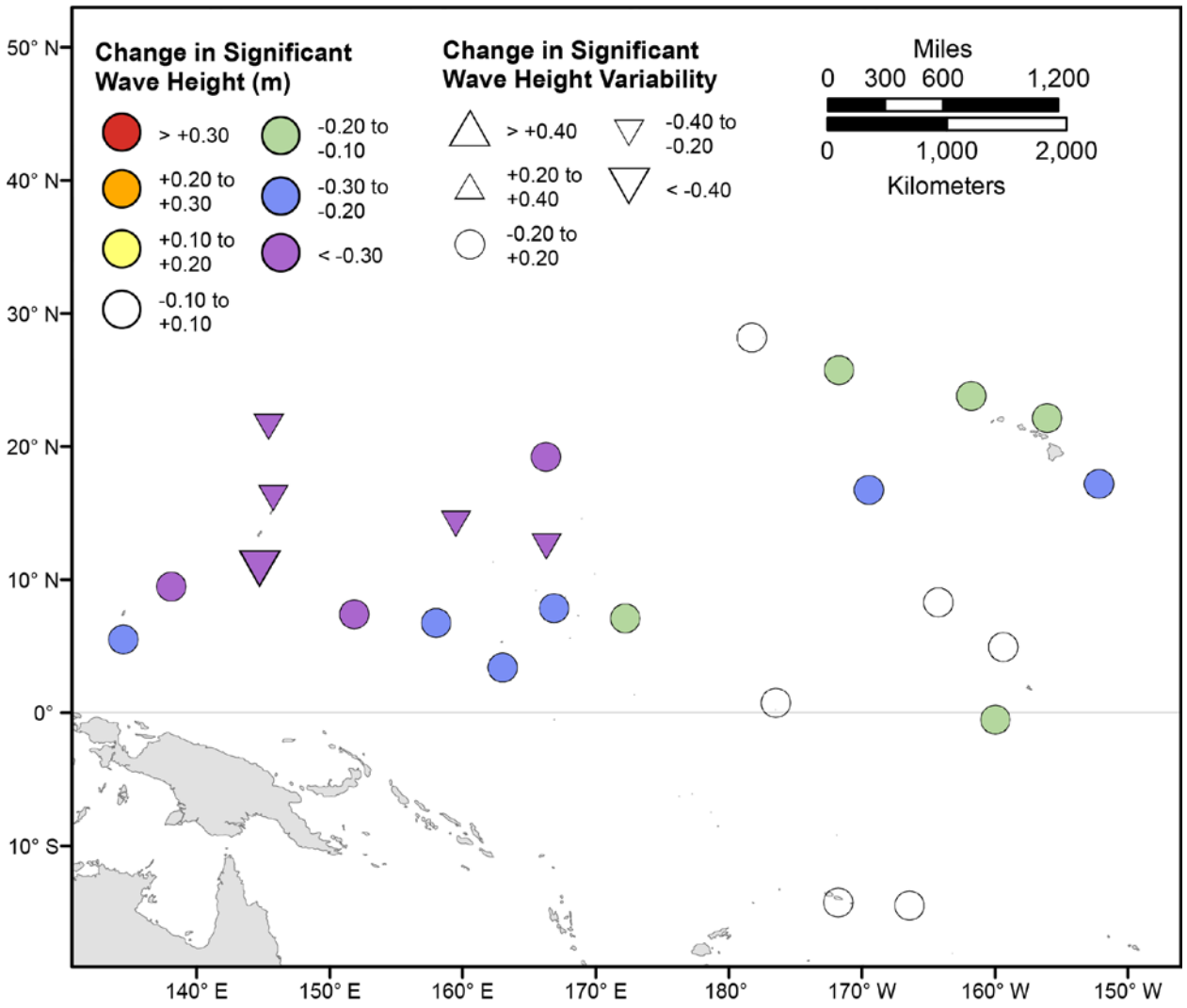

Figure 35. Map showing forecasted differences in the mean of the top 5 percent of significant wave heights and variance in the top 5 percent of significant wave heights for the years 2081–2100 from hindcasted values during the March-May season under the RCP8.5 future climatic scenario. The colors correspond to the magnitude of change in modeled mean significant wave heights during 2081–2100 from those hindcasted for 1976–2005. The shapes correspond to the magnitude of change in modeled variance in significant wave height during 2081–2100 from those hindcasted for 1976–2005. Units are in meters.

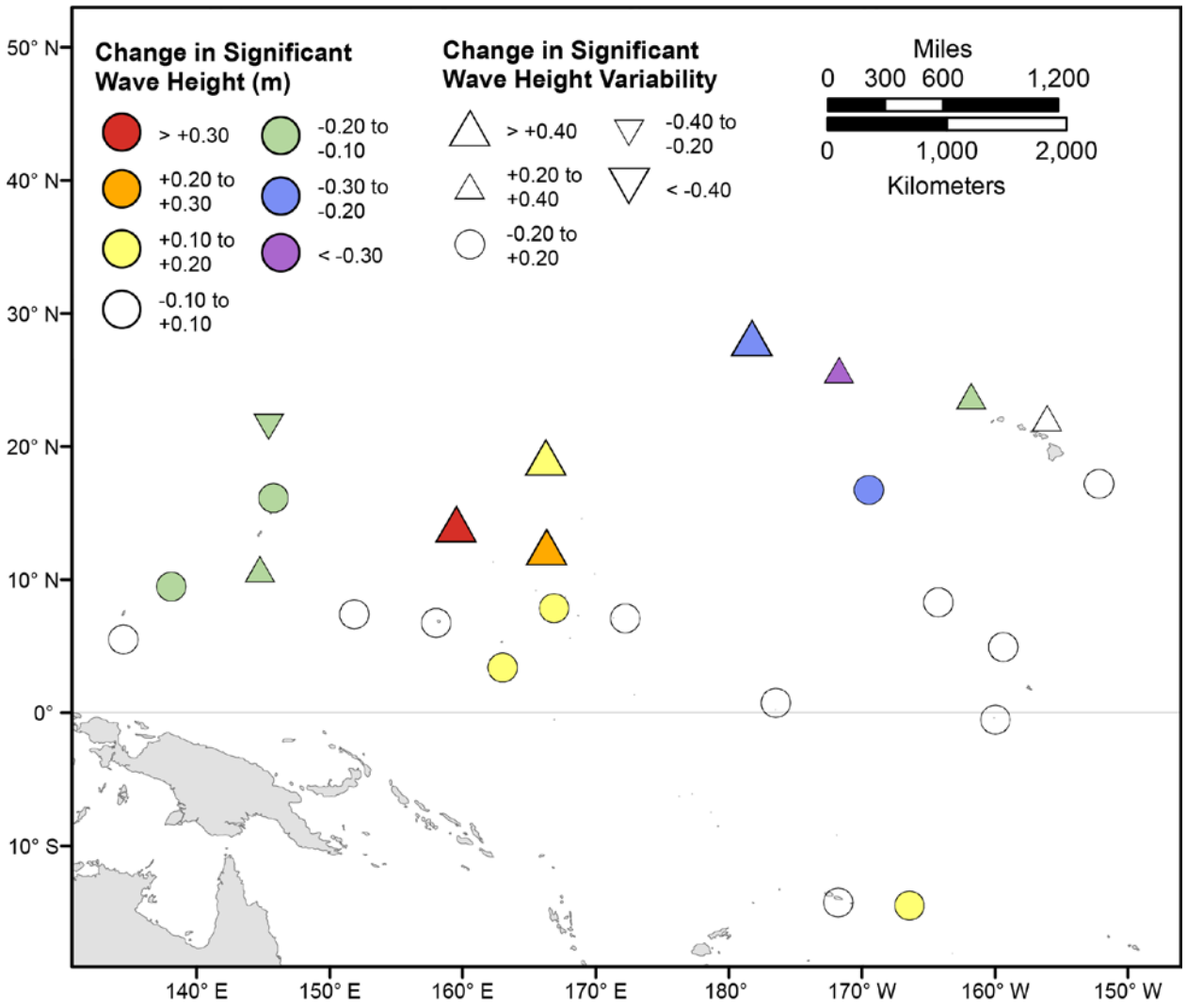

Figure 36. Map showing forecasted differences in the mean of the top 5 percent of significant wave heights and variance in the top 5 percent of significant wave heights for the years 2081–2100 from hindcasted values during the June-August season under the RCP8.5 future climatic scenario. The colors correspond to the magnitude of change in modeled mean significant wave heights during 2081–2100 from those hindcasted for 1976–2005. The shapes correspond to the magnitude of change in modeled variance in significant wave height during 2081–2100 from those hindcasted for 1976–2005. Units are in meters.

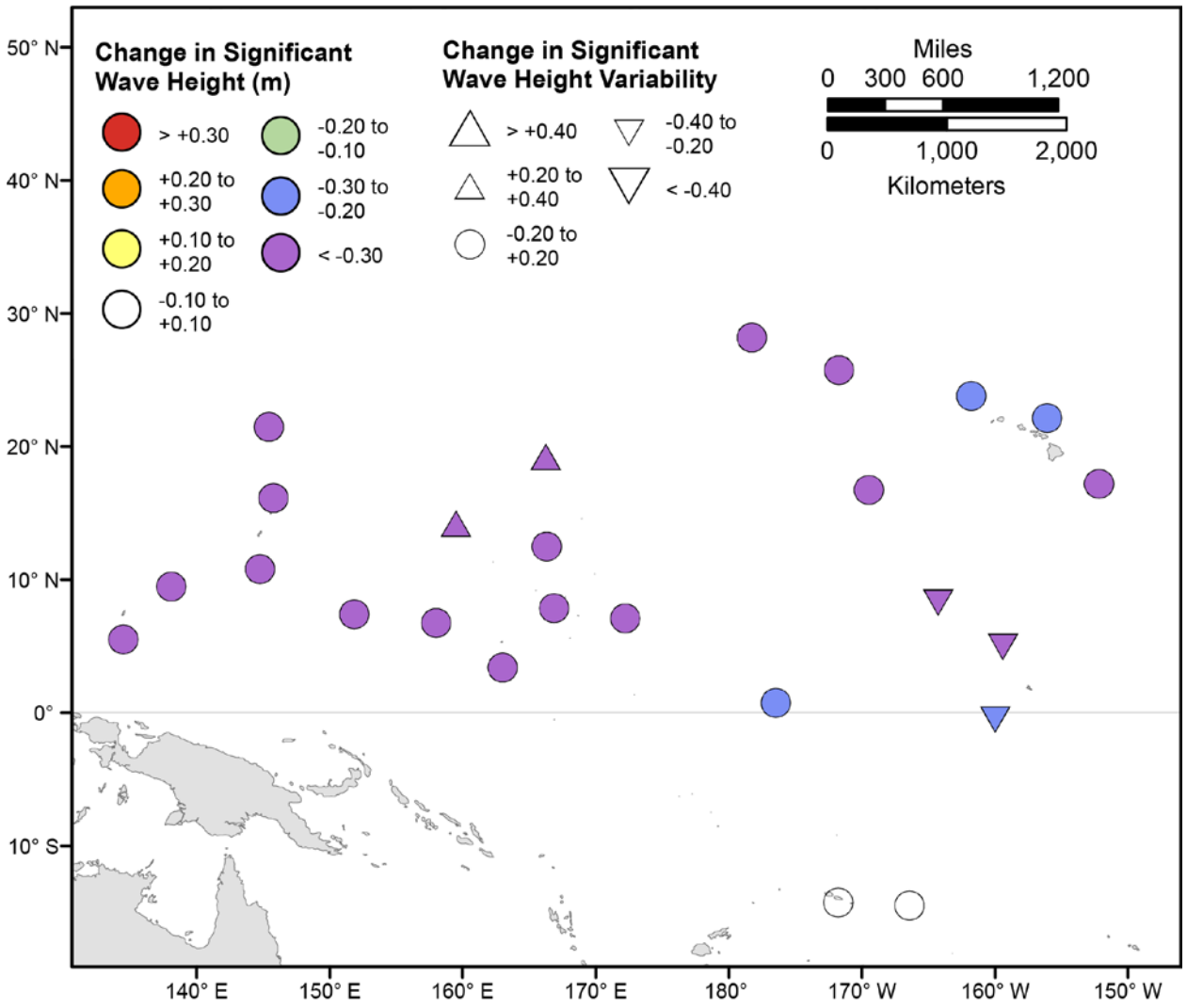

Figure 37. Map showing forecasted differences in the mean of the top 5 percent of significant wave heights and variance in the top 5 percent of significant wave heights for the years 2081–2100 from hindcasted values during the September-November season under the RCP8.5 future climatic scenario. The colors correspond to the magnitude of change in modeled mean significant wave heights during 2081–2100 from those hindcasted for 1976–2005. The shapes correspond to the magnitude of change in modeled variance in significant wave height during 2081–2100 from those hindcasted for 1976–2005. Units are in meters.

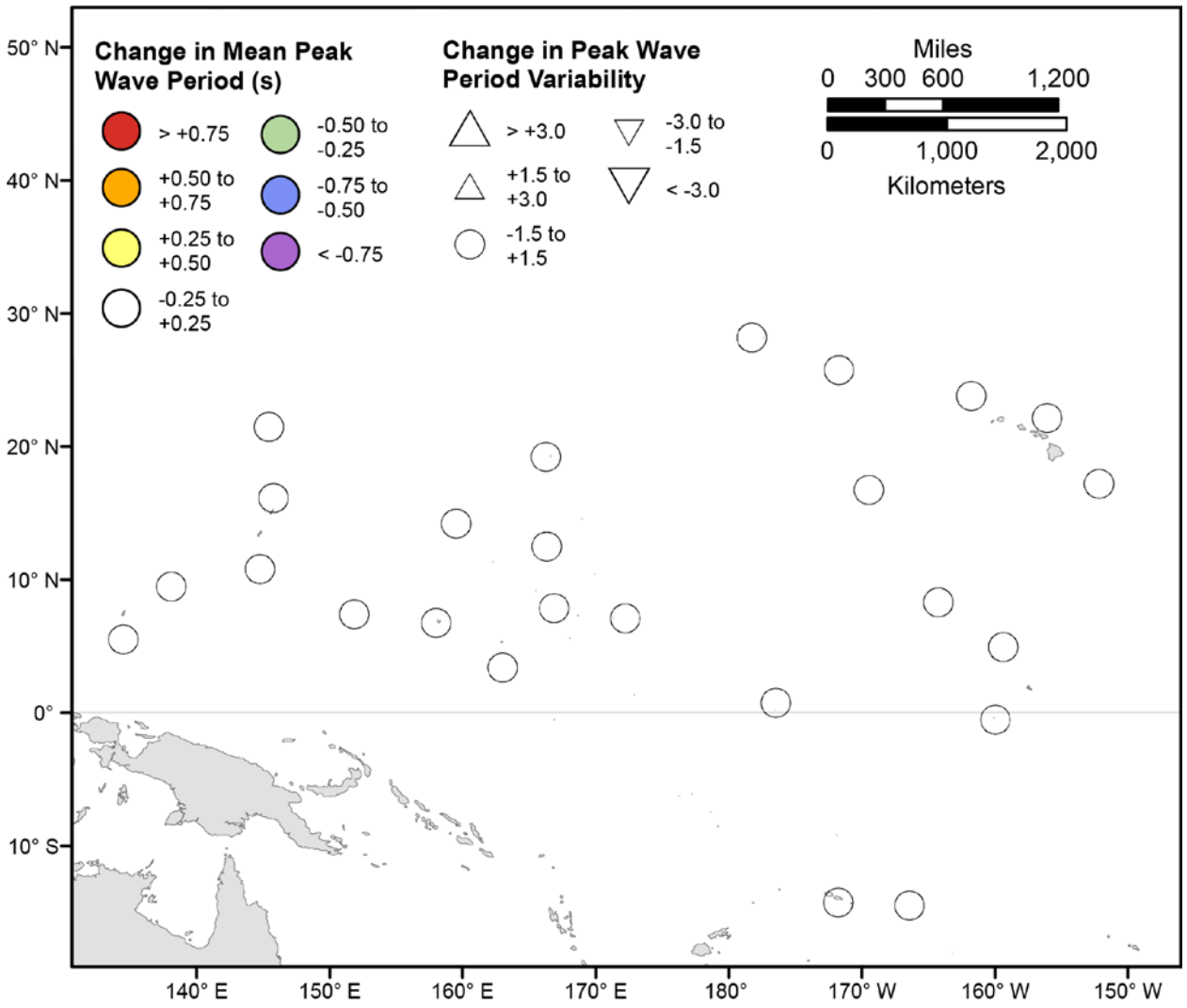

Figure 38. Map showing forecasted differences in mean peak wave period and variance in peak wave period for the years 2026–2045 from hindcasted values during the December-February season under the RCP4.5 future climatic scenario. The colors correspond to the magnitude of change in modeled mean peak wave periods during 2026–2045 from those hindcasted for 1976–2005. The shapes correspond to the magnitude of change in modeled variance in peak wave period during 2026–2045 from those hindcasted for 1976–2005. Units are in seconds.

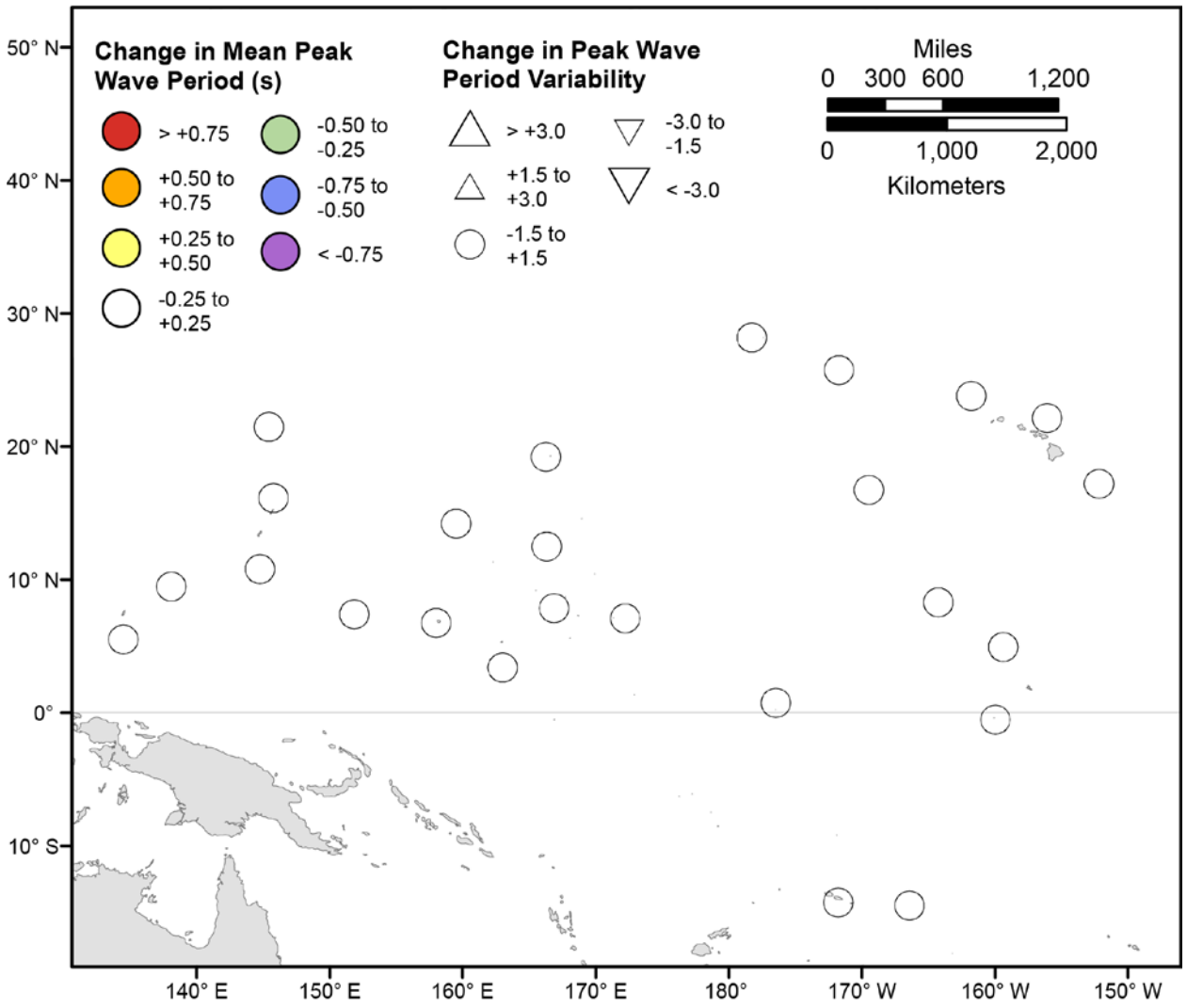

Figure 39. Map showing forecasted differences in mean peak wave period and variance in peak wave period for the years 2026–2045 from hindcasted values during the March-May season under the RCP4.5 future climatic scenario. The colors correspond to the magnitude of change in modeled mean peak wave periods during 2026–2045 from those hindcasted for 1976–2005. The shapes correspond to the magnitude of change in modeled variance in peak wave period during 2026–2045 from those hindcasted for 1976–2005. Units are in seconds.

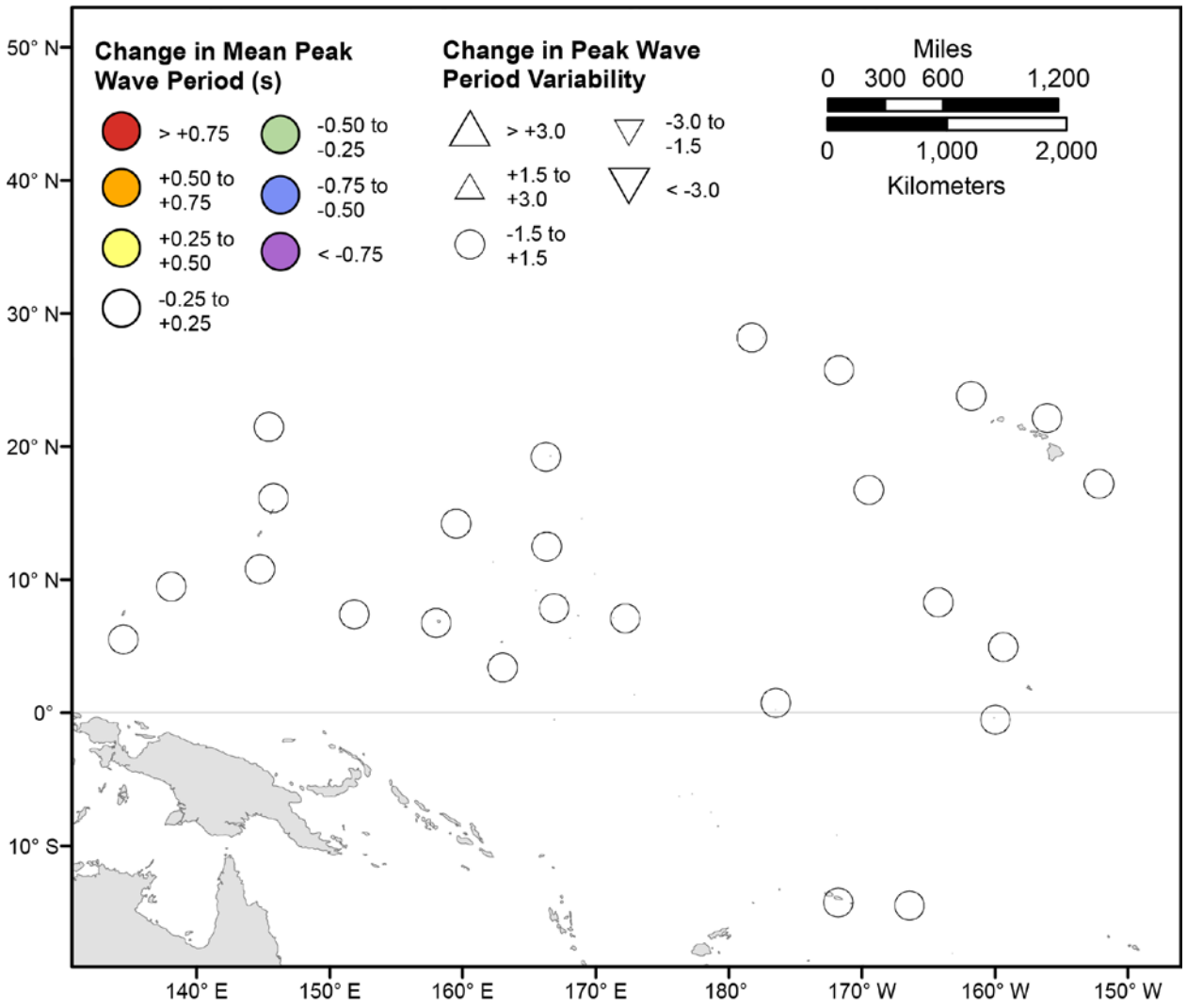

Figure 40. Map showing forecasted differences in mean peak wave period and variance in peak wave period for the years 2026–2045 from hindcasted values during the June-August season under the RCP4.5 future climatic scenario. The colors correspond to the magnitude of change in modeled mean peak wave periods during 2026–2045 from those hindcasted for 1976–2005. The shapes correspond to the magnitude of change in modeled variance in peak wave period during 2026–2045 from those hindcasted for 1976–2005. Units are in seconds.

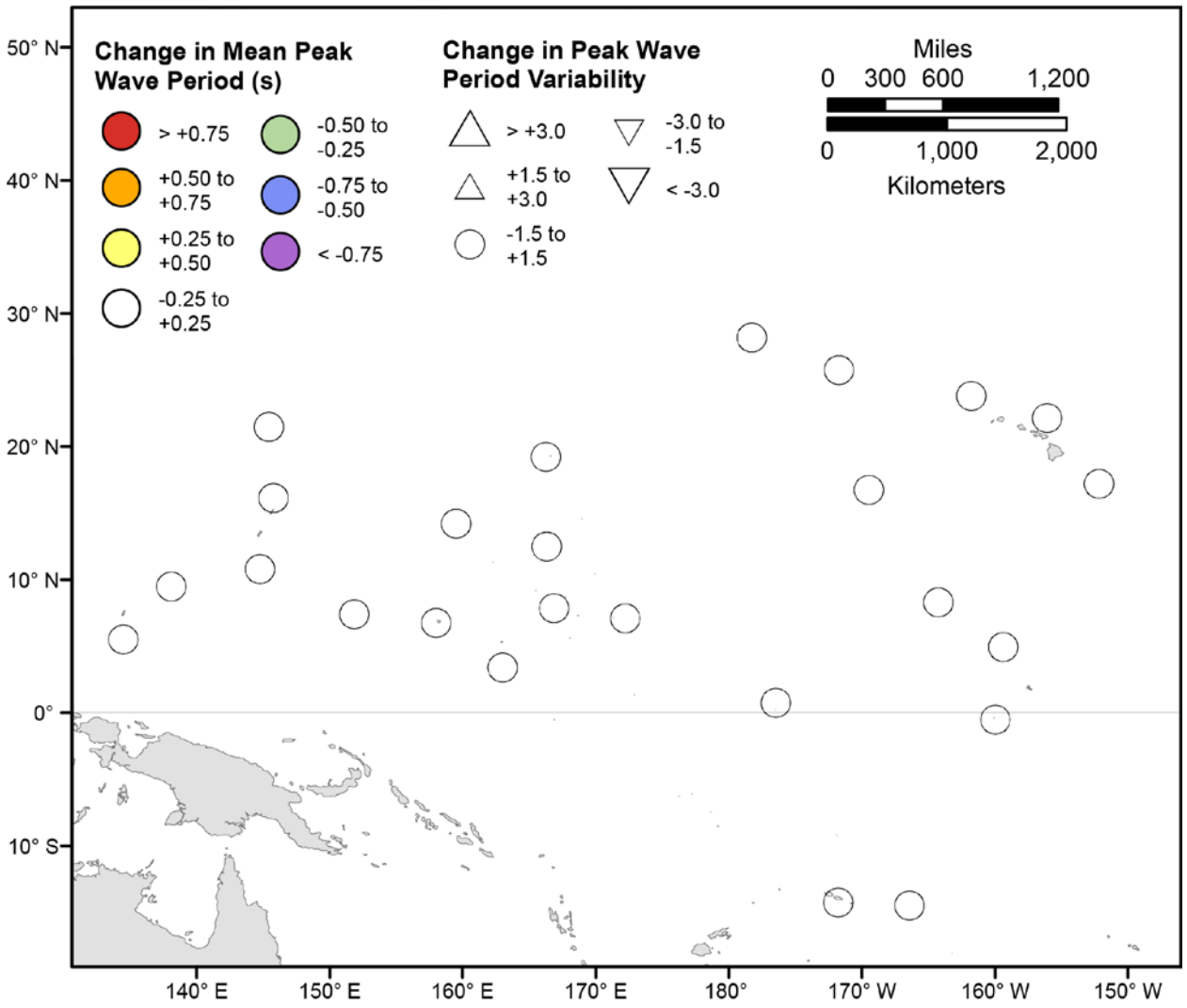

Figure 41. Map showing forecasted differences in mean peak wave period and variance in peak wave period for the years 2026–2045 from hindcasted values during the September-November season under the RCP4.5 future climatic scenario. The colors correspond to the magnitude of change in modeled mean peak wave periods during 2026–2045 from those hindcasted for 1976–2005. The shapes correspond to the magnitude of change in modeled variance in peak wave period during 2026–2045 from those hindcasted for 1976–2005. Units are in seconds.

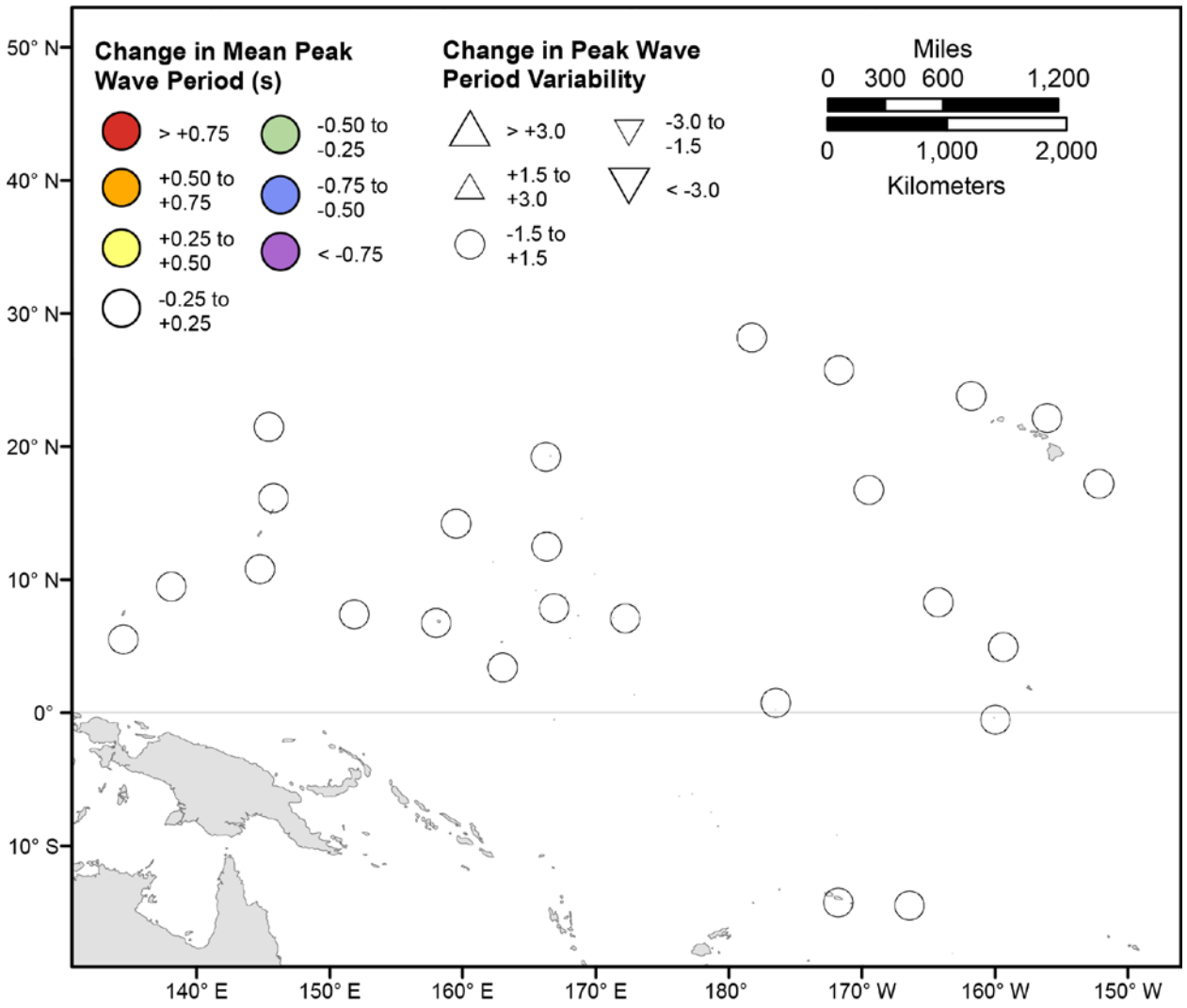

Figure 42. Map showing forecasted differences in the mean peak wave period of the top 5 percent of significant wave heights and variance in the peak wave period of top 5 percent of significant wave heights for the years 2026–2045 from hindcasted values during the December-February season under the RCP4.5 future climatic scenario. The colors correspond to the magnitude of change in modeled mean peak wave periods during 2026–2045 from those hindcasted for 1976–2005. The shapes correspond to the magnitude of change in modeled variance in peak wave period during 2026–2045 from those hindcasted for 1976–2005. Units are in seconds.

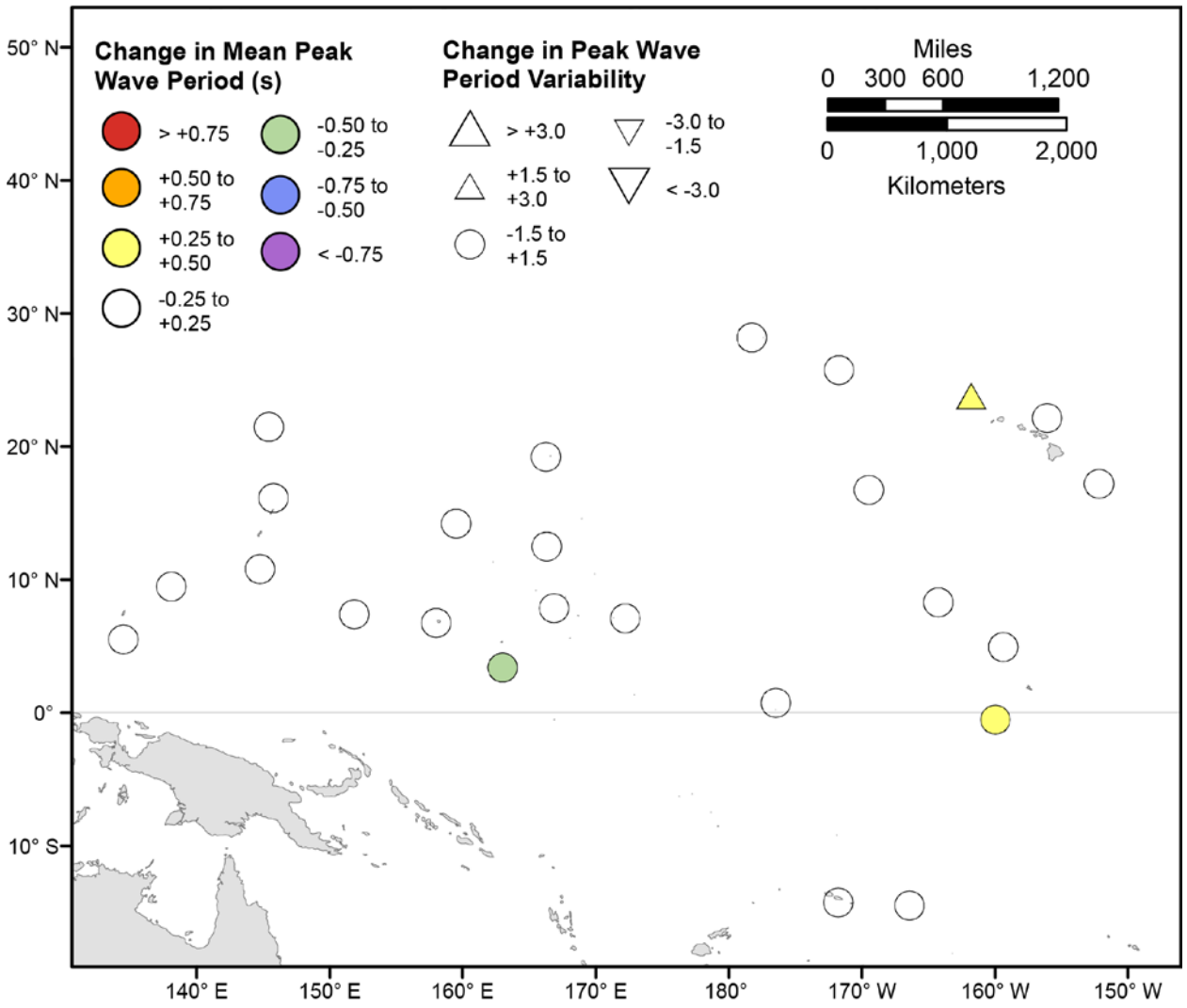

Figure 43. Map showing forecasted differences in the mean peak wave period of the top 5 percent of significant wave heights and variance in the peak wave period of top 5 percent of significant wave heights for the years 2026–2045 from hindcasted values during the March-May season under the RCP4.5 future climatic scenario. The colors correspond to the magnitude of change in modeled mean peak wave periods during 2026–2045 from those hindcasted for 1976–2005. The shapes correspond to the magnitude of change in modeled variance in peak wave period during 2026–2045 from those hindcasted for 1976–2005. Units are in seconds.

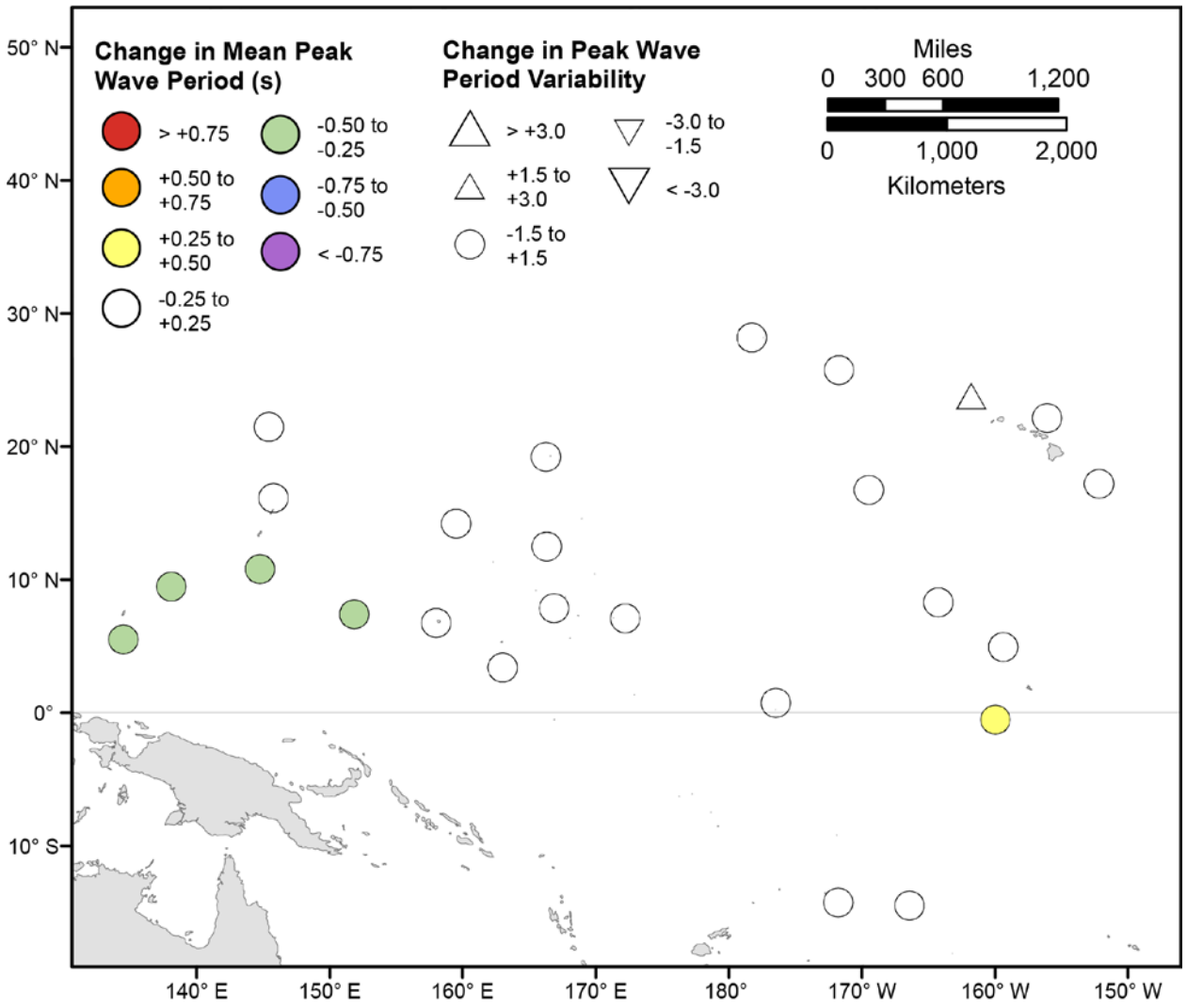

Figure 44. Map showing forecasted differences in the mean peak wave period of the top 5 percent of significant wave heights and variance in the peak wave period of top 5 percent of significant wave heights for the years 2026–2045 from hindcasted values during the June-August season under the RCP4.5 future climatic scenario. The colors correspond to the magnitude of change in modeled mean peak wave periods during 2026–2045 from those hindcasted for 1976–2005. The shapes correspond to the magnitude of change in modeled variance in peak wave period during 2026–2045 from those hindcasted for 1976–2005. Units are in seconds.

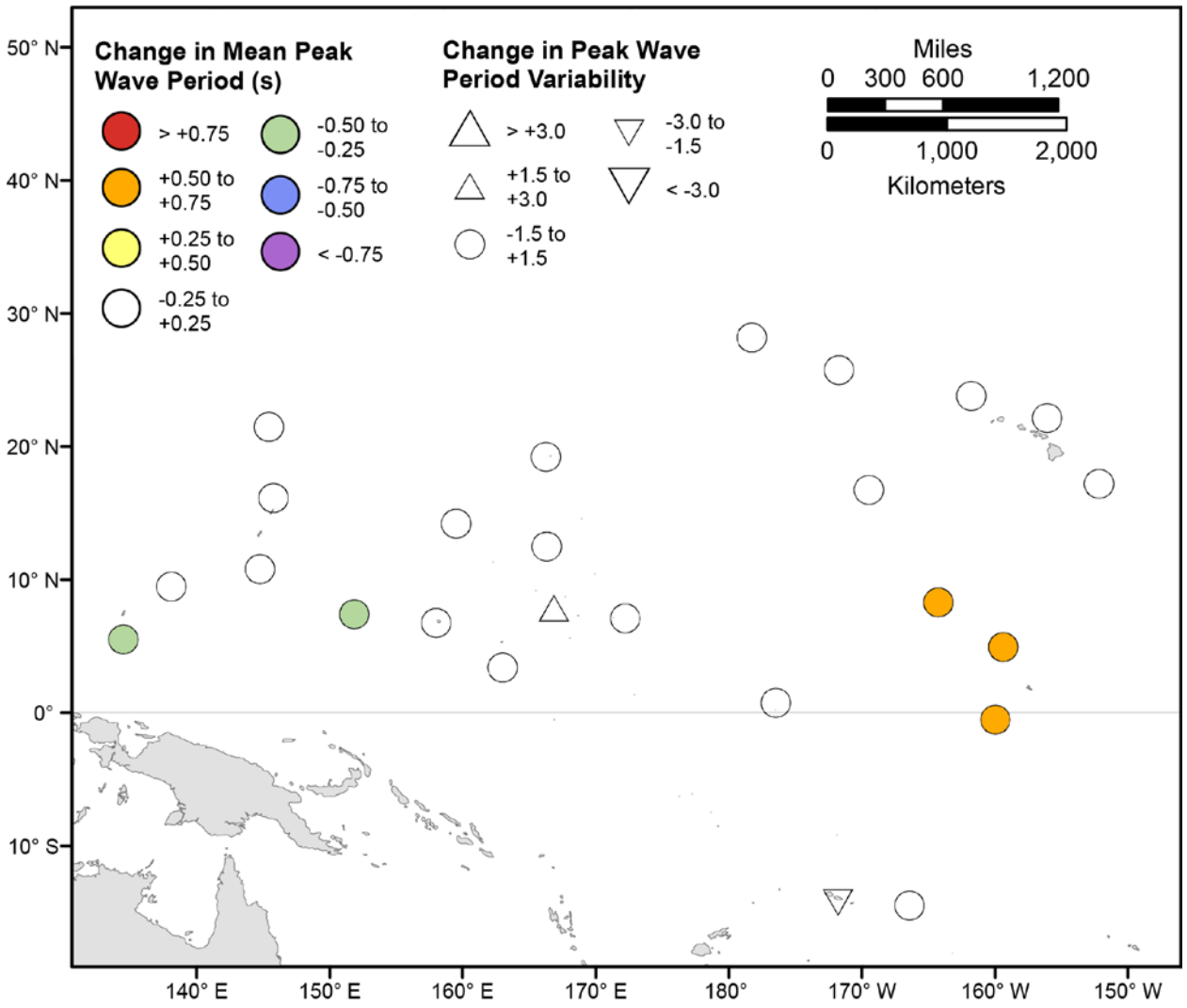

Figure 45. Map showing forecasted differences in the mean peak wave period of the top 5 percent of significant wave heights and variance in the peak wave period of top 5 percent of significant wave heights for the years 2026–2045 from hindcasted values during the September-November season under the RCP4.5 future climatic scenario. The colors correspond to the magnitude of change in modeled mean peak wave periods during 2026–2045 from those hindcasted for 1976–2005. The shapes correspond to the magnitude of change in modeled variance in peak wave period during 2026–2045 from those hindcasted for 1976–2005. Units are in seconds.

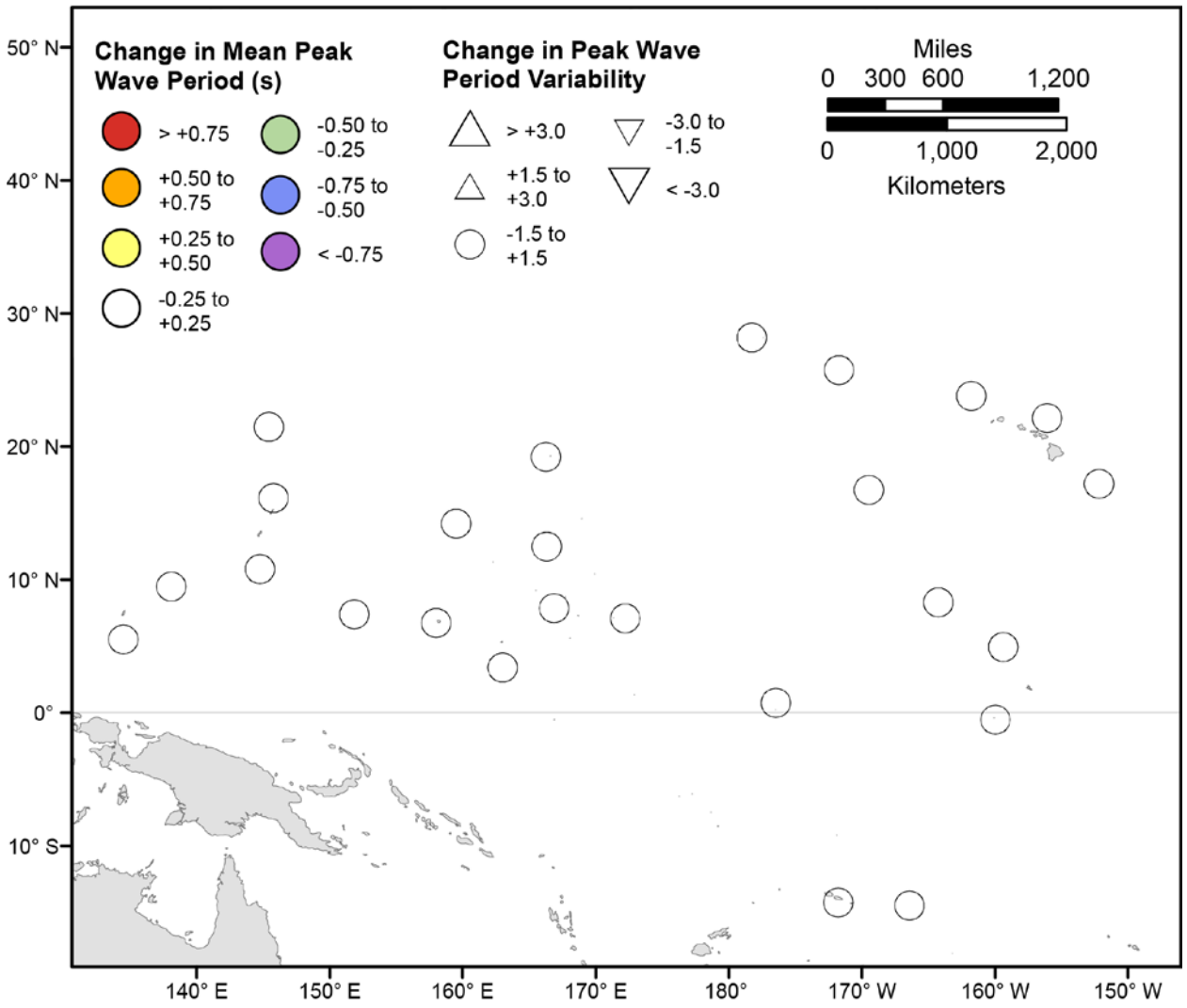

Figure 46. Map showing forecasted differences in mean peak wave period and variance in peak wave period for the years 2026–2045 from hindcasted values during the December-February season under the RCP8.5 future climatic scenario. The colors correspond to the magnitude of change in modeled mean peak wave periods during 2026–2045 from those hindcasted for 1976–2005. The shapes correspond to the magnitude of change in modeled variance in peak wave period during 2026–2045 from those hindcasted for 1976–2005. Units are in seconds.

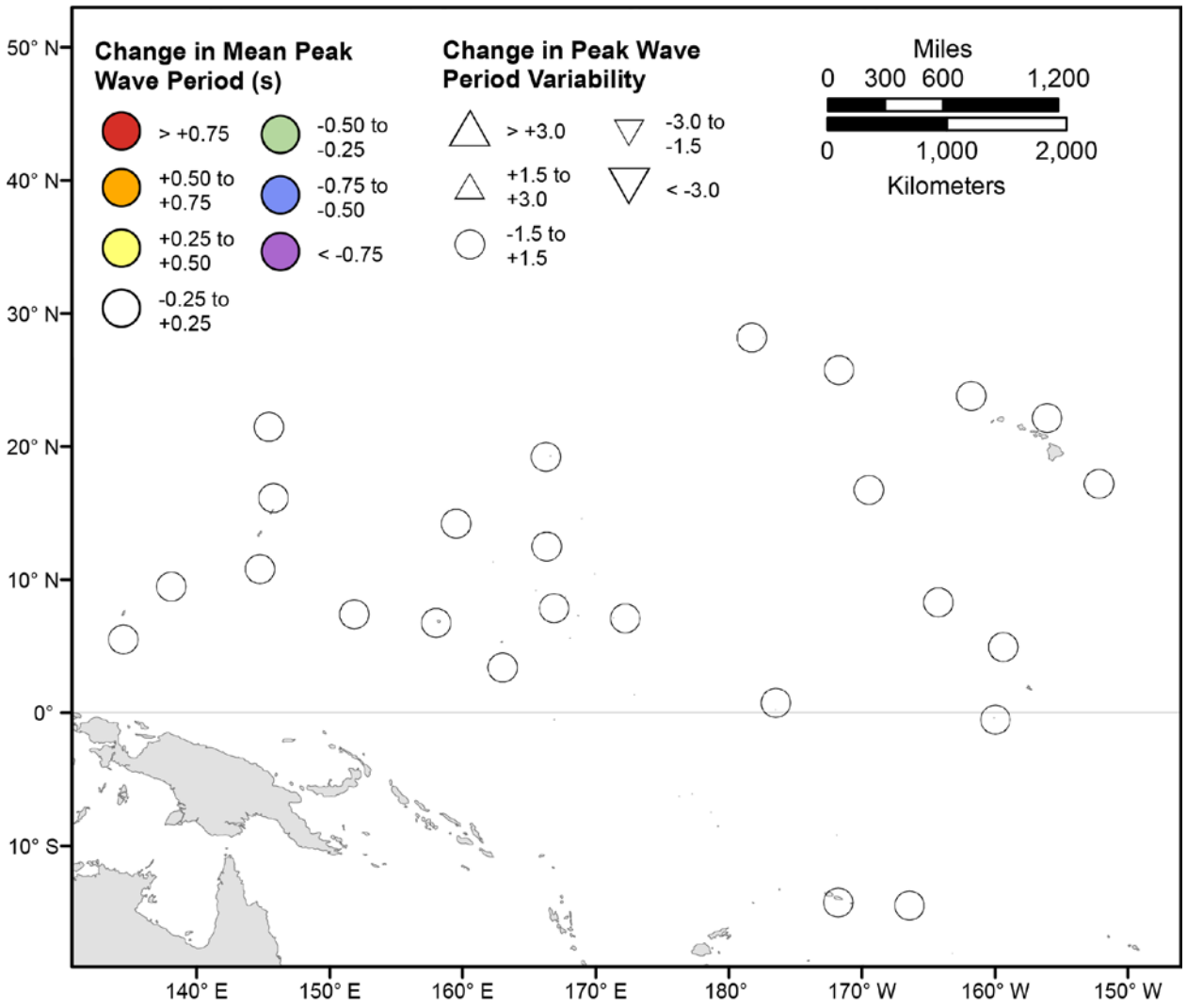

Figure 47. Map showing forecasted differences in mean peak wave period and variance in peak wave period for the years 2026–2045 from hindcasted values during the March-May season under the RCP8.5 future climatic scenario. The colors correspond to the magnitude of change in modeled mean peak wave periods during 2026–2045 from those hindcasted for 1976–2005. The shapes correspond to the magnitude of change in modeled variance in peak wave period during 2026–2045 from those hindcasted for 1976–2005. Units are in seconds.

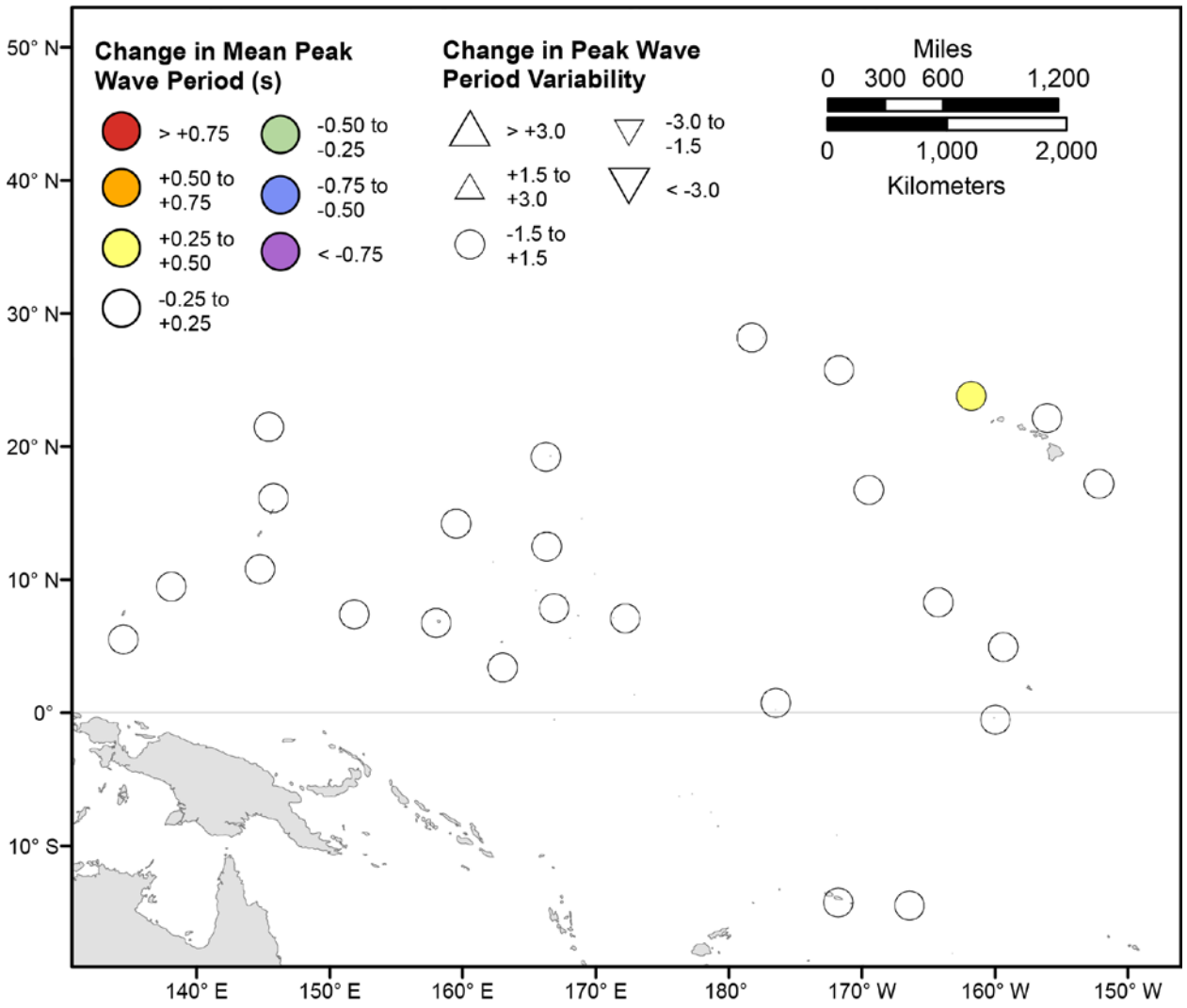

Figure 48. Map showing forecasted differences in mean peak wave period and variance in peak wave period for the years 2026–2045 from hindcasted values during the June-August season under the RCP8.5 future climatic scenario. The colors correspond to the magnitude of change in modeled mean peak wave periods during 2026–2045 from those hindcasted for 1976–2005. The shapes correspond to the magnitude of change in modeled variance in peak wave period during 2026–2045 from those hindcasted for 1976–2005. Units are in seconds.

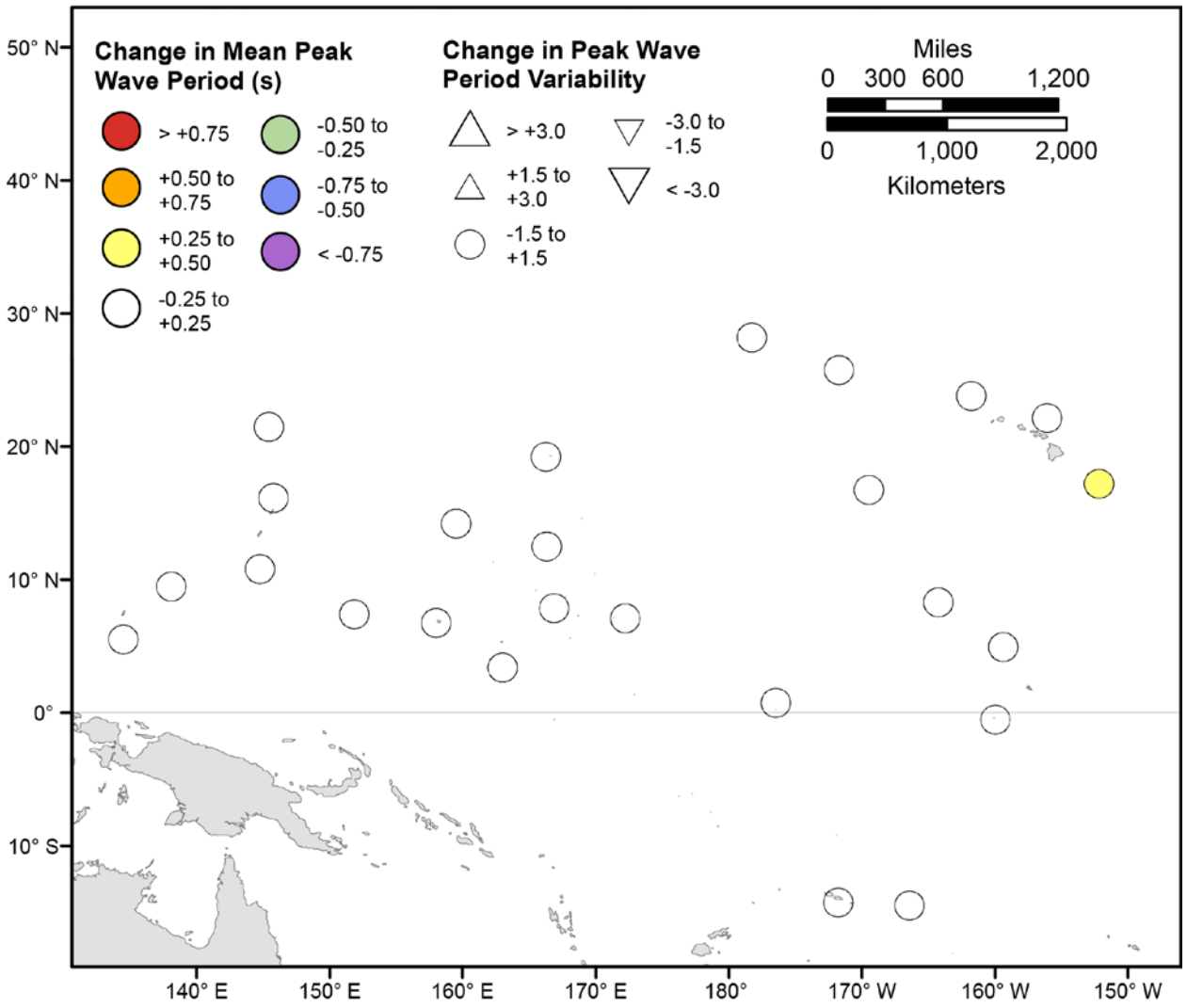

Figure 49. Map showing forecasted differences in mean peak wave period and variance in peak wave period for the years 2026–2045 from hindcasted values during the September-November season under the RCP8.5 future climatic scenario. The colors correspond to the magnitude of change in modeled mean peak wave periods during 2026–2045 from those hindcasted for 1976–2005. The shapes correspond to the magnitude of change in modeled variance in peak wave period during 2026–2045 from those hindcasted for 1976–2005. Units are in seconds.

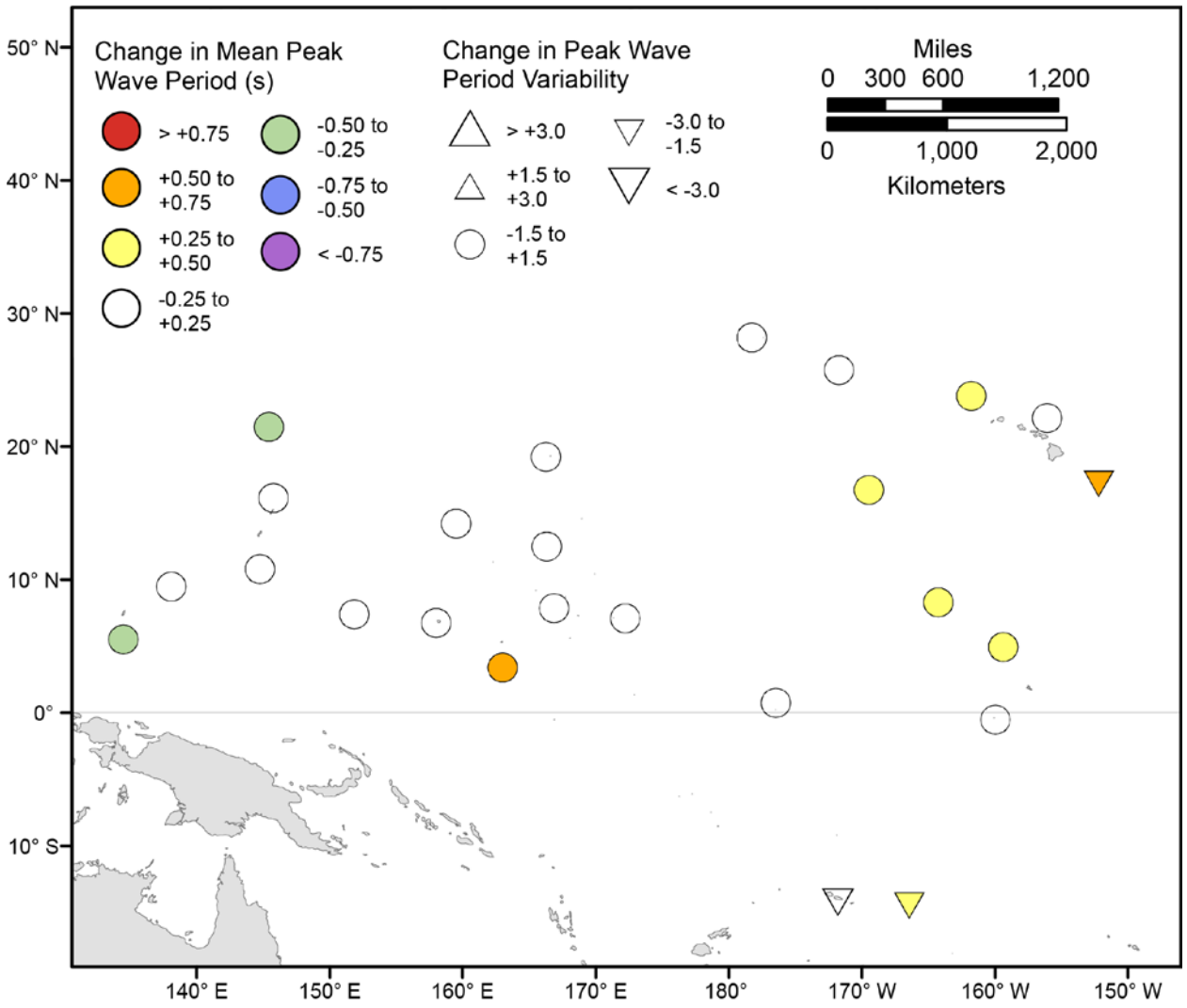

Figure 50. Map showing forecasted differences in the mean peak wave period of the top 5 percent of significant wave heights and variance in the peak wave period of top 5 percent of significant wave heights for the years 2026–2045 from hindcasted values during the December-February season under the RCP8.5 future climatic scenario. The colors correspond to the magnitude of change in modeled mean peak wave periods during 2026–2045 from those hindcasted for 1976–2005. The shapes correspond to the magnitude of change in modeled variance in peak wave period during 2026–2045 from those hindcasted for 1976–2005. Units are in seconds.

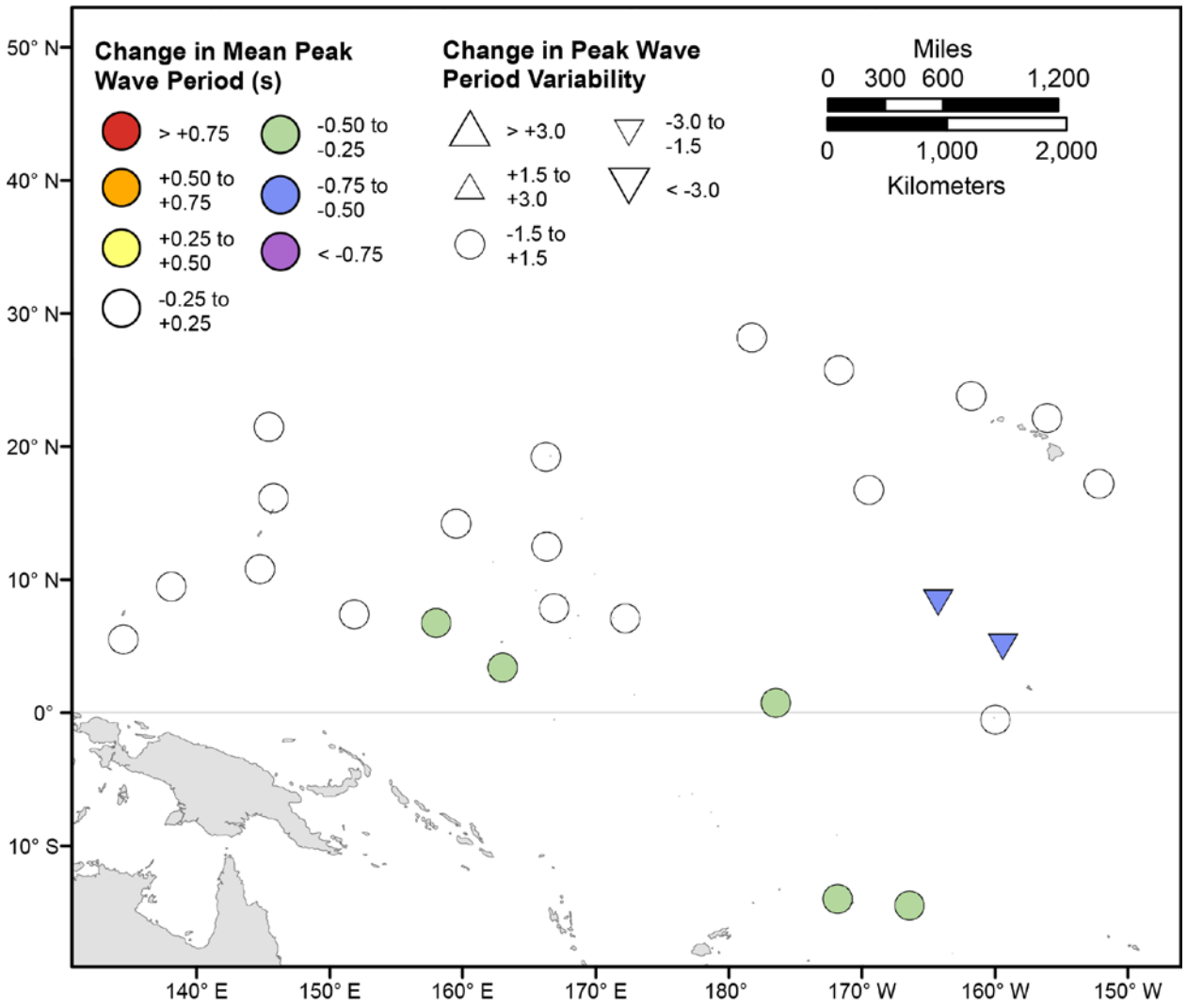

Figure 51. Map showing forecasted differences in the mean peak wave period of the top 5 percent of significant wave heights and variance in the peak wave period of top 5 percent of significant wave heights for the years 2026–2045 from hindcasted values during the March-May season under the RCP8.5 future climatic scenario. The colors correspond to the magnitude of change in modeled mean peak wave periods during 2026–2045 from those hindcasted for 1976–2005. The shapes correspond to the magnitude of change in modeled variance in peak wave period during 2026–2045 from those hindcasted for 1976–2005. Units are in seconds.

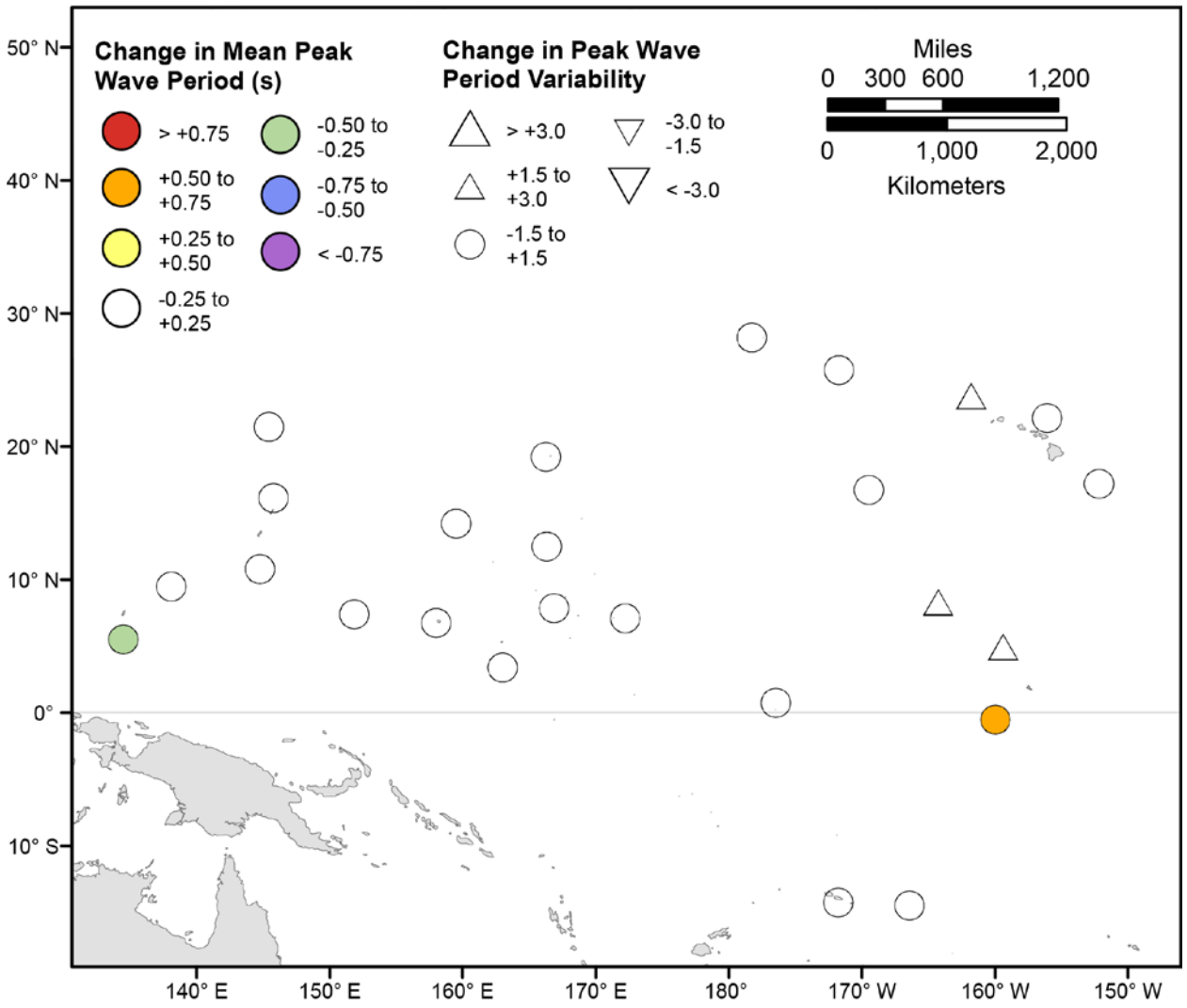

Figure 52. Map showing forecasted differences in the mean peak wave period of the top 5 percent of significant wave heights and variance in the peak wave period of top 5 percent of significant wave heights for the years 2026–2045 from hindcasted values during the June-August season under the RCP8.5 future climatic scenario. The colors correspond to the magnitude of change in modeled mean peak wave periods during 2026–2045 from those hindcasted for 1976–2005. The shapes correspond to the magnitude of change in modeled variance in peak wave period during 2026–2045 from those hindcasted for 1976–2005. Units are in seconds.

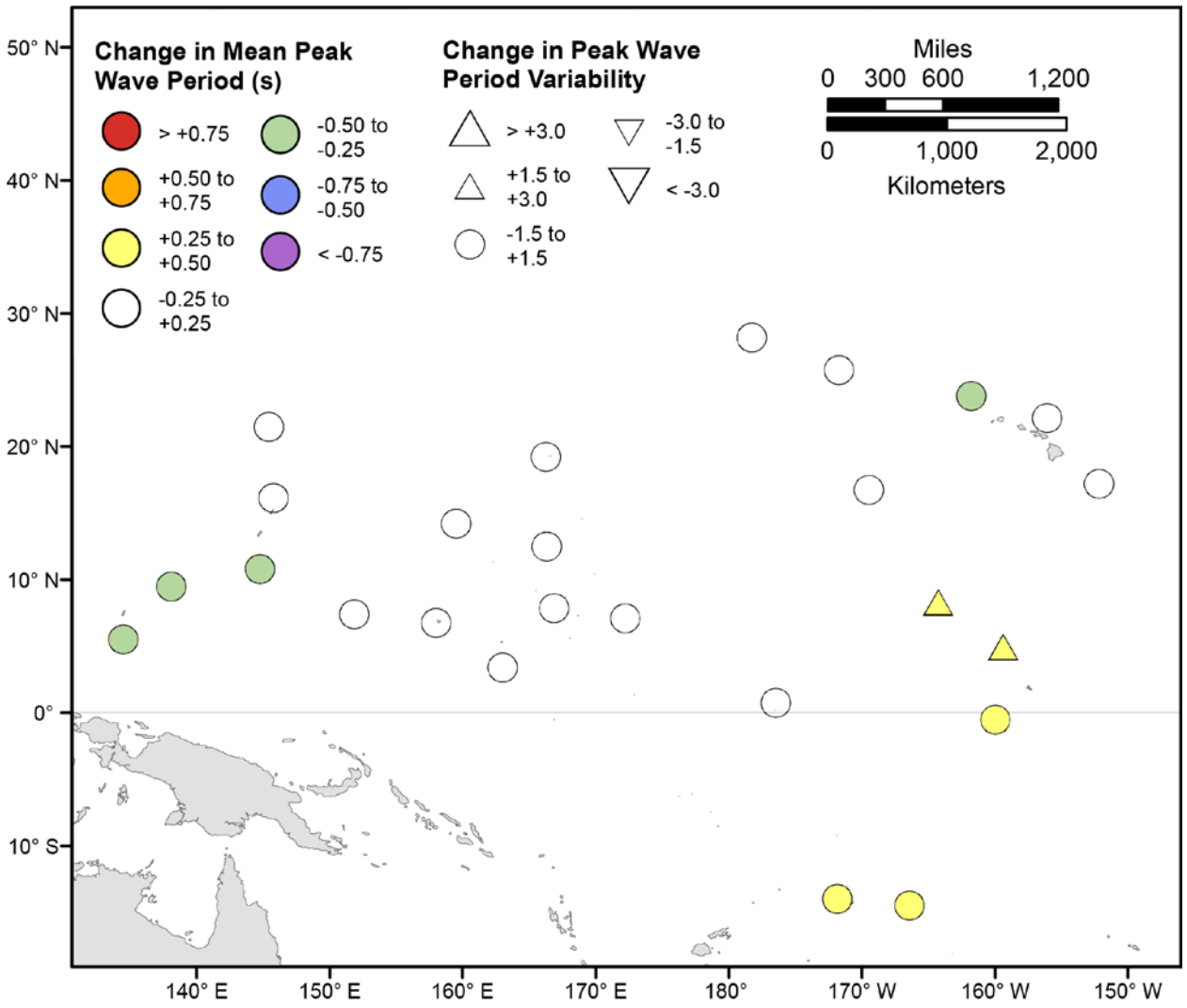

Figure 53. Map showing forecasted differences in the mean peak wave period of the top 5 percent of significant wave heights and variance in the peak wave period of top 5 percent of significant wave heights for the years 2026–2045 from hindcasted values during the September-November season under the RCP8.5 future climatic scenario. The colors correspond to the magnitude of change in modeled mean peak wave periods during 2026–2045 from those hindcasted for 1976–2005. The shapes correspond to the magnitude of change in modeled variance in peak wave period during 2026–2045 from those hindcasted for 1976–2005. Units are in seconds.

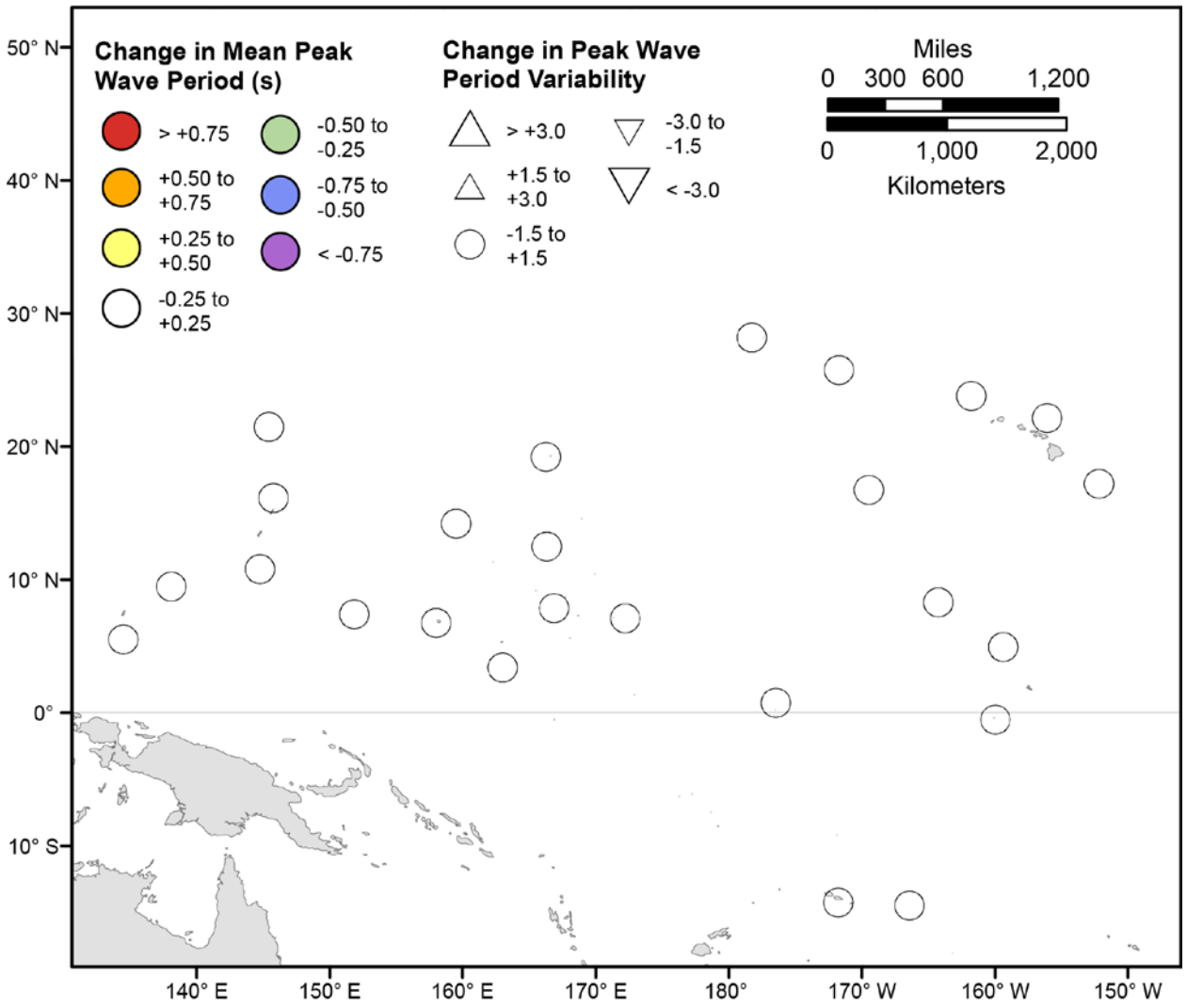

Figure 54. Map showing forecasted differences in mean peak wave period and variance in peak wave period for the years 2081–2100 from hindcasted values during the December-February season under the RCP4.5 future climatic scenario. The colors correspond to the magnitude of change in modeled mean peak wave periods during 2081–2100 from those hindcasted for 1976–2005. The shapes correspond to the magnitude of change in modeled variance in peak wave period during 2081–2100 from those hindcasted for 1976–2005. Units are in seconds.

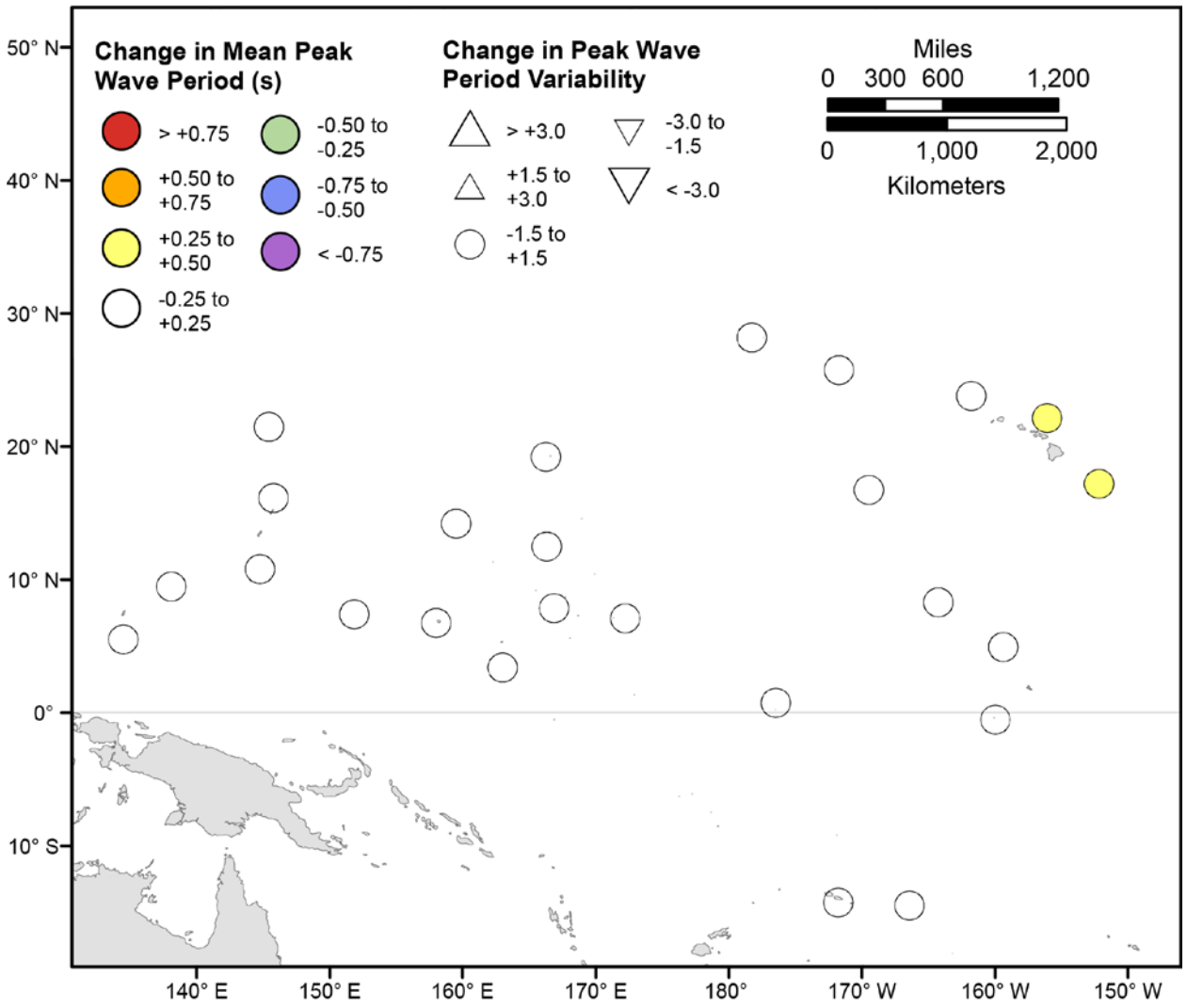

Figure 55. Map showing forecasted differences in mean peak wave period and variance in peak wave period for the years 2081–2100 from hindcasted values during the March-May season under the RCP4.5 future climatic scenario. The colors correspond to the magnitude of change in modeled mean peak wave periods during 2081–2100 from those hindcasted for 1976–2005. The shapes correspond to the magnitude of change in modeled variance in peak wave period during 2081–2100 from those hindcasted for 1976–2005. Units are in seconds.

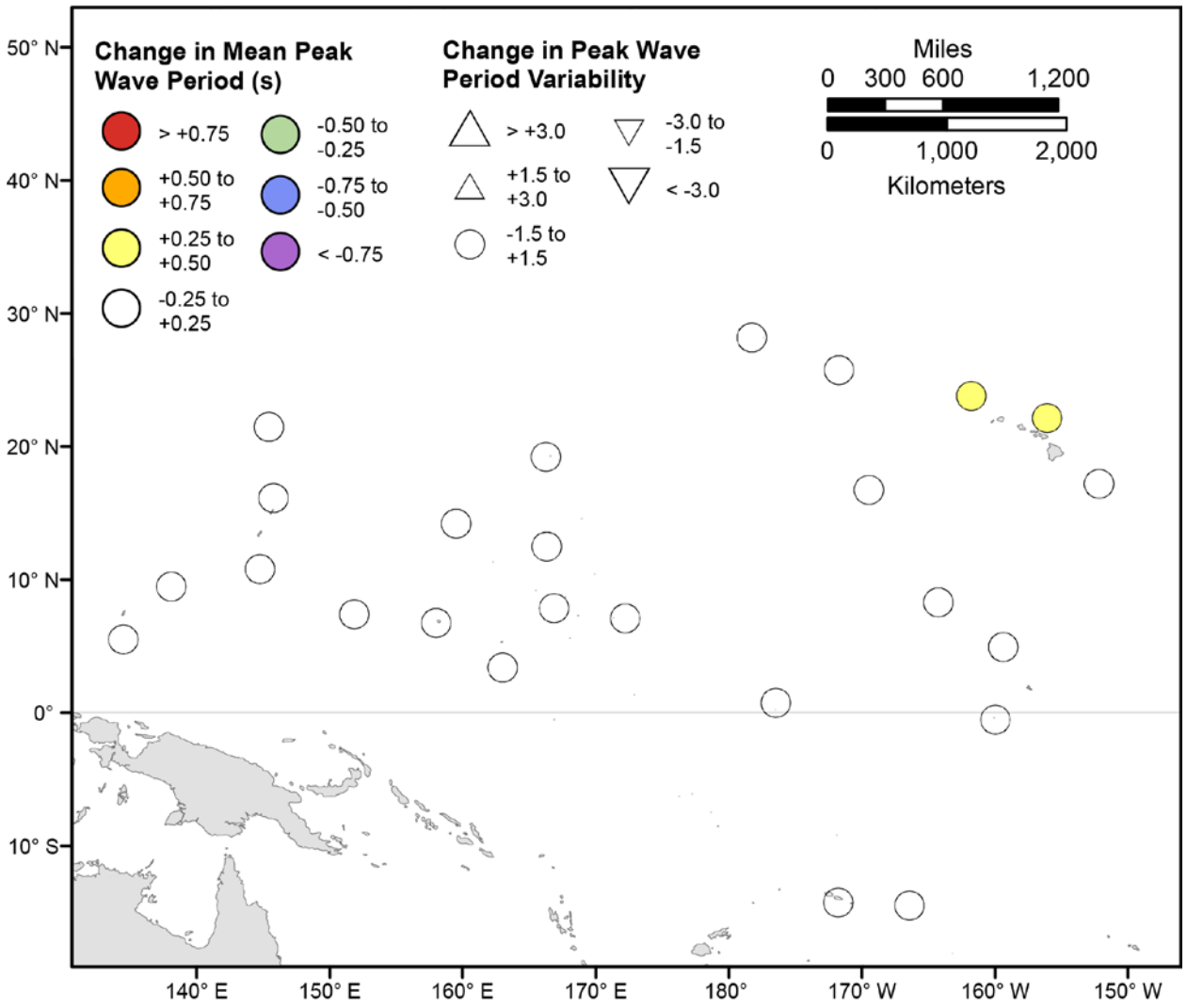

Figure 56. Map showing forecasted differences in mean peak wave period and variance in peak wave period for the years 2081–2100 from hindcasted values during the June-August season under the RCP4.5 future climatic scenario. The colors correspond to the magnitude of change in modeled mean peak wave periods during 2081–2100 from those hindcasted for 1976–2005. The shapes correspond to the magnitude of change in modeled variance in peak wave period during 2081–2100 from those hindcasted for 1976–2005. Units are in seconds.

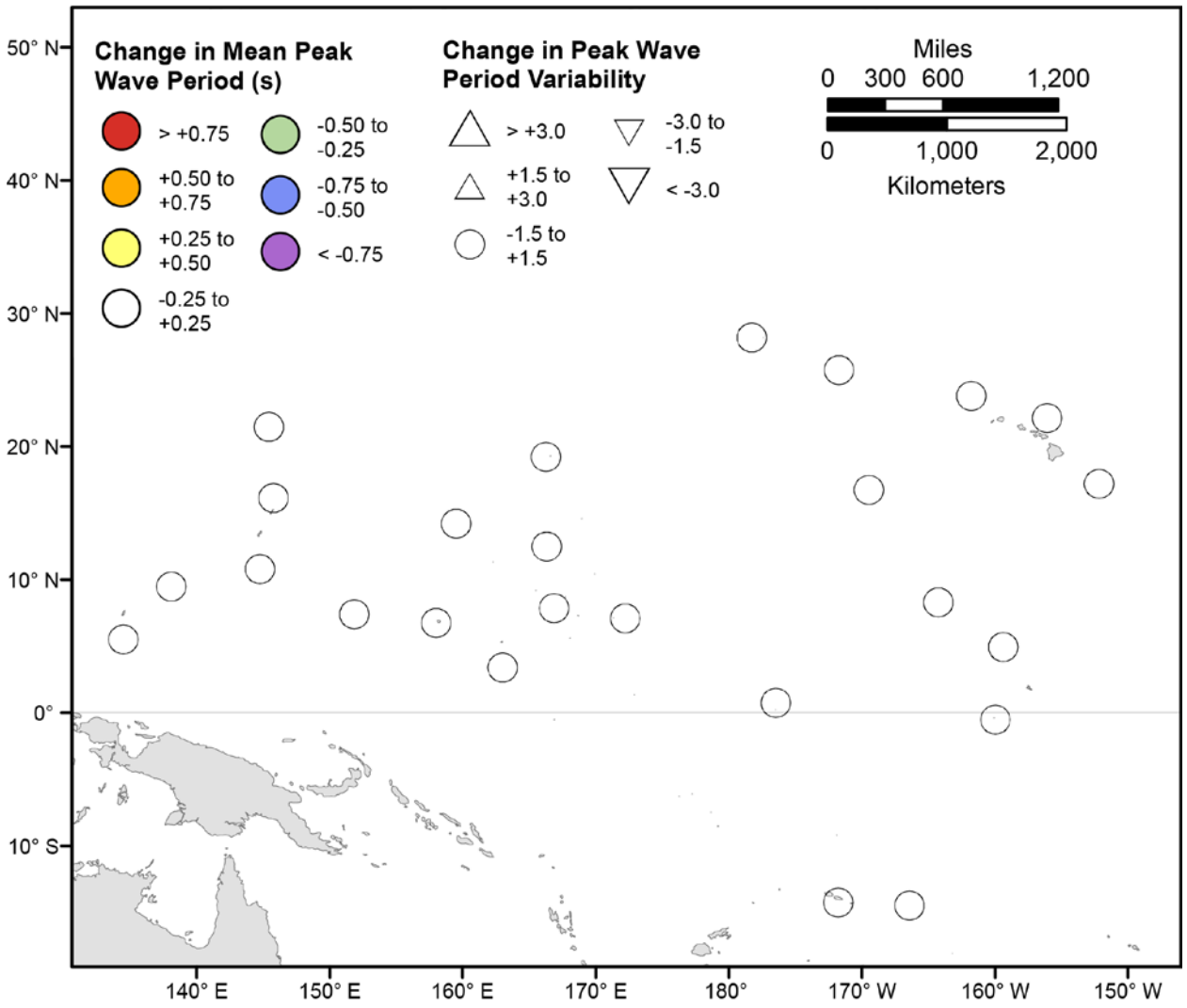

Figure 57. Map showing forecasted differences in mean peak wave period and variance in peak wave period for the years 2081–2100 from hindcasted values during the September-November season under the RCP4.5 future climatic scenario. The colors correspond to the magnitude of change in modeled mean peak wave periods during 2081–2100 from those hindcasted for 1976–2005. The shapes correspond to the magnitude of change in modeled variance in peak wave period during 2081–2100 from those hindcasted for 1976–2005. Units are in seconds.

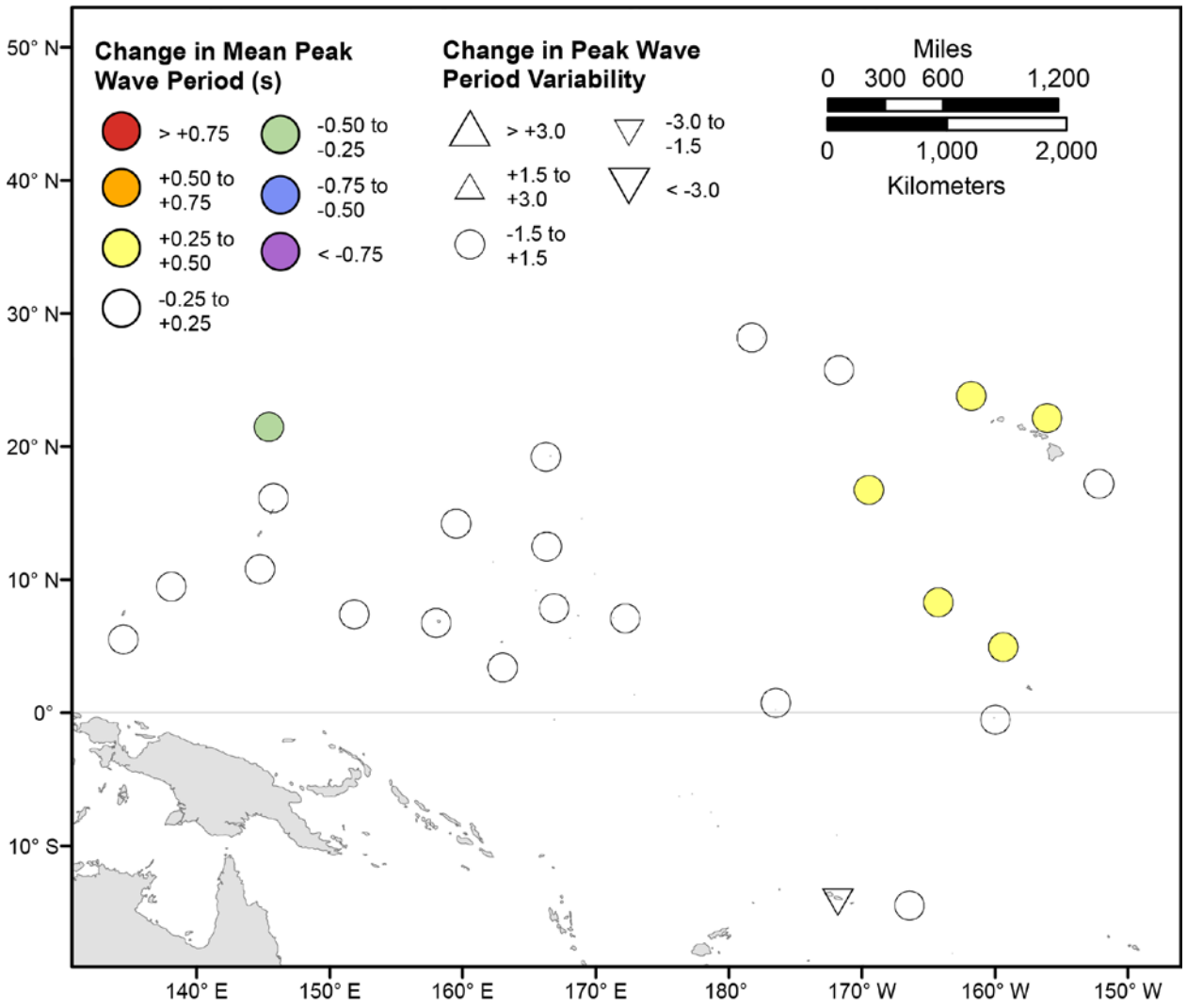

Figure 58. Map showing forecasted differences in the mean peak wave period of the top 5 percent of significant wave heights and variance in the peak wave period of top 5 percent of significant wave heights for the years 2081–2100 from hindcasted values during the December-February season under the RCP4.5 future climatic scenario. The colors correspond to the magnitude of change in modeled mean peak wave periods during 2081–2100 from those hindcasted for 1976–2005. The shapes correspond to the magnitude of change in modeled variance in peak wave period during 2081–2100 from those hindcasted for 1976–2005. Units are in seconds.

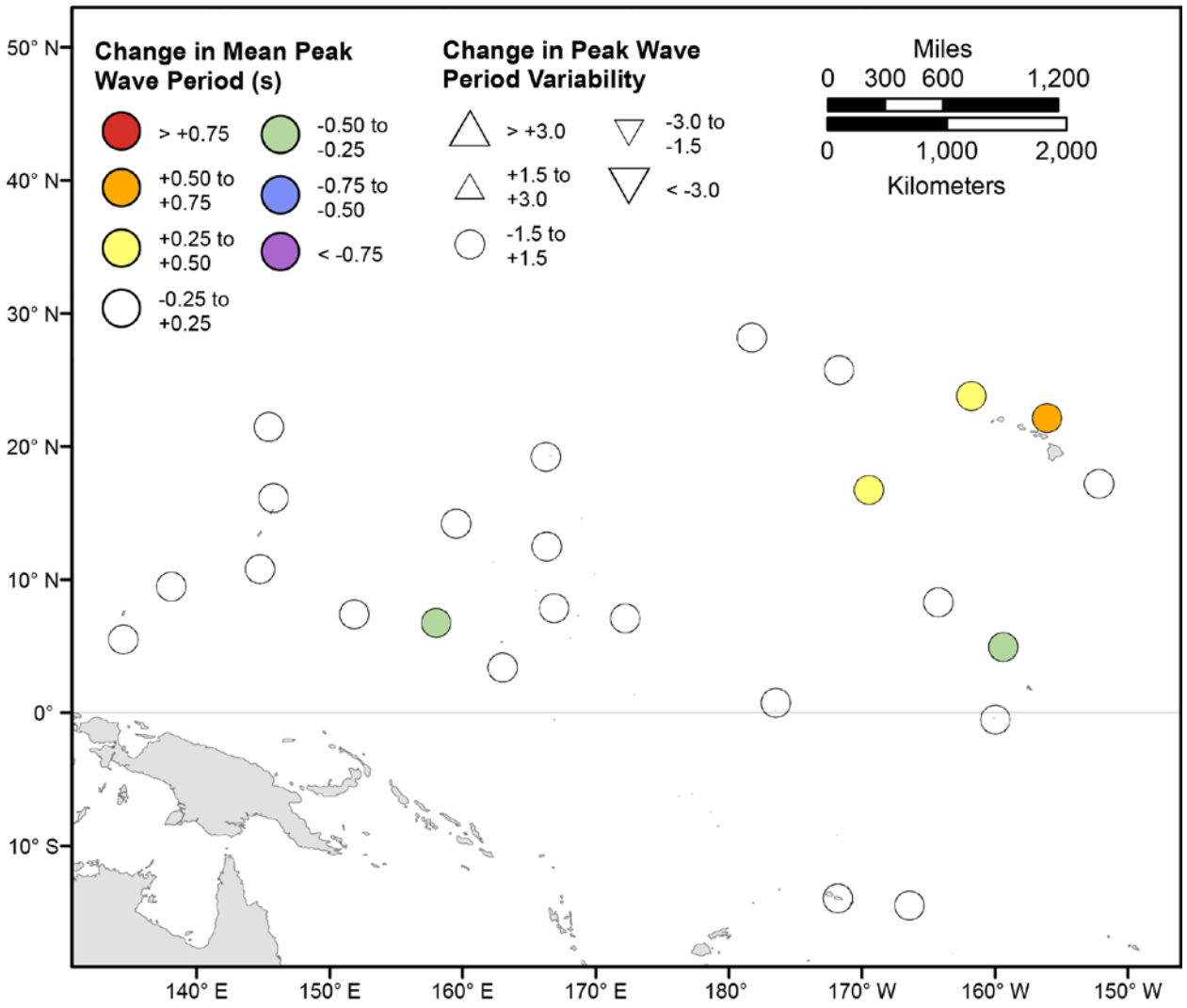

Figure 59. Map showing forecasted differences in the mean peak wave period of the top 5 percent of significant wave heights and variance in the peak wave period of top 5 percent of significant wave heights for the years 2081–2100 from hindcasted values during the March-May season under the RCP4.5 future climatic scenario. The colors correspond to the magnitude of change in modeled mean peak wave periods during 2081–2100 from those hindcasted for 1976–2005. The shapes correspond to the magnitude of change in modeled variance in peak wave period during 2081–2100 from those hindcasted for 1976–2005. Units are in seconds.

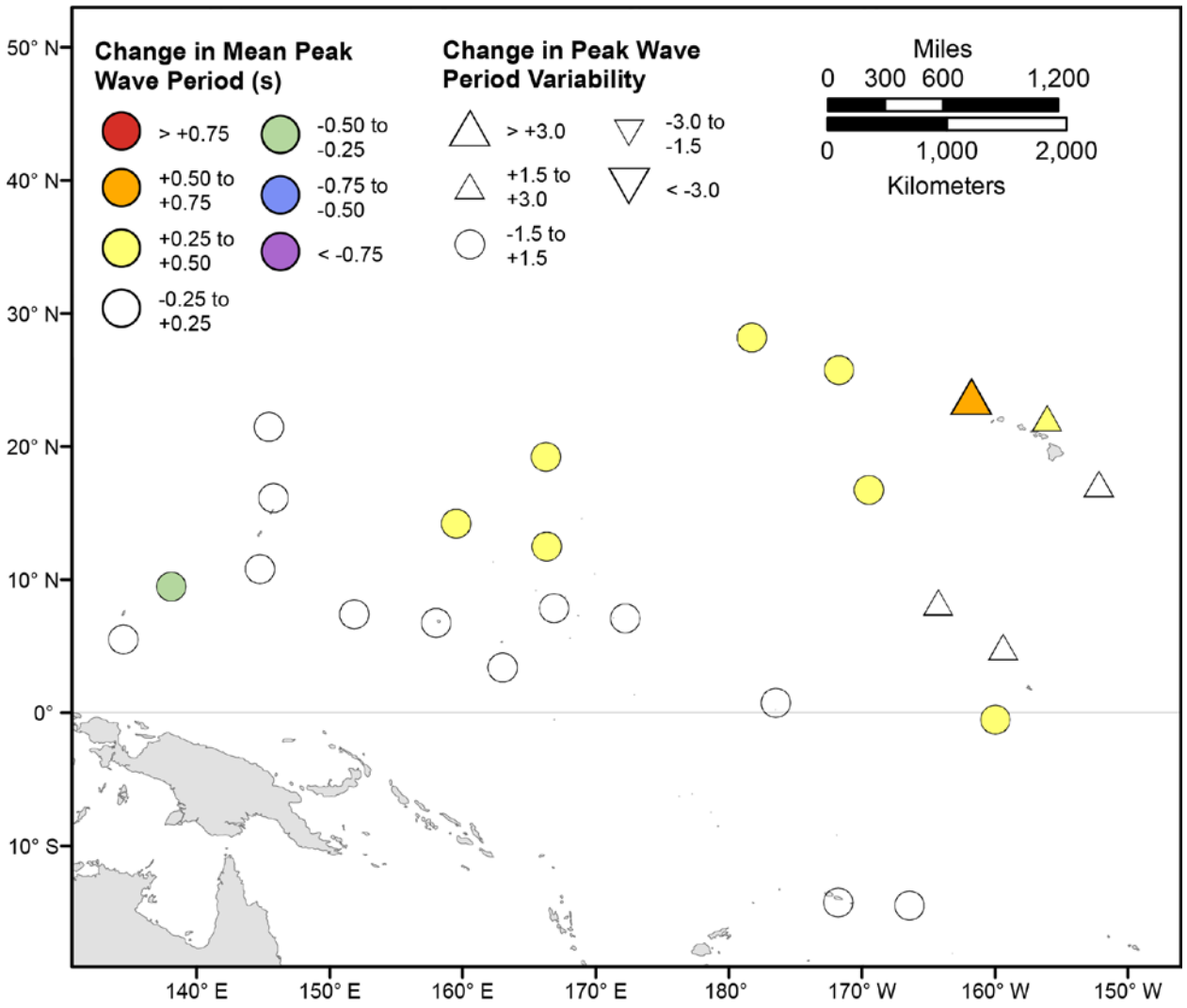

Figure 60. Map showing forecasted differences in the mean peak wave period of the top 5 percent of significant wave heights and variance in the peak wave period of top 5 percent of significant wave heights for the years 2081–2100 from hindcasted values during the June-August season under the RCP4.5 future climatic scenario. The colors correspond to the magnitude of change in modeled mean peak wave periods during 2081–2100 from those hindcasted for 1976–2005. The shapes correspond to the magnitude of change in modeled variance in peak wave period during 2081–2100 from those hindcasted for 1976–2005. Units are in seconds.

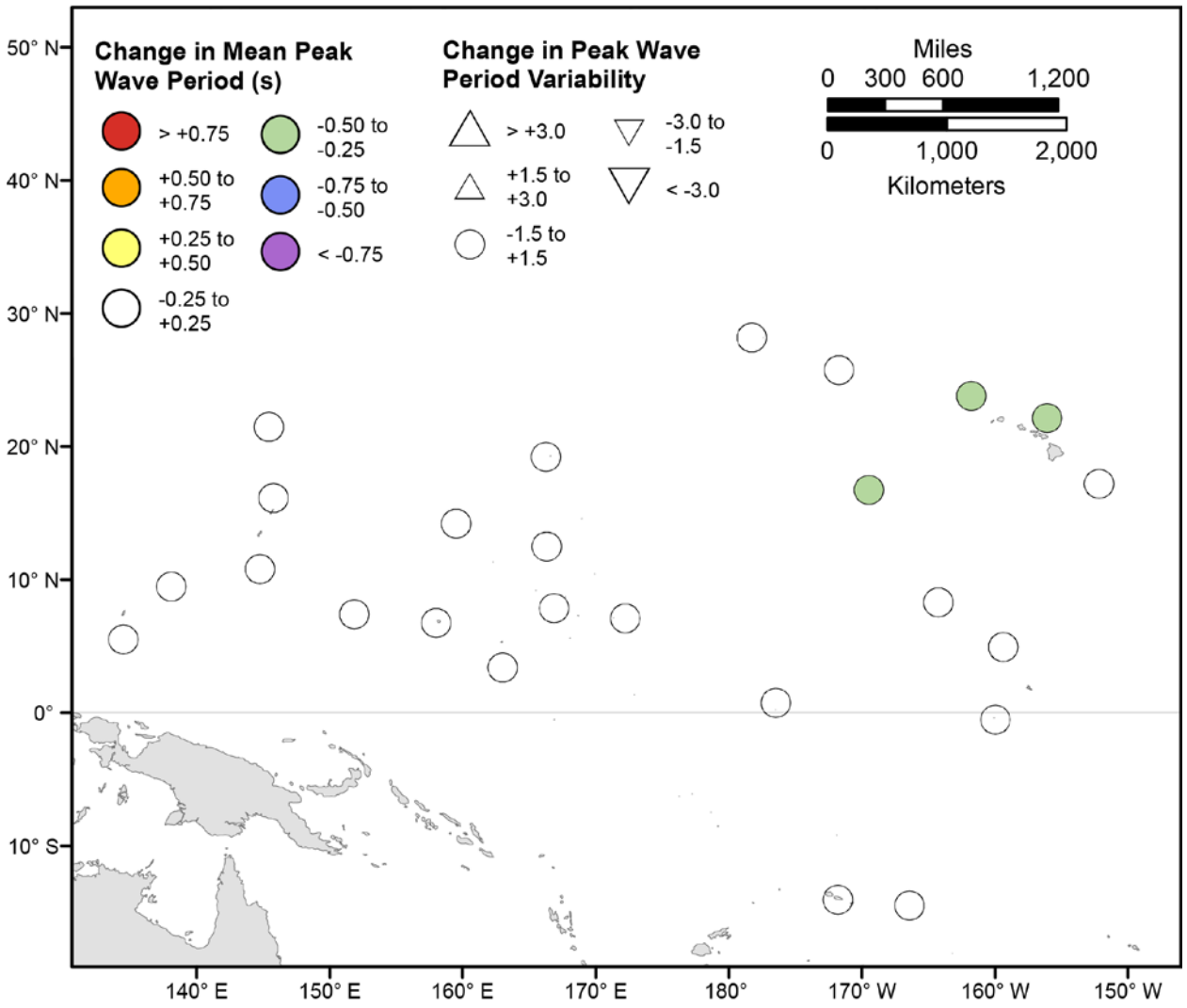

Figure 61. Map showing forecasted differences in the mean peak wave period of the top 5 percent of significant wave heights and variance in the peak wave period of top 5 percent of significant wave heights for the years 2081–2100 from hindcasted values during the September-November season under the RCP4.5 future climatic scenario. The colors correspond to the magnitude of change in modeled mean peak wave periods during 2081–2100 from those hindcasted for 1976–2005. The shapes correspond to the magnitude of change in modeled variance in peak wave period during 2081–2100 from those hindcasted for 1976–2005. Units are in seconds.

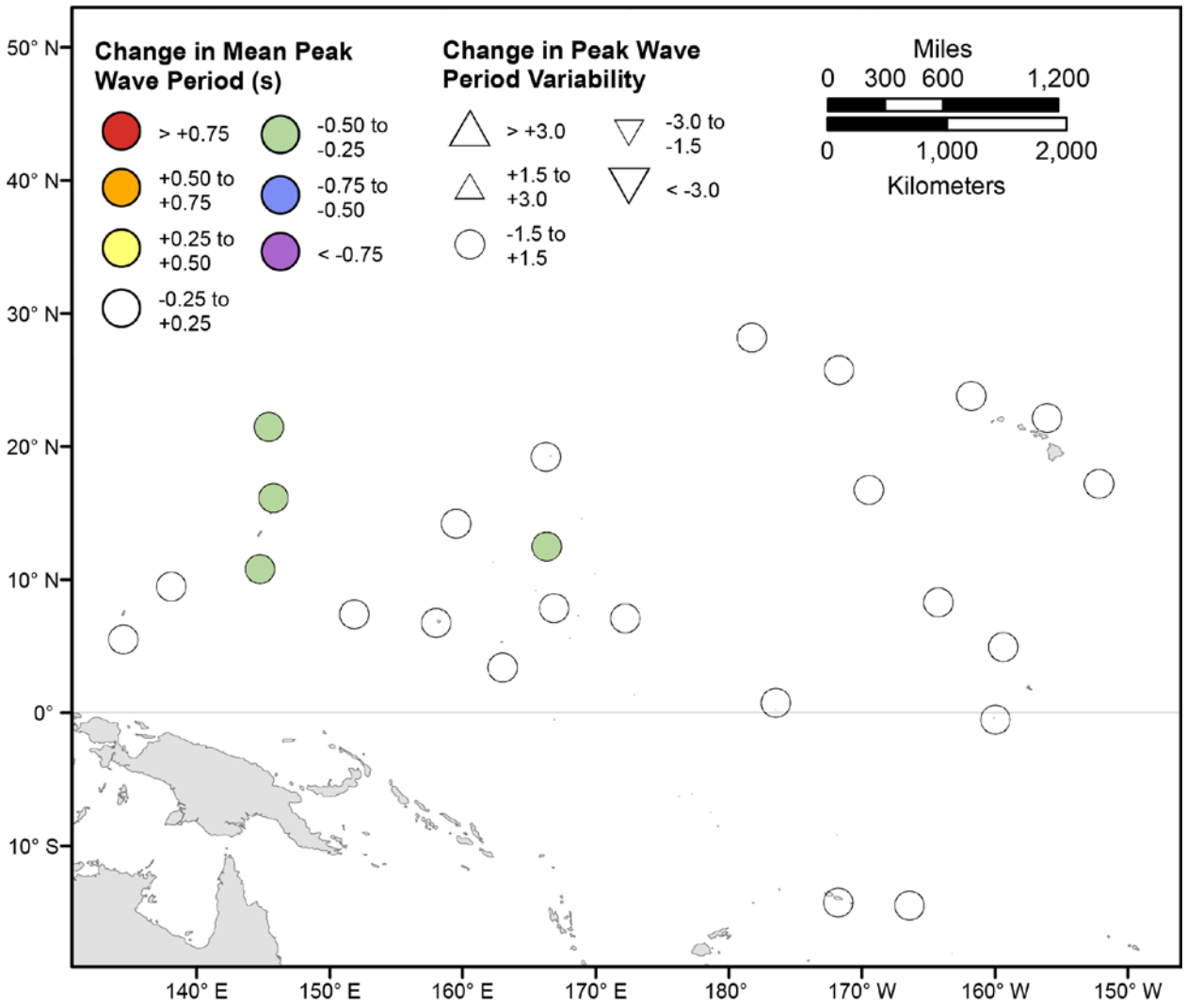

Figure 62. Map showing forecasted differences in mean peak wave period and variance in peak wave period for the years 2081–2100 from hindcasted values during the December-February season under the RCP8.5 future climatic scenario. The colors correspond to the magnitude of change in modeled mean peak wave periods during 2081–2100 from those hindcasted for 1976–2005. The shapes correspond to the magnitude of change in modeled variance in peak wave period during 2081–2100 from those hindcasted for 1976–2005. Units are in seconds.

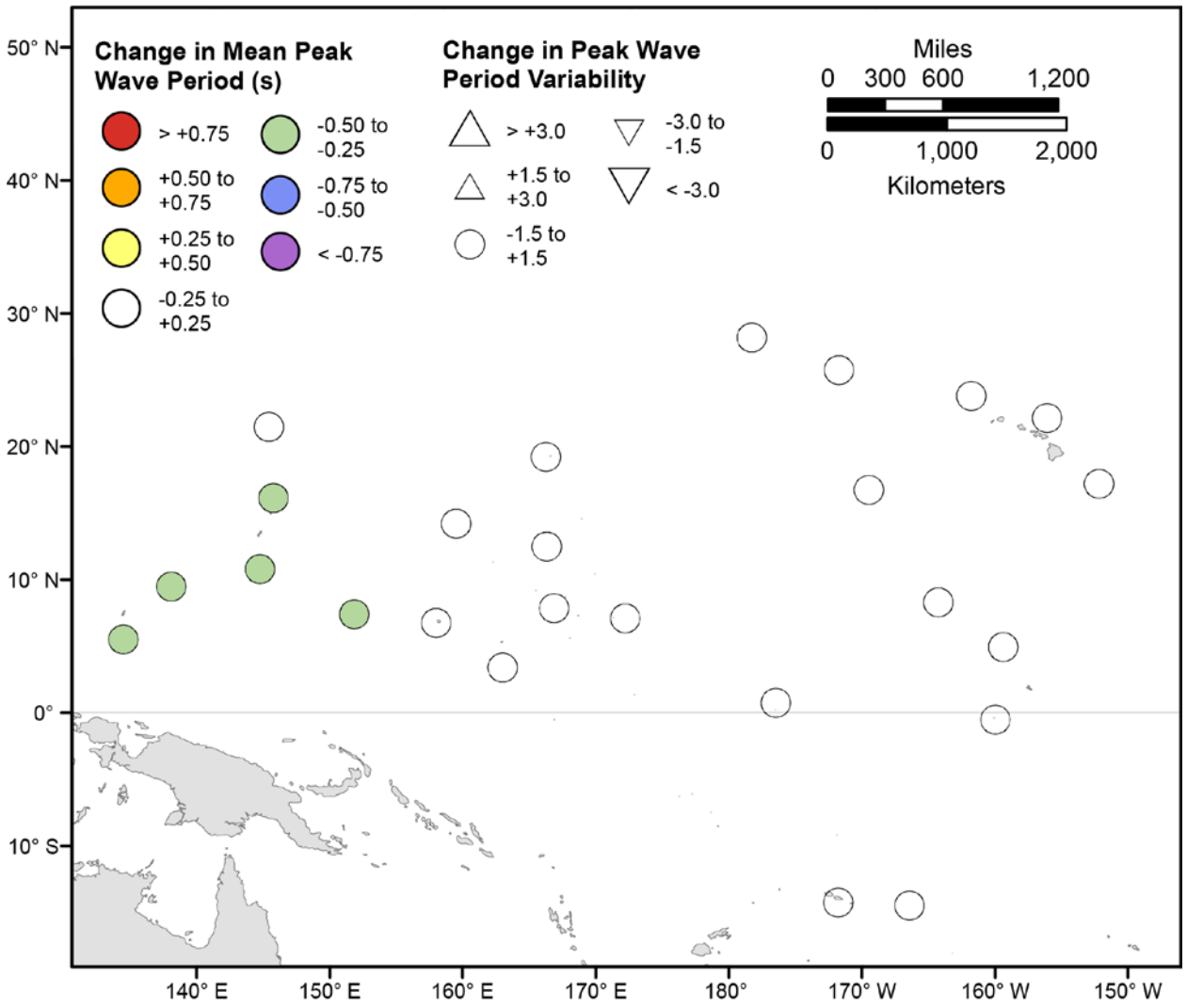

Figure 63. Map showing forecasted differences in mean peak wave period and variance in peak wave period for the years 2081–2100 from hindcasted values during the March-May season under the RCP8.5 future climatic scenario. The colors correspond to the magnitude of change in modeled mean peak wave periods during 2081–2100 from those hindcasted for 1976–2005. The shapes correspond to the magnitude of change in modeled variance in peak wave period during 2081–2100 from those hindcasted for 1976–2005. Units are in seconds.

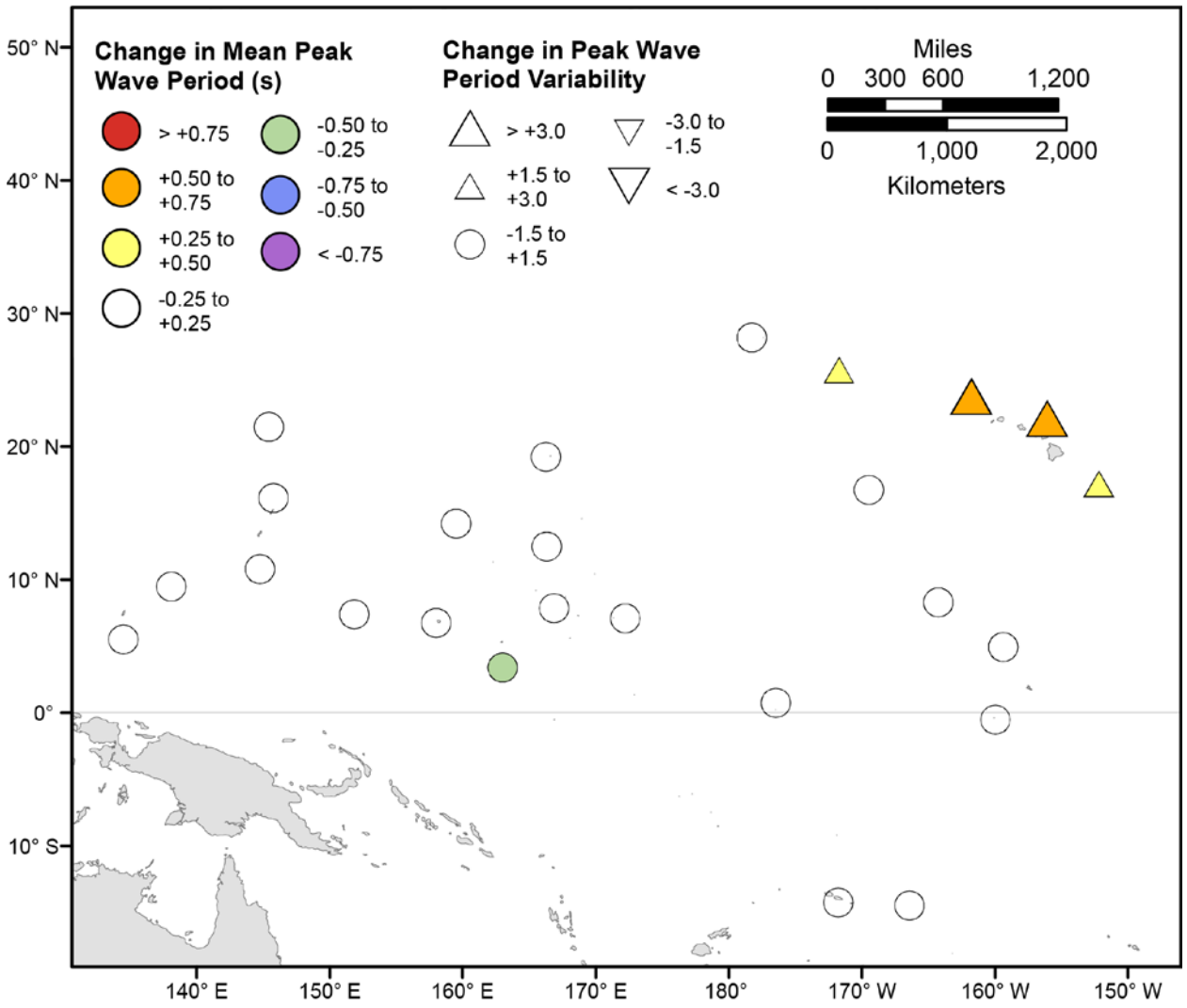

Figure 64. Map showing forecasted differences in mean peak wave period and variance in peak wave period for the years 2081–2100 from hindcasted values during the June-August season under the RCP8.5 future climatic scenario. The colors correspond to the magnitude of change in modeled mean peak wave periods during 2081–2100 from those hindcasted for 1976–2005. The shapes correspond to the magnitude of change in modeled variance in peak wave period during 2081–2100 from those hindcasted for 1976–2005. Units are in seconds.

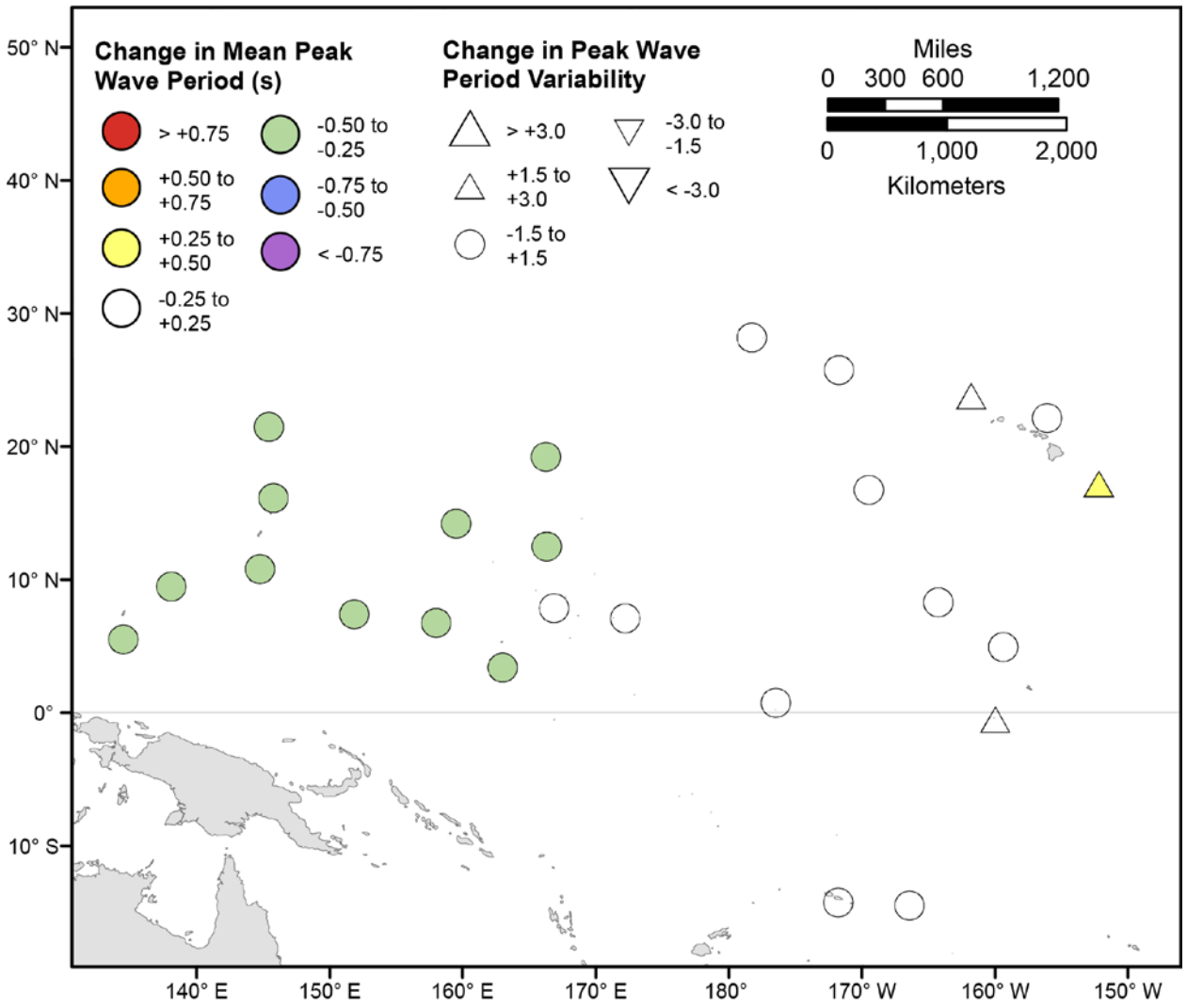

Figure 65. Map showing forecasted differences in mean peak wave period and variance in peak wave period for the years 2081–2100 from hindcasted values during the September-November season under the RCP8.5 future climatic scenario. The colors correspond to the magnitude of change in modeled mean peak wave periods during 2081–2100 from those hindcasted for 1976–2005. The shapes correspond to the magnitude of change in modeled variance in peak wave period during 2081–2100 from those hindcasted for 1976–2005. Units are in seconds.

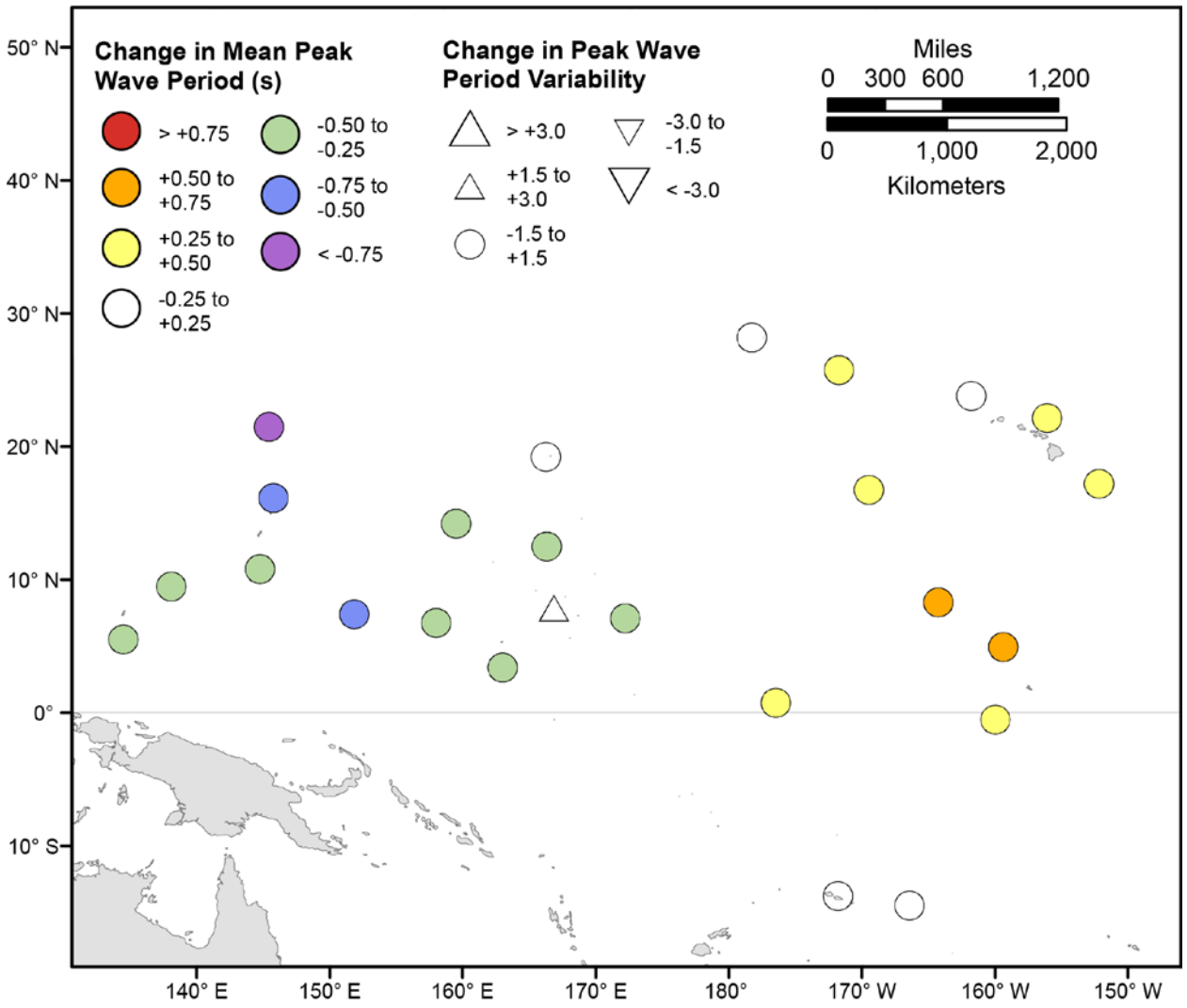

Figure 66. Map showing forecasted differences in the mean peak wave period of the top 5 percent of significant wave heights and variance in the peak wave period of top 5 percent of significant wave heights for the years 2081–2100 from hindcasted values during the December-February season under the RCP8.5 future climatic scenario. The colors correspond to the magnitude of change in modeled mean peak wave periods during 2081–2100 from those hindcasted for 1976–2005. The shapes correspond to the magnitude of change in modeled variance in peak wave period during 2081–2100 from those hindcasted for 1976–2005. Units are in seconds.

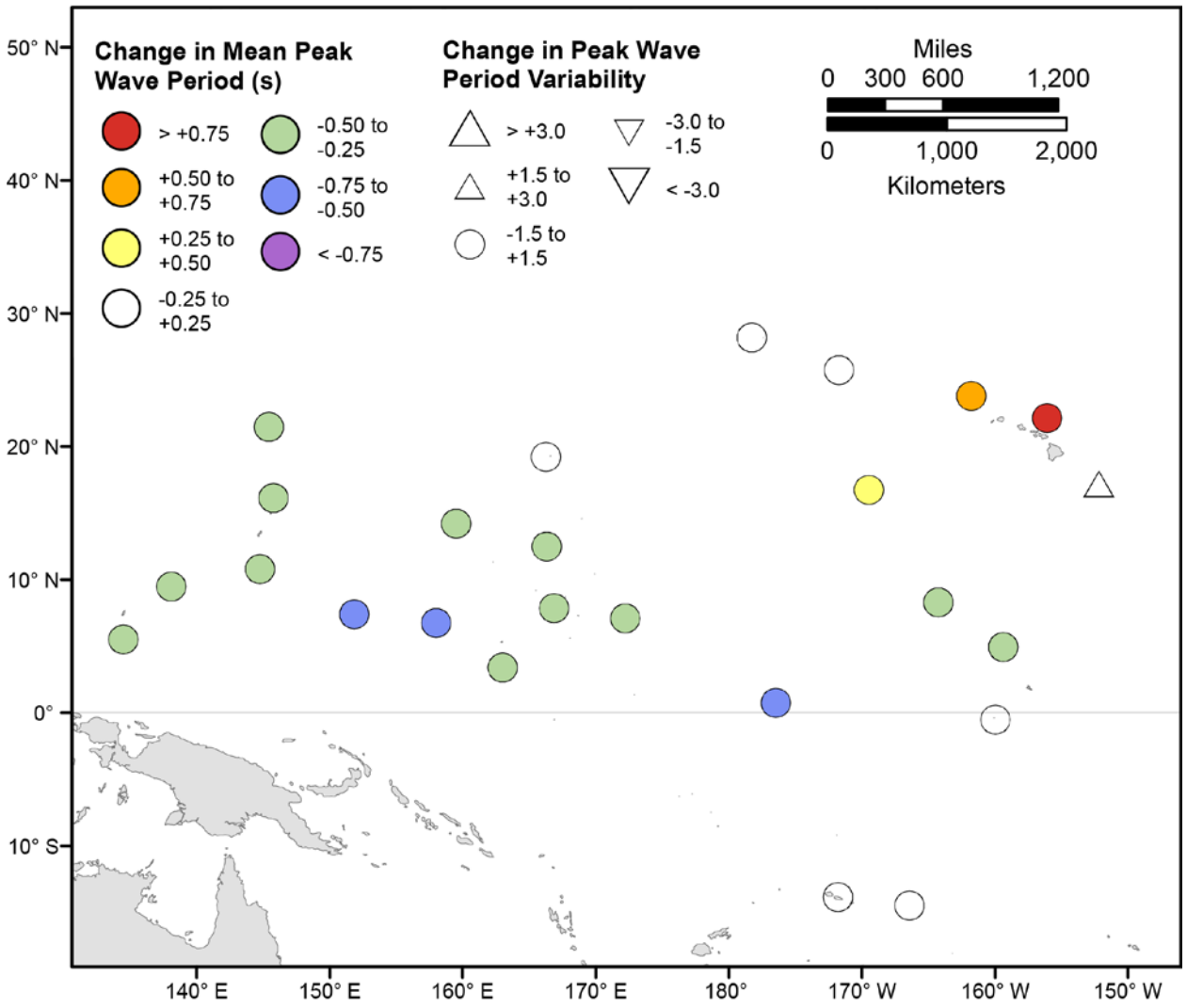

Figure 67. Map showing forecasted differences in the mean peak wave period of the top 5 percent of significant wave heights and variance in the peak wave period of top 5 percent of significant wave heights for the years 2081–2100 from hindcasted values during the March-May season under the RCP8.5 future climatic scenario. The colors correspond to the magnitude of change in modeled mean peak wave periods during 2081–2100 from those hindcasted for 1976–2005. The shapes correspond to the magnitude of change in modeled variance in peak wave period during 2081–2100 from those hindcasted for 1976–2005. Units are in seconds.

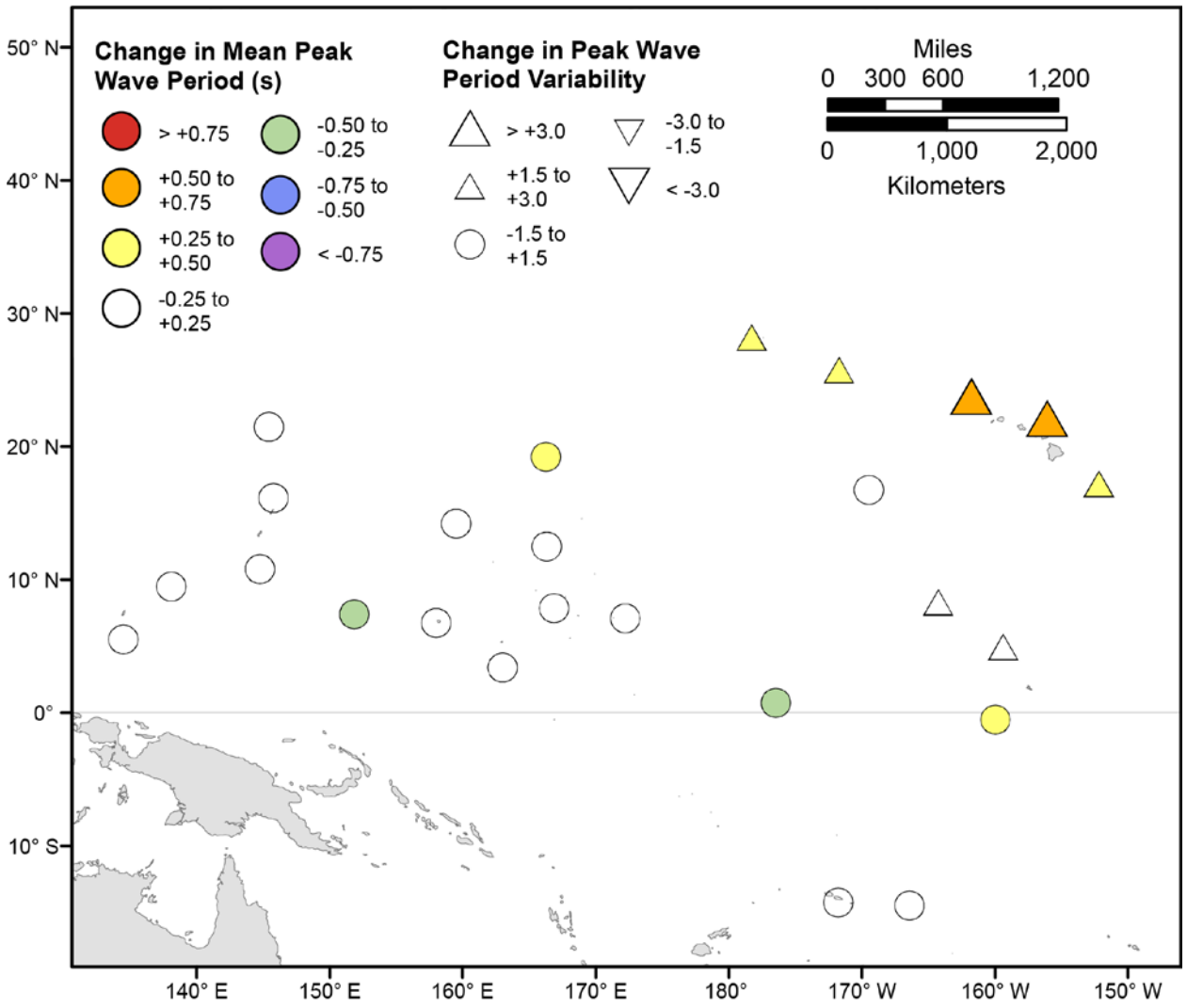

Figure 68. Map showing forecasted differences in the mean peak wave period of the top 5 percent of significant wave heights and variance in the peak wave period of top 5 percent of significant wave heights for the years 2081–2100 from hindcasted values during the June-August season under the RCP8.5 future climatic scenario. The colors correspond to the magnitude of change in modeled mean peak wave periods during 2081–2100 from those hindcasted for 1976–2005. The shapes correspond to the magnitude of change in modeled variance in peak wave period during 2081–2100 from those hindcasted for 1976–2005. Units are in seconds.

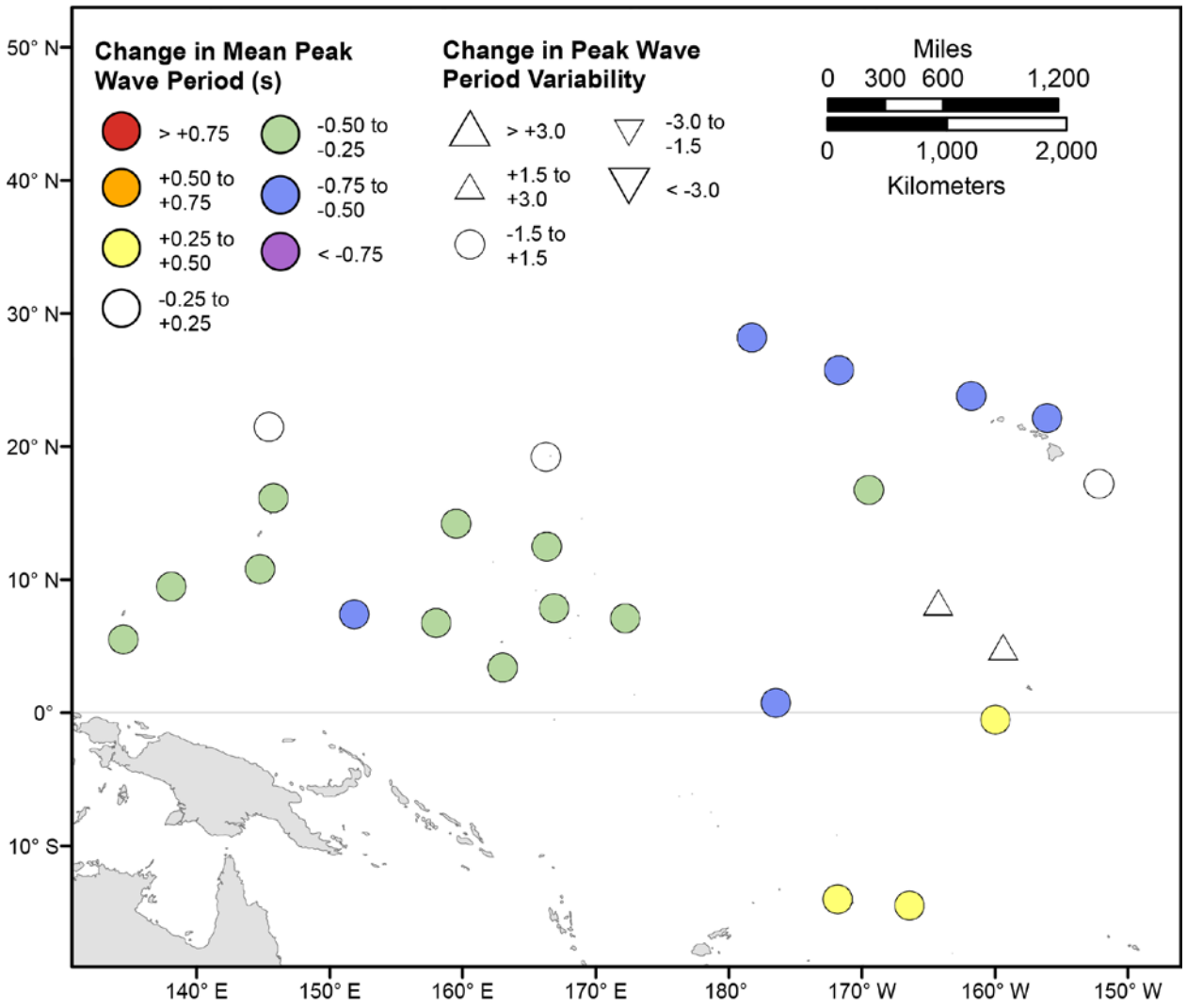

Figure 69. Map showing forecasted differences in the mean peak wave period of the top 5 percent of significant wave heights and variance in the peak wave period of top 5 percent of significant wave heights for the years 2081–2100 from hindcasted values during the September-November season under the RCP8.5 future climatic scenario. The colors correspond to the magnitude of change in modeled mean peak wave periods during 2081–2100 from those hindcasted for 1976–2005. The shapes correspond to the magnitude of change in modeled variance in peak wave period during 2081–2100 from those hindcasted for 1976–2005. Units are in seconds.

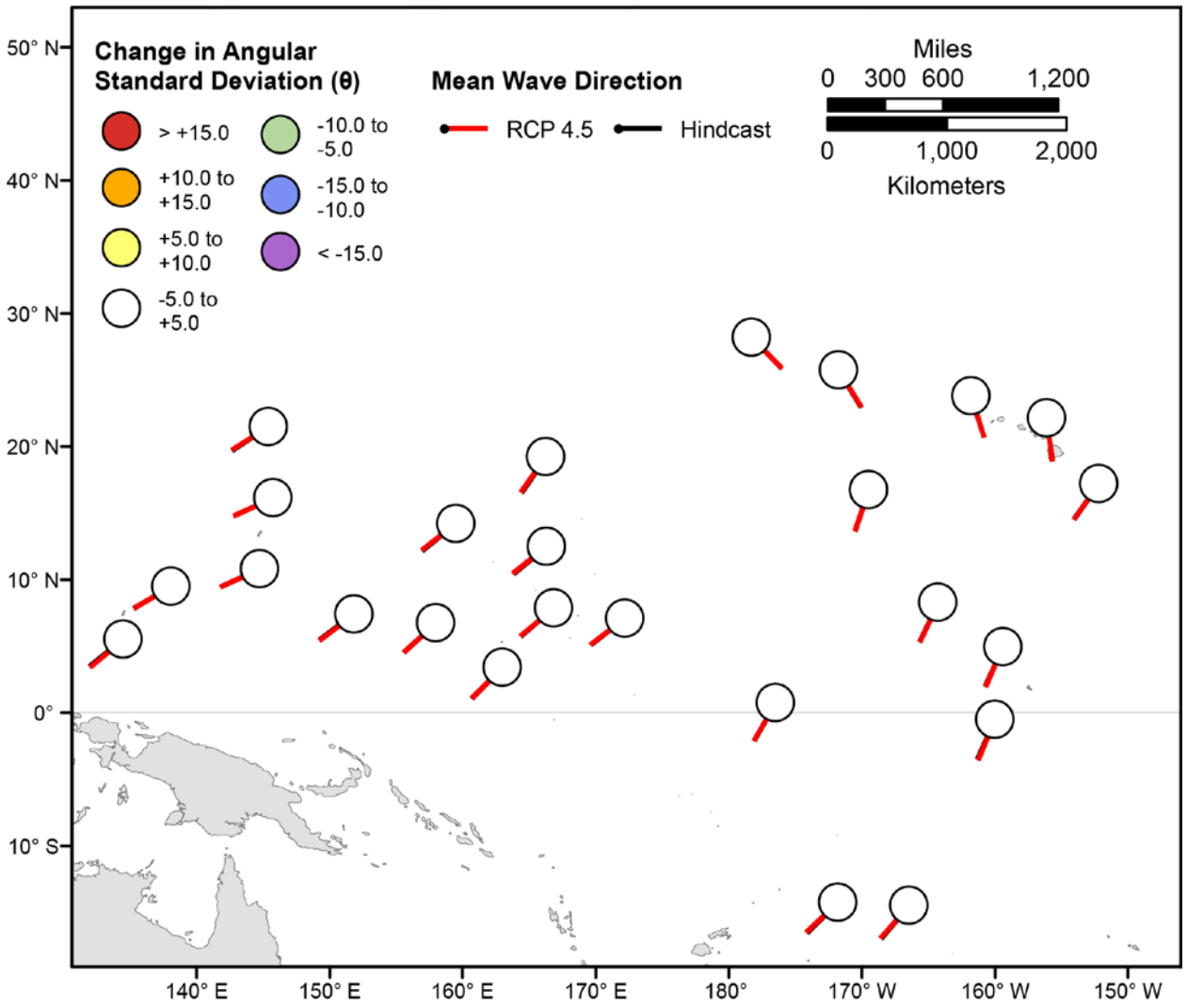

Figure 70. Map showing forecasted differences in the mean wave directions of significant wave heights and the standard deviation of wave directions of significant wave heights for the years 2026–2045 from hindcasted values during the December-February season under the RCP4.5 future climatic scenario. Mean wave directions at each point are indicated by lines radiating from the center of each point where RCP 2026–2045 mean wave directions are red and 1976–2005 hindcasted mean wave directions are black. The colors correspond to the magnitude of change in modeled mean wave direction standard deviation during 2026–2045 from those hindcasted for 1976–2005. Angular standard deviation units are in degrees. Mean wave directions are “heading towards”.

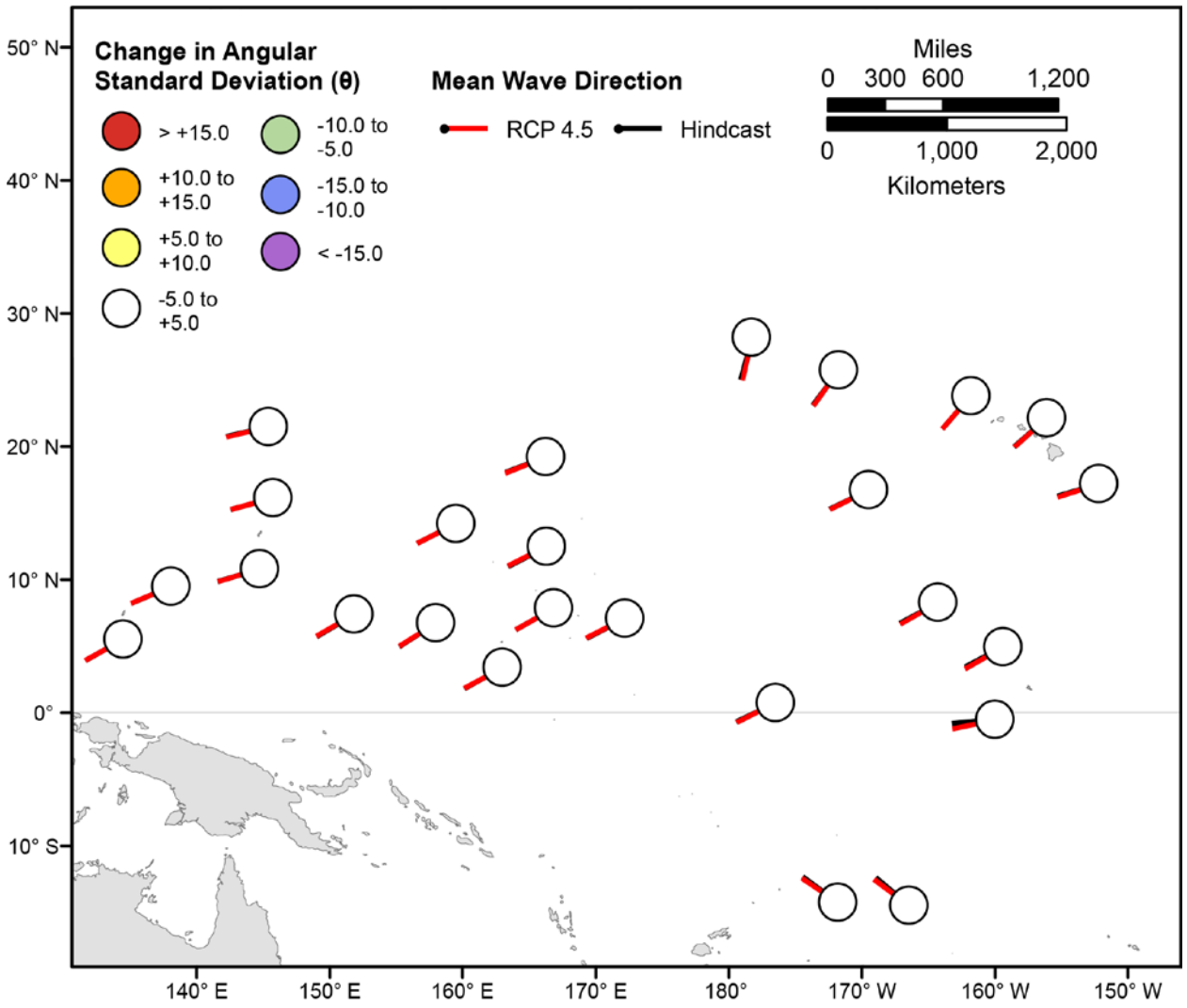

Figure 71. Map showing forecasted differences in the mean wave directions of significant wave heights and the standard deviation of wave directions of significant wave heights for the years 2026–2045 from hindcasted values during the March-May season under the RCP4.5 future climatic scenario. Mean wave directions at each point are indicated by lines radiating from the center of each point where RCP 2026–2045 mean wave directions are red and 1976–2005 hindcasted mean wave directions are black. The colors correspond to the magnitude of change in modeled mean wave direction standard deviation during 2026–2045 from those hindcasted for 1976–2005. Angular standard deviation units are in degrees. Mean wave directions are “heading towards”.

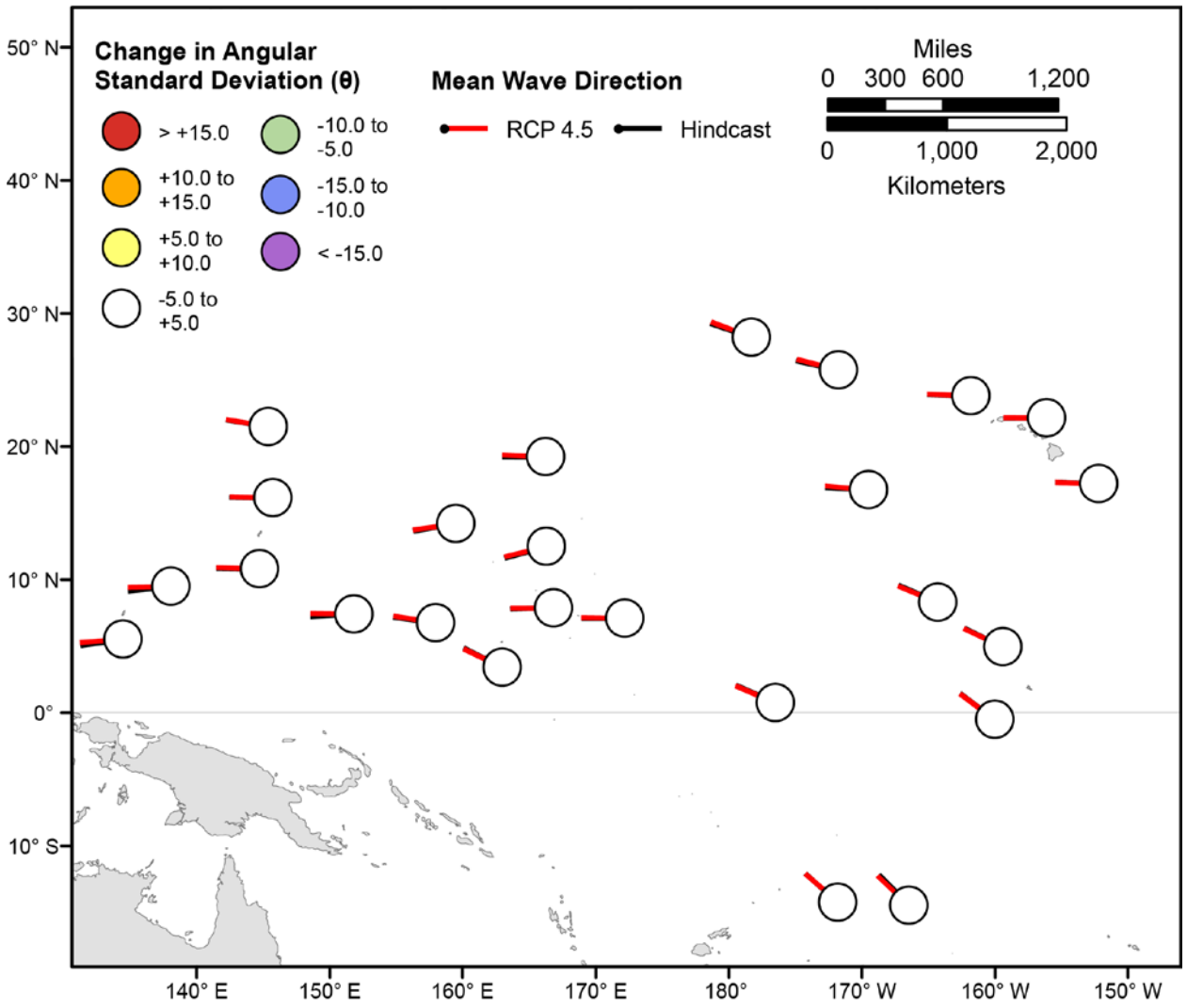

Figure 72. Map showing forecasted differences in the mean wave directions of significant wave heights and the standard deviation of wave directions of significant wave heights for the years 2026–2045 from hindcasted values during the June-July season under the RCP4.5 future climatic scenario. Mean wave directions at each point are indicated by lines radiating from the center of each point where RCP 2026–2045 mean wave directions are red and 1976–2005 hindcasted mean wave directions are black. The colors correspond to the magnitude of change in modeled mean wave direction standard deviation during 2026–2045 from those hindcasted for 1976–2005. Angular standard deviation units are in degrees. Mean wave directions are “heading towards”.

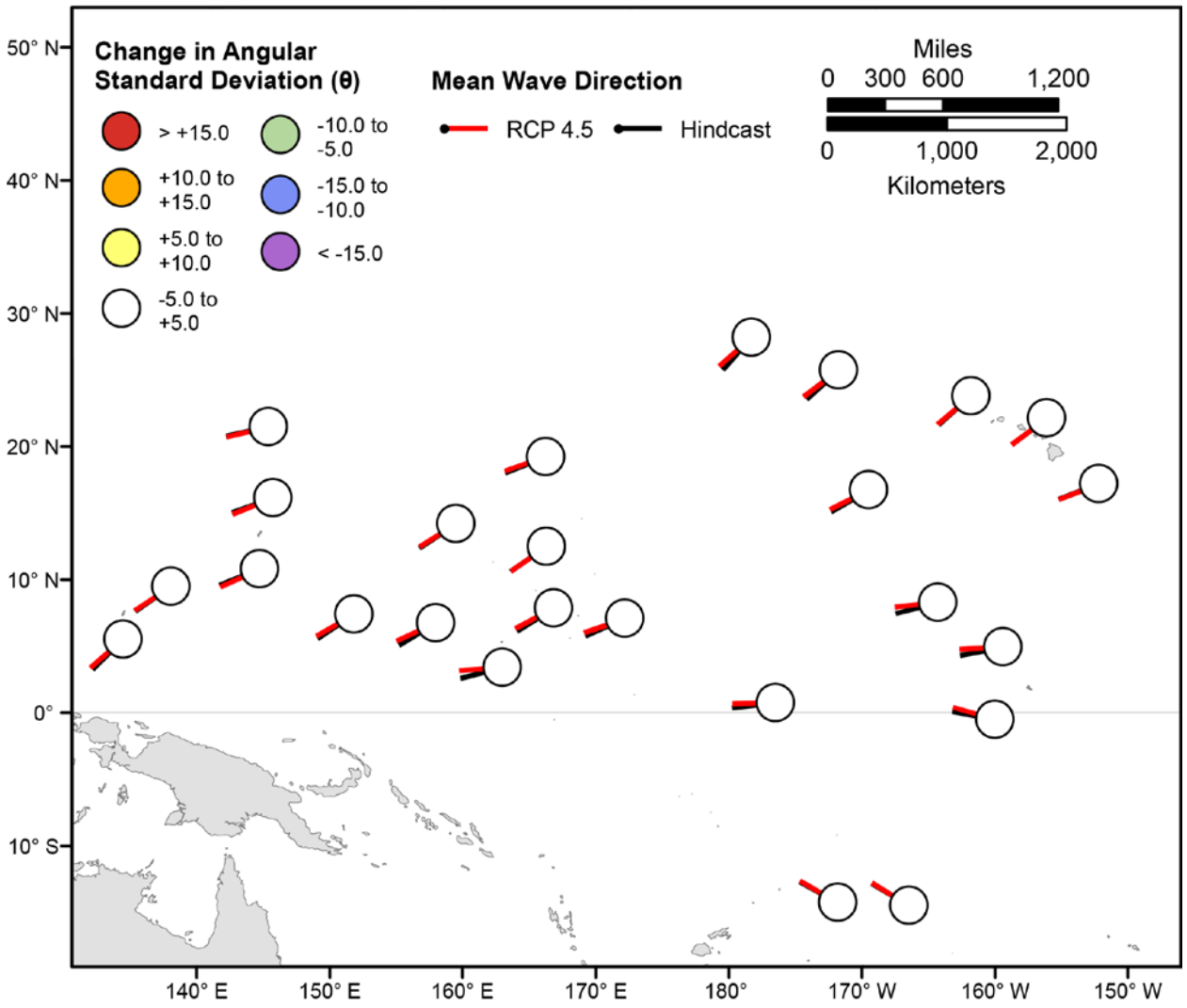

Figure 73. Map showing forecasted differences in the mean wave directions of significant wave heights and the standard deviation of wave directions of significant wave heights for the years 2026–2045 from hindcasted values during the September-November season under the RCP4.5 future climatic scenario. Mean wave directions at each point are indicated by lines radiating from the center of each point where RCP 2026–2045 mean wave directions are red and 1976–2005 hindcasted mean wave directions are black. The colors correspond to the magnitude of change in modeled mean wave direction standard deviation during 2026–2045 from those hindcasted for 1976–2005. Angular standard deviation units are in degrees. Mean wave directions are “heading towards”.

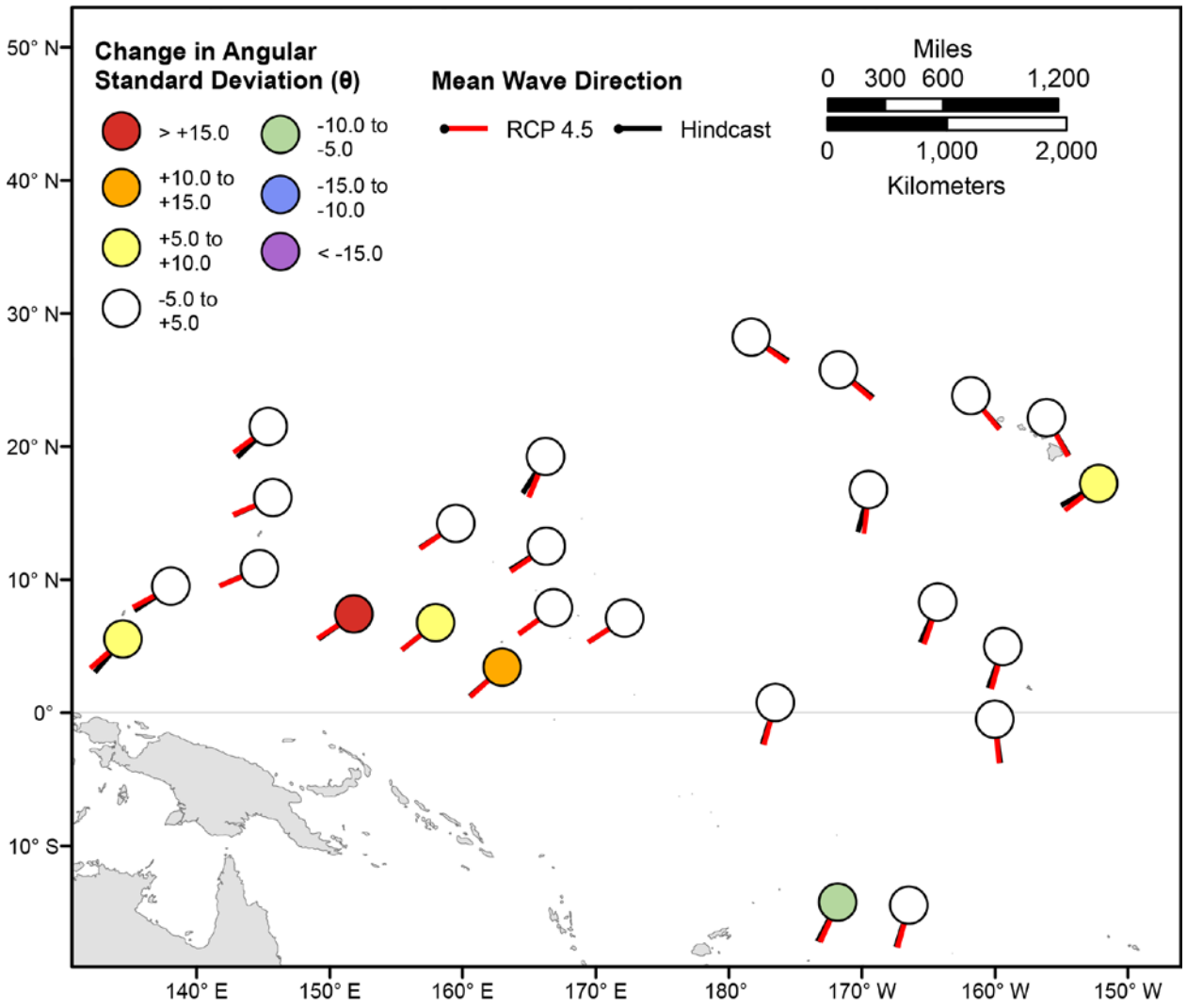

Figure 74. Map showing forecasted differences in the mean wave directions of the top 5 percent of significant wave heights and the standard deviation of wave directions of the top 5 percent of significant wave heights for the years 2026–2045 from hindcasted values during the December-February season under the RCP4.5 future climatic scenario. Mean wave directions at each point are indicated by lines radiating from the center of each point where RCP 2026–2045 mean wave directions are red and 1976–2005 hindcasted mean wave directions are black. The colors correspond to the magnitude of change in modeled mean wave direction standard deviation during 2026–2045 from those hindcasted for 1976–2005. Angular standard deviation units are in degrees. Mean wave directions are “heading towards”.

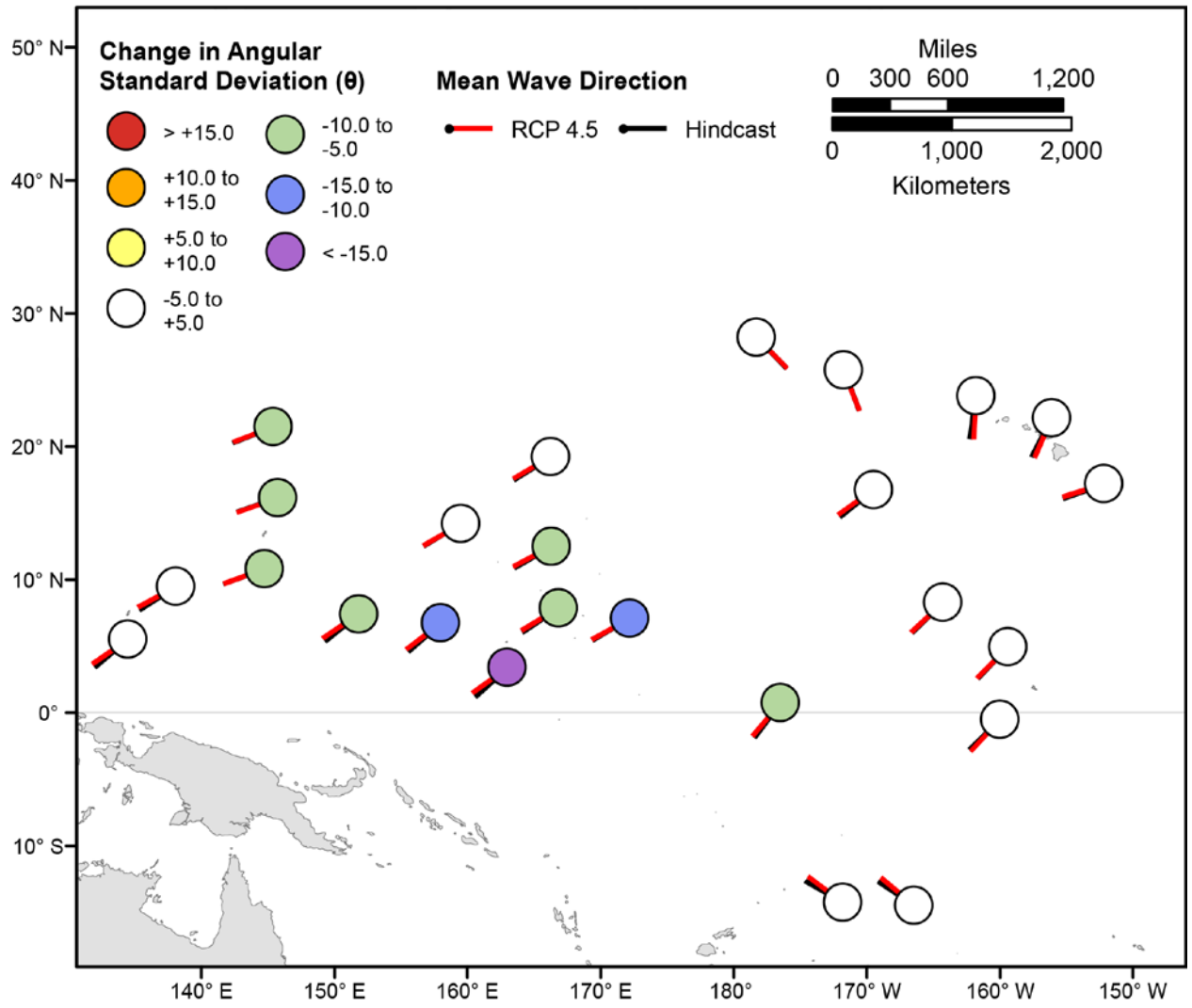

Figure 75. Map showing forecasted differences in the mean wave directions of the top 5 percent of significant wave heights and the standard deviation of wave directions of the top 5 percent of significant wave heights for the years 2026–2045 from hindcasted values during the March-May season under the RCP4.5 future climatic scenario. Mean wave directions at each point are indicated by lines radiating from the center of each point where RCP 2026–2045 mean wave directions are red and 1976–2005 hindcasted mean wave directions are black. The colors correspond to the magnitude of change in modeled mean wave direction standard deviation during 2026–2045 from those hindcasted for 1976–2005. Angular standard deviation units are in degrees. Mean wave directions are “heading towards”.

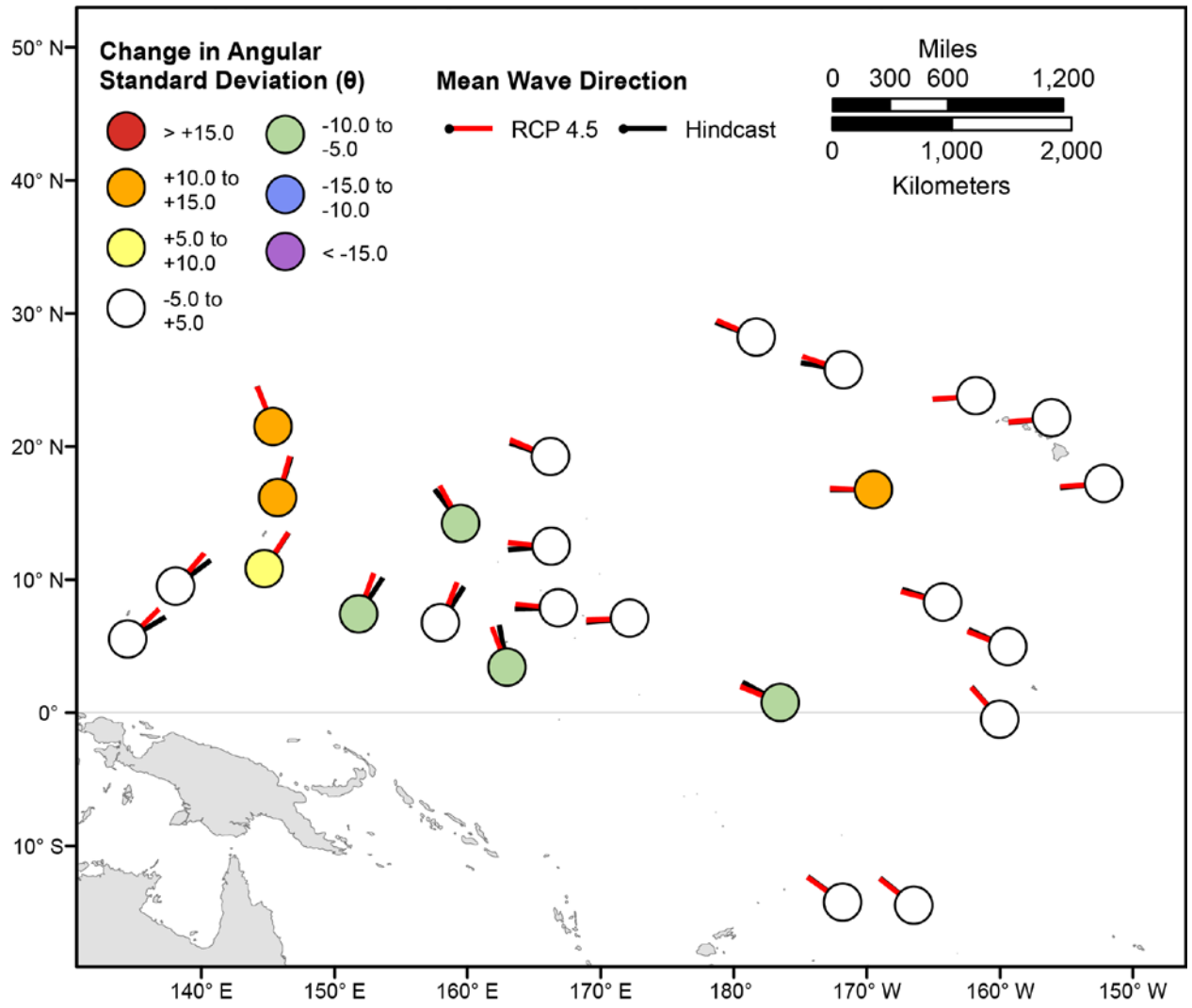

Figure 76. Map showing forecasted differences in the mean wave directions of the top 5 percent of significant wave heights and the standard deviation of wave directions of the top 5 percent of significant wave heights for the years 2026–2045 from hindcasted values during the June-August season under the RCP4.5 future climatic scenario. Mean wave directions at each point are indicated by lines radiating from the center of each point where RCP 2026–2045 mean wave directions are red and 1976–2005 hindcasted mean wave directions are black. The colors correspond to the magnitude of change in modeled mean wave direction standard deviation during 2026–2045 from those hindcasted for 1976–2005. Angular standard deviation units are in degrees. Mean wave directions are “heading towards”.

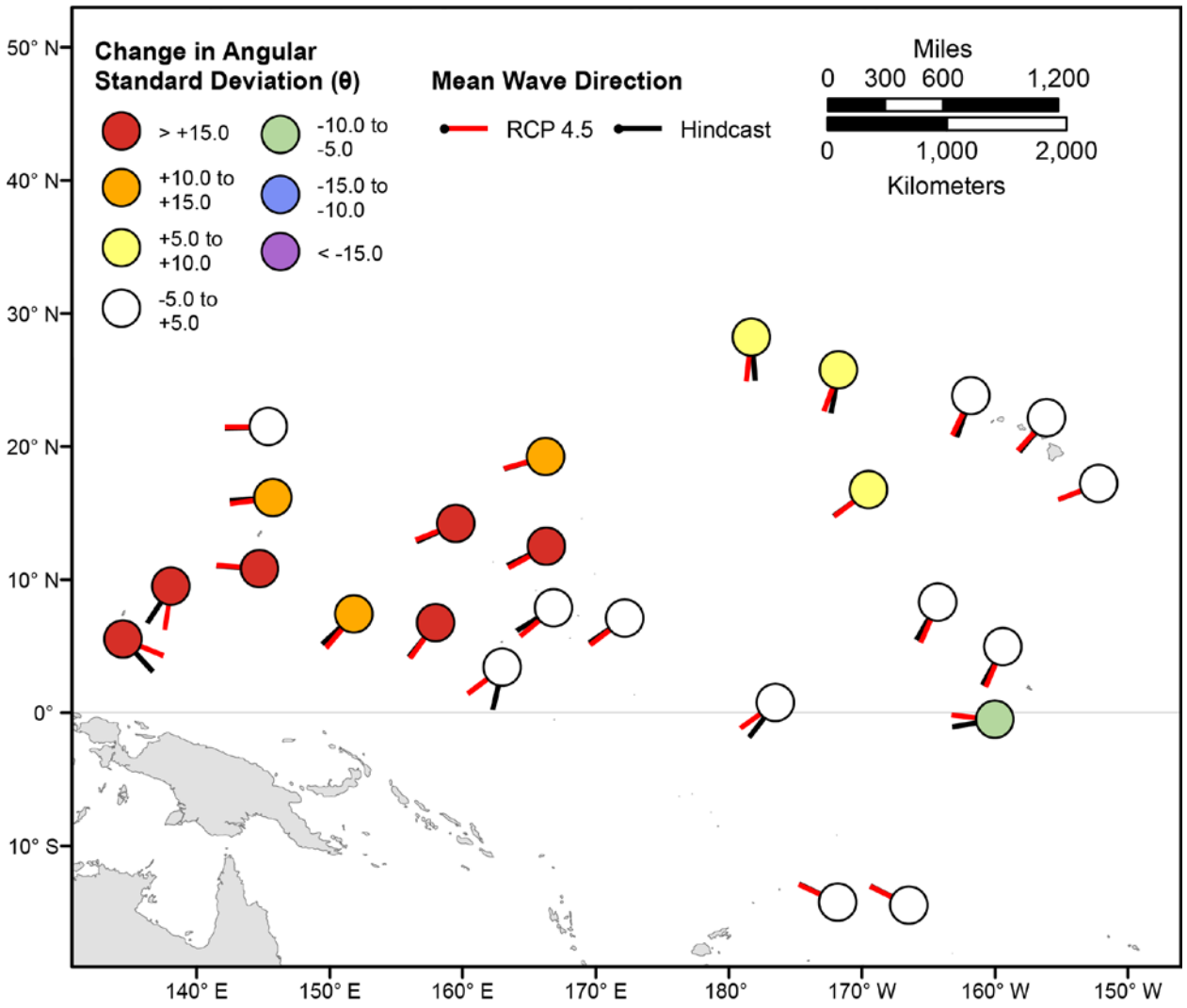

Figure 77. Map showing forecasted differences in the mean wave directions of the top 5 percent of significant wave heights and the standard deviation of wave directions of the top 5 percent of significant wave heights for the years 2026–2045 from hindcasted values during the September-November season under the RCP4.5 future climatic scenario. Mean wave directions at each point are indicated by lines radiating from the center of each point where RCP 2026–2045 mean wave directions are red and 1976–2005 hindcasted mean wave directions are black. The colors correspond to the magnitude of change in modeled mean wave direction standard deviation during 2026–2045 from those hindcasted for 1976–2005. Angular standard deviation units are in degrees. Mean wave directions are “heading towards”.

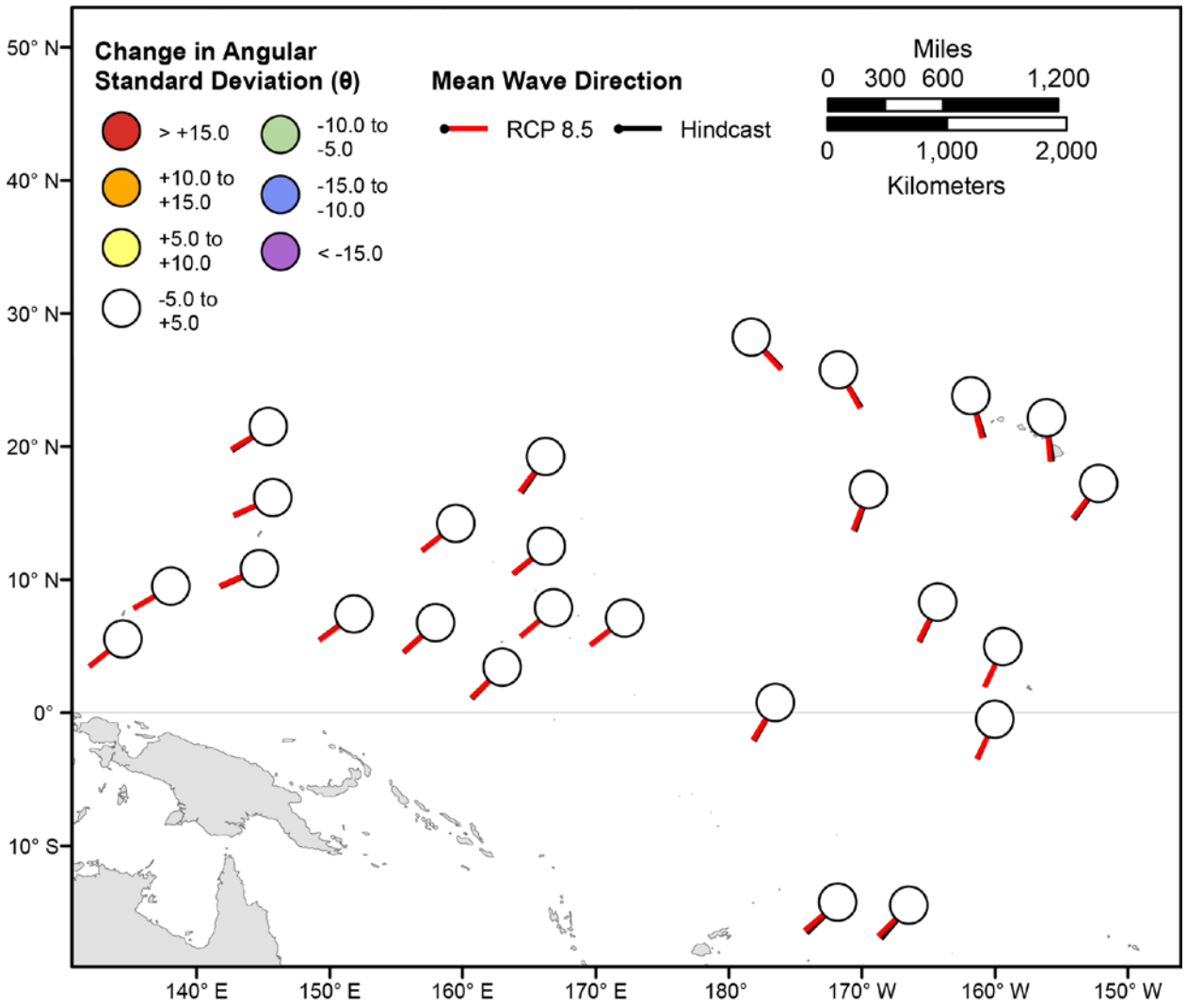

Figure 78. Map showing forecasted differences in the mean wave directions of significant wave heights and the standard deviation of wave directions of significant wave heights for the years 2026–2045 from hindcasted values during the December-February season under the RCP8.5 future climatic scenario. Mean wave directions at each point are indicated by lines radiating from the center of each point where RCP 2026–2045 mean wave directions are red and 1976–2005 hindcasted mean wave directions are black. The colors correspond to the magnitude of change in modeled mean wave direction standard deviation during 2026–2045 from those hindcasted for 1976–2005. Angular standard deviation units are in degrees. Mean wave directions are “heading towards”.

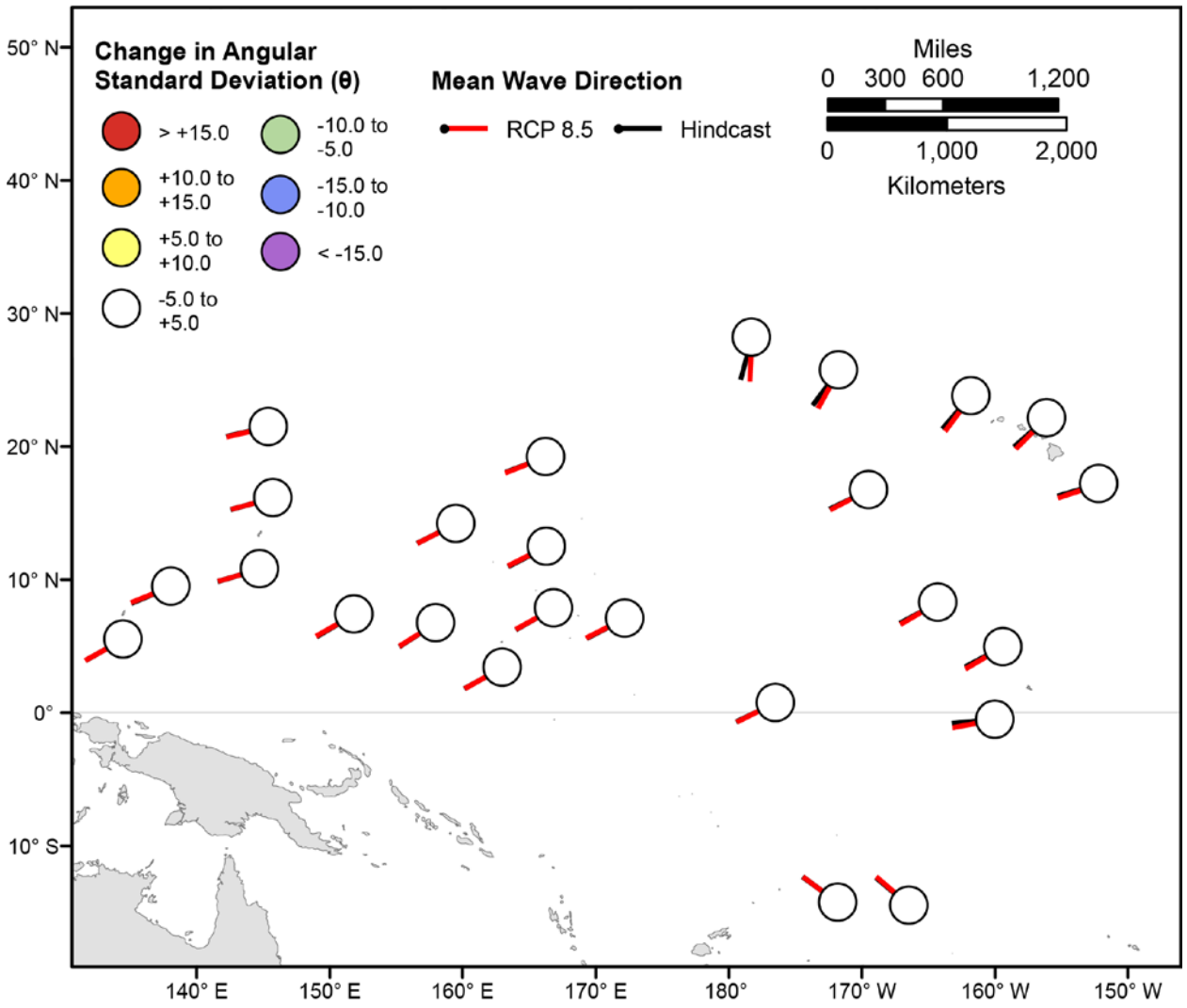

Figure 79. Map showing forecasted differences in the mean wave directions of significant wave heights and the standard deviation of wave directions of significant wave heights for the years 2026–2045 from hindcasted values during the March-May season under the RCP8.5 future climatic scenario. Mean wave directions at each point are indicated by lines radiating from the center of each point where RCP 2026–2045 mean wave directions are red and 1976–2005 hindcasted mean wave directions are black. The colors correspond to the magnitude of change in modeled mean wave direction standard deviation during 2026–2045 from those hindcasted for 1976–2005. Angular standard deviation units are in degrees. Mean wave directions are “heading towards”.

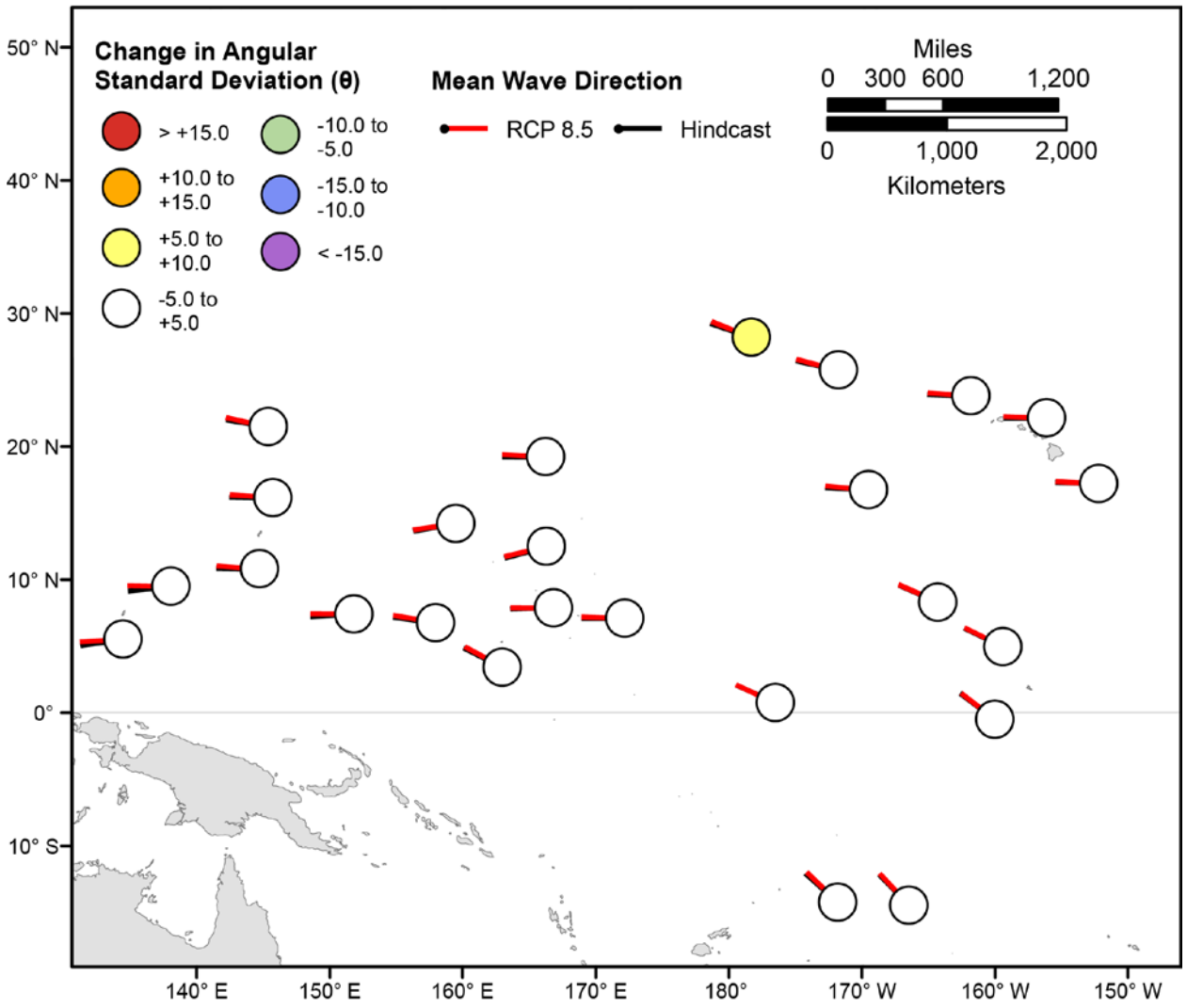

Figure 80. Map showing forecasted differences in the mean wave directions of significant wave heights and the standard deviation of wave directions of significant wave heights for the years 2026–2045 from hindcasted values during the June-July season under the RCP8.5 future climatic scenario. Mean wave directions at each point are indicated by lines radiating from the center of each point where RCP 2026–2045 mean wave directions are red and 1976–2005 hindcasted mean wave directions are black. The colors correspond to the magnitude of change in modeled mean wave direction standard deviation during 2026–2045 from those hindcasted for 1976–2005. Angular standard deviation units are in degrees. Mean wave directions are “heading towards”.

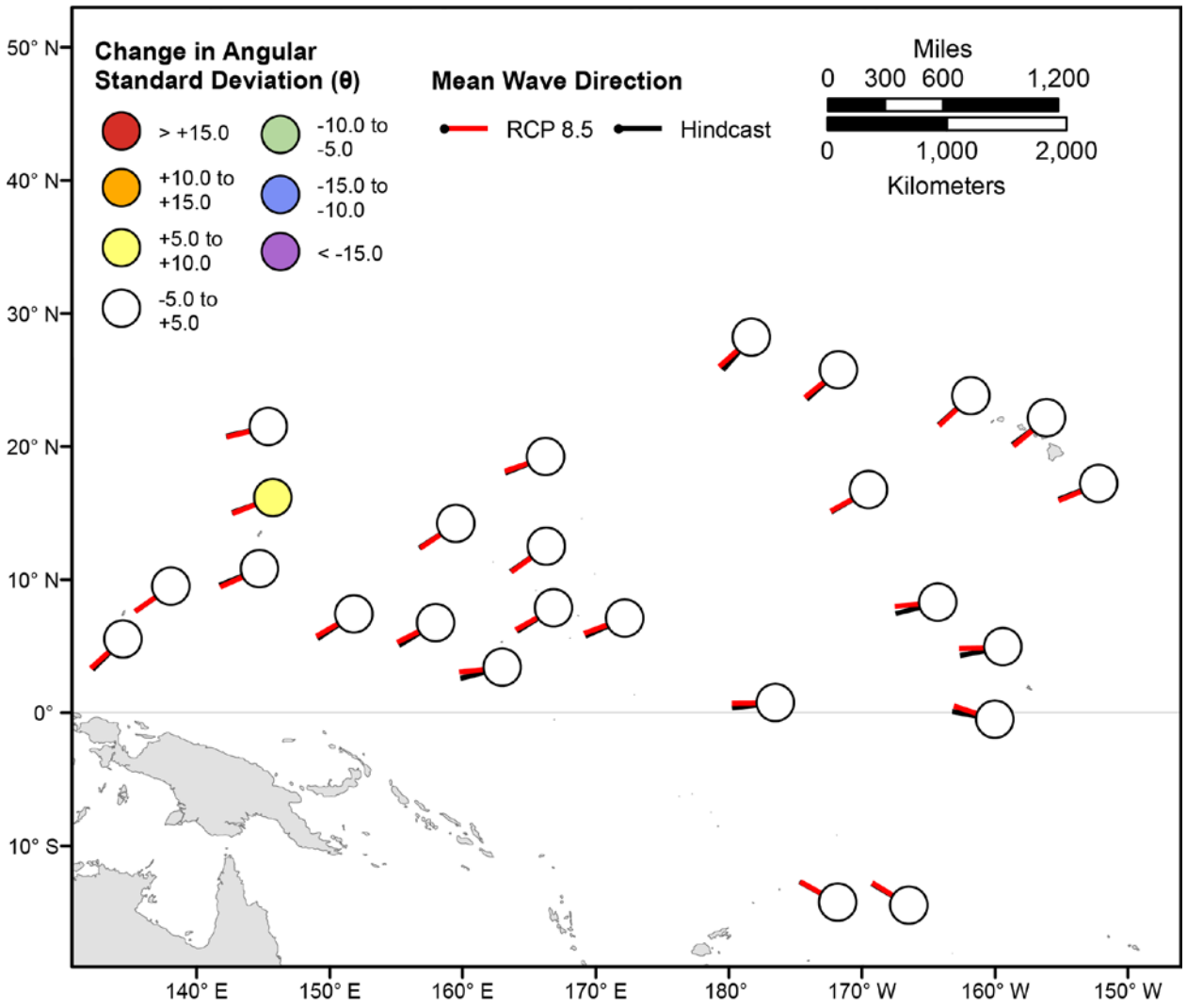

Figure 81. Map showing forecasted differences in the mean wave directions of significant wave heights and the standard deviation of wave directions of significant wave heights for the years 2026–2045 from hindcasted values during the September-November season under the RCP8.5 future climatic scenario. Mean wave directions at each point are indicated by lines radiating from the center of each point where RCP 2026–2045 mean wave directions are red and 1976–2005 hindcasted mean wave directions are black. The colors correspond to the magnitude of change in modeled mean wave direction standard deviation during 2026–2045 from those hindcasted for 1976–2005. Angular standard deviation units are in degrees. Mean wave directions are “heading towards”.

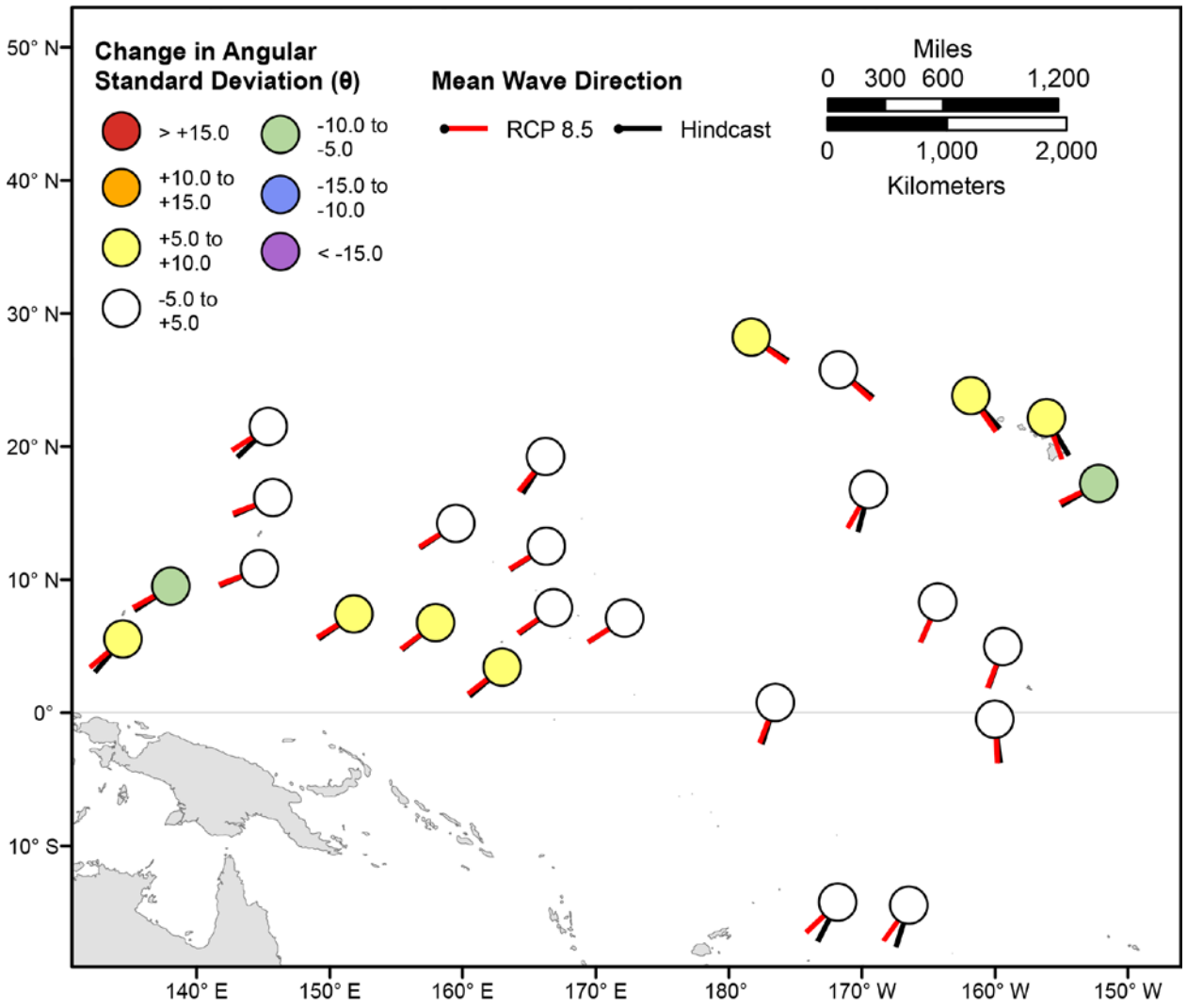

Figure 82. Map showing forecasted differences in the mean wave directions of the top 5 percent of significant wave heights and the standard deviation of wave directions of the top 5 percent of significant wave heights for the years 2026–2045 from hindcasted values during the December-February season under the RCP8.5 future climatic scenario. Mean wave directions at each point are indicated by lines radiating from the center of each point where RCP 2026–2045 mean wave directions are red and 1976–2005 hindcasted mean wave directions are black. The colors correspond to the magnitude of change in modeled mean wave direction standard deviation during 2026–2045 from those hindcasted for 1976–2005. Angular standard deviation units are in degrees. Mean wave directions are “heading towards”.

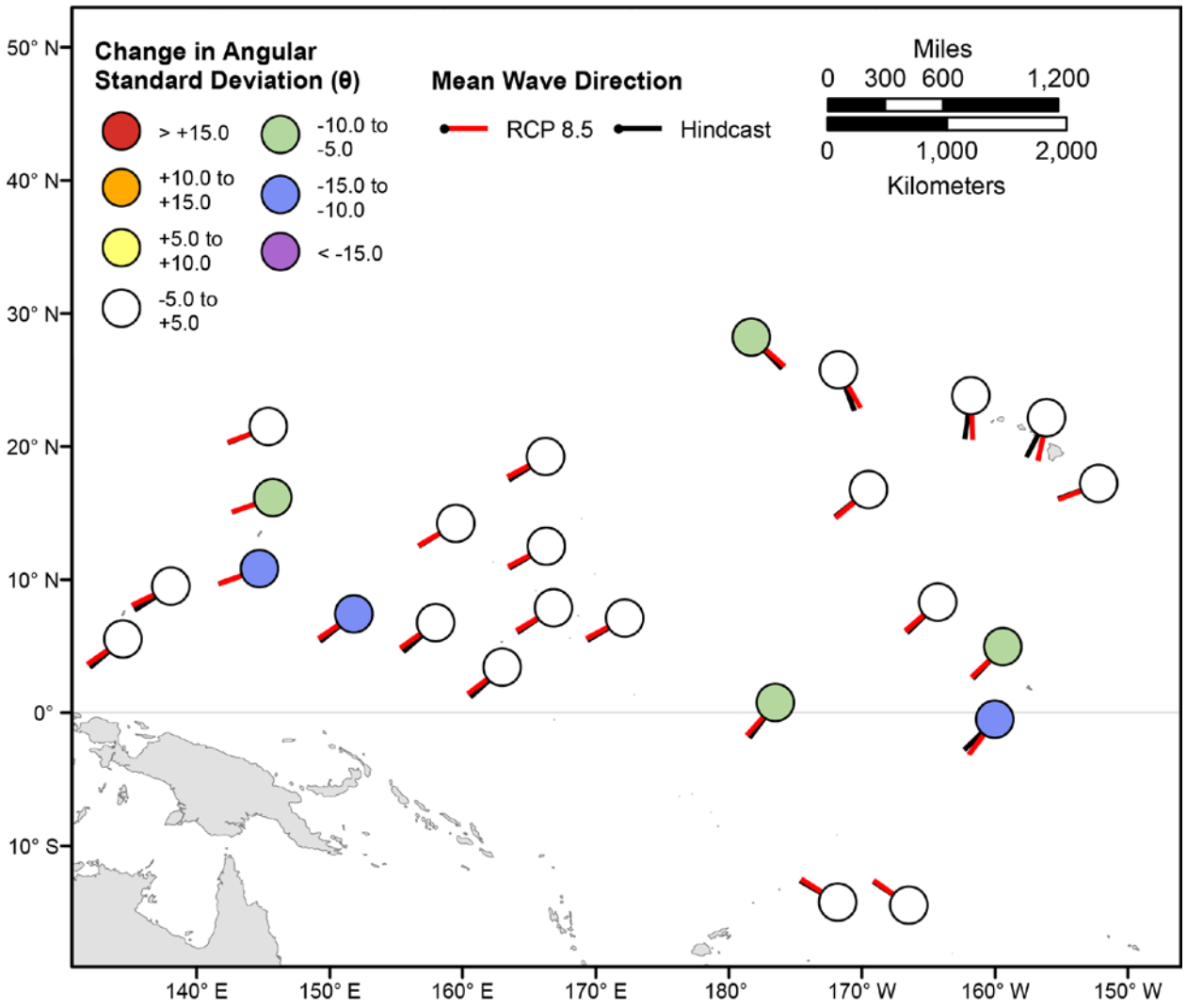

Figure 83. Map showing forecasted differences in the mean wave directions of the top 5 percent of significant wave heights and the standard deviation of wave directions of the top 5 percent of significant wave heights for the years 2026–2045 from hindcasted values during the March-May season under the RCP8.5 future climatic scenario. Mean wave directions at each point are indicated by lines radiating from the center of each point where RCP 2026–2045 mean wave directions are red and 1976–2005 hindcasted mean wave directions are black. The colors correspond to the magnitude of change in modeled mean wave direction standard deviation during 2026–2045 from those hindcasted for 1976–2005. Angular standard deviation units are in degrees. Mean wave directions are “heading towards”.

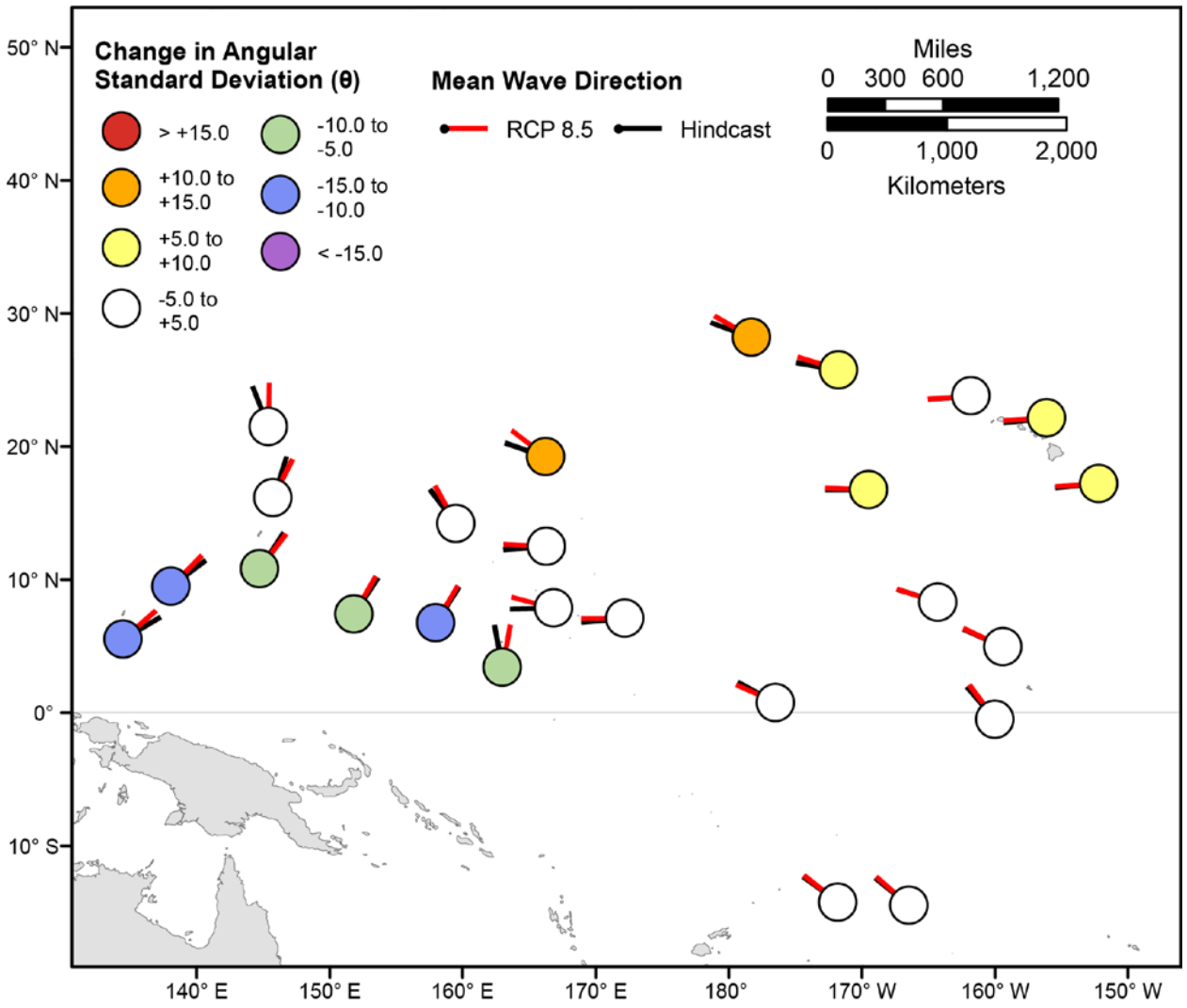

Figure 84. Map showing forecasted differences in the mean wave directions of the top 5 percent of significant wave heights and the standard deviation of wave directions of the top 5 percent of significant wave heights for the years 2026–2045 from hindcasted values during the June-August season under the RCP8.5 future climatic scenario. Mean wave directions at each point are indicated by lines radiating from the center of each point where RCP 2026–2045 mean wave directions are red and 1976–2005 hindcasted mean wave directions are black. The colors correspond to the magnitude of change in modeled mean wave direction standard deviation during 2026–2045 from those hindcasted for 1976–2005. Angular standard deviation units are in degrees. Mean wave directions are “heading towards”.

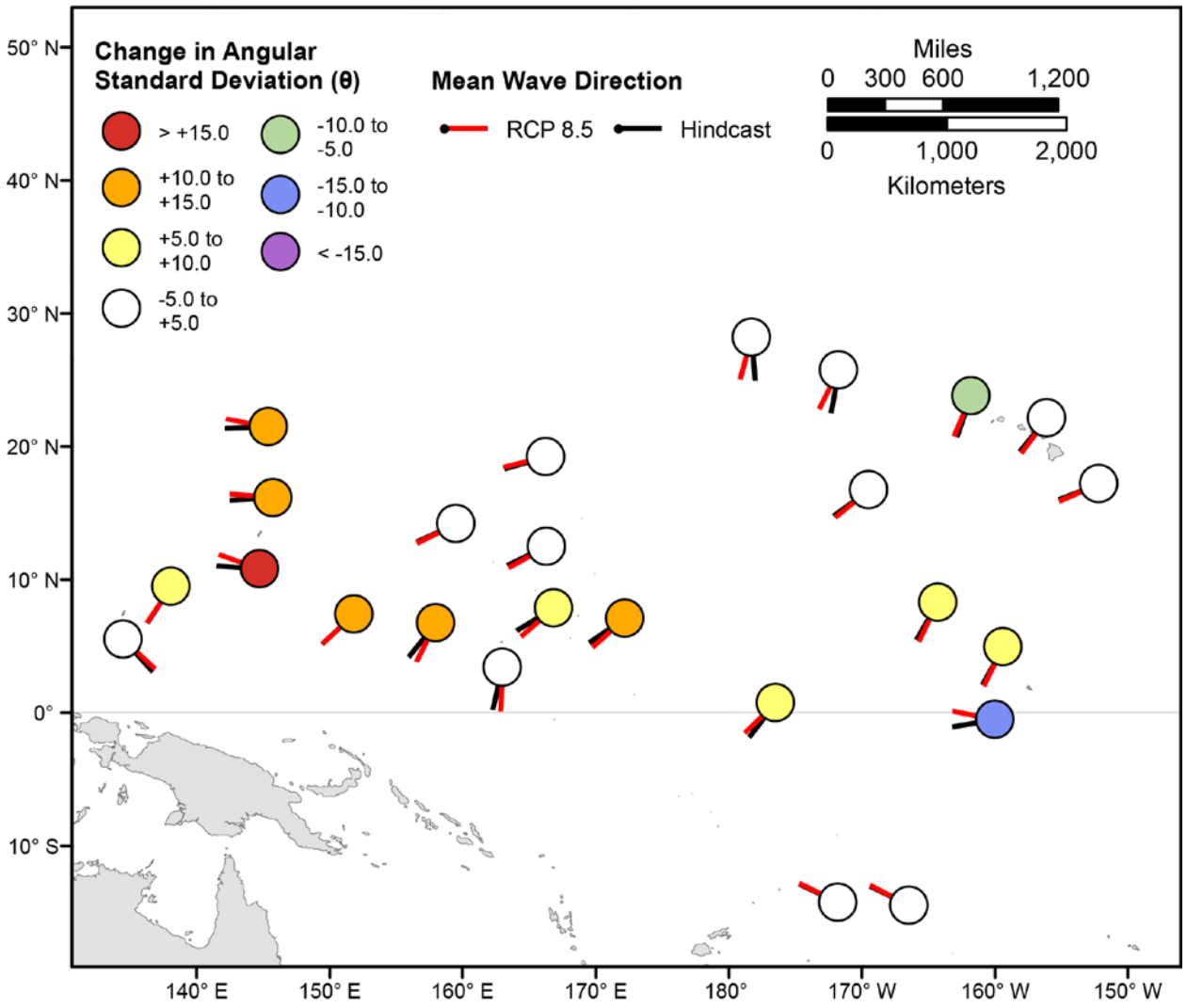

Figure 85. Map showing forecasted differences in the mean wave directions of the top 5 percent of significant wave heights and the standard deviation of wave directions of the top 5 percent of significant wave heights for the years 2026–2045 from hindcasted values during the September-November season under the RCP8.5 future climatic scenario. Mean wave directions at each point are indicated by lines radiating from the center of each point where RCP 2026–2045 mean wave directions are red and 1976–2005 hindcasted mean wave directions are black. The colors correspond to the magnitude of change in modeled mean wave direction standard deviation during 2026–2045 from those hindcasted for 1976–2005. Angular standard deviation units are in degrees. Mean wave directions are “heading towards”.

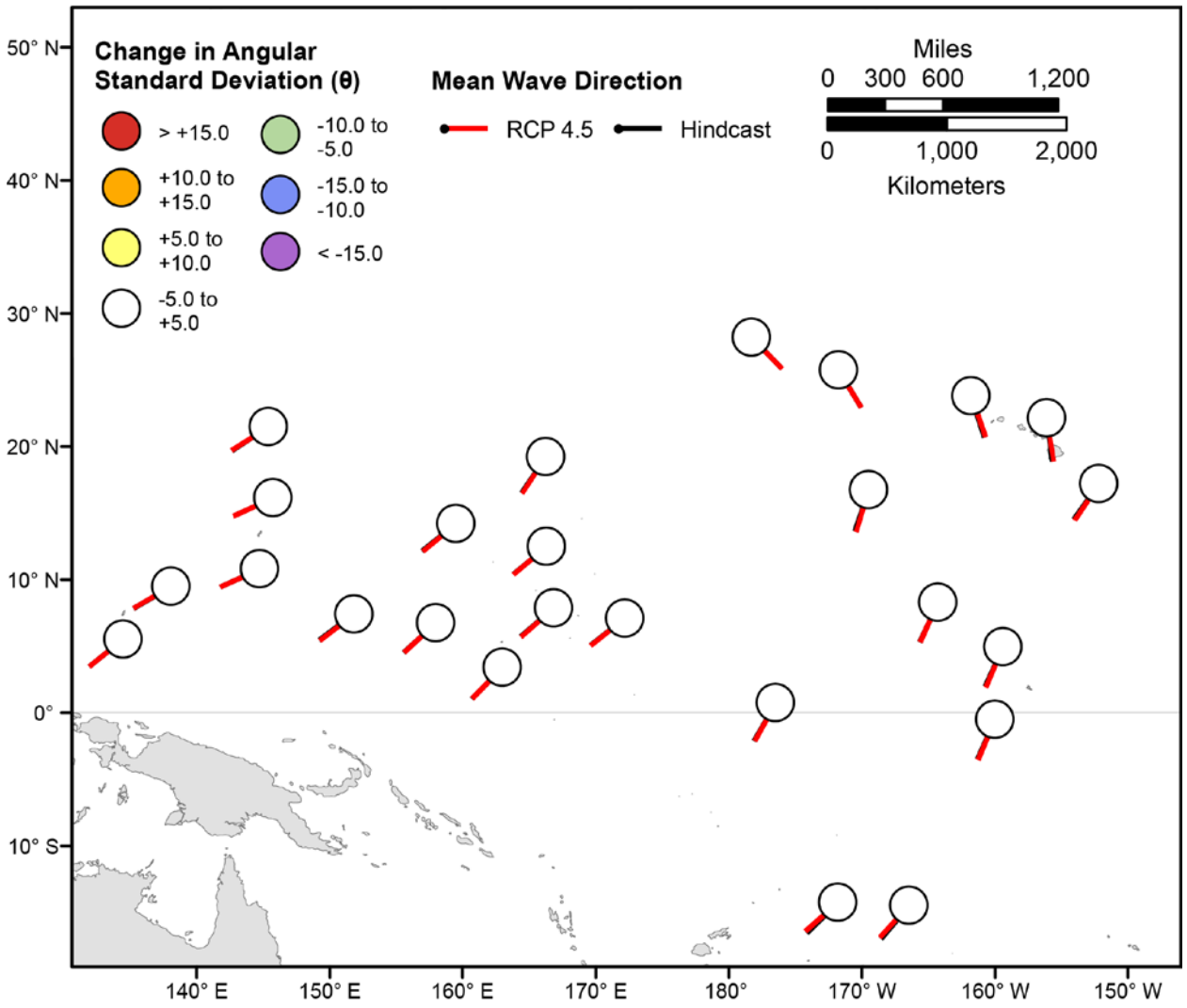

Figure 86. Map showing forecasted differences in the mean wave directions of significant wave heights and the standard deviation of wave directions of significant wave heights for the years 2081–2100 from hindcasted values during the December-February season under the RCP4.5 future climatic scenario. Mean wave directions at each point are indicated by lines radiating from the center of each point where RCP 2081–2100 mean wave directions are red and 1976–2005 hindcasted mean wave directions are black. The colors correspond to the magnitude of change in modeled mean wave direction standard deviation during 2081–2100 from those hindcasted for 1976–2005. Angular standard deviation units are in degrees. Mean wave directions are “heading towards”.

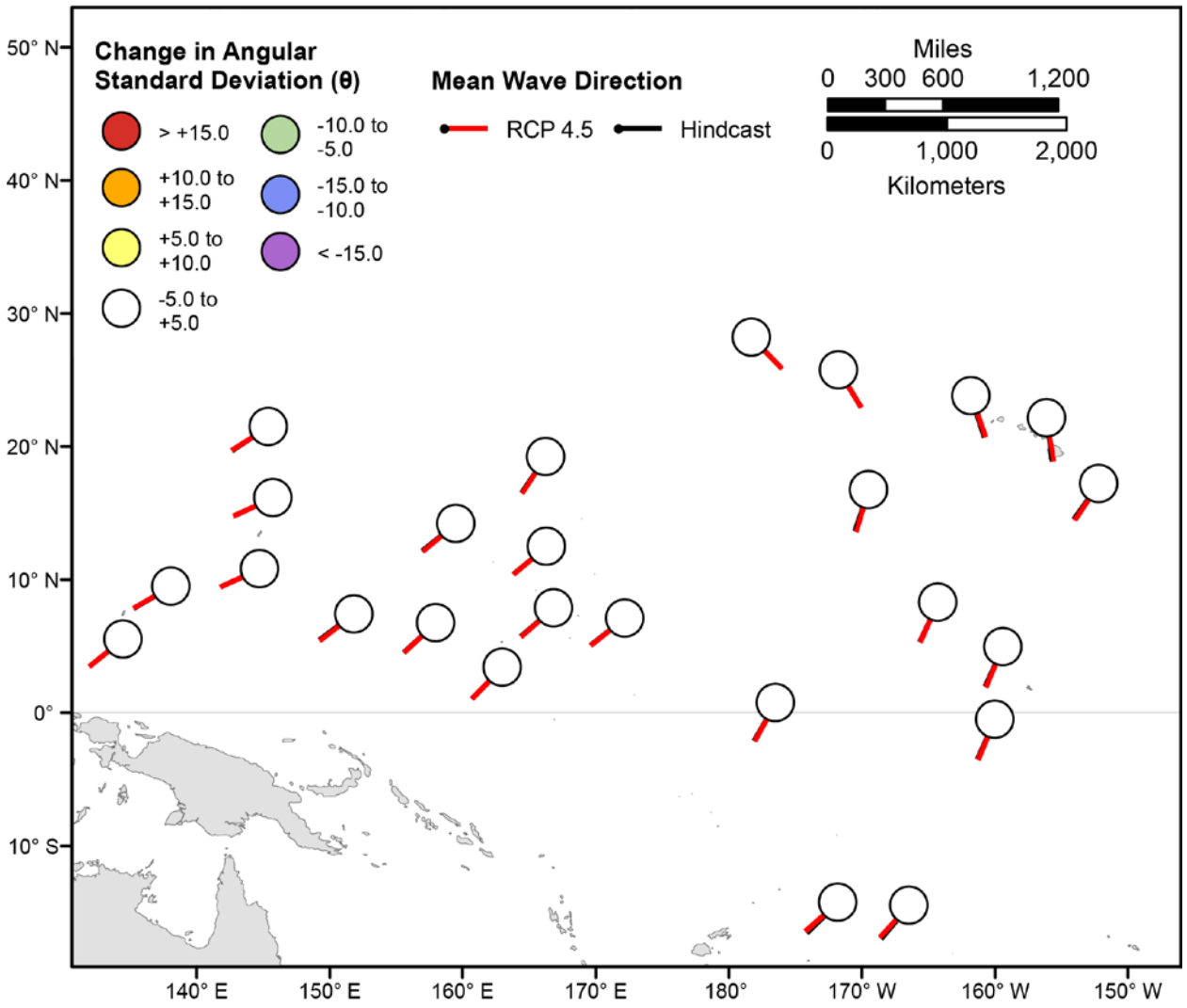

Figure 87. Map showing forecasted differences in the mean wave directions of significant wave heights and the standard deviation of wave directions of significant wave heights for the years 2081–2100 from hindcasted values during the March-May season under the RCP4.5 future climatic scenario. Mean wave directions at each point are indicated by lines radiating from the center of each point where RCP 2081–2100 mean wave directions are red and 1976–2005 hindcasted mean wave directions are black. The colors correspond to the magnitude of change in modeled mean wave direction standard deviation during 2081–2100 from those hindcasted for 1976–2005. Angular standard deviation units are in degrees. Mean wave directions are “heading towards”.

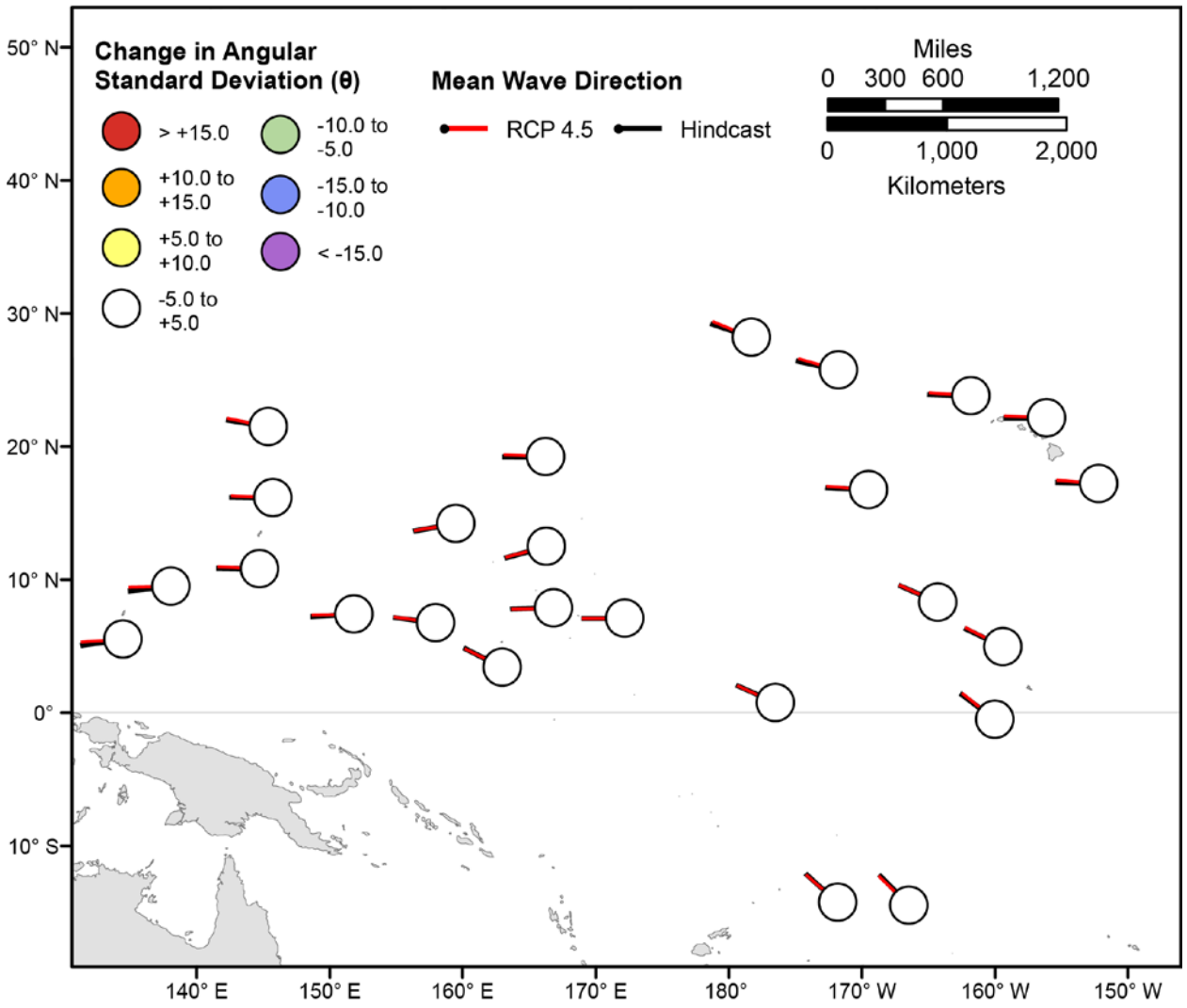

Figure 88. Map showing forecasted differences in the mean wave directions of significant wave heights and the standard deviation of wave directions of significant wave heights for the years 2081–2100 from hindcasted values during the June-July season under the RCP4.5 future climatic scenario. Mean wave directions at each point are indicated by lines radiating from the center of each point where RCP 2081–2100 mean wave directions are red and 1976–2005 hindcasted mean wave directions are black. The colors correspond to the magnitude of change in modeled mean wave direction standard deviation during 2081–2100 from those hindcasted for 1976–2005. Angular standard deviation units are in degrees. Mean wave directions are “heading towards”.

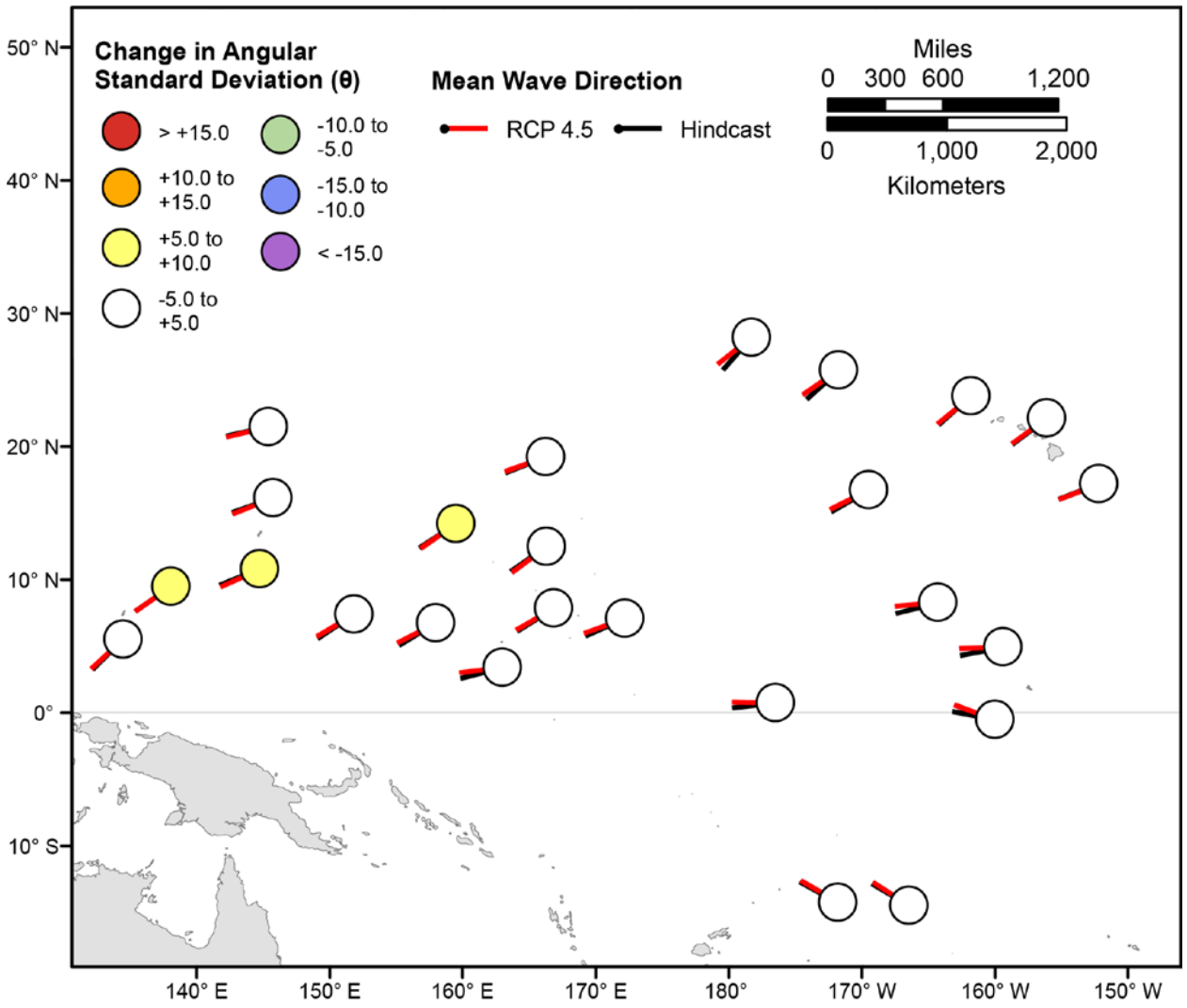

Figure 89. Map showing forecasted differences in the mean wave directions of significant wave heights and the standard deviation of wave directions of significant wave heights for the years 2081–2100 from hindcasted values during the September-November season under the RCP4.5 future climatic scenario. Mean wave directions at each point are indicated by lines radiating from the center of each point where RCP 2081–2100 mean wave directions are red and 1976–2005 hindcasted mean wave directions are black. The colors correspond to the magnitude of change in modeled mean wave direction standard deviation during 2081–2100 from those hindcasted for 1976–2005. Angular standard deviation units are in degrees. Mean wave directions are “heading towards”.

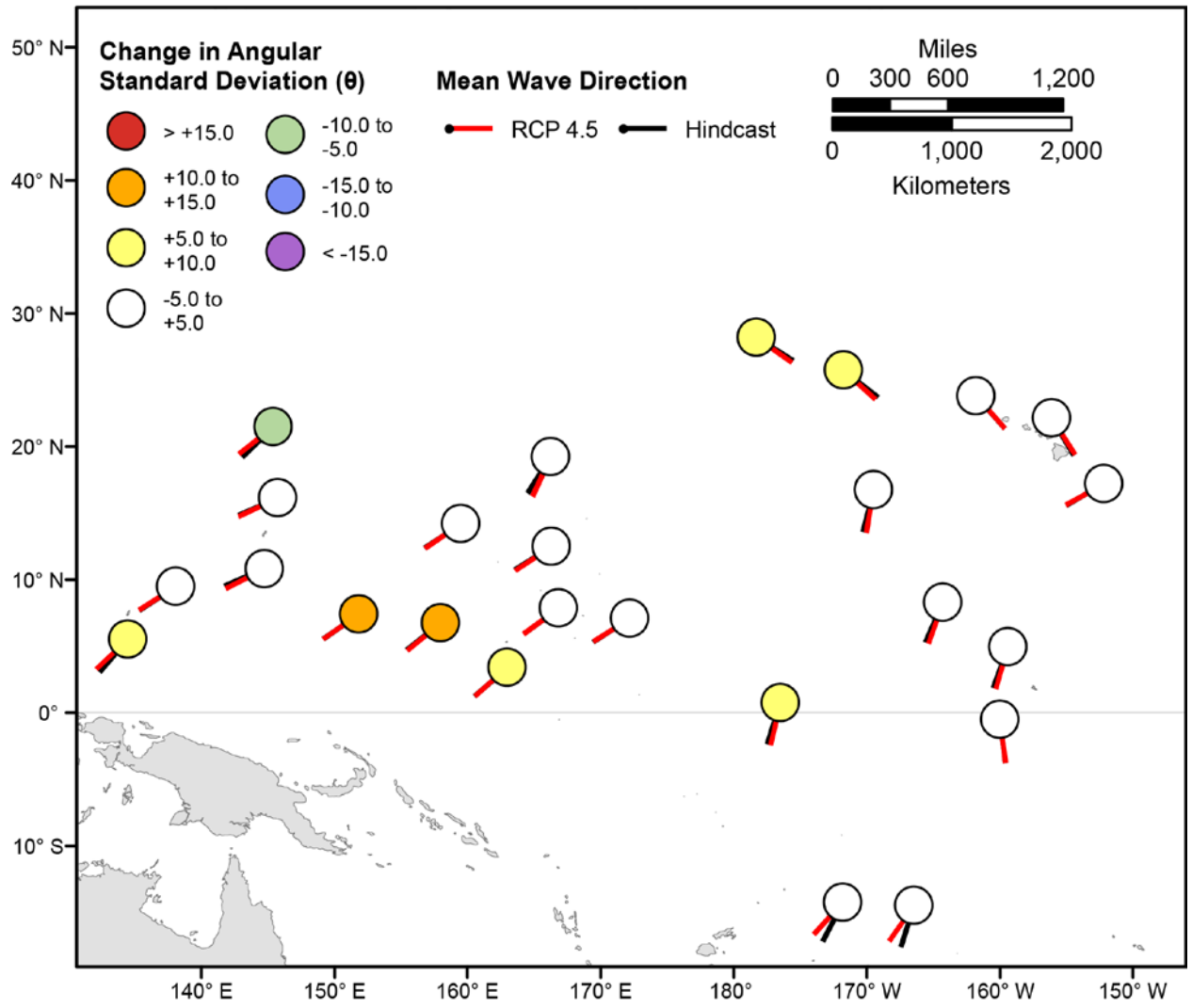

Figure 90. Map showing forecasted differences in the mean wave directions of the top 5 percent of significant wave heights and the standard deviation of wave directions of the top 5 percent of significant wave heights for the years 2081–2100 from hindcasted values during the December-February season under the RCP4.5 future climatic scenario. Mean wave directions at each point are indicated by lines radiating from the center of each point where RCP 2081–2100 mean wave directions are red and 1976–2005 hindcasted mean wave directions are black. The colors correspond to the magnitude of change in modeled mean wave direction standard deviation during 2081–2100 from those hindcasted for 1976–2005. Angular standard deviation units are in degrees. Mean wave directions are “heading towards”.

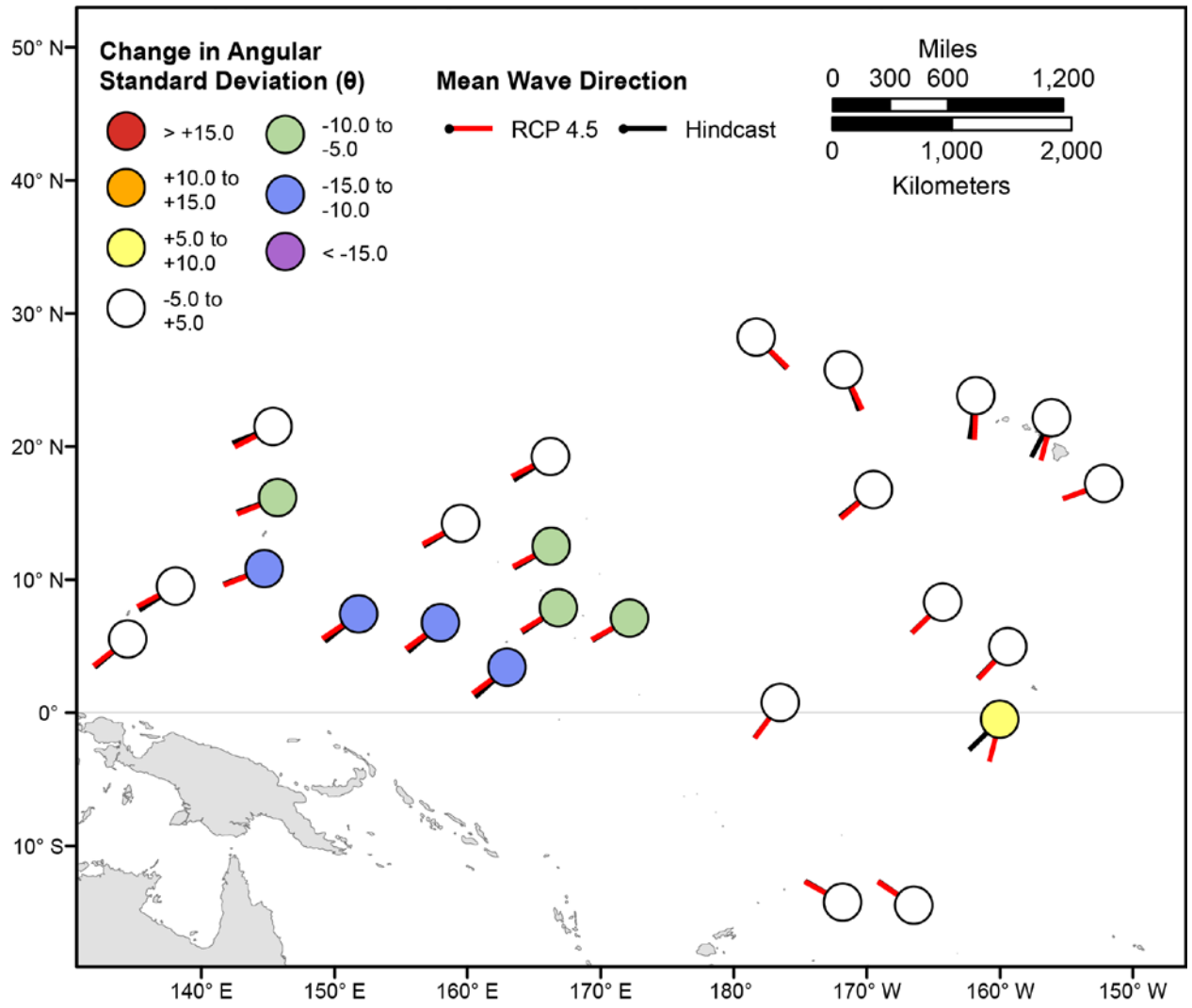

Figure 91. Map showing forecasted differences in the mean wave directions of the top 5 percent of significant wave heights and the standard deviation of wave directions of the top 5 percent of significant wave heights for the years 2081–2100 from hindcasted values during the March-May season under the RCP4.5 future climatic scenario. Mean wave directions at each point are indicated by lines radiating from the center of each point where RCP 2081–2100 mean wave directions are red and 1976–2005 hindcasted mean wave directions are black. The colors correspond to the magnitude of change in modeled mean wave direction standard deviation during 2081–2100 from those hindcasted for 1976–2005. Angular standard deviation units are in degrees. Mean wave directions are “heading towards”.

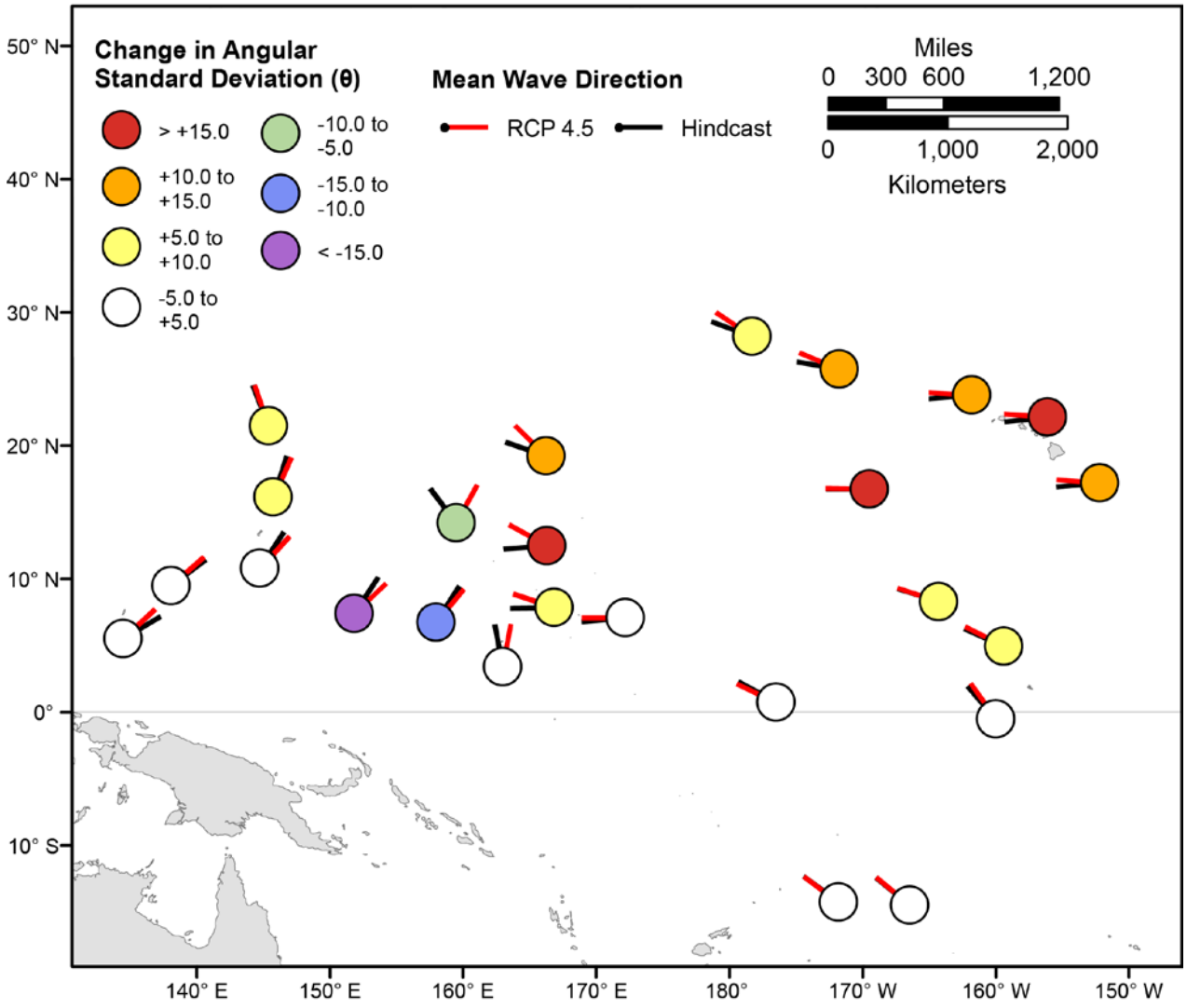

Figure 92. Map showing forecasted differences in the mean wave directions of the top 5 percent of significant wave heights and the standard deviation of wave directions of the top 5 percent of significant wave heights for the years 2081–2100 from hindcasted values during the June-August season under the RCP4.5 future climatic scenario. Mean wave directions at each point are indicated by lines radiating from the center of each point where RCP 2081–2100 mean wave directions are red and 1976–2005 hindcasted mean wave directions are black. The colors correspond to the magnitude of change in modeled mean wave direction standard deviation during 2081–2100 from those hindcasted for 1976–2005. Angular standard deviation units are in degrees. Mean wave directions are “heading towards”.

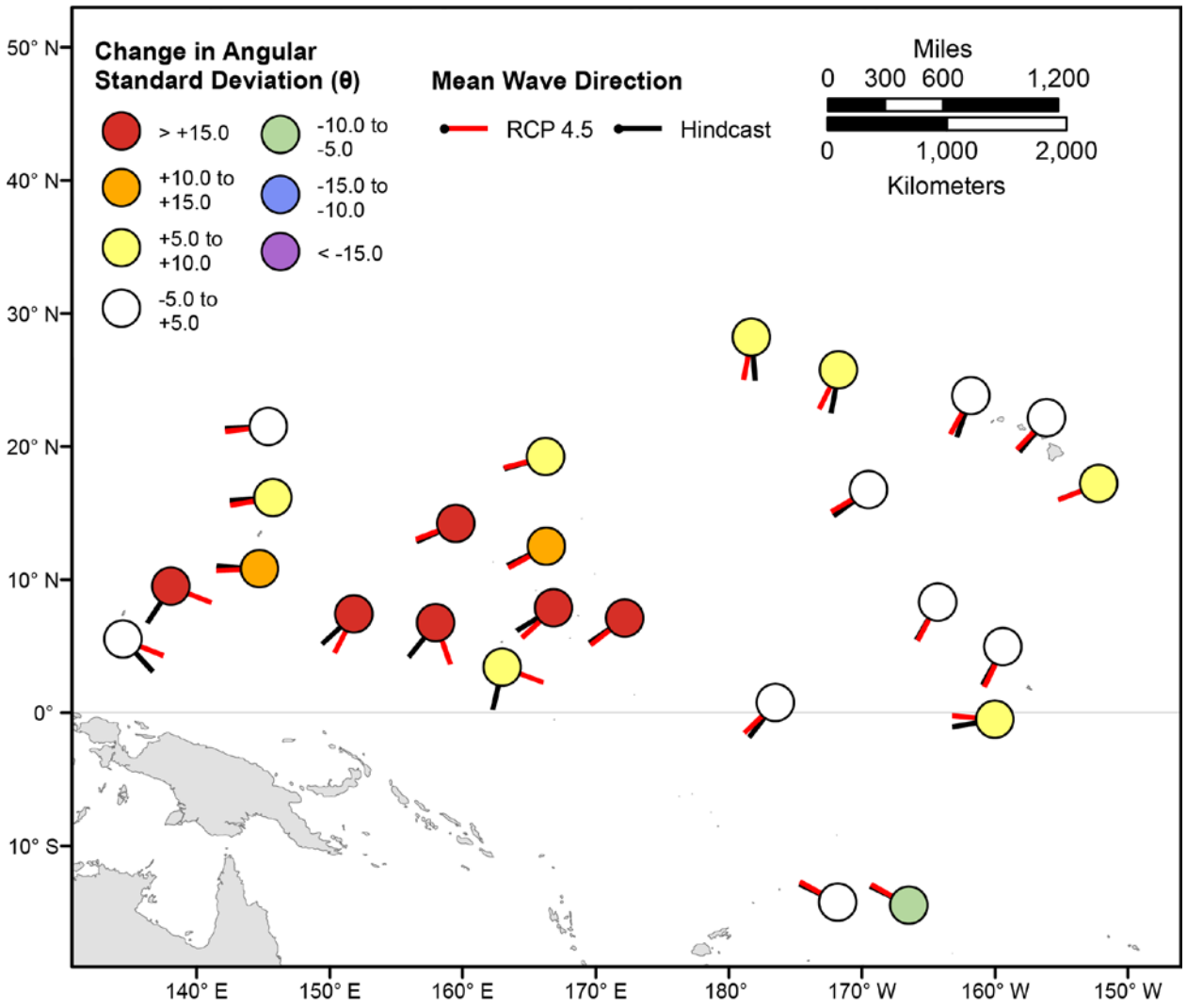

Figure 93. Map showing forecasted differences in the mean wave directions of the top 5 percent of significant wave heights and the standard deviation of wave directions of the top 5 percent of significant wave heights for the years 2081–2100 from hindcasted values during the September-November season under the RCP4.5 future climatic scenario. Mean wave directions at each point are indicated by lines radiating from the center of each point where RCP 2081–2100 mean wave directions are red and 1976–2005 hindcasted mean wave directions are black. The colors correspond to the magnitude of change in modeled mean wave direction standard deviation during 2081–2100 from those hindcasted for 1976–2005. Angular standard deviation units are in degrees. Mean wave directions are “heading towards”.

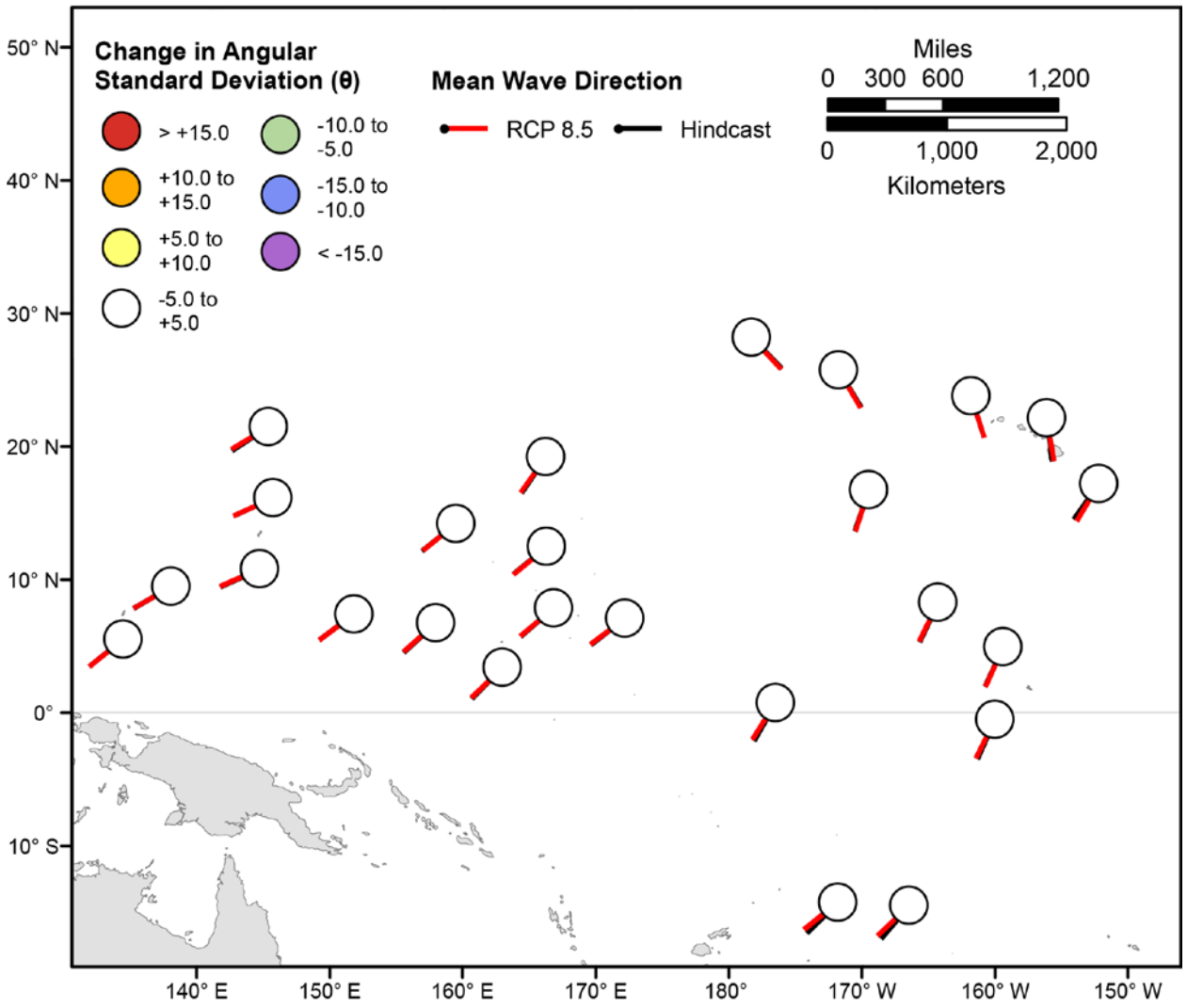

Figure 94. Map showing forecasted differences in the mean wave directions of significant wave heights and the standard deviation of wave directions of significant wave heights for the years 2081–2100 from hindcasted values during the December-February season under the RCP8.5 future climatic scenario. Mean wave directions at each point are indicated by lines radiating from the center of each point where RCP 2081–2100 mean wave directions are red and 1976–2005 hindcasted mean wave directions are black. The colors correspond to the magnitude of change in modeled mean wave direction standard deviation during 2081–2100 from those hindcasted for 1976–2005. Angular standard deviation units are in degrees. Mean wave directions are “heading towards”.

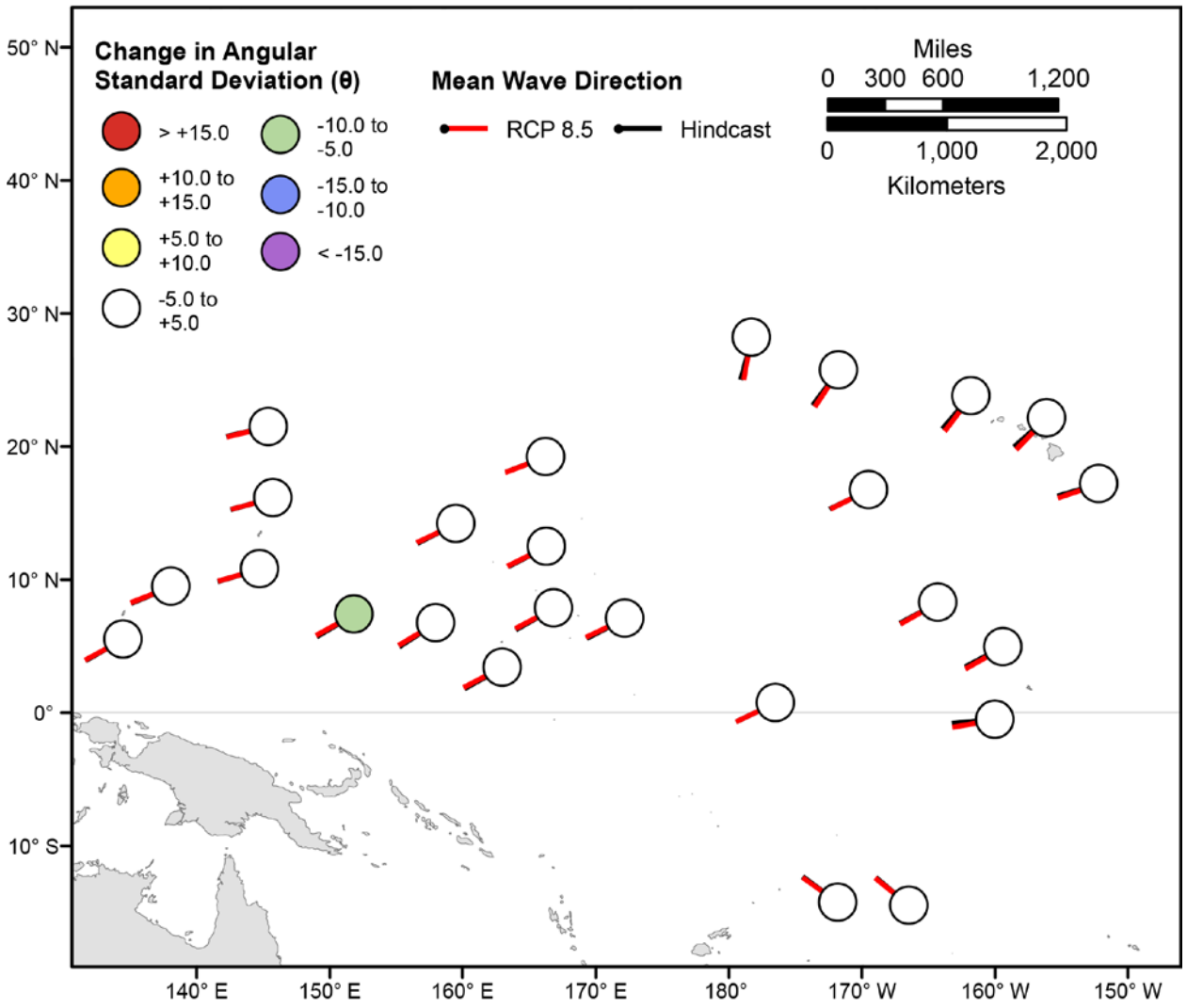

Figure 95. Map showing forecasted differences in the mean wave directions of significant wave heights and the standard deviation of wave directions of significant wave heights for the years 2081–2100 from hindcasted values during the March-May season under the RCP8.5 future climatic scenario. Mean wave directions at each point are indicated by lines radiating from the center of each point where RCP 2081–2100 mean wave directions are red and 1976–2005 hindcasted mean wave directions are black. The colors correspond to the magnitude of change in modeled mean wave direction standard deviation during 2081–2100 from those hindcasted for 1976–2005. Angular standard deviation units are in degrees. Mean wave directions are “heading towards”.

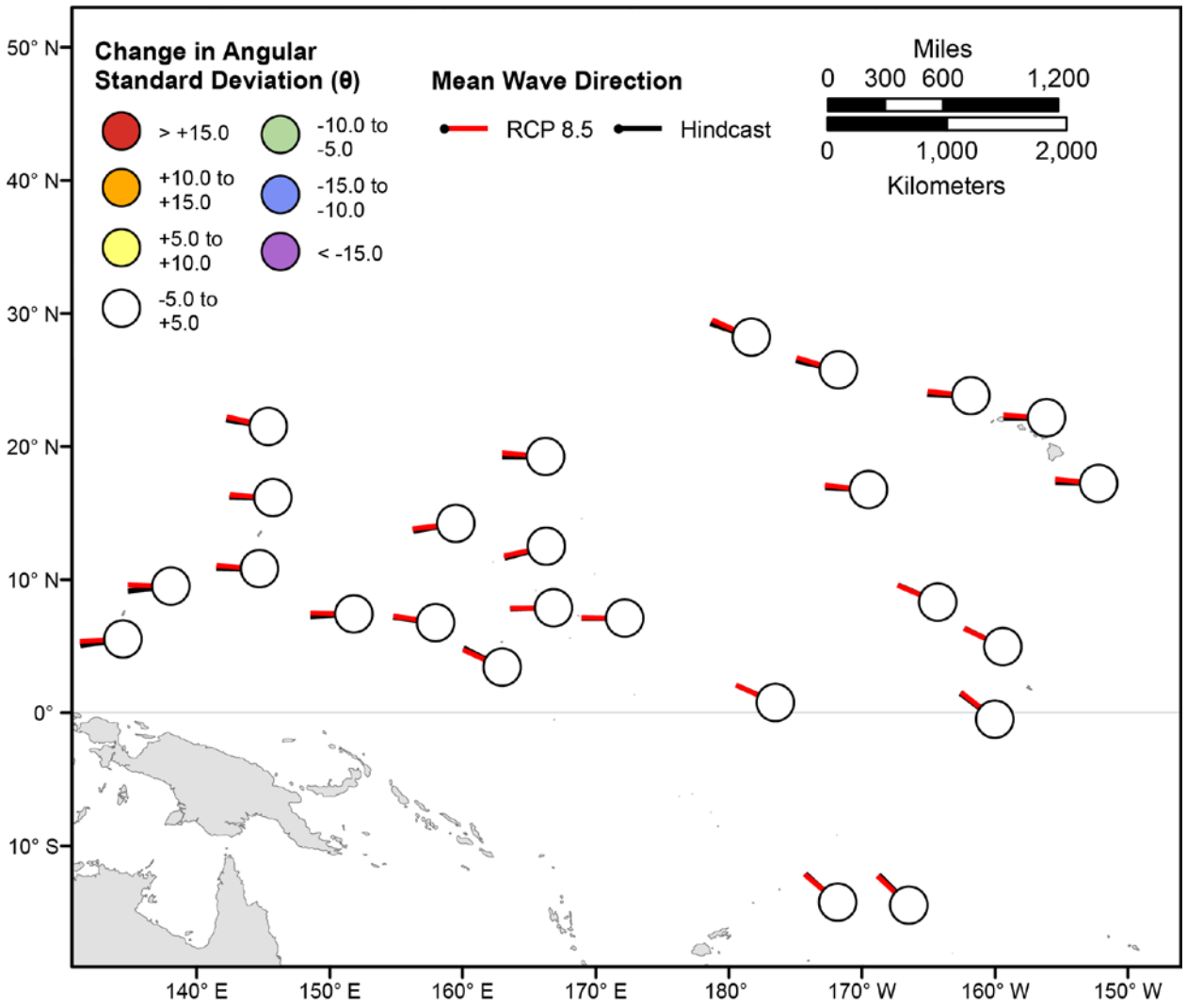

Figure 96. Map showing forecasted differences in the mean wave directions of significant wave heights and the standard deviation of wave directions of significant wave heights for the years 2081–2100 from hindcasted values during the June-July season under the RCP8.5 future climatic scenario. Mean wave directions at each point are indicated by lines radiating from the center of each point where RCP 2081–2100 mean wave directions are red and 1976–2005 hindcasted mean wave directions are black. The colors correspond to the magnitude of change in modeled mean wave direction standard deviation during 2081–2100 from those hindcasted for 1976–2005. Angular standard deviation units are in degrees. Mean wave directions are “heading towards”.

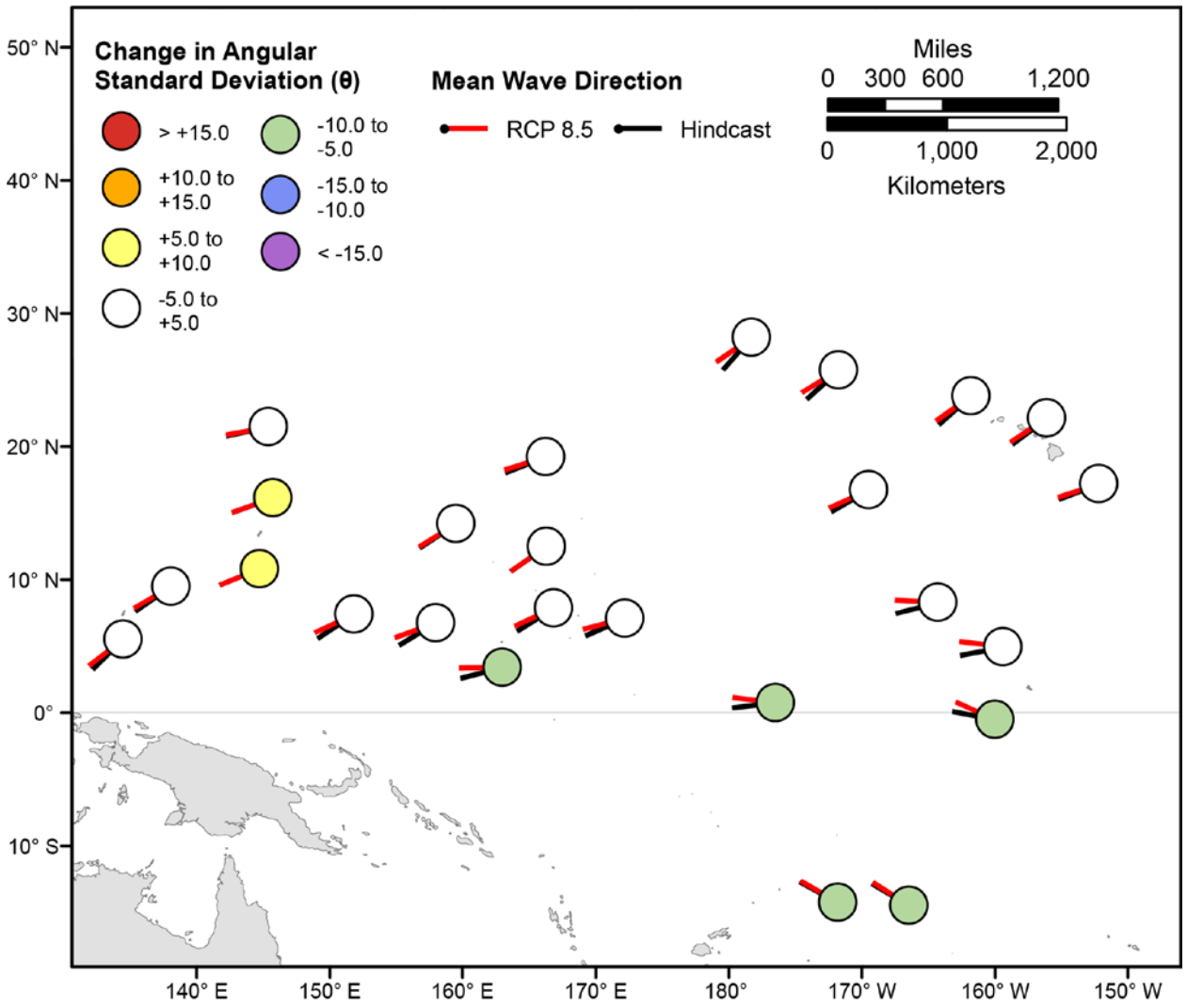

Figure 97. Map showing forecasted differences in the mean wave directions of significant wave heights and the standard deviation of wave directions of significant wave heights for the years 2081–2100 from hindcasted values during the September-November season under the RCP8.5 future climatic scenario. Mean wave directions at each point are indicated by lines radiating from the center of each point where RCP 2081–2100 mean wave directions are red and 1976–2005 hindcasted mean wave directions are black. The colors correspond to the magnitude of change in modeled mean wave direction standard deviation during 2081–2100 from those hindcasted for 1976–2005. Angular standard deviation units are in degrees. Mean wave directions are “heading towards”.

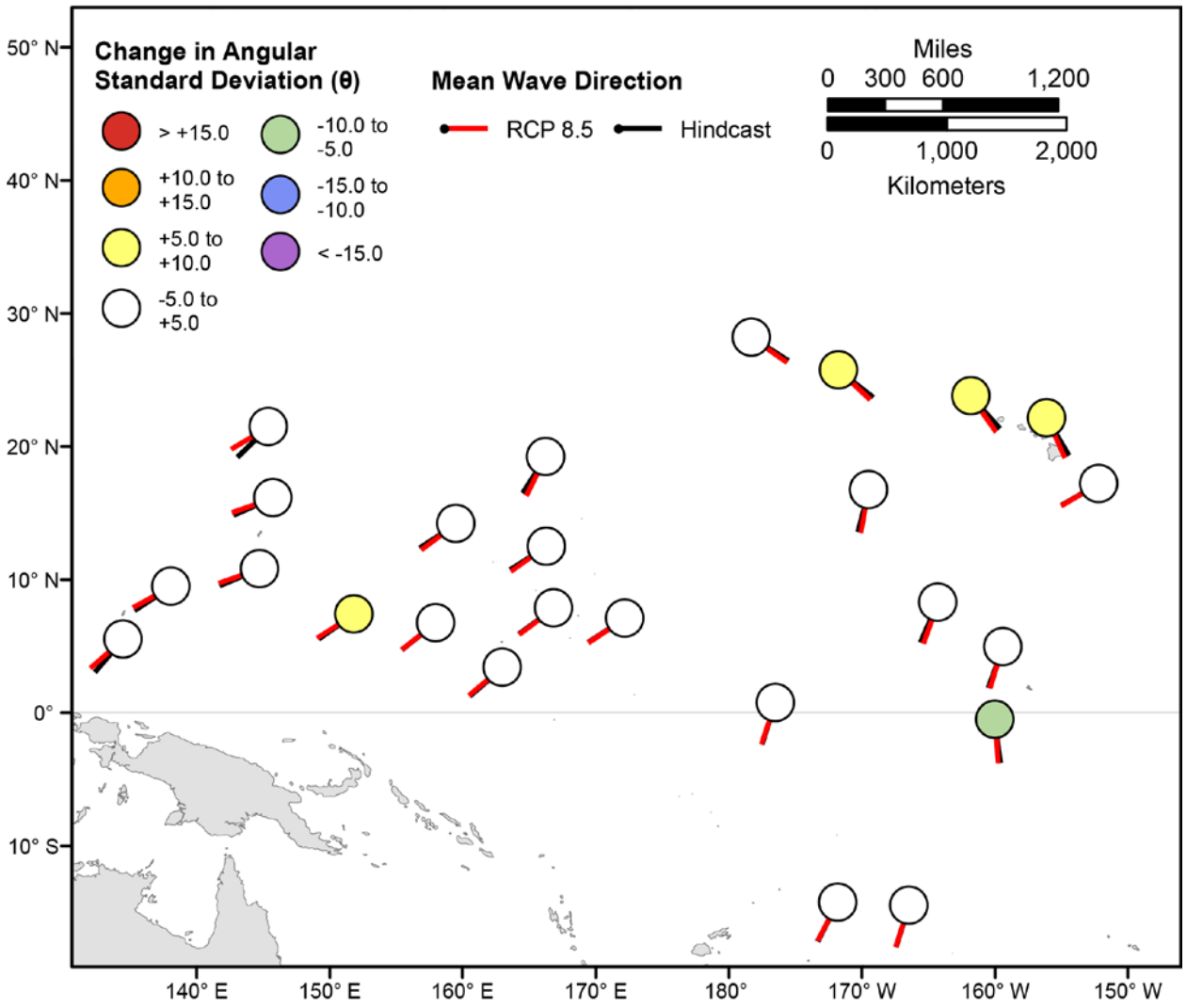

Figure 98. Map showing forecasted differences in the mean wave directions of the top 5 percent of significant wave heights and the standard deviation of wave directions of the top 5 percent of significant wave heights for the years 2081–2100 from hindcasted values during the December-February season under the RCP8.5 future climatic scenario. Mean wave directions at each point are indicated by lines radiating from the center of each point where RCP 2081–2100 mean wave directions are red and 1976–2005 hindcasted mean wave directions are black. The colors correspond to the magnitude of change in modeled mean wave direction standard deviation during 2081–2100 from those hindcasted for 1976–2005. Angular standard deviation units are in degrees. Mean wave directions are “heading towards”.

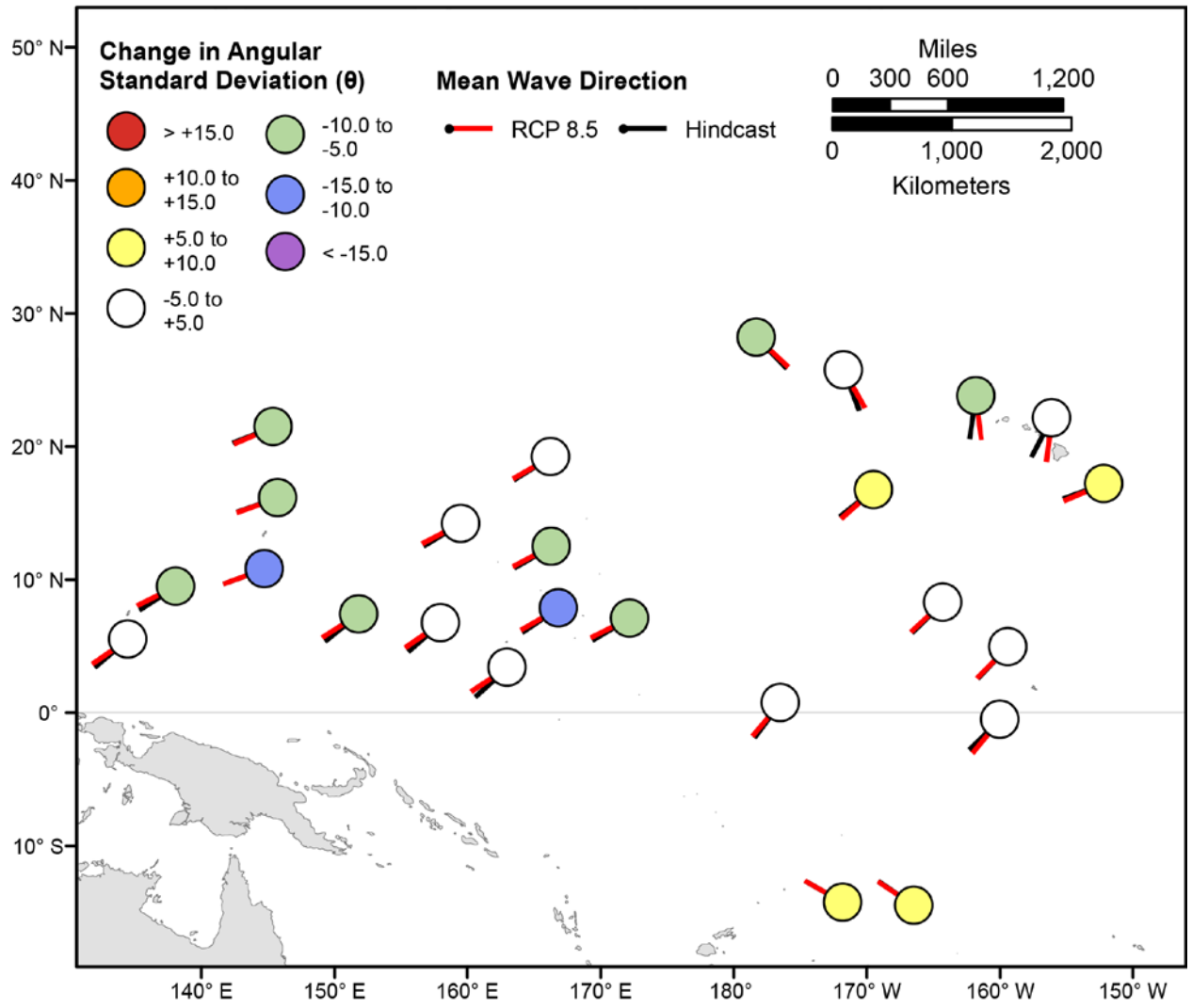

Figure 99. Map showing forecasted differences in the mean wave directions of the top 5 percent of significant wave heights and the standard deviation of wave directions of the top 5 percent of significant wave heights for the years 2081–2100 from hindcasted values during the March-May season under the RCP8.5 future climatic scenario. Mean wave directions at each point are indicated by lines radiating from the center of each point where RCP 2081–2100 mean wave directions are red and 1976–2005 hindcasted mean wave directions are black. The colors correspond to the magnitude of change in modeled mean wave direction standard deviation during 2081–2100 from those hindcasted for 1976–2005. Angular standard deviation units are in degrees. Mean wave directions are “heading towards”.

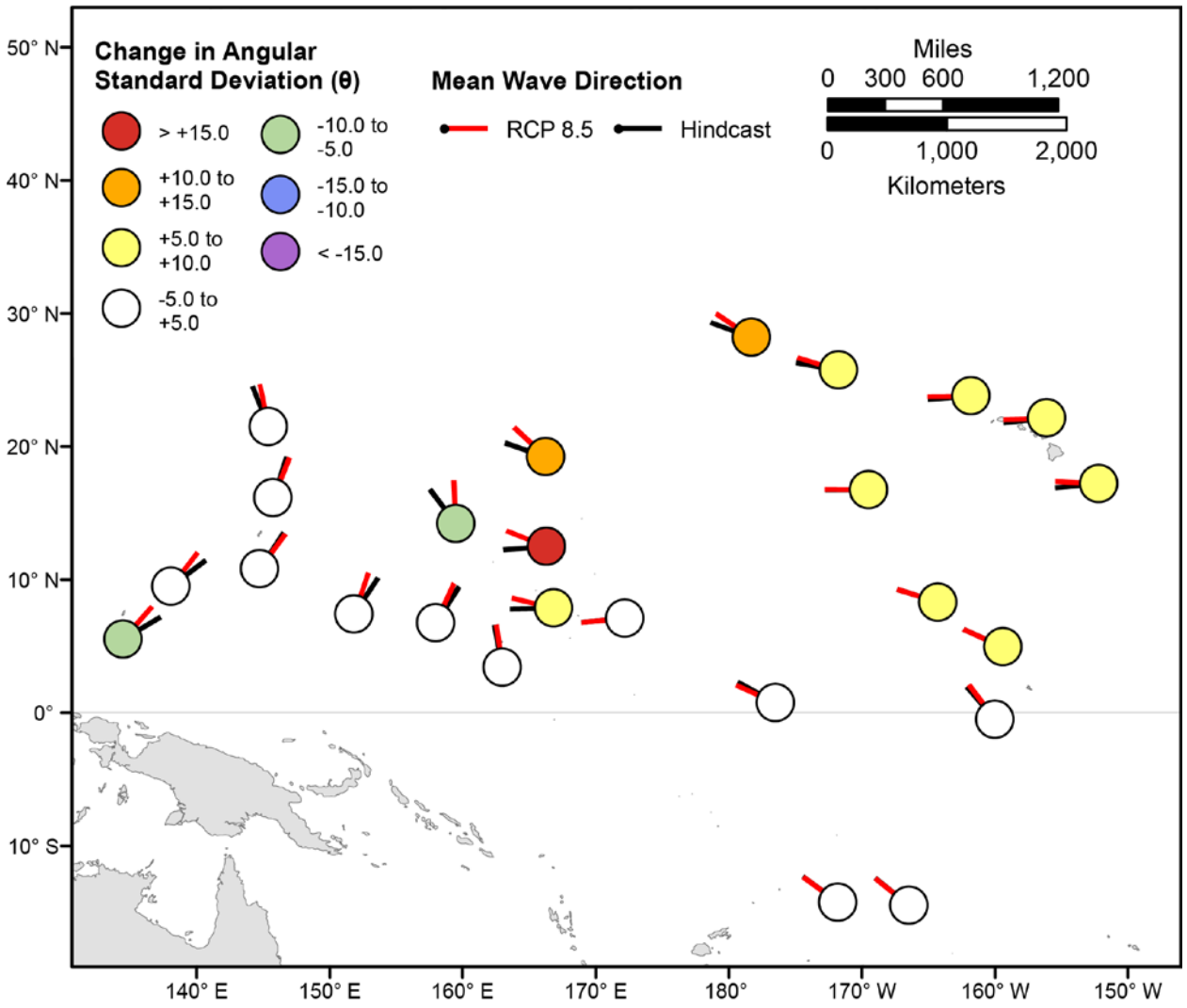

Figure 100. Map showing forecasted differences in the mean wave directions of the top 5 percent of significant wave heights and the standard deviation of wave directions of the top 5 percent of significant wave heights for the years 2081–2100 from hindcasted values during the June-August season under the RCP8.5 future climatic scenario. Mean wave directions at each point are indicated by lines radiating from the center of each point where RCP 2081–2100 mean wave directions are red and 1976–2005 hindcasted mean wave directions are black. The colors correspond to the magnitude of change in modeled mean wave direction standard deviation during 2081–2100 from those hindcasted for 1976–2005. Angular standard deviation units are in degrees. Mean wave directions are “heading towards”.

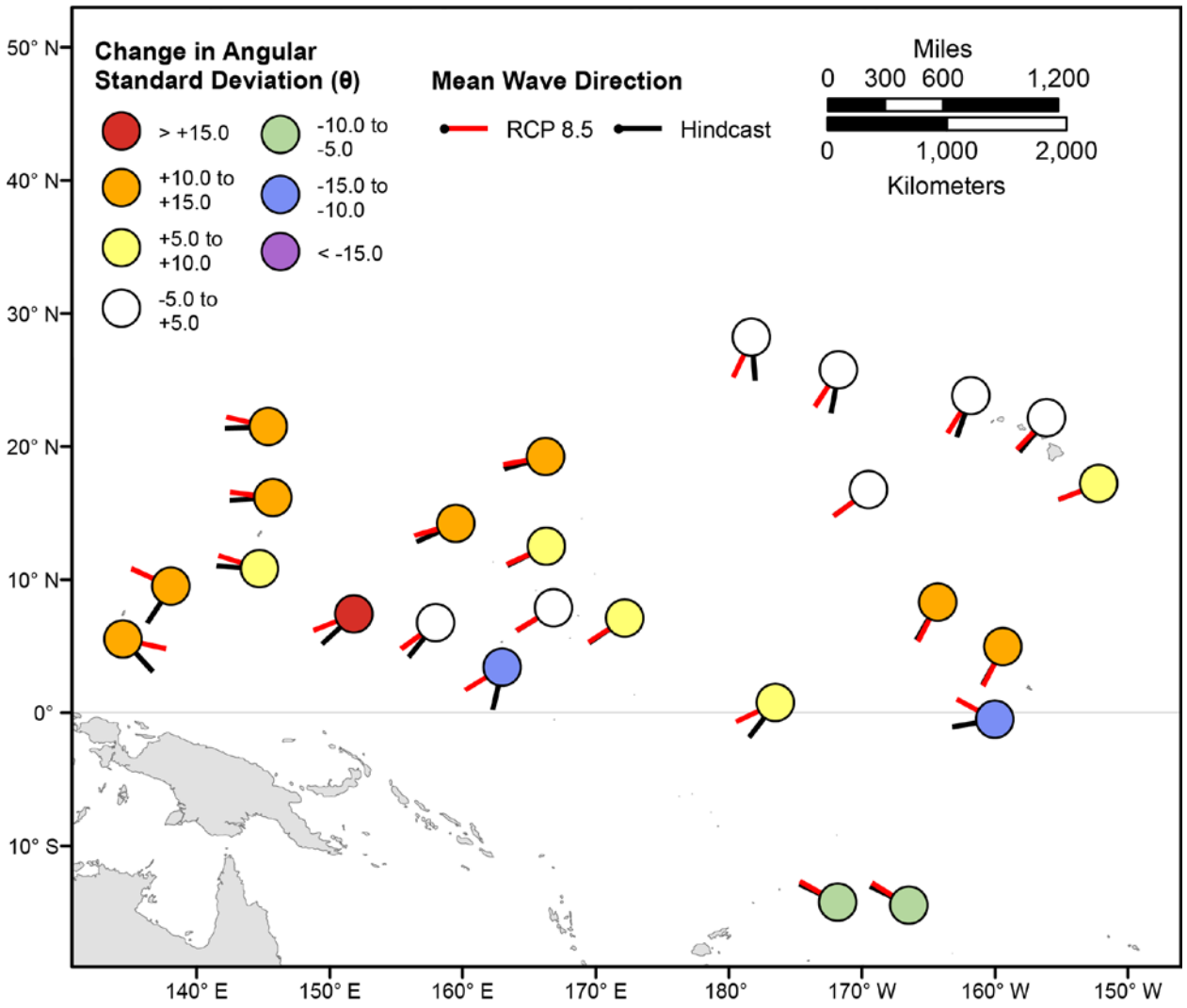

Figure 101. Map showing forecasted differences in the mean wave directions of the top 5 percent of significant wave heights and the standard deviation of wave directions of the top 5 percent of significant wave heights for the years 2081–2100 from hindcasted values during the September-November season under the RCP8.5 future climatic scenario. Mean wave directions at each point are indicated by lines radiating from the center of each point where RCP 2081–2100 mean wave directions are red and 1976–2005 hindcasted mean wave directions are black. The colors correspond to the magnitude of change in modeled mean wave direction standard deviation during 2081–2100 from those hindcasted for 1976–2005. Angular standard deviation units are in degrees. Mean wave directions are “heading towards”.

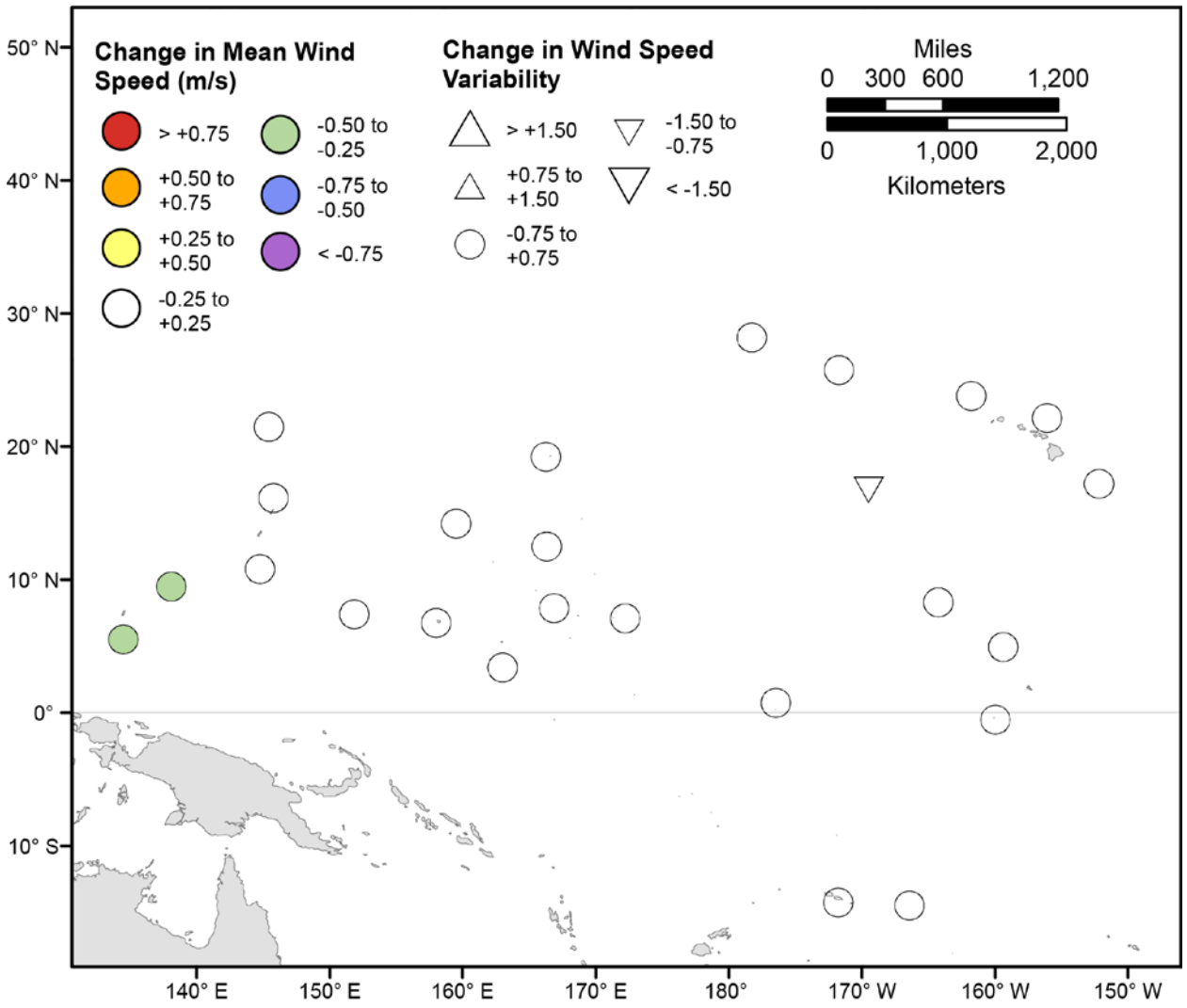

Figure 102. Map showing forecasted differences in mean wind speed and variance in wind speed for the years 2026–2045 from hindcasted values during the December-February season under the RCP4.5 future climatic scenario. The colors correspond to the magnitude of change in modeled mean wind speeds during 2026–2045 from those hindcasted for 1976–2005. The shapes correspond to the magnitude of change in modeled variance in wind speed during 2026–2045 from those hindcasted for 1976–2005. Units are in meters per second.

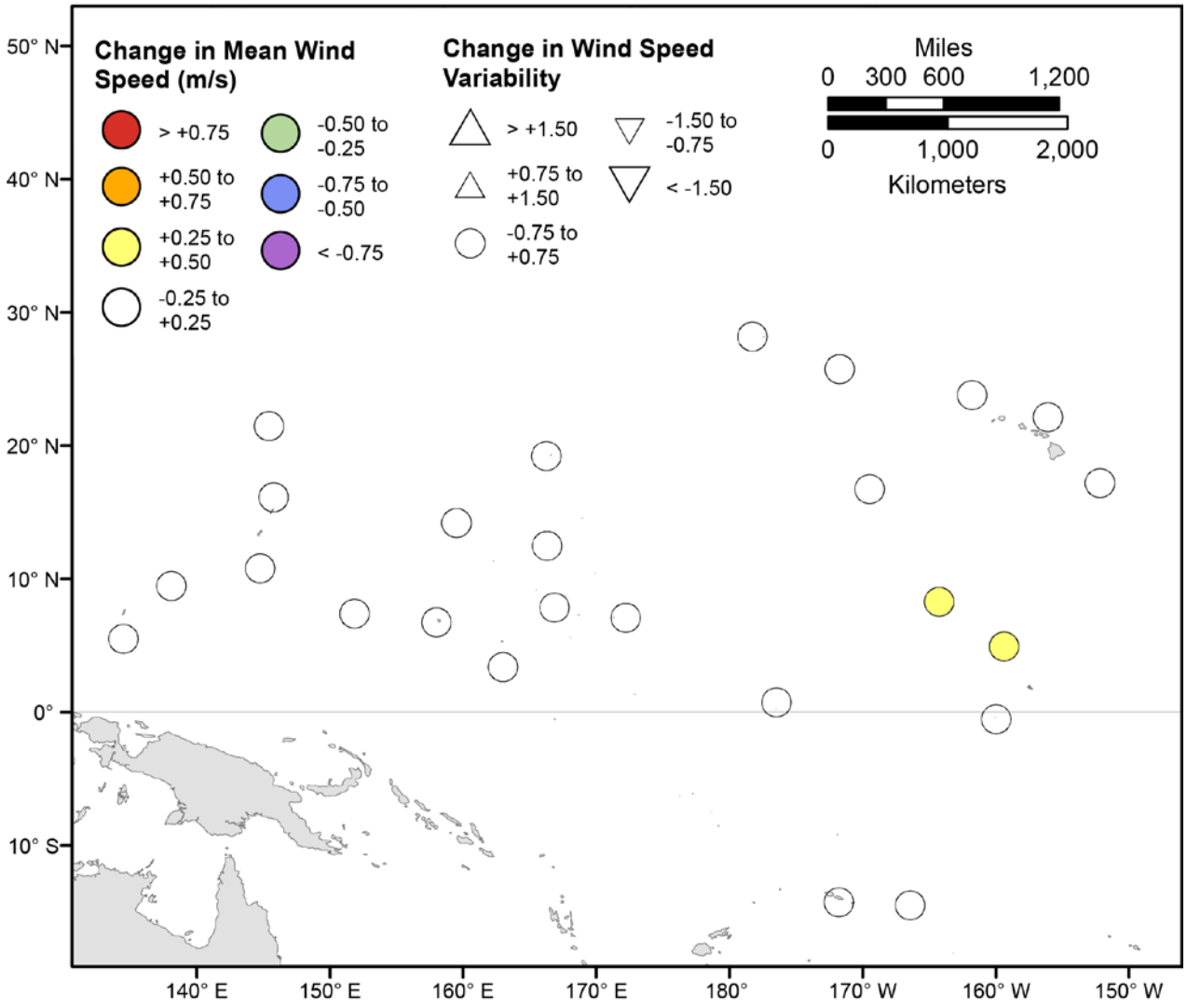

Figure 103. Map showing forecasted differences in mean wind speed and variance in wind speed for the years 2026–2045 from hindcasted values during the March-May season under the RCP4.5 future climatic scenario. The colors correspond to the magnitude of change in modeled mean wind speeds during 2026–2045 from those hindcasted for 1976–2005. The shapes correspond to the magnitude of change in modeled variance in wind speed during 2026–2045 from those hindcasted for 1976–2005. Units are in meters per second.

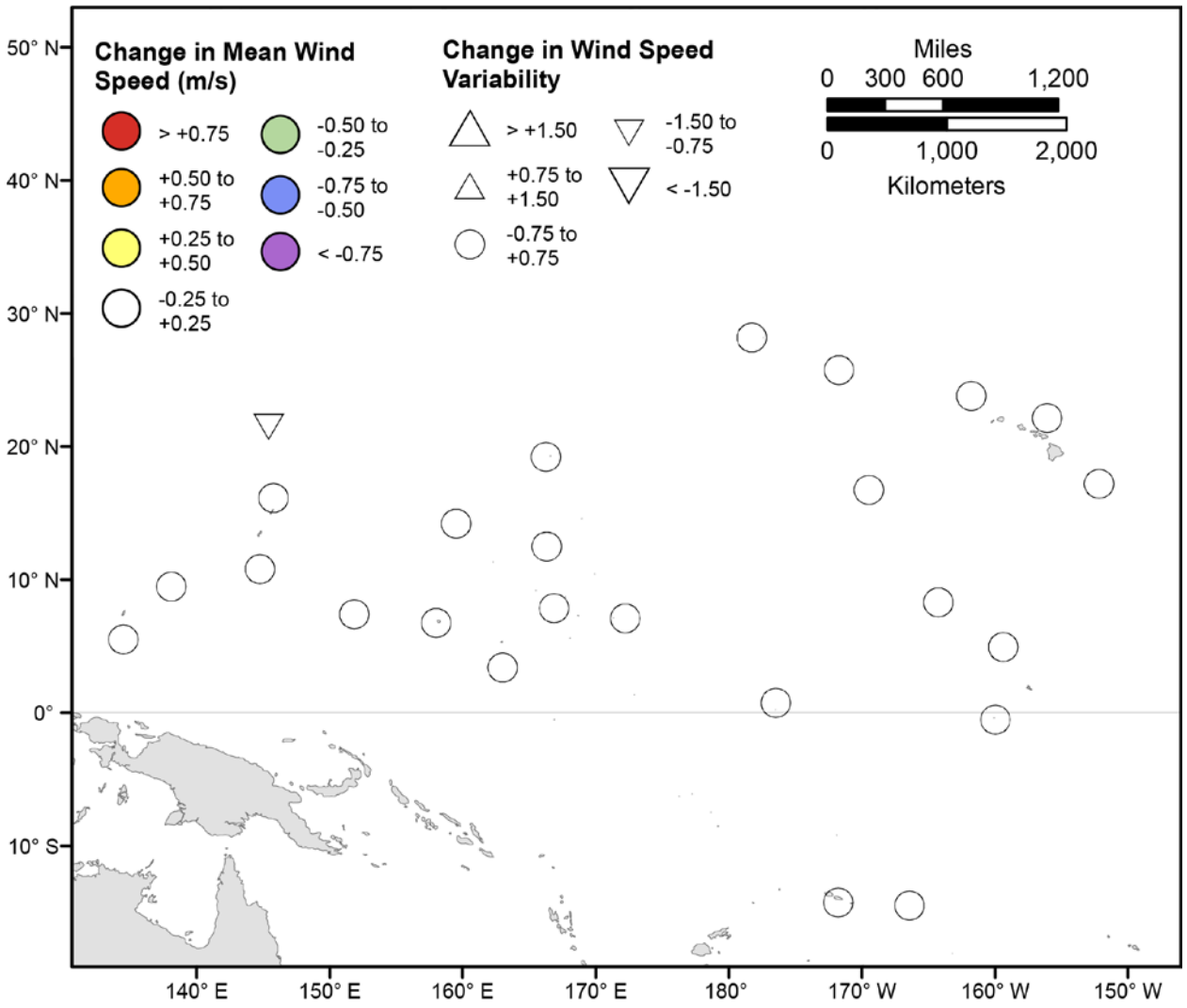

Figure 104. Map showing forecasted differences in mean wind speed and variance in wind speed for the years 2026–2045 from hindcasted values during the June-August season under the RCP4.5 future climatic scenario. The colors correspond to the magnitude of change in modeled mean wind speeds during 2026–2045 from those hindcasted for 1976–2005. The shapes correspond to the magnitude of change in modeled variance in wind speed during 2026–2045 from those hindcasted for 1976–2005. Units are in meters per second.

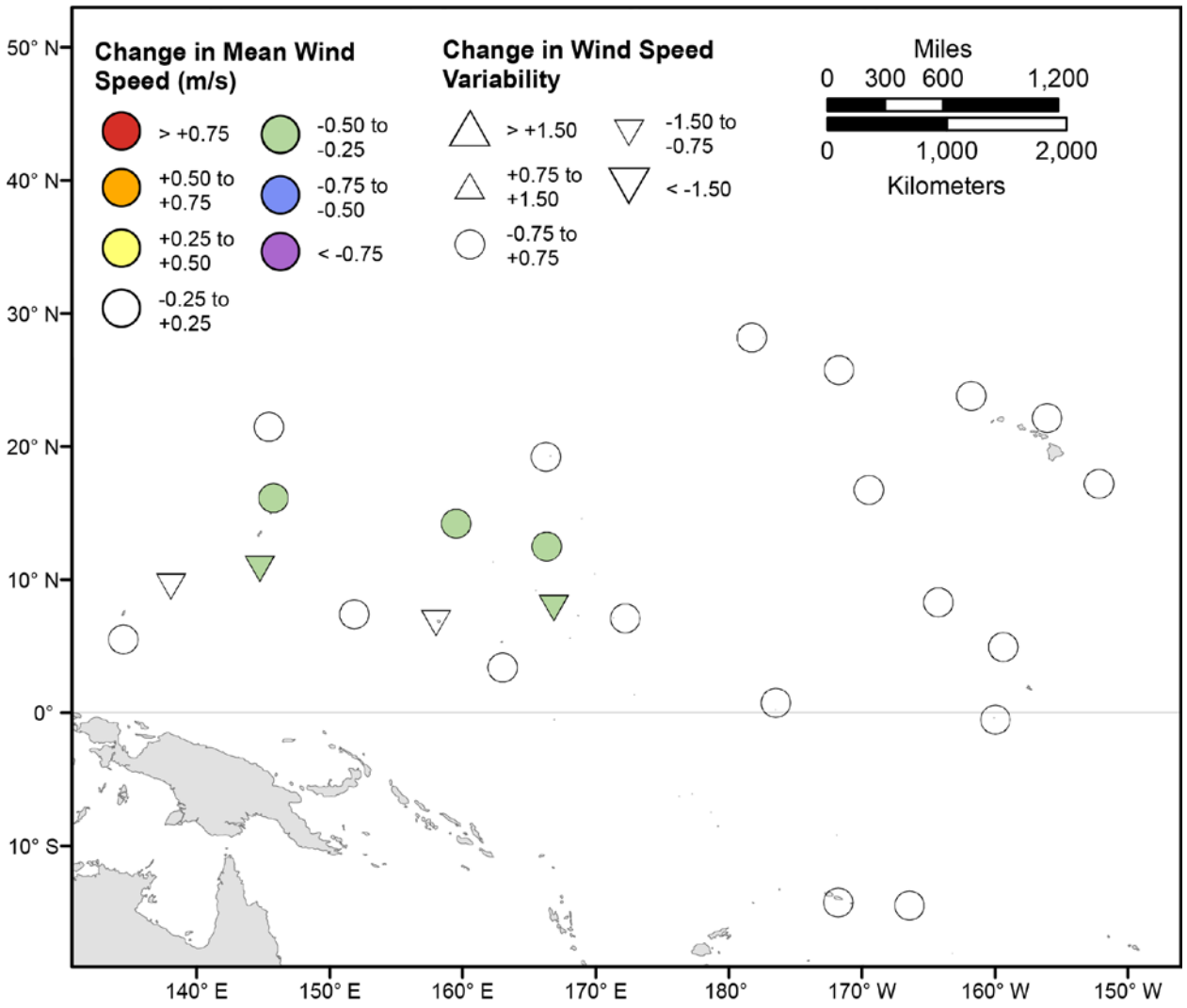

Figure 105. Map showing forecasted differences in mean wind speed and variance in wind speed for the years 2026–2045 from hindcasted values during the September-November season under the RCP4.5 future climatic scenario. The colors correspond to the magnitude of change in modeled mean wind speeds during 2026–2045 from those hindcasted for 1976–2005. The shapes correspond to the magnitude of change in modeled variance in wind speed during 2026–2045 from those hindcasted for 1976–2005. Units are in meters per second.

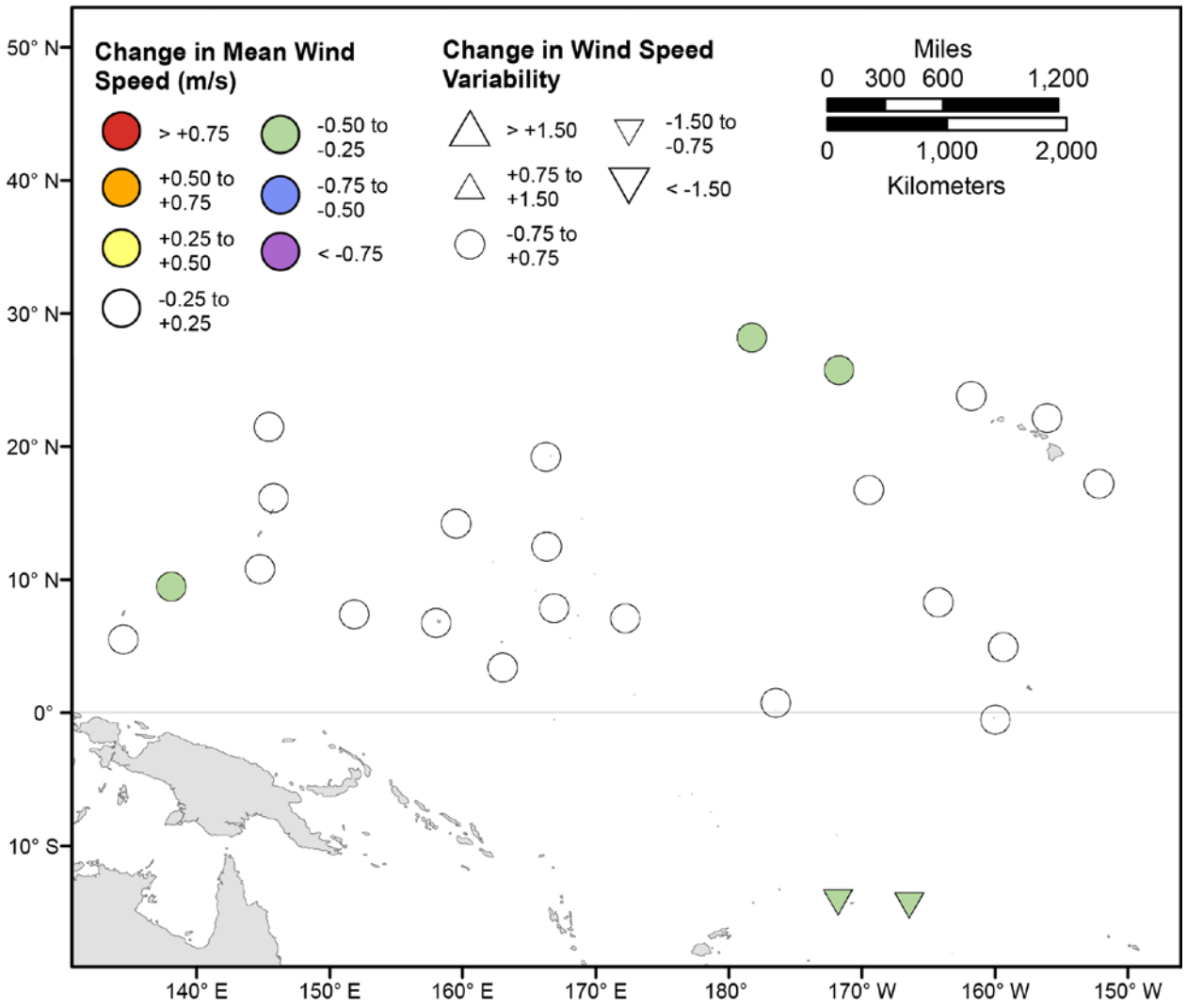

Figure 106. Map showing forecasted differences in the mean of the top 5 percent of wind speeds and variance in the top 5 percent of wind speeds for the years 2026–2045 from hindcasted values during the December-February season under the RCP4.5 future climatic scenario. The colors correspond to the magnitude of change in modeled mean wind speeds during 2026–2045 from those hindcasted for 1976–2005. The shapes correspond to the magnitude of change in modeled variance in wind speed during 2026–2045 from those hindcasted for 1976–2005. Units are in meters per second.

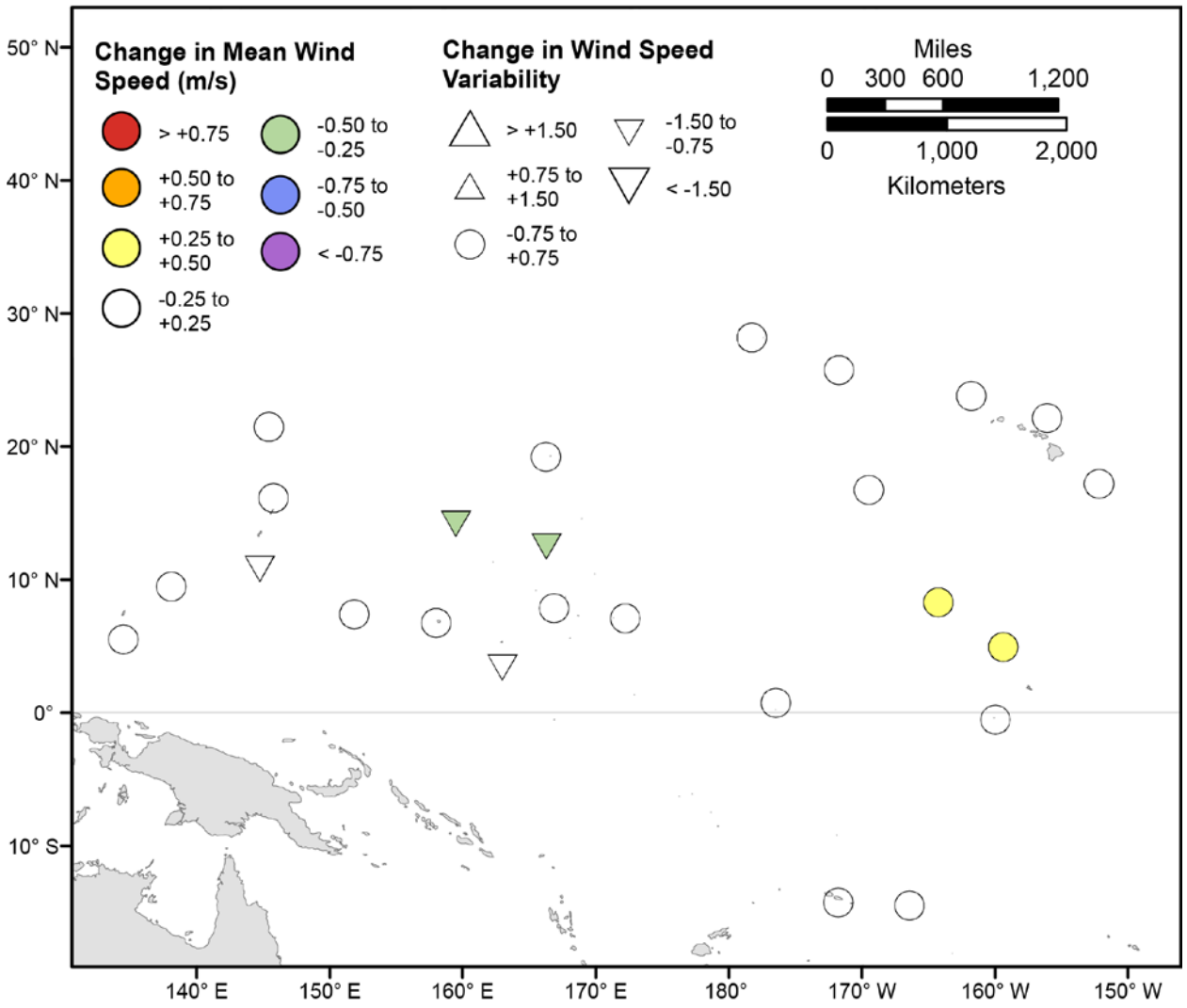

Figure 107. Map showing forecasted differences in the mean of the top 5 percent of wind speeds and variance in the top 5 percent of wind speeds for the years 2026–2045 from hindcasted values during the March-May season under the RCP4.5 future climatic scenario. The colors correspond to the magnitude of change in modeled mean wind speeds during 2026–2045 from those hindcasted for 1976–2005. The shapes correspond to the magnitude of change in modeled variance in wind speed during 2026–2045 from those hindcasted for 1976–2005. Units are in meters per second.

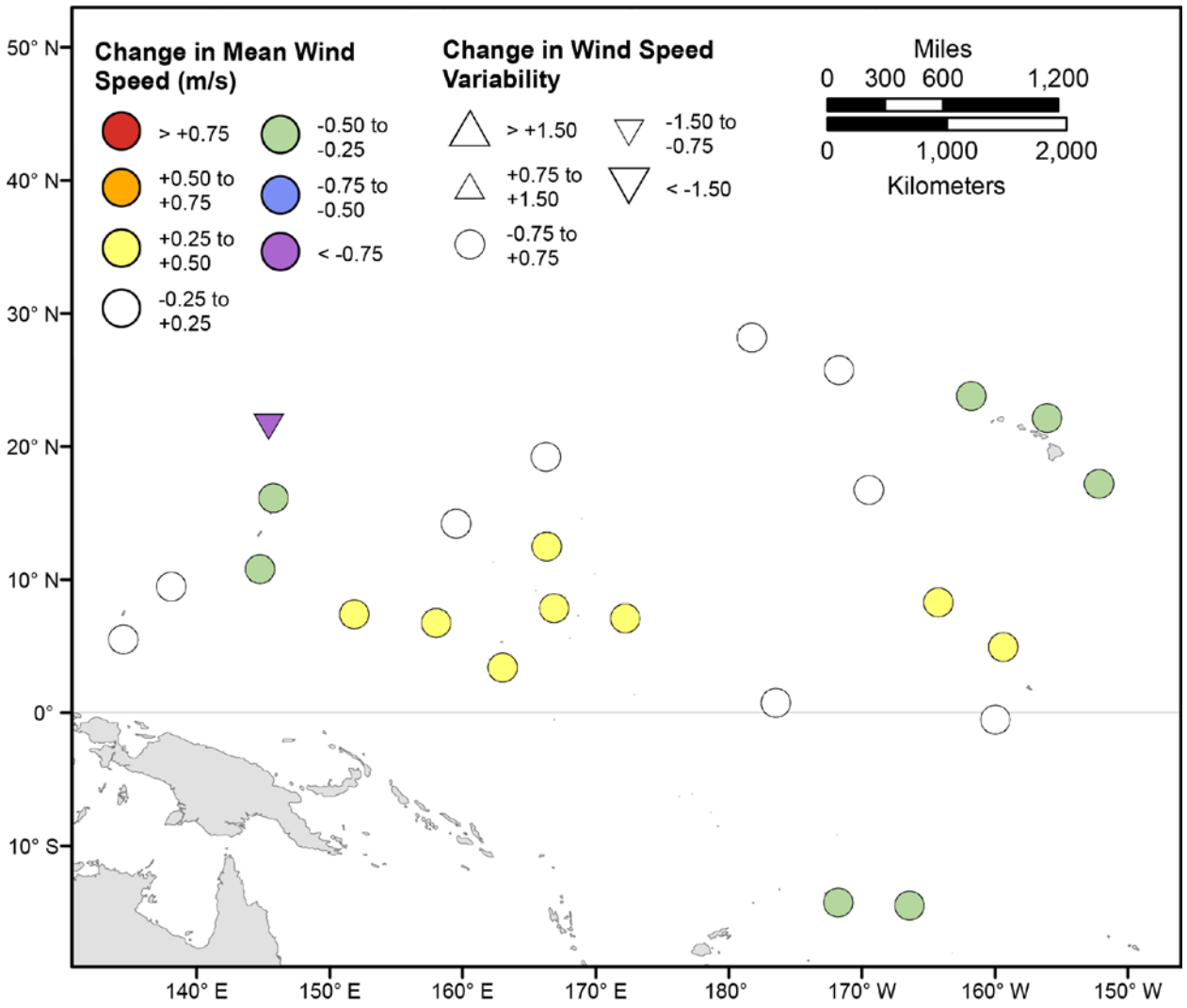

Figure 108. Map showing forecasted differences in the mean of the top 5 percent of wind speeds and variance in the top 5 percent of wind speeds for the years 2026–2045 from hindcasted values during the June-August season under the RCP4.5 future climatic scenario. The colors correspond to the magnitude of change in modeled mean wind speeds during 2026–2045 from those hindcasted for 1976–2005. The shapes correspond to the magnitude of change in modeled variance in wind speed during 2026–2045 from those hindcasted for 1976–2005. Units are in meters per second.

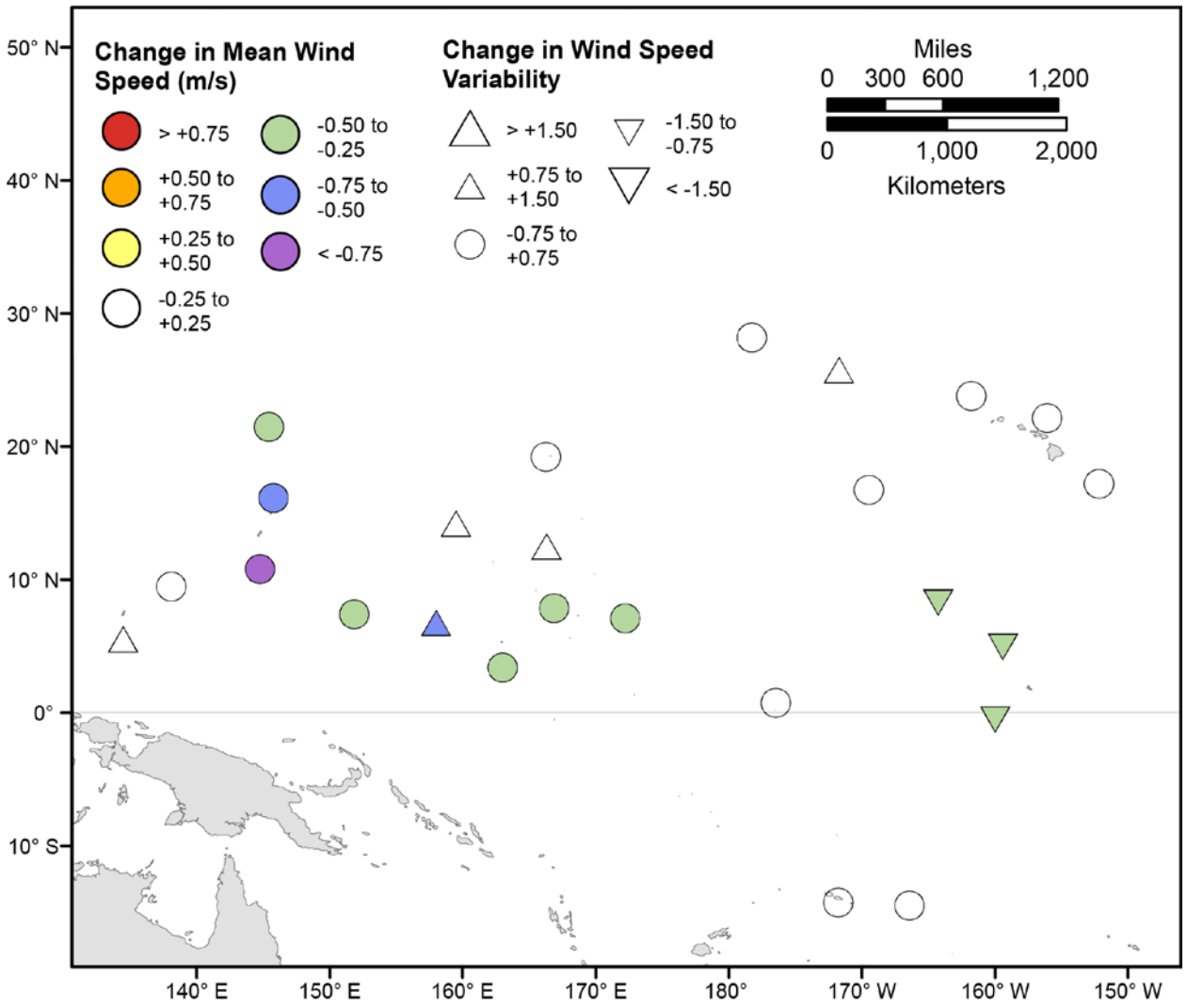

Figure 109. Map showing forecasted differences in the mean of the top 5 percent of wind speeds and variance in the top 5 percent of wind speeds for the years 2026–2045 from hindcasted values during the September-November season under the RCP4.5 future climatic scenario. The colors correspond to the magnitude of change in modeled mean wind speeds during 2026–2045 from those hindcasted for 1976–2005. The shapes correspond to the magnitude of change in modeled variance in wind speed during 2026–2045 from those hindcasted for 1976–2005. Units are in meters per second.

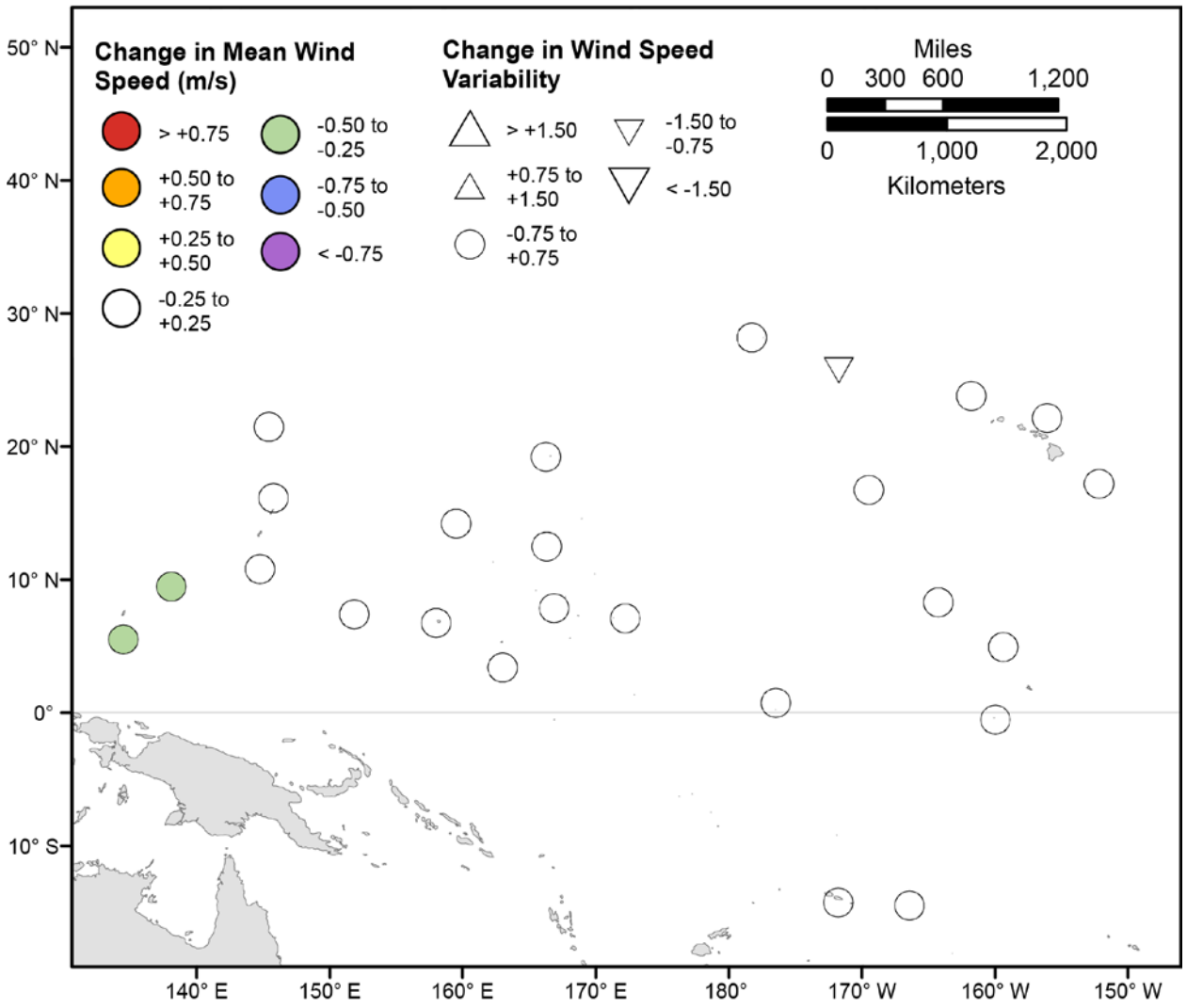

Figure 110. Map showing forecasted differences in mean wind speed and variance in wind speed for the years 2026–2045 from hindcasted values during the December-February season under the RCP8.5 future climatic scenario. The colors correspond to the magnitude of change in modeled mean wind speeds during 2026–2045 from those hindcasted for 1976–2005. The shapes correspond to the magnitude of change in modeled variance in wind speed during 2026–2045 from those hindcasted for 1976–2005. Units are in meters per second.

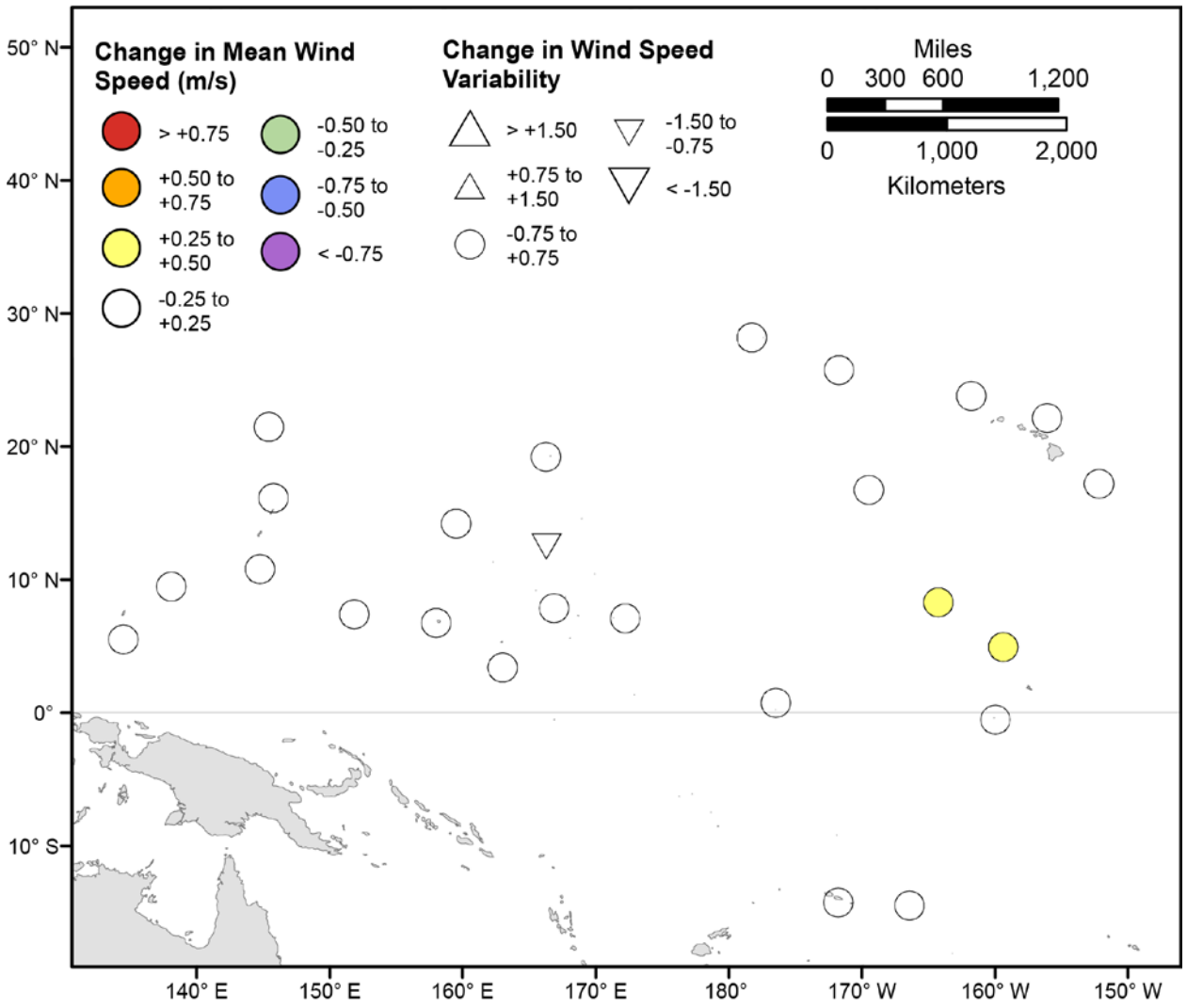

Figure 111. Map showing forecasted differences in mean wind speed and variance in wind speed for the years 2026–2045 from hindcasted values during the March-May season under the RCP8.5 future climatic scenario. The colors correspond to the magnitude of change in modeled mean wind speeds during 2026–2045 from those hindcasted for 1976–2005. The shapes correspond to the magnitude of change in modeled variance in wind speed during 2026–2045 from those hindcasted for 1976–2005. Units are in meters per second.

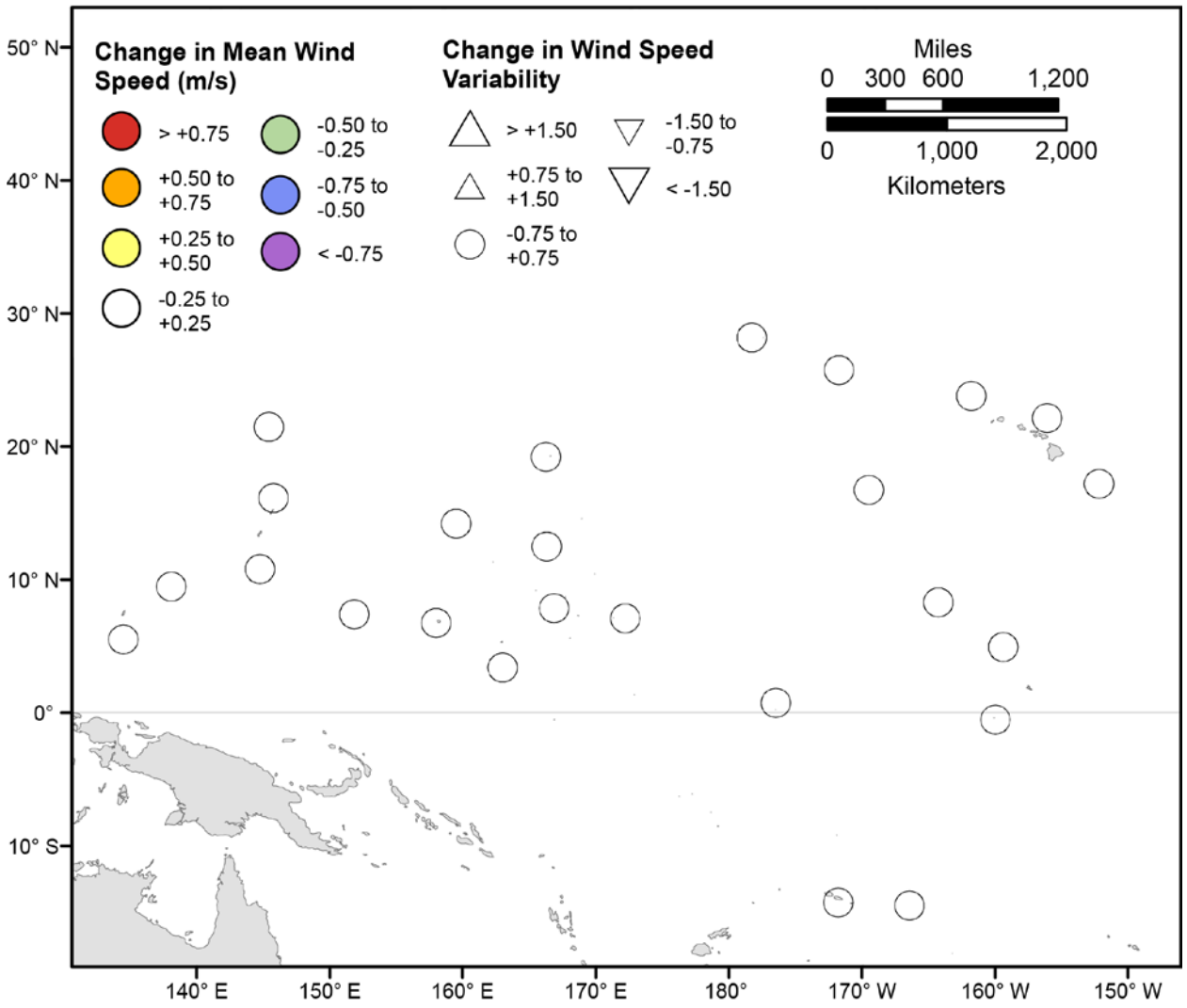

Figure 112. Map showing forecasted differences in mean wind speed and variance in wind speed for the years 2026–2045 from hindcasted values during the June-August season under the RCP8.5 future climatic scenario. The colors correspond to the magnitude of change in modeled mean wind speeds during 2026–2045 from those hindcasted for 1976–2005. The shapes correspond to the magnitude of change in modeled variance in wind speed during 2026–2045 from those hindcasted for 1976–2005. Units are in meters per second.

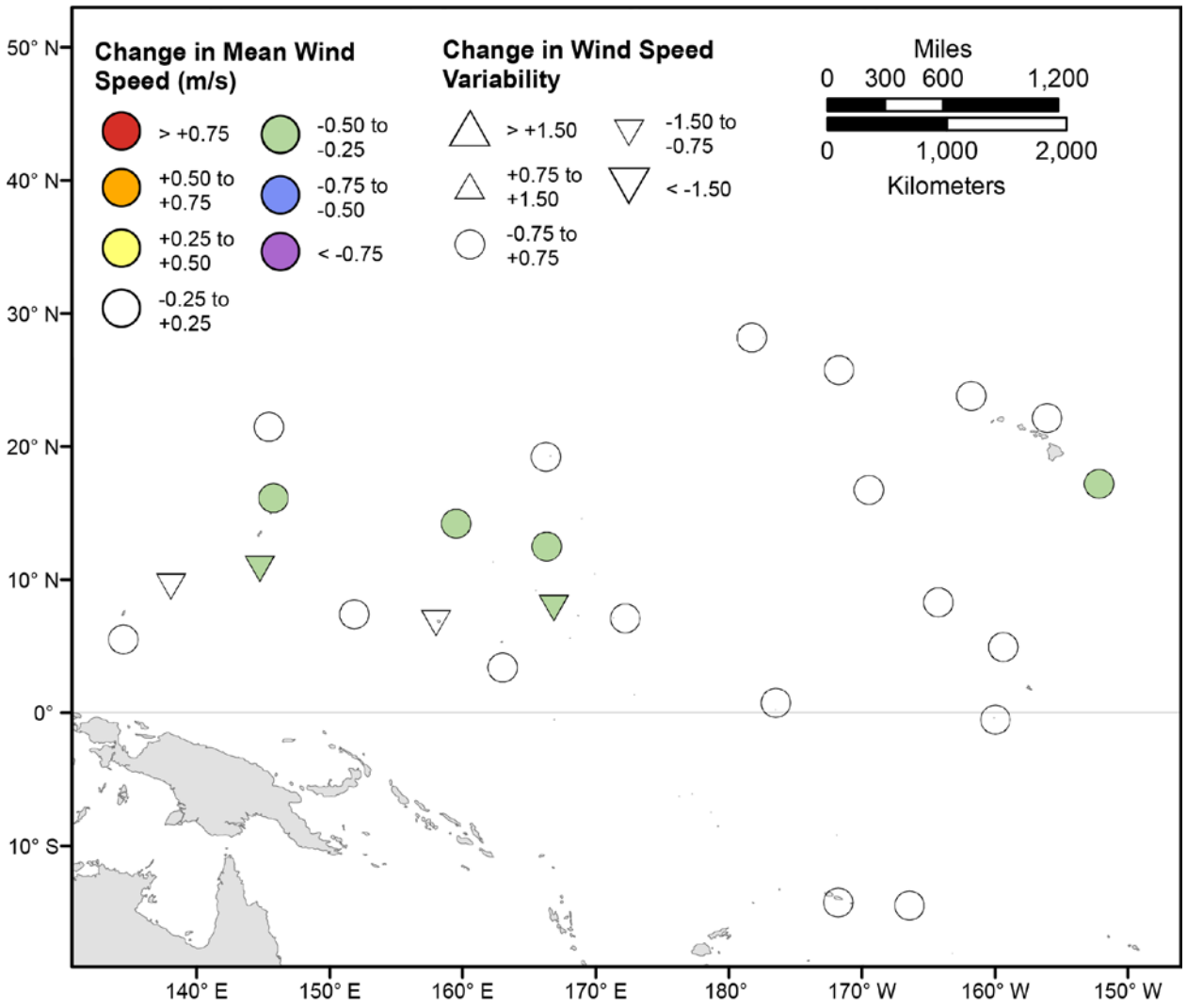

Figure 113. Map showing forecasted differences in mean wind speed and variance in wind speed for the years 2026–2045 from hindcasted values during the September-November season under the RCP8.5 future climatic scenario. The colors correspond to the magnitude of change in modeled mean wind speeds during 2026–2045 from those hindcasted for 1976–2005. The shapes correspond to the magnitude of change in modeled variance in wind speed during 2026–2045 from those hindcasted for 1976–2005. Units are in meters per second.

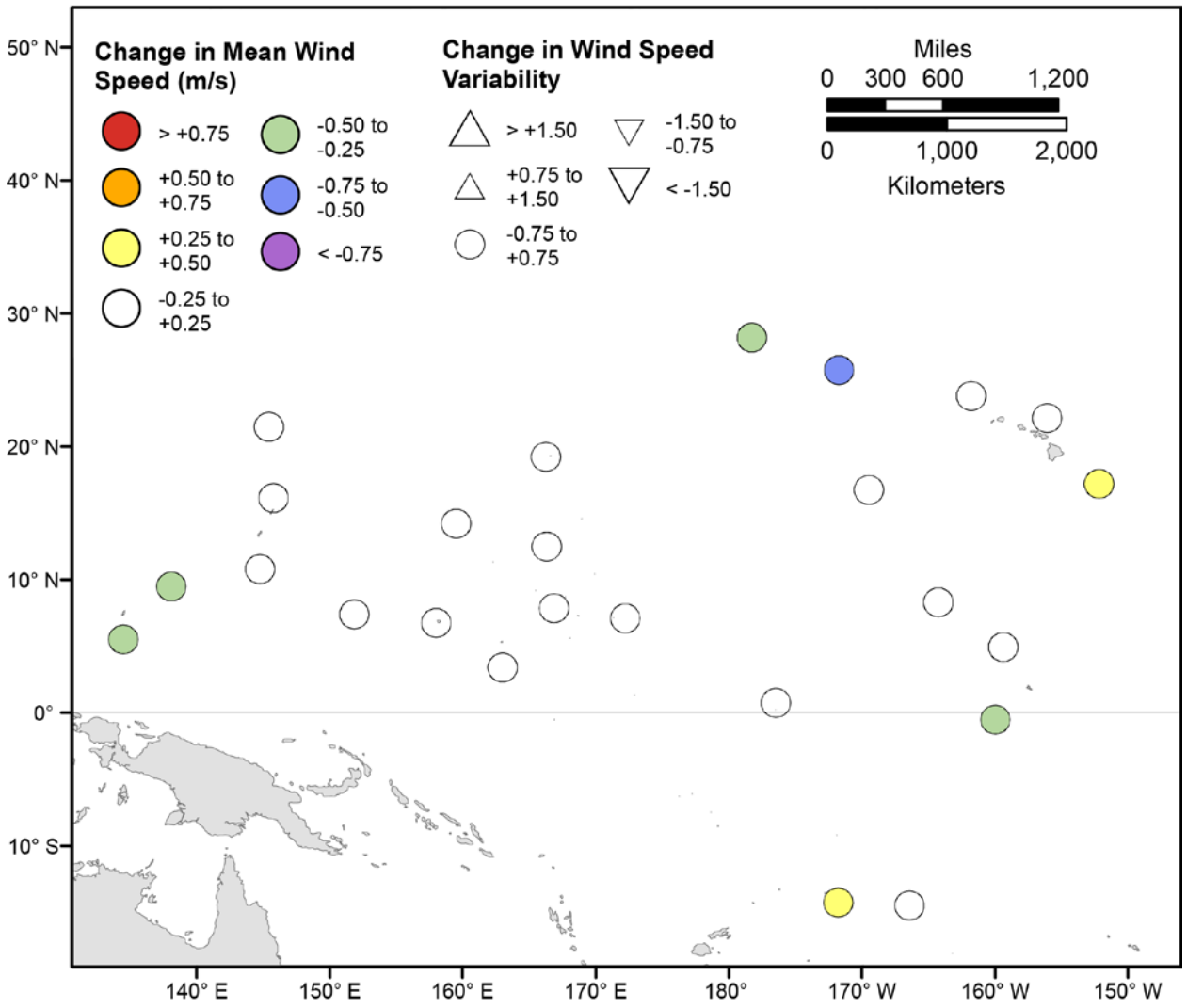

Figure 114. Map showing forecasted differences in the mean of the top 5 percent of wind speeds and variance in the top 5 percent of wind speeds for the years 2026–2045 from hindcasted values during the December-February season under the RCP8.5 future climatic scenario. The colors correspond to the magnitude of change in modeled mean wind speeds during 2026–2045 from those hindcasted for 1976–2005. The shapes correspond to the magnitude of change in modeled variance in wind speed during 2026–2045 from those hindcasted for 1976–2005. Units are in meters per second.

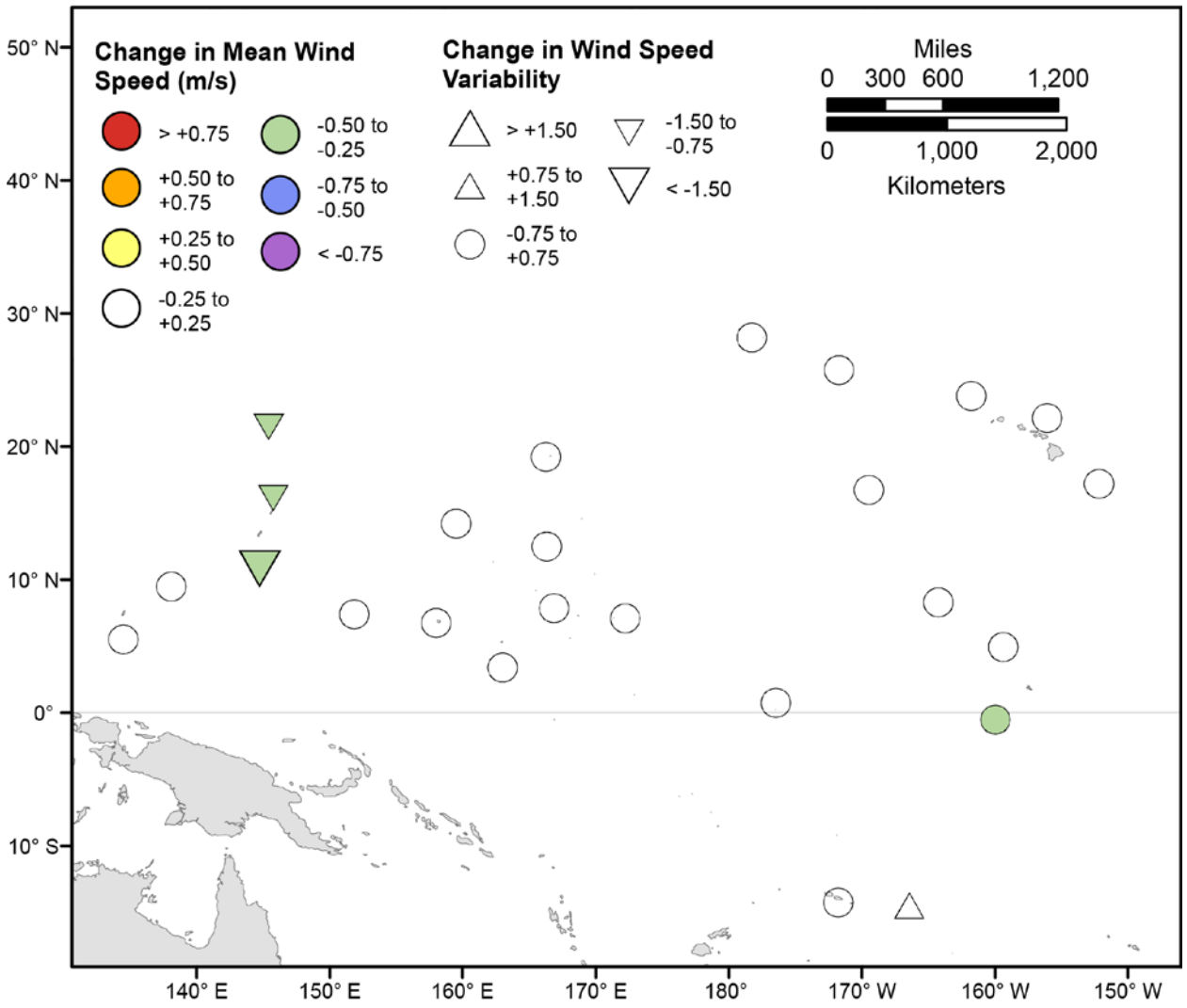

Figure 115. Map showing forecasted differences in the mean of the top 5 percent of wind speeds and variance in the top 5 percent of wind speeds for the years 2026–2045 from hindcasted values during the March-May season under the RCP8.5 future climatic scenario. The colors correspond to the magnitude of change in modeled mean wind speeds during 2026–2045 from those hindcasted for 1976–2005. The shapes correspond to the magnitude of change in modeled variance in wind speed during 2026–2045 from those hindcasted for 1976–2005. Units are in meters per second.

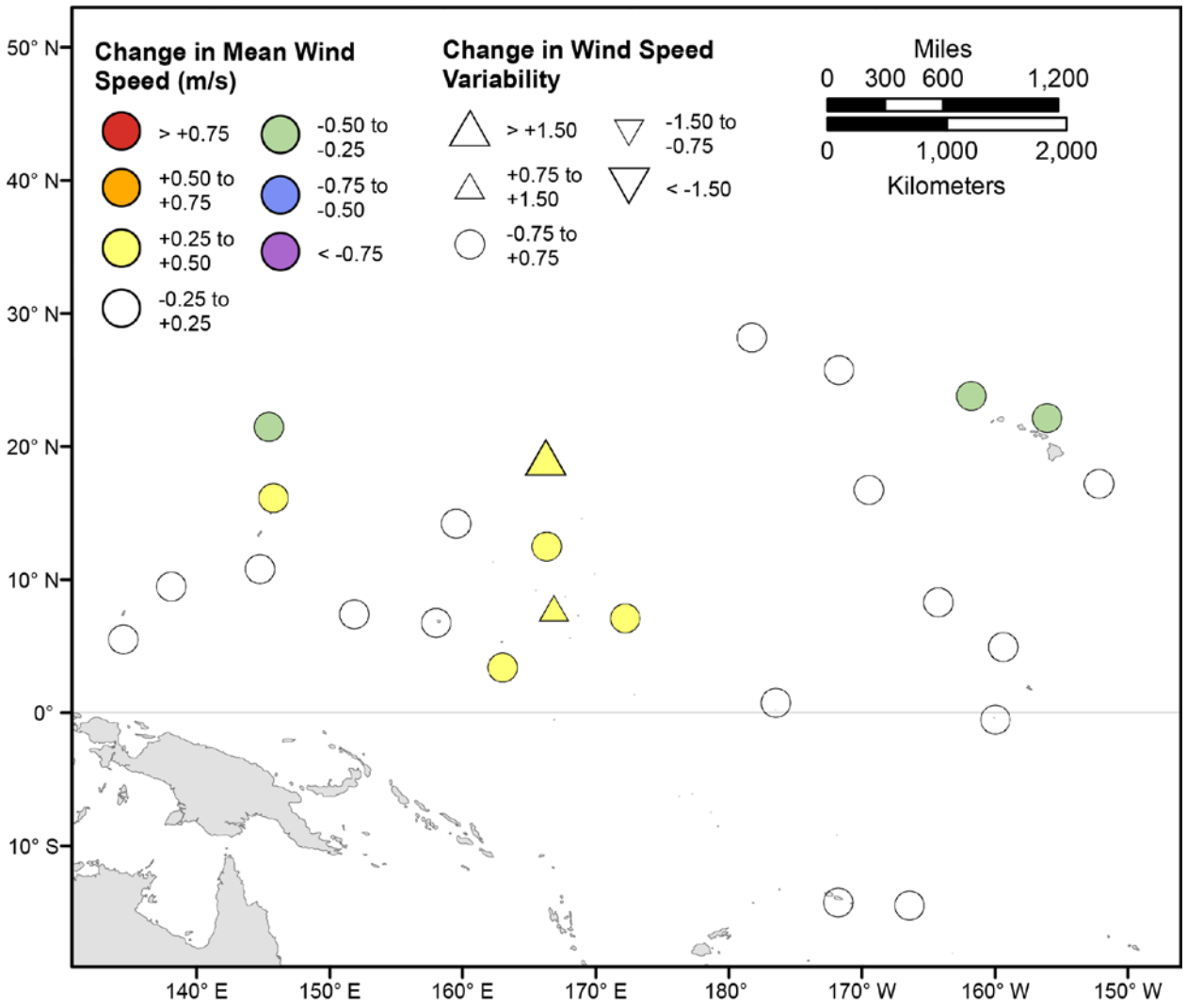

Figure 116. Map showing forecasted differences in the mean of the top 5 percent of wind speeds and variance in the top 5 percent of wind speeds for the years 2026–2045 from hindcasted values during the June-August season under the RCP8.5 future climatic scenario. The colors correspond to the magnitude of change in modeled mean wind speeds during 2026–2045 from those hindcasted for 1976–2005. The shapes correspond to the magnitude of change in modeled variance in wind speed during 2026–2045 from those hindcasted for 1976–2005. Units are in meters per second.

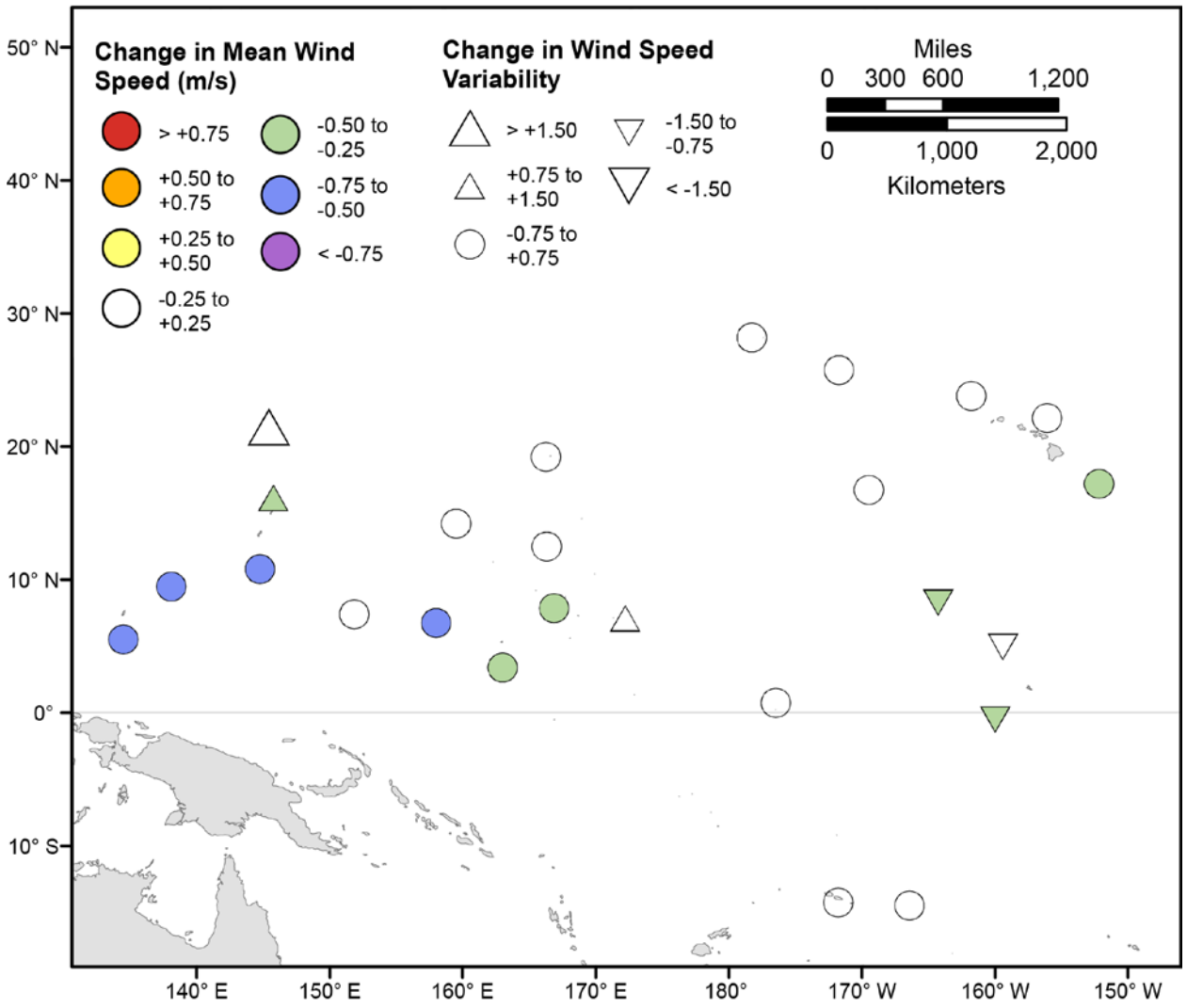

Figure 117. Map showing forecasted differences in the mean of the top 5 percent of wind speeds and variance in the top 5 percent of wind speeds for the years 2026–2045 from hindcasted values during the September-November season under the RCP8.5 future climatic scenario. The colors correspond to the magnitude of change in modeled mean wind speeds during 2026–2045 from those hindcasted for 1976–2005. The shapes correspond to the magnitude of change in modeled variance in wind speed during 2026–2045 from those hindcasted for 1976–2005. Units are in meters per second.

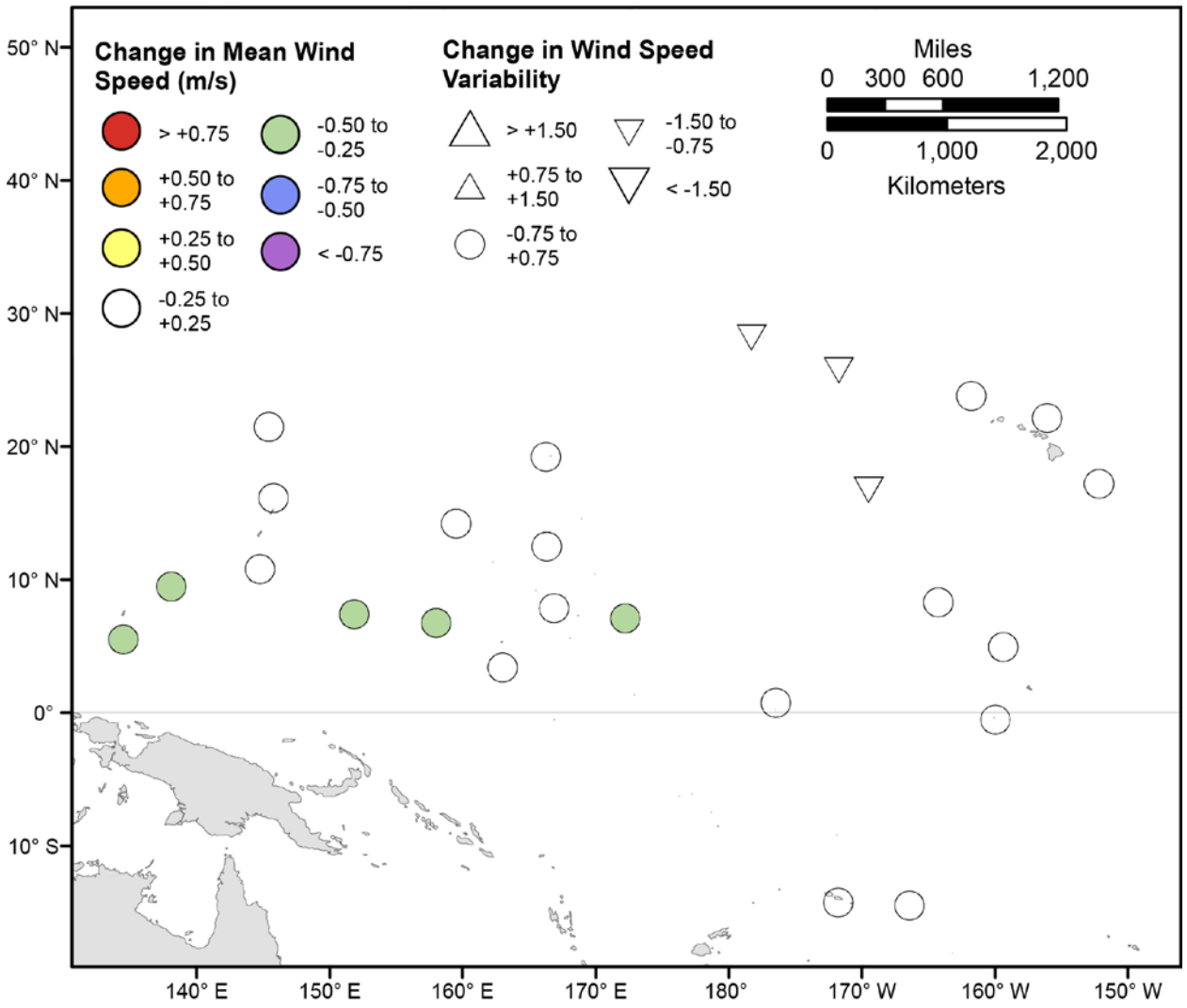

Figure 118. Map showing forecasted differences in mean wind speed and variance in wind speed for the years 2081–2100 from hindcasted values during the December-February season under the RCP4.5 future climatic scenario. The colors correspond to the magnitude of change in modeled mean wind speeds during 2081–2100 from those hindcasted for 1976–2005. The shapes correspond to the magnitude of change in modeled variance in wind speed during 2081–2100 from those hindcasted for 1976–2005. Units are in meters per second.

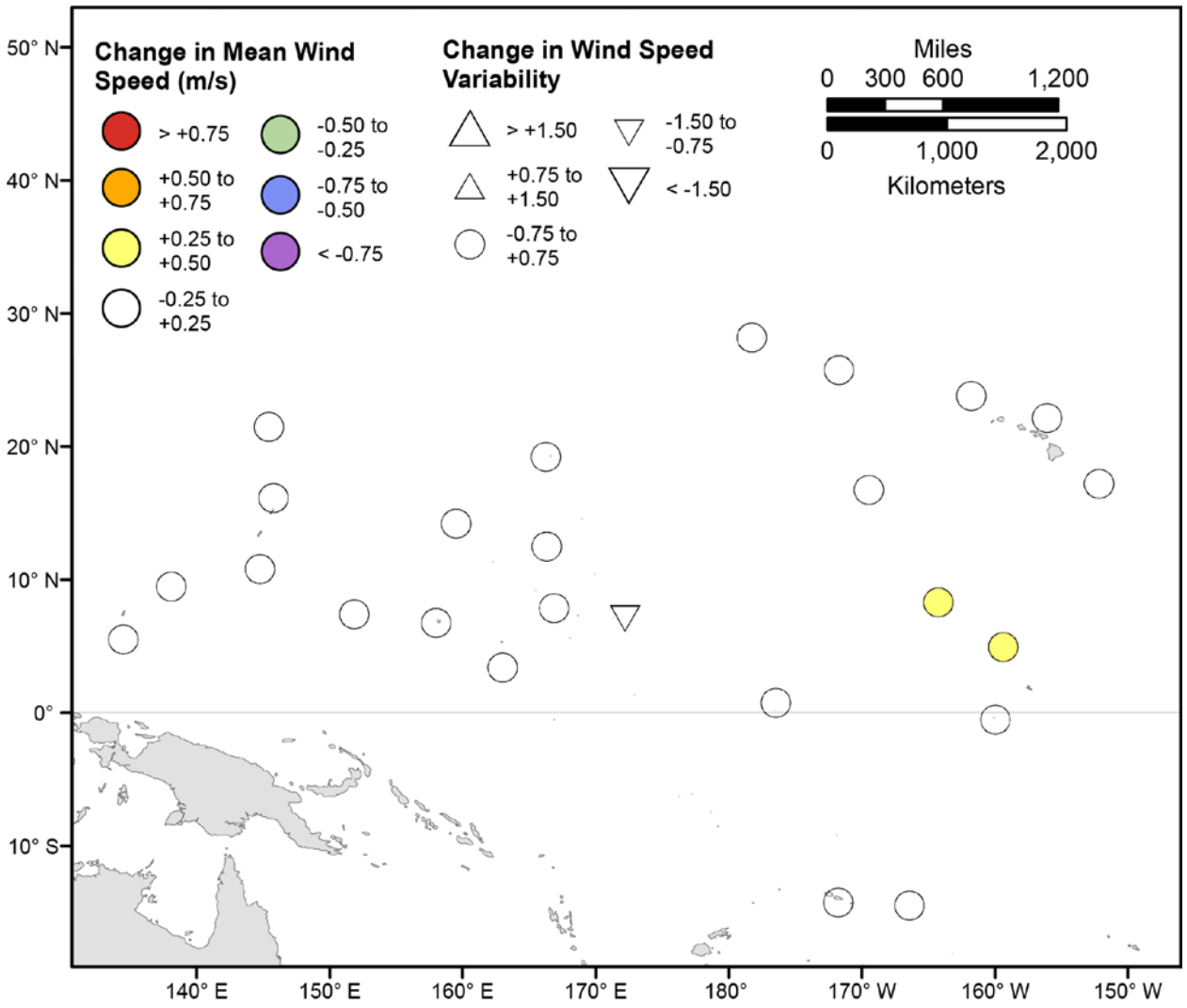

Figure 119. Map showing forecasted differences in mean wind speed and variance in wind speed for the years 2081–2100 from hindcasted values during the March-May season under the RCP4.5 future climatic scenario. The colors correspond to the magnitude of change in modeled mean wind speeds during 2081–2100 from those hindcasted for 1976–2005. The shapes correspond to the magnitude of change in modeled variance in wind speed during 2081–2100 from those hindcasted for 1976–2005. Units are in meters per second.

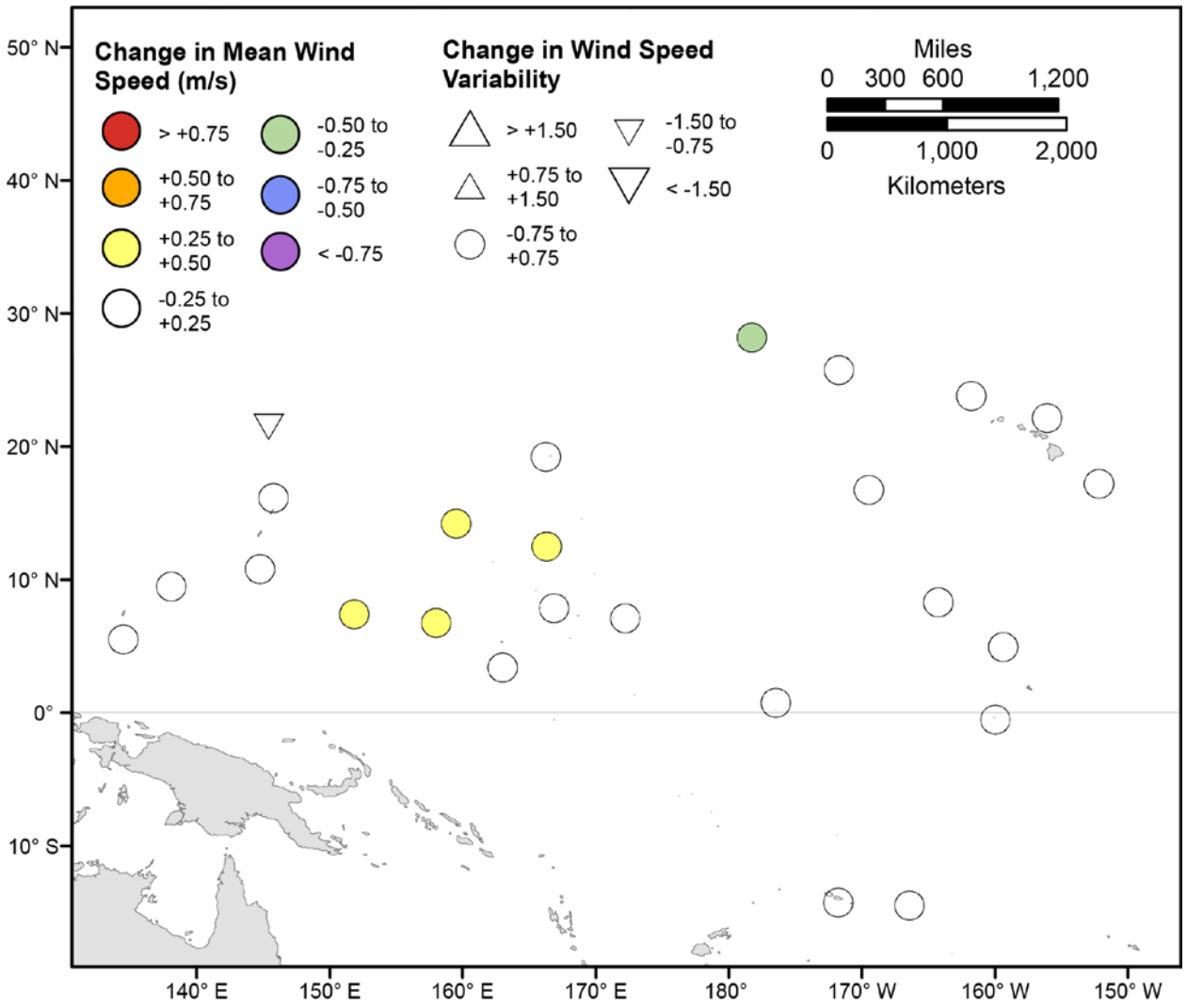

Figure 120. Map showing forecasted differences in mean wind speed and variance in wind speed for the years 2081–2100 from hindcasted values during the June-August season under the RCP4.5 future climatic scenario. The colors correspond to the magnitude of change in modeled mean wind speeds during 2081–2100 from those hindcasted for 1976–2005. The shapes correspond to the magnitude of change in modeled variance in wind speed during 2081–2100 from those hindcasted for 1976–2005. Units are in meters per second.

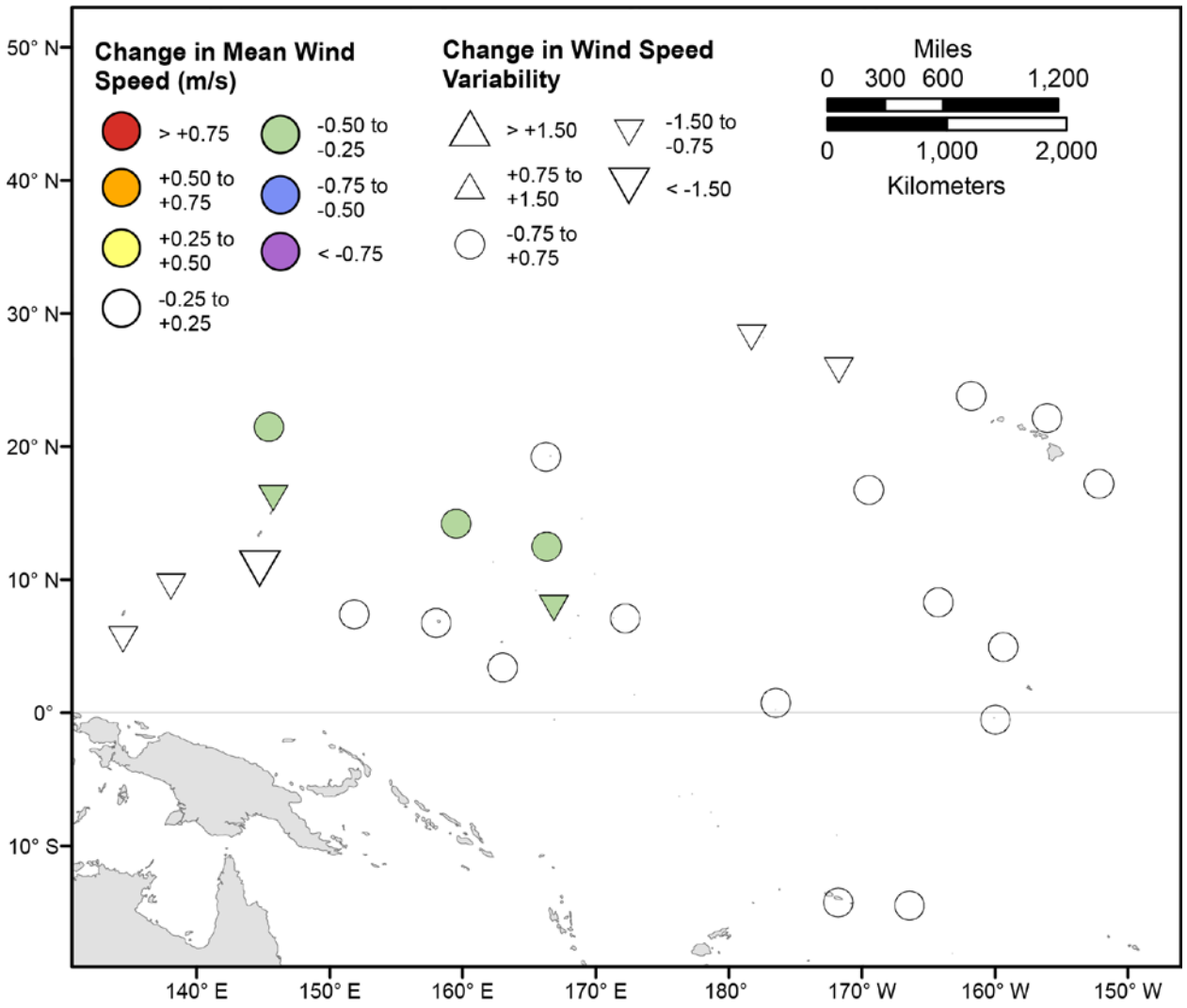

Figure 121. Map showing forecasted differences in mean wind speed and variance in wind speed for the years 2081–2100 from hindcasted values during the September-November season under the RCP4.5 future climatic scenario. The colors correspond to the magnitude of change in modeled mean wind speeds during 2081–2100 from those hindcasted for 1976–2005. The shapes correspond to the magnitude of change in modeled variance in wind speed during 2081–2100 from those hindcasted for 1976–2005. Units are in meters per second.

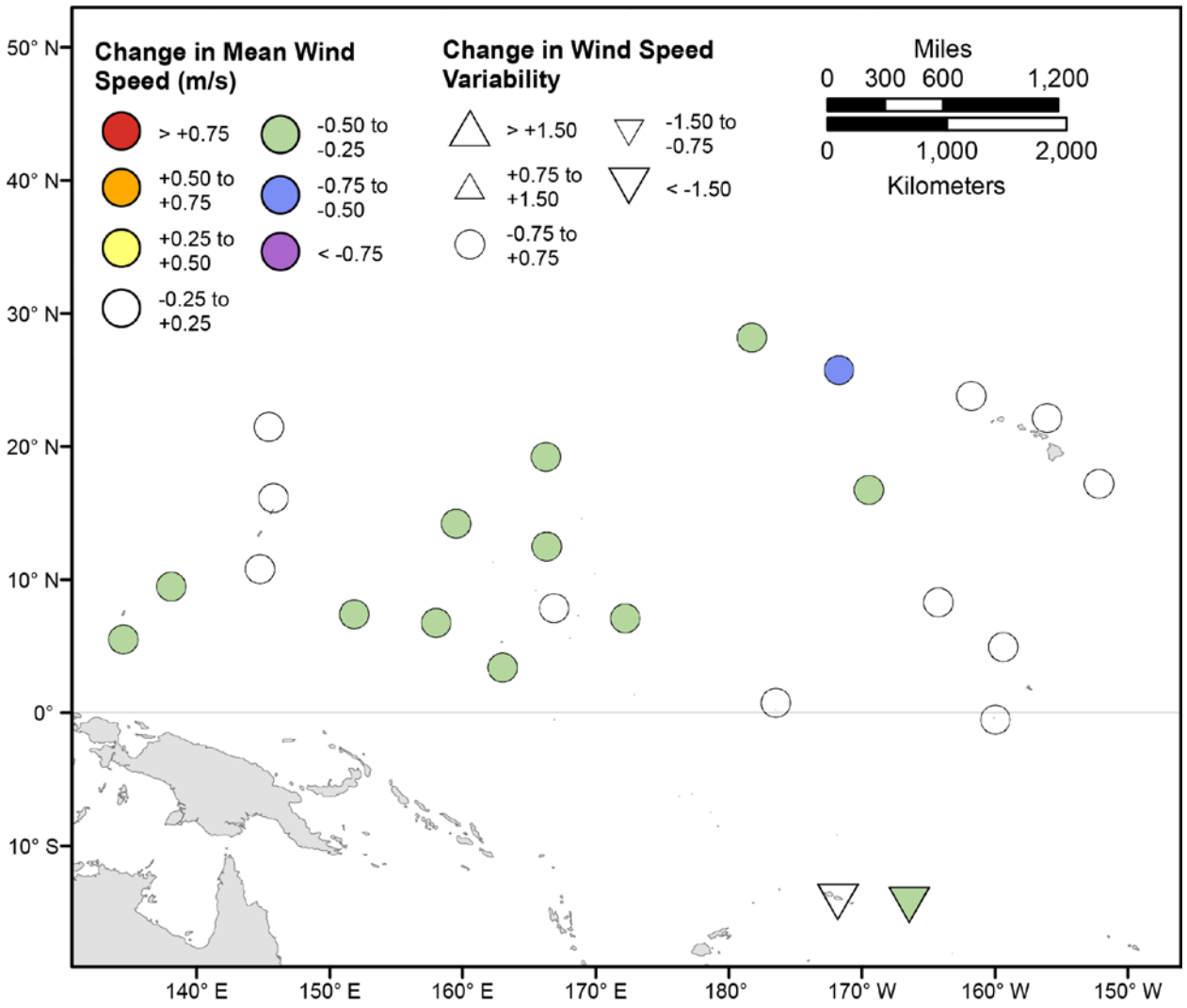

Figure 122. Map showing forecasted differences in the mean of the top 5 percent of wind speeds and variance in the top 5 percent of wind speeds for the years 2081–2100 from hindcasted values during the December-February season under the RCP4.5 future climatic scenario. The colors correspond to the magnitude of change in modeled mean wind speeds during 2081–2100 from those hindcasted for 1976–2005. The shapes correspond to the magnitude of change in modeled variance in wind speed during 2081–2100 from those hindcasted for 1976–2005. Units are in meters per second.

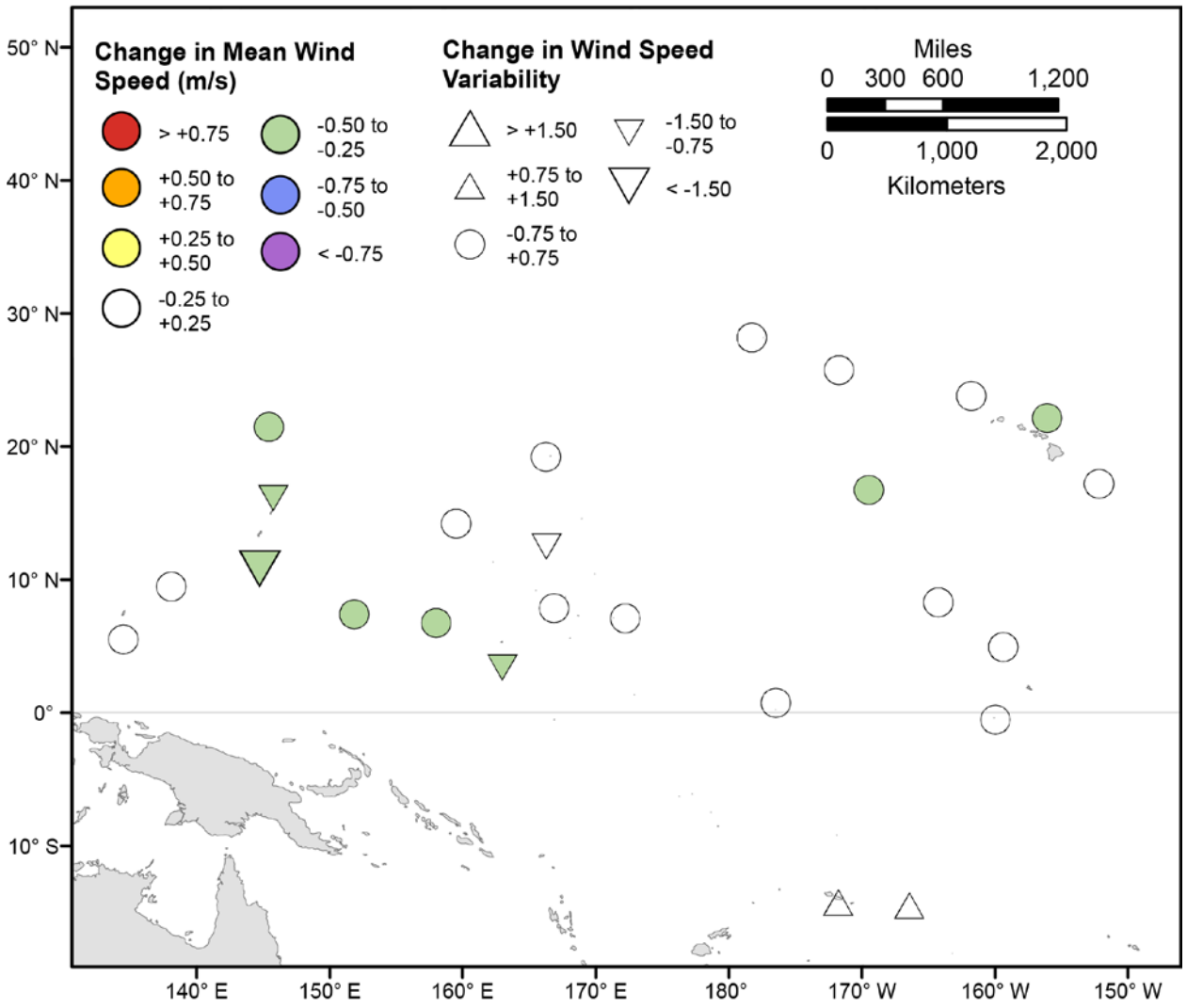

Figure 123. Map showing forecasted differences in the mean of the top 5 percent of wind speeds and variance in the top 5 percent of wind speeds for the years 2081–2100 from hindcasted values during the March-May season under the RCP4.5 future climatic scenario. The colors correspond to the magnitude of change in modeled mean wind speeds during 2081–2100 from those hindcasted for 1976–2005. The shapes correspond to the magnitude of change in modeled variance in wind speed during 2081–2100 from those hindcasted for 1976–2005. Units are in meters per second.

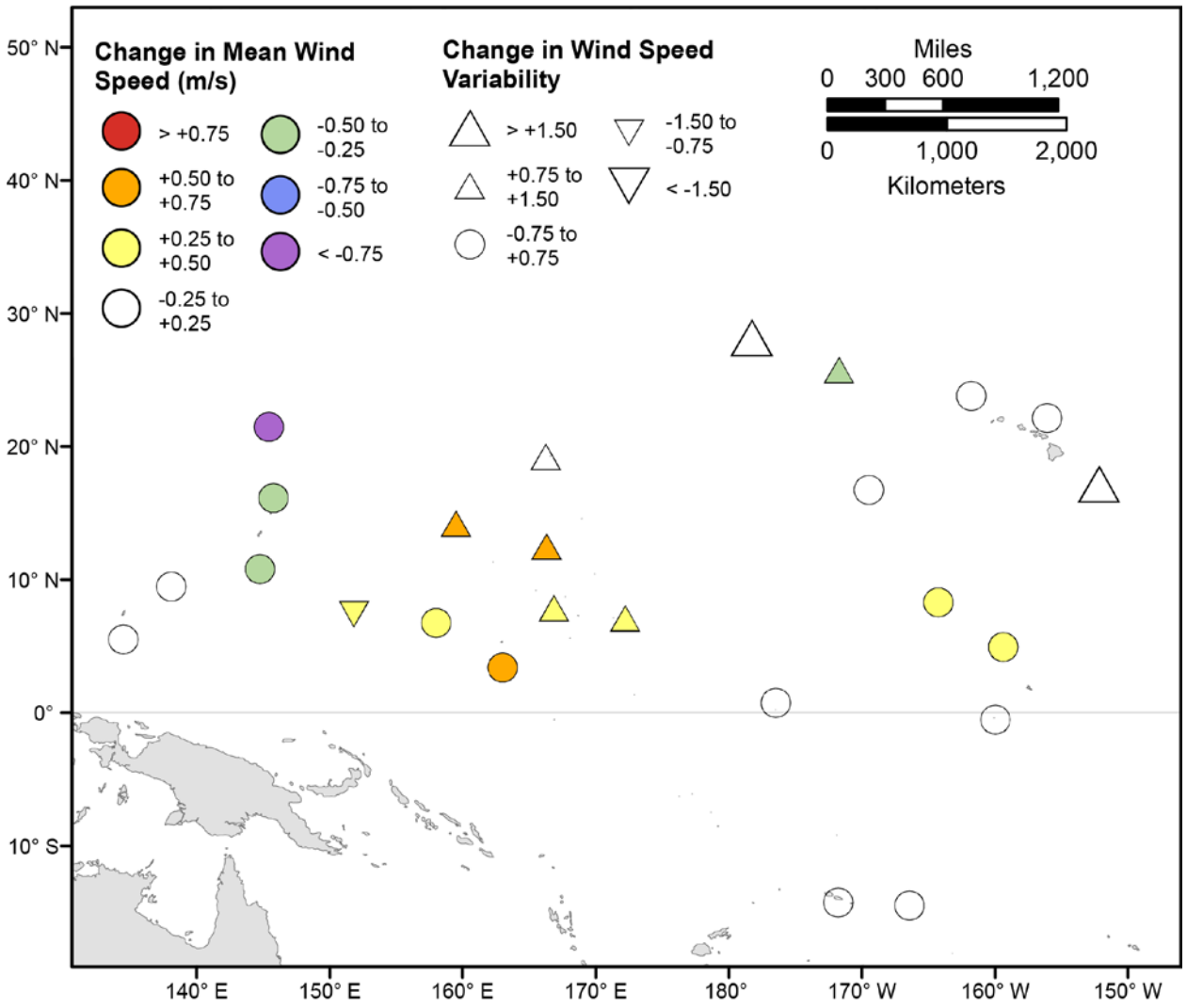

Figure 124. Map showing forecasted differences in the mean of the top 5 percent of wind speeds and variance in the top 5 percent of wind speeds for the years 2081–2100 from hindcasted values during the June-August season under the RCP4.5 future climatic scenario. The colors correspond to the magnitude of change in modeled mean wind speeds during 2081–2100 from those hindcasted for 1976–2005. The shapes correspond to the magnitude of change in modeled variance in wind speed during 2081–2100 from those hindcasted for 1976–2005. Units are in meters per second.

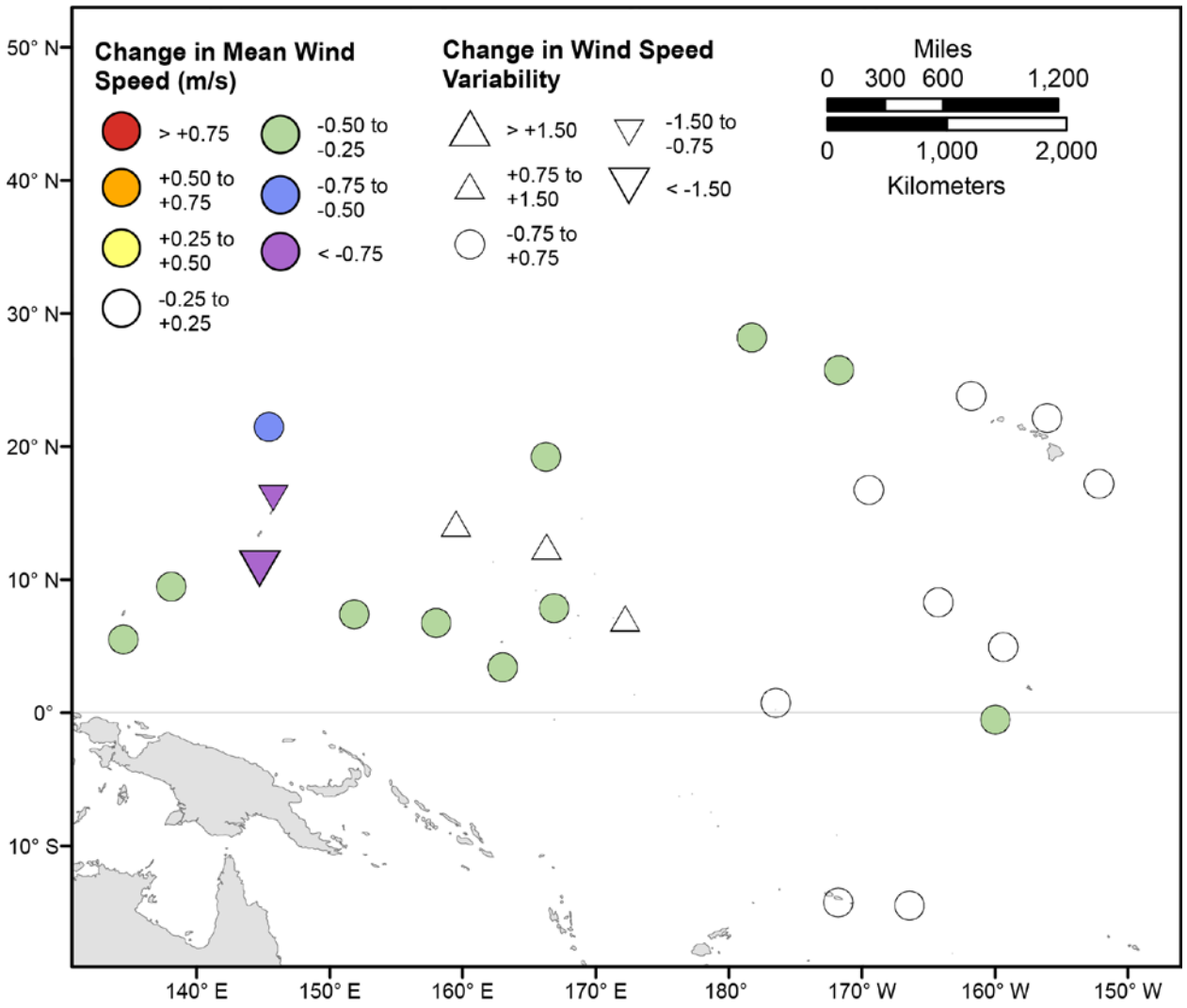

Figure 125. Map showing forecasted differences in the mean of the top 5 percent of wind speeds and variance in the top 5 percent of wind speeds for the years 2081–2100 from hindcasted values during the September-November season under the RCP4.5 future climatic scenario. The colors correspond to the magnitude of change in modeled mean wind speeds during 2081–2100 from those hindcasted for 1976–2005. The shapes correspond to the magnitude of change in modeled variance in wind speed during 2081–2100 from those hindcasted for 1976–2005. Units are in meters per second.

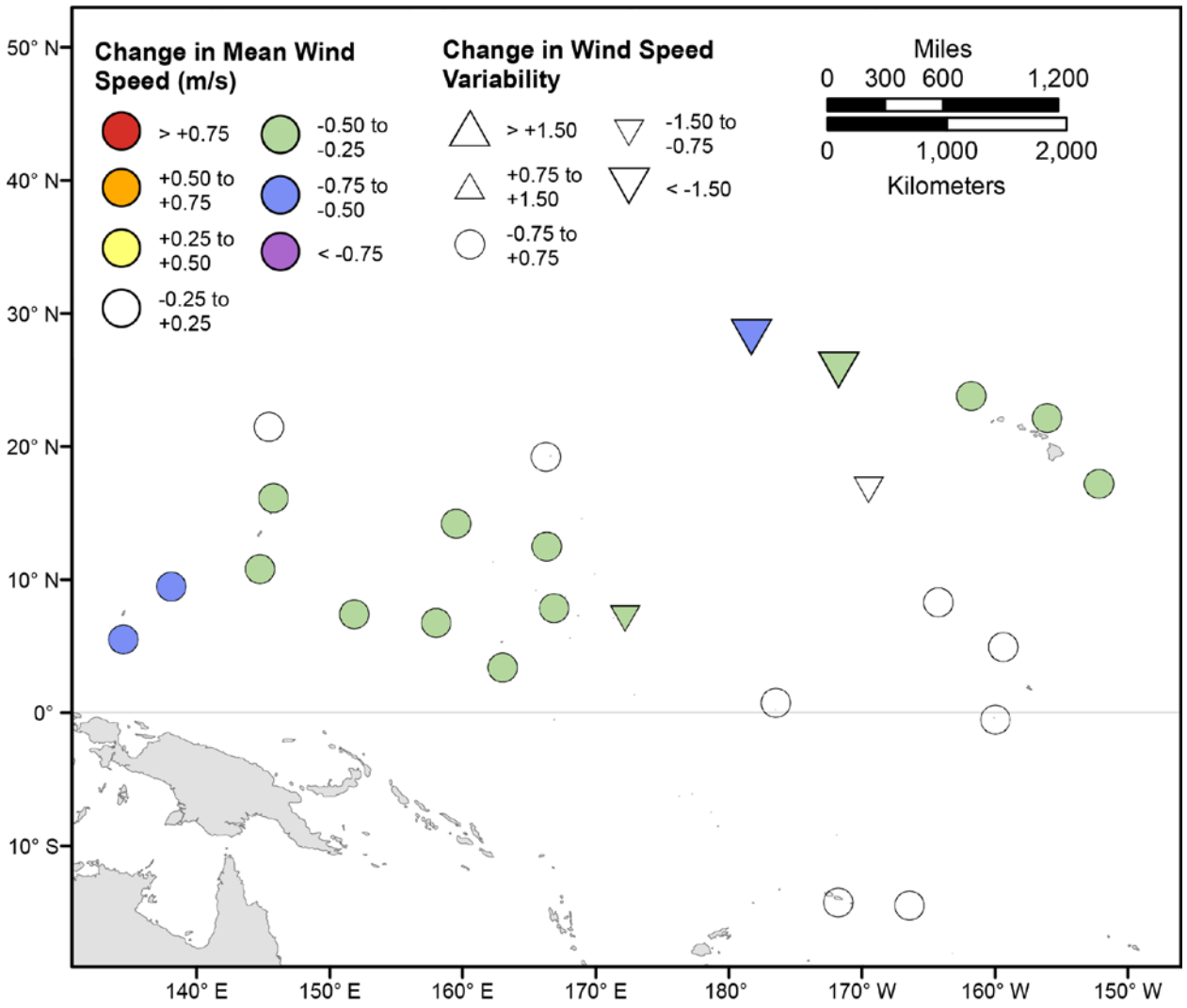

Figure 126. Map showing forecasted differences in mean wind speed and variance in wind speed for the years 2081–2100 from hindcasted values during the December-February season under the RCP8.5 future climatic scenario. The colors correspond to the magnitude of change in modeled mean wind speeds during 2081–2100 from those hindcasted for 1976–2005. The shapes correspond to the magnitude of change in modeled variance in wind speed during 2081–2100 from those hindcasted for 1976–2005. Units are in meters per second.

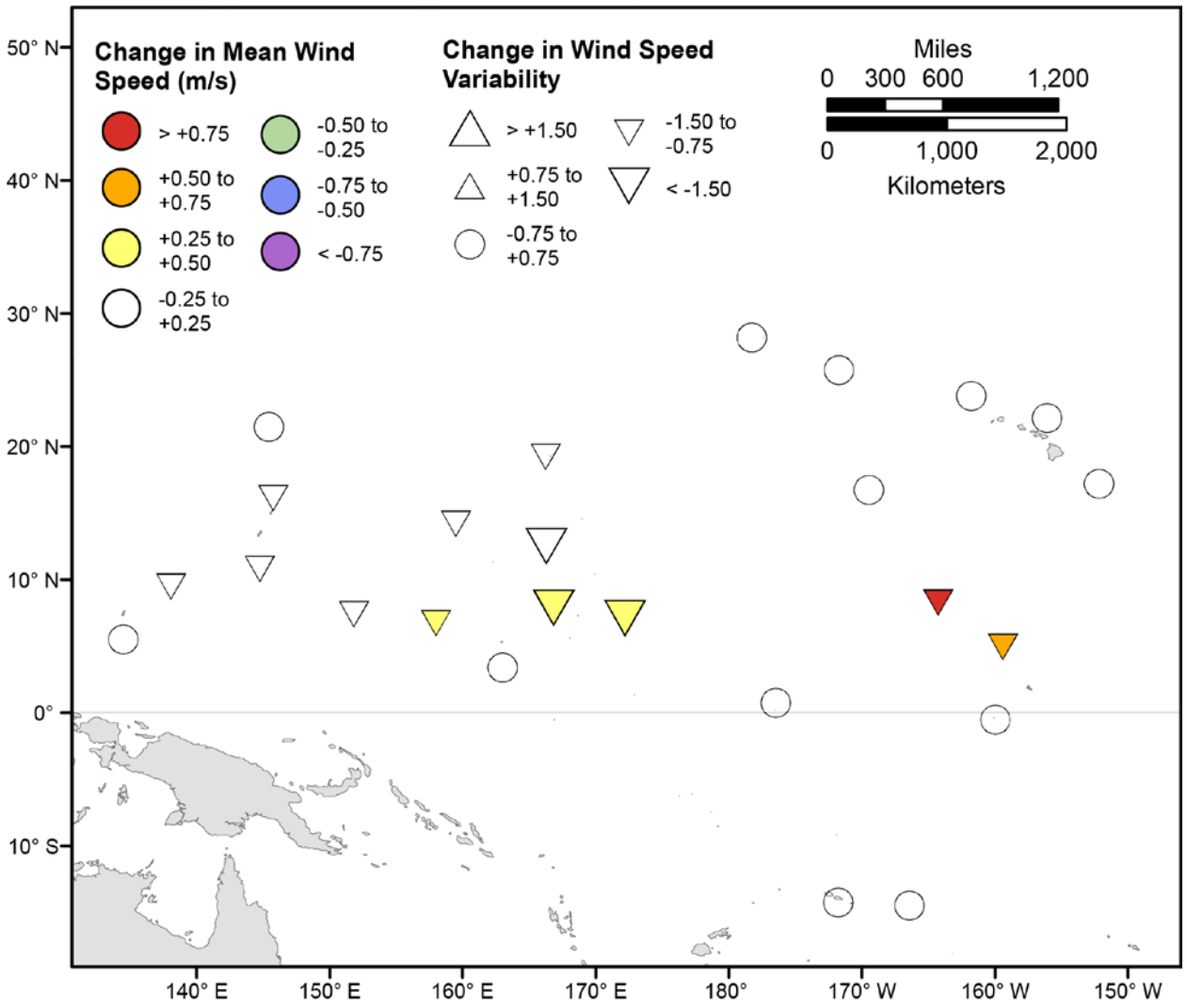

Figure 127. Map showing forecasted differences in mean wind speed and variance in wind speed for the years 2081–2100 from hindcasted values during the March-May season under the RCP8.5 future climatic scenario. The colors correspond to the magnitude of change in modeled mean wind speeds during 2081–2100 from those hindcasted for 1976–2005. The shapes correspond to the magnitude of change in modeled variance in wind speed during 2081–2100 from those hindcasted for 1976–2005. Units are in meters per second.

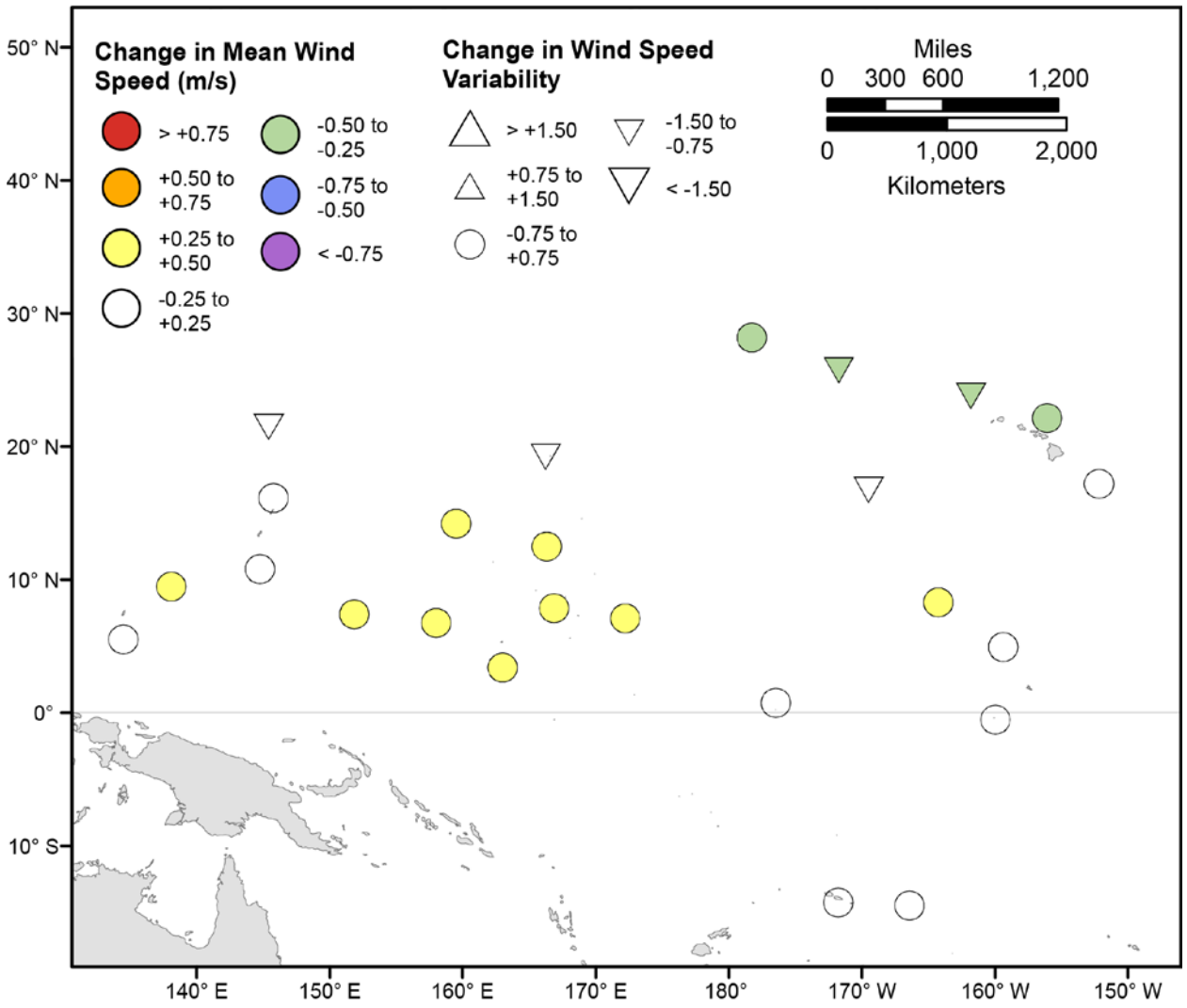

Figure 128. Map showing forecasted differences in mean wind speed and variance in wind speed for the years 2081–2100 from hindcasted values during the June-August season under the RCP8.5 future climatic scenario. The colors correspond to the magnitude of change in modeled mean wind speeds during 2081–2100 from those hindcasted for 1976–2005. The shapes correspond to the magnitude of change in modeled variance in wind speed during 2081–2100 from those hindcasted for 1976–2005. Units are in meters per second.

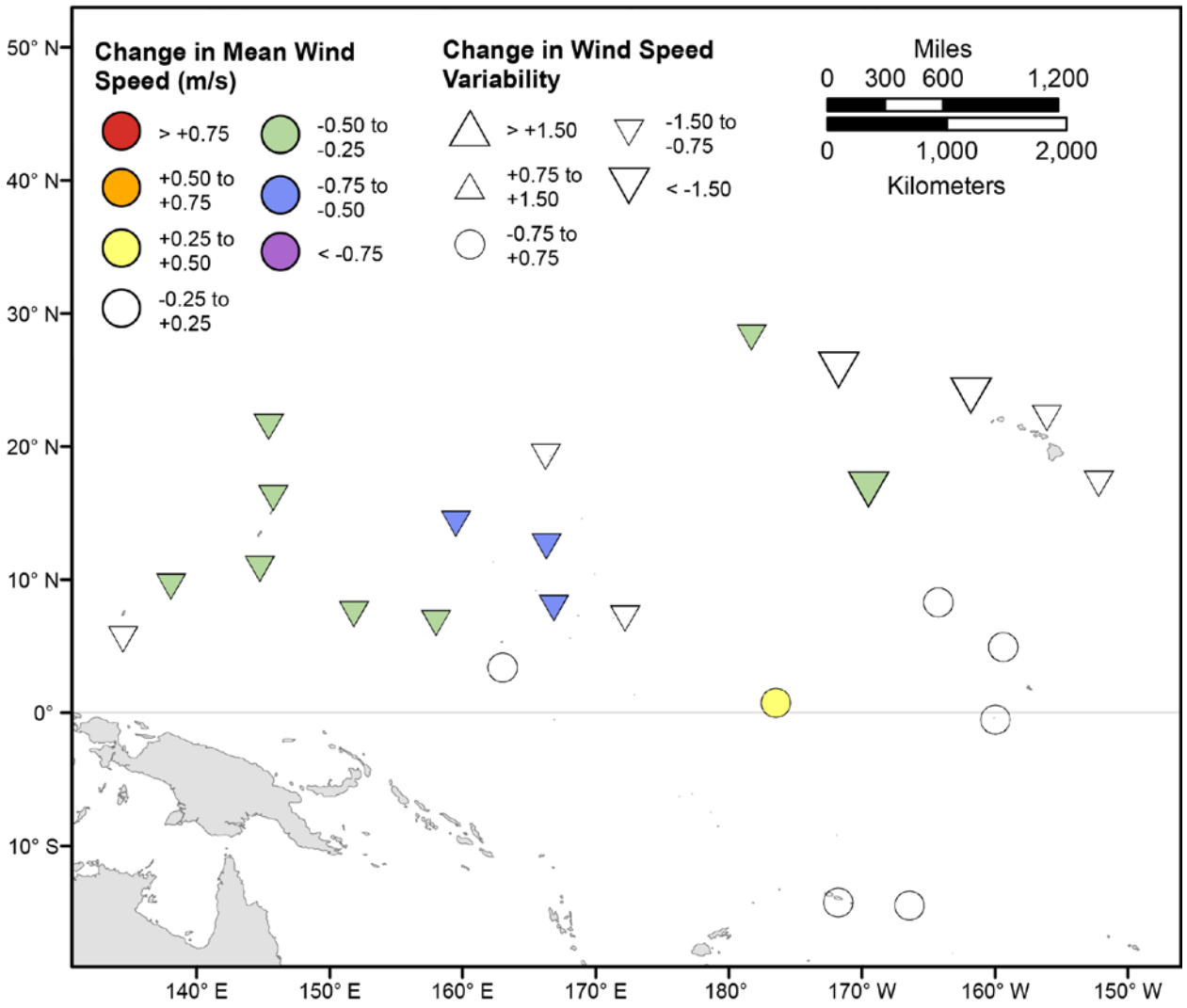

Figure 129. Map showing forecasted differences in mean wind speed and variance in wind speed for the years 2081–2100 from hindcasted values during the September-November season under the RCP8.5 future climatic scenario. The colors correspond to the magnitude of change in modeled mean wind speeds during 2081–2100 from those hindcasted for 1976–2005. The shapes correspond to the magnitude of change in modeled variance in wind speed during 2081–2100 from those hindcasted for 1976–2005. Units are in meters per second.

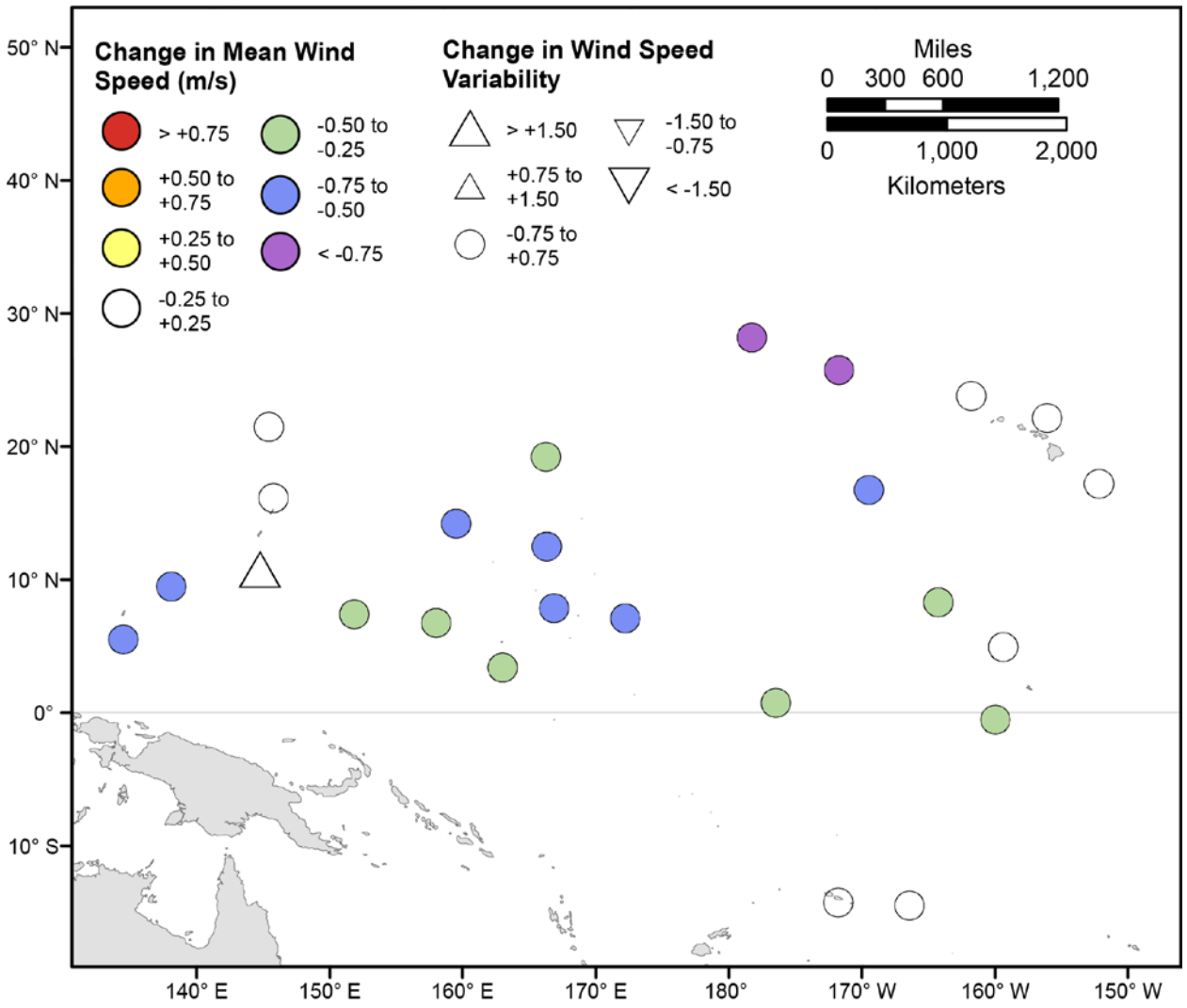

Figure 130. Map showing forecasted differences in the mean of the top 5 percent of wind speeds and variance in the top 5 percent of wind speeds for the years 2081–2100 from hindcasted values during the December-February season under the RCP8.5 future climatic scenario. The colors correspond to the magnitude of change in modeled mean wind speeds during 2081–2100 from those hindcasted for 1976–2005. The shapes correspond to the magnitude of change in modeled variance in wind speed during 2081–2100 from those hindcasted for 1976–2005. Units are in meters per second.

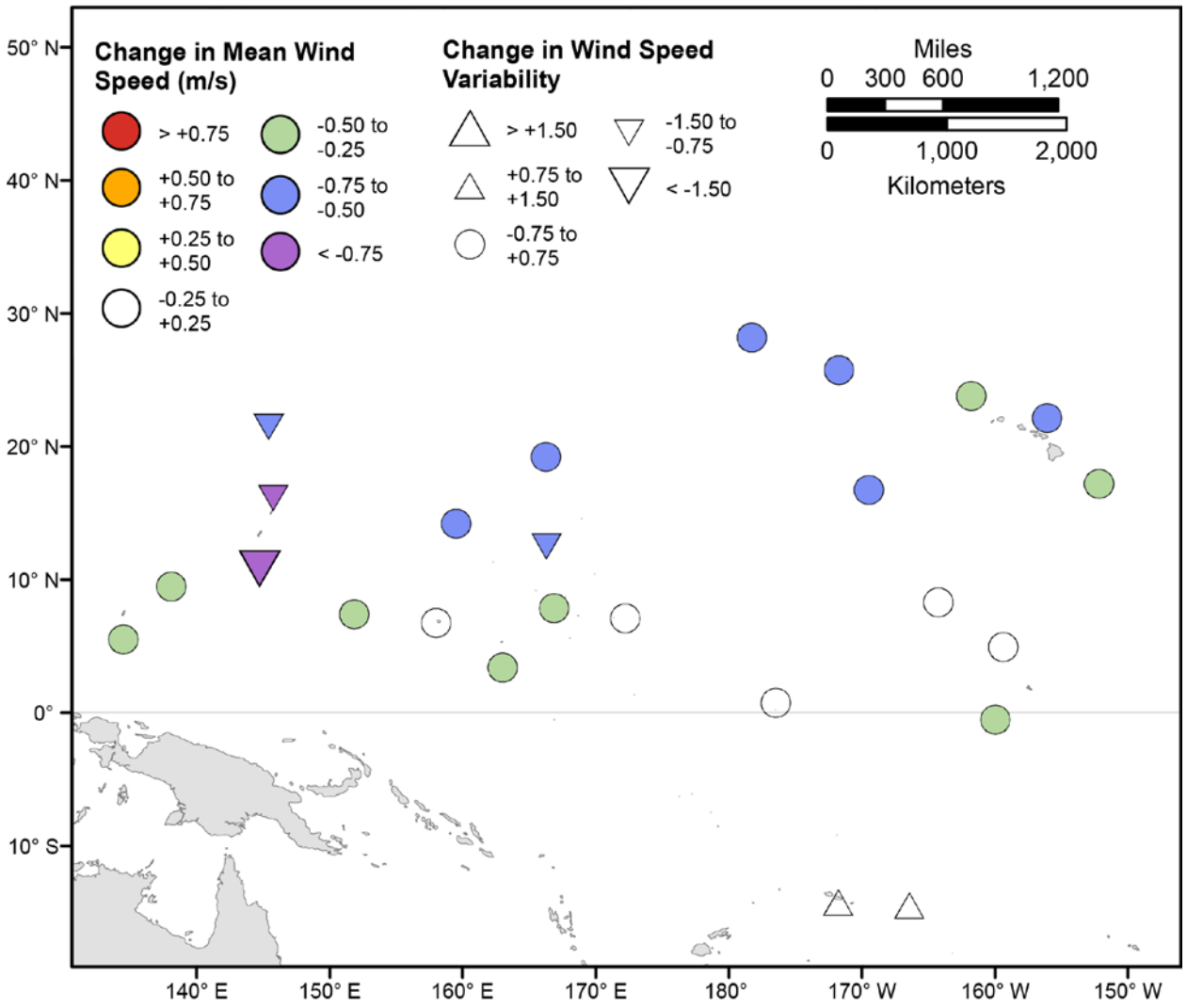

Figure 131. Map showing forecasted differences in the mean of the top 5 percent of wind speeds and variance in the top 5 percent of wind speeds for the years 2081–2100 from hindcasted values during the March-May season under the RCP8.5 future climatic scenario. The colors correspond to the magnitude of change in modeled mean wind speeds during 2081–2100 from those hindcasted for 1976–2005. The shapes correspond to the magnitude of change in modeled variance in wind speed during 2081–2100 from those hindcasted for 1976–2005. Units are in meters per second.

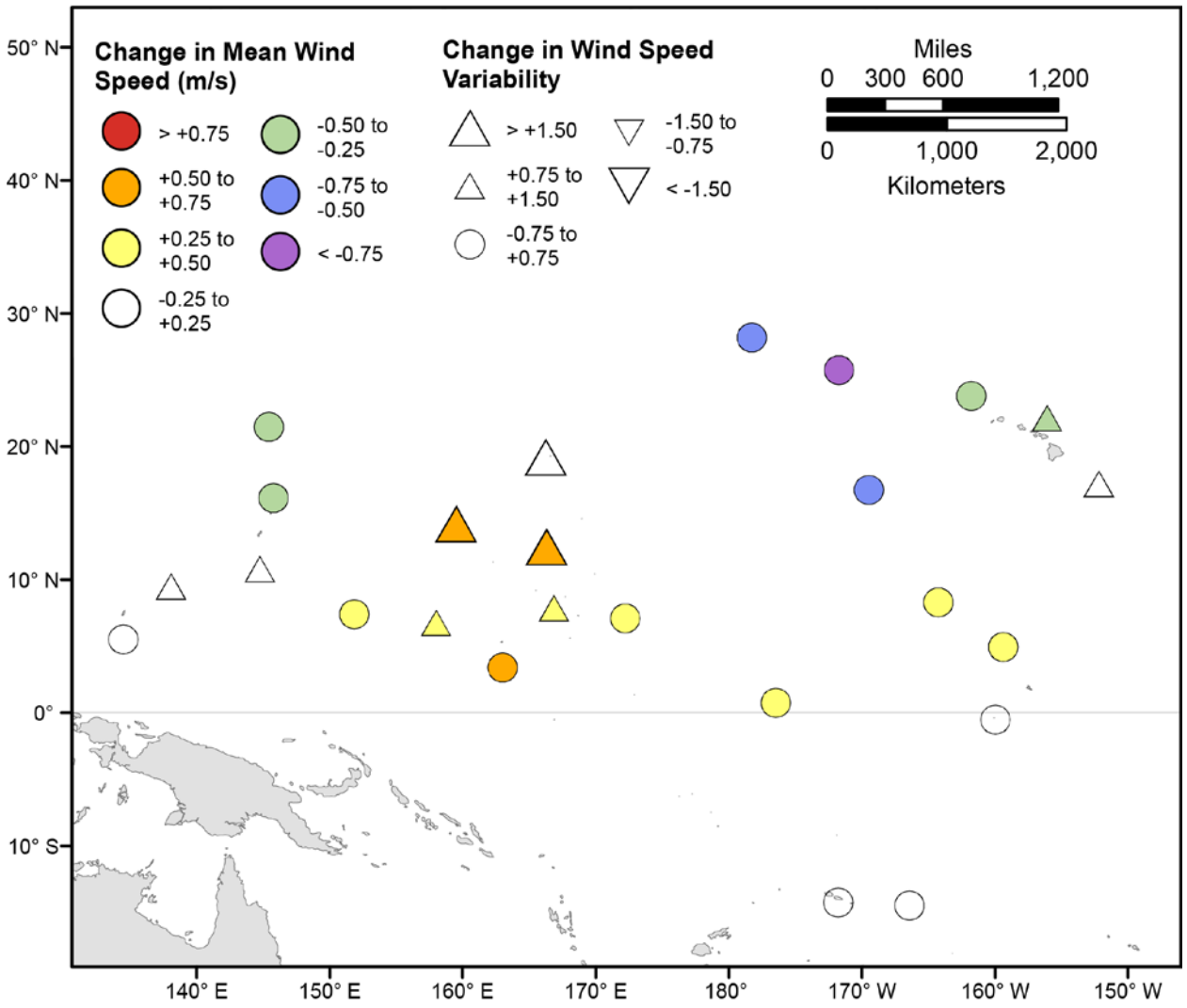

Figure 132. Map showing forecasted differences in the mean of the top 5 percent of wind speeds and variance in the top 5 percent of wind speeds for the years 2081–2100 from hindcasted values during the June-August season under the RCP8.5 future climatic scenario. The colors correspond to the magnitude of change in modeled mean wind speeds during 2081–2100 from those hindcasted for 1976–2005. The shapes correspond to the magnitude of change in modeled variance in wind speed during 2081–2100 from those hindcasted for 1976–2005. Units are in meters per second.

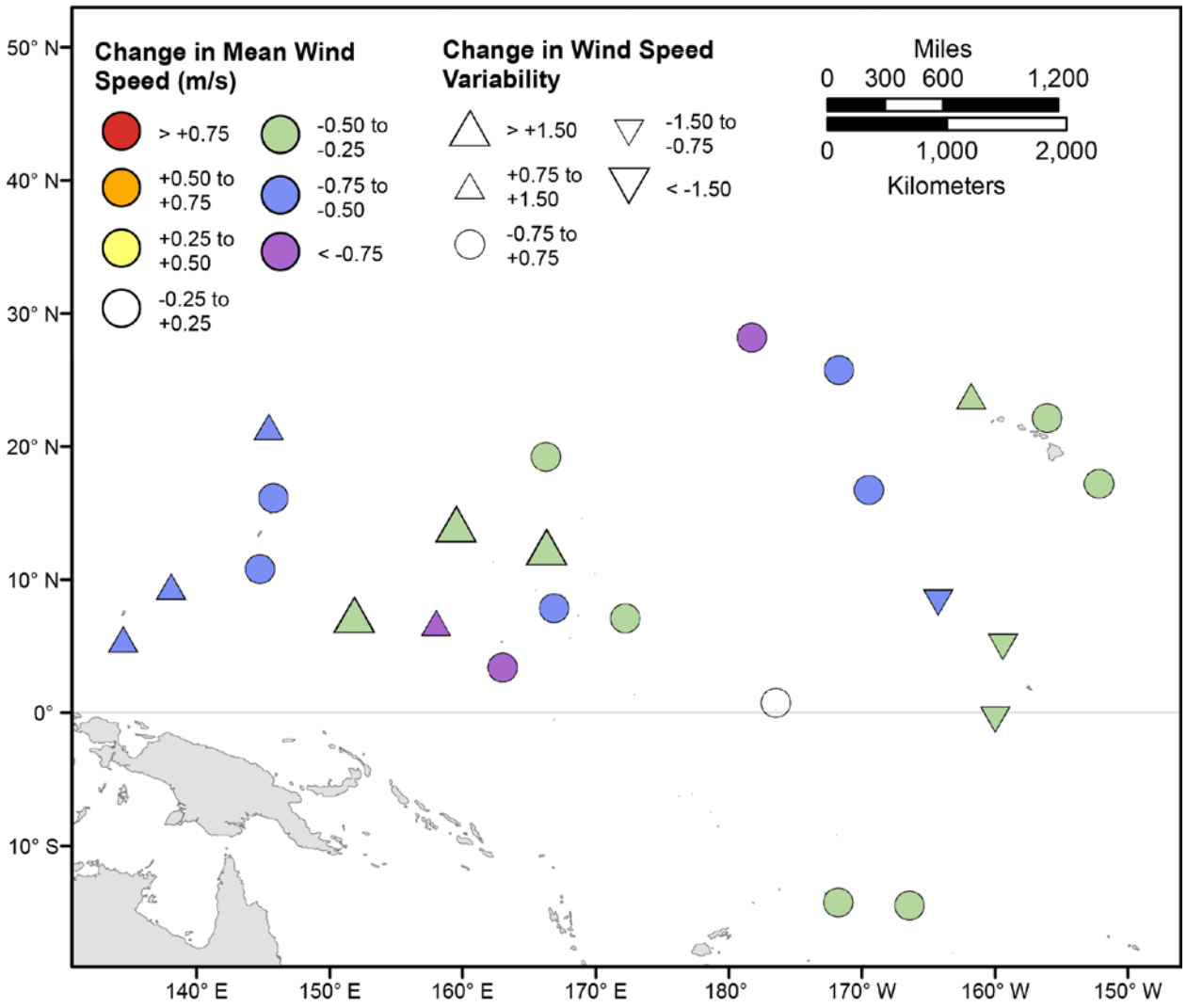

Figure 133. Map showing forecasted differences in the mean of the top 5 percent of wind speeds and variance in the top 5 percent of wind speeds for the years 2081–2100 from hindcasted values during the September-November season under the RCP8.5 future climatic scenario. The colors correspond to the magnitude of change in modeled mean wind speeds during 2081–2100 from those hindcasted for 1976–2005. The shapes correspond to the magnitude of change in modeled variance in wind speed during 2081–2100 from those hindcasted for 1976–2005. Units are in meters per second.

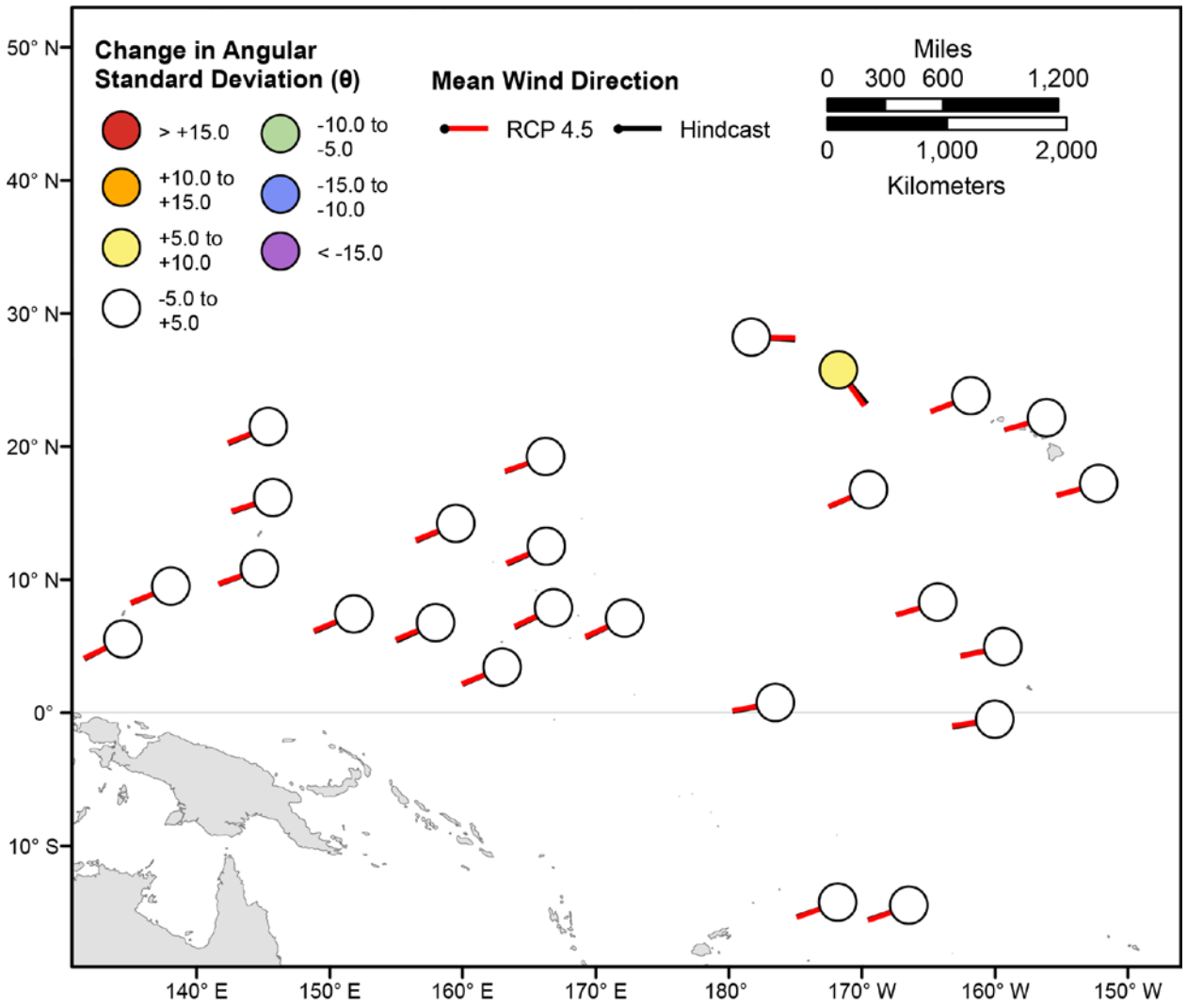

Figure 134. Map showing forecasted differences in mean wind directions and the standard deviation of wind directions for the years 2026–2045 from hindcasted values during the December-February season under the RCP4.5 future climatic scenario. Mean wind directions at each point are indicated by lines radiating from the center of each point where RCP4.5 2026–2045 mean wind directions are red and 1976–2005 hindcasted mean wind directions are black. The colors correspond to the magnitude of change in modeled mean wind direction standard deviation during 2026–2045 from those hindcasted for 1976–2005. Angular standard deviation units are in degrees. Mean wind directions are “heading towards”.

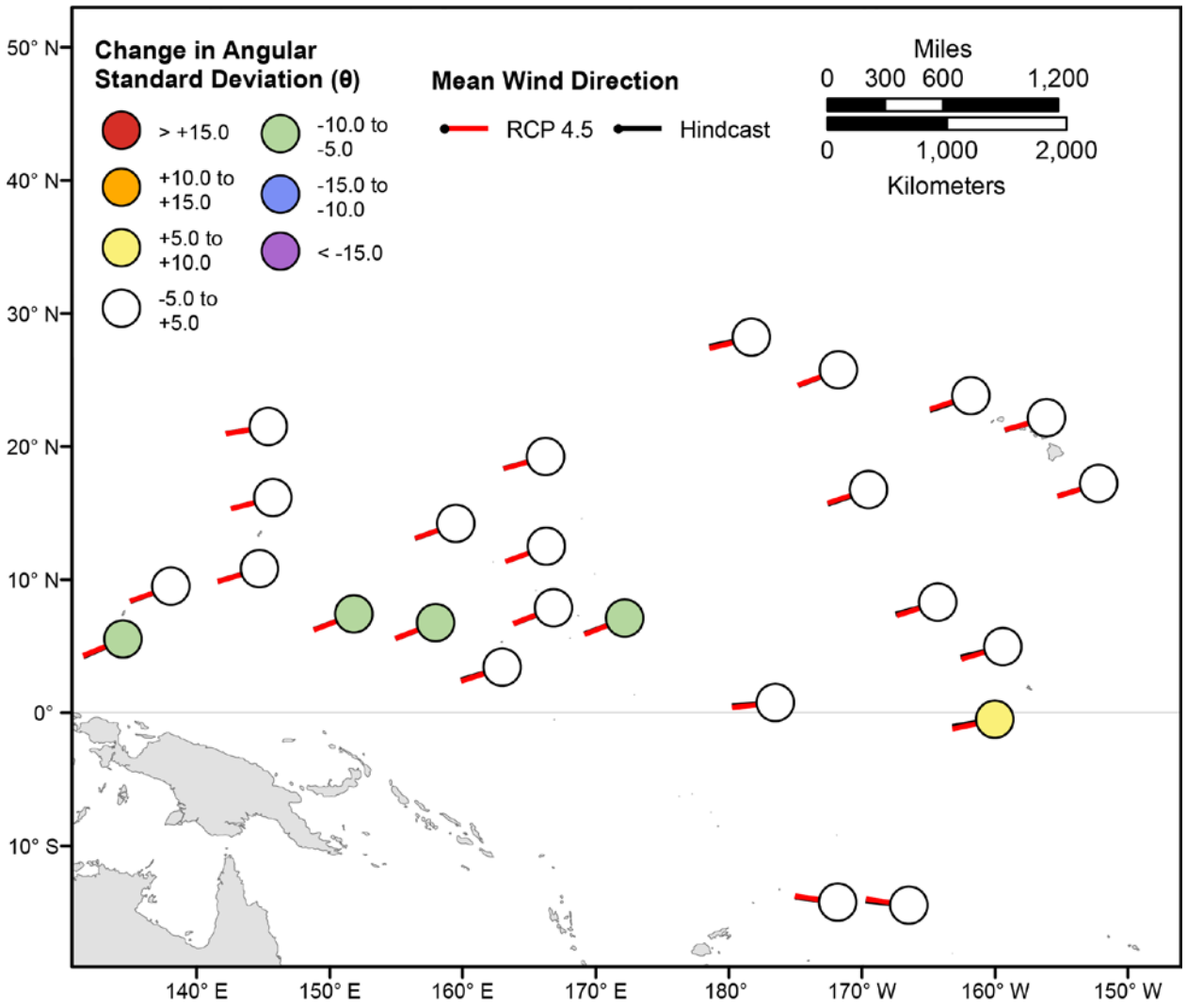

Figure 135. Map showing forecasted differences in mean wind directions and the standard deviation of wind directions for the years 2026–2045 from hindcasted values during the March-May season under the RCP4.5 future climatic scenario. Mean wind directions at each point are indicated by lines radiating from the center of each point where RCP4.5 2026–2045 mean wind directions are red and 1976–2005 hindcasted mean wind directions are black. The colors correspond to the magnitude of change in modeled mean wind direction standard deviation during 2026–2045 from those hindcasted for 1976–2005. Angular standard deviation units are in degrees. Mean wind directions are “heading towards”.

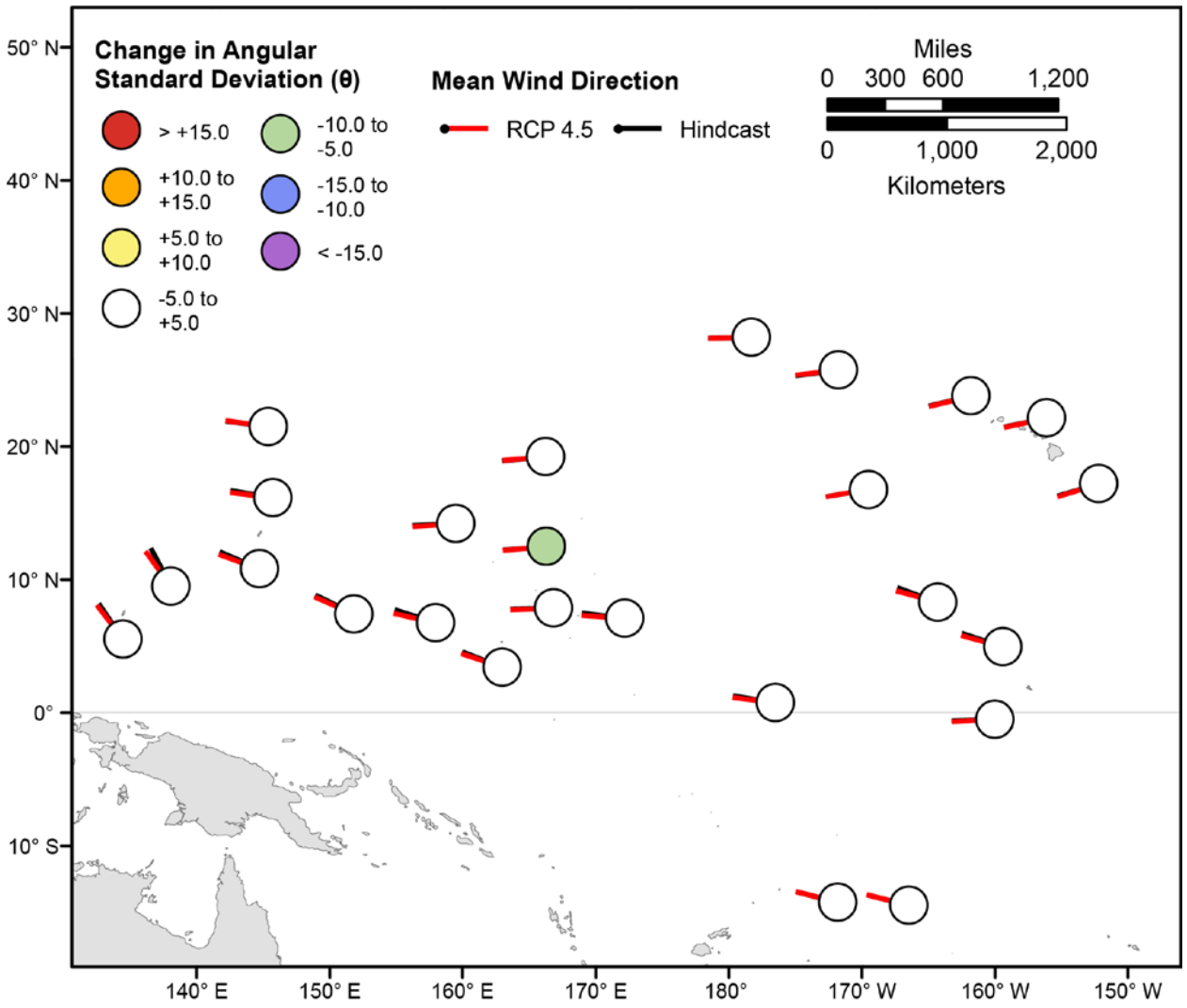

Figure 136. Map showing forecasted differences in mean wind directions and the standard deviation of wind directions for the years 2026–2045 from hindcasted values during the June-August season under the RCP4.5 future climatic scenario. Mean wind directions at each point are indicated by lines radiating from the center of each point where RCP4.5 2026–2045 mean wind directions are red and 1976–2005 hindcasted mean wind directions are black. The colors correspond to the magnitude of change in modeled mean wind direction standard deviation during 2026–2045 from those hindcasted for 1976–2005. Angular standard deviation units are in degrees. Mean wind directions are “heading towards”.

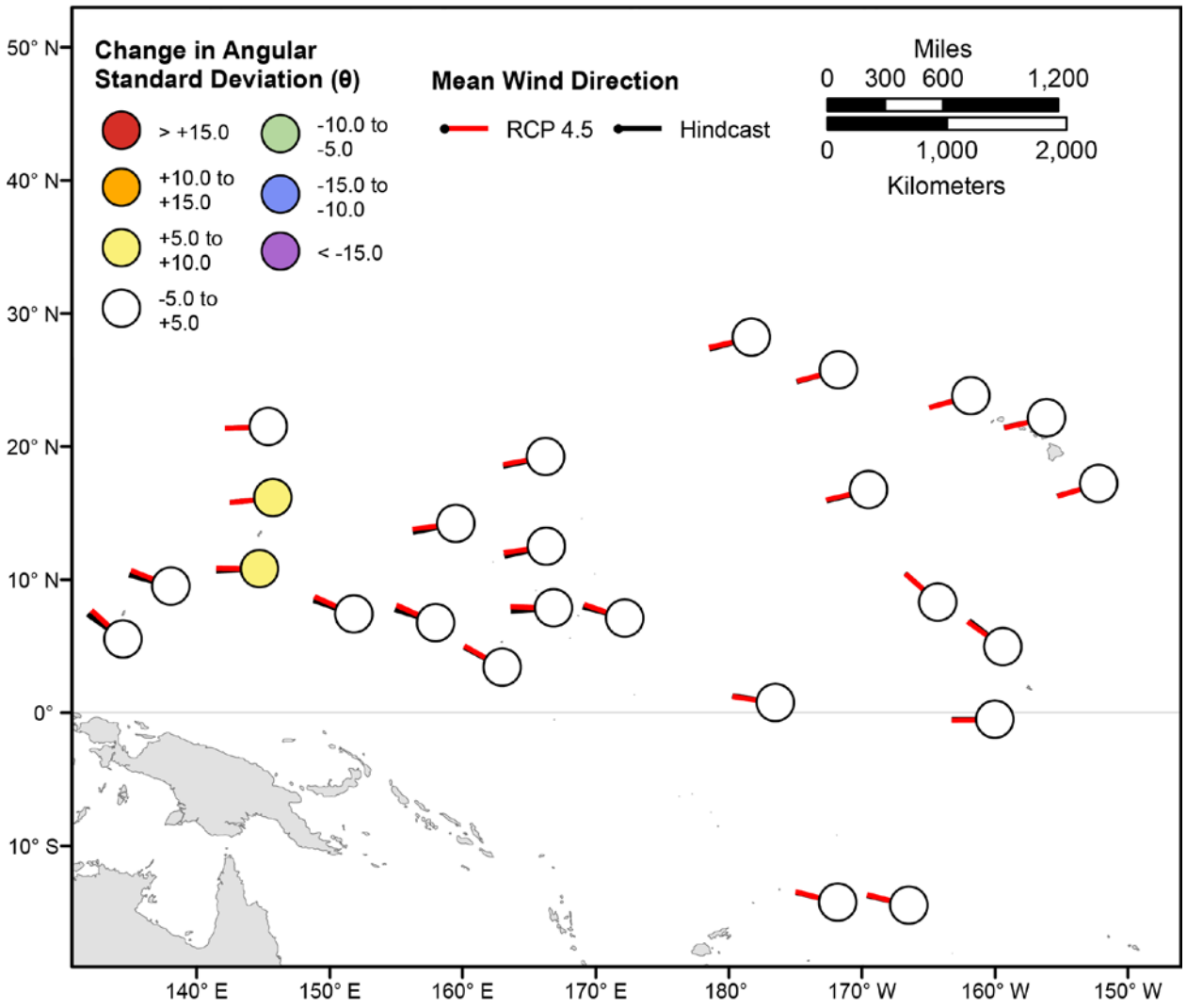

Figure 137. Map showing forecasted differences in mean wind directions and the standard deviation of wind directions for the years 2026–2045 from hindcasted values during the September-November season under the RCP4.5 future climatic scenario. Mean wind directions at each point are indicated by lines radiating from the center of each point where RCP4.5 2026–2045 mean wind directions are red and 1976–2005 hindcasted mean wind directions are black. The colors correspond to the magnitude of change in modeled mean wind direction standard deviation during 2026–2045 from those hindcasted for 1976–2005. Angular standard deviation units are in degrees. Mean wind directions are “heading towards”.

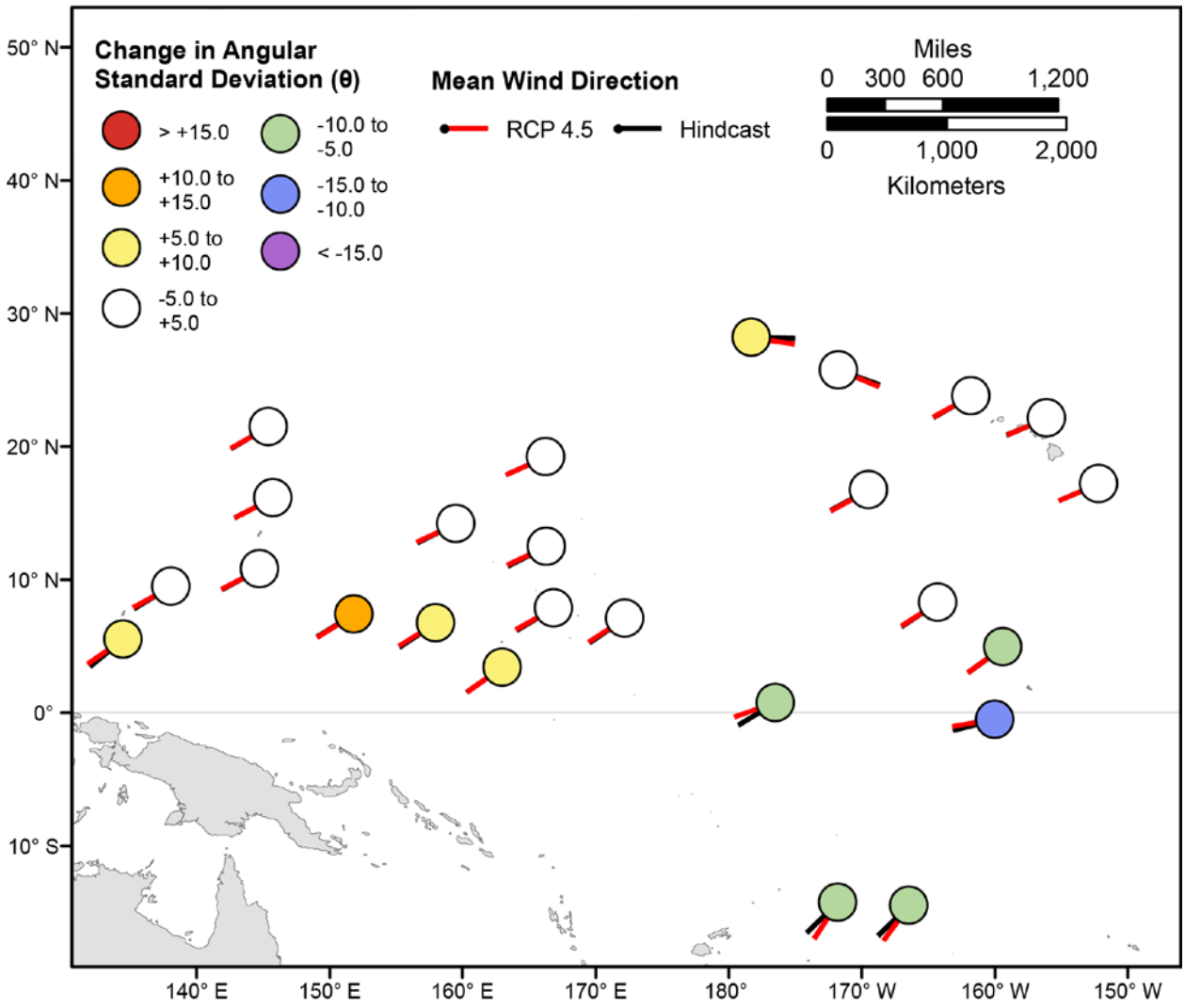

Figure 138. Map showing forecasted differences in the mean wind directions of the top 5 percent of wind speeds and the standard deviation of wind directions of the top 5 percent of wind speeds for the years 2026–2045 from hindcasted values during the December-February season under the RCP4.5 future climatic scenario. Mean wind directions at each point are indicated by lines radiating from the center of each point where RCP4.5 2026–2045 mean wind directions are red and 1976–2005 hindcasted mean wind directions are black. The colors correspond to the magnitude of change in modeled mean wind direction standard deviation during 2026–2045 from those hindcasted for 1976–2005. Angular standard deviation units are in degrees. Mean wind directions are “heading towards”.

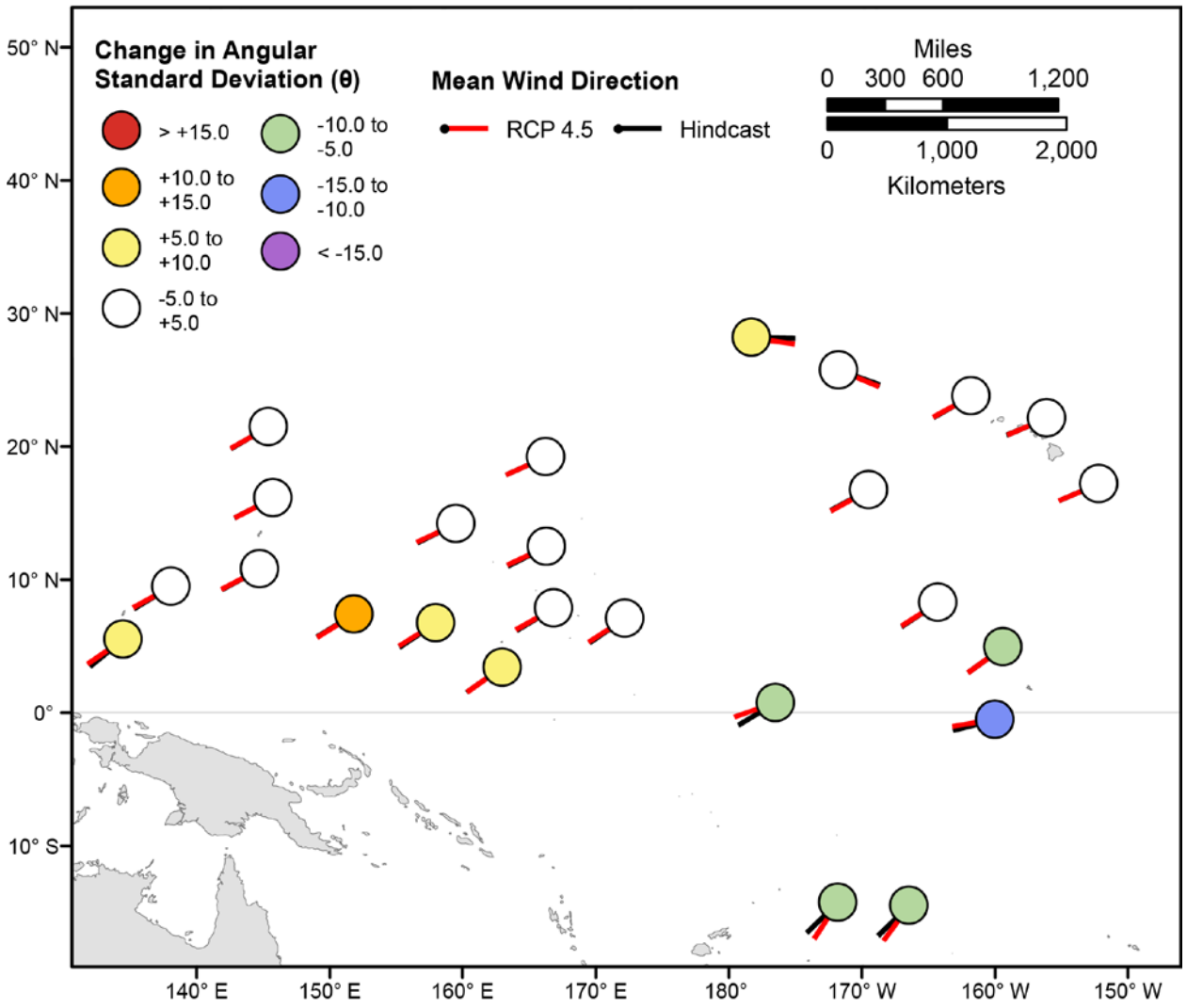

Figure 139. Map showing forecasted differences in the mean wind directions of the top 5 percent of wind speeds and the standard deviation of wind directions of the top 5 percent of wind speeds for the years 2026–2045 from hindcasted values during the March-May season under the RCP4.5 future climatic scenario. Mean wind directions at each point are indicated by lines radiating from the center of each point where RCP4.5 2026–2045 mean wind directions are red and 1976–2005 hindcasted mean wind directions are black. The colors correspond to the magnitude of change in modeled mean wind direction standard deviation during 2026–2045 from those hindcasted for 1976–2005. Angular standard deviation units are in degrees. Mean wind directions are “heading towards”.

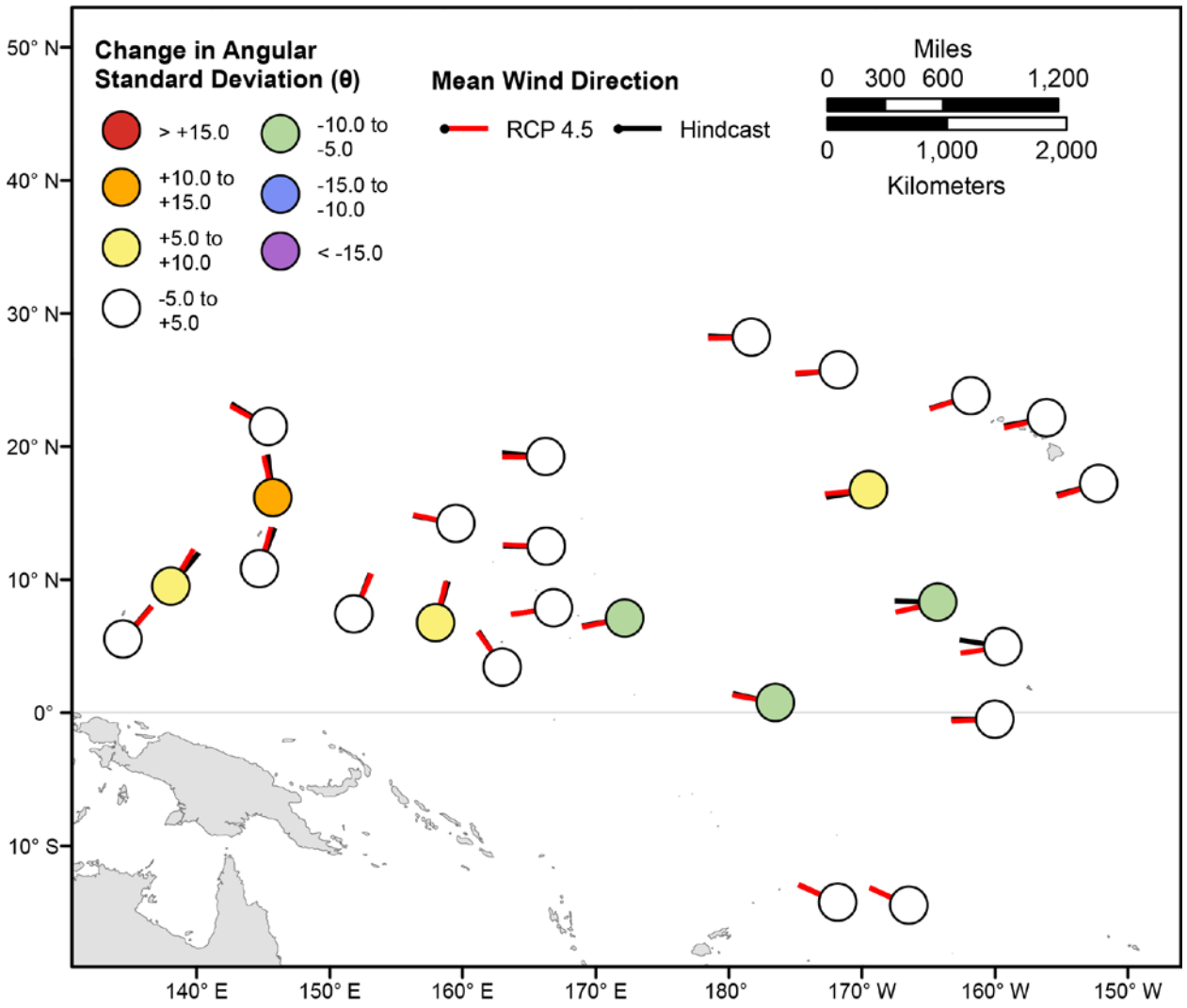

Figure 140. Map showing forecasted differences in the mean wind directions of the top 5 percent of wind speeds and the standard deviation of wind directions of the top 5 percent of wind speeds for the years 2026–2045 from hindcasted values during the June-August season under the RCP4.5 future climatic scenario. Mean wind directions at each point are indicated by lines radiating from the center of each point where RCP4.5 2026–2045 mean wind directions are red and 1976–2005 hindcasted mean wind directions are black. The colors correspond to the magnitude of change in modeled mean wind direction standard deviation during 2026–2045 from those hindcasted for 1976–2005. Angular standard deviation units are in degrees. Mean wind directions are “heading towards”.

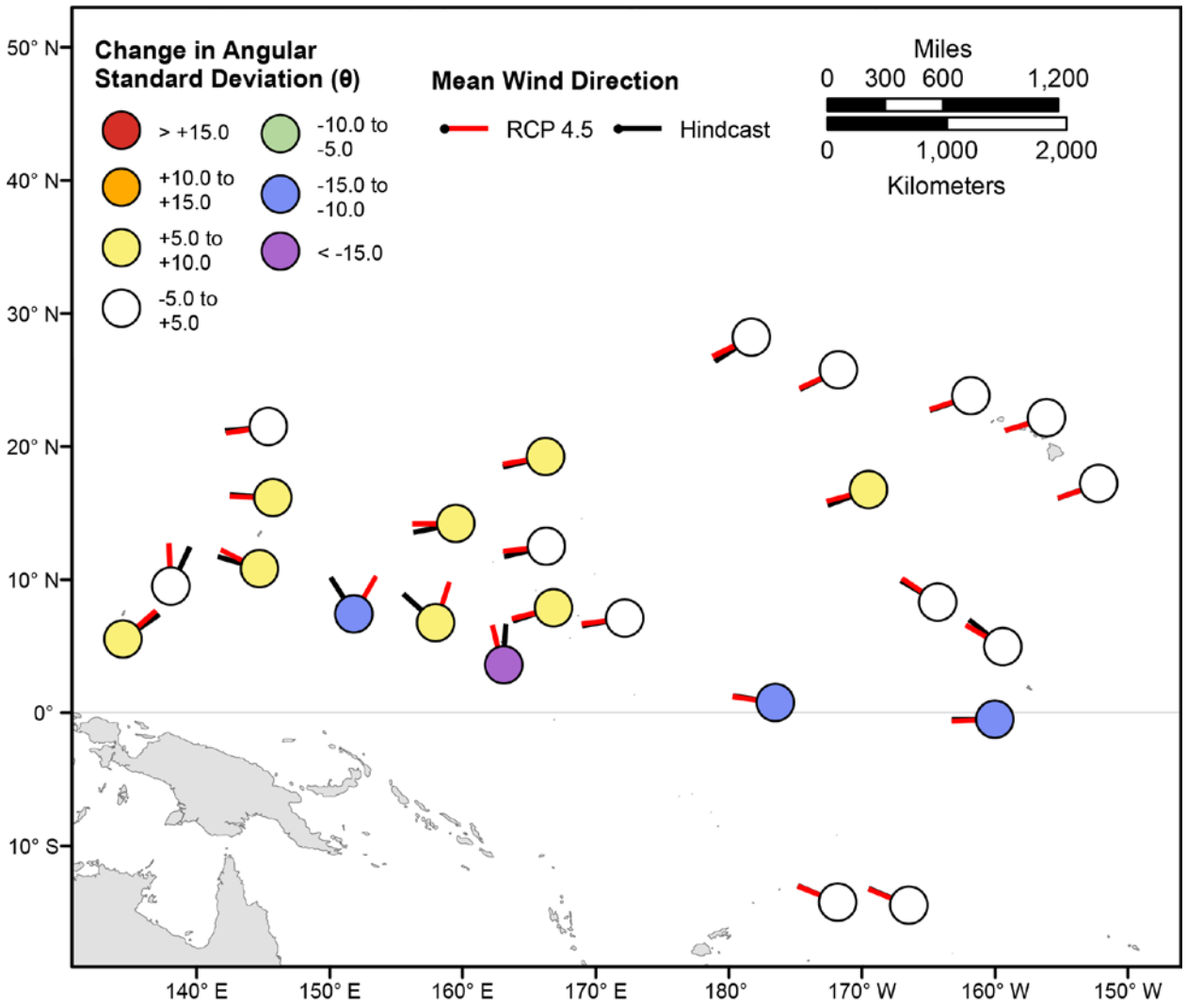

Figure 141. Map showing forecasted differences in the mean wind directions of the top 5 percent of wind speeds and the standard deviation of wind directions of the top 5 percent of wind speeds for the years 2026–2045 from hindcasted values during the September-November season under the RCP4.5 future climatic scenario. Mean wind directions at each point are indicated by lines radiating from the center of each point where RCP4.5 2026–2045 mean wind directions are red and 1976–2005 hindcasted mean wind directions are black. The colors correspond to the magnitude of change in modeled mean wind direction standard deviation during 2026–2045 from those hindcasted for 1976–2005. Angular standard deviation units are in degrees. Mean wind directions are “heading towards”.

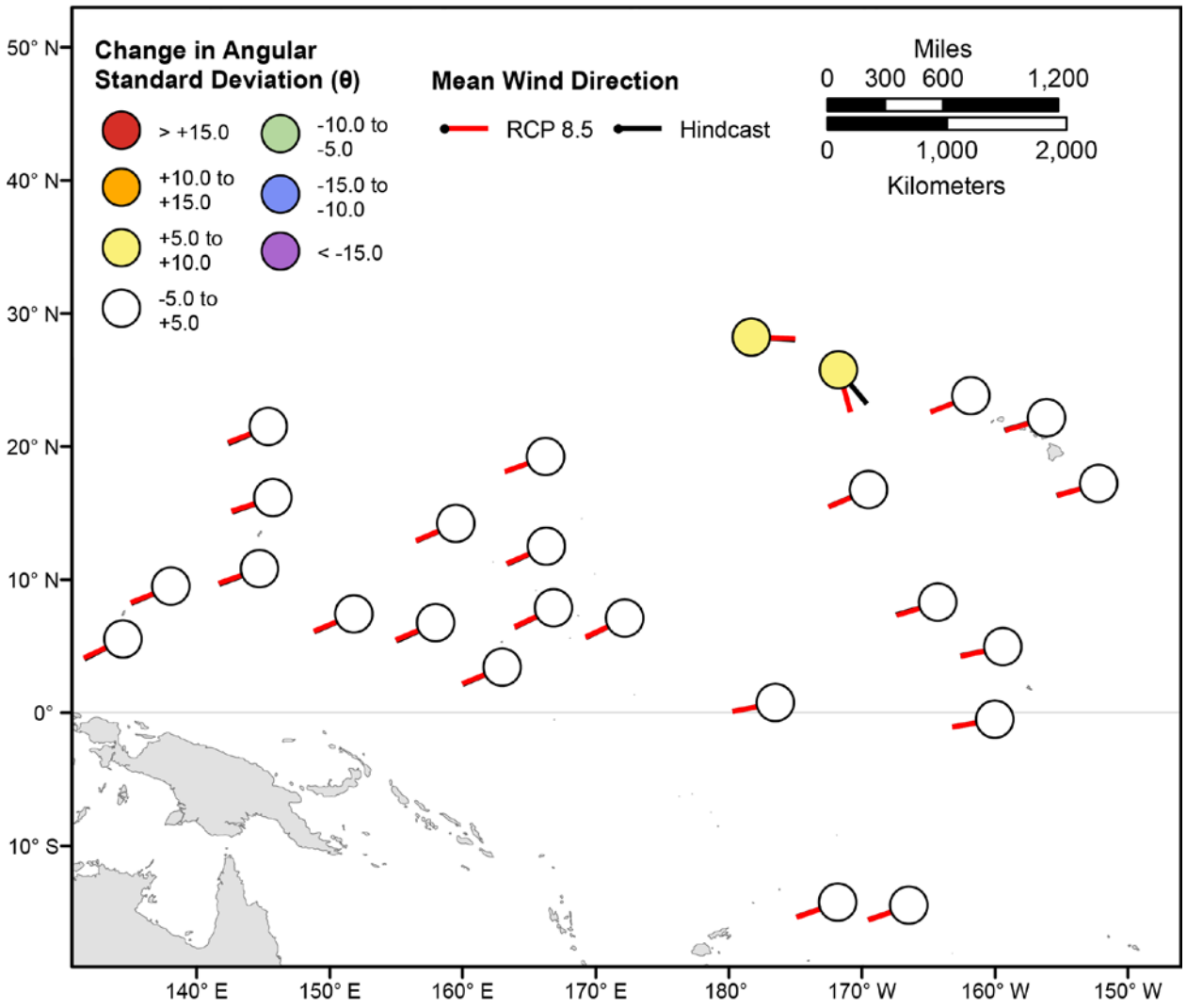

Figure 142. Map showing forecasted differences in mean wind directions and the standard deviation of wind directions for the years 2026–2045 from hindcasted values during the December-February season under the RCP8.5 future climatic scenario. Mean wind directions at each point are indicated by lines radiating from the center of each point where RCP8.5 2026–2045 mean wind directions are red and 1976–2005 hindcasted mean wind directions are black. The colors correspond to the magnitude of change in modeled mean wind direction standard deviation during 2026–2045 from those hindcasted for 1976–2005. Angular standard deviation units are in degrees. Mean wind directions are “heading towards”.

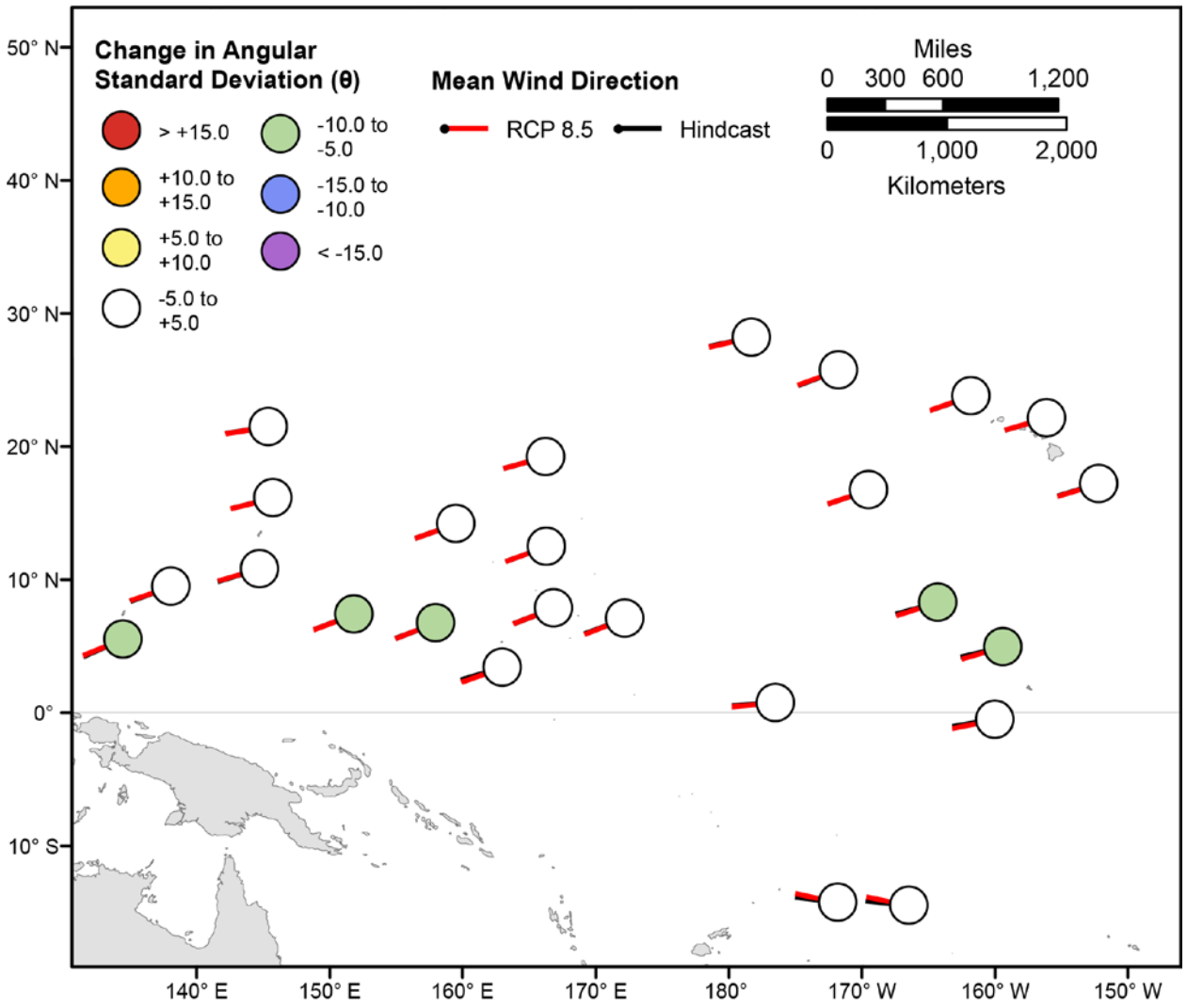

Figure 143. Map showing forecasted differences in mean wind directions and the standard deviation of wind directions for the years 2026–2045 from hindcasted values during the March-May season under the RCP8.5 future climatic scenario. Mean wind directions at each point are indicated by lines radiating from the center of each point where RCP8.5 2026–2045 mean wind directions are red and 1976–2005 hindcasted mean wind directions are black. The colors correspond to the magnitude of change in modeled mean wind direction standard deviation during 2026–2045 from those hindcasted for 1976–2005. Angular standard deviation units are in degrees. Mean wind directions are “heading towards”.

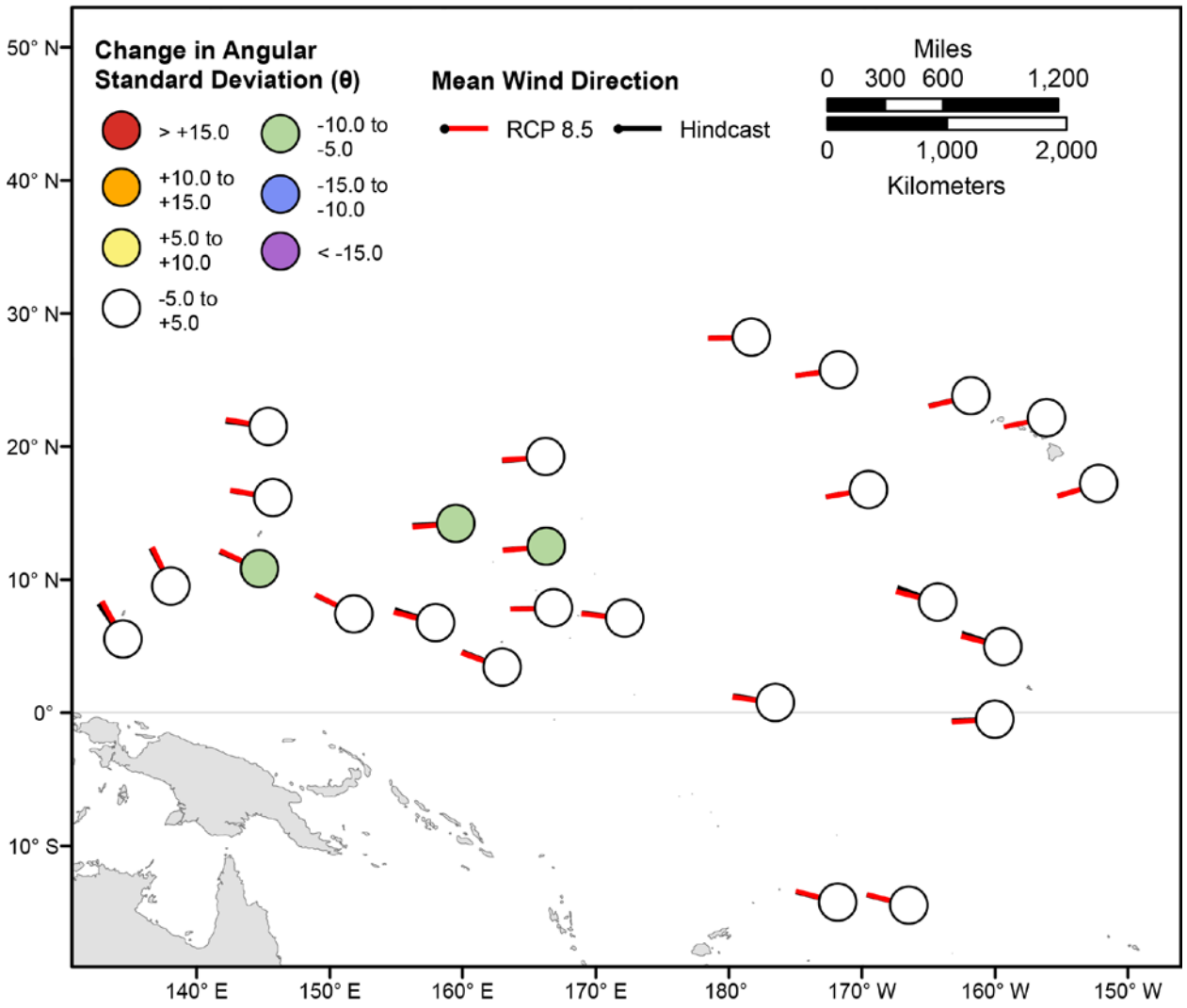

Figure 144. Map showing forecasted differences in mean wind directions and the standard deviation of wind directions for the years 2026–2045 from hindcasted values during the June-August season under the RCP8.5 future climatic scenario. Mean wind directions at each point are indicated by lines radiating from the center of each point where RCP8.5 2026–2045 mean wind directions are red and 1976–2005 hindcasted mean wind directions are black. The colors correspond to the magnitude of change in modeled mean wind direction standard deviation during 2026–2045 from those hindcasted for 1976–2005. Angular standard deviation units are in degrees. Mean wind directions are “heading towards”.

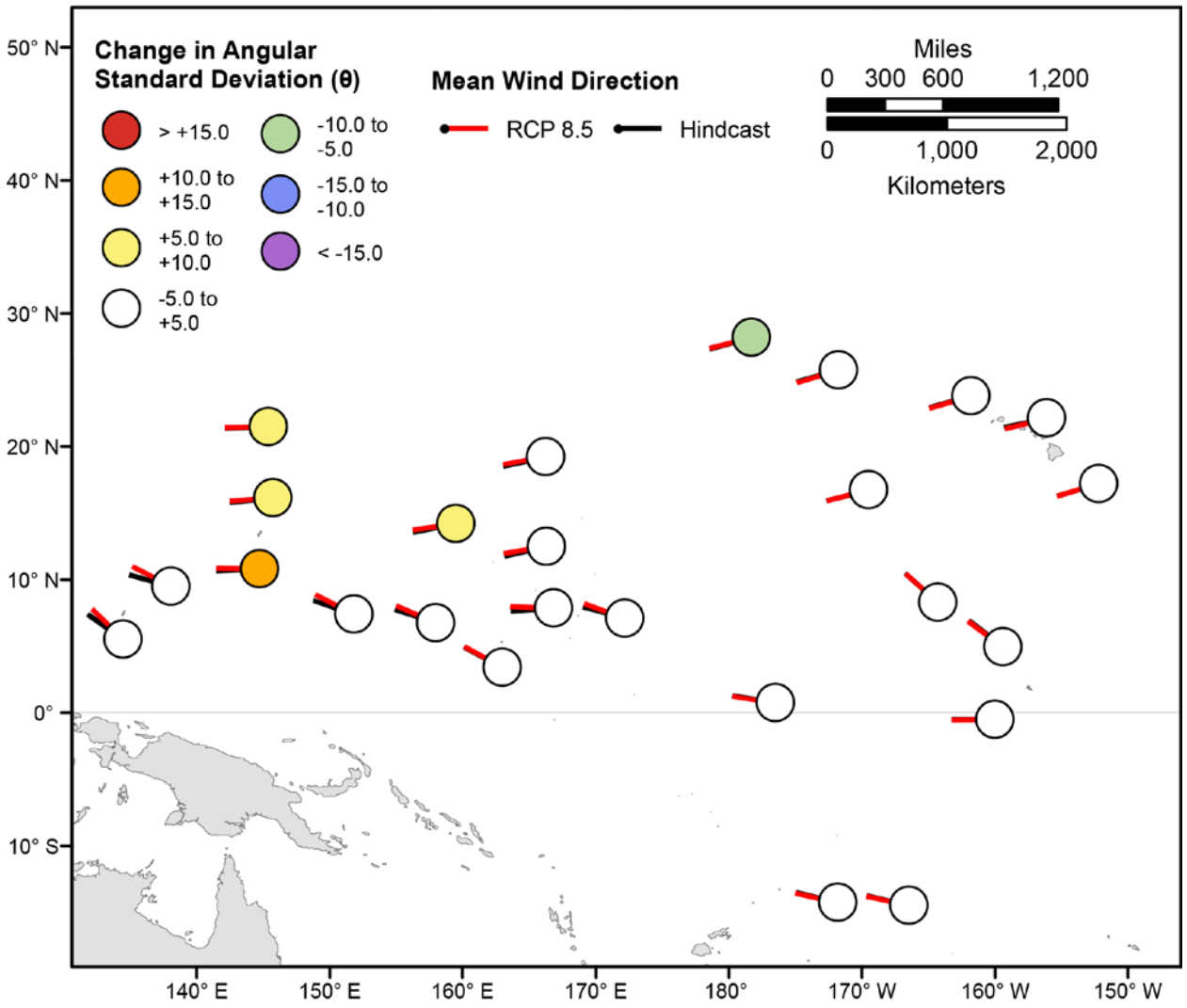

Figure 145. Map showing forecasted differences in mean wind directions and the standard deviation of wind directions for the years 2026–2045 from hindcasted values during the September-November season under the RCP8.5 future climatic scenario. Mean wind directions at each point are indicated by lines radiating from the center of each point where RCP8.5 2026–2045 mean wind directions are red and 1976–2005 hindcasted mean wind directions are black. The colors correspond to the magnitude of change in modeled mean wind direction standard deviation during 2026–2045 from those hindcasted for 1976–2005. Angular standard deviation units are in degrees. Mean wind directions are “heading towards”.

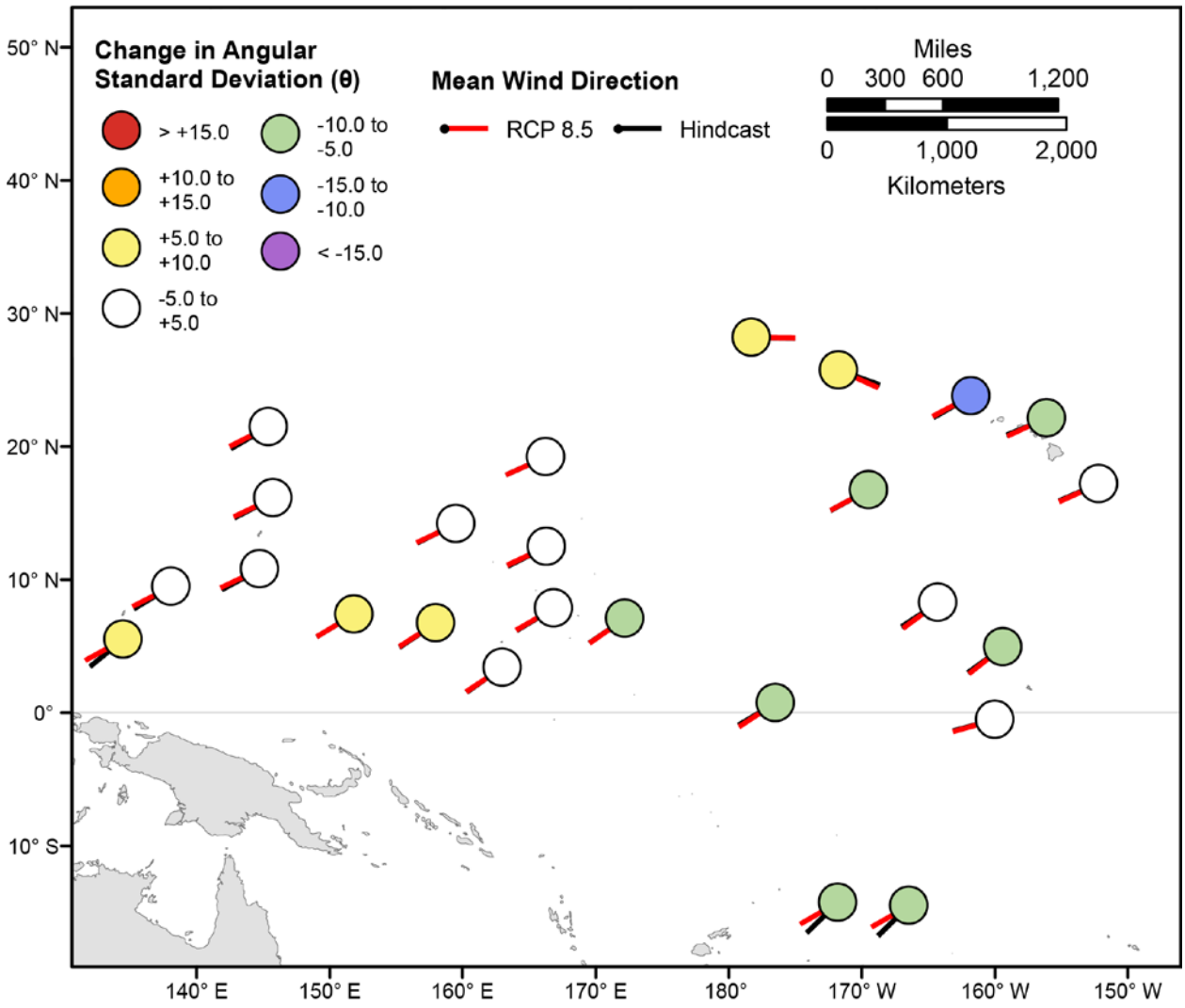

Figure 146. Map showing forecasted differences in the mean wind directions of the top 5 percent of wind speeds and the standard deviation of wind directions of the top 5 percent of wind speeds for the years 2026–2045 from hindcasted values during the December-February season under the RCP8.5 future climatic scenario. Mean wind directions at each point are indicated by lines radiating from the center of each point where RCP8.5 2026–2045 mean wind directions are red and 1976–2005 hindcasted mean wind directions are black. The colors correspond to the magnitude of change in modeled mean wind direction standard deviation during 2026–2045 from those hindcasted for 1976–2005. Angular standard deviation units are in degrees. Mean wind directions are “heading towards”.

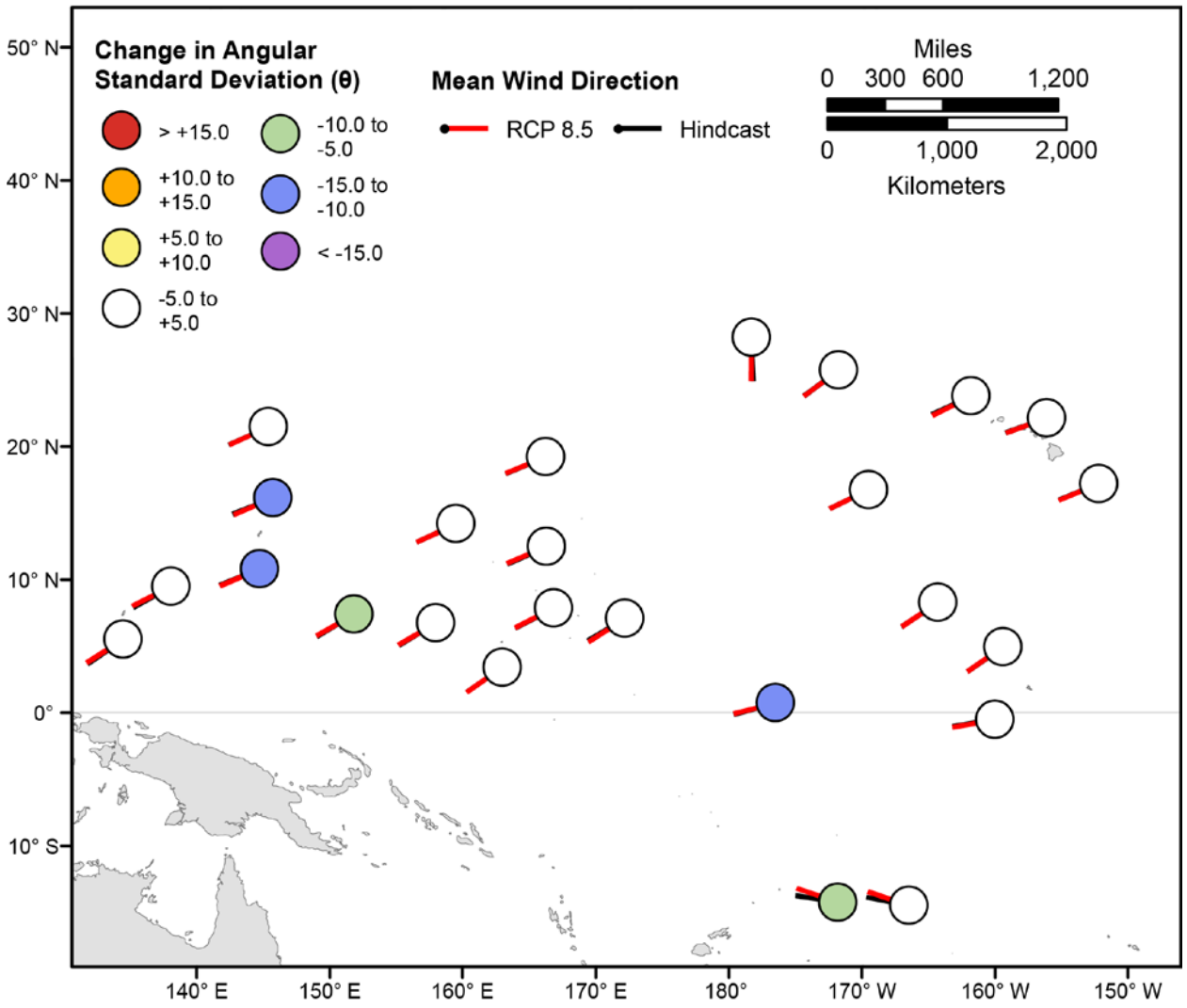

Figure 147. Map showing forecasted differences in the mean wind directions of the top 5 percent of wind speeds and the standard deviation of wind directions of the top 5 percent of wind speeds for the years 2026–2045 from hindcasted values during the March-May season under the RCP8.5 future climatic scenario. Mean wind directions at each point are indicated by lines radiating from the center of each point where RCP8.5 2026–2045 mean wind directions are red and 1976–2005 hindcasted mean wind directions are black. The colors correspond to the magnitude of change in modeled mean wind direction standard deviation during 2026–2045 from those hindcasted for 1976–2005. Angular standard deviation units are in degrees. Mean wind directions are “heading towards”.

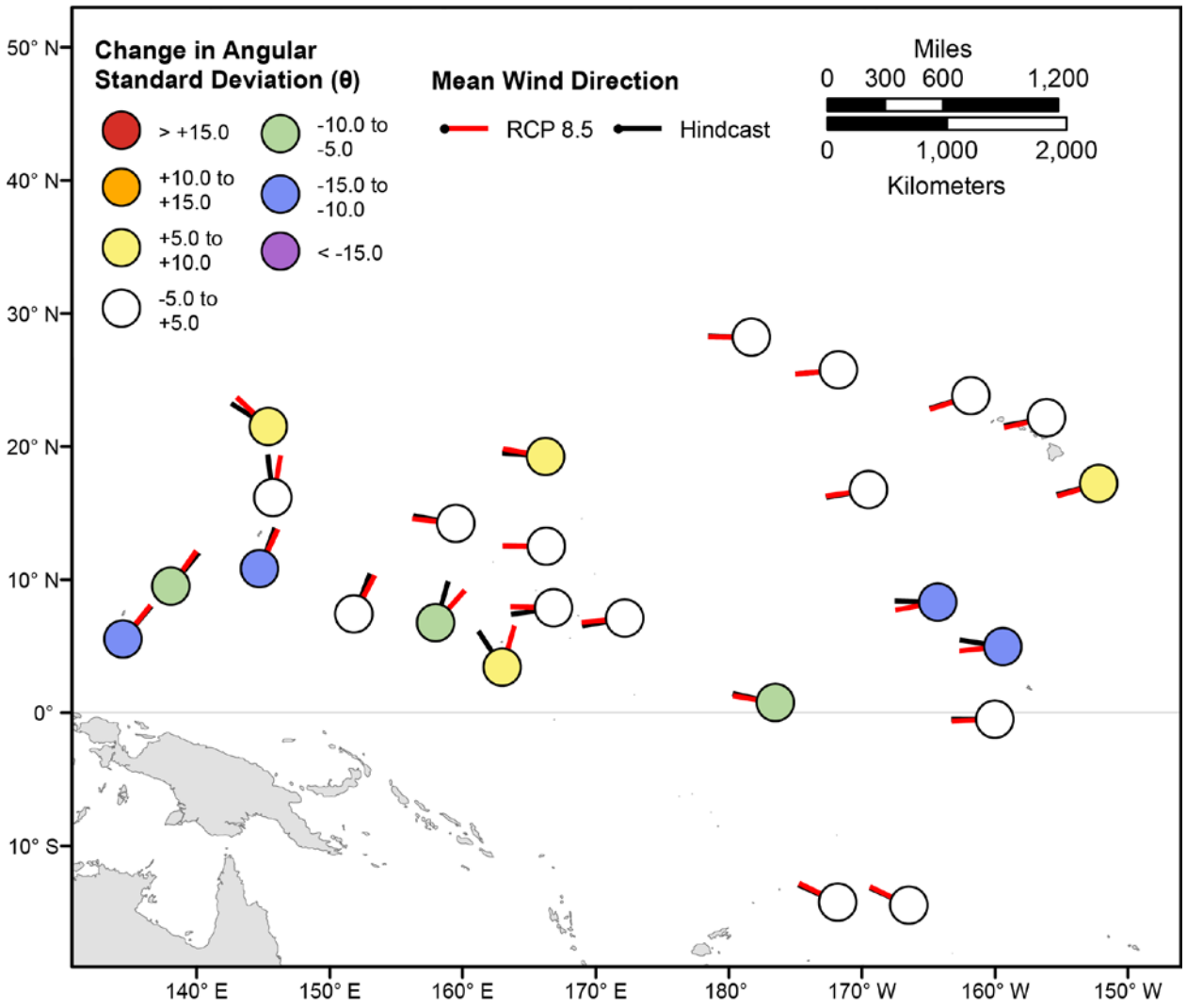

Figure 148. Map showing forecasted differences in the mean wind directions of the top 5 percent of wind speeds and the standard deviation of wind directions of the top 5 percent of wind speeds for the years 2026–2045 from hindcasted values during the June-August season under the RCP8.5 future climatic scenario. Mean wind directions at each point are indicated by lines radiating from the center of each point where RCP8.5 2026–2045 mean wind directions are red and 1976–2005 hindcasted mean wind directions are black. The colors correspond to the magnitude of change in modeled mean wind direction standard deviation during 2026–2045 from those hindcasted for 1976–2005. Angular standard deviation units are in degrees. Mean wind directions are “heading towards”.

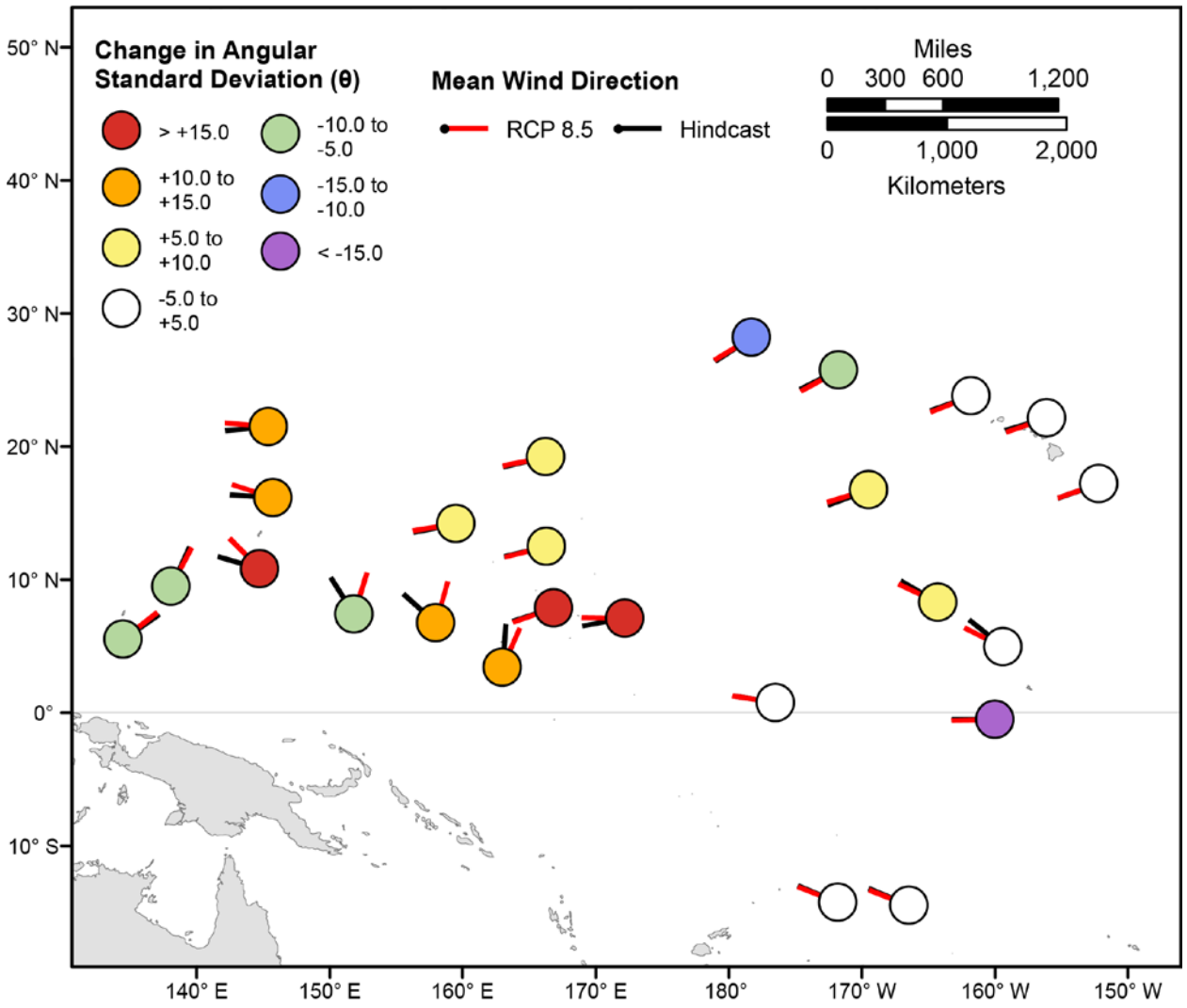

Figure 149. Map showing forecasted differences in the mean wind directions of the top 5 percent of wind speeds and the standard deviation of wind directions of the top 5 percent of wind speeds for the years 2026–2045 from hindcasted values during the September-November season under the RCP8.5 future climatic scenario. Mean wind directions at each point are indicated by lines radiating from the center of each point where RCP8.5 2026–2045 mean wind directions are red and 1976–2005 hindcasted mean wind directions are black. The colors correspond to the magnitude of change in modeled mean wind direction standard deviation during 2026–2045 from those hindcasted for 1976–2005. Angular standard deviation units are in degrees. Mean wind directions are “heading towards”.

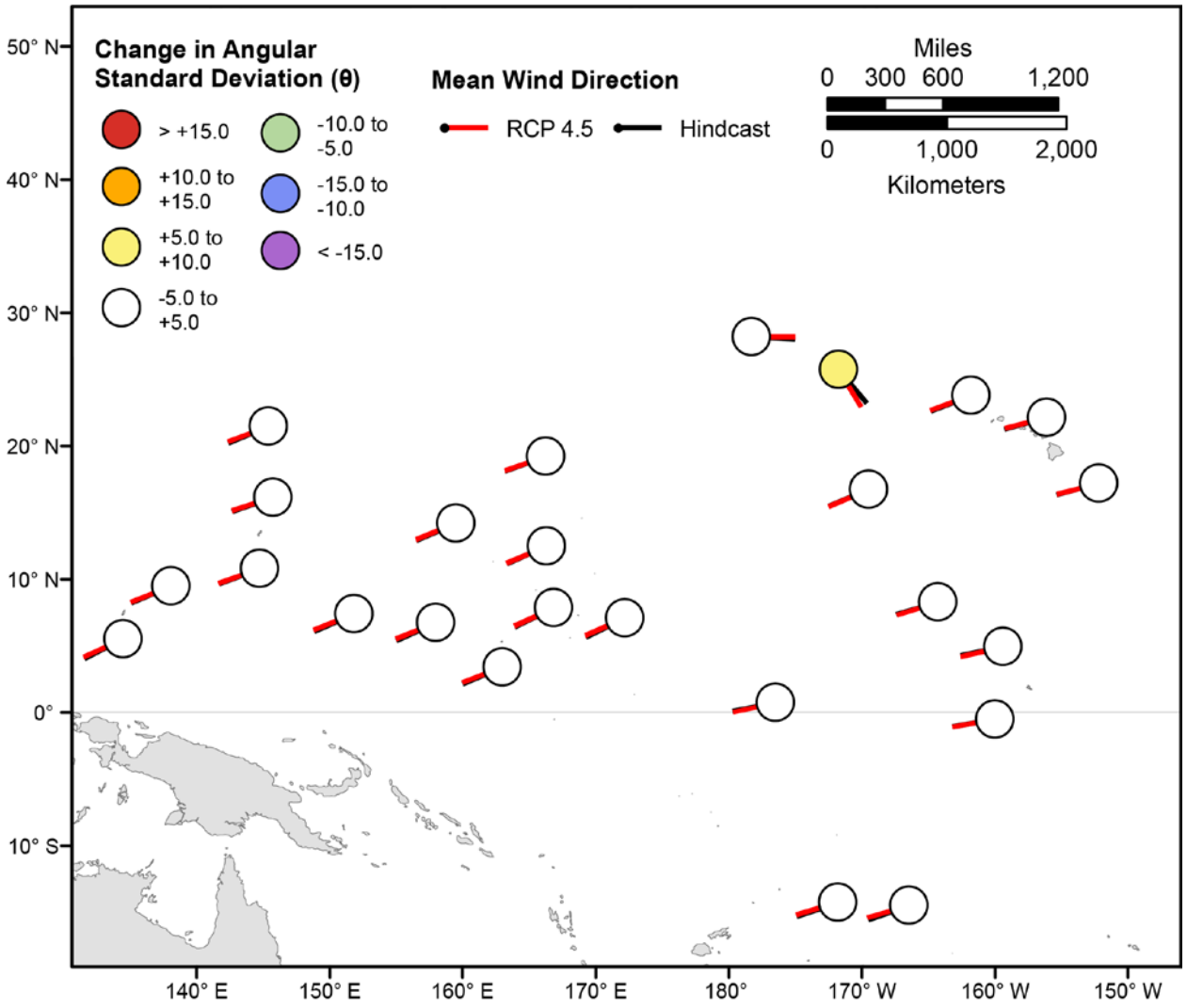

Figure 150. Map showing forecasted differences in mean wind directions and the standard deviation of wind directions for the years 2081–2100 from hindcasted values during the December-February season under the RCP4.5 future climatic scenario. Mean wind directions at each point are indicated by lines radiating from the center of each point where RCP4.5 2081–2100 mean wind directions are red and 1976–2005 hindcasted mean wind directions are black. The colors correspond to the magnitude of change in modeled mean wind direction standard deviation during 2081–2100 from those hindcasted for 1976–2005. Angular standard deviation units are in degrees. Mean wind directions are “heading towards”.

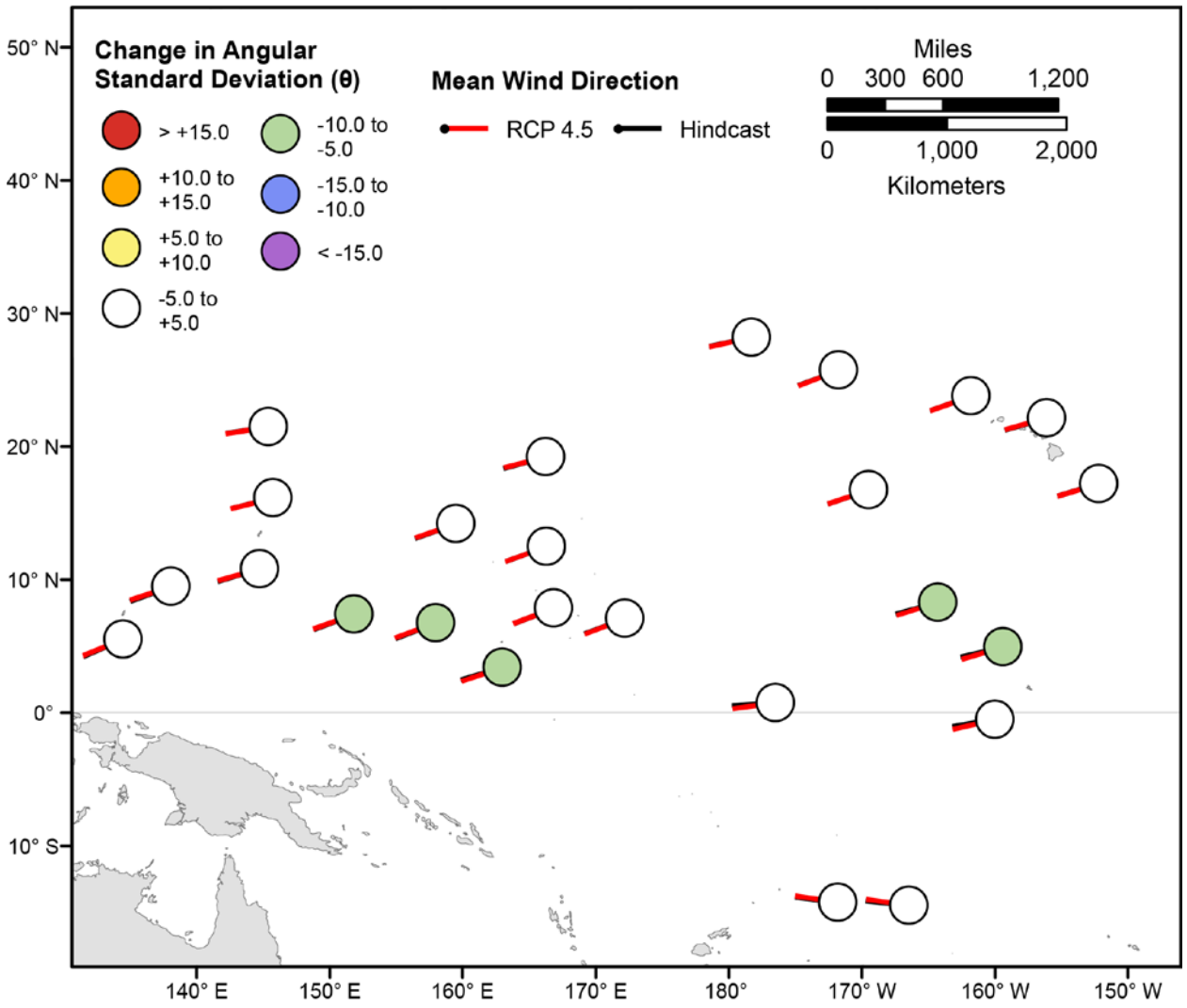

Figure 151. Map showing forecasted differences in mean wind directions and the standard deviation of wind directions for the years 2081–2100 from hindcasted values during the March-May season under the RCP4.5 future climatic scenario. Mean wind directions at each point are indicated by lines radiating from the center of each point where RCP4.5 2081–2100 mean wind directions are red and 1976–2005 hindcasted mean wind directions are black. The colors correspond to the magnitude of change in modeled mean wind direction standard deviation during 2081–2100 from those hindcasted for 1976–2005. Angular standard deviation units are in degrees. Mean wind directions are “heading towards”.

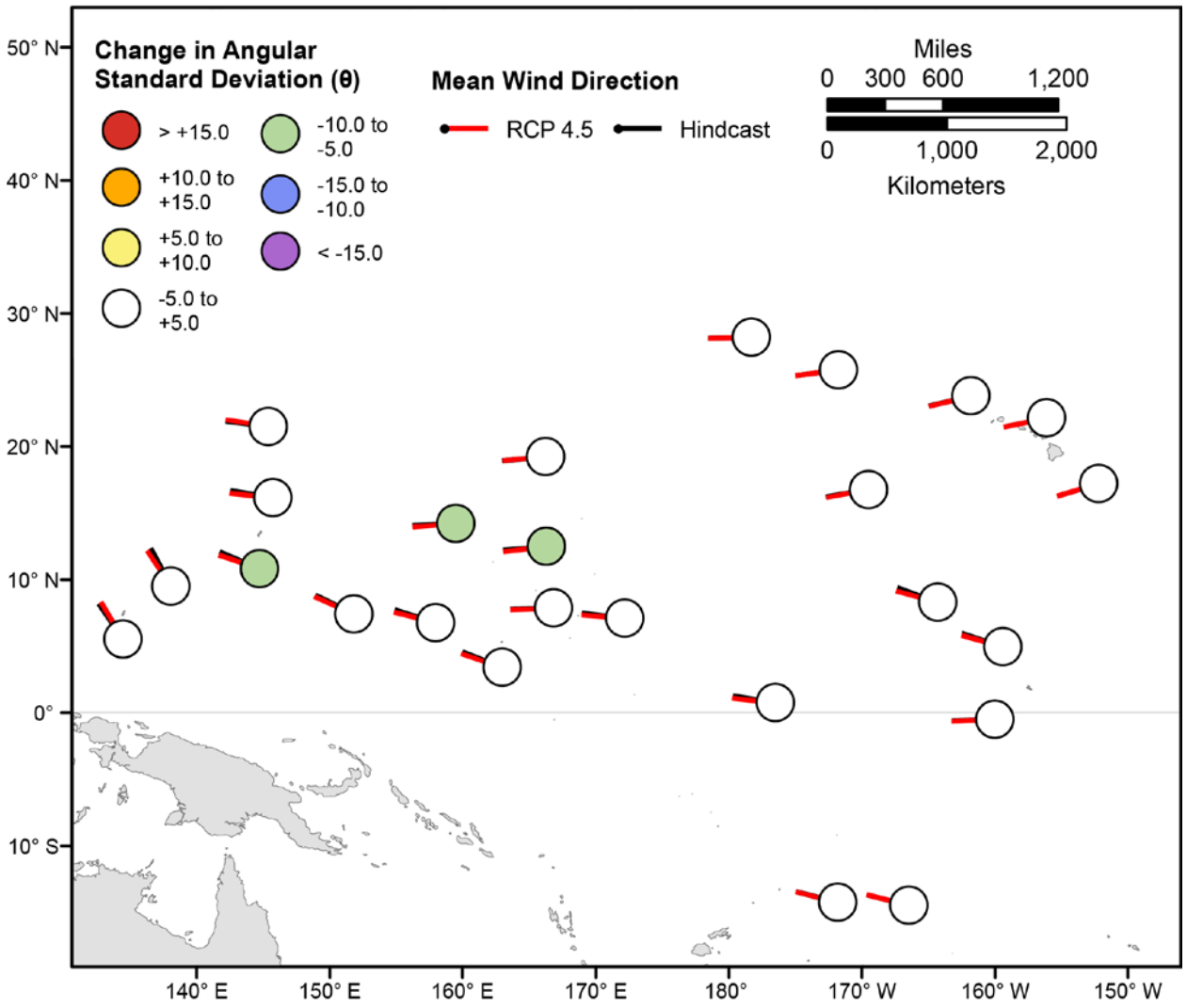

Figure 152. Map showing forecasted differences in mean wind directions and the standard deviation of wind directions for the years 2081–2100 from hindcasted values during the June-August season under the RCP4.5 future climatic scenario. Mean wind directions at each point are indicated by lines radiating from the center of each point where RCP4.5 2081–2100 mean wind directions are red and 1976–2005 hindcasted mean wind directions are black. The colors correspond to the magnitude of change in modeled mean wind direction standard deviation during 2081–2100 from those hindcasted for 1976–2005. Angular standard deviation units are in degrees. Mean wind directions are “heading towards”.

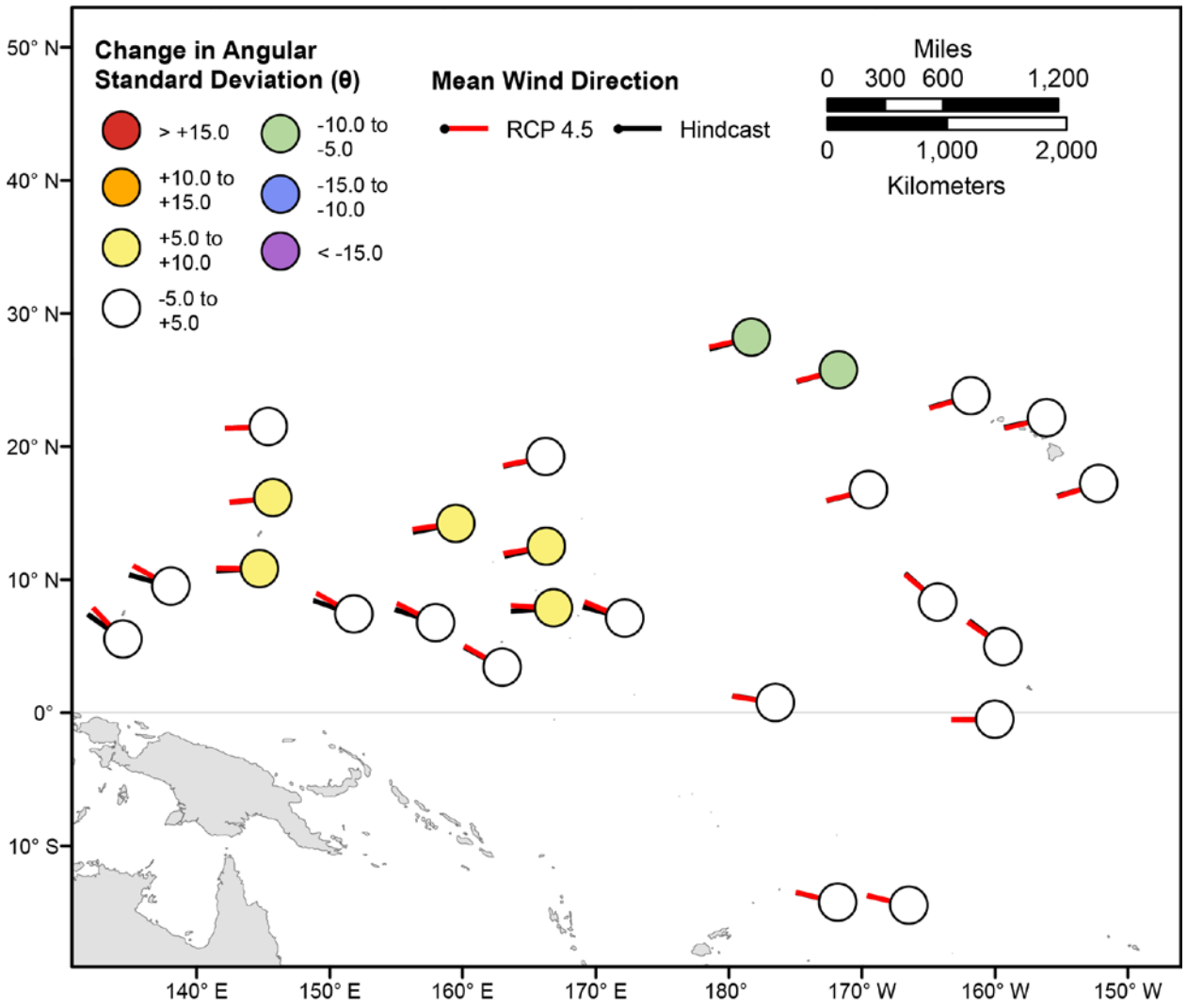

Figure 153. Map showing forecasted differences in mean wind directions and the standard deviation of wind directions for the years 2081–2100 from hindcasted values during the September-November season under the RCP4.5 future climatic scenario. Mean wind directions at each point are indicated by lines radiating from the center of each point where RCP4.5 2081–2100 mean wind directions are red and 1976–2005 hindcasted mean wind directions are black. The colors correspond to the magnitude of change in modeled mean wind direction standard deviation during 2081–2100 from those hindcasted for 1976–2005. Angular standard deviation units are in degrees. Mean wind directions are “heading towards”.

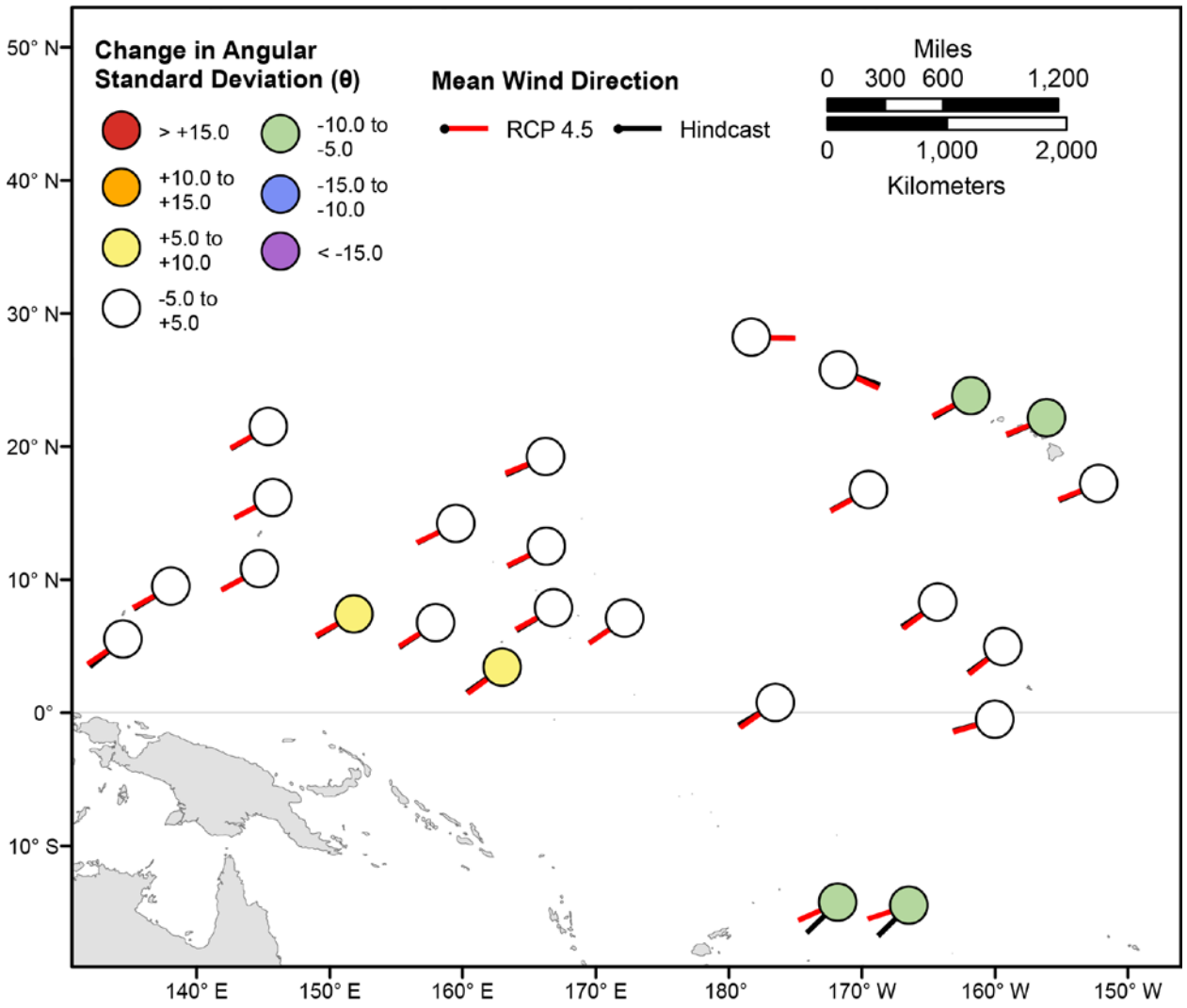

Figure 154. Map showing forecasted differences in the mean wind directions of the top 5 percent of wind speeds and the standard deviation of wind directions of the top 5 percent of wind speeds for the years 2081–2100 from hindcasted values during the December-February season under the RCP4.5 future climatic scenario. Mean wind directions at each point are indicated by lines radiating from the center of each point where RCP4.5 2081–2100 mean wind directions are red and 1976–2005 hindcasted mean wind directions are black. The colors correspond to the magnitude of change in modeled mean wind direction standard deviation during 2081–2100 from those hindcasted for 1976–2005. Angular standard deviation units are in degrees. Mean wind directions are “heading towards”.

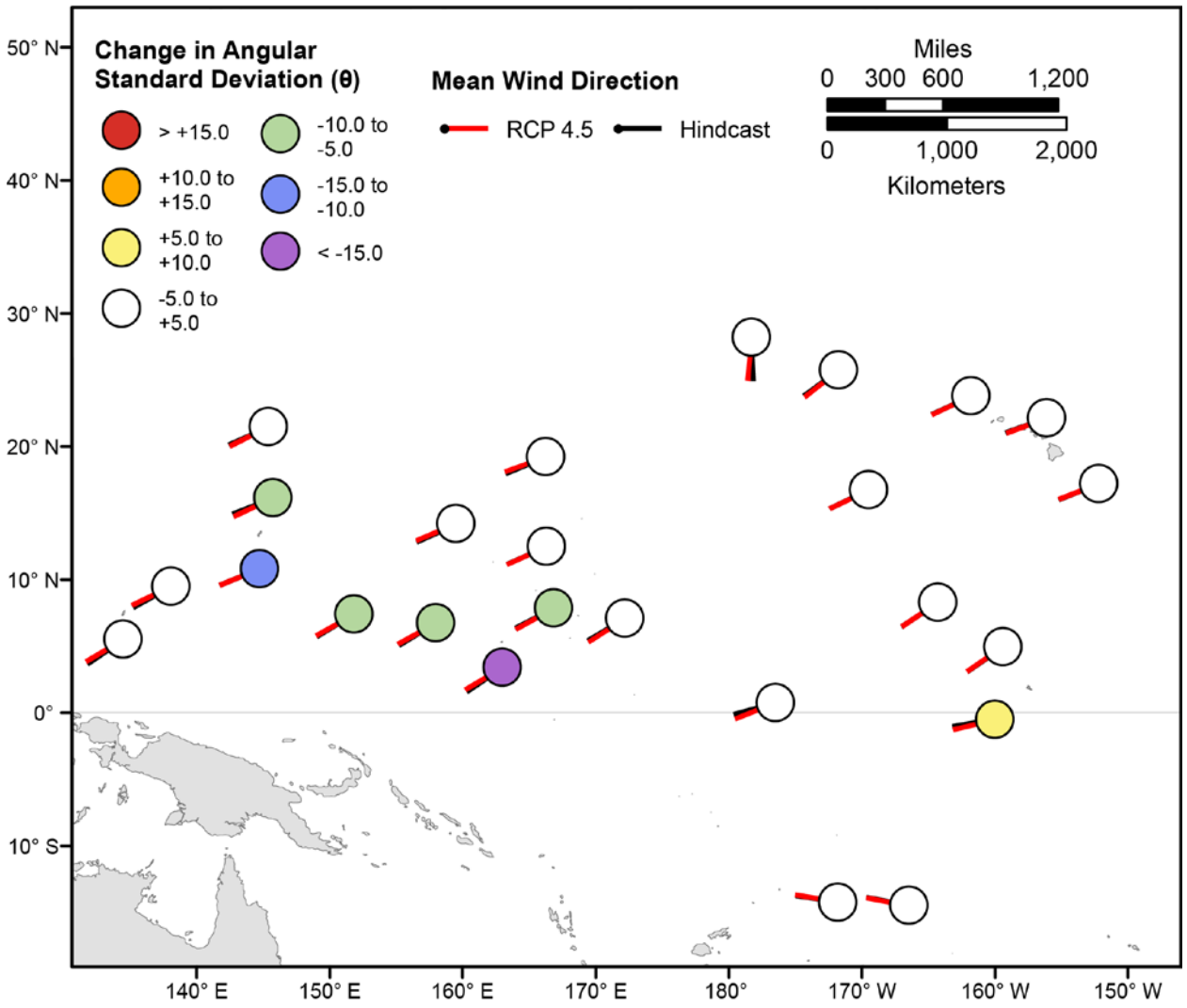

Figure 155. Map showing forecasted differences in the mean wind directions of the top 5 percent of wind speeds and the standard deviation of wind directions of the top 5 percent of wind speeds for the years 2081–2100 from hindcasted values during the March-May season under the RCP4.5 future climatic scenario. Mean wind directions at each point are indicated by lines radiating from the center of each point where RCP4.5 2081–2100 mean wind directions are red and 1976–2005 hindcasted mean wind directions are black. The colors correspond to the magnitude of change in modeled mean wind direction standard deviation during 2081–2100 from those hindcasted for 1976–2005. Angular standard deviation units are in degrees. Mean wind directions are “heading towards”.

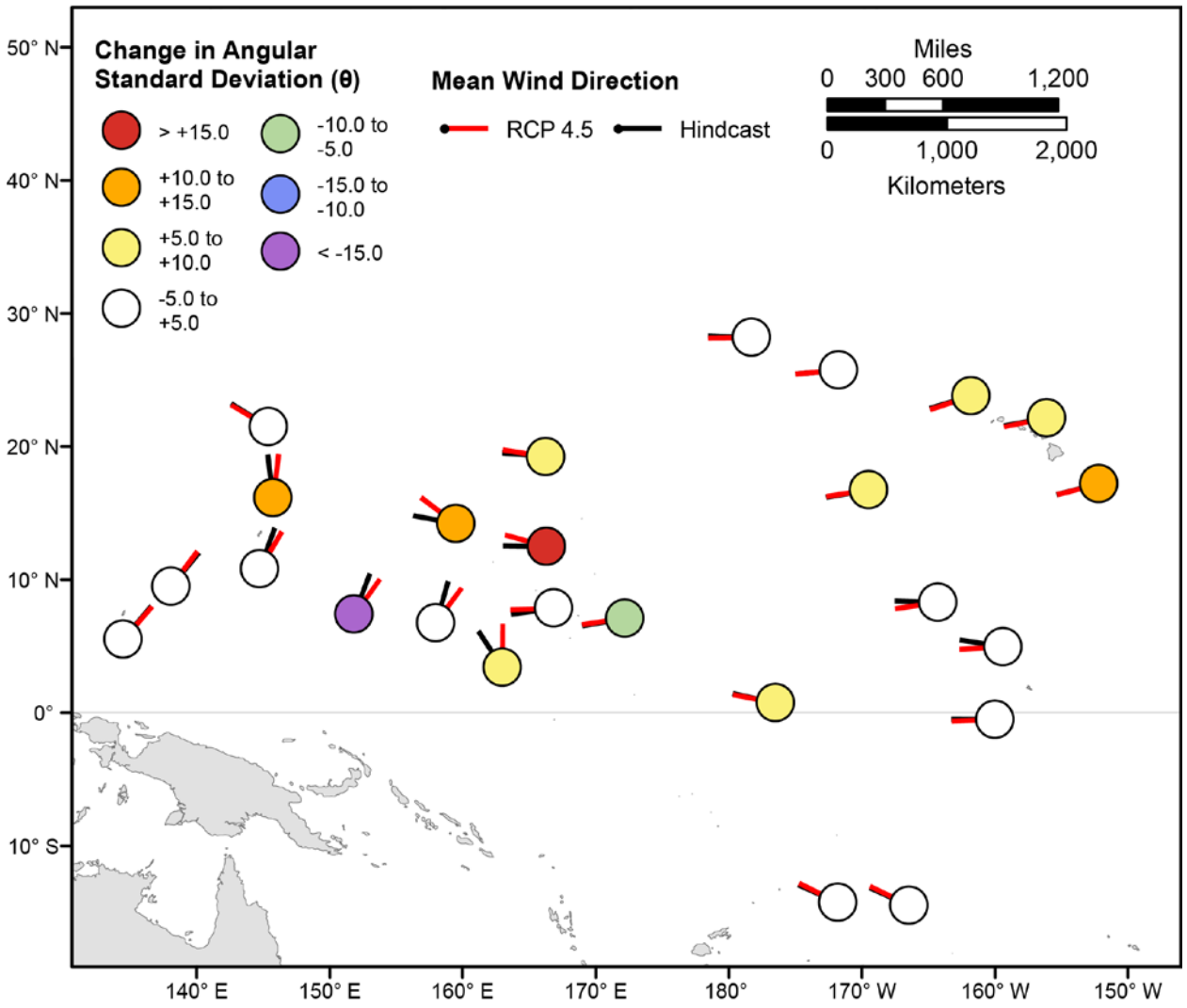

Figure 156. Map showing forecasted differences in the mean wind directions of the top 5 percent of wind speeds and the standard deviation of wind directions of the top 5 percent of wind speeds for the years 2081–2100 from hindcasted values during the June-August season under the RCP4.5 future climatic scenario. Mean wind directions at each point are indicated by lines radiating from the center of each point where RCP4.5 2081–2100 mean wind directions are red and 1976–2005 hindcasted mean wind directions are black. The colors correspond to the magnitude of change in modeled mean wind direction standard deviation during 2081–2100 from those hindcasted for 1976–2005. Angular standard deviation units are in degrees. Mean wind directions are “heading towards”.

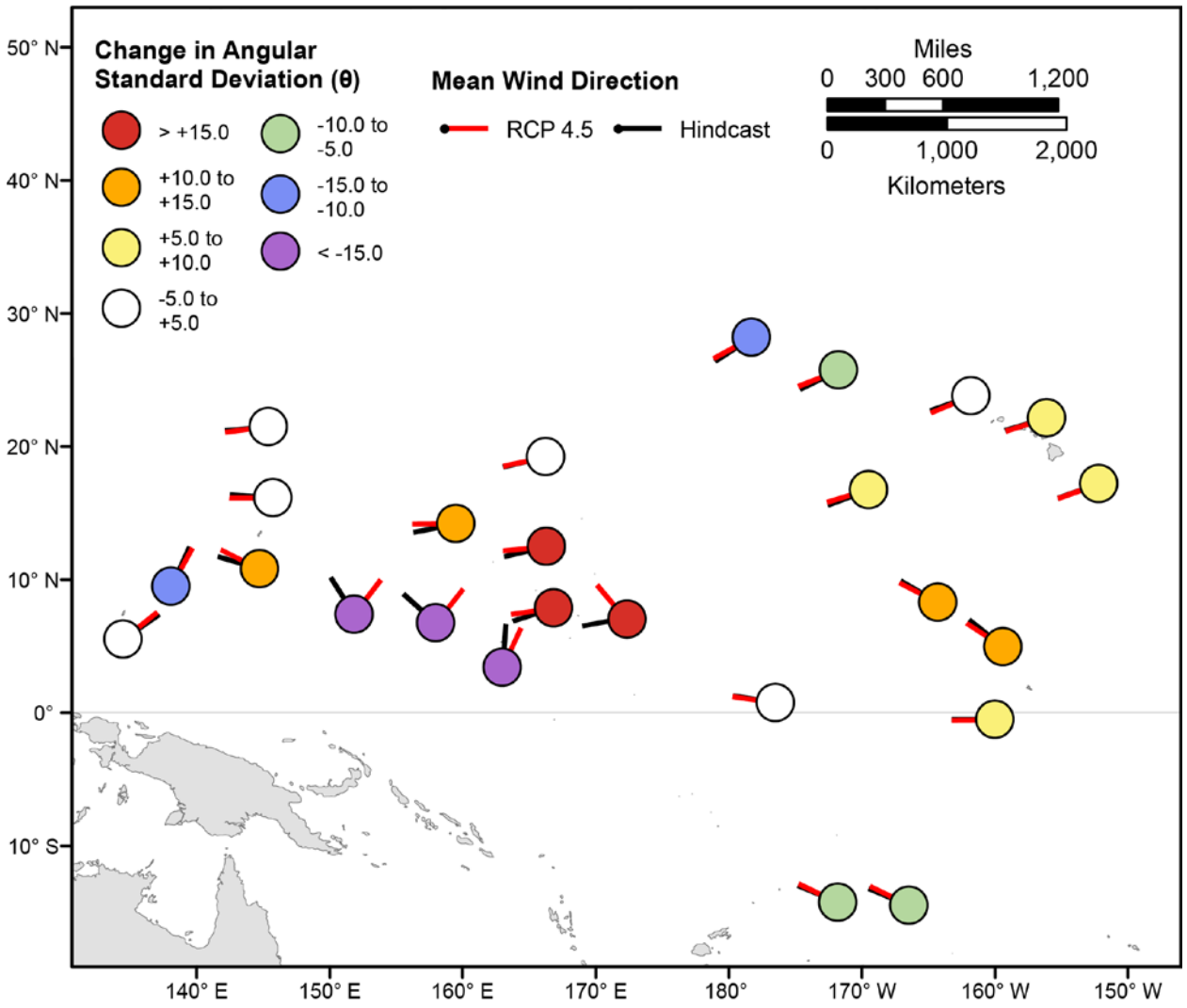

Figure 157. Map showing forecasted differences in the mean wind directions of the top 5 percent of wind speeds and the standard deviation of wind directions of the top 5 percent of wind speeds for the years 2081–2100 from hindcasted values during the September-November season under the RCP4.5 future climatic scenario. Mean wind directions at each point are indicated by lines radiating from the center of each point where RCP4.5 2081–2100 mean wind directions are red and 1976–2005 hindcasted mean wind directions are black. The colors correspond to the magnitude of change in modeled mean wind direction standard deviation during 2081–2100 from those hindcasted for 1976–2005. Angular standard deviation units are in degrees. Mean wind directions are “heading towards”.

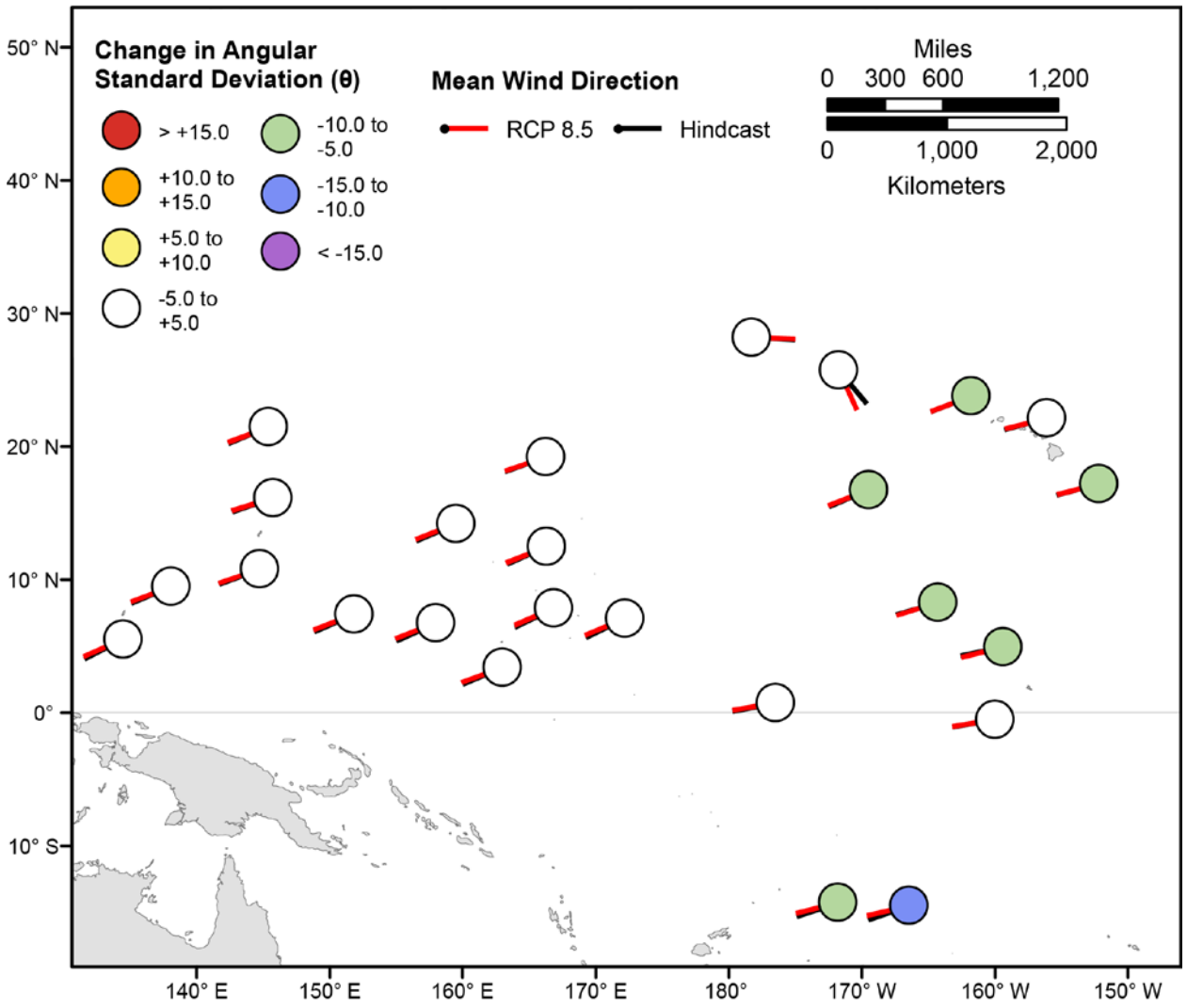

Figure 158. Map showing forecasted differences in mean wind directions and the standard deviation of wind directions for the years 2081–2100 from hindcasted values during the December-February season under the RCP8.5 future climatic scenario. Mean wind directions at each point are indicated by lines radiating from the center of each point where RCP8.5 2081–2100 mean wind directions are red and 1976–2005 hindcasted mean wind directions are black. The colors correspond to the magnitude of change in modeled mean wind direction standard deviation during 2081–2100 from those hindcasted for 1976–2005. Angular standard deviation units are in degrees. Mean wind directions are “heading towards”.

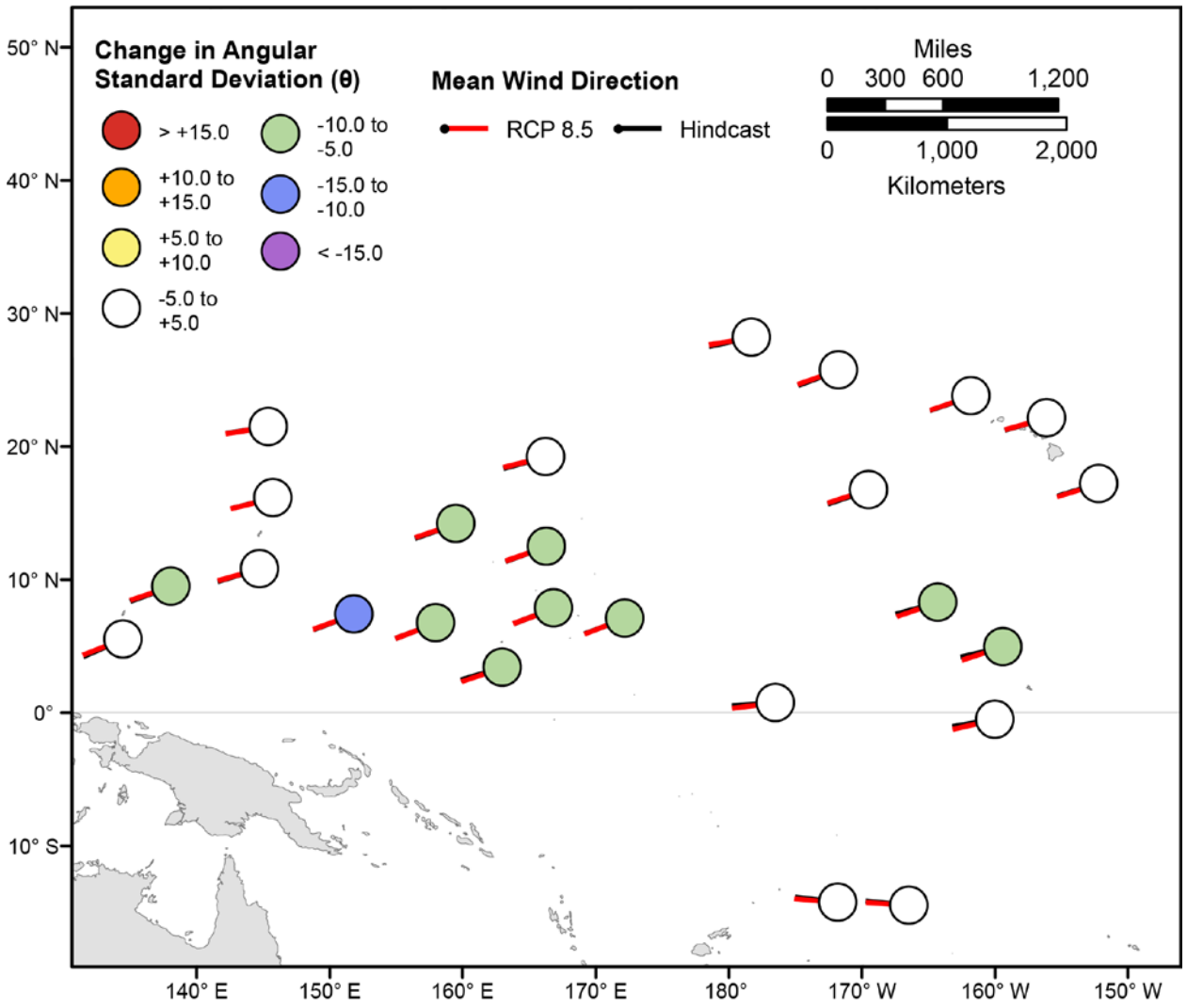

Figure 159. Map showing forecasted differences in mean wind directions and the standard deviation of wind directions for the years 2081–2100 from hindcasted values during the March-May season under the RCP8.5 future climatic scenario. Mean wind directions at each point are indicated by lines radiating from the center of each point where RCP8.5 2081–2100 mean wind directions are red and 1976–2005 hindcasted mean wind directions are black. The colors correspond to the magnitude of change in modeled mean wind direction standard deviation during 2081–2100 from those hindcasted for 1976–2005. Angular standard deviation units are in degrees. Mean wind directions are “heading towards”.

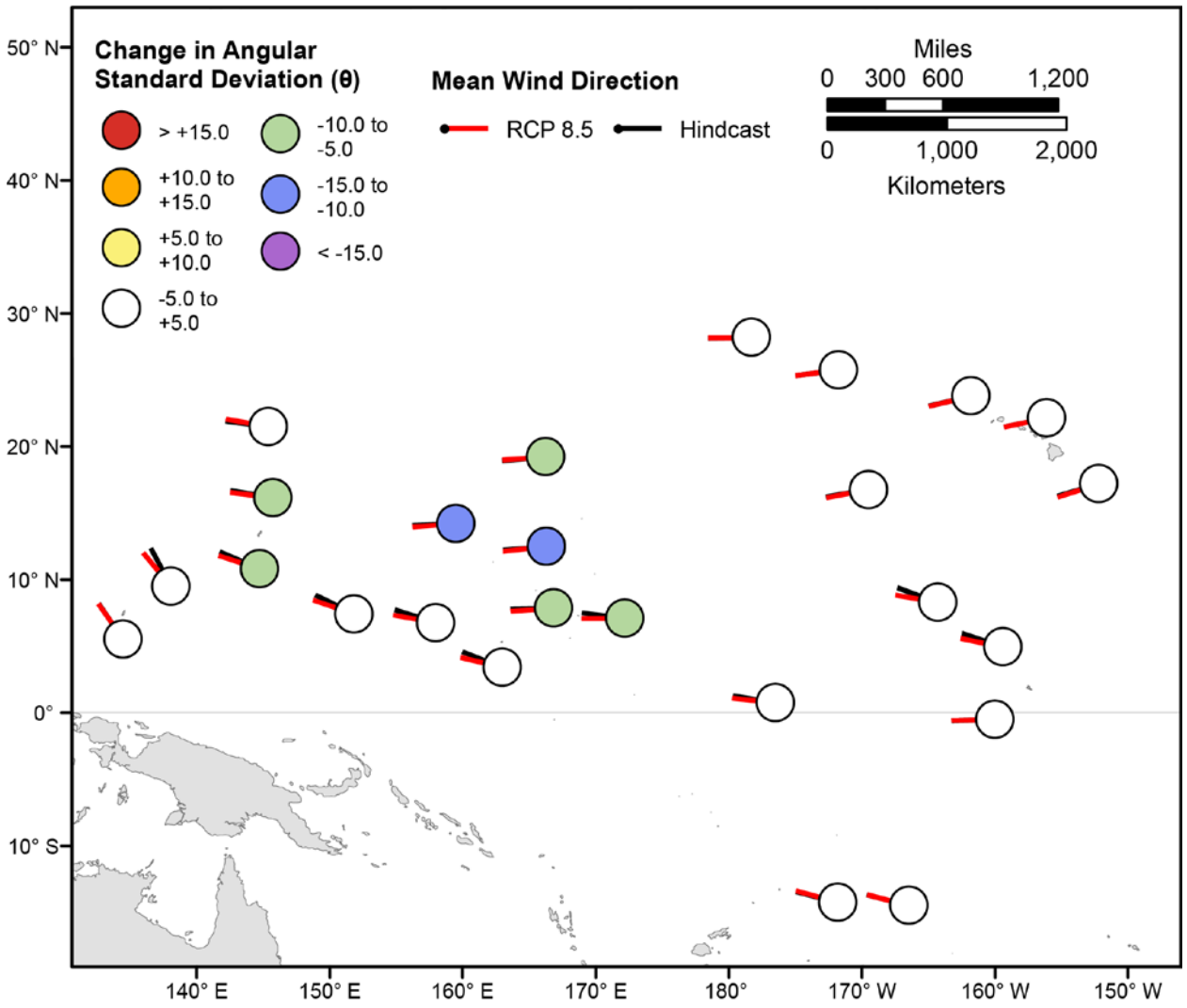

Figure 160. Map showing forecasted differences in mean wind directions and the standard deviation of wind directions for the years 2081–2100 from hindcasted values during the June-August season under the RCP8.5 future climatic scenario. Mean wind directions at each point are indicated by lines radiating from the center of each point where RCP8.5 2081–2100 mean wind directions are red and 1976–2005 hindcasted mean wind directions are black. The colors correspond to the magnitude of change in modeled mean wind direction standard deviation during 2081–2100 from those hindcasted for 1976–2005. Angular standard deviation units are in degrees. Mean wind directions are “heading towards”.

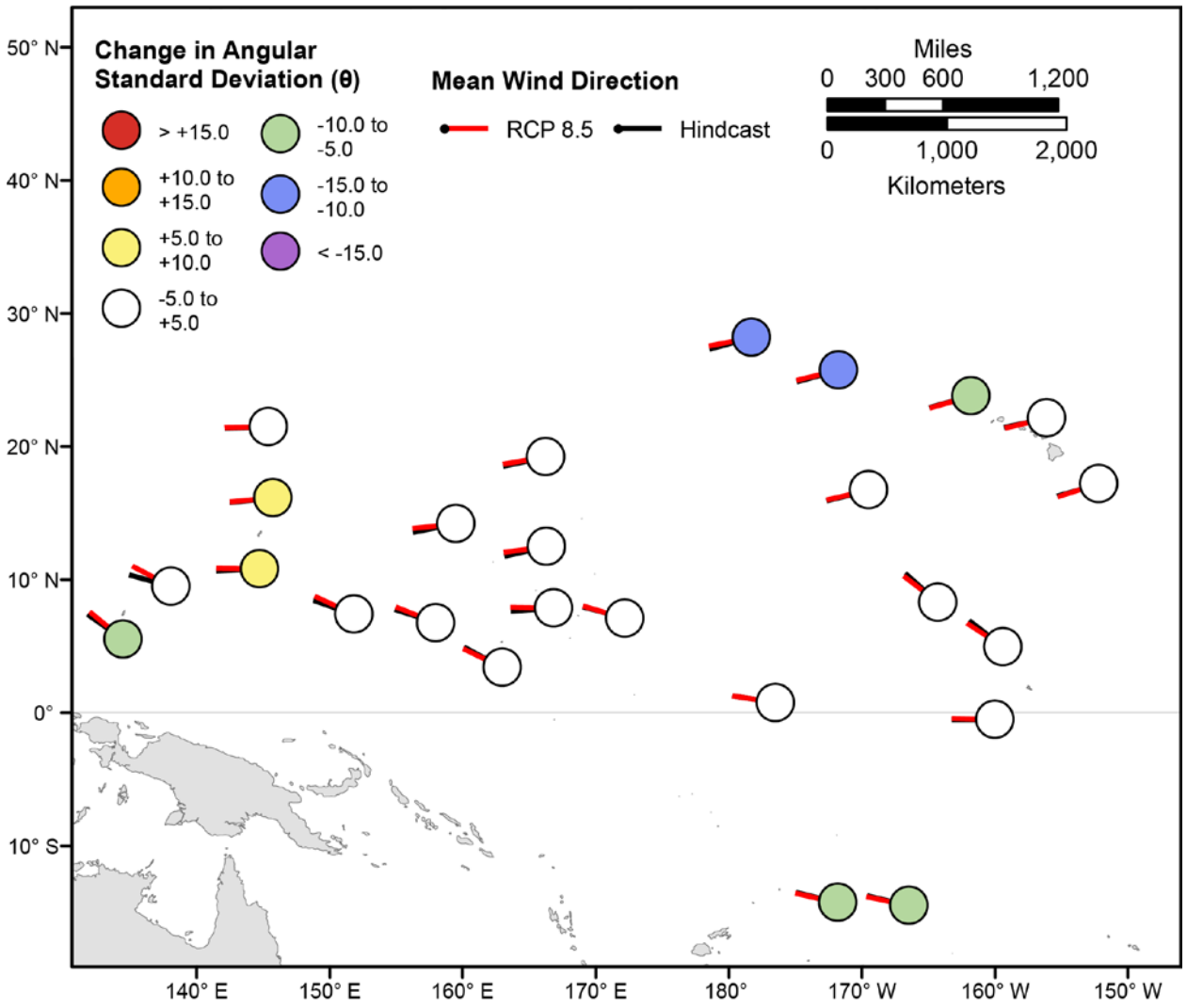

Figure 161. Map showing forecasted differences in mean wind directions and the standard deviation of wind directions for the years 2081–2100 from hindcasted values during the September-November season under the RCP8.5 future climatic scenario. Mean wind directions at each point are indicated by lines radiating from the center of each point where RCP8.5 2081–2100 mean wind directions are red and 1976–2005 hindcasted mean wind directions are black. The colors correspond to the magnitude of change in modeled mean wind direction standard deviation during 2081–2100 from those hindcasted for 1976–2005. Angular standard deviation units are in degrees. Mean wind directions are “heading towards”.

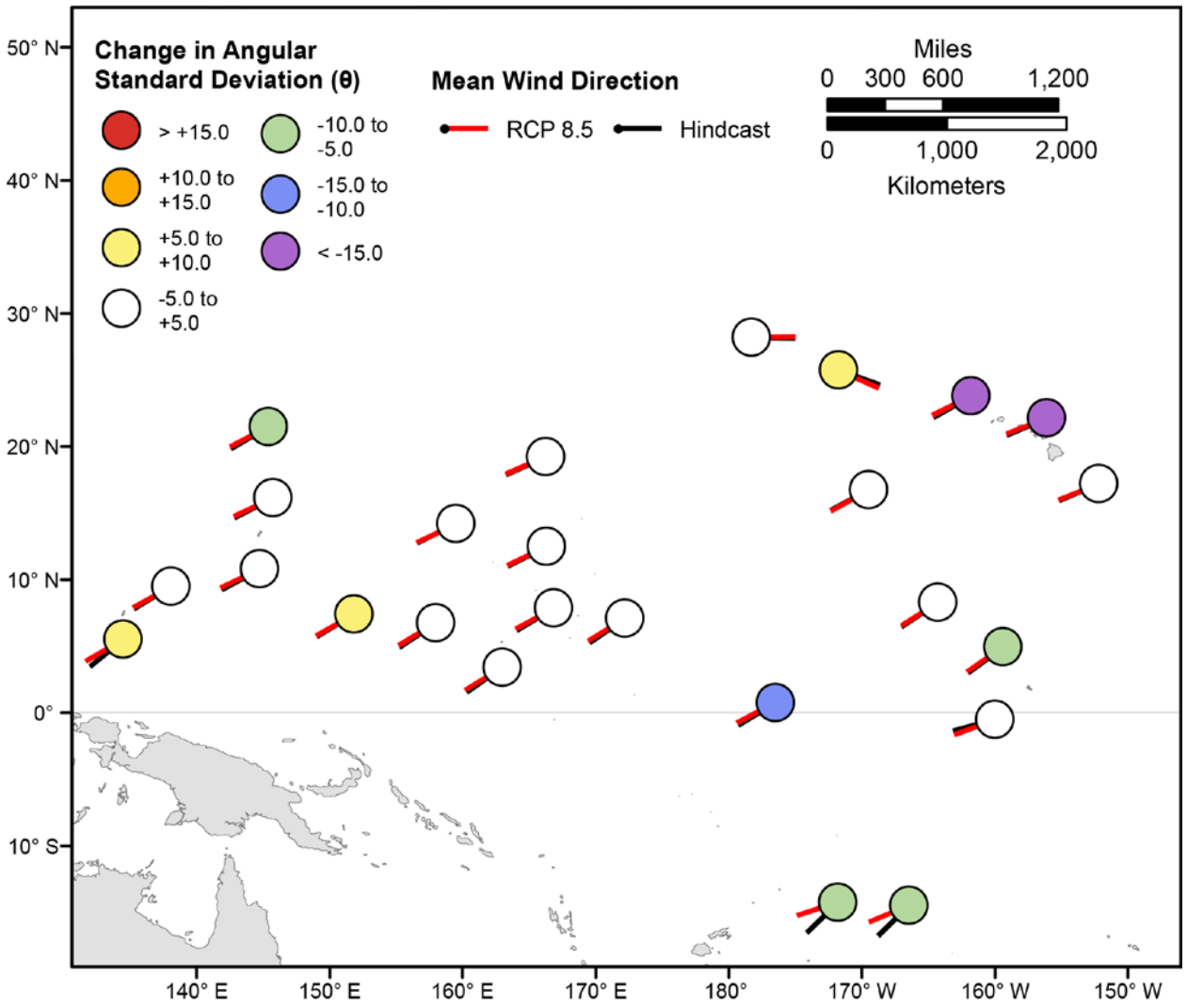

Figure 162. Map showing forecasted differences in the mean wind directions of the top 5 percent of wind speeds and the standard deviation of wind directions of the top 5 percent of wind speeds for the years 2081–2100 from hindcasted values during the December-February season under the RCP8.5 future climatic scenario. Mean wind directions at each point are indicated by lines radiating from the center of each point where RCP8.5 2081–2100 mean wind directions are red and 1976–2005 hindcasted mean wind directions are black. The colors correspond to the magnitude of change in modeled mean wind direction standard deviation during 2081–2100 from those hindcasted for 1976–2005. Angular standard deviation units are in degrees. Mean wind directions are “heading towards”.

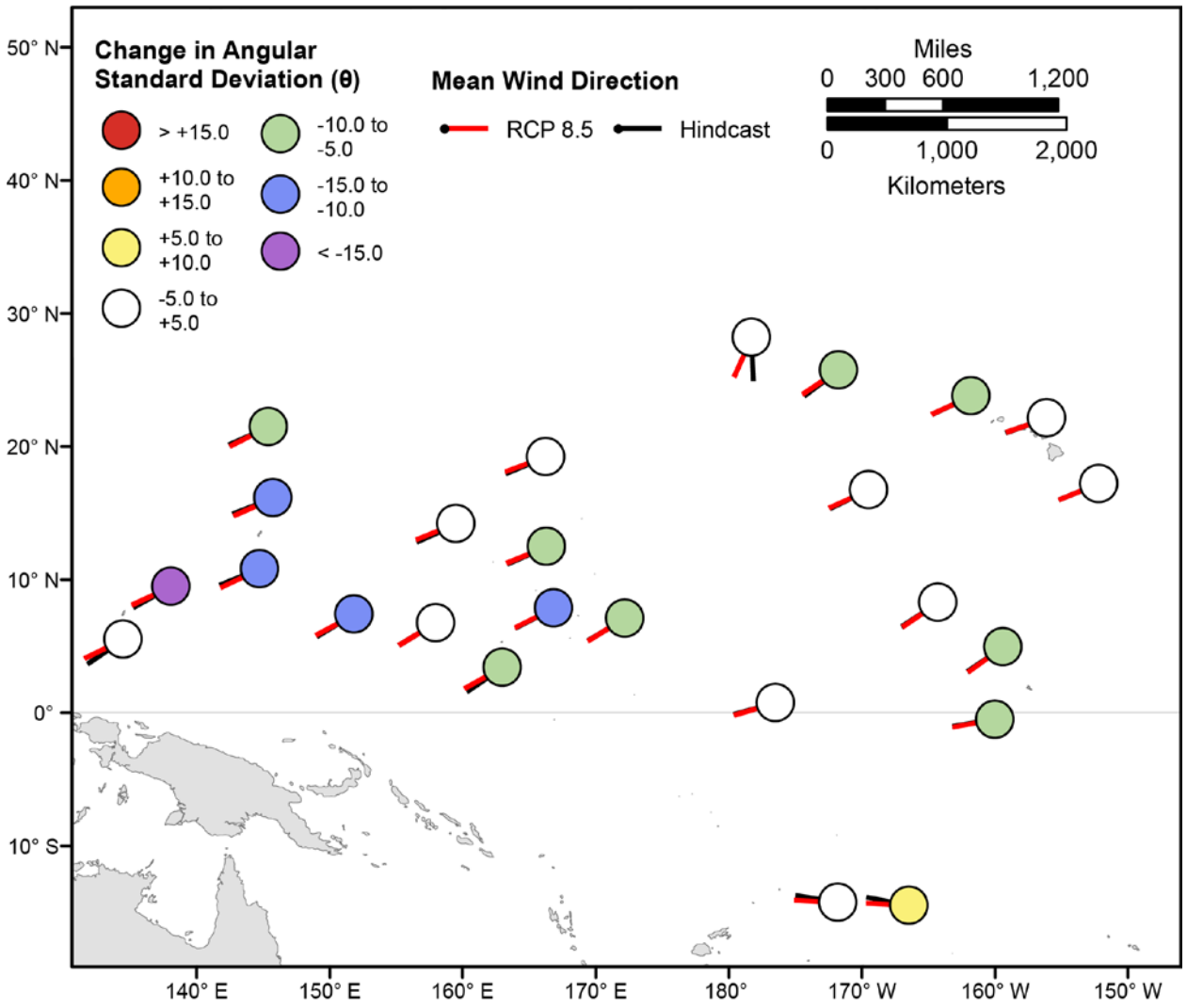

Figure 163. Map showing forecasted differences in the mean wind directions of the top 5 percent of wind speeds and the standard deviation of wind directions of the top 5 percent of wind speeds for the years 2081–2100 from hindcasted values during the March-May season under the RCP8.5 future climatic scenario. Mean wind directions at each point are indicated by lines radiating from the center of each point where RCP8.5 2081–2100 mean wind directions are red and 1976–2005 hindcasted mean wind directions are black. The colors correspond to the magnitude of change in modeled mean wind direction standard deviation during 2081–2100 from those hindcasted for 1976–2005. Angular standard deviation units are in degrees. Mean wind directions are “heading towards”.

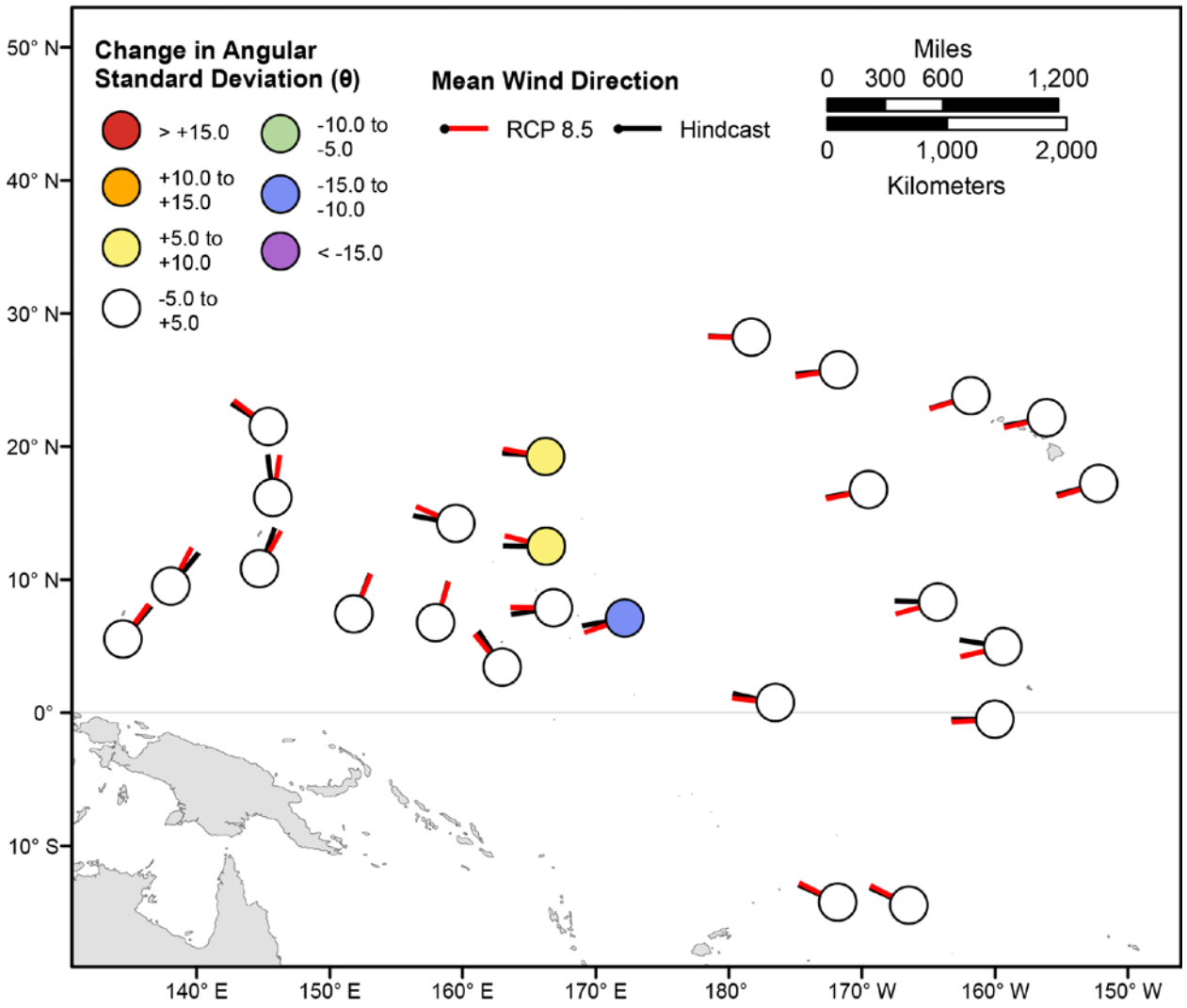

Figure 164. Map showing forecasted differences in the mean wind directions of the top 5 percent of wind speeds and the standard deviation of wind directions of the top 5 percent of wind speeds for the years 2081–2100 from hindcasted values during the June-August season under the RCP8.5 future climatic scenario. Mean wind directions at each point are indicated by lines radiating from the center of each point where RCP8.5 2081–2100 mean wind directions are red and 1976–2005 hindcasted mean wind directions are black. The colors correspond to the magnitude of change in modeled mean wind direction standard deviation during 2081–2100 from those hindcasted for 1976–2005. Angular standard deviation units are in degrees. Mean wind directions are “heading towards”.

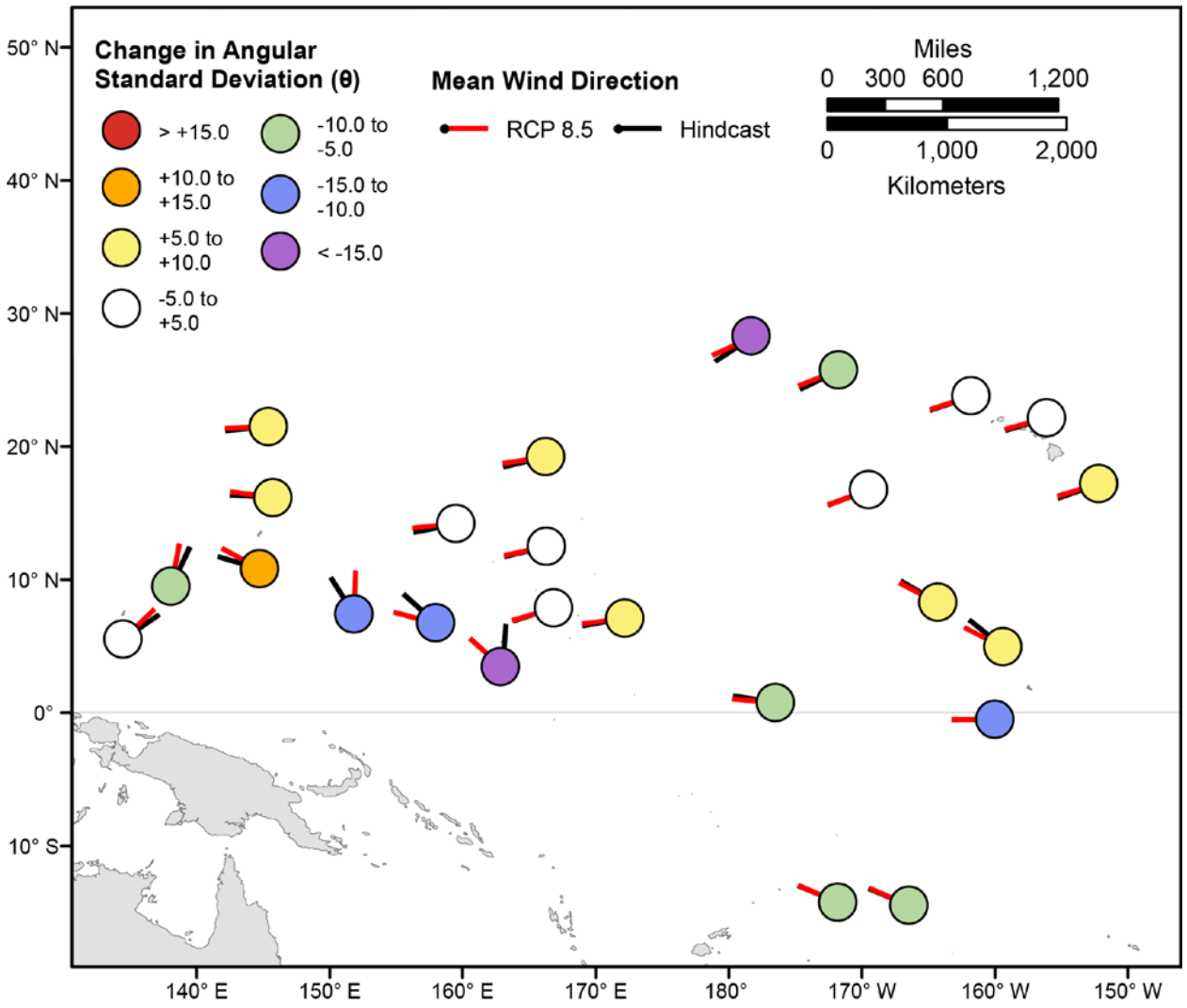

Figure 165. Map showing forecasted differences in the mean wind directions of the top 5 percent of wind speeds and the standard deviation of wind directions of the top 5 percent of wind speeds for the years 2081–2100 from hindcasted values during the September-November season under the RCP8.5 future climatic scenario. Mean wind directions at each point are indicated by lines radiating from the center of each point where RCP8.5 2081–2100 mean wind directions are red and 1976–2005 hindcasted mean wind directions are black. The colors correspond to the magnitude of change in modeled mean wind direction standard deviation during 2081–2100 from those hindcasted for 1976–2005. Angular standard deviation units are in degrees. Mean wind directions are “heading towards”.

Appendix A. Wave Height, Wave Period, and Wave Direction Statistics

Appendix A1. Table showing American Samoa monthly means and mean of the top 5 percent for significant wave height, peak wave period, and peak wave direction.

[Years: Hindcast = 1976–2005; RCP mid = 2026–2045; RCP end = 2081–2100. Wave directions are "coming from"]

Month	Jan	Feb	Mar	Apr	May	Jun	July	Aug	Sep	Oct	Nov	Dec
Mean Wave Height (m)												
Hindcast	2.0±0.7	2.0±0.7	2.1±0.6	2.1±0.6	2.3±0.7	2.4±0.7	2.3±0.6	2.3±0.6	2.3±0.6	2.0±0.6	2.1±0.6	2.0±0.5
RCP4.5 - mid	2.0±0.6	2.0±0.6	2.0±0.6	2.0±0.6	2.3±0.6	2.4±0.6	2.4±0.6	2.3±0.6	2.4±0.6	2.0±0.6	2.1±0.6	2.0±0.5
RCP8.5 - mid	2.0±0.6	2.0±0.6	2.0±0.6	2.1±0.6	2.3±0.6	2.3±0.6	2.4±0.7	2.4±0.6	2.3±0.6	2.3±0.6	2.1±0.6	2.0±0.7
RCP4.5 - end	2.0±0.6	2.0±0.6	2.0±0.6	2.0±0.6	2.4±0.7	2.4±0.6	2.4±0.7	2.4±0.6	2.3±0.6	2.0±0.6	2.1±0.6	2.0±0.6
RCP8.5 - end	2.0±0.7	2.0±0.7	2.0±0.6	2.1±0.5	2.3±0.7	2.4±0.7	2.4±0.6	2.4±0.7	2.4±0.6	2.3±0.6	2.0±0.5	1.9±0.5
Top 5 percent Wave Height (m)												
Hindcast	4.2±1.1	4.0±1.5	3.8±0.8	3.7±0.6	4.1±0.6	4.1±0.5	4.0±0.5	4.0±0.4	3.8±0.4	3.8±0.4	3.7±0.5	3.4±0.8
RCP4.5 - mid	3.9±1.1	3.7±1.0	3.7±0.9	3.9±0.6	3.9±0.5	4.0±0.4	4.0±0.3	3.9±0.3	4.1±0.4	3.8±0.3	3.9±0.6	3.3±0.6
RCP8.5 - mid	3.8±0.9	4.1±1.0	4.0±1.0	3.7±0.5	3.9±0.4	4.0±0.4	4.1±0.4	4.1±0.5	4.0±0.4	3.9±0.4	3.7±0.6	4.2±1.2
RCP4.5 - end	3.8±0.9	3.9±0.9	3.7±0.9	4.0±0.7	4.3±0.6	4.0±0.4	4.1±0.5	4.0±0.4	4.0±0.4	3.9±0.5	3.7±0.6	3.9±1.1
RCP8.5 - end	4.2±1.3	4.3±1.0	3.7±0.9	3.5±0.5	4.1±0.6	4.2±0.4	4.0±0.4	4.2±0.4	4.1±0.4	3.8±0.4	3.4±0.5	3.4±0.5
Mean Wave Period (s)												
Hindcast	12±3	12±2	12±2	11±2	11±3	11±3	11±3	11±3	11±3	11±3	11±3	12±3
RCP4.5 - mid	12±3	12±3	12±2	11±2	11±3	11±3	11±3	11±3	11±3	11±3	11±3	12±3
RCP8.5 - mid	12±3	12±2	12±2	11±2	11±3	11±3	11±3	11±3	11±3	11±3	11±3	12±3
RCP4.5 - end	12±3	12±2	12±2	11±2	11±3	11±3	11±3	11±3	11±3	11±3	11±3	12±3
RCP8.5 - end	12±3	12±3	12±2	11±3	11±3	11±3	11±3	11±3	11±3	11±3	11±3	12±3
Top 5 percent Wave Period (s)												
Hindcast	10±2	11±2	11±2	11±2	10±2	10±2	11±2	10±2	10±2	9±2	10±1	10±3
RCP4.5 - mid	11±3	11±3	11±2	11±2	11±2	10±2	11±2	10±2	10±1	9±1	10±2	10±3
RCP8.5 - mid	10±2	10±2	10±2	10±2	10±2	10±2	10±2	10±2	10±2	10±2	10±2	10±2
RCP4.5 - end	10±2	10±2	10±2	10±2	10±2	10±2	10±2	10±2	10±2	10±1	10±1	10±2
RCP8.5 - end	10±2	10±2	10±2	11±2	10±2	11±2	10±2	10±2	10±2	10±2	10±2	10±3
Mean Wave Direction (°)												
Hindcast	35±50	37±63	90±75	130±43	138±31	134±28	133±27	129±27	128±25	122±28	101±43	60±46
RCP4.5 - mid	37±49	33±57	76±75	129±45	135±27	130±28	131±26	128±25	126±23	124±25	105±42	67±50
RCP8.5 - mid	43±45	38±59	89±79	131±40	136±26	137±27	132±28	133±26	127±24	123±25	103±38	64±50
RCP4.5 - end	40±49	30±62	74±76	129±45	135±27	131±26	131±27	129±25	128±22	125±26	104±40	67±49
RCP8.5 - end	44±47	38±60	79±79	130±41	136±27	131±24	131±25	128±24	127±22	123±23	108±34	66±44
Top 5 percent Wave Direction (°)												
Hindcast	11±78	1±92	84±96	128±39	121±33	126±23	130±22	122±16	118±23	118±25	106±35	70±58
RCP4.5 - mid	0±71	353±65	74±103	130±50	130±23	123±23	128±19	125±16	119±14	118±19	104±37	94±56
RCP8.5 - mid	37±71	345±82	57±93	130±34	128±24	129±23	127±24	128±17	122±16	117±23	100±40	87±52
RCP4.5 - end	22±83	352±75	61±90	116±56	125±21	129±26	125±18	125±23	122±17	118±18	109±32	88±54
RCP8.5 - end	16±76	340±70	358±06	127±48	122±28	129±18	124±19	125±19	123±20	116±17	110±31	89±39

Appendix A2. Table showing return values of ensemble-average significant wave heights of hindcast and forecast scenarios, including lower and higher 95 percent confidence intervals, at the American Samoa location.

[Years: Hindcast = 1976–2005; RCP mid = 2026–2045; RCP end = 2081–2100. Wave height values are in meters]

Scenario	Hindcast			RCP4.5 - mid			RCP8.5 - mid			RCP4.5 - end			RCP8.5 - end		
	Low	R_v	High	Low	R_v	High	Low	R_v	High	Low	R_v	High	Low	R_v	High
2-year	5.92	6.86	8.56	5.67	6.69	8.76	5.91	6.91	8.90	5.78	6.94	9.50	5.90	6.79	8.47
5-year	6.50	8.27	12.03	6.10	7.94	12.42	6.32	8.07	12.16	6.15	8.18	13.59	6.30	7.83	11.26
10-year	6.97	9.64	16.02	6.43	9.10	16.61	6.62	9.09	15.68	6.41	9.27	18.18	6.58	8.74	14.21
20-year	7.46	11.32	21.77	6.74	10.48	22.60	6.90	10.24	20.47	6.66	10.51	24.65	6.85	9.78	18.16
50-year	8.15	14.16	33.45	7.16	12.72	34.68	7.25	12.03	29.55	6.95	12.44	37.44	7.20	11.37	25.52
100-year	8.71	16.89	46.89	7.47	14.79	48.48	7.50	13.59	39.35	7.15	14.14	51.80	7.45	12.76	33.32

Appendix A3. Table showing Kauai monthly means and mean of the top 5 percent for significant wave height, peak wave period, and peak wave direction.

[Years: Hindcast = 1976–2005; RCP mid = 2026–2045; RCP end = 2081–2100. Wave directions are "coming from"]

Month	Jan	Feb	Mar	Apr	May	Jun	July	Aug	Sep	Oct	Nov	Dec
Mean Wave Height (m)												
Hindcast	3.5±1.0	3.4±1.0	2.9±0.8	2.5±0.7	2.1±0.6	2.1±0.5	2.1±0.5	2.1±0.5	2.2±0.6	2.6±0.7	3.0±0.8	3.3±0.9
RCP4.5 - mid	3.5±1.0	3.4±1.0	3.0±0.8	2.5±0.7	2.1±0.6	2.0±0.5	2.1±0.5	2.0±0.5	2.0±0.6	2.5±0.7	3.0±0.8	3.3±0.9
RCP8.5 - mid	3.4±1.0	3.3±1.0	2.9±0.8	2.5±0.7	2.1±0.5	2.0±0.5	2.0±0.5	2.1±0.5	2.1±0.6	2.5±0.8	3.0±0.8	3.3±0.9
RCP4.5 - end	3.4±1.0	3.4±1.0	3.0±0.8	2.5±0.7	2.1±0.5	2.0±0.5	2.0±0.5	2.0±0.6	2.1±0.6	2.5±0.7	3.0±0.8	3.3±0.9
RCP8.5 - end	3.3±1.0	3.2±1.0	2.8±0.8	2.4±0.6	2.0±0.5	1.9±0.4	2.0±0.5	1.9±0.5	2.0±0.5	2.4±0.7	2.8±0.8	3.2±0.9
Top 5 percent Wave Height (m)												
Hindcast	6.1±0.7	6.0±0.7	5.0±0.5	4.2±0.5	3.5±0.3	3.4±0.4	3.3±0.4	3.4±0.5	3.6±0.3	4.5±0.5	5.1±0.6	5.5±0.6
RCP4.5 - mid	6.2±0.8	5.9±0.6	5.0±0.6	4.2±0.3	3.6±0.6	3.1±0.2	3.3±0.5	3.4±0.4	3.5±0.5	4.5±0.7	5.0±0.4	5.8±0.7
RCP8.5 - mid	5.9±0.7	5.8±0.6	5.0±0.6	4.1±0.4	3.3±0.3	3.2±0.3	3.2±0.5	3.4±0.4	3.5±0.4	4.6±0.6	5.0±0.5	5.6±0.5
RCP4.5 - end	5.9±0.6	6.1±0.7	5.0±0.5	4.2±0.5	3.4±0.3	3.1±0.3	3.3±0.7	3.9±0.9	3.6±0.6	4.4±0.7	4.8±0.4	5.5±0.6
RCP8.5 - end	5.8±0.6	5.8±0.8	4.9±0.5	3.9±0.3	3.3±0.3	3.0±0.2	3.4±0.7	3.4±0.8	3.5±0.8	4.1±0.6	4.8±0.6	5.6±0.5
Mean Wave Period (s)												
Hindcast	13±2	12±2	12±2	10±3	10±3	10±3	10±3	10±3	10±3	11±3	12±2	12±2
RCP4.5 - mid	13±2	13±2	12±2	11±3	11±3	10±3	9±3	10±3	10±3	11±3	12±2	12±2
RCP8.5 - mid	13±2	12±2	12±2	11±3	10±3	10±3	10±3	10±3	10±3	11±3	12±2	12±2
RCP4.5 - end	13±2	13±2	12±2	11±3	11±3	10±3	9.8±3	9.9±3	10±3	11±3	12±2	12±2
RCP8.5 - end	13±2	12±2	12±2	11±3	11±3	11±4	10±3	10±4	11±3	11±3	11±2	12±2
Top 5 percent Wave Period (s)												
Hindcast	15±2	15±2	13±3	11±3	10±3	8±1	9±2	9±2	10±2	11±2	13±3	14±2
RCP4.5 - mid	15±2	15±2	14±3	11±3	10±3	8±2	9±2	10±2	9±2	11±2	13±3	15±2
RCP8.5 - mid	15±2	15±2	13±3	11±3	9±3	9±3	9±2	9±2	10±2	11±2	14±3	14±2
RCP4.5 - end	15±2	15±2	13±2	12±3	10±3	9±3	9±2	10±2	9±1	11±2	13±3	15±2
RCP8.5 - end	16±2	15±2	13±3	12±3	10±3	9±3	9±2	10±3	10±2	11±2	12±3	15±3
Mean Wave Direction (°)												
Hindcast	336±45	335±47	7±55	45±50	75±43	91±25	93±20	92±29	77±41	51±42	22±47	356±50
RCP4.5 - mid	334±43	340±48	6±54	49±47	74±47	92±27	92±19	93±28	83±40	51±46	24±46	354±47
RCP8.5 - mid	339±45	339±45	2±52	42±49	74±45	92±29	94±24	95±31	83±44	49±45	21±44	357±48
RCP4.5 - end	332±42	336±47	6±51	36±50	71±46	94±28	94±23	96±29	82±42	54±43	25±43	356±49
RCP8.5 - end	336±42	335±42	1±52	46±48	73±49	96±26	96±22	98±30	86±41	55±41	31±43	356±48
Top 5 percent Wave Direction (°)												
Hindcast	316±23	317±25	356±55	37±46	68±29	82±14	86±16	88±36	71±39	44±54	3±51	328±43
RCP4.5 - mid	316±23	321±33	339±47	52±41	68±29	81±16	89±24	87±35	82±44	55±51	7±51	328±34
RCP8.5 - mid	321±31	323±34	342±53	40±44	68±23	80±12	87±21	91±38	80±52	53±43	0±40	335±47
RCP4.5 - end	314±17	316±30	343±45	21±48	72±26	90±19	85±23	105±57	82±48	48±54	18±49	331±39
RCP8.5 - end	318±24	318±26	343±47	33±42	63±35	87±17	91±28	91±39	101±68	58±53	21±47	345±51

Appendix A4. Table showing return values of ensemble-average significant wave heights of hindcast and forecast scenarios, including lower and higher 95 percent confidence intervals, at the Kauai location.

[Years: Hindcast = 1976–2005; RCP mid = 2026–2045; RCP end = 2081–2100. Wave height values are in meters]

Scenario	Hindcast			RCP4.5 - mid			RCP8.5 - mid			RCP4.5 - end			RCP8.5 - end		
	Low	R_v	High	Low	R_v	High	Low	R_v	High	Low	R_v	High	Low	R_v	High
2-year	7.51	8.06	8.88	7.41	8.17	9.53	7.26	7.89	8.94	7.22	7.81	8.83	7.27	7.89	8.88
5-year	7.83	8.65	9.99	7.70	8.89	11.26	7.50	8.42	10.08	7.47	8.38	10.17	7.51	8.38	9.87
10-year	8.02	9.07	10.89	7.89	9.42	12.79	7.64	8.76	10.95	7.62	8.80	11.35	7.64	8.69	10.58
20-year	8.19	9.46	11.82	8.04	9.94	14.52	7.74	9.07	11.83	7.75	9.23	12.70	7.74	8.95	11.26
50-year	8.37	9.95	13.12	8.21	10.61	17.20	7.85	9.43	13.00	7.90	9.78	14.79	7.84	9.23	12.10
100-year	8.49	10.29	14.16	8.32	11.11	19.55	7.91	9.66	13.91	7.99	10.19	16.64	7.89	9.41	12.70

Appendix A5. Table showing Big Island of Hawaii monthly means and mean of the top 5 percent for significant wave height, peak wave period, and peak wave direction.

[Years: Hindcast = 1976–2005; RCP mid = 2026–2045; RCP end = 2081–2100. Wave directions are "coming from"]

Month	Jan	Feb	Mar	Apr	May	Jun	July	Aug	Sep	Oct	Nov	Dec
Mean Wave Height (m)												
Hindcast	2.8±0.7	2.7±0.7	2.6±0.7	2.4±0.6	2.2±0.5	2.2±0.5	2.2±0.5	2.1±0.5	2.1±0.6	2.4±0.7	2.8±0.8	2.9±0.8
RCP4.5 - mid	2.8±0.7	2.8±0.7	2.7±0.7	2.5±0.7	2.2±0.5	2.2±0.4	2.2±0.5	2.1±0.5	2.0±0.5	2.3±0.7	2.8±0.8	2.9±0.7
RCP8.5 - mid	2.8±0.7	2.7±0.7	2.6±0.7	2.4±0.6	2.1±0.5	2.1±0.4	2.2±0.4	2.1±0.5	2.0±0.5	2.3±0.7	2.7±0.7	2.9±0.8
RCP4.5 - end	2.7±0.6	2.7±0.7	2.6±0.7	2.4±0.6	2.2±0.5	2.2±0.5	2.2±0.5	2.1±0.6	2.1±0.5	2.3±0.6	2.7±0.8	2.9±0.7
RCP8.5 - end	2.7±0.7	2.6±0.6	2.5±0.6	2.3±0.6	2.1±0.4	2.1±0.4	2.2±0.5	2.0±0.5	2.0±0.5	2.2±0.6	2.6±0.7	2.8±0.8
Top 5 percent Wave Height (m)												
Hindcast	4.6±0.5	4.5±0.5	4.5±0.4	3.9±0.3	3.4±0.3	3.4±0.3	3.5±0.4	3.5±0.6	3.7±0.6	4.4±0.5	4.9±0.5	4.7±0.4
RCP4.5 - mid	4.5±0.5	4.7±0.6	4.3±0.3	4.1±0.3	3.4±0.4	3.2±0.3	3.4±0.5	3.4±0.5	3.4±0.5	4.2±0.7	4.8±0.4	4.7±0.5
RCP8.5 - mid	4.7±0.5	4.6±0.5	4.3±0.5	3.9±0.4	3.3±0.2	3.1±0.3	3.3±0.4	3.5±0.5	3.4±0.6	4.2±0.5	4.5±0.4	5.0±0.6
RCP4.5 - end	4.4±0.5	4.5±0.5	4.3±0.4	3.9±0.3	3.4±0.3	3.2±0.3	3.6±0.8	3.8±1.0	3.5±0.6	4.1±0.7	4.8±0.5	4.9±0.6
RCP8.5 - end	4.4±0.4	4.2±0.4	4.1±0.4	3.7±0.3	3.1±0.3	3.1±0.4	3.4±0.5	3.6±0.7	3.3±0.6	3.9±0.6	4.5±0.7	5.1±0.8
Mean Wave Period (s)												
Hindcast	12±3	12±3	11±3	10±3	10±3	10±3	10±3	10±3	10±3	10±3	11±3	12±3
RCP4.5 - mid	12±3	12±3	11±3	10±3	10±3	10±3	9±3	10±3	10±3	11±3	11±3	12±3
RCP8.5 - mid	12±3	12±3	11±3	10±3	10±3	10±3	10±3	10±3	10±3	11±3	11±3	12±3
RCP4.5 - end	12±3	12±3	11±3	11±3	10±3	9.9±3	9.7±3	9.7±3	10±3	11±3	11±3	12±3
RCP8.5 - end	12±3	12±3	11±3	10±3	11±3	10±4	10±3	10±3	11±3	11±3	11±3	12±3
Top 5 percent Wave Period (s)												
Hindcast	12±3	12±3	10±2	10±2	9±2	9±1	9±2	9±1	9±1	10±1	11±2	11±2
RCP4.5 - mid	13±3	11±3	10±2	10±1	10±2	9±2	9±1	10±2	9±1	10±1	11±2	12±3
RCP8.5 - mid	12±3	11±3	11±2	10±2	9±2	9±2	9±2	9±1	9±1	10±2	11±2	11±2
RCP4.5 - end	12±3	12±3	10±2	10±2	9±2	9±2	10±2	10±2	9±2	10±2	11±2	11±2
RCP8.5 - end	13±3	12±3	10±2	10±2	9±2	10±3	9±2	9±2	10±2	10±2	11±2	11±2
Mean Wave Direction (°)												
Hindcast	29±53	25±55	55±47	75±33	91±27	92±17	92±18	92±21	85±31	69±33	57±36	47±44
RCP4.5 - mid	28±51	31±52	55±45	72±31	89±26	94±18	92±16	92±23	90±29	70±36	53±35	44±42
RCP8.5 - mid	31±50	31±52	50±48	73±34	90±25	94±19	93±19	93±23	88±31	68±40	51±37	48±43
RCP4.5 - end	29±54	23±54	52±44	72±34	90±25	95±18	94±18	95±24	90±33	70±37	52±36	45±43
RCP8.5 - end	25±51	21±53	49±46	73±32	91±27	97±18	95±17	97±24	92±32	72±37	56±34	43±44
Top 5 percent Wave Direction (°)												
Hindcast	56±46	50±49	69±23	75±20	84±15	87±12	86±18	81±16	76±28	73±24	69±26	64±26
RCP4.5 - mid	33±54	59±43	70±28	74±14	84±14	87±12	92±22	82±18	87±29	74±30	68±20	56±37
RCP8.5 - mid	57±40	59±40	67±28	75±20	86±15	88±12	86±20	86±28	81±27	68±28	65±33	69±22
RCP4.5 - end	52±50	44±49	69±28	75±23	85±13	92±18	94±24	97±41	95±45	73±36	68±19	73±28
RCP8.5 - end	49±48	38±56	63±31	76±19	81±17	91±17	94±20	93±30	88±40	75±40	66±21	70±25

Appendix A6. Table showing return values of ensemble-average significant wave heights of hindcast and forecast scenarios, including lower and higher 95 percent confidence intervals, at the Big Island of Hawaii location.

[Years: Hindcast = 1976–2005; RCP mid = 2026–2045; RCP end = 2081–2100. Wave height values are in meters]

Scenario	Hindcast			RCP4.5 - mid			RCP8.5 - mid			RCP4.5 - end			RCP8.5 - end		
	Low	R_v	High	Low	R_v	High	Low	R_v	High	Low	R_v	High	Low	R_v	High
2-year	5.83	6.27	6.95	5.79	6.32	7.21	5.70	6.20	7.04	5.95	6.72	8.11	5.64	6.45	8.11
5-year	6.04	6.68	7.77	6.05	6.88	8.47	5.91	6.66	8.08	6.14	7.22	9.42	5.87	7.15	10.27
10-year	6.16	6.95	8.40	6.22	7.32	9.60	6.04	7.00	8.95	6.25	7.54	10.42	6.01	7.70	12.38
20-year	6.25	7.20	9.04	6.37	7.77	10.92	6.14	7.32	9.90	6.32	7.81	11.43	6.13	8.26	15.00
50-year	6.35	7.49	9.90	6.54	8.37	12.99	6.26	7.72	11.29	6.39	8.11	12.77	6.26	9.02	19.48
100-year	6.41	7.69	10.57	6.66	8.83	14.86	6.33	8.00	12.46	6.42	8.30	13.79	6.35	9.61	23.84

Appendix A7. Table showing Midway monthly means and mean of the top 5 percent for significant wave height, peak wave period, and peak wave direction.

[Years: Hindcast = 1976–2005; RCP mid = 2026–2045; RCP end = 2081–2100. Wave directions are "coming from"]

Month	Jan	Feb	Mar	Apr	May	Jun	July	Aug	Sep	Oct	Nov	Dec
Mean Wave Height (m)												
Hindcast	4.1±1.5	3.9±1.5	3.1±1.1	2.4±0.8	1.9±0.5	1.8±0.4	1.9±0.6	2.0±0.7	2.2±0.8	2.7±1.0	3.2±1.1	3.8±1.3
RCP4.5 - mid	4.2±1.5	3.9±1.4	3.2±1.1	2.5±0.8	1.9±0.5	1.7±0.4	1.9±0.6	1.9±0.7	2.1±0.7	2.5±0.9	3.1±1.1	3.7±1.4
RCP8.5 - mid	4.0±1.4	3.8±1.4	3.2±1.1	2.4±0.8	1.8±0.5	1.7±0.4	1.9±0.6	1.9±0.7	2.1±0.8	2.6±0.9	3.0±1.0	3.7±1.4
RCP4.5 - end	4.1±1.4	4.0±1.5	3.2±1.1	2.4±0.8	1.9±0.5	1.7±0.4	1.8±0.5	1.9±0.8	2.0±0.7	2.5±0.9	3.0±1.0	3.7±1.4
RCP8.5 - end	4.0±1.5	3.8±1.4	3.1±1.1	2.3±0.7	1.8±0.5	1.6±0.4	1.8±0.5	1.8±0.7	2.0±0.7	2.4±0.8	2.8±0.9	3.6±1.3
Top 5 percent Wave Height (m)												
Hindcast	8.1±1.2	7.9±0.9	6.2±0.8	4.6±0.7	3.3±0.4	2.9±0.4	3.5±0.7	4.0±0.9	4.5±0.7	5.3±0.8	6.1±0.9	7.4±0.9
RCP4.5 - mid	8.1±1.0	7.8±0.9	6.3±0.8	4.5±0.6	3.3±0.5	2.9±0.5	3.6±0.9	4.1±0.9	4.2±0.9	5.1±0.8	6.2±1.0	7.5±0.9
RCP8.5 - mid	7.7±0.9	7.4±0.8	6.3±0.8	4.5±0.7	3.2±0.5	2.7±0.3	3.4±0.7	4.1±0.8	4.6±1.0	5.0±0.7	5.9±0.9	7.5±1.0
RCP4.5 - end	7.9±1.0	8.0±1.2	6.2±0.8	4.6±0.7	3.3±0.4	2.7±0.3	3.3±0.7	4.5±1.2	4.2±1.1	5.1±0.9	5.9±1.0	7.3±1.0
RCP8.5 - end	7.9±1.2	7.5±1.1	6.2±0.8	4.3±0.6	3.1±0.4	2.6±0.4	3.1±0.6	4.0±1.3	4.2±0.8	4.7±0.9	5.3±0.7	7.0±0.8
Mean Wave Period (s)												
Hindcast	12±2	12±2	11±2	10±2	10±2	10±2	9±2	9±2	9±2	10±2	11±2	12±2
RCP4.5 - mid	12±2	12±2	11±2	10±2	10±2	10±2	9±2	10±2	10±2	10±2	11±2	12±2
RCP8.5 - mid	12±2	12±2	11±2	10±2	10±2	10±2	10±2	10±2	10±2	10±2	11±2	12±2
RCP4.5 - end	12±2	12±2	11±2	10±2	9.8±2	9.7±2	9.6±2	9.6±2	9.4±2	9.9±2	11±2	12±2
RCP8.5 - end	12±2	12±2	11±2	10±2	10±2	10±2	10±2	10±2	10±2	10±2	11±2	12±2
Top 5 percent Wave Period (s)												
Hindcast	14±2	14±1	14±2	12±2	10±2	10±1	10±1	10±2	10±1	11±2	14±2	14±2
RCP4.5 - mid	15±1	14±1	14±2	12±2	11±2	9±2	10±2	10±2	10±2	11±2	13±2	14±2
RCP8.5 - mid	14±2	14±2	14±2	12±2	10±2	10±2	10±1	11±2	10±1	11±2	13±2	14±2
RCP4.5 - end	15±2	15±1	13±2	13±2	11±2	10±2	10±2	11±2	10±2	11±2	13±2	14±2
RCP8.5 - end	15±2	14±1	14±2	12±2	11±2	10±2	10±2	11±2	11±2	11±2	13±2	15±2
Mean Wave Direction (°)												
Hindcast	313±44	310±49	330±67	34±71	79±64	110±39	109±23	108±34	82±48	49±53	359±61	326±54
RCP4.5 - mid	311±40	311±47	331±64	39±70	71±71	110±47	111±24	111±28	87±46	56±50	8±60	325±51
RCP8.5 - mid	314±46	314±49	326±60	22±75	70±70	109±51	111±27	113±35	84±50	58±49	11±55	326±50
RCP4.5 - end	310±38	312±47	331±62	18±72	69±72	110±48	113±28	113±30	87±46	61±49	12±60	329±52
RCP8.5 - end	311±41	310±43	330±64	32±72	75±68	113±45	113±27	116±32	93±46	62±48	19±56	330±51
Top 5 percent Wave Direction (°)												
Hindcast	302±19	300±16	310±29	349±61	40±64	98±37	109±29	120±60	81±51	38±53	329±39	308±25
RCP4.5 - mid	303±21	301±13	308±27	6±68	22±63	100±58	113±40	118±44	83±53	59±59	341±52	310±28
RCP8.5 - mid	306±36	302±17	307±33	342±55	36±56	98±51	111±39	137±71	73±49	56±49	347±50	308±26
RCP4.5 - end	301±17	302±25	311±40	332±52	35±75	100±53	121±48	133±54	86±61	56±53	335±54	315±29
RCP8.5 - end	301±12	303±20	307±20	353±60	14±63	97±47	110±40	155±72	95±69	59±51	357±51	315±22

Appendix A8. Table showing return values of ensemble-average significant wave heights of hindcast and forecast scenarios, including lower and higher 95 percent confidence intervals, at the Midway location.

[Years: Hindcast = 1976–2005; RCP mid = 2026–2045; RCP end = 2081–2100. Wave height values are in meters]

Scenario	Hindcast			RCP4.5 - mid			RCP8.5 - mid			RCP4.5 - end			RCP8.5 - end		
	Low	R_v	High	Low	R_v	High	Low	R_v	High	Low	R_v	High	Low	R_v	High
2-year	10.33	11.17	12.46	10.03	10.93	12.50	9.54	10.49	12.27	10.49	11.57	13.28	9.69	10.84	12.90
5-year	10.85	12.18	14.42	10.26	11.49	13.86	9.81	11.21	14.19	11.00	12.61	15.41	10.10	11.85	15.41
10-year	11.20	12.95	16.12	10.37	11.82	14.84	9.96	11.70	15.79	11.32	13.34	17.11	10.35	12.58	17.58
20-year	11.52	13.72	18.02	10.45	12.10	15.77	10.08	12.15	17.54	11.58	14.02	18.91	10.55	13.29	20.02
50-year	11.88	14.74	20.89	10.53	12.39	16.93	10.20	12.70	20.08	11.86	14.86	21.42	10.77	14.18	23.72
100-year	12.13	15.52	23.37	10.56	12.56	17.76	10.26	13.07	22.21	12.03	15.45	23.43	10.90	14.83	26.93

Appendix A9. Table showing Chuuk monthly means and mean of the top 5 percent for significant wave height, peak wave period, and peak wave direction.

[Years: Hindcast = 1976–2005; RCP mid = 2026–2045; RCP end = 2081–2100. Wave directions are "coming from"]

Month	Jan	Feb	Mar	Apr	May	Jun	July	Aug	Sep	Oct	Nov	Dec
Mean Wave Height (m)												
Hindcast	2.7±0.6	2.6±0.6	2.5±0.6	2.1±0.6	1.6±0.5	1.4±0.5	1.4±0.6	1.3±0.6	1.3±0.6	1.6±0.6	2.1±0.7	2.6±0.7
RCP4.5 - mid	2.7±0.7	2.6±0.6	2.5±0.6	2.1±0.6	1.6±0.5	1.4±0.5	1.4±0.6	1.3±0.6	1.3±0.5	1.5±0.5	2.0±0.6	2.5±0.7
RCP8.5 - mid	2.6±0.6	2.6±0.7	2.4±0.6	2.1±0.5	1.6±0.5	1.4±0.5	1.4±0.5	1.3±0.6	1.3±0.5	1.5±0.5	2.0±0.7	2.5±0.7
RCP4.5 - end	2.6±0.6	2.6±0.6	2.4±0.6	2.0±0.5	1.6±0.5	1.4±0.6	1.4±0.6	1.4±0.6	1.3±0.6	1.5±0.6	1.9±0.6	2.4±0.7
RCP8.5 - end	2.5±0.6	2.4±0.6	2.3±0.6	2.0±0.5	1.6±0.5	1.4±0.5	1.4±0.6	1.3±0.6	1.3±0.6	1.4±0.5	1.8±0.6	2.3±0.6
Top 5 percent Wave Height (m)												
Hindcast	4.2±0.4	4.1±0.5	4.0±0.6	3.6±0.5	2.9±0.5	2.9±0.7	2.9±0.7	3.2±0.9	3.1±0.6	3.4±0.5	4.1±0.6	4.3±0.6
RCP4.5 - mid	4.3±0.5	4.0±0.4	3.9±0.4	3.5±0.5	2.9±0.6	2.6±0.5	3.1±0.7	3.3±1.0	3.0±0.8	3.0±0.5	3.6±0.5	4.3±0.4
RCP8.5 - mid	4.1±0.4	4.3±0.6	3.9±0.5	3.4±0.4	2.8±0.5	2.8±0.7	2.9±0.7	3.2±0.8	2.9±0.8	3.0±0.5	3.9±0.6	4.4±0.6
RCP4.5 - end	3.9±0.3	4.1±0.5	3.9±0.5	3.3±0.4	2.7±0.3	3.0±0.7	3.1±0.7	3.2±0.6	3.1±0.7	3.1±0.5	3.6±0.6	4.1±0.5
RCP8.5 - end	3.9±0.4	3.9±0.5	3.7±0.4	3.2±0.4	2.8±0.4	2.7±0.5	3.1±0.9	3.2±0.7	3.1±0.9	2.9±0.8	3.6±0.5	3.9±0.5
Mean Wave Period (s)												
Hindcast	10±2	10±2	9±2	9±1	9±1	9±1	9±1	9±1	9±1	10±1	10±2	10±2
RCP4.5 - mid	10±2	10±2	9±2	9±1	9±1	9±1	9±1	9±1	9±1	9±1	10±1	10±2
RCP8.5 - mid	10±2	10±2	9±2	9±1	9±1	8±1	9±1	9±1	9±1	10±1	10±2	10±2
RCP4.5 - end	10±2	10±2	9±2	9±1	9±1	9±1	9±1	9±1	9±1	10±1	10±2	10±2
RCP8.5 - end	10±2	9±2	9±2	9±1	8±1	8±1	9±1	9±1	9±1	9±1	10±1	10±2
Top 5 percent Wave Period (s)												
Hindcast	11±1	11±2	11±1	10±1	9±1	9±1	9±2	9±2	9±2	11±2	11±1	11±1
RCP4.5 - mid	10±1	10±1	10±1	10±1	9±1	9±1	9±1	9±1	9±2	10±2	11±2	11±1
RCP8.5 - mid	10±2	10±1	10±0.9	10±1	9±1	9±1	9±2	9±2	9±2	10±2	11±2	10±1
RCP4.5 - end	10±1	11±2	10±1	10±1	9±0.8	9±1	9±2	9±2	9±2	10±2	11±2	10±0.9
RCP8.5 - end	10±1	10±1	10±1	9±0.8	9±0.8	9±1	8±1	9±2	9±2	10±2	10±1	10±0.9
Mean Wave Direction (°)												
Hindcast	54±14	53±16	55±17	60±16	66±22	76±30	87±43	103±51	80±48	51±38	50±26	54±16
RCP4.5 - mid	53±18	53±16	56±14	60±12	66±18	78±25	94±45	109±49	93±47	55±42	49±24	53±21
RCP8.5 - mid	53±15	54±15	56±16	60±15	67±17	78±29	92±46	110±54	94±52	54±40	51±22	54±17
RCP4.5 - end	53±15	51±17	56±14	59±15	66±17	77±28	91±50	108±53	93±51	54±43	50±23	54±18
RCP8.5 - end	52±17	53±17	56±14	62±11	68±14	80±27	91±44	110±48	101±50	61±38	53±21	55±17
Top 5 percent Wave Direction (°)												
Hindcast	54±13	52±20	48±34	54±34	62±58	95±101	220±102	216±52	258±90	32±85	54±52	58±13
RCP4.5 - mid	56±23	57±18	55±21	55±25	67±43	82±64	212±69	212±52	228±61	306±111	46±53	59±44
RCP8.5 - mid	56±12	54±13	52±25	57±18	66±46	128±85	222±80	221±53	226±47	324±98	51±57	63±31
RCP4.5 - end	55±12	49±33	56±17	57±29	68±44	96±96	232±52	229±41	245±51	298±104	51±54	60±30
RCP8.5 - end	53±22	57±20	53±28	63±17	68±38	93±68	204±84	219±47	219±59	343103	63±49	62±31

Appendix A10. Table showing return values of ensemble-average significant wave heights of hindcast and forecast scenarios, including lower and higher 95 percent confidence intervals, at the Chuuk location.

[Years: Hindcast = 1976–2005; RCP mid = 2026–2045; RCP end = 2081–2100. Wave height values are in meters]

Scenario	Hindcast			RCP4.5 - mid			RCP8.5 - mid			RCP4.5 - end			RCP8.5 - end		
	Low	R_v	High	Low	R_v	High	Low	R_v	High	Low	R_v	High	Low	R_v	High
2-year	5.56	6.25	7.41	5.38	6.03	7.19	5.46	6.34	8.08	5.06	5.70	6.94	5.15	5.94	7.53
5-year	5.95	7.12	9.34	5.59	6.55	8.47	5.72	7.09	10.24	5.32	6.39	8.81	5.45	6.80	10.05
10-year	6.23	7.84	11.23	5.71	6.91	9.52	5.88	7.66	12.24	5.49	6.96	10.71	5.66	7.55	12.73
20-year	6.50	8.63	13.58	5.81	7.24	10.64	6.02	8.22	14.63	5.65	7.59	13.16	5.85	8.39	16.36
50-year	6.83	9.78	17.61	5.91	7.63	12.23	6.16	8.96	18.51	5.84	8.49	17.54	6.09	9.66	23.17
100-year	7.06	10.75	21.55	5.96	7.90	13.54	6.24	9.51	22.11	5.97	9.25	22.00	6.26	10.76	30.45

Appendix A11. Table showing Saipan monthly means and mean of the top 5 percent for significant wave height, peak wave period, and peak wave direction.

[Years: Hindcast = 1976–2005; RCP mid = 2026–2045; RCP end = 2081–2100. Wave directions are "coming from"]

Month	Jan	Feb	Mar	Apr	May	Jun	July	Aug	Sep	Oct	Nov	Dec
Mean Wave Height (m)												
Hindcast	2.7±0.7	2.6±0.7	2.5±0.7	2.2±0.6	1.8±0.6	1.7±0.7	1.7±0.9	1.7±1.0	1.7±0.8	2.1±0.9	2.6±0.9	2.8±0.7
RCP4.5 - mid	2.7±0.7	2.6±0.6	2.5±0.7	2.2±0.6	1.8±0.6	1.7±0.6	1.7±0.9	1.6±0.8	1.6±0.9	1.9±0.7	2.5±0.8	2.7±0.8
RCP8.5 - mid	2.6±0.7	2.6±0.7	2.4±0.7	2.2±0.6	1.8±0.6	1.8±0.8	1.7±0.9	1.7±1.0	1.6±0.9	1.9±0.7	2.4±0.8	2.8±0.7
RCP4.5 - end	2.6±0.7	2.6±0.7	2.5±0.7	2.2±0.6	1.8±0.5	1.7±0.6	1.7±0.9	1.7±0.9	1.6±0.7	1.9±0.8	2.5±0.8	2.6±0.7
RCP8.5 - end	2.5±0.7	2.4±0.7	2.3±0.6	2.1±0.5	1.8±0.5	1.7±0.6	1.8±0.8	1.6±1.0	1.6±0.8	1.8±0.7	2.3±0.8	2.6±0.7
Top 5 percent Wave Height (m)												
Hindcast	4.3±0.4	4.3±0.4	4.4±0.8	3.9±0.6	3.5±0.8	3.5±0.9	4.5±1.0	4.9±1.3	4.3±1.0	4.6±0.9	5.0±1.0	4.6±0.7
RCP4.5 - mid	4.3±0.4	4.2±0.4	4.2±0.6	3.8±1.0	3.3±0.6	3.4±1.0	4.4±1.0	4.1±0.9	4.5±1.3	3.9±0.7	4.5±0.8	4.8±0.8
RCP8.5 - mid	4.3±0.5	4.3±0.5	4.2±0.6	3.7±0.4	3.2±0.5	4.2±1.4	4.5±1.0	4.7±1.1	4.4±1.3	4.0±0.8	4.7±1.0	4.8±0.7
RCP4.5 - end	4.2±0.4	4.4±0.5	4.2±0.4	3.7±0.4	2.9±0.4	3.4±1.0	4.5±1.2	4.7±1.1	3.9±0.8	4.0±0.9	4.6±0.9	4.4±0.6
RCP8.5 - end	4.3±0.4	4.1±0.4	3.9±0.6	3.4±0.4	3.1±0.5	3.4±1.2	4.3±0.9	4.7±1.3	4.3±0.9	3.8±0.8	4.5±0.7	4.4±0.7
Mean Wave Period (s)												
Hindcast	10±2	10±2	9±1	9±1	9±1	9±1	9±1	9±1	9±1	10±1	10±1	10±2
RCP4.5 - mid	10±2	10±2	9±1	9±1	9±1	8±1	9±1	9±1	9±1	9±1	10±1	10±2
RCP8.5 - mid	10±2	10±2	9±1	9±1	9±1	9±1	9±1	9±1	9±2	9±1	10±1	10±2
RCP4.5 - end	10±2	10±2	9±1	9±1	9±1	9±1	9±1	9±1	9±1	9±2	10±2	10±2
RCP8.5 - end	10±2	9±2	9±1	9±1	9±1	8±1	9±1	9±1	9±1	9±1	9±1	9±1
Top 5 percent Wave Period (s)												
Hindcast	10±1	10±2	10±1	10±1	10±1	9±1	10±2	10±1	10±1	11±1	11±1	11±1
RCP4.5 - mid	10±1	10±1	10±1	10±1	9±0.9	9±1	10±1	10±1	10±1	11±1	11±1	11±1
RCP8.5 - mid	10±2	10±1	10±1	10±1	10±0.9	10±1	10±1	10±1	10±1	11±1	11±1	11±1
RCP4.5 - end	10±2	10±2	10±1	10±1	9±1	10±1	10±1	10±1	10±1	11±2	11±1	10±1
RCP8.5 - end	10±1	9±1	10±1	10±0.9	9±0.8	9±1	10±1	10±1	10±1	11±1	11±1	10±1
Mean Wave Direction (°)												
Hindcast	64±23	61±23	69±20	76±13	81±15	85±24	92±50	102±68	75±59	66±35	72±23	70±21
RCP4.5 - mid	64±24	63±22	69±18	75±11	80±13	87±22	94±43	98±72	77±65	63±41	69±22	69±21
RCP8.5 - mid	64±23	64±22	70±18	75±14	81±10	89±26	93±47	111±72	77±73	63±37	70±21	70±22
RCP4.5 - end	64±24	62±23	69±17	75±13	81±12	87±20	95±49	108±69	78±72	63±37	70±19	70±18
RCP8.5 - end	63±24	63±23	68±17	76±12	82±11	89±24	93±43	107±61	83±73	65±41	71±18	70±19
Top 5 percent Wave Direction (°)												
Hindcast	63±18	57±27	67±23	72±19	85±28	108±68	204±64	205±55	194±93	81±53	81±40	75±25
RCP4.5 - mid	64±23	64±14	69±19	73±11	81±22	111±52	205±76	218±60	218±84	69±75	74±34	70±25
RCP8.5 - mid	62±18	64±16	68±15	73±13	82±14	128±63	210±64	224±45	229±52	83±63	82±35	77±21
RCP4.5 - end	66±16	54±26	66±15	71±11	82±17	103±55	193±76	224±53	235±67	78±70	76±35	73±21
RCP8.5 - end	65±18	66±16	68±14	74±11	82±12	112±50	202±73	213±53	209±68	76±70	82±28	78±23

Appendix A12. Table showing return values of ensemble-average significant wave heights of hindcast and forecast scenarios, including lower and higher 95 percent confidence intervals, at the Saipan location.

[Years: Hindcast = 1976–2005; RCP mid = 2026–2045; RCP end = 2081–2100. Wave height values are in meters]

Scenario	Hindcast			RCP4.5 - mid			RCP8.5 - mid			RCP4.5 - end			RCP8.5 - end		
	Low	R_v	High	Low	R_v	High	Low	R_v	High	Low	R_v	High	Low	R_v	High
2-year	7.39	8.27	9.59	6.95	8.04	9.89	7.06	8.17	10.12	6.70	7.81	9.86	6.90	7.96	9.74
5-year	7.90	9.22	11.32	7.45	9.14	12.34	7.50	9.21	12.59	7.04	8.71	12.18	7.36	8.97	11.98
10-year	8.22	9.86	12.64	7.77	9.96	14.46	7.77	9.98	14.76	7.24	9.33	14.15	7.65	9.70	13.87
20-year	8.48	10.46	13.99	8.04	10.77	16.86	8.00	10.73	17.22	7.40	9.92	16.31	7.89	10.41	15.94
50-year	8.76	11.17	15.79	8.34	11.83	20.50	8.26	11.70	20.97	7.57	10.64	19.52	8.15	11.30	18.99
100-year	8.93	11.65	17.17	8.54	12.61	23.66	8.41	12.42	24.26	7.66	11.14	22.24	8.31	11.95	21.57

Appendix A13. Table showing Asuncion monthly means and mean of the top 5 percent for significant wave height, peak wave period, and peak wave direction.

[Years: Hindcast = 1976–2005; RCP mid = 2026–2045; RCP end = 2081–2100. Wave directions are "coming from"]

Month	Jan	Feb	Mar	Apr	May	Jun	July	Aug	Sep	Oct	Nov	Dec
Mean Wave Height (m)												
Hindcast	2.5±0.6	2.4±0.7	2.3±0.7	2.0±0.6	1.7±0.6	1.7±0.7	1.9±1.0	1.9±1.0	1.9±0.9	2.2±0.9	2.5±0.8	2.6±0.7
RCP4.5 - mid	2.5±0.6	2.4±0.7	2.3±0.7	2.1±0.6	1.7±0.5	1.7±0.6	1.8±0.9	1.7±0.8	1.8±1.0	2.1±0.8	2.5±0.8	2.5±0.8
RCP8.5 - mid	2.5±0.7	2.4±0.7	2.2±0.6	2.0±0.6	1.7±0.5	1.7±0.8	1.8±1.0	1.8±1.0	1.8±1.0	2.1±0.8	2.5±0.9	2.6±0.7
RCP4.5 - end	2.4±0.6	2.4±0.7	2.3±0.7	2.0±0.6	1.7±0.5	1.7±0.6	1.8±0.9	1.8±1.0	1.7±0.8	2.1±0.9	2.5±0.8	2.5±0.7
RCP8.5 - end	2.4±0.7	2.3±0.6	2.1±0.6	1.9±0.5	1.6±0.5	1.6±0.6	1.8±0.9	1.8±1.0	1.8±0.9	2.0±0.8	2.3±0.7	2.4±0.7
Top 5 percent Wave Height (m)												
Hindcast	4.0±0.4	4.2±0.4	4.1±0.8	3.7±0.5	3.3±0.7	3.8±1.0	5.0±1.3	5.2±1.3	4.5±1.0	4.9±1.0	4.9±0.9	4.3±0.6
RCP4.5 - mid	4.1±0.4	4.0±0.3	4.0±0.5	3.7±0.9	3.1±0.4	3.5±1.1	4.8±1.1	4.4±1.1	4.9±1.5	4.3±0.8	4.7±0.7	4.7±0.6
RCP8.5 - mid	4.2±0.5	4.1±0.4	3.8±0.3	3.6±0.4	3.0±0.5	4.1±1.4	4.9±1.3	4.9±1.1	5.0±1.5	4.5±1.0	4.7±1.6	4.5±0.5
RCP4.5 - end	4.0±0.4	4.2±0.6	3.9±0.4	3.5±0.5	2.8±0.4	3.6±1.0	4.7±1.4	4.9±1.3	4.2±0.9	4.7±1.0	4.6±0.7	4.1±0.5
RCP8.5 - end	4.1±0.4	3.8±0.4	3.6±0.4	3.3±0.4	2.8±0.4	3.5±1.1	4.9±1.1	4.9±1.1	4.8±1.2	4.3±1.0	4.3±0.7	4.2±0.4
Mean Wave Period (s)												
Hindcast	10±2	10±2	10±1	9±1	9±1	9±1	9±1	9±1	9±1	10±1	10±1	10±2
RCP4.5 - mid	10±2	10±2	10±2	9±1	9±1	9±1	9±1	9±1	9±1	9±1	10±1	10±2
RCP8.5 - mid	10±2	10±2	10±1	9±1	9±1	9±1	9±1	9±1	9±2	9±1	10±1	10±2
RCP4.5 - end	10±2	10±2	10±1	9±1	9±1	9±1	9±1	9±1	9±1	9±1	10±1	10±2
RCP8.5 - end	10±2	10±2	9±1	9±1	9±1	9±1	9±1	9±1	9±2	9±1	9±1	10±1
Top 5 percent Wave Period (s)												
Hindcast	11±2	11±2	10±2	10±1	10±1	10±1	11±1	11±1	11±1	11±1	11±2	11±2
RCP4.5 - mid	11±2	11±2	11±2	10±1	9±1	10±1	11±1	11±1	11±1	11±2	11±1	11±2
RCP8.5 - mid	11±2	11±2	10±2	10±2	10±1	10±1	11±1	11±1	11±2	11±1	11±1	11±2
RCP4.5 - end	11±2	11±2	10±2	10±1	9±1	10±1	11±2	11±1	11±1	11±1	11±1	11±2
RCP8.5 - end	10±2	10±2	10±2	9±1	9±0.9	10±1	11±1	11±1	11±1	11±1	11±1	10±1
Mean Wave Direction (°)												
Hindcast	52±38	49±39	65±32	80±19	88±19	94±22	101±39	104±50	86±41	75±30	75±26	67±32
RCP4.5 - mid	55±37	52±37	65±30	79±18	87±19	97±22	101±35	101±52	87±44	75±34	74±26	65±33
RCP8.5 - mid	53±38	55±38	66±32	78±22	89±17	99±25	103±37	108±55	88±53	73±31	75±24	67±33
RCP4.5 - end	51±39	51±37	66±29	78±21	88±19	97±19	104±40	107±52	87±48	73±32	74±24	68±29
RCP8.5 - end	54±37	53±38	64±29	79±20	89±17	99±22	104±37	109±46	94±54	75±31	77±22	68±31
Top 5 percent Wave Direction (°)												
Hindcast	36±45	25±46	61±32	74±20	93±29	112±47	160±64	174±60	125±76	86±46	77±39	65±41
RCP4.5 - mid	36±48	42±39	63±32	74±16	84±24	124±45	152±72	186±87	141±82	83±55	76±35	67±36
RCP8.5 - mid	42±45	52±41	67±30	72±19	90±16	135±55	176±62	203±62	177±84	87±55	84±37	70±37
RCP4.5 - end	50±42	36±43	55±31	74±21	82±24	111±42	163±66	187±76	139±86	84±63	72±32	65±29
RCP8.5 - end	45±47	49±43	62±29	73±20	84±13	117±48	169±69	184±61	173±82	88±57	85±34	73±37

Appendix A14. Table showing return values of ensemble-average significant wave heights of hindcast and forecast scenarios, including lower and higher 95 percent confidence intervals, at the Asuncion location.

[Years: Hindcast = 1976–2005; RCP mid = 2026–2045; RCP end = 2081–2100. Wave height values are in meters]

Scenario	Hindcast			RCP4.5 - mid			RCP8.5 - mid			RCP4.5 - end			RCP8.5 - end		
	Low	R_v	High	Low	R_v	High	Low	R_v	High	Low	R_v	High	Low	R_v	High
2-year	7.86	8.86	10.32	7.29	8.62	10.93	7.58	9.11	11.79	7.01	8.31	10.64	7.05	8.29	10.41
5-year	8.37	9.79	12.02	7.81	9.83	13.74	8.22	10.62	15.36	7.45	9.39	13.32	7.48	9.28	12.67
10-year	8.67	10.39	13.23	8.12	10.69	16.11	8.63	11.77	18.53	7.70	10.15	15.58	7.72	9.93	14.43
20-year	8.89	10.90	14.39	8.38	11.52	18.73	8.99	12.91	22.20	7.91	10.86	18.07	7.91	10.51	16.23
50-year	9.12	11.47	15.83	8.66	12.55	22.59	9.39	14.42	27.92	8.12	11.74	21.73	8.10	11.18	18.69
100-year	9.25	11.84	16.86	8.83	13.29	25.85	9.65	15.56	33.02	8.25	12.36	24.81	8.20	11.63	20.61

Appendix A15. Table showing Kosrae monthly means and mean of the top 5 percent for significant wave height, peak wave period, and peak wave direction.

[Years: Hindcast = 1976–2005; RCP mid = 2026–2045; RCP end = 2081–2100. Wave directions are "coming from"]

Month	Jan	Feb	Mar	Apr	May	Jun	July	Aug	Sep	Oct	Nov	Dec
Mean Wave Height (m)												
Hindcast	2.3±0.5	2.3±0.5	2.1±0.5	1.7±0.5	1.4±0.4	1.3±0.4	1.3±0.4	1.3±0.4	1.3±0.5	1.4±0.5	1.7±0.6	2.1±0.7
RCP4.5 - mid	2.3±0.5	2.2±0.5	2.1±0.5	1.7±0.5	1.4±0.4	1.3±0.4	1.4±0.4	1.3±0.5	1.3±0.4	1.3±0.4	1.6±0.5	2.0±0.6
RCP8.5 - mid	2.2±0.5	2.3±0.6	2.1±0.5	1.8±0.5	1.4±0.5	1.3±0.4	1.4±0.4	1.4±0.5	1.3±0.4	1.3±0.4	1.6±0.5	2.0±0.6
RCP4.5 - end	2.2±0.5	2.2±0.5	2.1±0.5	1.7±0.5	1.4±0.4	1.3±0.5	1.3±0.4	1.4±0.5	1.3±0.5	1.3±0.5	1.6±0.5	2.0±0.6
RCP8.5 - end	2.1±0.5	2.1±0.5	2.0±0.5	1.7±0.5	1.4±0.5	1.3±0.5	1.4±0.4	1.4±0.5	1.3±0.4	1.3±0.4	1.4±0.5	1.9±0.5
Top 5 percent Wave Height (m)												
Hindcast	3.6±0.4	3.5±0.3	3.5±0.4	3.1±0.5	2.5±0.6	2.4±0.4	2.5±0.8	2.6±0.7	2.7±0.6	2.8±0.6	3.3±0.5	3.8±0.5
RCP4.5 - mid	3.5±0.4	3.5±0.5	3.3±0.4	3.0±0.3	2.5±0.3	2.5±0.5	2.5±0.5	2.7±0.7	2.4±0.4	2.6±0.6	3.0±0.5	3.7±0.4
RCP8.5 - mid	3.5±0.3	3.8±0.5	3.4±0.4	3.2±0.6	2.7±0.6	2.4±0.3	2.5±0.5	2.8±0.6	2.5±0.6	2.6±0.6	3.1±0.4	3.5±0.4
RCP4.5 - end	3.4±0.3	3.4±0.3	3.3±0.3	2.8±0.3	2.4±0.2	2.6±0.7	2.6±0.7	2.8±0.6	2.7±0.6	2.6±0.5	3.0±0.6	3.6±0.4
RCP8.5 - end	3.2±0.2	3.3±0.4	3.2±0.3	2.8±0.3	2.7±0.4	2.6±0.5	2.5±0.6	2.9±0.9	2.4±0.5	2.3±0.4	2.9±0.6	3.2±0.3
Mean Wave Period (s)												
Hindcast	10±2	10±2	10±2	9±2	9±2	9±2	9±2	9±2	9±2	10±2	10±2	10±2
RCP4.5 - mid	10±2	10±2	10±2	9±2	9±2	9±2	9±2	9±2	9±2	10±2	10±2	10±2
RCP8.5 - mid	10±2	10±2	10±2	9±2	9±2	9±2	9±2	9±2	9±2	10±2	10±2	10±2
RCP4.5 - end	10±2	10±2	9.8±2	9.5±2	9.2±2	9.1±2	9.2±2	9.3±2	9.1±1	9.6±2	10±2	10±2
RCP8.5 - end	10±2	10±2	10±2	9±2	9±1	9±2	9±1	9±2	9±2	9±2	10±2	10±2
Top 5 percent Wave Period (s)												
Hindcast	10±2	10±2	10±2	9±2	9±1	9±2	9±2	9±2	9±2	9±2	10±2	10±1
RCP4.5 - mid	10±2	10±2	10±2	9±1	9±1	8±2	9±2	9±2	10±2	9±2	10±2	10±2
RCP8.5 - mid	10±2	10±1	9±1	9±1	8±1	9±2	9±2	9±2	9±2	9±2	10±2	9±1
RCP4.5 - end	10±2	10±2	10±1	9±1	8±1	9±1	9±2	9±1	9±2	9±2	10±2	9±1
RCP8.5 - end	10±3	9±2	9±2	9±1	8±0.9	8±1	9±2	9±2	9±2	9±2	9±2	9±2
Mean Wave Direction (°)												
Hindcast	45±18	45±19	50±20	61±23	82±29	104±32	118±33	128±38	117±45	79±49	48±32	44±20
RCP4.5 - mid	45±21	45±19	50±17	61±21	80±27	101±27	119±35	128±36	125±35	90±48	53±34	45±26
RCP8.5 - mid	45±19	47±20	50±21	59±22	79±28	102±30	120±36	134±40	127±42	90±45	51±31	45±21
RCP4.5 - end	44±20	43±22	50±18	61±22	78±25	102±29	119±38	131±42	127±41	87±52	50±34	46±23
RCP8.5 - end	44±21	46±20	51±19	61±16	79±24	101±29	115±37	129±35	124±37	95±43	58±30	48±22
Top 5 percent Wave Direction (°)												
Hindcast	49±15	46±17	44±30	53±45	77±68	102±77	181±87	200±66	235±76	264±108	39±68	51±21
RCP4.5 - mid	49±21	48±21	53±15	57±36	69±57	94±63	164±78	202±68	197±68	219±110	48±62	47±41
RCP8.5 - mid	52±18	52±27	54±31	50±45	71±66	103±70	193±80	211±52	223±67	248±91	28±64	52±27
RCP4.5 - end	45±15	45±25	52±27	59±41	66±19	114±65	210±75	222±68	235±58	258±88	352±84	54±34
RCP8.5 - end	46±20	53±15	53±38	61±26	71±51	100±71	163±83	210±59	182±82	19±126	51±52	51±14

Appendix A16. Table showing return values of ensemble-average significant wave heights of hindcast and forecast scenarios, including lower and higher 95 percent confidence intervals, at the Kosrae location.

[Years: Hindcast = 1976–2005; RCP mid = 2026–2045; RCP end = 2081–2100. Wave height values are in meters]

Scenario	Hindcast			RCP4.5 - mid			RCP8.5 - mid			RCP4.5 - end			RCP8.5 - end		
	Low	R_v	High	Low	R_v	High	Low	R_v	High	Low	R_v	High	Low	R_v	High
2-year	4.82	5.41	6.36	4.54	5.12	6.17	4.51	5.07	6.13	4.61	5.16	6.08	4.25	4.90	6.20
5-year	5.22	6.22	8.07	4.79	5.75	7.73	4.74	5.67	7.70	4.89	5.76	7.39	4.51	5.64	8.30
10-year	5.50	6.92	9.75	4.97	6.26	9.24	4.89	6.16	9.23	5.08	6.23	8.55	4.69	6.29	10.54
20-year	5.79	7.70	11.86	5.13	6.80	11.10	5.04	6.68	11.17	5.24	6.70	9.90	4.87	7.01	13.56
50-year	6.16	8.85	15.51	5.31	7.57	14.27	5.20	7.43	14.51	5.43	7.34	12.01	5.09	8.12	19.25
100-year	6.43	9.84	19.11	5.44	8.19	17.33	5.31	8.03	17.81	5.56	7.83	13.89	5.24	9.09	25.33

Appendix A17. Table showing Palau monthly means and mean of the top 5 percent for significant wave height, peak wave period, and peak wave direction.

[Years: Hindcast = 1976–2005; RCP mid = 2026–2045; RCP end = 2081–2100. Wave directions are "coming from"]

Month	Jan	Feb	Mar	Apr	May	Jun	July	Aug	Sep	Oct	Nov	Dec
Mean Wave Height (m)												
Hindcast	2.5±0.7	2.5±0.7	2.2±0.6	1.7±0.5	1.2±0.5	1.0±0.5	1.0±0.5	1.0±0.6	1.1±0.6	1.4±0.6	1.9±0.7	2.3±0.7
RCP4.5 - mid	2.4±0.6	2.4±0.6	2.2±0.6	1.8±0.5	1.2±0.5	1.0±0.5	1.1±0.6	0.98±0.5	1.0±0.5	1.3±0.6	1.7±0.6	2.2±0.7
RCP8.5 - mid	2.4±0.7	2.4±0.6	2.2±0.6	1.7±0.5	1.2±0.4	1.0±0.5	1.0±0.5	1.0±0.6	1.0±0.5	1.3±0.6	1.7±0.6	2.2±0.7
RCP4.5 - end	2.4±0.7	2.4±0.6	2.2±0.6	1.7±0.5	1.2±0.4	1.0±0.5	1.1±0.5	1.0±0.6	1.0±0.6	1.3±0.6	1.7±0.6	2.1±0.7
RCP8.5 - end	2.3±0.6	2.3±0.6	2.0±0.6	1.6±0.4	1.2±0.5	1.0±0.5	1.1±0.5	1.0±0.6	1.0±0.6	1.2±0.5	1.6±0.6	2.0±0.6
Top 5 percent Wave Height (m)												
Hindcast	4.3±0.5	4.5±0.6	3.9±0.6	3.0±0.4	2.4±0.4	2.4±0.6	2.7±0.5	3.0±0.7	3.1±0.6	3.3±0.6	4.0±0.8	4.1±0.6
RCP4.5 - mid	4.1±0.4	4.0±0.6	3.8±0.6	3.0±0.4	2.3±0.5	2.3±0.6	3.0±0.6	2.5±0.7	2.6±0.7	3.3±0.7	3.5±0.7	4.1±0.6
RCP8.5 - mid	4.2±0.4	4.0±0.4	3.8±0.5	3.0±0.6	2.3±0.4	2.6±0.9	2.7±0.6	2.8±0.7	2.8±0.8	2.9±0.5	3.3±0.4	4.1±0.6
RCP4.5 - end	4.2±0.5	4.0±0.5	3.6±0.6	2.9±0.4	2.3±0.4	2.4±0.6	2.8±0.7	3.0±0.7	3.0±0.7	3.1±0.7	3.3±0.4	3.9±0.5
RCP8.5 - end	4.0±0.5	4.0±0.5	3.5±0.3	2.7±0.3	2.3±0.3	2.3±0.6	2.7±0.7	3.0±0.8	2.9±0.9	2.6±0.5	3.4±0.7	3.8±0.5
Mean Wave Period (s)												
Hindcast	9±1	9±1	9±1	9±1	9±1	9±1	9±1	9±1	9±1	10±2	10±1	10±1
RCP4.5 - mid	10±1	9±1	9±1	9±1	9±1	8±1	9±1	9±1	9±1	9±1	10±1	10±1
RCP8.5 - mid	9±1	9±2	9±1	9±1	9±1	8±1	9±1	9±1	9±2	10±2	10±2	10±2
RCP4.5 - end	9±1	9±1	9±1	9±1	9±1	8±1	8±1	9±1	9±1	10±2	10±2	10±1
RCP8.5 - end	9±1	9±1	9±1	9±1	8±1	8±1	9±1	8±1	9±2	9±1	10±1	9±1
Top 5 percent Wave Period (s)												
Hindcast	10±1	10±1	10±1	10±1	9±1	8±1	8±1	8±1	9±2	10±2	11±2	11±2
RCP4.5 - mid	10±0.8	10±0.9	10±1	10±1	9±1	7±1	8±1	8±1	9±2	9±2	10±2	10±1
RCP8.5 - mid	10±0.9	10±1	10±0.9	10±1	9±1	8±1	8±1	8±1	8±2	9±2	10±2	10±1
RCP4.5 - end	10±1	10±2	10±0.9	9±1	8±1	8±1	8±1	8±1	8±2	10±2	10±2	10±1
RCP8.5 - end	10±1	10±0.8	9±0.8	9±1	8±1	8±1	8±1	8±1	8±2	10±2	10±2	10±1
Mean Wave Direction (°)												
Hindcast	51±18	51±17	57±16	62±16	66±24	73±35	84±47	94±53	64±52	39±42	43±30	52±21
RCP4.5 - mid	50±19	53±16	57±15	63±14	66±18	76±30	92±51	94±50	79±51	41±46	43±32	48±25
RCP8.5 - mid	52±18	53±17	58±16	62±14	67±17	77±37	88±50	102±54	78±55	40±44	43±31	50±24
RCP4.5 - end	51±19	52±15	57±14	62±16	66±19	76±32	88±53	102±55	81±56	38±44	43±29	51±21
RCP8.5 - end	51±18	53±18	57±15	63±13	68±21	76±35	89±49	104±52	86±55	47±43	46±30	50±23
Top 5 percent Wave Direction (°)												
Hindcast	43±23	35±27	44±23	57±33	63±60	250±109	239±57	235±50	259±48	284±73	350±79	46±37
RCP4.5 - mid	51±23	52±25	52±25	64±30	69±39	168±97	232±42	229±66	239±68	260±75	351±102	43±56
RCP8.5 - mid	49±25	48±27	56±27	57±29	61±44	216±71	233±47	231±33	238±46	278±71	350±81	51±54
RCP4.5 - end	45±38	46±17	51±25	59±41	65±53	169±99	223±50	235±37	244±44	276±76	348±78	48±48
RCP8.5 - end	49±22	46±23	53±29	62±22	73±53	16±100	220±52	226±36	234±46	279±83	349±94	52±47

Appendix A18. Table showing return values of ensemble-average significant wave heights of hindcast and forecast scenarios, including lower and higher 95 percent confidence intervals, at the Palau location.

[Years: Hindcast = 1976–2005; RCP mid = 2026–2045; RCP end = 2081–2100. Wave height values are in meters]

Scenario	Hindcast			RCP4.5 - mid			RCP8.5 - mid			RCP4.5 - end			RCP8.5 - end		
	Low	R_v	High	Low	R_v	High	Low	R_v	High	Low	R_v	High	Low	R_v	High
2-year	5.61	6.16	6.98	5.27	5.85	6.80	5.20	6.01	7.62	5.16	5.74	6.73	5.17	5.75	6.75
5-year	5.96	6.81	8.19	5.50	6.35	7.91	5.44	6.71	9.63	5.41	6.31	8.00	5.38	6.24	7.89
10-year	6.19	7.28	9.19	5.64	6.69	8.79	5.59	7.23	11.51	5.57	6.72	9.08	5.50	6.58	8.82
20-year	6.39	7.75	10.26	5.75	7.01	9.72	5.71	7.75	13.75	5.70	7.12	10.28	5.60	6.89	9.82
50-year	6.62	8.35	11.82	5.86	7.39	11.01	5.84	8.44	17.41	5.85	7.63	12.07	5.70	7.27	11.24
100-year	6.77	8.78	13.10	5.93	7.66	12.04	5.92	8.96	20.82	5.94	8.01	13.59	5.76	7.53	12.39

Appendix A19. Table showing Pohnpei monthly means and mean of the top 5 percent for significant wave height, peak wave period, and peak wave direction.

[Years: Hindcast = 1976–2005; RCP mid = 2026–2045; RCP end = 2081–2100. Wave directions are "coming from"]

Month	Jan	Feb	Mar	Apr	May	Jun	July	Aug	Sep	Oct	Nov	Dec
Mean Wave Height (m)												
Hindcast	2.6±0.6	2.6±0.6	2.4±0.6	2.0±0.6	1.5±0.5	1.4±0.5	1.4±0.5	1.3±0.5	1.4±0.6	1.6±0.6	2.0±0.7	2.5±0.7
RCP4.5 - mid	2.6±0.6	2.5±0.6	2.4±0.6	2.0±0.5	1.6±0.5	1.4±0.5	1.4±0.5	1.3±0.6	1.3±0.5	1.5±0.6	1.9±0.6	2.4±0.7
RCP8.5 - mid	2.6±0.6	2.6±0.7	2.3±0.6	2.0±0.6	1.6±0.5	1.4±0.5	1.4±0.5	1.4±0.6	1.3±0.5	1.4±0.5	1.9±0.6	2.4±0.7
RCP4.5 - end	2.5±0.5	2.5±0.5	2.4±0.6	2.0±0.5	1.6±0.5	1.4±0.6	1.4±0.5	1.4±0.6	1.3±0.6	1.5±0.6	1.8±0.6	2.3±0.7
RCP8.5 - end	2.4±0.5	2.4±0.5	2.2±0.6	1.9±0.5	1.6±0.5	1.4±0.5	1.4±0.5	1.4±0.6	1.3±0.5	1.4±0.5	1.7±0.6	2.2±0.6
Top 5 percent Wave Height (m)												
Hindcast	4.1±0.4	4.0±0.3	3.9±0.4	3.5±0.5	2.8±0.6	2.8±0.7	2.9±0.8	3.0±0.7	3.2±0.8	3.3±0.5	3.8±0.4	4.3±0.6
RCP4.5 - mid	4.0±0.5	3.9±0.3	3.7±0.4	3.4±0.3	2.8±0.4	2.7±0.6	2.9±0.6	3.1±0.9	2.9±0.7	3.1±0.9	3.6±0.6	4.2±0.4
RCP8.5 - mid	3.9±0.4	4.3±0.7	3.8±0.5	3.5±0.6	2.9±0.5	2.6±0.4	2.9±0.6	3.2±0.9	2.8±0.7	3.0±0.5	3.7±0.5	4.1±0.6
RCP4.5 - end	3.8±0.3	3.9±0.4	3.7±0.4	3.2±0.4	2.7±0.3	3.0±0.7	2.9±0.7	3.3±1.0	3.1±0.7	3.1±0.6	3.6±0.6	4.0±0.4
RCP8.5 - end	3.7±0.3	3.7±0.4	3.7±0.6	3.1±0.3	2.9±0.5	2.7±0.5	2.9±0.7	3.3±0.9	2.9±0.9	2.8±0.6	3.5±0.6	3.6±0.3
Mean Wave Period (s)												
Hindcast	10±2	10±2	10±2	9±1	9±1	9±1	9±1	9±1	9±1	10±2	10±2	10±2
RCP4.5 - mid	10±2	10±2	10±2	9±1	9±1	9±1	9±1	9±1	9±1	9±1	10±2	10±2
RCP8.5 - mid	10±2	10±2	9±2	9±1	9±1	9±1	9±1	9±2	9±1	10±1	10±2	10±2
RCP4.5 - end	10±2	9.9±2	9.5±2	9.1±1	8.7±1	8.7±1	8.8±1	9±1	9±1	9.6±1	10±2	10±2
RCP8.5 - end	10±2	10±2	9±2	9±1	9±1	9±1	9±1	9±1	9±1	9±1	10±2	10±2
Top 5 percent Wave Period (s)												
Hindcast	10±2	11±2	10±1	10±1	9±1	9±1	9±2	9±2	9±2	10±2	10±1	10±1
RCP4.5 - mid	10±2	10±2	10±1	10±1	9±1	9±1	9±1	9±2	9±2	10±2	10±2	10±1
RCP8.5 - mid	10±2	10±1	10±1	10±2	9±1	8±1	8±1	9±2	9±2	10±2	11±2	10±1
RCP4.5 - end	10±2	11±2	10±1	9±1	9±1	9±1	9±2	9±1	9±2	10±2	10±2	10±1
RCP8.5 - end	10±2	10±1	10±1	9±1	8±0.8	8±1	9±1	9±2	9±2	10±2	10±2	10±1
Mean Wave Direction (°)												
Hindcast	48±16	47±18	51±18	58±18	67±24	84±33	99±41	113±47	94±49	55±43	46±27	48±17
RCP4.5 - mid	47±20	48±17	52±15	58±15	68±21	83±27	103±43	118±46	108±45	63±47	46±27	48±23
RCP8.5 - mid	48±17	49±17	52±18	57±17	68±21	84±31	102±43	122±51	106±51	62±43	47±24	48±18
RCP4.5 - end	47±17	45±19	51±16	57±17	67±19	84±30	100±46	118±50	107±49	61±48	46±26	48±19
RCP8.5 - end	46±19	48±19	52±17	59±12	69±18	84±27	98±43	121±45	111±46	69±41	51±23	50±18
Top 5 percent Wave Direction (°)												
Hindcast	51±15	47±18	47±33	52±35	57±54	119±94	223±106	224±62	255±80	12±107	50±49	54±14
RCP4.5 - mid	52±24	51±16	53±19	53±29	67±49	81±63	213±82	224±58	223±61	238±117	46±51	52±31
RCP8.5 - mid	53±15	52±19	55±28	51±27	66±53	92±71	219±83	225±47	229±53	269±96	43±54	56±28
RCP4.5 - end	49±14	44±30	54±21	57±35	65±26	108±78	234±68	235±53	245±48	272±96	36±64	58±28
RCP8.5 - end	48±22	53±17	53±34	62±16	66±43	79±58	204±93	229±46	221±64	28±102	52±46	56±17

Appendix A20. Table showing return values of ensemble-average significant wave heights of hindcast and forecast scenarios, including lower and higher 95 percent confidence intervals, at the Pohnpei location.

[Years: Hindcast = 1976–2005; RCP mid = 2026–2045; RCP end = 2081–2100. Wave height values are in meters]

Scenario	Hindcast			RCP4.5 - mid			RCP8.5 - mid			RCP4.5 - end			RCP8.5 - end		
	Low	R_v	High	Low	R_v	High	Low	R_v	High	Low	R_v	High	Low	R_v	High
2-year	5.41	5.88	6.60	5.36	6.04	7.20	5.12	5.83	7.24	5.11	5.86	7.28	4.97	5.70	7.11
5-year	5.79	6.59	7.90	5.62	6.64	8.56	5.42	6.66	9.54	5.41	6.65	9.42	5.20	6.34	8.88
10-year	6.07	7.17	9.11	5.78	7.06	9.67	5.63	7.38	12.01	5.61	7.31	11.58	5.34	6.82	10.51
20-year	6.34	7.80	10.54	5.91	7.45	10.85	5.83	8.21	15.36	5.79	8.02	14.35	5.46	7.29	12.45
50-year	6.70	8.70	12.86	6.04	7.92	12.53	6.09	9.47	21.69	6.01	9.05	19.26	5.59	7.92	15.58
100-year	6.95	9.44	15.01	6.12	8.25	13.91	6.27	10.58	28.49	6.16	9.91	24.21	5.67	8.39	18.47

Appendix A21. Table showing Yap monthly means and mean of the top 5 percent for significant wave height, peak wave period, and peak wave direction.

[Years: Hindcast = 1976–2005; RCP mid = 2026–2045; RCP end = 2081–2100. Wave directions are "coming from"]

Month	Jan	Feb	Mar	Apr	May	Jun	July	Aug	Sep	Oct	Nov	Dec
Mean Wave Height (m)												
Hindcast	2.7±0.7	2.7±0.7	2.4±0.7	2.0±0.6	1.5±0.5	1.3±0.6	1.3±0.7	1.3±0.8	1.3±0.7	1.6±0.7	2.2±0.8	2.6±0.7
RCP4.5 - mid	2.7±0.7	2.7±0.7	2.5±0.7	2.0±0.6	1.5±0.5	1.3±0.6	1.3±0.8	1.2±0.6	1.2±0.6	1.5±0.7	2.0±0.7	2.5±0.8
RCP8.5 - mid	2.7±0.7	2.7±0.7	2.4±0.7	2.0±0.5	1.5±0.5	1.3±0.7	1.3±0.7	1.3±0.8	1.2±0.7	1.4±0.6	1.9±0.7	2.5±0.7
RCP4.5 - end	2.6±0.7	2.7±0.7	2.4±0.7	2.0±0.5	1.5±0.5	1.3±0.6	1.3±0.7	1.3±0.8	1.2±0.7	1.4±0.6	2.0±0.7	2.4±0.7
RCP8.5 - end	2.5±0.7	2.5±0.7	2.2±0.6	1.9±0.5	1.5±0.5	1.3±0.5	1.3±0.7	1.3±0.8	1.2±0.7	1.3±0.5	1.8±0.7	2.3±0.7
Top 5 percent Wave Height (m)												
Hindcast	4.5±0.5	4.7±0.7	4.3±0.7	3.4±0.4	2.9±0.6	2.9±0.7	3.5±0.7	3.8±1.0	3.5±0.8	3.6±0.8	4.4±0.9	4.5±0.7
RCP4.5 - mid	4.4±0.5	4.4±0.6	4.2±0.6	3.4±0.6	2.7±0.4	2.8±0.9	3.7±0.8	3.2±0.9	3.2±0.8	3.6±0.8	3.9±0.7	4.6±0.9
RCP8.5 - mid	4.5±0.5	4.4±0.4	4.2±0.7	3.4±0.6	2.8±0.6	3.3±1.1	3.4±0.7	3.7±0.9	3.4±0.9	3.1±0.7	3.7±0.6	4.5±0.7
RCP4.5 - end	4.5±0.6	4.3±0.5	4.1±0.6	3.3±0.5	2.7±0.6	2.8±0.7	3.4±0.8	3.7±0.9	3.5±0.9	3.4±0.8	3.7±0.6	4.3±0.6
RCP8.5 - end	4.4±0.7	4.3±0.5	3.7±0.3	3.1±0.5	2.7±0.5	2.7±0.8	3.3±0.9	3.8±0.9	3.3±0.9	2.9±0.6	3.9±0.9	4.3±0.8
Mean Wave Period (s)												
Hindcast	9±1	9±1	9±1	9±1	9±1	9±1	9±1	9±1	9±1	10±1	10±1	10±1
RCP4.5 - mid	9±2	9±1	9±1	9±1	9±1	9±1	9±1	9±1	9±1	9±1	10±1	10±1
RCP8.5 - mid	9±2	9±2	9±1	9±1	9±1	8±1	9±1	9±1	9±1	10±2	10±1	10±2
RCP4.5 - end	9±1	9±1	9±1	9±1	9±1	9±1	9±1	9±1	9±1	10±2	10±2	10±1
RCP8.5 - end	9±2	9±1	9±1	9±1	8±1	8±1	9±1	9±1	9±1	9±1	9±1	9±1
Top 5 percent Wave Period (s)												
Hindcast	10±1	10±1	10±1	10±1	9±1	9±1	9±1	9±1	9±1	10±2	11±1	10±1
RCP4.5 - mid	10±0.8	10±0.7	10±1	10±1	9±1	8±1	9±1	8±1	9±2	10±2	10±1	10±1
RCP8.5 - mid	10±0.9	10±0.9	10±0.9	10±1	9±1	8±1	9±1	9±1	9±1	10±2	10±1	11±1
RCP4.5 - end	10±1	10±1	10±0.8	10±1	9±0.9	8±1	9±1	9±1	9±1	10±2	10±2	10±1
RCP8.5 - end	10±1	10±0.7	9±0.9	9±0.9	9±0.8	8±1	8±1	9±1	9±1	10±2	10±1	10±1
Mean Wave Direction (°)												
Hindcast	59±17	59±16	63±15	68±15	72±21	77±34	85±52	98±61	67±58	48±42	56±29	61±19
RCP4.5 - mid	59±17	60±16	64±14	68±11	71±16	81±30	97±52	95±62	79±58	48±48	54±29	59±23
RCP8.5 - mid	60±17	61±15	65±14	68±13	73±14	81±34	92±52	113±64	78±65	47±44	54±27	60±22
RCP4.5 - end	60±19	59±15	63±13	68±14	72±16	80±30	90±56	108±62	83±68	46±46	54±28	60±18
RCP8.5 - end	59±18	60±16	64±13	69±11	73±14	81±34	93±49	111±60	87±65	53±43	58±26	61±18
Top 5 percent Wave Direction (°)												
Hindcast	56±20	51±22	52±22	64±22	72±54	207±121	237±51	229±47	244±57	287±106	50±80	65±35
RCP4.5 - mid	62±16	60±15	58±28	67±12	70±37	140±80	224±42	234±49	231±66	245±88	52±76	63±45
RCP8.5 - mid	59±16	57±16	61±23	69±34	74±35	205±77	232±46	225±29	231±40	299±88	55±69	67±27
RCP4.5 - end	62±25	53±16	62±14	67±35	78±46	142±83	232±45	229±40	239±41	267±87	47±68	57±30
RCP8.5 - end	60±25	57±18	61±18	67±16	77±26	136±81	217±42	224±40	227±47	273±104	73±76	67±38

Appendix A22. Table showing return values of ensemble-average significant wave heights of hindcast and forecast scenarios, including lower and higher 95 percent confidence intervals, at the Yap location.

[Years: Hindcast = 1976–2005; RCP mid = 2026–2045; RCP end = 2081–2100. Wave height values are in meters]

Scenario	Hindcast			RCP4.5 - mid			RCP8.5 - mid			RCP4.5 - end			RCP8.5 - end		
	Low	R_v	High	Low	R_v	High	Low	R_v	High	Low	R_v	High	Low	R_v	High
2-year	6.22	7.05	8.44	5.85	6.80	8.74	5.98	6.84	8.46	5.88	6.69	8.12	6.11	7.05	8.71
5-year	6.64	7.98	10.53	6.15	7.70	11.47	6.29	7.65	10.59	6.20	7.44	9.93	6.39	7.73	10.37
10-year	6.92	8.71	12.45	6.35	8.43	14.23	6.49	8.28	12.57	6.39	7.99	11.52	6.54	8.17	11.67
20-year	7.17	9.47	14.74	6.52	9.21	17.79	6.65	8.91	14.93	6.55	8.54	13.33	6.65	8.56	13.00
50-year	7.47	10.51	18.45	6.71	10.31	24.10	6.84	9.75	18.76	6.73	9.24	16.10	6.76	9.00	14.80
100-year	7.66	11.33	21.87	6.84	11.21	30.48	6.96	10.40	22.32	6.84	9.76	18.54	6.82	9.28	16.20

Appendix A23. Table showing Majuro monthly means and mean of the top 5 percent for significant wave height, peak wave period, and peak wave direction.

[Years: Hindcast = 1976–2005; RCP mid = 2026–2045; RCP end = 2081–2100. Wave directions are "coming from"]

Month	Jan	Feb	Mar	Apr	May	Jun	July	Aug	Sep	Oct	Nov	Dec
Mean Wave Height (m)												
Hindcast	2.7±0.6	2.6±0.6	2.5±0.6	2.1±0.6	1.7±0.5	1.6±0.4	1.5±0.4	1.4±0.4	1.4±0.4	1.6±0.5	2.1±0.6	2.6±0.7
RCP4.5 - mid	2.6±0.6	2.6±0.6	2.5±0.6	2.2±0.5	1.8±0.5	1.6±0.5	1.6±0.4	1.4±0.4	1.3±0.3	1.5±0.4	2.0±0.6	2.5±0.6
RCP8.5 - mid	2.6±0.6	2.6±0.6	2.4±0.6	2.2±0.6	1.8±0.5	1.6±0.5	1.6±0.4	1.4±0.4	1.3±0.4	1.5±0.4	2.0±0.7	2.5±0.6
RCP4.5 - end	2.5±0.5	2.5±0.6	2.5±0.6	2.2±0.5	1.8±0.5	1.7±0.5	1.5±0.4	1.4±0.4	1.3±0.4	1.5±0.5	1.9±0.6	2.4±0.7
RCP8.5 - end	2.4±0.5	2.4±0.6	2.3±0.5	2.1±0.5	1.8±0.5	1.7±0.5	1.6±0.4	1.4±0.4	1.3±0.3	1.4±0.4	1.8±0.6	2.3±0.6
Top 5 percent Wave Height (m)												
Hindcast	4.1±0.5	4.0±0.3	3.9±0.4	3.5±0.4	2.8±0.3	2.7±0.3	2.6±0.4	2.4±0.5	2.4±0.5	3.1±0.5	3.8±0.4	4.4±0.7
RCP4.5 - mid	4±0.3	3.9±0.4	3.9±0.4	3.5±0.2	2.8±0.2	2.7±0.3	2.6±0.3	2.6±0.5	2.2±0.4	2.7±0.4	3.5±0.5	4.0±0.4
RCP8.5 - mid	4.1±0.5	4.3±0.4	3.9±0.3	3.6±0.5	2.9±0.3	2.7±0.3	2.7±0.5	2.5±0.4	2.4±0.7	2.7±0.4	3.8±0.6	4.0±0.4
RCP4.5 - end	3.8±0.3	4.0±0.4	3.9±0.4	3.4±0.2	2.9±0.2	2.8±0.4	2.7±0.5	2.5±0.5	2.4±0.5	2.8±0.5	3.5±0.7	4.2±0.5
RCP8.5 - end	3.6±0.2	3.8±0.4	3.7±0.2	3.3±0.3	2.9±0.2	2.8±0.3	2.7±0.5	2.5±0.7	2.2±0.5	2.7±0.5	3.3±0.4	3.7±0.3
Mean Wave Period (s)												
Hindcast	10±2	10±2	10±2	9±1	9±1	9±1	9±1	9±1	9±1	10±1	10±2	11±2
RCP4.5 - mid	10±2	10±2	10±2	9±1	9±1	9±1	9±1	9±1	9±1	10±1	10±2	10±2
RCP8.5 - mid	10±2	10±2	10±2	9±1	9±1	9±1	9±1	9±1	9±2	10±2	10±2	10±2
RCP4.5 - end	11±2	10±2	9.9±2	9.4±1	8.9±1	8.8±1	8.8±1	9±1	9.1±1	9.6±2	10±2	10±2
RCP8.5 - end	10±2	10±2	10±2	9±1	9±0.9	9±1	9±1	9±1	9±1	9±1	10±2	10±2
Top 5 percent Wave Period (s)												
Hindcast	11±1	11±2	11±1	10±1	9±0.8	9±0.8	9±1	9±1	9±2	10±2	11±1	11±1
RCP4.5 - mid	11±2	11±2	11±0.9	10±0.9	9±0.8	9±0.8	9±1	9±2	9±2	10±2	11±2	10±1
RCP8.5 - mid	11±1	11±1	10±0.9	10±0.9	9±0.8	9±0.7	9±0.9	9±1	9±2	11±2	10±1	11±1
RCP4.5 - end	10±1	11±1	11±1	10±0.8	9±0.6	9±0.9	9±1	9±2	9±2	10±2	11±2	11±1
RCP8.5 - end	11±2	11±1	10±0.8	10±0.9	9±0.7	9±0.8	9±1	9±1	9±2	10±2	10±2	11±1
Mean Wave Direction (°)												
Hindcast	52±15	53±16	57±15	62±14	71±15	82±20	90±23	99±30	93±36	65±32	52±21	51±16
RCP4.5 - mid	52±15	54±15	57±13	63±12	72±14	82±18	90±21	102±26	100±27	72±33	53±20	53±16
RCP8.5 - mid	53±15	54±15	57±14	63±14	72±14	82±17	91±23	104±31	101±34	71±32	51±22	52±16
RCP4.5 - end	51±17	51±17	57±13	62±12	71±13	81±15	91±23	102±33	102±33	70±37	51±24	53±17
RCP8.5 - end	52±16	54±16	58±13	64±11	73±12	83±16	90±24	103±26	103±30	76±31	57±20	54±16
Top 5 percent Wave Direction (°)												
Hindcast	58±10	58±12	58±16	61±22	70±27	77±33	87±52	117±73	70±90	55±62	58±28	56±16
RCP4.5 - mid	56±14	58±13	59±10	62±8	68±10	76±37	87±38	128±67	107±66	55±76	52±31	57±11
RCP8.5 - mid	59±10	58±10	60±8	66±35	70±22	77±30	99±53	128±72	184±100	40±69	49±49	56±11
RCP4.5 - end	58±12	58±9	60±10	64±9	68±11	78±28	101±50	139±86	177±88	24±103	52±45	58±19
RCP8.5 - end	56±14	57±11	63±7	66±15	69±7	77±28	86±58	122±66	115±88	53±71	55±34	58±10

Appendix A24. Table showing return values of ensemble-average significant wave heights of hindcast and forecast scenarios, including lower and higher 95 percent confidence intervals, at the Majuro location.

[Years: Hindcast = 1976–2005; RCP mid = 2026–2045; RCP end = 2081–2100. Wave height values are in meters]

Scenario	Hindcast			RCP4.5 - mid			RCP8.5 - mid			RCP4.5 - end			RCP8.5 - end		
	Low	R_v	High	Low	R_v	High	Low	R_v	High	Low	R_v	High	Low	R_v	High
2-year	5.06	5.56	6.38	4.71	5.14	5.89	4.94	5.41	6.23	4.91	5.54	6.68	4.48	4.96	5.88
5-year	5.39	6.25	7.85	4.92	5.62	6.99	5.16	5.92	7.39	5.13	6.11	8.13	4.68	5.49	7.33
10-year	5.63	6.84	9.31	5.06	6.00	8.03	5.31	6.31	8.45	5.27	6.53	9.40	4.81	5.94	8.83
20-year	5.87	7.51	11.16	5.18	6.40	9.27	5.44	6.72	9.70	5.39	6.94	10.87	4.94	6.44	10.82
50-year	6.17	8.50	14.41	5.34	6.95	11.31	5.59	7.27	11.69	5.52	7.48	13.15	5.10	7.19	14.44
100-year	6.40	9.36	17.64	5.44	7.39	13.22	5.69	7.70	13.52	5.59	7.88	15.17	5.20	7.83	18.20

Appendix A25. Table showing Enewetak monthly means and mean of the top 5 percent for significant wave height, peak wave period, and peak wave direction.

[Years: Hindcast = 1976–2005; RCP mid = 2026–2045; RCP end = 2081–2100. Wave directions are "coming from"]

Month	Jan	Feb	Mar	Apr	May	Jun	July	Aug	Sep	Oct	Nov	Dec
Mean Wave Height (m)												
Hindcast	2.9±0.6	2.7±0.6	2.6±0.6	2.4±0.6	1.9±0.6	1.7±0.6	1.6±0.6	1.5±0.7	1.5±0.7	1.9±0.8	2.5±0.8	2.9±0.7
RCP4.5 - mid	2.8±0.6	2.7±0.6	2.6±0.6	2.4±0.6	1.9±0.5	1.7±0.6	1.6±0.7	1.5±0.7	1.4±0.6	1.8±0.7	2.4±0.7	2.8±0.7
RCP8.5 - mid	2.8±0.6	2.8±0.7	2.6±0.6	2.4±0.6	1.9±0.5	1.7±0.5	1.6±0.6	1.5±0.8	1.4±0.6	1.7±0.6	2.4±0.8	2.8±0.7
RCP4.5 - end	2.8±0.6	2.7±0.6	2.7±0.6	2.4±0.6	1.9±0.5	1.8±0.6	1.6±0.7	1.6±0.8	1.4±0.7	1.7±0.7	2.4±0.8	2.8±0.7
RCP8.5 - end	2.6±0.6	2.6±0.6	2.5±0.6	2.3±0.5	1.9±0.5	1.7±0.5	1.7±0.7	1.5±0.8	1.4±0.6	1.6±0.6	2.2±0.8	2.6±0.6
Top 5 percent Wave Height (m)												
Hindcast	4.4±0.5	4.3±0.3	4.3±0.5	4.0±0.8	3.2±0.5	3.0±0.5	3.2±0.7	3.5±0.9	3.6±0.9	4.0±0.7	4.5±0.6	4.7±0.6
RCP4.5 - mid	4.2±0.3	4.2±0.5	4.1±0.5	3.9±0.5	3.1±0.3	3.0±0.6	3.4±0.8	3.6±0.9	3.5±0.9	3.8±0.9	4.3±0.6	4.4±0.5
RCP8.5 - mid	4.2±0.4	4.4±0.3	4.1±0.4	4.1±1.0	3.2±0.6	3.0±0.4	3.3±0.7	3.7±1.3	3.4±0.7	3.6±0.6	4.5±0.7	4.4±0.5
RCP4.5 - end	4.1±0.4	4.2±0.4	4.2±0.3	3.8±0.4	3.0±0.2	3.1±0.7	3.5±0.9	4.0±1.0	3.8±1.0	3.7±0.7	4.3±0.7	4.3±0.5
RCP8.5 - end	4.0±0.3	4.0±0.3	3.9±0.4	3.4±0.2	3.0±0.4	3.0±0.7	3.5±1.0	4.1±1.4	3.5±1.0	3.5±0.8	4.3±0.8	4.1±0.4
Mean Wave Period (s)												
Hindcast	10±2	10±2	10±2	9±1	9±1	9±1	9±1	9±1	9±1	10±2	10±2	10±2
RCP4.5 - mid	10±2	10±2	10±2	9±1	9±1	8±1	9±1	9±1	9±1	9±1	10±2	10±2
RCP8.5 - mid	10±2	10±2	10±2	9±1	9±1	8±1	9±1	9±1	9±2	9±2	10±2	10±2
RCP4.5 - end	10±2	10±2	9.9±2	9.3±1	8.6±1	8.5±1	8.6±1	8.7±1	8.8±1	9.5±2	10±2	10±2
RCP8.5 - end	10±2	10±2	10±2	9±1	8±1	8±1	9±1	9±1	9±2	9±1	10±2	10±2
Top 5 percent Wave Period (s)												
Hindcast	11±2	11±2	11±1	10±1	9±0.9	9±1	9±1	10±2	10±2	10±1	11±1	11±1
RCP4.5 - mid	11±2	11±2	11±2	10±1	9±0.9	9±1	10±1	10±2	10±2	10±2	11±1	11±1
RCP8.5 - mid	11±2	11±2	11±1	11±1	9±0.7	9±0.9	9±1	10±2	10±1	10±2	11±1	11±1
RCP4.5 - end	11±2	11±2	11±1	10±0.9	9±0.9	9±1	10±2	10±1	10±1	10±2	11±1	11±2
RCP8.5 - end	11±2	11±2	10±1	10±0.8	9±0.8	9±1	10±1	10±2	10±2	10±1	11±1	11±2
Mean Wave Direction (°)												
Hindcast	51±21	48±23	56±19	64±13	71±14	77±23	81±37	85±56	64±55	54±35	56±21	54±19
RCP4.5 - mid	50±22	50±22	56±18	65±12	70±11	77±18	84±38	88±52	74±57	53±38	56±20	56±19
RCP8.5 - mid	50±22	51±22	56±19	64±15	70±12	77±19	83±38	89±60	66±67	52±39	56±19	55±19
RCP4.5 - end	48±22	47±23	57±17	64±15	70±12	77±17	81±37	88±57	70±62	50±45	54±22	56±18
RCP8.5 - end	48±24	49±24	57±19	65±11	72±11	79±18	81±37	95±51	75±59	52±39	56±17	55±17
Top 5 percent Wave Direction (°)												
Hindcast	55±18	50±25	56±21	59±15	77±27	89±55	101±85	234±65	247±88	68±62	63±28	59±14
RCP4.5 - mid	50±22	53±21	56±17	67±23	70±15	80±38	168±94	215±72	224±76	124±113	62±26	60±21
RCP8.5 - mid	53±23	57±18	59±14	60±22	71±20	80±38	130±96	229±64	242±66	66±86	63±28	61±17
RCP4.5 - end	53±22	48±26	61±13	67±24	69±14	89±45	199±105	231±51	232±61	59±112	62±34	62±16
RCP8.5 - end	45±28	53±20	62±19	65±8	74±22	85±40	162±99	222±57	228±61	72±76	67±25	59±12

Appendix A26. Table showing return values of ensemble-average significant wave heights of hindcast and forecast scenarios, including lower and higher 95 percent confidence intervals, at the Enewetak location.

[Years: Hindcast = 1976–2005; RCP mid = 2026–2045; RCP end = 2081–2100. Wave height values are in meters]

Scenario	Hindcast			RCP4.5 - mid			RCP8.5 - mid			RCP4.5 - end			RCP8.5 - end		
	Low	R_v	High	Low	R_v	High	Low	R_v	High	Low	R_v	High	Low	R_v	High
2-year	6.10	6.78	7.88	5.95	6.88	8.58	5.75	6.69	8.67	6.06	6.91	8.36	5.80	7.03	9.60
5-year	6.47	7.54	9.47	6.25	7.64	10.50	6.12	7.83	12.12	6.42	7.73	10.22	6.21	8.29	13.46
10-year	6.71	8.12	10.85	6.42	8.16	12.11	6.40	8.87	16.08	6.65	8.33	11.81	6.49	9.35	17.54
20-year	6.92	8.69	12.41	6.56	8.66	13.88	6.67	10.11	21.78	6.84	8.91	13.59	6.74	10.52	22.98
50-year	7.16	9.45	14.78	6.70	9.26	16.48	7.02	12.12	33.33	7.05	9.66	16.25	7.04	12.25	33.08
100-year	7.32	10.02	16.84	6.78	9.68	18.67	7.28	13.97	46.61	7.18	10.21	18.54	7.24	13.71	43.73

Appendix A27. Table showing Bikini monthly means and mean of the top 5 percent for significant wave height, peak wave period, and peak wave direction.

[Years: Hindcast = 1976–2005; RCP mid = 2026–2045; RCP end = 2081–2100. Wave directions are "coming from"]

Month	Jan	Feb	Mar	Apr	May	Jun	July	Aug	Sep	Oct	Nov	Dec
Mean Wave Height (m)												
Hindcast	3.0±0.7	2.9±0.7	2.8±0.7	2.5±0.7	2.0±0.6	1.8±0.6	1.6±0.6	1.5±0.6	1.5±0.6	2.0±0.8	2.7±0.8	3.0±0.8
RCP4.5 - mid	3.0±0.7	2.8±0.6	2.8±0.6	2.5±0.6	2.0±0.5	1.8±0.6	1.7±0.6	1.5±0.6	1.4±0.6	1.8±0.7	2.5±0.7	2.9±0.7
RCP8.5 - mid	2.9±0.6	2.9±0.7	2.7±0.7	2.5±0.7	2.0±0.6	1.8±0.6	1.7±0.6	1.5±0.7	1.4±0.6	1.8±0.6	2.6±0.8	2.9±0.7
RCP4.5 - end	2.9±0.6	2.8±0.6	2.8±0.7	2.5±0.6	2.1±0.5	1.9±0.6	1.7±0.6	1.6±0.7	1.4±0.6	1.8±0.7	2.5±0.8	2.9±0.7
RCP8.5 - end	2.8±0.6	2.7±0.6	2.6±0.6	2.4±0.5	2.0±0.5	1.8±0.5	1.7±0.6	1.5±0.7	1.4±0.6	1.7±0.6	2.3±0.8	2.8±0.7
Top 5 percent Wave Height (m)												
Hindcast	4.6±0.5	4.5±0.4	4.4±0.6	4.2±0.7	3.3±0.4	3.0±0.3	3.1±0.6	3.2±0.8	3.3±0.7	4.1±0.7	4.7±0.6	4.9±0.6
RCP4.5 - mid	4.4±0.4	4.4±0.5	4.3±0.5	4.1±0.4	3.2±0.3	3.1±0.5	3.2±0.6	3.4±0.9	3.1±0.7	3.8±0.6	4.5±0.5	4.6±0.4
RCP8.5 - mid	4.5±0.4	4.6±0.4	4.3±0.4	4.2±1.0	3.3±0.7	3.1±0.4	3.2±0.6	3.5±1.1	3.2±0.6	3.6±0.5	4.8±0.9	4.6±0.5
RCP4.5 - end	4.4±0.4	4.5±0.4	4.5±0.4	3.9±0.3	3.2±0.2	3.1±0.6	3.3±0.7	3.7±1.0	3.4±0.9	3.7±0.6	4.4±0.7	4.5±0.5
RCP8.5 - end	4.2±0.3	4.2±0.3	4.0±0.3	3.6±0.2	3.1±0.2	3.1±0.6	3.3±0.7	3.7±1.2	3.1±1.0	3.4±0.7	4.4±0.6	4.3±0.4
Mean Wave Period (s)												
Hindcast	11±2	11±2	10±2	9±1	9±0.9	9±0.9	9±1	9±1	9±1	10±1	10±2	11±2
RCP4.5 - mid	11±2	11±2	10±2	9±1	9±1	8±0.9	9±1	9±1	9±1	9±1	10±2	10±2
RCP8.5 - mid	11±2	10±2	10±2	9±1	9±1	8±0.8	9±1	9±1	9±1	9±2	10±2	10±2
RCP4.5 - end	11±2	11±2	10±2	9.4±1	8.6±1	8.4±0.8	8.5±1	8.6±1	8.8±1	9.5±2	10±2	10±2
RCP8.5 - end	11±2	10±2	10±2	9±1	8±0.9	8±0.9	9±1	9±1	9±1	9±1	10±2	10±2
Top 5 percent Wave Period (s)												
Hindcast	11±2	11±2	11±1	10±0.9	10±0.8	9±0.8	9±1	10±2	10±2	10±1	11±1	11±1
RCP4.5 - mid	11±2	11±2	11±1	10±0.9	9±0.7	9±0.8	9±1	10±2	10±2	11±1	11±1	11±1
RCP8.5 - mid	12±2	11±1	11±1	11±1	9±0.7	9±0.6	9±0.9	10±2	10±2	11±2	11±1	11±1
RCP4.5 - end	11±2	11±2	11±1	10±0.8	9±0.8	9±1	10±2	10±2	10±2	10±2	11±1	11±2
RCP8.5 - end	11±2	11±2	11±1	10±0.8	9±0.7	9±0.8	9±1	10±2	10±2	10±1	11±1	11±2
Mean Wave Direction (°)												
Hindcast	50±22	48±24	56±20	64±13	70±12	74±18	74±30	75±47	57±49	53±30	56±19	54±19
RCP4.5 - mid	49±22	50±23	56±19	65±11	69±10	75±15	77±31	78±45	64±46	52±32	55±19	55±19
RCP8.5 - mid	49±23	51±23	56±20	65±15	70±11	75±14	78±31	76±52	57±57	51±33	55±17	54±20
RCP4.5 - end	48±24	47±24	57±18	64±14	69±10	75±13	76±31	77±50	61±52	48±40	54±20	55±18
RCP8.5 - end	47±24	49±24	57±19	65±12	71±11	77±14	76±30	82±42	64±49	51±34	55±16	55±18
Top 5 percent Wave Direction (°)												
Hindcast	56±18	53±25	57±17	63±23	74±19	76±29	80±56	220±104	282±118	67±44	64±21	59±14
RCP4.5 - mid	50±23	55±21	58±16	67±11	70±13	78±32	98±70	162±99	202±124	68±83	57±24	60±19
RCP8.5 - mid	55±23	59±18	60±12	64±25	71±18	77±23	89±52	208±98	252±95	58±65	63±20	60±13
RCP4.5 - end	54±24	51±26	62±13	67±12	69±11	81±32	98±83	232±68	223±93	45±80	62±23	62±15
RCP8.5 - end	47±24	56±17	62±18	65±8	72±15	81±28	91±78	211±81	233±96	66±53	62±19	59±13

Appendix A28. Table showing return values of ensemble-average significant wave heights of hindcast and forecast scenarios, including lower and higher 95 percent confidence intervals, at the Bikini location.

[Years: Hindcast = 1976–2005; RCP mid = 2026–2045; RCP end = 2081–2100. Wave height values are in meters]

Scenario	Hindcast			RCP4.5 - mid			RCP8.5 - mid			RCP4.5 - end			RCP8.5 - end		
	Low	R_v	High	Low	R_v	High	Low	R_v	High	Low	R_v	High	Low	R_v	High
2-year	6.10	6.73	7.74	5.51	6.21	7.66	5.77	6.66	8.54	5.80	6.54	7.93	5.61	6.52	8.39
5-year	6.46	7.47	9.28	5.72	6.84	9.61	6.15	7.83	12.11	6.06	7.22	9.71	5.98	7.62	11.64
10-year	6.70	8.04	10.64	5.85	7.34	11.56	6.45	8.96	16.42	6.22	7.74	11.33	6.26	8.63	15.32
20-year	6.92	8.63	12.22	5.96	7.86	14.03	6.75	10.36	22.91	6.36	8.26	13.24	6.53	9.82	20.55
50-year	7.17	9.42	14.69	6.08	8.58	18.34	7.17	12.74	36.78	6.52	8.93	16.28	6.88	11.73	31.00
100-year	7.34	10.03	16.89	6.16	9.16	22.63	7.48	15.05	53.56	6.61	9.45	19.05	7.14	13.47	42.84

Appendix A29. Table showing Molokai monthly means and mean of the top 5 percent for significant wave height, peak wave period, and peak wave direction.

[Years: Hindcast = 1976–2005; RCP mid = 2026–2045; RCP end = 2081–2100. Wave directions are "coming from"]

Month	Jan	Feb	Mar	Apr	May	Jun	July	Aug	Sep	Oct	Nov	Dec
Mean Wave Height (m)												
Hindcast	3.2±0.9	3.1±0.9	2.7±0.8	2.4±0.6	2.0±0.5	2.0±0.5	2.0±0.5	2.0±0.5	2.1±0.6	2.5±0.7	2.9±0.8	3.1±0.8
RCP4.5 - mid	3.2±0.9	3.1±0.9	2.8±0.7	2.4±0.6	2.0±0.5	1.9±0.4	2.0±0.4	2.0±0.5	1.9±0.5	2.4±0.7	2.9±0.8	3.1±0.8
RCP8.5 - mid	3.2±0.9	3.1±0.9	2.8±0.7	2.4±0.6	2.0±0.5	1.9±0.4	1.9±0.4	2.0±0.5	2.0±0.5	2.4±0.7	2.9±0.8	3.1±0.8
RCP4.5 - end	3.1±0.8	3.1±0.9	2.8±0.7	2.4±0.6	2.0±0.5	2.0±0.4	2.0±0.5	2.0±0.6	2.0±0.5	2.4±0.7	2.8±0.8	3.1±0.8
RCP8.5 - end	3.0±0.9	3.0±0.8	2.7±0.7	2.3±0.6	1.9±0.4	1.9±0.4	1.9±0.5	1.8±0.5	1.9±0.5	2.3±0.7	2.7±0.7	3.0±0.9
Top 5 percent Wave Height (m)												
Hindcast	5.5±0.6	5.4±0.6	4.6±0.4	3.9±0.4	3.2±0.3	3.1±0.4	3.2±0.4	3.3±0.4	3.5±0.4	4.3±0.5	4.8±0.5	5.0±0.5
RCP4.5 - mid	5.5±0.7	5.3±0.5	4.6±0.5	4.0±0.4	3.3±0.5	2.9±0.3	3.1±0.5	3.2±0.4	3.2±0.4	4.3±0.6	4.8±0.4	5.3±0.6
RCP8.5 - mid	5.3±0.6	5.3±0.6	4.6±0.5	3.8±0.4	3.0±0.2	2.9±0.3	3.1±0.5	3.3±0.5	3.3±0.5	4.4±0.6	4.7±0.4	5.1±0.4
RCP4.5 - end	5.2±0.5	5.5±0.6	4.5±0.4	3.9±0.4	3.1±0.3	2.9±0.4	3.3±0.9	3.7±0.8	3.4±0.6	4.1±0.7	4.6±0.4	5.1±0.5
RCP8.5 - end	5.2±0.4	5.1±0.7	4.5±0.4	3.6±0.3	3.0±0.3	2.7±0.2	3.2±0.7	3.4±0.7	3.2±0.6	4.0±0.6	4.6±0.5	5.2±0.6
Mean Wave Period (s)												
Hindcast	13±2	12±2	11±2	10±3	10±3	10±3	10±3	10±3	10±3	10±3	12±2	12±2
RCP4.5 - mid	13±2	13±2	12±2	11±3	10±3	10±3	9±3	10±3	10±3	11±3	12±2	12±2
RCP8.5 - mid	13±2	12±2	12±2	11±3	10±3	10±3	10±3	10±3	10±3	11±3	12±2	12±2
RCP4.5 - end	13±2	13±2	12±2	11±3	11±3	10±3	9.7±3	9.7±3	10±3	11±3	12±3	12±2
RCP8.5 - end	13±2	13±2	12±2	11±3	11±3	11±4	10±3	10±4	11±3	11±3	11±3	12±2
Top 5 percent Wave Period (s)												
Hindcast	15±2	15±2	13±3	11±2	10±3	9±2	9±1	9±1	10±2	11±2	13±3	14±3
RCP4.5 - mid	15±2	14±2	13±3	11±2	10±3	9±2	9±1	10±2	9±2	11±2	13±3	15±3
RCP8.5 - mid	15±2	14±2	13±3	11±3	10±3	9±2	9±2	9±1	10±2	11±2	13±3	14±3
RCP4.5 - end	15±2	15±2	13±3	12±3	10±3	9±3	10±2	10±2	9±1	11±2	12±3	14±3
RCP8.5 - end	15±2	15±2	13±3	12±3	10±3	10±3	9±2	10±3	10±2	11±2	12±3	14±3
Mean Wave Direction (°)												
Hindcast	345±49	343±49	18±54	53±46	78±39	90±21	91±18	89±25	77±37	55±39	31±45	9±51
RCP4.5 - mid	343±47	349±50	17±54	53±44	77±41	91±24	90±17	90±25	81±35	55±43	30±44	5±48
RCP8.5 - mid	348±47	348±48	12±53	49±46	78±39	92±25	92±21	92±25	81±38	51±44	27±43	10±50
RCP4.5 - end	342±47	343±49	15±51	44±48	75±41	93±24	93±21	93±26	82±38	56±41	31±42	7±50
RCP8.5 - end	344±46	341±45	10±52	52±44	77±43	95±23	94±19	95±27	84±38	57±40	37±41	6±49
Top 5 percent Wave Direction (°)												
Hindcast	323±35	324±39	21±55	48±43	70±31	85±11	85±15	83±26	70±37	57±42	30±52	352±49
RCP4.5 - mid	321±30	332±46	359±56	58±33	71±30	85±13	88±19	83±26	81±34	62±41	28±51	343±45
RCP8.5 - mid	331±45	331±44	2±55	46±41	72±26	84±13	87±20	90±37	77±37	58±40	19±44	4±57
RCP4.5 - end	319±28	326±43	359±52	29±47	74±23	93±20	89±22	101±52	86±48	56±49	40±44	349±54
RCP8.5 - end	327±39	321±32	353±50	42±41	65±37	88±19	92±24	86±34	84±57	61±51	36±46	7±57

Appendix A30. Table showing return values of ensemble-average significant wave heights of hindcast and forecast scenarios, including lower and higher 95 percent confidence intervals, at the Molokai location.

[Years: Hindcast = 1976–2005; RCP mid = 2026–2045; RCP end = 2081–2100. Wave height values are in meters]

Scenario	Hindcast			RCP4.5 - mid			RCP8.5 - mid			RCP4.5 - end			RCP8.5 - end		
	Low	R_v	High	Low	R_v	High	Low	R_v	High	Low	R_v	High	Low	R_v	High
2-year	6.65	7.11	7.83	6.59	7.26	8.46	6.45	7.01	7.97	6.47	7.06	8.16	6.36	6.83	7.62
5-year	6.95	7.69	8.93	6.86	7.91	10.08	6.65	7.47	9.01	6.65	7.55	9.43	6.51	7.17	8.41
10-year	7.15	8.13	9.89	7.03	8.41	11.56	6.77	7.78	9.84	6.76	7.89	10.52	6.60	7.40	9.00
20-year	7.33	8.57	10.96	7.18	8.92	13.31	6.86	8.06	10.70	6.85	8.22	11.73	6.66	7.59	9.59
50-year	7.54	9.16	12.58	7.34	9.60	16.10	6.95	8.39	11.88	6.94	8.62	13.53	6.72	7.81	10.37
100-year	7.69	9.61	13.98	7.45	10.12	18.66	7.00	8.61	12.82	6.99	8.90	15.08	6.75	7.94	10.95

Appendix A31. Table showing Northwest Hawaiian Islands monthly means and mean of the top 5 percent for significant wave height, peak wave period, and peak wave direction.

[Years: Hindcast = 1976–2005; RCP mid = 2026–2045; RCP end = 2081–2100. Wave directions are "coming from"]

Month	Jan	Feb	Mar	Apr	May	Jun	July	Aug	Sep	Oct	Nov	Dec
Mean Wave Height (m)												
Hindcast	3.9±1.3	3.7±1.3	3.1±1.0	2.5±0.8	2.0±0.5	2.0±0.5	2.1±0.6	2.1±0.6	2.2±0.7	2.7±0.9	3.2±1.0	3.6±1.1
RCP4.5 - mid	3.9±1.3	3.7±1.2	3.2±1.0	2.6±0.7	2.0±0.5	1.9±0.5	2.1±0.5	2.0±0.7	2.1±0.7	2.6±0.9	3.1±1.0	3.6±1.2
RCP8.5 - mid	3.8±1.2	3.6±1.2	3.1±1.0	2.4±0.7	2.0±0.5	1.9±0.5	2.0±0.6	2.1±0.7	2.1±0.7	2.7±0.9	3.1±1.0	3.5±1.2
RCP4.5 - end	3.8±1.2	3.7±1.3	3.1±1.0	2.5±0.8	2.0±0.5	1.9±0.4	2.0±0.5	2.0±0.7	2.1±0.6	2.6±0.9	3.0±0.9	3.5±1.2
RCP8.5 - end	3.7±1.3	3.5±1.2	3.0±1.0	2.4±0.7	1.9±0.5	1.8±0.4	1.9±0.5	1.9±0.6	2.0±0.6	2.5±0.8	2.9±0.9	3.4±1.1
Top 5 percent Wave Height (m)												
Hindcast	7.4±1.0	7.1±0.8	5.6±0.6	4.5±0.6	3.4±0.4	3.2±0.5	3.7±0.7	3.9±0.8	4.2±0.6	5.1±0.6	5.7±0.7	6.7±0.7
RCP4.5 - mid	7.3±0.9	6.9±0.8	5.8±0.7	4.4±0.6	3.4±0.4	3.1±0.4	3.5±0.7	4.0±0.9	4.2±1.0	5.3±1.1	5.7±0.8	6.8±0.8
RCP8.5 - mid	6.9±0.8	6.7±0.7	5.6±0.7	4.2±0.4	3.4±0.6	2.9±0.2	3.4±0.7	3.9±0.9	4.4±1.1	5.1±0.7	5.6±0.7	6.7±0.8
RCP4.5 - end	7.1±0.8	7.2±1.0	5.8±0.8	4.5±0.5	3.4±0.5	2.9±0.3	3.3±0.6	4.3±1.2	4.0±0.7	5.0±0.9	5.3±0.6	6.6±0.8
RCP8.5 - end	7.1±0.9	6.8±1.1	5.6±0.7	4.2±0.5	3.2±0.3	2.8±0.4	3.2±0.6	3.7±1.2	3.9±0.8	4.7±0.7	5.2±0.6	6.4±0.7
Mean Wave Period (s)												
Hindcast	12±2	12±2	11±2	10±2	10±2	9±2	9±2	9±2	10±2	10±2	11±2	12±2
RCP4.5 - mid	12±2	12±2	11±2	10±2	10±2	10±2	9±3	9±2	10±2	10±2	11±2	12±2
RCP8.5 - mid	12±2	12±2	11±2	10±2	10±2	10±2	9±3	10±3	10±2	10±2	11±2	12±2
RCP4.5 - end	12±2	12±2	11±2	11±2	10±2	9.7±3	9.5±3	9.5±2	9.5±2	10±2	11±2	12±2
RCP8.5 - end	12±2	12±2	11±2	10±2	10±2	10±3	10±3	10±3	10±3	10±2	11±2	12±2
Top 5 percent Wave Period (s)												
Hindcast	14±2	15±1	14±2	12±2	10±2	9±1	9±1	10±2	10±1	11±2	13±2	14±2
RCP4.5 - mid	15±2	15±2	14±2	11±2	10±2	9±1	9±1	10±2	10±2	11±2	13±2	15±2
RCP8.5 - mid	15±2	15±2	14±2	12±2	10±2	9±2	9±1	10±2	10±1	11±2	13±2	15±2
RCP4.5 - end	15±2	15±2	13±2	12±2	11±2	9±2	9±2	11±2	10±2	11±2	13±2	14±2
RCP8.5 - end	15±2	14±2	14±2	12±2	10±2	9±3	10±2	11±2	10±2	11±2	12±2	15±2
Mean Wave Direction (°)												
Hindcast	324±45	322±49	351±63	47±58	80±50	102±29	103±20	102±30	83±42	53±46	13±54	341±53
RCP4.5 - mid	322±40	325±50	351±60	51±56	77±54	103±35	104±21	107±26	89±41	56±44	20±54	339±50
RCP8.5 - mid	326±46	327±49	347±58	41±61	76±53	102±36	105±25	108±33	87±46	57±43	20±49	340±50
RCP4.5 - end	320±40	325±48	352±59	35±60	74±55	103±34	106±23	108±28	87±41	62±43	23±52	343±52
RCP8.5 - end	323±43	323±44	349±59	49±57	77±52	105±31	106±21	110±29	93±42	63±42	29±48	344±50
Top 5 percent Wave Direction (°)												
Hindcast	307±20	306±18	329±46	24±58	63±44	94±21	102±29	104±54	82±46	43±50	347±48	314±26
RCP4.5 - mid	309±20	309±24	326±45	46±59	54±46	93±24	108±44	122±48	90±57	53±54	352±54	316±28
RCP8.5 - mid	312±31	311±25	318±42	13±61	61±42	93±20	101±34	124±63	79±54	51±41	0±49	313±25
RCP4.5 - end	307±17	310±30	330±48	10±58	66±50	97±21	104±41	133±62	93±66	62±47	352±56	325±37
RCP8.5 - end	308±17	310±23	319±35	23±58	51±48	96±23	98±26	132±66	97±67	62±52	16±47	328±41

Appendix A32. Table showing return values of ensemble-average significant wave heights of hindcast and forecast scenarios, including lower and higher 95 percent confidence intervals, at the Northwest Hawaiian Islands location.

[Years: Hindcast = 1976–2005; RCP mid = 2026–2045; RCP end = 2081–2100. Wave height values are in meters]

Scenario	Hindcast			RCP4.5 - mid			RCP8.5 - mid			RCP4.5 - end			RCP8.5 - end		
	Low	R_v	High	Low	R_v	High	Low	R_v	High	Low	R_v	High	Low	R_v	High
2-year	9.18	9.95	11.16	8.89	9.79	11.46	8.61	9.47	11.04	9.10	10.11	11.86	8.68	9.59	11.12
5-year	9.65	10.88	13.01	9.20	10.61	13.63	8.85	10.10	12.67	9.51	11.07	14.09	8.98	10.27	12.67
10-year	9.96	11.60	14.63	9.40	11.23	15.62	8.99	10.52	13.98	9.77	11.77	16.02	9.15	10.71	13.83
20-year	10.25	12.32	16.47	9.57	11.85	17.98	9.09	10.90	15.37	9.99	12.46	18.18	9.27	11.08	14.99
50-year	10.58	13.29	19.29	9.75	12.68	21.78	9.19	11.34	17.32	10.23	13.34	21.45	9.39	11.51	16.51
100-year	10.81	14.03	21.76	9.86	13.31	25.27	9.25	11.63	18.89	10.38	13.99	24.29	9.45	11.78	17.65

Appendix A33. Table showing Guam monthly means and mean of the top 5 percent for significant wave height, peak wave period, and peak wave direction.

[Years: Hindcast = 1976–2005; RCP mid = 2026–2045; RCP end = 2081–2100. Wave directions are "coming from"]

Month	Jan	Feb	Mar	Apr	May	Jun	July	Aug	Sep	Oct	Nov	Dec
Mean Wave Height (m)												
Hindcast	2.7±0.6	2.6±0.7	2.5±0.7	2.2±0.6	1.8±0.6	1.6±0.6	1.6±0.9	1.6±1.0	1.5±0.8	1.9±0.8	2.5±0.9	2.7±0.7
RCP4.5 - mid	2.7±0.6	2.5±0.6	2.5±0.7	2.2±0.6	1.7±0.6	1.6±0.6	1.6±0.8	1.5±0.8	1.5±0.8	1.7±0.7	2.3±0.7	2.6±0.7
RCP8.5 - mid	2.6±0.6	2.6±0.7	2.4±0.7	2.1±0.6	1.7±0.5	1.6±0.8	1.6±0.9	1.6±1.0	1.5±0.8	1.7±0.7	2.3±0.8	2.7±0.7
RCP4.5 - end	2.6±0.6	2.6±0.7	2.5±0.6	2.1±0.6	1.7±0.5	1.6±0.6	1.6±0.9	1.6±0.9	1.5±0.7	1.7±0.7	2.3±0.8	2.6±0.7
RCP8.5 - end	2.5±0.7	2.4±0.6	2.2±0.6	2.0±0.5	1.7±0.5	1.6±0.7	1.6±0.8	1.6±1.0	1.5±0.8	1.6±0.6	2.1±0.8	2.5±0.7
Top 5 percent Wave Height (m)												
Hindcast	4.3±0.5	4.2±0.5	4.3±0.9	3.7±0.7	3.4±0.9	3.4±0.9	4.4±1.0	4.8±1.3	4.2±1.1	4.2±0.8	4.9±0.9	4.6±0.7
RCP4.5 - mid	4.2±0.3	4.1±0.5	4.1±0.8	3.6±0.9	3.2±0.7	3.3±1.0	4.2±0.9	4.2±0.9	4.2±1.3	3.7±0.6	4.3±1.0	4.7±0.9
RCP8.5 - mid	4.2±0.5	4.2±0.4	4.1±0.6	3.6±0.5	3.0±0.5	4.0±1.4	4.3±0.9	4.7±1.1	4.2±1.3	3.7±0.8	4.3±0.8	4.8±0.8
RCP4.5 - end	4.2±0.4	4.3±0.4	4.1±0.4	3.6±0.5	2.9±0.5	3.2±0.9	4.5±1.4	4.6±1.1	3.9±0.8	3.7±0.8	4.3±0.8	4.3±0.7
RCP8.5 - end	4.2±0.5	4.1±0.5	3.8±0.5	3.2±0.4	3.0±0.6	3.3±1.3	4.0±0.8	4.8±1.3	4.1±0.9	3.4±0.7	4.4±0.9	4.5±1.0
Mean Wave Period (s)												
Hindcast	10±2	10±2	9±1	9±1	9±1	9±1	9±1	9±1	9±1	10±1	10±1	10±2
RCP4.5 - mid	10±2	9±2	9±1	9±1	9±1	8±1	9±1	9±1	9±1	9±1	10±1	10±2
RCP8.5 - mid	10±2	10±2	9±1	9±1	9±1	9±1	9±1	9±1	9±2	9±1	10±1	10±2
RCP4.5 - end	9±2	9±2	9±1	9±1	9±1	9±1	9±1	9±1	9±1	9±2	10±2	10±2
RCP8.5 - end	9±2	9±2	9±1	9±1	9±1	8±1	9±1	9±1	9±2	9±1	9±1	9±1
Top 5 percent Wave Period (s)												
Hindcast	10±1	10±2	10±1	10±1	10±1	9±1	10±1	10±1	10±1	11±1	11±1	11±1
RCP4.5 - mid	10±1	10±1	10±1	10±1	9±0.9	9±1	10±1	10±1	10±2	11±2	11±1	11±1
RCP8.5 - mid	10±1	10±1	10±1	10±1	9±0.9	10±1	10±1	10±1	10±1	10±2	11±1	11±1
RCP4.5 - end	10±1	10±2	10±1	10±0.9	9±0.9	9±1	10±1	10±1	10±1	10±2	11±1	10±1
RCP8.5 - end	10±1	9±0.9	10±1	10±0.9	9±0.8	9±1	10±1	10±1	10±1	10±2	11±1	10±0.9
Mean Wave Direction (°)												
Hindcast	65±20	63±20	69±18	74±13	79±17	84±28	92±55	111±76	74±67	62±39	70±25	69±19
RCP4.5 - mid	65±21	64±19	69±16	74±10	78±14	85±27	96±49	107±82	78±72	59±48	67±25	68±21
RCP8.5 - mid	65±20	65±19	69±16	74±13	79±11	88±29	93±52	126±78	77±81	59±42	68±23	69±20
RCP4.5 - end	65±21	63±20	69±15	73±12	80±13	85±23	95±54	118±76	77±81	58±45	68±21	69±18
RCP8.5 - end	64±21	64±20	68±15	75±11	80±10	88±28	93±48	116±68	87±81	60±46	69±21	70±17
Top 5 percent Wave Direction (°)												
Hindcast	64±15	57±23	68±28	71±24	86±40	134±94	217±57	214±50	208±79	83±79	81±52	76±23
RCP4.5 - mid	65±20	63±12	69±19	70±14	81±29	116±64	218±59	224±48	232±69	88±122	78±47	72±28
RCP8.5 - mid	63±15	64±14	65±16	74±17	82±17	154±77	223±50	223±34	233±37	89±83	78±44	78±25
RCP4.5 - end	67±14	54±24	66±13	70±14	85±27	116±68	218±60	229±37	239±49	88±113	76±41	68±27
RCP8.5 - end	66±18	65±16	65±13	73±12	82±15	128±68	221±60	220±41	220±55	84±96	84±39	79±29

Appendix A34. Table showing return values of ensemble-average significant wave heights of hindcast and forecast scenarios, including lower and higher 95 percent confidence intervals, at the Guam location.

[Years: Hindcast = 1976–2005; RCP mid = 2026–2045; RCP end = 2081–2100. Wave height values are in meters]

Scenario	Hindcast			RCP4.5 - mid			RCP8.5 - mid			RCP4.5 - end			RCP8.5 - end		
	Low	R_v	High	Low	R_v	High	Low	R_v	High	Low	R_v	High	Low	R_v	High
2-year	7.34	8.32	9.84	6.83	8.05	10.19	6.73	7.88	10.04	6.58	7.80	10.09	6.67	8.09	11.01
5-year	7.89	9.38	11.88	7.31	9.20	12.90	7.19	9.07	13.11	6.97	8.82	12.78	7.09	9.35	14.83
10-year	8.22	10.13	13.54	7.62	10.04	15.26	7.49	10.01	16.07	7.20	9.56	15.12	7.35	10.34	18.54
20-year	8.51	10.84	15.30	7.87	10.87	17.91	7.76	11.01	19.73	7.38	10.26	17.77	7.57	11.34	23.14
50-year	8.83	11.72	17.78	8.15	11.92	21.95	8.08	12.40	25.91	7.58	11.14	21.80	7.81	12.71	30.98
100-year	9.03	12.35	19.79	8.32	12.70	25.45	8.28	13.52	31.86	7.69	11.77	25.30	7.96	13.78	38.60

Appendix A35. Table showing Kwajalein monthly means and mean of the top 5 percent for significant wave height, peak wave period, and peak wave direction.

[Years: Hindcast = 1976–2005; RCP mid = 2026–2045; RCP end = 2081–2100. Wave directions are "coming from"]

Month	Jan	Feb	Mar	Apr	May	Jun	July	Aug	Sep	Oct	Nov	Dec
Mean Wave Height (m)												
Hindcast	2.4±0.5	2.3±0.5	2.2±0.5	1.9±0.5	1.5±0.4	1.3±0.4	1.2±0.4	1.1±0.4	1.1±0.4	1.4±0.5	1.9±0.6	2.3±0.6
RCP4.5 - mid	2.3±0.5	2.3±0.5	2.2±0.5	1.9±0.5	1.5±0.4	1.3±0.4	1.3±0.4	1.1±0.5	1.1±0.4	1.3±0.5	1.7±0.5	2.2±0.6
RCP8.5 - mid	2.3±0.5	2.3±0.5	2.1±0.5	1.9±0.5	1.5±0.5	1.3±0.4	1.3±0.5	1.2±0.5	1.1±0.4	1.3±0.4	1.8±0.6	2.2±0.6
RCP4.5 - end	2.3±0.5	2.2±0.5	2.2±0.5	1.8±0.5	1.5±0.4	1.4±0.5	1.2±0.4	1.2±0.5	1.1±0.4	1.3±0.5	1.7±0.6	2.2±0.6
RCP8.5 - end	2.2±0.5	2.2±0.5	2.0±0.5	1.8±0.4	1.5±0.4	1.4±0.4	1.3±0.4	1.2±0.5	1.1±0.4	1.2±0.4	1.6±0.5	2.1±0.5
Top 5 percent Wave Height (m)												
Hindcast	3.6±0.4	3.5±0.3	3.4±0.5	3.1±0.4	2.5±0.3	2.3±0.3	2.4±0.4	2.3±0.7	2.3±0.6	2.9±0.7	3.5±0.5	3.8±0.6
RCP4.5 - mid	3.5±0.3	3.5±0.4	3.3±0.3	3.0±0.2	2.5±0.3	2.4±0.3	2.4±0.4	2.5±0.7	2.2±0.5	2.6±0.6	3.2±0.4	3.6±0.4
RCP8.5 - mid	3.5±0.3	3.7±0.4	3.3±0.3	3.2±0.7	2.6±0.5	2.4±0.3	2.5±0.5	2.5±0.7	2.3±0.5	2.5±0.5	3.5±0.6	3.5±0.4
RCP4.5 - end	3.4±0.3	3.4±0.3	3.4±0.3	2.9±0.2	2.5±0.2	2.4±0.4	2.4±0.7	2.6±0.8	2.5±0.6	2.6±0.5	3.2±0.6	3.5±0.4
RCP8.5 - end	3.2±0.3	3.3±0.3	3.1±0.2	2.8±0.3	2.4±0.2	2.4±0.3	2.4±0.5	2.6±0.9	2.1±0.7	2.5±0.6	3.1±0.4	3.2±0.3
Mean Wave Period (s)												
Hindcast	11±2	10±2	10±2	9±2	9±1	9±2	9±2	9±2	9±2	10±2	10±2	11±2
RCP4.5 - mid	11±2	10±2	10±2	9±1	9±1	9±2	9±2	9±2	9±2	10±2	10±2	10±2
RCP8.5 - mid	11±2	10±2	10±2	9±2	9±1	9±2	9±1	9±2	9±2	10±2	10±2	11±2
RCP4.5 - end	11±2	11±2	10±2	9.5±2	8.9±1	8.7±1	8.9±1	9.1±2	9.2±2	9.8±2	10±2	11±2
RCP8.5 - end	11±2	10±2	10±2	9±2	9±1	9±1	9±1	9±2	9±2	10±2	10±2	10±2
Top 5 percent Wave Period (s)												
Hindcast	11±2	11±2	10±2	10±1	9±1	8±1	9±1	9±2	9±2	10±2	10±1	11±1
RCP4.5 - mid	11±3	11±2	10±2	10±1	9±1	8±1	8±1	9±2	9±2	10±2	10±2	10±2
RCP8.5 - mid	11±2	11±2	10±1	10±1	9±1	8±1	8±1	8±2	9±2	10±2	10±2	11±1
RCP4.5 - end	11±2	11±2	10±1	10±1	9±1	8±1	9±2	9±2	9±2	10±2	10±2	10±2
RCP8.5 - end	11±3	10±2	10±2	9±1	9±1	8±1	8±1	9±2	9±2	9±2	10±2	11±2
Mean Wave Direction (°)												
Hindcast	50±17	49±18	55±16	61±15	69±18	80±25	89±32	100±43	85±49	56±37	49±22	49±17
RCP4.5 - mid	49±17	50±18	55±15	62±14	69±15	80±21	90±33	104±39	95±41	60±39	48±22	51±18
RCP8.5 - mid	49±17	51±17	54±16	62±16	69±16	79±20	92±33	108±46	95±51	60±38	48±22	50±17
RCP4.5 - end	48±19	48±19	55±15	61±15	68±14	79±19	90±33	104±47	98±49	56±44	47±24	51±18
RCP8.5 - end	48±19	50±19	56±15	62±11	71±14	81±20	88±33	105±38	98±43	63±38	51±20	51±16
Top 5 percent Wave Direction (°)												
Hindcast	55±14	52±17	54±19	59±28	69±31	73±32	90±67	191±103	267±110	67±68	59±32	54±18
RCP4.5 - mid	49±18	57±17	56±12	62±18	69±18	74±40	93±56	172±89	194±127	47±105	49±28	55±17
RCP8.5 - mid	54±16	57±13	57±11	62±34	73±26	77±33	111±65	192±83	239±94	34±90	52±45	54±13
RCP4.5 - end	51±20	53±16	57±12	62±17	66±9	79±37	113±75	209±74	214±78	355±109	49±45	57±18
RCP8.5 - end	49±17	55±12	60±15	62±12	70±15	80±44	86±75	194±78	170±133	67±75	55±27	54±13

Appendix A36. Table showing return values of ensemble-average significant wave heights of hindcast and forecast scenarios, including lower and higher 95 percent confidence intervals, at the Kwajalein location.

[Years: Hindcast = 1976–2005; RCP mid = 2026–2045; RCP end = 2081–2100. Wave height values are in meters]

Scenario	Hindcast			RCP4.5 - mid			RCP8.5 - mid			RCP4.5 - end			RCP8.5 - end		
	Low	R_v	High	Low	R_v	High	Low	R_v	High	Low	R_v	High	Low	R_v	High
2-year	4.73	5.35	6.42	4.28	4.80	5.92	4.50	5.16	6.51	4.45	5.07	6.22	4.21	4.77	5.80
5-year	5.15	6.30	8.55	4.45	5.35	7.64	4.76	5.91	8.70	4.74	5.81	8.11	4.48	5.46	7.58
10-year	5.48	7.18	10.87	4.57	5.82	9.51	4.94	6.56	11.10	4.95	6.45	10.09	4.69	6.08	9.48
20-year	5.83	8.23	14.07	4.68	6.34	12.07	5.11	7.31	14.39	5.15	7.17	12.71	4.89	6.79	12.03
50-year	6.31	9.94	20.21	4.81	7.13	16.96	5.32	8.47	20.72	5.40	8.27	17.50	5.14	7.90	16.83
100-year	6.69	11.54	26.92	4.90	7.82	22.27	5.47	9.49	27.63	5.59	9.23	22.51	5.33	8.89	21.95

Appendix A37. Table showing Wake monthly means and mean of the top 5 percent for significant wave height, peak wave period, and peak wave direction.

[Years: Hindcast = 1976–2005; RCP mid = 2026–2045; RCP end = 2081–2100. Wave directions are "coming from"]

Month	Jan	Feb	Mar	Apr	May	Jun	July	Aug	Sep	Oct	Nov	Dec
Mean Wave Height (m)												
Hindcast	3.0±0.8	2.9±0.8	2.8±0.8	2.6±0.7	2.2±0.6	2.1±0.6	2.1±0.7	2.1±0.7	2.1±0.8	2.7±0.9	2.9±0.8	3.1±0.8
RCP4.5 - mid	3.0±0.8	2.9±0.7	2.8±0.8	2.6±0.7	2.2±0.6	2.0±0.6	2.1±0.7	2.0±0.7	2.0±0.8	2.6±0.9	2.9±0.8	3.0±0.8
RCP8.5 - mid	3.0±0.8	2.9±0.8	2.7±0.7	2.6±0.7	2.2±0.6	2.0±0.5	2.1±0.6	2.1±0.8	2.1±0.8	2.5±0.9	3.0±0.9	3.0±0.8
RCP4.5 - end	3.0±0.8	2.9±0.8	2.8±0.7	2.6±0.7	2.2±0.5	2.1±0.5	2.1±0.7	2.1±0.8	2.0±0.8	2.5±0.9	2.9±0.9	3.0±0.8
RCP8.5 - end	2.9±0.8	2.8±0.7	2.6±0.7	2.5±0.6	2.1±0.5	2.0±0.5	2.1±0.6	2.0±0.9	2.0±0.8	2.4±0.8	2.8±0.8	2.9±0.8
Top 5 percent Wave Height (m)												
Hindcast	5.0±0.6	5.0±0.6	4.7±0.5	4.4±0.5	3.6±0.3	3.7±0.7	3.9±0.8	4.2±0.9	4.6±1.0	5.2±0.8	5.0±0.6	5.3±0.7
RCP4.5 - mid	5.0±0.5	4.8±0.5	4.8±0.6	4.3±0.4	3.6±0.4	3.5±0.6	4.0±0.7	3.9±0.8	4.4±0.9	5.3±1.0	5.1±0.6	4.9±0.5
RCP8.5 - mid	.05±0.5	4.9±0.5	4.6±0.5	4.5±0.9	3.6±0.5	3.3±0.4	3.8±0.9	4.6±1.3	4.6±1.2	5.0±0.9	5.3±0.6	5.0±0.5
RCP4.5 - end	4.8±0.5	4.9±0.5	4.7±0.4	4.4±0.5	3.5±0.3	3.4±0.7	4.0±1.0	4.6±0.9	4.4±1.0	4.9±0.9	5.1±0.7	4.8±0.5
RCP8.5 - end	4.8±0.5	4.6±0.3	4.2±0.4	4.0±0.4	3.3±0.3	3.3±0.8	3.8±1.0	4.9±1.4	4.4±1.2	4.6±0.9	4.9±0.9	4.8±0.4
Mean Wave Period (s)												
Hindcast	11±2	11±2	10±2	9±1	9±1	9±1	9±1	9±1	9±1	10±1	10±2	11±2
RCP4.5 - mid	11±2	11±2	10±2	10±1	9±1	9±1	9±1	9±1	9±1	9±1	10±2	11±2
RCP8.5 - mid	11±2	11±2	10±2	10±1	9±1	9±1	9±1	9±1	9±1	9±1	10±2	11±2
RCP4.5 - end	11±2	11±2	10±2	9.6±1	8.9±1	8.7±1	8.7±1	8.8±1	8.8±1	9.4±1	10±2	11±2
RCP8.5 - end	11±2	11±2	10±2	9±1	9±1	9±1	9±1	9±1	9±2	9±1	10±2	11±2
Top 5 percent Wave Period (s)												
Hindcast	13±2	13±2	11±2	10±1	10±0.8	10±0.9	10±1	10±2	10±1	11±0.9	11±1	12±2
RCP4.5 - mid	13±2	13±2	12±2	10±1	10±1	9±1	10±1	11±2	11±2	11±1	11±2	12±2
RCP8.5 - mid	13±2	12±2	11±2	11±1	9±0.7	9±0.7	10±1	11±2	10±1	11±1	11±1	12±2
RCP4.5 - end	13±2	13±2	12±2	10±1	10±1	9±1	10±1	11±1	10±1	11±1	11±1	12±2
RCP8.5 - end	13±2	12±2	11±2	10±1	9±0.8	9±1	10±2	11±2	10±1	10±1	11±1	12±2
Mean Wave Direction (°)												
Hindcast	29±43	26±46	51±39	73±21	83±15	89±15	90±25	92±36	77±36	70±24	62±28	45±38
RCP4.5 - mid	27±43	28±43	50±39	73±21	82±16	90±15	93±27	95±36	82±35	71±27	63±25	47±38
RCP8.5 - mid	29±43	33±44	49±41	73±25	83±15	90±14	93±27	97±43	83±41	70±23	66±23	47±38
RCP4.5 - end	22±44	24±44	53±38	73±25	82±16	91±12	93±25	96±37	83±36	69±26	64±26	49±37
RCP8.5 - end	26±43	28±44	50±39	73±23	84±15	92±13	94±24	99±34	86±39	71±29	66±22	49±35
Top 5 percent Wave Direction (°)												
Hindcast	24±52	6±52	48±41	70±17	83±19	91±25	100±52	153±78	91±63	79±35	64±27	54±37
RCP4.5 - mid	3±46	17±49	52±40	73±18	76±17	89±26	124±67	133±70	113±79	83±50	62±23	43±43
RCP8.5 - mid	29±53	40±52	56±41	70±24	79±13	90±15	117±64	180±79	118±74	74±36	70±22	45±40
RCP4.5 - end	9±49	11±54	55±41	73±25	77±18	92±17	122±59	190±75	132±77	73±41	68±28	49±40
RCP8.5 - end	3±45	23±52	52±43	71±19	76±13	90±17	112±58	194±70	152±86	79±44	69±22	47±36

Appendix A38. Table showing return values of ensemble-average significant wave heights of hindcast and forecast scenarios, including lower and higher 95 percent confidence intervals, at the Wake location.

[Years: Hindcast = 1976–2005; RCP mid = 2026–2045; RCP end = 2081–2100. Wave height values are in meters]

Scenario	Hindcast			RCP4.5 - mid			RCP8.5 - mid			RCP4.5 - end			RCP8.5 - end		
	Low	R_v	High	Low	R_v	High	Low	R_v	High	Low	R_v	High	Low	R_v	High
2-year	7.14	7.90	9.11	6.68	7.37	8.58	6.96	7.89	9.54	6.76	7.75	9.73	6.73	8.09	11.02
5-year	7.54	8.72	10.77	6.97	8.07	10.27	7.37	8.87	11.89	7.08	8.70	12.48	7.24	9.69	16.11
10-year	7.80	9.32	12.15	7.17	8.61	11.81	7.64	9.64	14.09	7.30	9.46	15.21	7.61	11.17	22.03
20-year	8.02	9.89	13.67	7.33	9.17	13.63	7.88	10.43	16.73	7.48	10.25	18.66	7.97	12.93	30.65
50-year	8.26	10.62	15.87	7.53	9.92	16.56	8.16	11.53	21.05	7.69	11.37	24.64	8.43	15.78	48.34
100-year	8.42	11.16	17.72	7.65	10.50	19.25	8.35	12.40	25.10	7.83	12.27	30.56	8.77	18.42	68.94

Appendix A39. Table showing Johnston Atoll monthly means and mean of the top 5 percent for significant wave height, peak wave period, and peak wave direction.

[Years: Hindcast = 1976–2005; RCP mid = 2026–2045; RCP end = 2081–2100. Wave directions are "coming from"]

Month	Jan	Feb	Mar	Apr	May	Jun	July	Aug	Sep	Oct	Nov	Dec
Mean Wave Height (m)												
Hindcast	3.4±0.8	3.2±0.8	3.1±0.8	2.8±0.7	2.4±0.6	2.4±0.5	2.3±0.5	2.1±0.5	2.1±0.5	2.5±0.8	3.1±0.8	3.3±0.8
RCP4.5 - mid	3.3±0.8	3.3±0.8	3.1±0.7	2.9±0.7	2.4±0.5	2.3±0.5	2.3±0.5	2.1±0.5	2.0±0.5	2.4±0.7	3.0±0.8	3.3±0.8
RCP8.5 - mid	3.3±0.8	3.2±0.8	3.0±0.8	2.8±0.6	2.3±0.5	2.3±0.5	2.3±0.5	2.1±0.5	2.0±0.5	2.4±0.7	3.0±0.8	3.3±0.8
RCP4.5 - end	3.3±0.7	3.2±0.8	3.1±0.7	2.8±0.6	2.4±0.5	2.3±0.5	2.2±0.5	2.2±0.6	2.0±0.5	2.4±0.8	3.0±0.8	3.3±0.8
RCP8.5 - end	3.2±0.8	3.1±0.8	2.9±0.7	2.7±0.6	2.3±0.5	2.2±0.4	2.3±0.5	2.1±0.5	2.0±0.5	2.3±0.6	2.8±0.7	3.2±0.8
Top 5 percent Wave Height (m)												
Hindcast	5.4±0.5	5.2±0.5	4.9±0.4	4.4±0.4	3.7±0.4	3.6±0.5	3.6±0.5	3.4±0.7	3.5±0.5	4.7±0.7	5.2±0.5	5.3±0.5
RCP4.5 - mid	5.3±0.5	5.2±0.4	4.9±0.4	4.7±0.4	3.7±0.4	3.4±0.4	3.4±0.4	3.6±0.9	3.5±0.6	4.3±0.6	5.0±0.6	5.2±0.4
RCP8.5 - mid	5.3±0.5	5.3±0.4	4.9±0.4	4.3±0.4	3.5±0.3	3.3±0.3	3.5±0.5	3.5±0.8	3.5±0.7	4.5±0.7	4.9±0.5	5.4±0.4
RCP4.5 - end	5.1±0.4	5.3±0.5	4.8±0.5	4.2±0.3	3.7±0.5	3.5±0.3	3.5±0.5	3.8±1.0	3.3±0.6	4.6±1.0	5.1±0.5	5.1±0.3
RCP8.5 - end	5.1±0.5	5.1±0.6	4.7±0.4	4.1±0.3	3.4±0.3	3.3±0.4	3.5±0.6	3.4±0.6	3.4±1.0	4.0±0.9	4.7±0.5	5.1±0.4
Mean Wave Period (s)												
Hindcast	12±2	12±2	11±2	10±2	9±2	9±2	9±2	9±2	10±2	10±2	11±2	12±2
RCP4.5 - mid	12±2	12±2	11±2	10±2	9±2	9±2	9±2	9±2	10±3	10±2	11±2	12±2
RCP8.5 - mid	12±2	12±2	11±2	10±2	9±2	9±2	9±3	9±3	10±3	10±2	11±2	12±2
RCP4.5 - end	12±2	12±2	11±2	10±2	9.4±2	9.2±2	9.2±2	9.3±2	9.7±2	10±2	11±2	12±2
RCP8.5 - end	12±2	12±2	11±2	10±2	9±2	9±3	9±2	9±3	10±3	10±2	11±2	12±2
Top 5 percent Wave Period (s)												
Hindcast	14±3	14±3	11±2	10±2	10±1	9±0.6	9±0.8	9±2	10±2	11±2	12±2	13±3
RCP4.5 - mid	15±2	14±3	12±3	10±1	10±1	9±0.6	9±1	9±2	10±2	11±2	12±2	13±3
RCP8.5 - mid	13±3	13±3	11±2	10±2	9±1	9±1	9±0.7	9±2	10±2	11±2	12±2	13±3
RCP4.5 - end	14±3	13±3	12±2	11±2	10±2	9±1	9±0.8	10±2	10±2	10±1	11±2	13±3
RCP8.5 - end	14±3	13±3	12±3	10±2	9±2	9±1	9±1	10±2	10±2	10±2	12±2	13±3
Mean Wave Direction (°)												
Hindcast	14±41	13±44	43±39	67±27	83±18	91±14	94±19	96±28	85±39	61±36	44±33	28±40
RCP4.5 - mid	9±39	18±42	40±39	68±25	84±20	93±16	94±18	98±28	92±36	61±37	47±33	28±38
RCP8.5 - mid	16±41	17±41	38±41	67±26	84±19	93±14	95±20	99±32	91±41	60±35	45±31	30±38
RCP4.5 - end	7±41	11±43	41±38	63±28	83±19	93±14	95±19	98±32	89±39	63±41	47±32	30±38
RCP8.5 - end	11±40	12±42	38±40	67±27	85±19	96±14	95±16	99±29	95±39	65±34	49±29	28±38
Top 5 percent Wave Direction (°)												
Hindcast	6±43	8±50	47±35	62±24	74±14	87±12	89±22	96±41	78±50	65±42	52±39	27±46
RCP4.5 - mid	352±36	10±48	46±39	71±14	77±15	88±16	88±32	106±52	102±70	65±54	48±42	19±43
RCP8.5 - mid	26±45	28±47	49±36	63±23	79±14	87±10	90±27	106±47	100±76	60±45	45±36	33±46
RCP4.5 - end	354±45	10±50	43±36	60±26	77±14	87±14	88±23	102±71	97±71	71±63	61±28	23±44
RCP8.5 - end	353±40	8±46	40±44	66±22	76±17	90±12	89±25	97±52	113±71	68±44	47±34	28±47

Appendix A40. Table showing return values of ensemble-average significant wave heights of hindcast and forecast scenarios, including lower and higher 95 percent confidence intervals, at the Johnston Atoll location.

[Years: Hindcast = 1976–2005; RCP mid = 2026–2045; RCP end = 2081–2100. Wave height values are in meters]

Scenario	Hindcast			RCP4.5 - mid			RCP8.5 - mid			RCP4.5 - end			RCP8.5 - end		
	Low	R_v	High	Low	R_v	High	Low	R_v	High	Low	R_v	High	Low	R_v	High
2-year	6.50	7.00	7.86	6.47	6.98	7.83	6.32	6.78	7.60	6.44	7.13	8.45	6.39	6.95	7.87
5-year	6.75	7.58	9.15	6.71	7.50	9.00	6.49	7.18	8.61	6.76	7.96	10.66	6.66	7.53	9.12
10-year	6.92	8.03	10.33	6.86	7.90	10.03	6.58	7.47	9.48	6.99	8.70	13.02	6.83	7.96	10.18
20-year	7.08	8.49	11.74	6.99	8.30	11.19	6.66	7.75	10.46	7.21	9.54	16.21	6.99	8.39	11.37
50-year	7.26	9.14	14.01	7.15	8.82	12.99	6.75	8.11	11.95	7.49	10.83	22.20	7.16	8.94	13.15
100-year	7.38	9.64	16.10	7.25	9.21	14.57	6.80	8.37	13.24	7.69	11.98	28.60	7.27	9.35	14.67

Appendix A41. Table showing Kingman Reef monthly means and mean of the top 5 percent for significant wave height, peak wave period, and peak wave direction.

[Years: Hindcast = 1976–2005; RCP mid = 2026–2045; RCP end = 2081–2100. Wave directions are "coming from"]

Month	Jan	Feb	Mar	Apr	May	Jun	July	Aug	Sep	Oct	Nov	Dec
Mean Wave Height (m)												
Hindcast	2.9±0.6	2.9±0.6	2.7±0.6	2.4±0.5	2.1±0.5	2.1±0.4	2.0±0.4	1.9±0.4	1.8±0.4	1.9±0.4	2.3±0.6	2.7±0.6
RCP4.5 - mid	2.9±0.6	2.9±0.6	2.8±0.6	2.5±0.5	2.2±0.5	2.1±0.4	2.0±0.4	1.9±0.4	1.8±0.3	1.9±0.4	2.3±0.5	2.7±0.6
RCP8.5 - mid	2.9±0.6	2.9±0.6	2.7±0.6	2.5±0.5	2.2±0.5	2.1±0.4	2.0±0.4	1.9±0.4	1.8±0.3	1.9±0.4	2.2±0.5	2.7±0.6
RCP4.5 - end	2.8±0.6	2.9±0.6	2.7±0.6	2.4±0.5	2.2±0.5	2.1±0.4	2.0±0.4	1.9±0.4	1.8±0.3	1.9±0.4	2.2±0.6	2.7±0.6
RCP8.5 - end	2.8±0.6	2.8±0.6	2.6±0.6	2.4±0.5	2.2±0.4	2.1±0.4	2.0±0.3	1.9±0.3	1.8±0.3	1.8±0.3	2.1±0.5	2.6±0.6
Top 5 percent Wave Height (m)												
Hindcast	4.4±0.4	4.3±0.3	4.1±0.3	3.6±0.3	3.2±0.2	3.1±0.2	2.9±0.2	2.8±0.2	2.6±0.2	3.1±0.4	4.0±0.9	4.2±0.4
RCP4.5 - mid	4.3±0.3	4.3±0.3	4.2±0.3	3.8±0.3	3.4±0.5	3.1±0.2	2.9±0.2	2.8±0.3	2.6±0.2	2.8±0.2	3.6±0.3	4.2±0.3
RCP8.5 - mid	4.4±0.4	4.3±0.3	4.2±0.4	3.6±0.3	3.3±0.3	3.0±0.2	2.9±0.2	2.7±0.2	2.6±0.2	2.9±0.3	3.5±0.4	4.2±0.3
RCP4.5 - end	4.3±0.3	4.4±0.3	4.0±0.2	3.8±0.3	3.3±0.4	3.2±0.3	2.8±0.2	2.8±0.3	2.5±0.2	2.8±0.3	3.7±0.7	4.1±0.4
RCP8.5 - end	4.1±0.3	4.2±0.4	4.0±0.3	3.6±0.2	3.2±0.2	3.1±0.2	2.8±0.2	2.8±0.4	2.5±0.3	2.7±0.3	3.3±0.3	4.2±0.4
Mean Wave Period (s)												
Hindcast	12±3	12±3	11±2	11±3	11±3	10±3	10±3	11±3	11±3	11±2	12±2	12±2
RCP4.5 - mid	13±3	12±3	11±3	11±3	10±3	10±3	10±3	10±3	11±3	11±3	12±2	12±3
RCP8.5 - mid	12±3	12±3	11±3	10±3	10±3	10±3	10±3	11±3	11±3	12±3	12±2	12±3
RCP4.5 - end	12±3	12±3	11±2	11±3	10±3	10±3	11±3	11±3	11±3	11±3	12±2	12±3
RCP8.5 - end	12±3	12±3	11±3	10±3	10±3	10±3	10±3	11±3	11±3	11±3	11±3	12±3
Top 5 percent Wave Period (s)												
Hindcast	13±3	13±3	11±2	10±2	11±3	11±3	12±3	12±3	12±3	12±2	12±3	13±3
RCP4.5 - mid	14±3	13±3	11±2	11±2	11±3	10±3	11±3	12±3	13±3	13±3	13±3	14±3
RCP8.5 - mid	13±3	13±3	11±2	10±2	10±2	11±3	12±3	12±3	13±3	13±3	13±3	13±3
RCP4.5 - end	14±3	13±3	11±2	11±2	10±3	11±3	12±4	12±3	12±3	12±3	12±2	14±3
RCP8.5 - end	15±3	13±3	12±3	10±2	10±3	11±4	11±3	12±3	12±3	13±3	13±3	14±3
Mean Wave Direction (°)												
Hindcast	24±28	25±31	41±29	62±29	88±31	101±28	116±25	124±25	123±35	82±50	35±38	27±29
RCP4.5 - mid	21±28	28±27	41±27	61±26	84±30	100±27	114±23	124±23	128±26	92±51	37±40	25±29
RCP8.5 - mid	26±27	28±28	38±29	60±26	85±29	100±26	116±23	126±24	129±30	96±49	36±39	26±28
RCP4.5 - end	22±29	23±29	39±27	60±28	85±29	101±27	117±24	127±28	130±29	97±53	36±39	27±30
RCP8.5 - end	23±28	27±29	39±28	62±26	84±25	99±25	114±24	127±25	132±28	105±47	45±40	26±29
Top 5 percent Wave Direction (°)												
Hindcast	20±33	27±32	44±23	54±21	76±28	91±29	120±36	127±25	127±39	42±51	30±47	21±36
RCP4.5 - mid	11±35	25±32	44±23	57±16	70±33	90±25	112±30	129±30	132±35	55±67	17±39	21±32
RCP8.5 - mid	24±30	27±32	47±21	56±11	76±25	97±32	117±30	124±27	136±32	65±68	18±34	21±39
RCP4.5 - end	20±35	23±36	45±23	50±22	76±32	92±36	123±32	139±42	142±42	29±67	30±37	18±34
RCP8.5 - end	7±32	25±35	41±25	59±17	73±27	94±39	113±35	137±43	142±42	59±85	25±31	26±33

Appendix A42. Table showing return values of ensemble-average significant wave heights of hindcast and forecast scenarios, including lower and higher 95 percent confidence intervals, at the Kingman Reef location.

[Years: Hindcast = 1976–2005; RCP mid = 2026–2045; RCP end = 2081–2100. Wave height values are in meters]

Scenario	Hindcast			RCP4.5 - mid			RCP8.5 - mid			RCP4.5 - end			RCP8.5 - end		
	Low	R_v	High	Low	R_v	High	Low	R_v	High	Low	R_v	High	Low	R_v	High
2-year	5.01	5.37	5.96	5.01	5.36	5.93	4.88	5.26	5.96	4.94	5.35	6.10	4.81	5.13	5.64
5-year	5.26	5.91	7.13	5.21	5.78	6.80	5.02	5.63	6.91	5.14	5.83	7.24	4.97	5.47	6.35
10-year	5.46	6.41	8.36	5.35	6.10	7.57	5.11	5.91	7.79	5.28	6.22	8.35	5.08	5.72	6.95
20-year	5.67	6.99	9.99	5.48	6.44	8.48	5.19	6.20	8.83	5.41	6.65	9.73	5.17	5.97	7.62
50-year	5.95	7.91	13.00	5.63	6.91	9.92	5.28	6.59	10.54	5.56	7.26	12.10	5.28	6.29	8.62
100-year	6.17	8.74	16.16	5.73	7.28	11.22	5.34	6.89	12.12	5.67	7.76	14.41	5.34	6.53	9.47

Appendix A43. Table showing Palmyra monthly means and mean of the top 5 percent for significant wave height, peak wave period, and peak wave direction.

[Years: Hindcast = 1976–2005; RCP mid = 2026–2045; RCP end = 2081–2100. Wave directions are "coming from"]

Month	Jan	Feb	Mar	Apr	May	Jun	July	Aug	Sep	Oct	Nov	Dec
Mean Wave Height (m)												
Hindcast	2.9±0.6	2.8±0.6	2.6±0.5	2.3±0.5	2.1±0.4	2±0.4	2.0±0.4	1.9±0.4	1.8±0.4	1.9±0.4	2.3±0.6	2.7±0.6
RCP4.5 - mid	2.8±0.6	2.9±0.6	2.7±0.6	2.4±0.5	2.2±0.5	2.1±0.4	2.0±0.4	1.9±0.4	1.8±0.3	1.9±0.4	2.2±0.5	2.6±0.6
RCP8.5 - mid	2.8±0.6	2.8±0.6	2.6±0.6	2.4±0.5	2.1±0.4	2.0±0.4	2.0±0.4	1.9±0.4	1.8±0.3	1.9±0.4	2.2±0.5	2.6±0.6
RCP4.5 - end	2.8±0.6	2.8±0.6	2.7±0.5	2.4±0.5	2.2±0.5	2.1±0.4	2.0±0.4	1.9±0.4	1.8±0.3	1.9±0.4	2.2±0.6	2.6±0.6
RCP8.5 - end	2.7±0.5	2.7±0.6	2.6±0.5	2.4±0.5	2.2±0.4	2.1±0.4	2.0±0.3	1.9±0.3	1.8±0.3	1.8±0.3	2.1±0.4	2.6±0.6
Top 5 percent Wave Height (m)												
Hindcast	4.3±0.4	4.2±0.3	4.0±0.3	3.5±0.3	3.1±0.2	3.0±0.2	2.9±0.2	2.8±0.2	2.6±0.2	3.0±0.4	3.9±0.9	4.1±0.4
RCP4.5 - mid	4.2±0.3	4.2±0.3	4.1±0.3	3.7±0.3	3.3±0.4	3.1±0.2	2.9±0.2	2.8±0.2	2.6±0.2	2.7±0.2	3.5±0.3	4.1±0.3
RCP8.5 - mid	4.2±0.4	4.2±0.3	4.1±0.4	3.5±0.3	3.2±0.3	2.9±0.2	2.9±0.2	2.7±0.2	2.6±0.2	2.8±0.3	3.4±0.4	4.0±0.3
RCP4.5 - end	4.2±0.3	4.3±0.3	3.9±0.2	3.7±0.3	3.2±0.3	3.1±0.3	2.8±0.2	2.8±0.3	2.5±0.3	2.8±0.4	3.6±0.7	4.0±0.4
RCP8.5 - end	4.0±0.3	4.1±0.4	3.9±0.3	3.5±0.2	3.1±0.2	3.0±0.2	2.8±0.2	2.8±0.4	2.5±0.2	2.7±0.3	3.2±0.3	4.1±0.4
Mean Wave Period (s)												
Hindcast	12±3	12±3	11±2	11±3	11±3	10±3	11±3	11±3	11±3	11±3	12±2	12±2
RCP4.5 - mid	13±3	12±3	11±3	11±3	11±3	10±3	10±3	11±3	11±3	11±3	12±2	12±3
RCP8.5 - mid	12±3	12±3	11±3	11±3	11±3	10±3	10±3	11±3	11±3	12±3	12±2	12±2
RCP4.5 - end	12±3	12±3	11±2	11±3	11±3	11±3	11±3	11±3	11±3	12±3	12±2	12±3
RCP8.5 - end	12±3	12±3	11±3	11±3	11±3	11±3	10±3	11±3	11±3	12±3	12±3	12±3
Top 5 percent Wave Period (s)												
Hindcast	14±3	13±3	12±2	11±2	11±3	11±3	12±3	12±3	12±3	12±2	13±3	13±3
RCP4.5 - mid	14±3	13±3	12±3	11±2	11±3	11±3	12±3	12±3	13±3	13±3	14±3	14±3
RCP8.5 - mid	13±3	13±3	11±2	10±2	11±3	12±3	12±3	12±3	13±3	13±3	13±3	14±3
RCP4.5 - end	14±3	13±3	11±2	11±2	11±3	11±3	12±4	12±3	12±3	12±3	12±2	14±3
RCP8.5 - end	15±3	13±3	12±3	10±2	11±3	12±4	11±3	12±3	13±3	13±3	13±3	14±3
Mean Wave Direction (°)												
Hindcast	23±28	24±31	40±29	62±31	91±32	104±28	118±24	125±24	124±33	86±50	36±39	27±29
RCP4.5 - mid	20±28	26±27	39±28	61±28	87±32	103±27	116±22	125±22	130±25	96±50	38±42	24±29
RCP8.5 - mid	24±27	27±28	37±30	60±28	87±31	103±26	118±22	127±22	130±28	101±48	37±41	25±29
RCP4.5 - end	21±29	22±29	38±27	60±30	88±31	104±27	120±23	129±26	131±28	101±52	37±41	26±31
RCP8.5 - end	22±29	26±29	37±28	62±28	86±27	103±25	117±23	128±24	133±26	109±45	47±41	26±30
Top 5 percent Wave Direction (°)												
Hindcast	17±34	24±32	41±23	53±25	80±34	96±31	125±34	128±22	129±34	47±56	25±47	17±36
RCP4.5 - mid	7±36	22±32	41±24	57±19	75±40	95±28	118±27	130±26	135±32	72±71	15±38	17±31
RCP8.5 - mid	20±31	24±32	45±21	54±12	79±28	103±34	123±28	128±25	136±28	71±71	15±34	17±39
RCP4.5 - end	17±34	20±35	43±26	48±24	79±38	100±39	128±30	140±37	145±38	34±70	23±40	13±34
RCP8.5 - end	5±32	22±35	38±26	58±18	75±31	99±42	121±32	137±37	142±36	75±84	23±32	23±33

Appendix A44. Table showing return values of ensemble-average significant wave heights of hindcast and forecast scenarios, including lower and higher 95 percent confidence intervals, at the Palmyra location.

[Years: Hindcast = 1976–2005; RCP mid = 2026–2045; RCP end = 2081–2100. Wave height values are in meters]

Scenario	Hindcast			RCP4.5 - mid			RCP8.5 - mid			RCP4.5 - end			RCP8.5 - end		
	Low	R_v	High	Low	R_v	High	Low	R_v	High	Low	R_v	High	Low	R_v	High
2-year	4.91	5.24	5.78	4.85	5.19	5.78	4.76	5.12	5.76	4.79	5.20	5.93	4.68	4.99	5.50
5-year	5.17	5.76	6.81	5.02	5.58	6.63	4.89	5.43	6.54	4.98	5.66	7.07	4.83	5.31	6.16
10-year	5.37	6.22	7.86	5.14	5.88	7.42	4.97	5.66	7.21	5.12	6.05	8.21	4.93	5.54	6.72
20-year	5.57	6.75	9.20	5.24	6.19	8.35	5.03	5.88	7.97	5.24	6.48	9.66	5.01	5.76	7.34
50-year	5.85	7.56	11.58	5.37	6.62	9.86	5.10	6.16	9.13	5.40	7.10	12.20	5.10	6.05	8.24
100-year	6.07	8.27	13.97	5.45	6.96	11.24	5.14	6.37	10.12	5.51	7.63	14.74	5.16	6.26	9.00

Appendix A45. Table showing Rose Atoll monthly means and mean of the top 5 percent for significant wave height, peak wave period, and peak wave direction.

[Years: Hindcast = 1976–2005; RCP mid = 2026–2045; RCP end = 2081–2100. Wave directions are "coming from"]

Month	Jan	Feb	Mar	Apr	May	Jun	July	Aug	Sep	Oct	Nov	Dec
Mean Wave Height (m)												
Hindcast	2.2±0.7	2.2±0.7	2.2±0.6	2.2±0.6	2.4±0.7	2.5±0.7	2.5±0.7	2.4±0.7	2.4±0.6	2.3±0.6	2.2±0.6	2.1±0.5
RCP4.5 - mid	2.2±0.7	2.1±0.6	2.2±0.6	2.3±0.6	2.4±0.6	2.5±0.7	2.5±0.7	2.4±0.6	2.5±0.7	2.3±0.6	2.2±0.6	2.1±0.5
RCP8.5 - mid	2.1±0.6	2.2±0.7	2.2±0.7	2.3±0.6	2.4±0.6	2.4±0.7	2.5±0.7	2.5±0.7	2.4±0.7	2.4±0.6	2.2±0.6	2.2±0.7
RCP4.5 - end	2.1±0.6	2.2±0.6	2.1±0.6	2.3±0.7	2.5±0.7	2.5±0.7	2.5±0.7	2.5±0.6	2.4±0.6	2.3±0.6	2.2±0.6	2.2±0.7
RCP8.5 - end	2.1±0.7	2.2±0.7	2.1±0.6	2.2±0.5	2.4±0.7	2.5±0.7	2.5±0.6	2.5±0.7	2.5±0.7	2.4±0.6	2.1±0.5	2.1±0.5
Top 5 percent Wave Height (m)												
Hindcast	4.4±1.0	4.3±1.4	4.0±0.7	3.9±0.7	4.3±0.6	4.2±0.5	4.1±0.5	4.1±0.4	3.9±0.4	3.9±0.4	3.9±0.6	3.5±0.7
RCP4.5 - mid	4.1±1.3	3.9±1.1	3.9±1.0	4.1±0.7	4.1±0.5	4.2±0.4	4.2±0.3	4.1±0.4	4.2±0.4	3.9±0.3	4.0±0.6	3.5±0.6
RCP8.5 - mid	4.0±1.0	4.4±1.1	4.2±1.0	3.9±0.6	4.1±0.4	4.2±0.4	4.2±0.4	4.2±0.4	4.2±0.4	4.0±0.4	3.8±0.6	4.3±1.3
RCP4.5 - end	4.0±1.0	4.1±0.9	3.9±1.2	4.2±0.7	4.5±0.6	4.2±0.4	4.3±0.5	4.1±0.4	4.2±0.4	4.0±0.5	3.9±0.7	4.1±1.1
RCP8.5 - end	4.4±1.6	4.6±1.0	3.9±1.0	3.7±0.6	4.3±0.5	4.4±0.5	4.2±0.4	4.3±0.4	4.2±0.4	3.9±0.4	3.5±0.5	3.6±0.5
Mean Wave Period (s)												
Hindcast	12±3	12±2	12±2	11±2	11±3	11±3	11±3	11±3	11±3	11±3	11±3	12±3
RCP4.5 - mid	12±3	12±3	12±2	12±2	11±3	11±3	11±3	11±3	11±3	11±3	12±3	12±3
RCP8.5 - mid	12±3	12±2	12±2	11±2	11±3	11±3	11±3	11±3	11±3	11±3	12±3	12±3
RCP4.5 - end	12±3	12±2	12±2	12±2	11±3	11±3	11±3	11±3	11±3	11±3	11±3	12±3
RCP8.5 - end	12±3	12±3	12±2	12±3	11±3	11±3	11±3	11±3	11±3	11±3	11±3	12±3
Top 5 percent Wave Period (s)												
Hindcast	11±2	11±2	11±2	11±2	11±2	10±2	11±3	10±2	10±2	10±2	10±2	10±3
RCP4.5 - mid	11±3	11±2	11±2	11±2	11±2	10±2	11±2	11±2	10±1	10±2	10±2	11±3
RCP8.5 - mid	11±2	10±2	11±2	10±2	11±2	11±2	11±2	10±2	10±2	10±2	10±2	10±2
RCP4.5 - end	10±2	11±2	11±2	11±2	10±2	11±2	11±3	10±2	10±2	10±2	10±1	10±2
RCP8.5 - end	10±2	10±2	10±2	11±2	10±2	11±3	10±2	10±2	10±2	10±2	10±2	11±3
Mean Wave Direction (°)												
Hindcast	30±51	31±65	91±81	134±45	141±31	137±29	136±29	132±28	131±27	124±30	101±47	56±49
RCP4.5 - mid	33±50	28±59	76±79	133±48	139±28	134±30	135±28	131±26	129±25	126±28	105±46	62±53
RCP8.5 - mid	40±46	34±61	89±86	135±43	139±26	140±29	136±29	136±27	130±25	126±27	104±42	60±52
RCP4.5 - end	36±50	23±63	72±82	133±47	138±28	135±28	135±28	132±26	130±24	128±28	106±43	63±52
RCP8.5 - end	40±49	32±61	77±84	134±42	139±28	134±26	134±26	131±26	129±23	126±24	110±37	63±47
Top 5 percent Wave Direction (°)												
Hindcast	5±73	357±88	84±106	132±41	124±34	127±29	135±24	125±17	121±26	120±29	105±38	60±60
RCP4.5 - mid	357±66	350±65	61±115	132±49	133±24	125±27	130±21	128±17	121±16	121±20	102±42	89±66
RCP8.5 - mid	37±72	345±79	57±98	133±39	129±27	133±24	131±26	130±19	123±17	120±24	102±43	75±57
RCP4.5 - end	24±80	347±74	47±100	121±54	128±22	132±29	128±19	128±25	123±19	119±19	111±33	82±58
RCP8.5 - end	9±75	338±61	349±111	134±50	123±32	131±20	128±22	128±21	125±19	119±20	115±30	87±44

Appendix A46. Table showing return values of ensemble-average significant wave heights of hindcast and forecast scenarios, including lower and higher 95 percent confidence intervals, at the Rose Atoll location.

[Years: Hindcast = 1976–2005; RCP mid = 2026–2045; RCP end = 2081–2100. Wave height values are in meters]

Scenario	Hindcast			RCP4.5 - mid			RCP8.5 - mid			RCP4.5 - end			RCP8.5 - end		
	Low	R_v	High	Low	R_v	High	Low	R_v	High	Low	R_v	High	Low	R_v	High
2-year	6.14	6.99	8.46	5.82	7.02	9.82	6.04	7.34	10.47	6.00	7.30	10.26	6.11	7.17	9.39
5-year	6.71	8.26	11.29	6.29	8.68	15.74	6.47	8.95	16.49	6.49	8.96	16.01	6.56	8.53	13.46
10-year	7.15	9.42	14.32	6.68	10.43	23.75	6.81	10.57	24.32	6.87	10.63	23.36	6.90	9.81	18.27
20-year	7.61	10.79	18.41	7.08	12.76	37.08	7.15	12.62	36.88	7.25	12.74	34.96	7.25	11.38	25.36
50-year	8.23	12.97	26.09	7.66	17.06	69.15	7.60	16.22	65.81	7.78	16.44	61.19	7.72	14.00	40.14
100-year	8.72	14.97	34.30	8.14	21.58	112.59	7.94	19.81	103.41	8.19	20.13	94.68	8.07	16.48	57.60

Appendix A47. Table showing Howland monthly means and mean of the top 5 percent for significant wave height, peak wave period, and peak wave direction.

[Years: Hindcast = 1976–2005; RCP mid = 2026–2045; RCP end = 2081–2100. Wave directions are "coming from"]

Month	Jan	Feb	Mar	Apr	May	Jun	July	Aug	Sep	Oct	Nov	Dec
Mean Wave Height (m)												
Hindcast	2.4±0.5	2.4±0.4	2.2±0.4	2.0±0.4	1.8±0.4	1.9±0.4	1.9±0.4	1.9±0.4	1.8±0.4	1.9±0.4	2.1±0.5	2.3±0.5
RCP4.5 - mid	2.4±0.5	2.4±0.4	2.3±0.4	2.1±0.4	1.8±0.3	1.8±0.4	2.0±0.4	1.9±0.4	1.8±0.4	1.8±0.4	2.0±0.5	2.3±0.4
RCP8.5 - mid	2.4±0.4	2.4±0.5	2.2±0.4	2.0±0.4	1.8±0.3	1.8±0.3	1.9±0.4	1.9±0.4	1.8±0.3	1.8±0.4	2.0±0.4	2.3±0.5
RCP4.5 - end	2.4±0.4	2.4±0.5	2.3±0.4	2.0±0.4	1.9±0.3	1.9±0.4	1.9±0.3	1.9±0.4	1.8±0.3	1.8±0.4	2.0±0.5	2.3±0.5
RCP8.5 - end	2.3±0.4	2.3±0.4	2.2±0.4	2.0±0.4	1.8±0.3	1.9±0.3	2.0±0.3	2.0±0.3	1.9±0.3	1.8±0.4	1.9±0.4	2.2±0.5
Top 5 percent Wave Height (m)												
Hindcast	3.6±0.5	3.5±0.2	3.3±0.2	2.9±0.2	2.7±0.4	2.6±0.2	2.8±0.3	2.8±0.2	2.6±0.2	2.9±0.5	3.2±0.3	3.5±0.4
RCP4.5 - mid	3.5±0.3	3.5±0.3	3.4±0.4	3.0±0.2	2.6±0.2	2.7±0.2	2.9±0.1	2.8±0.2	2.7±0.6	2.7±0.1	3.1±0.6	3.3±0.2
RCP8.5 - mid	3.5±0.4	3.6±0.3	3.3±0.3	2.9±0.2	2.6±0.2	2.6±0.2	2.8±0.2	2.8±0.2	2.6±0.1	2.7±0.3	3.1±0.3	3.5±0.4
RCP4.5 - end	3.5±0.3	3.6±0.3	3.2±0.2	2.9±0.2	2.6±0.2	2.7±0.2	2.7±0.2	2.7±0.1	2.6±0.2	2.7±0.2	3.3±0.6	3.5±0.3
RCP8.5 - end	3.3±0.3	3.4±0.3	3.1±0.2	2.9±0.4	2.7±0.4	2.7±0.2	2.8±0.2	2.8±0.2	2.6±0.2	2.8±0.6	2.9±0.2	3.3±0.3
Mean Wave Period (s)												
Hindcast	12±2	12±2	11±2	10±2	11±3	10±3	10±3	10±2	10±2	11±2	11±2	12±2
RCP4.5 - mid	12±2	12±2	11±2	10±2	10±2	10±2	10±2	10±2	10±3	11±2	11±2	12±2
RCP8.5 - mid	12±2	12±2	11±2	10±2	10±2	10±3	10±3	10±3	11±3	11±3	11±2	12±2
RCP4.5 - end	12±2	12±2	11±2	11±2	10±3	10±3	10±3	10±3	10±3	11±3	11±2	12±2
RCP8.5 - end	12±2	12±2	11±2	10±2	10±3	10±3	10±2	10±3	10±3	11±3	11±2	12±2
Top 5 percent Wave Period (s)												
Hindcast	13±3	13±3	12±2	11±2	11±2	11±3	11±2	10±2	10±2	12±2	13±2	13±2
RCP4.5 - mid	14±2	13±3	12±2	11±1	11±2	10±2	11±3	10±2	11±2	11±3	13±3	13±2
RCP8.5 - mid	13±2	13±2	12±2	11±2	11±2	11±2	10±3	11±2	10±2	12±3	12±3	13±2
RCP4.5 - end	14±3	13±2	12±2	11±2	11±2	11±2	11±2	10±2	10±3	11±3	12±2	13±3
RCP8.5 - end	14±3	13±2	12±2	11±2	10±1	11±2	10±2	10±3	11±2	11±2	12±2	13±3
Mean Wave Direction (°)												
Hindcast	27±23	29±24	41±26	65±27	97±30	111±22	114±19	117±18	114±26	88±37	48±34	32±26
RCP4.5 - mid	27±25	29±24	39±23	63±26	95±28	109±23	113±17	116±16	118±20	95±32	53±34	34±26
RCP8.5 - mid	29±23	31±22	38±25	62±27	96±26	111±21	114±18	119±18	119±21	97±33	51±35	33±26
RCP4.5 - end	27±26	26±25	37±25	62±28	96±28	110±22	115±19	119±19	120±20	99±37	52±37	33±29
RCP8.5 - end	28±25	30±24	40±25	65±28	96±27	110±21	114±19	119±18	120±21	104±31	64±32	38±29
Top 5 percent Wave Direction (°)												
Hindcast	18±23	19±26	32±26	53±32	98±60	118±26	122±28	114±12	110±22	56±58	23±38	16±33
RCP4.5 - mid	11±24	10±33	32±25	54±31	94±38	109±21	114±12	109±12	117±34	81±37	29±42	26±24
RCP8.5 - mid	23±24	26±21	37±21	46±29	101±27	110±22	110±15	120±24	117±17	71±48	4±58	14±32
RCP4.5 - end	13±28	18±28	25±27	52±30	101±46	107±33	120±19	118±26	122±29	82±52	20±56	8±40
RCP8.5 - end	8±23	22±25	35±24	53±36	91±42	110±24	113±22	118±22	125±36	91±63	40±33	24±25

Appendix A48. Table showing return values of ensemble-average significant wave heights of hindcast and forecast scenarios, including lower and higher 95 percent confidence intervals, at the Howland location.

[Years: Hindcast = 1976–2005; RCP mid = 2026–2045; RCP end = 2081–2100. Wave height values are in meters]

Scenario	Hindcast			RCP4.5 - mid			RCP8.5 - mid			RCP4.5 - end			RCP8.5 - end		
	Low	R_v	High	Low	R_v	High	Low	R_v	High	Low	R_v	High	Low	R_v	High
2-year	4.10	4.40	4.88	4.05	4.40	5.03	4.06	4.41	5.01	4.01	4.36	4.99	3.88	4.34	5.26
5-year	4.32	4.84	5.79	4.26	4.90	6.18	4.22	4.78	5.83	4.17	4.75	5.97	4.07	4.88	6.82
10-year	4.48	5.22	6.70	4.43	5.35	7.39	4.33	5.06	6.56	4.28	5.08	6.96	4.21	5.37	8.54
20-year	4.64	5.66	7.88	4.60	5.88	9.01	4.42	5.34	7.39	4.38	5.44	8.21	4.34	5.93	10.94
50-year	4.86	6.33	9.96	4.83	6.71	12.01	4.53	5.71	8.67	4.51	5.97	10.41	4.51	6.82	15.60
100-year	5.02	6.92	12.05	5.01	7.45	15.19	4.60	5.99	9.81	4.60	6.41	12.62	4.64	7.62	20.75

Appendix A49. Table showing Jarvis monthly means and mean of the top 5 percent for significant wave height, peak wave period, and peak wave direction.

[Years: Hindcast = 1976–2005; RCP mid = 2026–2045; RCP end = 2081–2100. Wave directions are "coming from"]

Month	Jan	Feb	Mar	Apr	May	Jun	July	Aug	Sep	Oct	Nov	Dec
Mean Wave Height (m)												
Hindcast	2.4±0.5	2.4±0.4	2.2±0.4	2.0±0.4	1.9±0.4	2.0±0.4	2.1±0.4	2.1±0.4	2.0±0.4	1.9±0.4	2.1±0.5	2.3±0.4
RCP4.5 - mid	2.4±0.4	2.4±0.4	2.2±0.4	2.1±0.4	2.0±0.4	2.0±0.4	2.1±0.4	2.0±0.4	2.0±0.4	1.9±0.4	2.1±0.4	2.3±0.4
RCP8.5 - mid	2.4±0.4	2.3±0.4	2.2±0.4	2.0±0.3	1.9±0.3	2.0±0.4	2.1±0.4	2.0±0.4	2.0±0.4	1.9±0.4	2.0±0.4	2.3±0.4
RCP4.5 - end	2.4±0.4	2.4±0.4	2.2±0.4	2.0±0.4	2.0±0.4	2.1±0.4	2.1±0.4	2.1±0.4	2.0±0.3	2.0±0.4	2.0±0.4	2.3±0.4
RCP8.5 - end	2.3±0.4	2.3±0.4	2.1±0.4	2.0±0.3	1.9±0.3	2.1±0.4	2.1±0.4	2.1±0.4	2.0±0.3	1.9±0.3	2.0±0.3	2.2±0.4
Top 5 percent Wave Height (m)												
Hindcast	3.5±0.3	3.4±0.3	3.1±0.2	3.0±0.4	2.9±0.2	2.9±0.2	3.1±0.2	3.1±0.2	2.9±0.2	2.8±0.2	3.4±0.9	3.3±0.3
RCP4.5 - mid	3.5±0.3	3.4±0.3	3.2±0.2	2.9±0.2	2.9±0.3	2.9±0.2	3.0±0.2	3.0±0.2	2.8±0.2	2.7±0.2	3.0±0.3	3.3±0.2
RCP8.5 - mid	3.4±0.3	3.4±0.3	3.1±0.2	2.8±0.2	2.8±0.2	2.9±0.2	3.1±0.2	2.9±0.2	2.8±0.2	2.8±0.2	3.0±0.3	3.3±0.2
RCP4.5 - end	3.4±0.3	3.4±0.3	3.1±0.3	3.0±0.3	2.9±0.2	3.0±0.3	3.0±0.2	2.9±0.2	2.8±0.2	2.8±0.4	3.1±0.4	3.3±0.3
RCP8.5 - end	3.3±0.3	3.3±0.3	3.0±0.2	2.8±0.2	2.8±0.2	3.0±0.2	3.0±0.2	2.9±0.2	2.7±0.2	2.8±0.3	2.8±0.2	3.3±0.3
Mean Wave Period (s)												
Hindcast	13±2	13±2	12±2	12±3	12±3	12±3	11±3	11±3	12±3	12±3	12±2	13±2
RCP4.5 - mid	13±2	13±2	12±2	12±3	12±3	11±3	11±3	11±3	12±3	12±3	12±3	13±3
RCP8.5 - mid	13±2	13±2	12±2	12±3	12±3	12±3	11±3	11±3	12±3	12±3	12±2	13±2
RCP4.5 - end	13±2	13±2	12±2	12±3	12±3	12±3	11±3	11±3	12±3	12±3	12±3	13±3
RCP8.5 - end	13±3	13±2	12±2	12±3	12±3	12±3	11±3	11±3	12±3	12±3	12±3	13±3
Top 5 percent Wave Period (s)												
Hindcast	15±2	15±2	14±2	14±2	14±2	13±3	13±3	13±3	13±3	13±3	13±3	15±2
RCP4.5 - mid	16±2	15±2	14±3	14±3	14±3	13±3	13±3	13±3	14±3	14±3	14±3	15±2
RCP8.5 - mid	15±2	15±2	13±2	13±3	14±2	14±3	13±3	13±3	13±3	14±3	14±3	15±3
RCP4.5 - end	15±3	15±2	13±3	14±3	14±3	13±3	13±3	13±3	12±3	14±3	13±3	15±2
RCP8.5 - end	16±2	15±2	14±2	13±3	14±2	14±3	12±3	13±3	13±3	14±3	14±3	15±2
Mean Wave Direction (°)												
Hindcast	21±33	21±35	41±43	87±48	126±36	127±26	127±21	127±20	127±24	109±39	54±50	30±35
RCP4.5 - mid	19±34	20±32	36±40	81±48	123±39	128±26	125±20	127±19	130±19	116±36	59±50	29±37
RCP8.5 - mid	24±32	23±33	36±41	81±51	124±36	128±25	126±21	130±20	130±21	120±35	59±51	29±37
RCP4.5 - end	21±35	19±35	33±39	80±52	126±37	128±26	128±22	129±20	132±20	120±36	61±52	29±39
RCP8.5 - end	22±33	22±34	35±41	82±48	123±35	129±24	127±21	129±19	132±20	124±32	77±46	34±39
Top 5 percent Wave Direction (°)												
Hindcast	344±32	355±28	15±43	114±89	162±34	143±26	143±24	134±17	137±19	104±59	4±68	2±35
RCP4.5 - mid	349±27	350±32	7±49	113±80	157±40	141±28	135±18	140±18	144±22	128±42	28±59	7±31
RCP8.5 - mid	358±26	357±29	13±36	76±74	151±36	146±23	141±24	145±22	140±17	130±49	32±50	357±40
RCP4.5 - end	351±29	352±26	351±53	92±109	160±35	146±28	146±19	141±23	141±22	135±60	6±67	355±38
RCP8.5 - end	347±18	355±26	4±36	100±81	160±30	150±27	138±21	141±24	142±21	140±56	48±59	6±29

Appendix A50. Table showing return values of ensemble-average significant wave heights of hindcast and forecast scenarios, including lower and higher 95 percent confidence intervals, at the Jarvis location.

[Years: Hindcast = 1976–2005; RCP mid = 2026–2045; RCP end = 2081–2100. Wave height values are in meters]

Scenario	Hindcast			RCP4.5 - mid			RCP8.5 - mid			RCP4.5 - end			RCP8.5 - end		
	Low	R_v	High	Low	R_v	High	Low	R_v	High	Low	R_v	High	Low	R_v	High
2-year	4.05	4.34	4.81	3.96	4.24	4.75	3.86	4.09	4.47	3.97	4.30	4.91	3.84	4.07	4.47
5-year	4.28	4.80	5.74	4.06	4.49	5.32	3.96	4.31	4.95	4.11	4.66	5.81	3.94	4.29	4.94
10-year	4.46	5.22	6.72	4.12	4.66	5.79	4.02	4.47	5.36	4.21	4.96	6.68	4.00	4.44	5.32
20-year	4.65	5.71	8.01	4.17	4.81	6.29	4.08	4.62	5.80	4.30	5.26	7.76	4.04	4.58	5.72
50-year	4.91	6.49	10.36	4.22	5.00	7.01	4.14	4.82	6.46	4.41	5.70	9.59	4.09	4.75	6.29
100-year	5.11	7.20	12.82	4.25	5.13	7.60	4.17	4.96	7.00	4.48	6.06	11.37	4.12	4.87	6.76

Appendix B. Wind Speed and Wind Direction Statistics

Appendix B1. Table showing American Samoa monthly means and mean of the top 5 percent for wind speed and mean wind direction.

[Years: Hindcast = 1976–2005; RCP mid = 2026–2045; RCP end = 2081–2100. Wind directions are "coming from"]

Month	Jan	Feb	Mar	Apr	May	Jun	July	Aug	Sep	Oct	Nov	Dec
Mean Wind Speed (m/s)												
Hindcast	5.2±2.9	5.0±2.8	5.1±2.8	5.4±2.7	6.3±2.9	6.9±2.7	6.9±2.7	7.1±2.7	7.1±2.7	6.8±2.7	6.0±2.8	5.3±2.6
RCP4.5 - mid	5.3±2.8	5.1±2.8	5.2±2.7	5.5±2.7	6.5±2.9	7.0±2.7	7.1±2.7	7.1±2.6	7.4±2.7	7.0±2.7	6.2±2.9	5.4±2.6
RCP8.5 - mid	5.2±2.8	5.1±2.8	5.1±2.9	5.5±2.8	6.3±2.9	6.8±2.7	6.9±2.7	7.1±2.8	7.3±2.6	6.9±2.7	6.0±2.7	5.4±3.0
RCP4.5 - end	5.2±2.7	5.2±2.7	4.8±2.7	5.4±2.8	6.6±3.0	7.2±2.6	6.9±2.8	7.2±2.6	7.3±2.6	6.9±2.7	6.1±2.7	5.5±2.8
RCP8.5 - end	5.4±2.8	5.3±2.8	5.2±2.8	5.2±2.6	6.2±2.9	7.0±2.8	7.0±2.7	7.3±2.6	7.3±2.6	7±2.6	6.1±2.7	5.3±2.5
Top 5 percent Wind Speed (m/s)												
Hindcast	13.2±2.5	12.5±2.9	12.4±2.1	11.7±1.3	12.9±1.6	12.8±1.5	12.6±1.0	12.8±1.1	12.6±1.0	12.6±1.2	12.4±1.3	11.7±2.0
RCP4.5 - mid	12.6±2.3	12.6±2.6	11.6±2.1	11.9±1.3	12.6±1.4	12.5±1.0	12.5±0.8	12.4±0.9	12.9±1.0	12.6±0.8	12.7±1.5	11.5±1.7
RCP8.5 - mid	12.3±2.5	12.5±2.3	12.6±2.7	12.1±1.2	12.4±1.0	12.4±1.2	12.8±1.4	12.8±1.0	12.5±0.8	12.6±1.1	12.2±1.5	13.5±2.7
RCP4.5 - end	12.2±2.3	12.1±2.3	11.9±2.4	12.4±2.3	12.8±1.8	12.5±1.1	12.6±1.1	12.5±1.0	12.6±1.0	12.6±1.1	11.9±1.3	12.4±2.1
RCP8.5 - end	12.7±2.9	13.0±2.6	12.6±2.8	11.4±1.5	12.7±1.6	13.0±1.1	12.6±0.9	12.9±1.0	12.7±1.0	12.1±0.8	11.8±1.2	11.4±1.4
Mean Wind Direction (°)												
Hindcast	242±83	217±98	233±104	281±68	284±53	285±43	286±43	283±39	285±38	285±39	280±52	268±66
RCP4.5 - mid	243±79	207±97	219±106	283±72	286±49	284±43	285±43	285±38	285±34	286±37	284±48	271±67
RCP8.5 - mid	249±71	214±96	235±108	285±70	288±49	287±44	283±44	286±41	285±37	283±38	279±49	266±70
RCP4.5 - end	250±76	214±94	233±106	279±73	286±48	283±40	284±43	285±37	286±33	285±36	280±48	269±63
RCP8.5 - end	250±70	229±93	232±97	278±70	283±50	285±41	286±39	285±34	286±31	284±34	277±45	269±55
Top 5 percent Wind Direction (°)												
Hindcast	205±93	182±89	183±89	289±54	291±36	296±31	296±24	292±24	294±27	295±24	287±40	280±63
RCP4.5 - mid	196±79	164±67	164±85	292±53	294±33	290±32	295±23	296±23	294±23	293±19	289±39	281±57
RCP8.5 - mid	226±72	152±76	178±102	294±45	294±32	297±33	293±31	298±23	294±22	294±25	283±33	284±57
RCP4.5 - end	218±82	169±84	166±82	266±76	296±33	295±25	298±25	296±22	297±18	296±17	290±33	286±53
RCP8.5 - end	234±85	160±94	173±78	280±65	292±40	297±25	297±23	298±24	297±18	294±16	286±33	285±37

Appendix B2. Table showing return values of ensemble-average wind speeds of hindcast and forecast scenarios, including lower and higher 95 percent confidence intervals, at the American Samoa location.

[Years: Hindcast = 1976–2005; RCP mid = 2026–2045; RCP end = 2081–2100. Wind speeds are in meters per second]

Scenario	Hindcast			RCP4.5 - mid			RCP8.5 - mid			RCP4.5 - end			RCP8.5 - end		
	Low	R_v	High	Low	R_v	High	Low	R_v	High	Low	R_v	High	Low	R_v	High
2-year	18.63	20.53	23.67	18.06	19.99	23.26	18.84	20.96	24.46	17.77	20.54	26.43	18.16	20.54	25.11
5-year	19.71	22.87	28.72	18.90	21.87	27.47	19.79	22.99	28.82	18.62	23.23	34.98	18.99	22.82	31.32
10-year	20.47	24.76	33.47	19.43	23.25	31.07	20.37	24.43	32.42	19.18	25.46	43.94	19.53	24.60	37.24
20-year	21.18	26.77	39.22	19.88	24.59	35.09	20.85	25.81	36.31	19.68	27.89	55.82	20.00	26.44	44.50
50-year	22.04	29.63	48.71	20.38	26.31	41.09	21.38	27.52	41.92	20.25	31.41	77.66	20.53	28.96	56.65
100-year	22.63	31.94	57.64	20.69	27.57	46.23	21.70	28.75	46.56	20.62	34.33	100.54	20.86	30.94	68.25

Appendix B3. Table showing Kauai monthly means and mean of the top 5 percent for wind speed and mean wind direction.

[Years: Hindcast = 1976–2005; RCP mid = 2026–2045; RCP end = 2081–2100. Wind directions are "coming from"]

Month	Jan	Feb	Mar	Apr	May	Jun	July	Aug	Sep	Oct	Nov	Dec
Mean Wind Speed (m/s)												
Hindcast	6.9±3.1	6.9±3.1	7.5±3.1	8.0±2.7	8.1±2.4	8.6±2.0	8.5±1.9	8.2±2.2	7.8±2.5	8.1±2.9	7.9±3.1	7.3±3.2
RCP4.5 - mid	6.8±3.1	6.9±3.1	7.6±3.1	8.4±2.8	7.9±2.4	8.4±2.0	8.8±1.7	8.2±2.0	7.7±2.4	8.0±2.8	8.1±3.0	7.3±3.1
RCP8.5 - mid	6.9±3.2	6.9±3.2	7.5±3.1	8.1±2.6	7.8±2.3	8.2±2.0	8.5±1.8	8.2±2.1	7.6±2.4	8.0±2.8	8.1±2.9	7.5±3.1
RCP4.5 - end	6.4±3.0	6.9±3.2	7.6±3.1	8.0±2.7	8.0±2.3	8.4±1.9	8.5±1.8	8.2±2.1	7.7±2.4	8.1±2.8	8.1±3.0	7.3±3.1
RCP8.5 - end	6.4±3.1	6.5±3.1	7.4±3.0	8.1±2.6	7.6±2.3	8.1±1.8	8.5±1.7	8.0±1.9	7.6±2.2	8.0±2.6	8.2±2.8	7.0±3.2
Top 5 percent Wind Speed (m/s)												
Hindcast	13.5±1.2	13.5±1.2	13.6±1.0	13.0±0.8	12.3±0.7	12.5±1.0	12.1±1.1	12.4±1.4	12.5±1.1	13.7±1.4	14.0±1.0	13.8±1.2
RCP4.5 - mid	13.4±1.2	13.5±1.0	13.4±0.9	13.4±0.8	12.6±0.9	12.0±0.8	12.1±1.1	11.9±0.9	12.8±1.5	13.6±1.4	13.8±1.1	13.6±1.1
RCP8.5 - mid	13.9±1.1	13.7±1.2	13.8±1.0	13.0±0.8	12.0±0.7	11.9±0.6	12.0±1.3	12.4±1.2	12.4±1.1	13.9±1.3	13.5±0.8	13.9±1.0
RCP4.5 - end	12.8±1.1	13.7±1.0	13.5±0.7	13.1±0.8	12.4±0.8	11.9±0.9	12.2±1.3	12.7±1.5	12.5±1.3	13.6±1.6	13.8±0.8	13.6±1.0
RCP8.5 - end	13.1±1.3	13.5±1.2	13.2±0.8	12.7±0.6	11.7±0.7	11.5±0.7	12.1±1.5	12.0±1.6	12.1±1.9	13.1±1.7	13.7±1.3	13.7±1.3
Mean Wind Direction (°)												
Hindcast	248±77	243±78	248±50	250±35	253±24	256±17	256±17	258±24	258±30	255±34	251±41	254±59
RCP4.5 - mid	247±76	249±69	250±52	251±32	254±24	256±16	256±15	257±22	258±28	254±35	251±37	251±54
RCP8.5 - mid	248±72	244±73	248±52	249±29	254±23	256±16	256±17	257±24	259±29	253±35	249±37	252±55
RCP4.5 - end	252±78	244±72	247±50	250±33	254±22	256±15	256±18	257±24	257±32	254±33	250±37	252±50
RCP8.5 - end	250±70	243±75	248±50	250±31	254±23	257±14	256±15	257±21	257±28	253±30	252±32	253±53
Top 5 percent Wind Direction (°)												
Hindcast	232±66	238±51	244±26	245±17	247±13	251±15	252±13	258±31	255±24	253±31	247±22	246±39
RCP4.5 - mid	234±68	246±39	246±22	246±16	246±15	252±18	252±23	251±26	256±31	255±34	248±22	241±38
RCP8.5 - mid	241±46	240±41	243±25	244±12	245±10	247±7	253±20	257±33	259±35	250±28	242±19	245±32
RCP4.5 - end	243±65	238±50	243±22	245±16	246±12	248±10	250±20	257±41	252±37	250±32	244±19	246±27
RCP8.5 - end	240±37	236±42	244±18	246±11	248±12	249±10	253±23	255±25	264±40	251±28	246±23	250±26

Appendix B4. Table showing return values of ensemble-average wind speeds of hindcast and forecast scenarios, including lower and higher 95 percent confidence intervals, at the Kauai location.

[Years: Hindcast = 1976–2005; RCP mid = 2026–2045; RCP end = 2081–2100. Wind speeds are in meters per second]

Scenario	Hindcast			RCP4.5 - mid			RCP8.5 - mid			RCP4.5 - end			RCP8.5 - end		
	Low	R_v	High	Low	R_v	High	Low	R_v	High	Low	R_v	High	Low	R_v	High
2-year	17.80	18.92	20.66	17.25	18.57	20.94	16.99	18.05	20.04	17.24	18.45	20.50	17.54	19.22	22.16
5-year	18.44	20.16	23.07	17.67	19.62	23.58	17.42	19.17	22.95	17.66	19.41	22.68	18.31	21.02	26.41
10-year	18.85	21.06	25.05	17.91	20.34	25.76	17.71	20.08	25.81	17.90	20.05	24.37	18.82	22.45	30.38
20-year	19.20	21.92	27.17	18.10	21.01	28.11	17.97	21.05	29.39	18.08	20.61	26.09	19.29	23.94	35.14
50-year	19.59	23.01	30.21	18.29	21.82	31.50	18.28	22.43	35.53	18.27	21.26	28.42	19.83	25.99	42.92
100-year	19.83	23.80	32.71	18.40	22.38	34.30	18.49	23.55	41.56	18.37	21.69	30.22	20.20	27.62	50.18

Appendix B5. Table showing Big Island of Hawaii monthly means and mean of the top 5 percent for wind speed and mean wind direction.

[Years: Hindcast = 1976–2005; RCP mid = 2026–2045; RCP end = 2081–2100. Wind directions are "coming from"]

Month	Jan	Feb	Mar	Apr	May	Jun	July	Aug	Sep	Oct	Nov	Dec
Mean Wind Speed (m/s)												
Hindcast	7.0±3.0	6.8±3.1	7.7±2.9	8.2±2.5	8±2.1	8.5±1.8	8.2±1.8	7.9±2.0	7.4±2.3	7.7±2.6	8.1±2.8	7.7±3.0
RCP4.5 - mid	6.9±3.0	7.1±3.1	7.7±3.0	8.4±2.6	8.0±2.0	8.3±1.7	8.4±1.7	7.8±2.0	7.2±2.2	7.5±2.6	8.2±2.8	7.7±3.0
RCP8.5 - mid	7.0±3.1	7.0±3.1	7.6±2.9	8.2±2.4	7.9±2.0	8.2±1.7	8.2±1.7	8.0±2.0	7.1±2.2	7.3±2.6	8.0±2.6	7.9±2.9
RCP4.5 - end	6.7±2.9	6.9±3.0	7.7±2.9	8.1±2.4	8.0±1.9	8.5±1.7	8.3±1.8	7.9±2.0	7.3±2.3	7.5±2.6	8.1±2.8	7.8±2.9
RCP8.5 - end	6.6±2.9	6.4±2.9	7.5±2.8	8.1±2.4	7.6±1.9	8.2±1.5	8.4±1.6	7.7±1.9	7.1±2.1	7.4±2.5	8.0±2.7	7.6±3.0
Top 5 percent Wind Speed (m/s)												
Hindcast	12.8±0.9	12.9±0.8	13.2±0.9	12.5±0.7	11.7±0.7	11.7±0.9	11.7±0.9	11.8±1.1	11.9±1.3	13.0±1.1	13.7±1.1	13.5±0.9
RCP4.5 - mid	12.9±1.1	13.3±1.0	13.1±0.7	12.9±0.7	11.8±1.3	11.3±0.7	11.7±1.1	11.4±1.0	11.8±1.3	13.0±1.4	13.5±1.1	13.2±1.0
RCP8.5 - mid	13.3±1.0	13.2±1.0	13.0±0.8	12.3±0.8	11.3±0.6	11.1±0.5	11.4±0.8	12.1±1.2	11.3±1.4	12.8±1.3	13.0±0.9	13.7±1.0
RCP4.5 - end	12.4±0.9	13.0±1.0	12.9±0.6	12.3±0.6	11.4±0.7	11.6±1.2	12.0±1.6	12.1±1.8	12.0±1.3	12.9±1.7	13.5±0.9	13.4±1.1
RCP8.5 - end	12.6±1.2	12.5±0.9	12.7±0.7	12.0±0.6	10.9±0.5	11.1±0.8	11.9±1.7	11.8±1.5	11.3±1.6	12.4±1.5	13.3±1.4	13.5±1.2
Mean Wind Direction (°)												
Hindcast	256±51	253±53	251±35	253±24	254±19	254±14	253±16	253±23	255±29	254±32	253±31	255±37
RCP4.5 - mid	256±50	254±46	254±36	251±22	254±17	254±14	252±16	252±25	255±28	253±32	252±28	254±35
RCP8.5 - mid	255±46	253±48	252±37	252±23	255±17	254±14	252±16	253±24	253±31	254±36	252±30	254±38
RCP4.5 - end	259±48	255±51	254±36	253±23	254±16	254±13	252±18	253±27	254±32	253±32	251±30	254±31
RCP8.5 - end	258±42	254±50	253±35	252±22	254±15	253±12	252±16	251±23	252±30	252±33	252±28	255±32
Top 5 percent Wind Direction (°)												
Hindcast	249±30	246±21	246±14	249±12	252±11	255±12	255±19	255±20	256±31	251±22	249±20	245±19
RCP4.5 - mid	248±32	248±18	246±13	247±10	252±11	254±13	253±15	251±24	255±29	255±36	249±16	246±18
RCP8.5 - mid	245±23	243±22	245±16	248±12	253±10	253±9	254±20	253±34	254±30	256±37	247±20	248±15
RCP4.5 - end	252±22	244±28	247±13	250±12	252±12	257±22	256±27	255±40	263±50	253±31	244±19	251±18
RCP8.5 - end	251±22	244±22	246±16	249±11	250±7	251±9	257±21	251±30	261±41	256±37	249±14	250±16

Appendix B6. Table showing return values of ensemble-average wind speeds of hindcast and forecast scenarios, including lower and higher 95 percent confidence intervals, at the Big Island of Hawaii location.

[Years: Hindcast = 1976–2005; RCP mid = 2026–2045; RCP end = 2081–2100. Wind speeds are in meters per second]

Scenario	Hindcast			RCP4.5 - mid			RCP8.5 - mid			RCP4.5 - end			RCP8.5 - end		
	Low	R_v	High	Low	R_v	High	Low	R_v	High	Low	R_v	High	Low	R_v	High
2-year	16.30	17.25	18.75	16.40	17.73	20.24	16.14	17.16	19.03	16.76	18.15	20.62	16.68	18.14	20.63
5-year	16.83	18.33	20.96	16.82	18.85	23.24	16.56	18.22	21.68	17.33	19.53	23.95	17.22	19.37	23.46
10-year	17.19	19.15	22.89	17.07	19.66	25.90	16.85	19.06	24.20	17.70	20.59	26.99	17.53	20.22	25.75
20-year	17.50	19.98	25.05	17.27	20.45	28.94	17.10	19.94	27.26	18.02	21.66	30.55	17.78	20.99	28.17
50-year	17.86	21.06	28.35	17.49	21.45	33.65	17.39	21.16	32.35	18.39	23.09	36.23	18.04	21.93	31.58
100-year	18.10	21.89	31.21	17.61	22.18	37.81	17.58	22.13	37.19	18.62	24.19	41.39	18.19	22.57	34.33

Appendix B7. Table showing Midway monthly means and mean of the top 5 percent for wind speed and mean wind direction.

[Years: Hindcast = 1976–2005; RCP mid = 2026–2045; RCP end = 2081–2100. Wind directions are "coming from"]

Month	Jan	Feb	Mar	Apr	May	Jun	July	Aug	Sep	Oct	Nov	Dec
Mean Wind Speed (m/s)												
Hindcast	8.7±4.0	8.3±3.8	7.0±3.1	6.4±2.7	5.7±2.4	5.9±2.2	6.8±2.3	6.8±2.5	6.8±2.9	7.3±3.2	7.2±3.3	8.0±3.7
RCP4.5 - mid	8.6±4.0	8.1±3.7	7.1±3.1	6.5±2.8	5.5±2.4	5.6±2.2	6.9±2.2	6.5±2.4	6.6±2.7	7.2±3.1	7.1±3.4	7.8±3.7
RCP8.5 - mid	8.5±3.9	8.2±3.6	7.0±3.2	6.1±2.7	5.5±2.5	5.4±2.2	6.9±2.2	6.7±2.5	6.6±2.9	7.4±3.1	7.1±3.4	7.6±3.8
RCP4.5 - end	8.6±3.8	8.2±3.7	7.1±3.2	6.2±2.8	5.7±2.4	5.5±2.1	6.6±2.2	6.5±2.5	6.5±2.6	7.3±3.0	7.0±3.3	7.6±3.6
RCP8.5 - end	8.2±3.8	8.0±3.5	6.8±3.0	6.2±2.6	5.4±2.4	5.5±2.1	6.5±2.1	6.3±2.2	6.5±2.6	7.1±2.9	6.8±3.1	7.3±3.5
Top 5 percent Wind Speed (m/s)												
Hindcast	17.9±1.9	16.9±1.5	14.3±1.6	12.4±1.5	10.7±1.0	10.1±0.9	11.5±1.5	12.1±1.8	13.5±1.7	14.4±1.7	14.5±1.6	16.6±1.8
RCP4.5 - mid	17.4±1.6	16.6±1.8	14.1±1.5	12.5±1.3	10.5±1.2	10.1±1.3	11.6±1.6	12.2±2.1	12.5±1.7	13.9±1.7	15.0±1.7	16.6±2.0
RCP8.5 - mid	17.4±1.8	16.4±1.7	14.4±1.7	12.2±1.6	10.9±1.2	9.9±1.1	11.2±1.5	12.4±2.0	13.5±2.0	14.0±1.6	14.6±1.6	16.5±1.9
RCP4.5 - end	17.1±1.7	16.8±2.0	14.5±1.7	12.1±1.4	10.8±1.0	9.8±0.8	11.0±1.5	12.4±2.7	12.4±2.0	14.0±1.7	14.4±1.8	16.0±1.9
RCP8.5 - end	16.8±1.8	16.4±1.7	13.5±1.4	12.0±1.3	10.4±1.0	9.7±1.1	10.7±1.3	11.4±2.2	12.7±2.0	13.2±1.4	13.8±1.6	15.4±1.7
Mean Wind Direction (°)												
Hindcast	92±86	87±89	283±134	255±67	261±54	270±43	267±32	269±37	262±49	252±57	241±92	108±117
RCP4.5 - mid	92±85	84±93	206±136	256±65	260±60	270±47	268±29	270±34	262±46	255±50	250±88	99±117
RCP8.5 - mid	88±92	88±97	203±139	257±71	258±58	270±49	268±33	271±39	262±49	256±50	245±78	106±129
RCP4.5 - end	88±81	87±94	227±126	257±69	262±55	269±46	268±33	270±37	264±43	256±48	250±78	105±130
RCP8.5 - end	88±87	86±88	257±121	259±63	262±55	271±45	268±29	271±34	266±45	258±45	251±71	122±125
Top 5 percent Wind Direction (°)												
Hindcast	88±42	90±43	107±82	232±58	249±32	266±32	268±25	279±39	260±37	236±42	190±96	97±60
RCP4.5 - mid	100±55	95±48	109±84	239±45	248±39	265±43	268±27	269±30	256±32	252±39	219±80	100±63
RCP8.5 - mid	89±57	89±47	113±82	236±54	243±37	263±32	270±32	277±44	252±38	244±30	218±68	95±57
RCP4.5 - end	86±42	93±49	117±87	242±53	255±39	261±28	270±27	274±39	260±38	243±36	225±68	98±64
RCP8.5 - end	87±38	88±45	111±90	240±51	251±38	262±28	269±25	282±49	257±43	248±32	237±51	99±75

Appendix B8. Table showing return values of ensemble-average wind speeds of hindcast and forecast scenarios, including lower and higher 95 percent confidence intervals, at the Midway location.

[Years: Hindcast = 1976–2005; RCP mid = 2026–2045; RCP end = 2081–2100. Wind speeds are in meters per second]

Scenario	Hindcast			RCP4.5 - mid			RCP8.5 - mid			RCP4.5 - end			RCP8.5 - end		
	Low	R_v	High	Low	R_v	High	Low	R_v	High	Low	R_v	High	Low	R_v	High
2-year	22.76	24.25	26.65	22.56	24.09	26.51	22.07	23.70	26.72	22.39	24.33	27.82	21.44	23.30	26.62
5-year	23.54	25.87	30.01	23.16	25.30	28.96	22.46	24.76	29.57	23.10	26.10	32.21	22.09	24.89	30.56
10-year	24.04	27.07	32.88	23.48	26.06	30.72	22.67	25.43	31.78	23.55	27.41	36.10	22.47	26.02	33.92
20-year	24.48	28.25	36.07	23.73	26.71	32.39	22.82	26.01	34.04	23.92	28.70	40.53	22.78	27.10	37.64
50-year	24.97	29.77	40.84	23.97	27.41	34.49	22.95	26.65	37.09	24.33	30.36	47.38	23.11	28.44	43.19
100-year	25.28	30.91	44.91	24.10	27.86	35.99	23.03	27.06	39.46	24.58	31.59	53.42	23.30	29.40	47.92

Appendix B9. Table showing Chuuk monthly means and mean of the top 5 percent for wind speed and mean wind direction.

[Years: Hindcast = 1976–2005; RCP mid = 2026–2045; RCP end = 2081–2100. Wind directions are "coming from"]

Month	Jan	Feb	Mar	Apr	May	Jun	July	Aug	Sep	Oct	Nov	Dec
Mean Wind Speed (m/s)												
Hindcast	8.5±2.0	8.5±1.9	8.0±2.0	6.8±2.4	5.2±2.4	4.4±2.4	4.2±2.4	4.3±2.5	4.0±2.3	4.2±2.4	5.3±2.8	7.5±2.6
RCP4.5 - mid	8.4±2.2	8.3±2.0	8.0±2.0	6.9±2.2	5.2±2.4	4.4±2.4	4.5±2.6	4.3±2.5	4.1±2.3	4.1±2.3	4.9±2.5	7.1±2.6
RCP8.5 - mid	8.3±2.1	8.4±1.9	7.9±1.9	7.0±2.0	5.2±2.4	4.5±2.4	4.4±2.4	4.4±2.5	4.2±2.3	4.1±2.4	4.9±2.6	7.1±2.7
RCP4.5 - end	8.2±2.0	8.3±1.9	7.9±2.0	6.7±2.1	5.2±2.4	4.7±2.5	4.5±2.5	4.5±2.6	4.2±2.4	4.1±2.4	4.9±2.5	6.9±2.6
RCP8.5 - end	8.1±2.0	8.0±1.9	7.9±1.7	7.0±2.0	5.5±2.4	4.7±2.5	4.7±2.6	4.5±2.5	4.2±2.5	3.8±2.2	4.6±2.5	7.0±2.5
Top 5 percent Wind Speed (m/s)												
Hindcast	12.2±0.8	12.3±1.2	11.7±1.3	11.2±1.3	10.3±1.2	10.2±1.7	10.7±2.1	11.3±2.2	10.7±1.9	10.5±1.9	11.7±1.6	12.4±1.0
RCP4.5 - mid	12.7±1.1	12.1±0.8	11.6±1.3	10.9±0.8	10.2±1.2	10.1±1.6	11.3±2.0	11.8±2.3	11.0±2.1	10.5±1.6	11.1±1.7	12.5±1.6
RCP8.5 - mid	12.5±1.2	12.2±0.9	11.6±1.0	10.9±0.7	10.1±1.3	10.5±2.2	10.6±2.0	11.5±2.2	10.9±2.1	10.5±1.8	11.5±1.6	12.9±1.5
RCP4.5 - end	11.7±0.6	11.9±1.0	11.6±1.4	10.6±0.8	10.2±1.0	10.6±1.8	11.2±1.8	11.7±1.6	11.0±2.0	10.8±1.7	10.7±1.7	12.3±1.3
RCP8.5 - end	12.2±1.3	11.7±1.0	11.3±1.0	10.9±0.9	10.5±1.6	10.3±1.5	11.5±2.3	11.6±1.8	11.4±2.5	9.9±2.3	10.8±1.7	12.1±1.5
Mean Wind Direction (°)												
Hindcast	245±18	244±18	245±23	250±31	257±53	269±71	299±73	324±68	324±74	317±90	263±63	249±30
RCP4.5 - mid	247±23	245±19	246±19	248±26	255±45	268±69	300±73	321±72	322±73	318±85	265±70	252±37
RCP8.5 - mid	247±17	244±16	247±21	249±24	254±44	269±69	302±79	328±72	325±71	328±87	264±68	252±33
RCP4.5 - end	248±17	245±19	247±20	250±25	256±42	265±74	301±76	325±71	327±73	332±87	267±67	253±35
RCP8.5 - end	248±19	246±17	246±17	250±19	256±40	267±68	290±71	317±70	325±70	311±82	267±65	253±31
Top 5 percent Wind Direction (°)												
Hindcast	239±16	237±18	237±30	239±37	249±64	275±97	24±80	28±47	41±62	48±73	258±72	240±25
RCP4.5 - mid	237±32	236±16	239±27	240±30	244±33	262±73	33±64	30±54	34±53	55±57	242±77	243±46
RCP8.5 - mid	241±19	233±20	238±28	241±18	247±52	300±82	43±72	37±45	34±43	57±61	251±74	242±39
RCP4.5 - end	239±11	241±29	238±21	241±34	246±47	263±94	41±49	35±35	46±40	50±54	254±79	243±36
RCP8.5 - end	239±24	240±23	238±28	242±16	247±35	274±70	34±67	35±39	29±39	47±80	250±58	245±35

Appendix B10. Table showing return values of ensemble-average wind speeds of hindcast and forecast scenarios, including lower and higher 95 percent confidence intervals, at the Chuuk location.

[Years: Hindcast = 1976–2005; RCP mid = 2026–2045; RCP end = 2081–2100. Wind speeds are in meters per second]

Scenario	Hindcast			RCP4.5 - mid			RCP8.5 - mid			RCP4.5 - end			RCP8.5 - end		
	Low	R_v	High	Low	R_v	High	Low	R_v	High	Low	R_v	High	Low	R_v	High
2-year	16.86	18.81	22.23	17.32	19.05	21.90	16.86	18.91	22.75	16.13	17.76	20.62	17.63	19.65	22.95
5-year	17.82	21.07	27.64	18.04	20.60	25.22	17.44	20.45	26.90	16.74	19.20	24.03	18.33	21.15	26.21
10-year	18.48	22.94	32.94	18.47	21.66	27.86	17.76	21.51	30.38	17.10	20.22	26.91	18.70	22.10	28.58
20-year	19.09	24.96	39.57	18.82	22.64	30.60	18.01	22.48	34.17	17.40	21.19	30.07	18.98	22.90	30.87
50-year	19.83	27.86	50.97	19.18	23.81	34.41	18.26	23.65	39.71	17.71	22.40	34.74	19.25	23.78	33.78
100-year	20.35	30.25	62.13	19.39	24.62	37.42	18.40	24.46	44.35	17.90	23.26	38.67	19.39	24.33	35.90

Appendix B11. Table showing Saipan monthly means and mean of the top 5 percent for wind speed and mean wind direction.

[Years: Hindcast = 1976–2005; RCP mid = 2026–2045; RCP end = 2081–2100. Wind directions are "coming from"]

Month	Jan	Feb	Mar	Apr	May	Jun	July	Aug	Sep	Oct	Nov	Dec
Mean Wind Speed (m/s)												
Hindcast	8.7±2.3	8.6±2.4	8.4±2.3	7.9±2.1	7.1±2.2	6.4±2.5	5.9±3.2	5.8±3.3	5.5±3.0	6.2±3.0	8.4±2.6	8.9±2.2
RCP4.5 - mid	8.8±2.3	8.5±2.4	8.5±2.2	8.0±1.9	7.1±2.2	6.7±2.5	5.9±3.1	5.6±3.0	5.4±3.0	5.7±2.8	7.9±2.5	8.7±2.4
RCP8.5 - mid	8.7±2.3	8.6±2.3	8.4±2.2	7.9±1.8	7.0±2.0	6.8±2.6	6.1±3.2	5.7±3.3	5.6±3.0	5.7±2.8	7.8±2.6	8.9±2.4
RCP4.5 - end	8.6±2.3	8.7±2.2	8.4±2.2	7.8±2.0	7.2±2.0	6.7±2.4	6.2±3.0	5.9±3.3	5.5±2.7	5.7±2.8	8.0±2.6	8.7±2.2
RCP8.5 - end	8.5±2.4	8.3±2.4	8.1±2.1	7.8±1.8	7.1±2.0	6.6±2.5	6.2±3.1	5.7±3.3	5.6±3.0	5.7±2.7	7.8±2.6	8.6±2.3
Top 5 percent Wind Speed (m/s)												
Hindcast	13.2±0.8	13.2±1.0	13.2±1.7	12.0±1.2	11.8±1.7	12.0±2.1	14.0±2.4	14.6±2.5	13.4±2.8	13.5±2.5	14.1±1.8	13.3±1.2
RCP4.5 - mid	13.1±0.7	13.2±0.8	13.0±1.3	11.9±1.8	11.3±1.3	12.4±2.5	13.6±2.4	13.3±2.3	13.8±3.2	12.2±1.9	13.2±1.9	13.8±1.4
RCP8.5 - mid	13.3±0.9	13.2±0.7	13.0±1.2	11.7±1.0	10.8±1.1	13.2±3.1	14.2±2.5	14.3±2.3	14.0±3.0	12.2±2.2	13.5±2.1	13.8±1.7
RCP4.5 - end	13.0±0.8	13.2±1.0	12.9±0.8	11.8±0.8	10.7±0.7	11.6±2.0	13.6±2.9	14.4±2.5	12.3±2.1	12.4±2.2	13.5±1.8	13.2±1.4
RCP8.5 - end	13.3±0.9	13.0±0.8	12.3±0.9	11.2±0.8	11.0±1.3	11.9±2.3	13.6±2.4	14.3±2.6	13.8±2.4	11.8±1.9	13.3±1.8	13.3±1.6
Mean Wind Direction (°)												
Hindcast	251±21	247±21	251±20	256±20	262±25	266±40	283±79	330±108	294±103	263±63	260±32	255±22
RCP4.5 - mid	251±22	249±21	251±18	255±15	262±27	268±39	281±72	330±115	323±119	263±74	259±34	256±22
RCP8.5 - mid	251±21	250±20	251±18	256±16	261±23	269±37	282±76	342±110	355±125	265±74	260±33	257±22
RCP4.5 - end	251±21	248±20	251±19	256±18	262±24	266±37	280±77	319±105	318±110	265±76	258±31	256±20
RCP8.5 - end	252±21	249±22	251±17	256±14	262±21	268±43	278±69	308±97	338±115	264±74	258±29	257±20
Top 5 percent Wind Direction (°)												
Hindcast	240±14	238±12	245±26	248±22	260±33	278±52	357±70	12±57	8±79	278±64	258±39	249±20
RCP4.5 - mid	242±13	239±11	243±19	247±18	260±25	279±51	356±80	28±66	30±76	259±68	256±37	247±27
RCP8.5 - mid	243±12	241±11	243±17	250±12	258±21	282±59	15±63	29±55	40±47	285±70	257±34	251±28
RCP4.5 - end	243±14	237±15	241±12	248±20	259±18	272±51	344±84	36±51	40±57	275±66	255±33	246±19
RCP8.5 - end	243±14	241±13	240±11	251±13	257±14	283±56	12±77	27±55	27±66	269±76	256±24	251±19

Appendix B12. Table showing return values of ensemble-average wind speeds of hindcast and forecast scenarios, including lower and higher 95 percent confidence intervals, at the Saipan location.

[Years: Hindcast = 1976–2005; RCP mid = 2026–2045; RCP end = 2081–2100. Wind speeds are in meters per second]

Scenario	Hindcast			RCP4.5 - mid			RCP8.5 - mid			RCP4.5 - end			RCP8.5 - end		
	Low	R_v	High	Low	R_v	High	Low	R_v	High	Low	R_v	High	Low	R_v	High
2-year	20.87	22.67	25.25	20.13	22.46	26.21	20.39	22.84	26.87	19.76	21.64	24.46	19.87	22.11	25.83
5-year	21.91	24.49	28.42	21.15	24.58	30.63	21.51	25.23	32.02	20.56	23.13	27.25	20.67	23.87	29.74
10-year	22.52	25.66	30.70	21.76	26.03	34.10	22.21	26.97	36.32	20.98	24.02	29.13	21.11	25.02	32.71
20-year	23.01	26.69	32.86	22.25	27.36	37.69	22.80	28.63	41.00	21.30	24.76	30.83	21.45	26.03	35.70
50-year	23.50	27.85	35.58	22.77	28.96	42.63	23.45	30.74	47.84	21.60	25.54	32.85	21.79	27.18	39.67
100-year	23.79	28.60	37.52	23.08	30.05	46.52	23.86	32.26	53.55	21.76	26.00	34.21	21.98	27.93	42.69

Appendix B13. Table showing Asuncion monthly means and mean of the top 5 percent for wind speed and mean wind direction.

[Years: Hindcast = 1976–2005; RCP mid = 2026–2045; RCP end = 2081–2100. Wind directions are "coming from"]

Month	Jan	Feb	Mar	Apr	May	Jun	July	Aug	Sep	Oct	Nov	Dec
Mean Wind Speed (m/s)												
Hindcast	7.3±2.8	7.1±2.8	6.9±2.8	6.6±2.4	6.4±2.3	6.4±2.4	6.3±3.0	6.1±3.0	6.1±2.8	6.9±3.0	7.8±2.7	7.7±2.8
RCP4.5 - mid	7.5±2.7	7.2±2.9	7.0±2.7	6.7±2.5	6.3±2.2	6.6±2.3	6.4±2.7	5.8±2.8	5.8±2.9	6.6±2.7	7.7±2.6	7.5±2.8
RCP8.5 - mid	7.4±2.8	7.2±2.8	6.9±2.7	6.7±2.3	6.2±2.1	6.5±2.4	6.4±2.8	5.8±3.0	6.0±3.0	6.5±2.8	7.6±2.7	7.8±2.7
RCP4.5 - end	7.2±2.8	7.3±2.8	7.0±2.7	6.7±2.4	6.2±2.1	6.5±2.2	6.4±2.8	5.9±2.9	5.7±2.7	6.5±2.9	7.7±2.6	7.4±2.7
RCP8.5 - end	7.3±2.9	7.2±2.8	6.9±2.7	6.4±2.3	6.0±2.0	6.3±2.3	6.5±2.7	6.0±2.8	5.9±2.9	6.5±2.6	7.5±2.5	7.4±2.8
Top 5 percent Wind Speed (m/s)												
Hindcast	13.0±1.0	12.7±0.9	12.8±1.4	11.7±1.1	11.3±1.6	12.1±2.1	14.2±2.8	14.4±2.7	12.9±2.2	14.0±2.5	13.9±1.6	13.3±1.2
RCP4.5 - mid	12.8±0.9	13.0±0.9	12.6±1.1	12.0±1.5	10.7±1.0	12.2±2.5	13.2±2.5	13.1±2.5	13.6±2.9	12.7±1.8	13.4±1.6	13.7±1.2
RCP8.5 - mid	13.0±0.9	13.0±1.1	12.3±0.9	11.5±0.9	10.4±1.1	12.2±2.6	13.7±2.8	13.5±2.5	14.1±3.1	13.1±2.0	13.2±2.5	13.4±1.2
RCP4.5 - end	12.8±0.9	12.7±0.8	12.6±0.8	11.5±1.1	10.3±1.2	11.5±2.0	13.3±2.7	13.4±2.7	12.2±2.4	13.3±2.1	13.2±1.6	12.9±1.1
RCP8.5 - end	13.2±0.8	12.7±0.8	12.1±0.8	11.2±0.9	9.9±0.8	11.8±2.3	13.7±2.5	13.7±2.6	13.6±2.7	12.4±2.4	12.9±1.5	13.1±1.0
Mean Wind Direction (°)												
Hindcast	245±51	240±52	251±43	262±34	270±33	273±35	279±52	284±67	274±59	268±46	265±37	255±41
RCP4.5 - mid	246±49	243±50	250±40	260±30	271±35	276±31	277±47	284±67	275±63	268±49	264±36	255±43
RCP8.5 - mid	245±48	244±49	251±42	261±32	271±31	277±33	278±50	288±73	279±71	267±50	265±35	256±43
RCP4.5 - end	246±51	242±45	251±42	260±32	272±33	275±30	279±51	287±67	275±62	268±49	264±34	259±41
RCP8.5 - end	246±49	242±48	249±40	261±31	272±30	277±33	280±47	286±61	282±68	268±48	264±32	259±39
Top 5 percent Wind Direction (°)												
Hindcast	236±29	236±26	239±21	245±21	265±30	276±40	307±66	320±70	289±70	268±48	255±38	244±26
RCP4.5 - mid	240±24	236±18	239±19	244±17	261±26	287±37	287±66	344±86	290±77	264±54	250±36	244±26
RCP8.5 - mid	242±27	241±25	241±22	247±20	264±25	284±40	313±67	346±86	342±84	268±50	259±36	246±27
RCP4.5 - end	240±25	237±24	239±19	247±18	260±25	277±32	304±64	328±78	295±75	267±54	251±35	244±22
RCP8.5 - end	240±21	238±20	238±15	249±15	263±20	282±40	312±64	327±75	343±92	263±49	255±29	248±24

Appendix B14. Table showing return values of ensemble-average wind speeds of hindcast and forecast scenarios, including lower and higher 95 percent confidence intervals, at the Asuncion location.

[Years: Hindcast = 1976–2005; RCP mid = 2026–2045; RCP end = 2081–2100. Wind speeds are in meters per second]

Scenario	Hindcast			RCP4.5 - mid			RCP8.5 - mid			RCP4.5 - end			RCP8.5 - end		
	Low	R_v	High	Low	R_v	High	Low	R_v	High	Low	R_v	High	Low	R_v	High
2-year	20.83	22.81	25.78	19.32	21.91	26.53	20.13	22.84	27.40	19.02	21.50	25.87	18.95	21.21	25.18
5-year	22.00	24.98	29.81	20.23	24.13	32.01	21.35	25.53	33.36	19.84	23.48	30.67	19.55	22.69	28.85
10-year	22.73	26.51	33.00	20.77	25.72	36.66	22.12	27.52	38.49	20.31	24.84	34.56	19.87	23.62	31.56
20-year	23.35	27.94	36.30	21.21	27.24	41.82	22.79	29.47	44.20	20.68	26.07	38.70	20.10	24.40	34.23
50-year	24.03	29.70	40.86	21.68	29.12	49.48	23.52	31.98	52.78	21.06	27.55	44.56	20.30	25.24	37.69
100-year	24.45	30.93	44.45	21.96	30.46	56.00	23.99	33.83	60.15	21.27	28.55	49.31	20.41	25.76	40.25

Appendix B15. Table showing Kosrae monthly means and mean of the top 5 percent for wind speed and mean wind direction.

[Years: Hindcast = 1976–2005; RCP mid = 2026–2045; RCP end = 2081–2100. Wind directions are "coming from"]

Month	Jan	Feb	Mar	Apr	May	Jun	July	Aug	Sep	Oct	Nov	Dec
Mean Wind Speed (m/s)												
Hindcast	7.5±2.1	7.4±2.0	6.8±2.0	5.7±2.1	4.4±2.0	4.1±2.0	4.2±1.9	4.4±1.9	4.4±2.0	4.3±2.1	4.6±2.4	6.3±2.6
RCP4.5 - mid	7.5±2.0	7.4±2.0	7.0±2.0	5.8±2.1	4.5±2.0	4.2±2.1	4.3±1.9	4.5±2.0	4.5±2.0	4.3±2.1	4.5±2.2	6.1±2.4
RCP8.5 - mid	7.3±2.1	7.5±2.1	7.0±2.0	5.9±2.1	4.5±2.2	4.1±2.0	4.4±2.0	4.5±2.0	4.6±1.9	4.3±2.1	4.4±2.2	5.9±2.5
RCP4.5 - end	7.2±2.0	7.3±1.9	6.9±1.9	5.7±2.0	4.5±2.0	4.2±2.1	4.3±2.0	4.5±2.1	4.5±2.1	4.2±2.1	4.5±2.2	5.9±2.4
RCP8.5 - end	7.1±2.0	7.2±1.9	6.9±1.8	5.9±1.9	4.7±2.1	4.3±2.1	4.4±1.9	4.8±2.0	4.6±2.0	4.2±2.0	4.3±2.0	5.9±2.3
Top 5 percent Wind Speed (m/s)												
Hindcast	11.3±0.8	10.9±0.6	10.9±1.1	10.1±1.2	9.0±1.4	8.8±1.3	9.0±2.1	9.3±2.0	9.6±1.7	9.7±1.7	10.4±1.7	11.5±1.2
RCP4.5 - mid	11.3±0.9	11.0±1.2	10.6±0.7	10.0±0.8	9.0±1.0	9.3±1.7	9.1±1.8	9.7±1.9	9.2±1.5	9.6±1.7	9.9±1.7	11.2±1.3
RCP8.5 - mid	11.2±0.7	11.6±1.5	10.8±0.8	10.5±1.4	9.6±1.6	8.7±1.2	9.5±1.8	9.8±1.7	9.4±1.5	9.5±1.8	10.0±1.3	11.0±0.9
RCP4.5 - end	10.7±0.6	10.6±0.6	10.4±0.8	9.7±0.8	9.1±0.8	9.2±1.9	9.4±2.0	10.1±1.7	9.9±1.5	9.3±1.4	9.9±1.7	11.1±1.2
RCP8.5 - end	10.8±0.7	10.9±1.0	10.4±0.8	9.8±0.6	9.6±1.4	9.5±1.9	9.2±1.9	10.0±2.2	9.2±1.5	9.1±1.5	9.2±1.4	10.6±1.0
Mean Wind Direction (°)												
Hindcast	245±21	245±19	247±25	253±33	267±53	278±60	292±55	301±51	306±55	311±65	278±60	251±38
RCP4.5 - mid	246±23	244±22	246±21	253±31	261±44	272±59	288±55	303±53	304±54	309±62	284±64	256±42
RCP8.5 - mid	246±22	245±21	247±20	250±31	258±47	275±59	289±59	304±57	305±54	309±66	281±64	255±39
RCP4.5 - end	247±23	245±21	247±21	252±31	258±45	273±58	288±57	304±57	307±59	308±66	283±64	256±40
RCP8.5 - end	248±22	247±18	248±19	251±24	259±40	267±55	282±54	299±52	302±52	303±60	281±58	257±35
Top 5 percent Wind Direction (°)												
Hindcast	236±14	235±12	232±29	236±31	246±63	262±82	346±92	355±75	18±82	38±80	261±91	233±27
RCP4.5 - mid	234±17	235±25	238±13	238±29	238±43	258±74	330±96	3±71	337±73	8±68	282±105	235±43
RCP8.5 - mid	238±14	237±29	236±17	233±49	233±57	258±89	30±100	30±68	30±82	33±83	226±85	234±25
RCP4.5 - end	232±14	236±20	236±17	242±26	240±24	274±67	30±98	31±74	30±76	33±83	319±114	232±41
RCP8.5 - end	238±16	242±21	240±28	241±20	242±42	251±79	322±99	3±79	329±83	355±91	261±74	235±24

Appendix B16. Table showing return values of ensemble-average wind speeds of hindcast and forecast scenarios, including lower and higher 95 percent confidence intervals, at the Kosrae location.

[Years: Hindcast = 1976–2005; RCP mid = 2026–2045; RCP end = 2081–2100. Wind speeds are in meters per second]

Scenario	Hindcast			RCP4.5 - mid			RCP8.5 - mid			RCP4.5 - end			RCP8.5 - end		
	Low	R_v	High	Low	R_v	High	Low	R_v	High	Low	R_v	High	Low	R_v	High
2-year	15.25	17.04	20.24	15.02	16.86	20.33	14.77	16.36	19.19	14.70	16.54	19.99	14.45	16.35	20.20
5-year	16.20	19.32	25.71	15.67	18.58	24.92	15.43	17.94	23.03	15.35	18.26	24.51	15.19	18.49	26.46
10-year	16.89	21.30	31.37	16.08	19.91	29.21	15.85	19.16	26.52	15.77	19.58	28.70	15.71	20.38	33.25
20-year	17.56	23.52	38.77	16.43	21.25	34.35	16.22	20.38	30.61	16.13	20.91	33.67	16.21	22.52	42.55
50-year	18.42	26.90	52.19	16.83	23.06	42.75	16.63	22.03	37.15	16.52	22.68	41.72	16.82	25.82	60.30
100-year	19.04	29.83	66.03	17.07	24.45	50.58	16.90	23.29	43.10	16.77	24.04	49.15	17.26	28.72	79.58

Appendix B17. Table showing Palau monthly means and mean of the top 5 percent for wind speed and mean wind direction.

[Years: Hindcast = 1976–2005; RCP mid = 2026–2045; RCP end = 2081–2100. Wind directions are "coming from"]

Month	Jan	Feb	Mar	Apr	May	Jun	July	Aug	Sep	Oct	Nov	Dec
Mean Wind Speed (m/s)												
Hindcast	7.7±2.5	8.1±2.3	7.3±2.2	6.2±2.2	4.7±2.3	4.0±2.3	4.0±2.5	4.1±2.7	4.0±2.6	4.2±2.6	4.9±2.7	6.5±2.8
RCP4.5 - mid	7.3±2.6	7.7±2.3	7.3±2.1	6.3±2.1	4.7±2.2	4.1±2.3	4.3±2.7	4.0±2.3	3.9±2.3	4.2±2.6	4.7±2.7	6.0±2.8
RCP8.5 - mid	7.5±2.5	7.6±2.3	7.4±2.1	6.3±2.0	4.6±2.2	4.2±2.4	4.2±2.6	4.3±2.6	4.0±2.5	4.1±2.5	4.7±2.6	6.1±2.8
RCP4.5 - end	7.4±2.5	7.8±2.1	7.2±2.2	6.1±2.2	4.7±2.2	4.1±2.3	4.4±2.5	4.3±2.7	4.1±2.6	4.0±2.4	4.5±2.5	5.9±2.7
RCP8.5 - end	7.1±2.4	7.4±2.2	7.2±2.0	6.2±1.9	4.6±2.3	4.2±2.3	4.4±2.6	4.3±2.6	4.2±2.5	4.0±2.3	4.5±2.6	5.8±2.6
Top 5 percent Wind Speed (m/s)												
Hindcast	12.6±1.1	13.0±1.3	11.8±1.2	10.5±1.3	9.7±1.3	9.9±1.6	10.9±1.4	11.8±1.8	11.5±1.6	11.2±1.5	11.9±2.1	12.3±1.5
RCP4.5 - mid	12.7±1.5	12.2±1.1	11.5±1.1	10.3±1.2	9.6±1.4	10.2±1.8	11.7±1.5	10.3±1.7	10.4±2.0	11.7±2.1	11.8±2.0	12.4±1.9
RCP8.5 - mid	12.3±1.2	12.1±0.9	11.8±1.3	10.5±1.3	9.3±1.0	10.6±2.1	11.0±1.5	11.4±1.7	11.0±2.0	10.9±1.3	11.1±1.5	12.2±1.7
RCP4.5 - end	12.4±1.5	12.1±1.4	11.4±1.2	10.7±1.3	9.5±1.4	10.2±1.8	11.1±1.8	11.6±1.7	11.6±1.8	11.0±2.2	10.8±1.7	11.9±1.6
RCP8.5 - end	11.9±1.1	12.1±1.1	11.7±1.3	10.0±1.0	9.6±1.3	9.9±1.7	11.0±1.8	11.6±1.9	11.5±2.3	10.1±1.5	11.3±2.1	11.8±1.7
Mean Wind Direction (°)												
Hindcast	243±30	239±27	241±33	246±36	257±62	283±85	333±82	350±75	354±86	341±105	255±81	249±47
RCP4.5 - mid	244±37	242±29	243±27	248±33	256±52	287±86	345±83	330±74	339±80	358±103	259±84	248±50
RCP8.5 - mid	244±32	243±28	244±29	248±32	255±52	295±91	345±88	343±77	342±77	348±100	261±87	249±54
RCP4.5 - end	246±32	243±24	244±27	248±37	258±61	288±92	340±87	348±76	347±80	354±103	258±87	250±51
RCP8.5 - end	245±35	243±27	245±26	248±27	258±61	287±91	337±88	342±77	344±77	319±93	264±82	254±51
Top 5 percent Wind Direction (°)												
Hindcast	233±29	222±38	232±37	241±39	247±74	44±97	38±51	36±34	53±36	54±46	69±115	241±48
RCP4.5 - mid	236±34	236±31	236±34	246±42	250±50	8±102	45±34	40±44	37±47	55±45	55±119	234±80
RCP8.5 - mid	238±36	242±33	239±40	236±41	245±45	33±61	41±40	37±32	47±35	55±48	55±93	246±68
RCP4.5 - end	235±48	235±26	236±33	244±48	250±63	22±97	37±40	44±35	45±36	55±52	78±130	240±52
RCP8.5 - end	239±36	236±40	244±38	246±31	256±60	10±90	36±42	37±30	41±40	49±63	58±91	253±70

Appendix B18. Table showing return values of ensemble-average wind speeds of hindcast and forecast scenarios, including lower and higher 95 percent confidence intervals, at the Palau location.

[Years: Hindcast = 1976–2005; RCP mid = 2026–2045; RCP end = 2081–2100. Wind speeds are in meters per second]

Scenario	Hindcast			RCP4.5 - mid			RCP8.5 - mid			RCP4.5 - end			RCP8.5 - end		
	Low	R_v	High	Low	R_v	High	Low	R_v	High	Low	R_v	High	Low	R_v	High
2-year	17.15	18.57	20.79	17.09	18.94	22.18	16.67	18.62	22.31	17.31	18.94	21.49	17.04	18.55	21.18
5-year	17.95	20.16	23.94	17.66	20.31	25.51	17.49	20.76	27.93	18.03	20.38	24.37	17.57	19.80	24.09
10-year	18.46	21.32	26.59	17.98	21.22	28.10	18.05	22.55	33.59	18.45	21.33	26.53	17.88	20.65	26.42
20-year	18.91	22.46	29.48	18.22	22.02	30.78	18.57	24.49	40.86	18.79	22.18	28.68	18.12	21.42	28.88
50-year	19.41	23.92	33.74	18.45	22.93	34.42	19.20	27.33	53.70	19.13	23.15	31.50	18.37	22.34	32.34
100-year	19.74	25.00	37.32	18.57	23.53	37.27	19.63	29.69	66.64	19.32	23.80	33.62	18.51	22.97	35.12

Appendix B19. Table showing Pohnpei monthly means and mean of the top 5 percent for wind speed and mean wind direction.

[Years: Hindcast = 1976–2005; RCP mid = 2026–2045; RCP end = 2081–2100. Wind directions are "coming from"]

Month	Jan	Feb	Mar	Apr	May	Jun	July	Aug	Sep	Oct	Nov	Dec
Mean Wind Speed (m/s)												
Hindcast	8.5±2.0	8.4±2.0	7.8±2.1	6.7±2.4	5.0±2.4	4.3±2.4	4.1±2.3	4.2±2.3	4.1±2.4	4.2±2.4	5.2±2.8	7.5±2.7
RCP4.5 - mid	8.4±2.2	8.3±2.0	8.0±2.0	6.8±2.3	5.2±2.4	4.5±2.4	4.3±2.4	4.3±2.4	4.1±2.3	4.1±2.3	4.9±2.5	7.2±2.7
RCP8.5 - mid	8.3±2.1	8.4±2.2	7.9±2.1	6.9±2.2	5.2±2.5	4.5±2.3	4.4±2.4	4.3±2.4	4.2±2.2	4.1±2.3	4.8±2.6	7.1±2.7
RCP4.5 - end	8.2±2.0	8.2±1.9	7.8±2.0	6.6±2.2	5.2±2.4	4.7±2.5	4.3±2.2	4.4±2.5	4.2±2.4	4.1±2.3	4.9±2.6	6.9±2.7
RCP8.5 - end	8.0±2.1	8.0±1.9	7.9±1.8	6.9±2.0	5.5±2.4	4.6±2.4	4.5±2.4	4.4±2.4	4.1±2.3	3.9±2.1	4.6±2.5	7.0±2.5
Top 5 percent Wind Speed (m/s)												
Hindcast	12.2±0.8	12.1±0.7	11.6±0.7	11.0±0.9	10.3±1.6	10.3±1.9	10.4±2.1	10.8±2.0	11.1±2.2	11.0±1.9	11.8±1.4	12.6±1.2
RCP4.5 - mid	12.6±1.0	11.9±0.6	11.6±0.8	10.8±0.5	10.1±0.9	10.2±1.7	10.9±2.2	11.4±2.2	10.8±2.2	10.5±2.3	11.0±1.6	12.7±1.1
RCP8.5 - mid	12.2±0.9	12.6±1.6	11.7±1.1	11.1±1.0	10.3±1.3	10.0±1.5	10.7±2.1	11.6±2.2	10.6±2.0	10.5±1.8	11.3±1.4	12.6±1.2
RCP4.5 - end	11.8±0.7	11.6±0.6	11.4±0.9	10.6±1.1	10.3±1.1	10.5±1.7	10.2±1.9	11.8±2.5	11.3±1.9	10.6±1.9	11.2±1.8	12.3±1.1
RCP8.5 - end	12.0±0.9	11.7±1.0	11.4±1.3	10.8±0.7	10.6±1.3	10.4±1.7	11.0±2.3	11.6±2.3	10.9±2.4	9.6±2.2	11.1±1.7	12.0±1.2
Mean Wind Direction (°)												
Hindcast	245±17	244±16	246±21	250±30	255±51	266±66	290±68	310±66	319±72	312±83	263±59	248±28
RCP4.5 - mid	247±21	245±18	246±17	249±27	255±41	263±62	285±65	312±70	316±70	317±81	266±65	252±35
RCP8.5 - mid	246±16	244±17	247±18	248±25	253±42	264±61	287±72	317±74	316±69	320±83	265±66	251±31
RCP4.5 - end	248±17	245±18	247±19	251±25	253±41	263±64	285±67	318±72	320±73	324±82	269±65	252±34
RCP8.5 - end	248±18	246±15	247±17	249±18	253±37	261±57	281±64	309±66	315±66	308±77	267±61	252±27
Top 5 percent Wind Direction (°)												
Hindcast	238±13	236±13	239±18	239±22	240±47	273±92	20±101	36±65	49±63	43±83	256±62	235±20
RCP4.5 - mid	239±21	238±12	240±16	241±27	239±28	250±64	35±90	37±64	32±64	44±64	230±67	237±31
RCP8.5 - mid	238±12	234±27	241±21	237±29	245±41	254±75	53±78	47±50	41±60	56±68	239±62	240±25
RCP4.5 - end	238±11	239±12	239±18	242±25	241±23	255±77	40±85	49±54	50±46	44±68	251±87	237±29
RCP8.5 - end	238±19	241±14	236±26	241±10	238±37	247±63	15±95	46±50	30±64	23±98	237±52	238±21

Appendix B20. Table showing return values of ensemble-average wind speeds of hindcast and forecast scenarios, including lower and higher 95 percent confidence intervals, at the Pohnpei location.

[Years: Hindcast = 1976–2005; RCP mid = 2026–2045; RCP end = 2081–2100. Wind speeds are in meters per second]

Scenario	Hindcast			RCP4.5 - mid			RCP8.5 - mid			RCP4.5 - end			RCP8.5 - end		
	Low	R_v	High	Low	R_v	High	Low	R_v	High	Low	R_v	High	Low	R_v	High
2-year	17.09	18.67	21.14	17.24	19.07	22.05	16.66	18.63	22.34	16.50	18.44	21.85	17.26	18.87	21.44
5-year	17.92	20.32	24.40	18.09	20.85	25.80	17.38	20.54	27.35	17.16	20.03	25.68	17.92	20.23	24.23
10-year	18.44	21.49	27.03	18.61	22.12	28.89	17.85	22.02	32.06	17.54	21.12	28.81	18.30	21.12	26.32
20-year	18.87	22.59	29.80	19.05	23.33	32.20	18.26	23.54	37.75	17.84	22.13	32.15	18.60	21.90	28.39
50-year	19.35	23.94	33.71	19.53	24.84	36.96	18.72	25.61	47.13	18.15	23.34	36.94	18.89	22.80	31.09
100-year	19.64	24.90	36.86	19.83	25.91	40.87	19.01	27.21	55.95	18.33	24.17	40.84	19.06	23.38	33.11

Appendix B21. Table showing Yap monthly means and mean of the top 5 percent for wind speed and mean wind direction.

[Years: Hindcast = 1976–2005; RCP mid = 2026–2045; RCP end = 2081–2100. Wind directions are "coming from"]

Month	Jan	Feb	Mar	Apr	May	Jun	July	Aug	Sep	Oct	Nov	Dec
Mean Wind Speed (m/s)												
Hindcast	8.6±2.4	8.9±2.2	8.2±2.1	7.1±2.1	5.5±2.3	4.6±2.5	4.5±2.9	4.6±3.1	4.4±2.8	4.6±2.6	6.0±3.0	7.8±2.7
RCP4.5 - mid	8.3±2.5	8.6±2.2	8.3±2.1	7.2±2.0	5.5±2.3	4.7±2.6	4.7±3.1	4.5±2.7	4.4±2.6	4.7±2.7	5.7±2.8	7.5±2.7
RCP8.5 - mid	8.5±2.3	8.5±2.1	8.2±2.1	7.2±1.9	5.4±2.3	4.8±2.7	4.6±2.9	4.7±3.0	4.4±2.8	4.4±2.4	5.4±2.7	7.5±2.8
RCP4.5 - end	8.4±2.4	8.7±2.0	8.1±2.0	7.0±2.1	5.6±2.2	4.7±2.6	4.9±2.9	4.8±3.0	4.5±2.8	4.4±2.5	5.5±2.6	7.3±2.6
RCP8.5 - end	8.2±2.3	8.3±2.0	7.9±1.9	7.1±1.7	5.6±2.3	4.8±2.5	4.8±2.9	4.8±3.0	4.6±2.7	4.2±2.3	5.3±2.8	7.2±2.6
Top 5 percent Wind Speed (m/s)												
Hindcast	13.2±1.2	13.4±1.3	12.3±1.4	11.0±0.9	10.3±1.4	10.8±2.0	12.5±2.1	13.4±1.9	12.5±2.1	11.4±1.8	12.8±2.2	13.1±1.6
RCP4.5 - mid	12.8±1.0	12.6±1.2	12.2±1.3	10.9±1.0	10.2±1.3	11.1±2.2	13.4±1.9	11.8±2.3	11.9±2.5	12.1±2.2	12.3±1.9	13.1±1.6
RCP8.5 - mid	13.1±1.2	12.5±0.8	12.5±1.4	11.0±1.4	10.0±1.3	12.2±2.6	12.5±1.7	13.1±2.2	12.5±2.3	10.8±1.9	11.5±1.6	13.0±1.6
RCP4.5 - end	13.2±1.4	12.4±1.0	12.0±1.3	11.1±1.4	10.1±1.4	10.8±1.9	12.7±2.1	12.9±1.9	12.4±2.1	11.5±2.5	11.5±1.8	12.6±1.4
RCP8.5 - end	12.8±1.2	12.4±0.9	11.7±0.9	10.5±1.1	10.0±1.3	10.7±1.9	12.7±2.5	13.3±2.1	12.1±2.7	10.4±2.1	12.1±2.1	12.5±1.7
Mean Wind Direction (°)												
Hindcast	246±24	243±22	246±25	250±29	259±49	276±83	345±93	10±85	14±95	308±107	260±63	251±33
RCP4.5 - mid	247±28	245±21	246±22	251±24	257±46	279±83	346±95	358±87	5±93	339±108	257±65	252±37
RCP8.5 - mid	247±23	246±21	247±23	252±25	258±44	283±86	349±93	8±86	8±91	345±115	260±70	252±38
RCP4.5 - end	249±23	245±19	247±21	252±26	260±43	275±84	343±95	5±86	6±89	352±112	259±65	253±35
RCP8.5 - end	248±25	246±21	248±19	251±20	258±47	277±86	328±91	359±86	8±87	320±103	262±64	255±35
Top 5 percent Wind Direction (°)												
Hindcast	237±22	233±27	236±35	249±38	253±63	12±110	44±44	34±38	48±51	45±74	285±92	248±41
RCP4.5 - mid	239±21	238±17	244±32	248±16	252±42	341±84	36±42	38±47	31±48	21±79	249±80	249±50
RCP8.5 - mid	238±29	242±24	243±33	245±40	249±41	22±67	38±44	35±30	38±40	51±77	252±83	249±46
RCP4.5 - end	245±32	236±17	240±19	253±44	257±47	335±92	37±45	40±32	38±43	38±72	247±77	242±34
RCP8.5 - end	238±32	237±22	242±19	246±20	255±31	336±90	25±32	33±36	35±45	32±77	282±93	253±44

Appendix B22. Table showing return values of ensemble-average wind speeds of hindcast and forecast scenarios, including lower and higher 95 percent confidence intervals, at the Yap location.

[Years: Hindcast = 1976–2005; RCP mid = 2026–2045; RCP end = 2081–2100. Wind speeds are in meters per second]

Scenario	Hindcast			RCP4.5 - mid			RCP8.5 - mid			RCP4.5 - end			RCP8.5 - end		
	Low	R_v	High	Low	R_v	High	Low	R_v	High	Low	R_v	High	Low	R_v	High
2-year	18.96	20.51	22.80	18.72	20.38	22.89	18.46	20.32	23.40	18.17	19.98	23.03	18.83	20.67	23.60
5-year	20.01	22.41	26.26	19.40	21.68	25.37	19.04	21.62	26.31	18.83	21.46	26.33	19.45	21.96	26.29
10-year	20.69	23.81	29.10	19.77	22.46	27.06	19.35	22.42	28.41	19.20	22.44	28.90	19.77	22.72	28.13
20-year	21.30	25.17	32.16	20.04	23.11	28.60	19.57	23.09	30.42	19.50	23.32	31.53	20.00	23.35	29.83
50-year	22.01	26.93	36.57	20.30	23.80	30.44	19.78	23.81	32.95	19.79	24.34	35.11	20.20	24.00	31.87
100-year	22.47	28.23	40.20	20.44	24.22	31.70	19.89	24.25	34.77	19.96	25.03	37.90	20.31	24.39	33.27

Appendix B23. Table showing Majuro monthly means and mean of the top 5 percent for wind speed and mean wind direction.

[Years: Hindcast = 1976–2005; RCP mid = 2026–2045; RCP end = 2081–2100. Wind directions are "coming from"]

Month	Jan	Feb	Mar	Apr	May	Jun	July	Aug	Sep	Oct	Nov	Dec
Mean Wind Speed (m/s)												
Hindcast	8.7±1.9	8.6±1.9	8.1±2.1	6.8±2.4	5.2±2.5	4.8±2.4	4.5±2.2	4.3±2.1	4.1±2.0	4.2±2.3	5.2±2.7	7.6±2.8
RCP4.5 - mid	8.6±1.9	8.5±1.9	8.3±2.0	6.9±2.3	5.6±2.5	5.1±2.5	4.7±2.3	4.3±2.2	4±1.9	4.2±2.2	4.9±2.6	7.4±2.7
RCP8.5 - mid	8.6±1.9	8.6±2.0	8.1±2.0	7.2±2.3	5.6±2.5	4.9±2.4	4.7±2.3	4.3±2.1	4.1±2.0	4.1±2.0	5.0±2.7	7.2±2.7
RCP4.5 - end	8.4±1.8	8.4±1.8	8.1±1.9	6.9±2.3	5.7±2.5	5.1±2.5	4.6±2.2	4.4±2.1	4.2±2.1	4.1±2.2	4.9±2.5	7.1±2.6
RCP8.5 - end	8.3±1.8	8.4±1.8	8.1±1.7	7.3±2.2	6.1±2.5	5.3±2.5	4.9±2.3	4.4±2.0	4.1±1.9	4.0±2.2	4.8±2.5	7.2±2.5
Top 5 percent Wind Speed (m/s)												
Hindcast	12.3±0.7	12.2±0.6	12.0±0.7	11.3±1.0	10.2±1.1	10.0±0.9	9.9±1.4	9.8±1.8	9.3±1.6	10.3±2.1	11.6±1.4	12.7±1.4
RCP4.5 - mid	12.2±0.6	12.1±0.9	11.8±0.7	11.1±0.6	10.5±0.8	10.5±1.1	10.1±1.2	10.1±1.9	8.8±1.7	9.9±2.0	11.2±1.6	12.5±0.9
RCP8.5 - mid	12.2±0.6	12.5±0.7	11.9±0.7	11.8±1.4	10.6±0.9	10.2±1.0	10.4±1.7	10.0±1.8	9.7±2.3	9.4±1.7	11.9±2.0	12.1±0.7
RCP4.5 - end	11.9±0.8	11.9±0.7	11.7±0.8	11.1±0.7	10.6±1.0	10.4±1.2	10.1±1.9	10.2±2.1	9.9±1.9	10.3±2.0	11.1±2.1	12.5±1.1
RCP8.5 - end	11.6±0.6	11.8±0.7	11.6±0.7	11.2±0.8	10.8±0.8	10.6±1.1	10.3±1.6	9.6±2.0	9.2±1.9	10.1±2.1	10.8±1.3	11.7±0.9
Mean Wind Direction (°)												
Hindcast	242±16	243±14	246±17	250±25	256±45	263±53	278±56	296±58	308±65	302±70	262±58	246±31
RCP4.5 - mid	244±16	244±15	244±14	250±22	253±36	261±49	273±51	295±56	302±61	305±67	267±62	250±32
RCP8.5 - mid	244±16	243±14	245±15	249±23	253±37	261±50	277±51	296±57	308±62	305±70	266±64	249±31
RCP4.5 - end	245±16	245±14	246±15	250±22	253±38	260±51	273±52	297±58	307±63	310±73	270±62	250±31
RCP8.5 - end	246±15	246±13	246±13	249±19	252±29	258±45	270±51	289±55	303±61	301±67	266±54	251±28
Top 5 percent Wind Direction (°)												
Hindcast	235±11	236±9	238±15	239±20	243±31	244±43	262±77	349±99	21±100	335±89	246±47	235±24
RCP4.5 - mid	237±10	239±17	236±9	240±13	238±23	243±45	256±64	325±82	317±87	359±86	239±48	236±15
RCP8.5 - mid	236±9	236±10	236±9	239±30	238±19	244±42	284±74	337±98	28±78	14±91	238±69	234±14
RCP4.5 - end	235±14	238±9	238±16	236±14	237±23	245±39	269±64	346±96	19±78	27±83	246±75	234±28
RCP8.5 - end	239±10	239±11	238±10	238±19	238±15	241±35	251±77	321±90	356±113	5±101	249±50	236±14

Appendix B24. Table showing return values of ensemble-average wind speeds of hindcast and forecast scenarios, including lower and higher 95 percent confidence intervals, at the Majuro location.

[Years: Hindcast = 1976–2005; RCP mid = 2026–2045; RCP end = 2081–2100. Wind speeds are in meters per second]

Scenario	Hindcast			RCP4.5 - mid			RCP8.5 - mid			RCP4.5 - end			RCP8.5 - end		
	Low	R_v	High	Low	R_v	High	Low	R_v	High	Low	R_v	High	Low	R_v	High
2-year	15.90	17.74	21.17	15.48	16.59	18.40	15.75	17.26	19.96	16.11	18.06	21.61	15.08	16.46	19.06
5-year	16.96	20.41	27.93	15.93	17.54	20.41	16.51	19.07	24.26	16.84	19.90	26.23	15.63	17.89	22.81
10-year	17.79	22.95	35.70	16.18	18.17	21.96	17.05	20.59	28.55	17.31	21.29	30.41	15.99	19.05	26.46
20-year	18.66	26.06	46.88	16.39	18.73	23.54	17.56	22.26	33.97	17.70	22.68	35.30	16.32	20.27	31.01
50-year	19.86	31.26	69.54	16.59	19.39	25.66	18.20	24.71	43.44	18.14	24.52	43.03	16.70	21.99	38.77
100-year	20.81	36.23	95.58	16.71	19.83	27.30	18.65	26.77	52.86	18.41	25.90	50.03	16.96	23.38	46.34

Appendix B25. Table showing Enewetak monthly means and mean of the top 5 percent for wind speed and mean wind direction.

[Years: Hindcast = 1976–2005; RCP mid = 2026–2045; RCP end = 2081–2100. Wind directions are "coming from"]

Month	Jan	Feb	Mar	Apr	May	Jun	July	Aug	Sep	Oct	Nov	Dec
Mean Wind Speed (m/s)												
Hindcast	9.4±1.8	9.1±1.9	9.0±1.8	8.5±2.0	7.1±2.5	6.0±2.8	5.4±2.9	5.2±2.9	5.0±2.6	5.7±3.0	8.0±2.8	9.4±2.1
RCP4.5 - mid	9.4±1.9	9.0±1.9	9.0±1.8	8.5±2.0	7.3±2.3	6.3±2.8	5.5±3.0	5.0±2.8	4.9±2.7	5.3±2.9	7.5±2.9	9.2±2.0
RCP8.5 - mid	9.3±1.9	9.2±1.9	8.9±1.8	8.5±1.9	7.4±2.3	6.4±2.7	5.6±2.9	5.1±2.9	4.8±2.7	5.2±2.7	7.3±3.0	9.2±2.1
RCP4.5 - end	9.2±1.8	9.1±1.8	9.1±1.8	8.4±2.0	7.4±2.3	6.4±2.8	5.7±3.0	5.5±3.0	4.9±2.8	5.3±2.7	7.3±2.9	9.2±2.0
RCP8.5 - end	9.0±1.9	8.8±1.9	8.7±1.7	8.4±1.7	7.6±2.2	6.5±2.7	5.7±3.0	5.2±3.1	4.7±2.7	4.9±2.6	7.0±2.9	9.0±1.9
Top 5 percent Wind Speed (m/s)												
Hindcast	12.8±0.7	12.7±0.7	12.6±1.0	12.3±1.4	11.6±1.4	11.1±1.3	11.4±1.7	12.4±2.5	11.8±2.3	12.7±1.8	13.4±1.5	13.3±1.0
RCP4.5 - mid	12.7±0.6	12.6±0.7	12.2±0.5	12.2±1.1	11.0±0.6	11.2±1.5	12.2±2.0	12.0±2.2	11.9±2.3	12.6±2.4	13.3±1.8	13.2±1.1
RCP8.5 - mid	12.6±0.6	12.9±0.7	12.4±0.7	12.1±1.5	11.5±1.2	11.2±1.1	11.8±1.8	12.2±2.7	12.0±2.3	12.1±2.1	13.2±1.4	13.1±0.9
RCP4.5 - end	12.5±0.5	12.5±0.7	12.6±0.7	11.9±1.2	11.0±0.6	11.3±1.6	11.9±2.3	13.2±2.3	12.6±2.6	12.1±2.1	12.9±1.7	13.1±1.3
RCP8.5 - end	12.4±0.6	12.3±0.7	12.3±1.1	11.4±0.5	11.1±1.2	11.0±1.3	12.2±2.3	13.2±2.9	11.7±2.6	11.8±2.7	13.0±2.1	12.5±0.8
Mean Wind Direction (°)												
Hindcast	246±12	246±14	248±13	250±16	254±29	259±48	268±71	294±99	294±111	263±78	252±34	248±15
RCP4.5 - mid	248±13	247±13	248±12	251±15	254±24	258±43	270±67	286±94	301±102	271±89	254±40	250±15
RCP8.5 - mid	247±11	246±12	248±11	250±16	254±22	258±38	268±67	293±97	312±109	271±89	253±39	249±15
RCP4.5 - end	247±12	246±13	248±11	252±15	253±23	258±38	267±64	290±95	307±105	274±92	253±41	250±15
RCP8.5 - end	248±13	248±13	249±10	251±11	255±21	258±38	265±58	285±81	305±102	271±89	254±39	250±14
Top 5 percent Wind Direction (°)												
Hindcast	244±9	243±9	242±11	244±16	254±24	260±39	273±60	9±91	11±95	265±62	250±30	244±12
RCP4.5 - mid	245±8	243±10	244±7	246±17	250±14	252±27	311±83	322±84	336±79	321±84	249±28	246±14
RCP8.5 - mid	245±8	243±9	245±9	243±23	250±22	255±32	288±78	351±100	36±75	288±85	247±32	246±13
RCP4.5 - end	245±8	243±10	244±8	250±16	251±17	259±27	300±73	33±69	16±76	308±101	246±31	245±16
RCP8.5 - end	245±14	244±14	246±12	249±7	252±16	256±32	289±70	9±75	11±70	273±81	250±25	246±9

Appendix B26. Table showing return values of ensemble-average wind speeds of hindcast and forecast scenarios, including lower and higher 95 percent confidence intervals, at the Enewetak location.

[Years: Hindcast = 1976–2005; RCP mid = 2026–2045; RCP end = 2081–2100. Wind speeds are in meters per second]

Scenario	Hindcast			RCP4.5 - mid			RCP8.5 - mid			RCP4.5 - end			RCP8.5 - end		
	Low	R_v	High	Low	R_v	High	Low	R_v	High	Low	R_v	High	Low	R_v	High
2-year	18.19	19.96	22.81	18.27	20.17	23.31	17.46	19.63	23.74	18.26	20.28	23.64	18.51	21.32	26.33
5-year	18.95	21.57	26.18	18.87	21.50	26.22	18.23	21.69	29.26	19.05	22.01	27.45	19.25	23.16	31.01
10-year	19.40	22.65	28.82	19.19	22.30	28.28	18.73	23.30	34.47	19.51	23.19	30.46	19.63	24.32	34.53
20-year	19.76	23.64	31.55	19.42	22.97	30.24	19.16	24.95	40.78	19.88	24.26	33.59	19.90	25.30	38.04
50-year	20.12	24.80	35.27	19.63	23.68	32.66	19.64	27.18	51.22	20.25	25.54	37.92	20.15	26.38	42.65
100-year	20.33	25.59	38.19	19.73	24.12	34.38	19.95	28.92	61.06	20.47	26.40	41.35	20.28	27.05	46.13

Appendix B27. Table showing Bikini monthly means and mean of the top 5 percent for wind speed and mean wind direction.

[Years: Hindcast = 1976–2005; RCP mid = 2026–2045; RCP end = 2081–2100. Wind directions are "coming from"]

Month	Jan	Feb	Mar	Apr	May	Jun	July	Aug	Sep	Oct	Nov	Dec
Mean Wind Speed (m/s)												
Hindcast	9.4±1.9	9.1±1.9	9.0±1.9	8.5±2.1	7.2±2.5	6.2±2.8	5.5±2.9	5.2±2.9	4.9±2.6	5.7±3	8.0±2.9	9.4±2.1
RCP4.5 - mid	9.4±1.9	9.1±1.9	9.1±1.8	8.6±2.0	7.5±2.3	6.4±2.8	5.6±3.0	5.1±2.8	4.8±2.6	5.3±2.8	7.5±2.9	9.2±2.1
RCP8.5 - mid	9.2±1.9	9.2±2.0	9.0±1.8	8.6±1.9	7.5±2.3	6.6±2.8	5.7±2.9	5.1±2.9	4.8±2.6	5.3±2.7	7.3±3.0	9.2±2.1
RCP4.5 - end	9.2±1.8	9.1±1.8	9.1±1.8	8.4±2.0	7.5±2.3	6.6±2.7	5.7±2.9	5.5±3.0	4.9±2.7	5.3±2.7	7.3±3.0	9.2±2.1
RCP8.5 - end	8.9±1.9	8.8±1.9	8.8±1.7	8.5±1.7	7.7±2.1	6.7±2.6	5.9±2.9	5.3±3.1	4.6±2.6	4.9±2.6	7.0±3.0	9.0±1.9
Top 5 percent Wind Speed (m/s)												
Hindcast	12.9±0.7	12.8±0.7	12.7±1.2	12.5±1.9	11.4±0.8	11.1±1.1	11.1±1.5	12.0±2.4	11.3±2.1	12.7±1.8	13.5±1.5	13.4±1.1
RCP4.5 - mid	12.7±0.5	12.8±1.0	12.3±0.7	12.3±1.1	11.2±0.8	11.3±1.4	11.7±1.8	12.0±2.1	11.3±2.2	12.5±2.3	13.2±1.5	13.2±0.9
RCP8.5 - mid	12.7±0.6	12.9±0.7	12.4±0.6	12.4±1.9	11.4±1.6	11.4±1.2	11.7±1.5	12.1±2.7	11.7±2.2	11.8±2.0	13.3±1.5	12.9±0.7
RCP4.5 - end	12.6±0.6	12.6±0.7	12.7±0.7	11.9±0.6	11.2±0.9	11.2±1.5	11.8±2.0	13.0±2.3	12.5±2.5	12.0±2.0	13.2±1.6	13.1±1.0
RCP8.5 - end	12.3±0.6	12.3±0.6	12.2±0.7	11.5±0.5	11.0±0.7	11.3±1.5	11.9±1.7	13.1±3.1	11.2±2.9	11.8±2.4	13.0±1.8	12.6±0.8
Mean Wind Direction (°)												
Hindcast	246±12	246±13	248±12	250±15	254±28	258±47	265±67	286±94	287±108	262±75	251±34	247±15
RCP4.5 - mid	247±13	246±13	247±12	250±15	253±23	257±41	267±61	280±86	291±98	269±86	252±38	249±15
RCP8.5 - mid	246±11	246±12	248±11	250±15	253±21	257±37	266±62	287±90	299±106	268±86	252±39	248±15
RCP4.5 - end	246±11	246±12	248±11	251±15	253±23	257±37	264±60	282±89	297±101	270±91	252±43	249±15
RCP8.5 - end	248±13	248±13	249±10	251±11	254±20	257±36	263±52	280±74	293±98	269±86	253±39	249±14
Top 5 percent Wind Direction (°)												
Hindcast	244±8	244±8	244±9	247±23	250±17	256±29	265±55	339±89	340±100	265±59	249±28	243±12
RCP4.5 - mid	245±7	243±10	244±7	248±13	249±11	252±26	282±65	312±77	324±77	295±74	247±25	246±11
RCP8.5 - mid	245±8	244±8	245±8	248±27	250±17	254±29	270±51	334±87	17±92	275±74	246±25	245±10
RCP4.5 - end	245±8	245±9	244±11	248±10	249±18	254±24	279±62	26±76	2±81	286±92	246±31	244±16
RCP8.5 - end	244±8	244±8	246±8	247±7	251±17	256±29	278±70	348±75	358±87	272±67	247±23	245±9

Appendix B28. Table showing return values of ensemble-average wind speeds of hindcast and forecast scenarios, including lower and higher 95 percent confidence intervals, at the Bikini location.

[Years: Hindcast = 1976–2005; RCP mid = 2026–2045; RCP end = 2081–2100. Wind speeds are in meters per second]

Scenario	Hindcast			RCP4.5 - mid			RCP8.5 - mid			RCP4.5 - end			RCP8.5 - end		
	Low	R_v	High	Low	R_v	High	Low	R_v	High	Low	R_v	High	Low	R_v	High
2-year	17.81	19.69	22.82	17.76	19.39	21.89	17.66	19.86	23.85	17.72	19.62	22.93	17.81	20.54	25.90
5-year	18.86	21.95	27.70	18.30	20.46	24.01	18.65	22.29	29.79	18.29	20.98	26.23	18.68	23.00	32.82
10-year	19.57	23.75	32.26	18.57	21.06	25.37	19.33	24.26	35.55	18.60	21.86	28.75	19.22	24.88	39.34
20-year	20.23	25.65	37.71	18.76	21.53	26.56	19.95	26.36	42.67	18.83	22.63	31.30	19.68	26.78	47.21
50-year	21.02	28.30	46.61	18.92	21.99	27.90	20.69	29.34	54.75	19.04	23.49	34.72	20.18	29.32	60.20
100-year	21.57	30.42	54.90	19.00	22.26	28.76	21.19	31.77	66.44	19.16	24.04	37.34	20.49	31.27	72.43

Appendix B29. Table showing Molokai monthly means and mean of the top 5 percent for wind speed and mean wind direction.

[Years: Hindcast = 1976–2005; RCP mid = 2026–2045; RCP end = 2081–2100. Wind directions are "coming from"]

Month	Jan	Feb	Mar	Apr	May	Jun	July	Aug	Sep	Oct	Nov	Dec
Mean Wind Speed (m/s)												
Hindcast	6.8±3.0	6.7±3.1	7.3±3.1	7.8±2.7	7.9±2.3	8.5±1.9	8.3±1.8	8.1±2.1	7.7±2.4	7.9±2.8	7.8±3.0	7.1±3.1
RCP4.5 - mid	6.7±3.1	6.9±3.1	7.4±3.1	8.2±2.8	7.7±2.3	8.2±1.9	8.5±1.7	8.0±1.9	7.6±2.3	7.9±2.7	8.0±3.0	7.1±3.1
RCP8.5 - mid	6.7±3.2	6.8±3.1	7.3±3.1	7.9±2.6	7.6±2.2	8.0±2.0	8.2±1.7	8.0±2.0	7.5±2.4	7.8±2.8	7.9±2.9	7.3±3.0
RCP4.5 - end	6.3±3.0	6.7±3.1	7.4±3.0	7.8±2.6	7.8±2.2	8.3±1.9	8.3±1.8	8.0±2.0	7.6±2.4	7.8±2.6	7.9±2.9	7.3±3.1
RCP8.5 - end	6.3±3.0	6.4±3.1	7.2±2.9	7.9±2.6	7.4±2.2	7.9±1.8	8.3±1.7	7.8±1.9	7.4±2.1	7.8±2.5	8.0±2.7	6.9±3.1
Top 5 percent Wind Speed (m/s)												
Hindcast	13.1±1.2	13.2±1.1	13.6±1.1	13.1±1.0	12.4±0.7	12.4±1.0	12.0±0.9	12.3±1.4	12.3±1.0	13.5±1.5	13.7±1.1	13.4±1.1
RCP4.5 - mid	13.2±1.2	13.4±1.1	13.0±0.9	13.3±0.9	12.6±1.1	11.8±0.6	12.1±1.1	11.8±0.8	12.5±1.1	13.6±1.6	13.7±1.2	13.4±1.1
RCP8.5 - mid	13.6±1.1	13.3±1.2	13.6±1.1	13.0±1.0	12.0±0.7	11.9±0.7	11.8±1.0	12.1±0.8	12.1±0.9	13.7±1.4	13.3±0.8	13.5±1.0
RCP4.5 - end	12.5±1.0	13.3±1.1	13.1±0.7	12.9±0.9	12.2±0.7	11.8±0.8	12.1±1.2	12.6±1.5	12.7±1.4	13.2±1.6	13.2±0.9	13.4±1.3
RCP8.5 - end	13.0±1.3	13.3±1.2	12.9±0.8	12.6±0.7	11.7±0.7	11.5±0.7	12.3±1.7	12.0±1.7	11.7±1.5	12.8±1.4	13.6±1.3	13.4±1.1
Mean Wind Direction (°)												
Hindcast	255±76	247±79	251±51	254±34	256±25	259±15	258±16	259±22	260±28	258±32	255±40	258±57
RCP4.5 - mid	254±75	253±69	253±52	253±32	257±23	259±16	257±13	258±21	260±26	257±33	255±36	255±53
RCP8.5 - mid	253±72	249±73	251±53	252±30	257±23	259±15	258±16	259±23	260±27	256±35	252±37	256±54
RCP4.5 - end	260±77	249±73	252±50	253±33	257±21	259±14	258±17	259±23	259±30	257±32	253±37	256±49
RCP8.5 - end	258±69	250±77	252±50	253±31	258±23	259±13	258±14	258±20	259±27	256±30	255±33	258±52
Top 5 percent Wind Direction (°)												
Hindcast	244±73	244±59	249±25	251±17	254±14	258±13	257±14	263±26	261±22	255±27	250±24	251±38
RCP4.5 - mid	244±73	249±42	247±21	249±19	255±14	257±11	258±18	258±25	258±19	256±32	250±22	246±42
RCP8.5 - mid	246±52	240±47	248±27	250±13	253±9	255±8	258±20	260±34	261±29	254±31	245±16	248±40
RCP4.5 - end	256±67	238±56	247±25	250±18	254±10	257±13	256±19	262±35	262±37	252±33	248±24	251±30
RCP8.5 - end	248±39	244±47	249±24	251±11	258±12	257±9	260±20	255±21	267±34	257±32	250±18	252±27

Appendix B30. Table showing return values of ensemble-average wind speeds of hindcast and forecast scenarios, including lower and higher 95 percent confidence intervals, at the Molokai location.

[Years: Hindcast = 1976–2005; RCP mid = 2026–2045; RCP end = 2081–2100. Wind speeds are in meters per second]

Scenario	Hindcast			RCP4.5 - mid			RCP8.5 - mid			RCP4.5 - end			RCP8.5 - end		
	Low	R_v	High	Low	R_v	High	Low	R_v	High	Low	R_v	High	Low	R_v	High
2-year	17.66	18.80	20.56	17.57	18.87	21.03	16.89	18.04	20.24	17.01	18.48	21.21	17.30	18.64	20.87
5-year	18.41	20.25	23.36	18.26	20.35	24.16	17.25	19.01	22.86	17.49	19.75	24.57	17.83	19.80	23.40
10-year	18.92	21.37	25.84	18.73	21.49	26.97	17.46	19.72	25.19	17.79	20.68	27.56	18.14	20.59	25.39
20-year	19.39	22.53	28.66	19.15	22.66	30.21	17.63	20.40	27.88	18.03	21.59	31.00	18.39	21.31	27.45
50-year	19.96	24.10	33.03	19.65	24.25	35.29	17.82	21.27	32.05	18.29	22.76	36.37	18.65	22.16	30.29
100-year	20.35	25.32	36.88	19.99	25.49	39.84	17.93	21.90	35.76	18.44	23.63	41.15	18.80	22.74	32.53

Appendix B31. Table showing Northwest Hawaiian Islands monthly means and mean of the top 5 percent for wind speed and mean wind direction.

[Years: Hindcast = 1976–2005; RCP mid = 2026–2045; RCP end = 2081–2100. Wind directions are "coming from"]

Month	Jan	Feb	Mar	Apr	May	Jun	July	Aug	Sep	Oct	Nov	Dec
Mean Wind Speed (m/s)												
Hindcast	7.7±3.7	7.5±3.5	6.9±3.0	7.1±2.8	6.7±2.3	7.0±2.2	7.6±2.2	7.3±2.4	7.3±2.7	7.7±3.1	7.4±3.2	7.4±3.5
RCP4.5 - mid	7.6±3.6	7.3±3.3	7.1±3.1	7.2±2.8	6.5±2.4	6.8±2.2	7.7±2.0	7.3±2.3	7.1±2.7	7.7±3.0	7.2±3.1	7.1±3.4
RCP8.5 - mid	7.6±3.6	7.5±3.3	6.9±3.1	6.7±2.6	6.4±2.4	6.5±2.2	7.5±2.1	7.3±2.4	6.9±2.7	8.0±3.0	7.5±3.2	7.1±3.4
RCP4.5 - end	7.5±3.5	7.4±3.4	7.1±3.0	7.0±2.8	6.7±2.4	6.7±2.2	7.4±2.0	7.2±2.4	7.1±2.4	7.7±2.9	7.3±3.1	7.1±3.3
RCP8.5 - end	7.2±3.4	7.2±3.2	6.9±2.9	6.9±2.6	6.4±2.3	6.6±2.0	7.3±1.8	6.9±2.1	7.0±2.4	7.7±2.7	7.1±3.0	6.8±3.3
Top 5 percent Wind Speed (m/s)												
Hindcast	16.4±1.9	15.3±1.5	13.4±1.2	12.8±1.2	11.3±1.0	10.9±1.0	11.9±1.4	12.3±2.0	13.4±1.6	14.3±1.6	14.1±1.3	15.3±1.7
RCP4.5 - mid	16.1±1.7	14.7±1.6	13.8±1.4	12.8±1.2	11.1±1.0	10.7±1.0	11.7±1.5	12.7±2.2	13.0±2.1	14.3±2.0	14.2±1.6	15.0±1.6
RCP8.5 - mid	15.7±1.8	14.8±1.5	13.6±1.4	12.1±1.0	11.3±1.2	10.4±0.5	11.6±1.6	12.4±2.0	13.0±2.2	14.2±1.6	14.2±1.3	14.9±1.6
RCP4.5 - end	15.4±1.6	15.3±1.6	13.9±1.4	12.9±1.1	11.2±0.9	10.6±0.8	11.2±1.2	12.5±2.5	12.5±2.0	14.2±1.7	13.8±1.2	14.7±1.8
RCP8.5 - end	15.1±1.8	14.6±1.6	12.9±1.4	12.2±1.0	10.9±0.9	10.3±1.0	10.6±0.9	11.4±2.2	12.5±1.8	13.6±1.7	13.8±1.3	14.3±1.5
Mean Wind Direction (°)												
Hindcast	117±113	119±118	242±87	248±49	254±36	262±27	262±25	265±31	263±40	253±46	244±68	207±114
RCP4.5 - mid	115±112	137±134	238±87	251±47	254±42	261±31	263±24	266±29	261±36	253±39	251±64	217±117
RCP8.5 - mid	118±130	145±128	242±87	251±49	254±39	261±30	262±25	266±32	262±40	252±40	245±59	222±107
RCP4.5 - end	108±108	132±130	238±84	249±48	254±37	261±31	262±23	265±29	261±35	255±38	249±59	228±105
RCP8.5 - end	111±121	122±118	244±81	252±44	254±35	262±27	262±22	264±27	263±35	256±36	250±53	224±101
Top 5 percent Wind Direction (°)												
Hindcast	103±62	104±66	220±76	237±39	247±20	259±19	265±25	269±39	266±36	244±34	227±55	144±90
RCP4.5 - mid	108±65	108±76	216±71	246±24	246±24	256±24	265±33	273±36	259±42	243±37	240±55	134±90
RCP8.5 - mid	106±76	119±78	216±75	244±31	245±24	257±15	262±30	273±44	256±35	240±29	234±43	126±91
RCP4.5 - end	103±61	114±66	205±81	239±31	249±21	255±14	262±29	277±46	263±40	249±30	240±49	167±99
RCP8.5 - end	94±57	106±67	219±68	246±26	246±21	256±19	258±23	272±47	264±39	253±32	236±35	207±87

Appendix B32. Table showing return values of ensemble-average wind speeds of hindcast and forecast scenarios, including lower and higher 95 percent confidence intervals, at the Northwest Hawaiian Islands location.

[Years: Hindcast = 1976–2005; RCP mid = 2026–2045; RCP end = 2081–2100. Wind speeds are in meters per second]

Scenario	Hindcast			RCP4.5 - mid			RCP8.5 - mid			RCP4.5 - end			RCP8.5 - end		
	Low	R_v	High	Low	R_v	High	Low	R_v	High	Low	R_v	High	Low	R_v	High
2-year	21.36	22.74	24.76	20.60	22.14	24.67	20.61	22.20	24.88	20.28	21.94	24.79	19.73	21.34	24.04
5-year	22.20	24.24	27.46	21.00	23.03	26.68	21.11	23.35	27.51	20.85	23.26	27.89	20.42	22.86	27.40
10-year	22.71	25.27	29.52	21.19	23.54	27.99	21.38	24.07	29.45	21.17	24.15	30.36	20.84	23.95	30.22
20-year	23.14	26.21	31.60	21.32	23.92	29.16	21.58	24.69	31.35	21.42	24.96	32.94	21.20	25.00	33.29
50-year	23.60	27.34	34.38	21.43	24.30	30.50	21.77	25.37	33.82	21.68	25.91	36.52	21.58	26.31	37.78
100-year	23.88	28.12	36.51	21.48	24.51	31.38	21.87	25.80	35.65	21.82	26.55	39.36	21.82	27.25	41.53

Appendix B33. Table showing Guam monthly means and mean of the top 5 percent for wind speed and mean wind direction.

[Years: Hindcast = 1976–2005; RCP mid = 2026–2045; RCP end = 2081–2100. Wind directions are "coming from"]

Month	Jan	Feb	Mar	Apr	May	Jun	July	Aug	Sep	Oct	Nov	Dec
Mean Wind Speed (m/s)												
Hindcast	9.1±2.1	9.0±2.1	8.8±2.0	8.0±2.0	6.8±2.4	5.7±2.7	5.5±3.2	5.6±3.2	5.3±2.9	5.6±2.9	7.8±2.8	8.9±2.3
RCP4.5 - mid	9.0±2.2	8.9±2.1	8.8±2.0	8.0±1.8	6.6±2.3	6.1±2.7	5.5±3.2	5.5±3.0	5.3±2.8	5.2±2.6	7.1±2.8	8.6±2.4
RCP8.5 - mid	9.0±2.2	8.9±2.1	8.7±1.9	8.0±1.7	6.6±2.2	6.0±2.7	5.6±3.2	5.6±3.3	5.3±2.9	5.1±2.6	6.9±2.8	8.8±2.4
RCP4.5 - end	9.0±2.1	9.1±2.0	8.7±2.0	7.9±1.9	6.9±2.2	6.0±2.6	5.8±3.1	5.7±3.2	5.4±2.8	5.3±2.6	7.1±2.7	8.6±2.3
RCP8.5 - end	8.8±2.2	8.6±2.2	8.4±1.9	7.8±1.6	6.8±2.2	6.0±2.7	5.8±3.2	5.6±3.3	5.3±2.9	5.1±2.6	6.9±2.9	8.4±2.4
Top 5 percent Wind Speed (m/s)												
Hindcast	13.2±0.8	13.3±1.0	13.2±1.9	11.9±1.6	11.8±2.5	11.7±1.9	13.9±2.3	14.5±2.4	13.2±2.8	12.8±2.6	13.9±2.0	13.4±1.5
RCP4.5 - mid	13.1±0.9	13.2±1.1	13.0±1.8	11.7±1.7	11.0±1.4	12.1±2.2	13.8±2.4	13.4±2.2	12.9±2.5	11.5±2.3	12.9±2.4	13.6±1.7
RCP8.5 - mid	13.4±1.2	12.9±0.7	12.9±1.2	11.5±1.1	10.8±1.7	12.6±2.9	13.8±2.3	14.4±2.3	13.3±2.9	11.8±2.6	12.9±2.1	13.7±1.7
RCP4.5 - end	13.1±0.8	13.1±0.9	12.7±0.9	11.8±1.4	11.0±1.3	11.3±1.7	13.5±2.6	14.2±2.3	12.6±1.9	11.8±2.5	12.6±1.6	13.1±1.5
RCP8.5 - end	13.3±1.3	13.0±0.9	12.2±0.8	11.0±0.8	10.7±1.0	11.8±2.4	13.3±2.4	14.5±2.5	13.3±2.4	11.5±2.1	13.2±2.5	13.5±2.5
Mean Wind Direction (°)												
Hindcast	249±18	246±18	249±18	253±21	260±33	266±58	301±100	12±103	355±117	267±85	259±39	253±23
RCP4.5 - mid	249±20	247±18	250±17	253±15	260±31	269±56	299±90	13±107	20±111	278±102	259±43	255±24
RCP8.5 - mid	249±18	248±17	249±16	254±16	260±29	270±54	301±95	16±103	33±107	274±102	259±43	255±24
RCP4.5 - end	250±18	246±17	249±16	254±18	261±29	267±55	295±93	3±105	13±110	279±102	258±40	255±21
RCP8.5 - end	250±19	248±18	250±15	254±13	260±28	269±59	289±86	357±105	26±105	277±98	258±41	256±22
Top 5 percent Wind Direction (°)												
Hindcast	241±15	236±14	244±28	248±26	263±44	290±76	24±67	26±47	14±65	302±91	263±52	248±23
RCP4.5 - mid	242±16	240±11	243±21	247±21	255±31	296±71	16±57	35±49	41±56	303±94	264±49	246±32
RCP8.5 - mid	243±15	242±11	241±19	251±15	259±19	322±81	27±52	29±37	42±35	318±104	259±51	250±30
RCP4.5 - end	242±14	238±17	242±11	251±22	263±26	284±68	29±65	36±36	40±49	333±94	257±43	245±27
RCP8.5 - end	245±18	239±14	240±12	250±16	256±21	291±83	24±59	36±42	39±49	328±103	256±39	251±27

Appendix B34. Table showing return values of ensemble-average wind speeds of hindcast and forecast scenarios, including lower and higher 95 percent confidence intervals, at the Guam location.

[Years: Hindcast = 1976–2005; RCP mid = 2026–2045; RCP end = 2081–2100. Wind speeds are in meters per second]

Scenario	Hindcast			RCP4.5 - mid			RCP8.5 - mid			RCP4.5 - end			RCP8.5 - end		
	Low	R_v	High	Low	R_v	High	Low	R_v	High	Low	R_v	High	Low	R_v	High
2-year	20.45	22.85	26.86	19.96	22.16	25.73	19.81	22.05	26.02	19.00	20.97	24.13	20.16	22.60	26.68
5-year	21.71	25.61	32.92	20.90	24.12	29.82	20.81	24.43	31.69	19.94	22.88	28.03	21.09	24.66	31.27
10-year	22.56	27.78	38.48	21.45	25.45	33.02	21.48	26.31	36.98	20.51	24.22	31.15	21.63	26.05	34.90
20-year	23.33	30.03	45.05	21.89	26.65	36.29	22.08	28.26	43.32	20.99	25.47	34.43	22.06	27.33	38.68
50-year	24.23	33.12	55.61	22.35	28.08	40.75	22.78	30.95	53.68	21.50	27.01	39.02	22.49	28.84	43.92
100-year	24.84	35.54	65.29	22.62	29.05	44.23	23.25	33.08	63.35	21.82	28.08	42.70	22.75	29.86	48.07

Appendix B35. Table showing Kwajalein monthly means and mean of the top 5 percent for wind speed and mean wind direction.

[Years: Hindcast = 1976–2005; RCP mid = 2026–2045; RCP end = 2081–2100. Wind directions are "coming from"]

Month	Jan	Feb	Mar	Apr	May	Jun	July	Aug	Sep	Oct	Nov	Dec
Mean Wind Speed (m/s)												
Hindcast	9.3±1.8	9.1±1.8	8.8±1.9	7.7±2.4	6.1±2.7	5.3±2.7	4.8±2.6	4.4±2.5	4.2±2.3	4.7±2.6	6.6±3.1	8.7±2.5
RCP4.5 - mid	9.3±1.9	9.0±1.9	8.9±1.8	7.8±2.2	6.4±2.7	5.6±2.7	4.9±2.7	4.4±2.6	4.2±2.3	4.5±2.4	5.9±3.0	8.5±2.5
RCP8.5 - mid	9.1±1.8	9.1±1.9	8.7±1.8	8.0±2.2	6.4±2.6	5.6±2.7	5.0±2.7	4.5±2.6	4.1±2.3	4.4±2.4	6.0±3.0	8.5±2.4
RCP4.5 - end	9.1±1.7	9.0±1.7	8.8±1.8	7.7±2.2	6.4±2.6	5.6±2.8	4.9±2.6	4.6±2.6	4.2±2.4	4.3±2.5	5.9±2.9	8.4±2.4
RCP8.5 - end	8.8±1.8	8.8±1.8	8.7±1.7	8.0±2.1	6.9±2.4	5.9±2.8	5.1±2.7	4.4±2.6	4.0±2.2	4.1±2.4	5.7±2.9	8.2±2.3
Top 5 percent Wind Speed (m/s)												
Hindcast	12.7±0.6	12.6±0.8	12.4±0.8	11.9±1.0	10.9±0.9	10.6±1.0	10.6±1.4	10.9±2.0	10.4±2.1	11.5±2.1	13.1±1.5	13.2±1.3
RCP4.5 - mid	12.6±0.5	12.7±1.2	12.1±0.5	11.7±0.7	11.1±1.0	11.0±1.3	11.0±1.4	11.4±2.2	10.6±2.1	11.0±2.3	12.5±1.4	13.1±1.2
RCP8.5 - mid	12.5±0.7	12.9±0.9	12.2±0.6	12.1±1.6	11.3±1.4	10.9±1.0	11.2±1.8	11.5±2.3	10.6±2.0	10.7±1.9	12.7±1.3	12.8±0.8
RCP4.5 - end	12.4±0.8	12.4±0.7	12.2±0.7	11.5±0.5	10.9±0.8	10.9±1.1	10.9±2.0	11.7±2.3	11.1±2.1	11.0±2.0	12.4±1.6	13.0±1.1
RCP8.5 - end	12.1±0.5	12.2±0.7	12.0±0.7	11.5±0.9	10.9±0.8	11.0±1.3	11.1±1.6	11.3±2.6	9.9±2.6	10.9±2.1	12.2±1.3	12.3±0.9
Mean Wind Direction (°)												
Hindcast	243±12	243±12	246±13	249±21	253±39	258±51	269±64	291±74	302±85	278±81	252±46	245±21
RCP4.5 - mid	244±13	244±13	245±11	249±19	252±31	258±49	268±58	288±73	301±79	289±83	255±52	248±23
RCP8.5 - mid	244±12	244±12	246±12	249±19	252±30	257±45	271±59	295±74	311±82	290±85	254±56	247±22
RCP4.5 - end	245±12	245±12	246±12	250±19	252±32	258±47	267±57	294±77	307±83	295±89	255±57	248±21
RCP8.5 - end	246±13	246±12	247±11	249±15	253±26	257±43	266±53	288±67	300±81	288±84	255±52	248±20
Top 5 percent Wind Direction (°)												
Hindcast	241±9	240±9	242±16	244±27	245±25	247±28	260±60	350±95	13±109	274±70	245±37	238±16
RCP4.5 - mid	240±9	242±13	240±8	243±15	244±15	248±35	258±56	325±89	325±92	318±94	240±36	241±12
RCP8.5 - mid	241±8	240±9	241±7	243±31	247±20	250±33	273±67	339±85	28±93	318±105	241±43	239±10
RCP4.5 - end	241±10	242±10	240±11	244±8	243±16	247±28	264±60	7±84	5±81	354±104	239±48	240±20
RCP8.5 - end	242±8	241±8	243±8	244±8	245±14	252±40	267±75	340±82	328±96	294±90	242±32	242±11

Appendix B36. Table showing return values of ensemble-average wind speeds of hindcast and forecast scenarios, including lower and higher 95 percent confidence intervals, at the Kwajalein location.

[Years: Hindcast = 1976–2005; RCP mid = 2026–2045; RCP end = 2081–2100. Wind speeds are in meters per second]

Scenario	Hindcast			RCP4.5 - mid			RCP8.5 - mid			RCP4.5 - end			RCP8.5 - end		
	Low	R_v	High	Low	R_v	High	Low	R_v	High	Low	R_v	High	Low	R_v	High
2-year	16.70	18.88	23.14	16.37	18.28	22.23	16.81	18.82	22.50	16.70	18.37	21.29	16.61	18.55	22.08
5-year	17.75	21.75	30.99	16.83	19.71	26.67	17.66	20.95	27.86	17.31	19.83	24.80	17.39	20.50	26.93
10-year	18.55	24.42	39.95	17.09	20.73	30.65	18.23	22.67	33.01	17.68	20.87	27.76	17.90	22.01	31.44
20-year	19.35	27.62	52.73	17.29	21.70	35.27	18.75	24.49	39.37	17.99	21.87	31.03	18.35	23.57	36.85
50-year	20.42	32.83	78.40	17.50	22.91	42.52	19.36	27.04	50.08	18.30	23.11	35.88	18.86	25.68	45.66
100-year	21.22	37.69	97.64	17.61	23.78	49.03	19.77	29.09	60.40	18.50	23.99	39.98	19.19	27.33	53.86

Appendix B37. Table showing Wake monthly means and mean of the top 5 percent for wind speed and mean wind direction.

[Years: Hindcast = 1976–2005; RCP mid = 2026–2045; RCP end = 2081–2100. Wind directions are "coming from"]

Month	Jan	Feb	Mar	Apr	May	Jun	July	Aug	Sep	Oct	Nov	Dec
Mean Wind Speed (m/s)												
Hindcast	7.3±2.8	7.2±2.8	7.7±2.6	8.3±2.3	8.0±1.9	7.6±2.1	7.2±2.4	6.8±2.7	6.7±2.8	7.8±2.9	8.6±2.6	8.2±2.8
RCP4.5 - mid	7.4±2.8	7.2±2.7	7.8±2.6	8.3±2.2	7.9±1.9	7.6±2.0	7.4±2.3	6.7±2.6	6.6±2.8	7.8±2.8	8.6±2.6	8.0±2.7
RCP8.5 - mid	7.3±2.8	7.4±2.9	7.7±2.6	8.2±2.3	8.0±1.9	7.7±2.0	7.4±2.5	6.7±2.8	6.6±2.9	7.5±2.8	8.8±2.5	8.0±2.8
RCP4.5 - end	7.1±2.7	7.2±2.7	7.8±2.7	8.2±2.3	7.9±1.9	7.7±1.8	7.4±2.4	6.9±2.6	6.7±2.8	7.5±2.8	8.6±2.5	8.1±2.6
RCP8.5 - end	7.2±2.8	7.0±2.8	7.5±2.5	8.2±2.0	7.8±1.8	7.5±1.8	7.5±2.2	7.2±2.5	6.6±2.6	7.5±2.7	8.6±2.4	8.0±2.5
Top 5 percent Wind Speed (m/s)												
Hindcast	12.9±1.2	12.7±0.8	12.9±1.0	12.9±1.3	11.6±0.9	11.8±1.3	12.0±1.7	12.8±1.8	13.0±2.1	14.1±2.1	13.9±1.4	13.5±0.9
RCP4.5 - mid	12.7±0.8	12.6±0.8	13.0±0.9	12.5±0.8	11.5±0.7	11.5±1.6	12.2±1.7	12.3±1.8	13.0±2.2	14.1±2.1	13.8±1.4	13.2±0.9
RCP8.5 - mid	12.8±0.8	13.0±0.8	12.7±0.9	12.7±1.7	11.6±1.2	11.3±0.9	12.5±1.9	13.5±2.6	13.6±2.8	13.3±1.5	14.0±1.3	13.2±1.0
RCP4.5 - end	12.5±0.9	12.6±0.9	12.7±0.7	12.4±0.9	11.3±0.8	11.2±1.4	12.3±2.1	12.8±2.2	13.2±2.4	13.4±1.8	13.6±1.2	12.9±0.8
RCP8.5 - end	12.6±0.8	12.7±0.9	12.3±0.8	11.9±0.6	11.1±0.6	11.1±1.4	11.8±1.8	13.5±2.7	12.7±2.6	13.4±2.3	13.4±1.2	12.8±0.6
Mean Wind Direction (°)												
Hindcast	249±39	249±43	252±32	254±21	257±17	261±24	265±36	270±48	262±48	258±35	254±24	251±29
RCP4.5 - mid	250±39	249±40	252±29	255±18	257±17	260±22	267±33	269±46	267±48	260±35	255±26	254±30
RCP8.5 - mid	249±40	248±41	252±29	255±20	257±15	260±21	268±35	273±50	267±50	260±36	256±22	253±30
RCP4.5 - end	250±40	249±38	253±30	256±20	257±15	261±17	266±34	270±47	266±48	259±39	255±24	253±25
RCP8.5 - end	250±39	250±41	254±28	256±16	259±15	262±20	266±32	270±40	269±46	260±37	255±21	253±25
Top 5 percent Wind Direction (°)												
Hindcast	246±16	245±20	244±15	246±11	255±16	264±24	268±44	300±66	271±51	259±38	250±23	245±13
RCP4.5 - mid	246±16	243±17	246±12	250±11	250±11	258±24	274±45	279±55	285±59	267±52	247±16	247±13
RCP8.5 - mid	247±14	246±15	245±13	247±15	253±10	260±18	283±55	311±78	291±71	259±42	251±17	245±13
RCP4.5 - end	247±14	248±17	247±12	253±15	253±9	262±19	281±47	314±84	282±61	257±35	250±22	249±11
RCP8.5 - end	245±16	247±15	249±11	250±10	252±8	259±22	277±48	329±80	304±73	263±39	248±18	247±10

Appendix B38. Table showing return values of ensemble-average wind speeds of hindcast and forecast scenarios, including lower and higher 95 percent confidence intervals, at the Wake location.

[Years: Hindcast = 1976–2005; RCP mid = 2026–2045; RCP end = 2081–2100. Wind speeds are in meters per second]

Scenario	Hindcast			RCP4.5 - mid			RCP8.5 - mid			RCP4.5 - end			RCP8.5 - end		
	Low	R_v	High	Low	R_v	High	Low	R_v	High	Low	R_v	High	Low	R_v	High
2-year	18.43	20.05	22.61	17.80	19.47	22.40	17.75	20.52	26.74	17.85	19.85	23.45	17.78	20.34	25.35
5-year	19.41	22.01	26.53	18.44	20.99	26.00	18.60	23.42	36.73	18.40	21.25	27.02	18.63	22.70	32.02
10-year	20.07	23.52	30.00	18.83	22.08	29.09	19.19	26.00	48.10	18.70	22.16	29.79	19.16	24.55	38.41
20-year	20.67	25.06	33.95	19.15	23.14	32.52	19.73	28.97	64.32	18.92	22.95	32.63	19.62	26.44	46.25
50-year	21.37	27.13	40.07	19.50	24.47	37.66	20.39	33.58	96.82	19.13	23.85	36.50	20.12	29.01	59.41
100-year	21.85	28.73	45.46	19.71	25.44	42.06	20.85	37.67	133.79	19.24	24.43	39.51	20.44	31.02	72.01

Appendix B39. Table showing Johnston Atoll monthly means and mean of the top 5 percent for wind speed and mean wind direction.

[Years: Hindcast = 1976–2005; RCP mid = 2026–2045; RCP end = 2081–2100. Wind directions are "coming from"]

Month	Jan	Feb	Mar	Apr	May	Jun	July	Aug	Sep	Oct	Nov	Dec
Mean Wind Speed (m/s)												
Hindcast	7.6±2.9	7.5±2.9	8.3±2.7	8.7±2.3	8.4±1.9	8.3±1.9	7.8±2.1	7.2±2.2	6.5±2.5	7.5±2.9	8.5±2.7	8.1±2.9
RCP4.5 - mid	7.6±2.7	7.6±2.8	8.2±2.7	8.8±2.4	8.2±1.9	8.2±1.8	8.1±1.8	7.4±2.3	6.6±2.4	7.3±2.7	8.6±2.6	8.3±2.6
RCP8.5 - mid	7.6±2.9	7.6±2.9	8.1±2.8	8.8±2.1	8.2±1.9	8.2±1.7	8.1±1.9	7.2±2.2	6.3±2.5	7.2±2.8	8.5±2.6	8.3±2.8
RCP4.5 - end	7.3±2.7	7.5±2.9	8.3±2.6	8.7±2.1	8.3±1.8	8.3±1.7	8.0±1.9	7.4±2.2	6.6±2.4	7.2±2.8	8.5±2.7	8.3±2.6
RCP8.5 - end	7.2±2.8	7.2±2.8	8.1±2.5	8.6±2.0	8.0±1.7	8.2±1.5	8.1±1.7	7.4±1.9	6.5±2.2	7.1±2.6	8.1±2.5	8.0±2.5
Top 5 percent Wind Speed (m/s)												
Hindcast	13.3±0.9	13.3±0.9	13.4±0.8	12.9±0.8	12.0±1.0	11.8±1.2	11.9±1.4	11.8±1.6	11.8±1.5	13.5±1.6	13.8±1.2	13.6±1.0
RCP4.5 - mid	13.0±0.9	13.2±0.9	13.2±0.7	13.2±0.7	11.6±0.8	11.5±1.1	11.6±1.0	12.6±2.0	11.7±1.7	13.2±1.7	13.6±1.3	13.5±1.0
RCP8.5 - mid	13.5±1.0	13.5±0.9	13.4±0.8	12.5±0.7	11.5±0.7	11.4±1.2	11.8±1.3	11.7±1.8	11.7±2.0	13.2±1.5	13.5±1.0	13.6±1.0
RCP4.5 - end	12.8±0.8	13.4±1.0	13.2±0.9	12.5±0.6	11.7±1.0	11.4±0.9	11.6±1.4	12.3±2.0	11.7±1.8	13.4±2.0	13.8±1.1	13.2±0.7
RCP8.5 - end	12.7±0.8	13.1±1.1	12.8±0.7	12.3±0.5	11.2±0.8	11.2±1.4	11.4±1.2	11.2±1.1	11.2±1.8	12.7±2.1	13.0±1.1	13.0±0.9
Mean Wind Direction (°)												
Hindcast	246±41	246±41	249±27	251±21	254±17	259±17	261±25	262±33	263±43	256±40	251±29	249±35
RCP4.5 - mid	245±40	248±36	249±29	252±21	255±18	258±17	260±21	264±31	264±43	257±38	252±27	249±29
RCP8.5 - mid	247±38	246±36	248±29	251±19	255±18	258±13	260±21	264±33	263±44	256±39	250±28	248±35
RCP4.5 - end	246±41	246±39	248±27	251±19	255±16	258±14	260±22	262±32	262±38	258±43	251±28	249±29
RCP8.5 - end	249±36	248±36	249±25	251±17	256±15	259±15	259±19	260±29	263±37	257±36	252±28	250±27
Top 5 percent Wind Direction (°)												
Hindcast	241±24	240±19	242±12	245±10	249±10	257±13	259±23	267±40	263±44	252±33	245±21	243±22
RCP4.5 - mid	239±26	244±15	245±11	247±9	249±12	256±19	259±27	282±47	274±52	259±44	249±21	241±19
RCP8.5 - mid	240±18	242±14	242±11	245±9	249±12	255±9	261±25	272±42	282±63	257±35	245±20	243±15
RCP4.5 - end	240±23	241±15	242±11	246±9	251±13	256±13	257±15	275±53	268±48	259±48	246±18	242±16
RCP8.5 - end	240±18	240±16	244±10	247±10	250±9	257±12	258±20	262±36	269±50	256±34	244±21	244±19

Appendix B40. Table showing return values of ensemble-average wind speeds of hindcast and forecast scenarios, including lower and higher 95 percent confidence intervals, at the Johnston Atoll location.

[Years: Hindcast = 1976–2005; RCP mid = 2026–2045; RCP end = 2081–2100. Wind speeds are in meters per second]

Scenario	Hindcast			RCP4.5 - mid			RCP8.5 - mid			RCP4.5 - end			RCP8.5 - end		
	Low	R_v	High	Low	R_v	High	Low	R_v	High	Low	R_v	High	Low	R_v	High
2-year	17.02	18.20	20.17	16.95	18.47	21.45	16.98	18.16	20.13	16.73	18.60	22.47	16.53	18.00	20.75
5-year	17.60	19.48	23.02	17.52	20.04	25.82	17.41	19.12	22.24	17.44	20.72	28.90	17.19	19.69	25.10
10-year	17.99	20.47	25.59	17.90	21.34	30.22	17.66	19.75	23.86	17.95	22.63	36.10	17.66	21.13	29.54
20-year	18.32	21.47	28.58	18.24	22.73	35.86	17.85	20.31	25.50	18.43	24.83	46.18	18.09	22.71	35.31
50-year	18.71	22.82	33.29	18.64	24.73	45.82	18.04	20.95	27.71	19.04	28.29	66.02	18.63	25.07	45.67
100-year	18.97	23.86	37.53	18.91	26.37	55.85	18.15	21.38	29.40	19.47	31.40	88.16	19.01	27.08	56.25

Appendix B41. Table showing Kingman Reef monthly means and mean of the top 5 percent for wind speed and mean wind direction.

[Years: Hindcast = 1976–2005; RCP mid = 2026–2045; RCP end = 2081–2100. Wind directions are "coming from"]

Month	Jan	Feb	Mar	Apr	May	Jun	July	Aug	Sep	Oct	Nov	Dec
Mean Wind Speed (m/s)												
Hindcast	6.9±2.6	7.2±2.4	7.1±2.5	6.4±2.4	5.5±2.3	5.0±2.1	4.8±1.8	4.7±1.7	4.5±1.8	4.3±1.9	4.4±2.2	5.7±2.4
RCP4.5 - mid	6.8±2.4	7.5±2.3	7.4±2.5	6.9±2.3	6.0±2.3	5.4±2.2	4.9±1.9	4.7±1.8	4.5±1.8	4.3±1.9	4.4±2.0	5.6±2.5
RCP8.5 - mid	7.0±2.4	7.3±2.4	7.2±2.4	6.9±2.3	6.1±2.3	5.4±2.1	4.9±1.7	4.6±1.7	4.5±1.7	4.3±1.9	4.4±2.0	5.5±2.4
RCP4.5 - end	6.8±2.4	7.3±2.3	7.3±2.3	6.8±2.3	6.2±2.3	5.4±2.1	4.8±1.7	4.6±1.8	4.5±1.8	4.3±1.9	4.3±2.1	5.7±2.6
RCP8.5 - end	7.0±2.3	7.6±2.1	7.4±2.2	7.2±2.2	6.7±2.1	5.7±2.2	4.9±1.8	4.8±1.8	4.4±1.7	4.1±1.8	4.1±1.9	5.6±2.3
Top 5 percent Wind Speed (m/s)												
Hindcast	11.8±1.0	11.7±0.7	11.7±0.7	11.0±0.6	10.4±0.7	9.9±1.0	8.8±1.0	8.8±1.4	8.5±1.1	8.6±1.3	10.0±1.9	11.0±1.2
RCP4.5 - mid	11.5±0.9	11.6±0.6	12.1±0.7	11.3±0.6	10.5±1.1	10.4±0.9	9.2±1.0	8.9±1.5	8.3±1.0	8.5±1.0	9.2±1.2	11.0±1.0
RCP8.5 - mid	11.7±1.1	11.9±0.8	11.9±0.7	11.3±0.6	10.7±0.9	9.9±0.7	8.9±0.9	8.4±0.9	8.3±1.1	8.6±1.3	9.4±1.2	10.8±0.9
RCP4.5 - end	11.5±0.8	11.8±0.6	11.5±0.6	11.3±0.8	11.0±0.9	10.3±1.0	9.0±1.3	9.1±1.6	8.6±1.2	8.9±1.5	9.6±1.8	11.4±1.0
RCP8.5 - end	11.3±0.6	11.5±0.7	11.7±0.6	11.3±0.7	10.8±0.7	10.5±0.9	9.1±1.2	8.9±1.3	8.3±1.2	8.4±1.2	8.9±1.3	10.8±1.0
Mean Wind Direction (°)												
Hindcast	251±30	249±26	251±25	254±29	261±33	273±41	291±41	307±39	317±41	319±48	297±57	264±42
RCP4.5 - mid	251±28	248±22	249±22	251±23	256±30	266±35	287±39	305±39	314±42	318±49	298±59	263±42
RCP8.5 - mid	250±28	249±24	249±21	251±22	257±27	265±34	286±37	307±39	316±42	320±49	297±57	263±42
RCP4.5 - end	251±28	249±26	250±21	252±21	256±26	266±35	287±39	308±42	315±43	318±50	295±58	261±42
RCP8.5 - end	251±25	249±18	249±18	250±18	254±23	261±31	282±37	301±41	315±43	317±49	289±54	260±38
Top 5 percent Wind Direction (°)												
Hindcast	237±12	234±14	234±10	237±13	244±21	254±44	283±48	317±47	324±44	321±44	270±58	240±25
RCP4.5 - mid	238±17	237±10	233±10	237±10	237±28	244±29	272±49	313±47	317±42	329±48	271±57	238±24
RCP8.5 - mid	234±14	233±10	235±9	237±10	241±18	246±21	271±47	309±41	322±49	322±54	255±54	234±18
RCP4.5 - end	233±13	234±12	235±11	237±10	239±20	245±28	278±53	326±58	324±52	335±68	247±57	233±25
RCP8.5 - end	239±12	238±11	234±10	236±11	239±13	240±26	266±51	321±57	324±51	333±70	258±48	237±15

Appendix B42. Table showing return values of ensemble-average wind speeds of hindcast and forecast scenarios, including lower and higher 95 percent confidence intervals, at the Kingman Reef location.

[Years: Hindcast = 1976–2005; RCP mid = 2026–2045; RCP end = 2081–2100. Wind speeds are in meters per second]

Scenario	Hindcast			RCP4.5 - mid			RCP8.5 - mid			RCP4.5 - end			RCP8.5 - end		
	Low	R_v	High	Low	R_v	High	Low	R_v	High	Low	R_v	High	Low	R_v	High
2-year	14.32	15.32	16.96	13.94	14.87	16.55	13.89	14.76	16.28	14.09	15.28	17.65	13.62	14.11	14.87
5-year	15.03	16.80	20.04	14.41	16.02	19.38	14.32	15.75	18.59	14.62	16.76	21.81	13.87	14.59	15.84
10-year	15.57	18.10	23.18	14.75	17.02	22.31	14.61	16.55	20.80	15.01	18.12	26.47	14.02	14.94	16.62
20-year	16.12	19.59	27.24	15.09	18.15	26.14	14.88	17.41	23.50	15.40	19.72	33.04	14.15	15.26	17.44
50-year	16.85	21.89	34.48	15.51	19.87	33.12	15.21	18.62	28.02	15.91	22.28	46.03	14.28	15.66	18.59
100-year	17.41	23.91	41.84	15.82	21.37	40.34	15.43	19.61	32.35	16.29	24.63	60.60	14.37	15.94	19.51

Appendix B43. Table showing Palmyra monthly means and mean of the top 5 percent for wind speed and mean wind direction.

[Years: Hindcast = 1976–2005; RCP mid = 2026–2045; RCP end = 2081–2100. Wind directions are "coming from"]

Month	Jan	Feb	Mar	Apr	May	Jun	July	Aug	Sep	Oct	Nov	Dec
Mean Wind Speed (m/s)												
Hindcast	6.4±2.4	6.7±2.3	6.8±2.4	6.1±2.3	5.5±2.1	5.3±2.0	5.3±1.8	5.2±1.7	5.0±1.7	4.7±1.8	4.6±2.1	5.3±2.2
RCP4.5 - mid	6.2±2.3	6.9±2.3	7.1±2.4	6.6±2.3	5.9±2.2	5.5±2.0	5.5±1.8	5.3±1.8	5.1±1.8	4.8±1.8	4.6±2.0	5.2±2.3
RCP8.5 - mid	6.4±2.3	6.9±2.4	6.9±2.4	6.6±2.3	5.9±2.2	5.6±1.9	5.5±1.7	5.2±1.8	5.1±1.8	4.7±1.8	4.6±2.0	5.2±2.3
RCP4.5 - end	6.4±2.3	6.8±2.3	7.0±2.2	6.6±2.2	6.1±2.1	5.5±2.0	5.4±1.7	5.2±1.8	5.1±1.8	4.8±1.8	4.5±2.1	5.4±2.4
RCP8.5 - end	6.5±2.2	7.2±2.0	7.1±2.2	6.9±2.1	6.4±2.1	5.7±2.0	5.4±1.8	5.4±1.8	5.1±1.7	4.6±1.8	4.4±1.9	5.2±2.2
Top 5 percent Wind Speed (m/s)												
Hindcast	11.5±1.2	11.5±0.8	11.6±0.7	10.9±0.7	10.3±0.8	9.8±1.1	8.9±1.0	8.9±1.3	8.6±1.0	8.6±1.2	9.9±2.2	10.4±1.1
RCP4.5 - mid	11.2±0.9	11.4±0.6	11.9±0.6	11.2±0.7	10.6±1.2	10.3±1.0	9.2±1.0	9.0±1.5	8.6±0.9	8.5±1.0	9.1±1.3	10.6±1.1
RCP8.5 - mid	11.3±0.9	11.7±0.9	11.8±0.8	11.2±0.7	10.6±0.9	9.9±0.7	9.0±0.8	8.7±0.8	8.6±1.0	8.7±1.3	9.2±1.3	10.6±1.0
RCP4.5 - end	11.3±0.9	11.5±0.7	11.4±0.7	11.1±0.8	10.9±0.9	10.3±1.0	9.0±1.2	9.2±1.5	8.8±1.2	8.9±1.3	9.5±2.0	11.2±1.0
RCP8.5 - end	11.0±0.8	11.2±0.7	11.6±0.7	11.3±0.7	10.8±0.8	10.4±0.9	9.1±1.1	9.1±1.2	8.5±1.0	8.5±1.1	8.9±1.3	10.7±1.0
Mean Wind Direction (°)												
Hindcast	255±32	252±27	253±25	256±30	264±32	275±38	289±37	301±34	310±35	312±40	299±48	270±42
RCP4.5 - mid	256±31	252±24	251±22	253±23	258±30	269±32	287±35	300±34	307±38	310±41	297±49	270±43
RCP8.5 - mid	255±31	251±26	251±22	253±22	258±26	268±31	286±33	302±35	308±38	312±42	298±48	270±43
RCP4.5 - end	254±29	252±26	251±22	253±21	257±26	269±33	287±35	303±38	307±38	309±42	297±49	267±42
RCP8.5 - end	254±26	251±18	250±18	251±18	255±23	263±30	284±35	299±37	308±39	309±42	291±45	266±38
Top 5 percent Wind Direction (°)												
Hindcast	234±20	232±17	233±11	236±16	244±23	257±47	286±44	311±43	316±41	319±43	289±66	238±31
RCP4.5 - mid	234±18	234±10	232±10	235±9	235±29	244±31	276±47	310±44	307±38	321±47	274±55	236±25
RCP8.5 - mid	230±16	232±10	233±9	236±9	240±19	246±22	276±44	305±35	312±43	313±48	261±58	232±19
RCP4.5 - end	230±16	231±11	234±19	235±10	239±19	245±27	282±48	319±53	314±49	328±65	259±63	231±28
RCP8.5 - end	235±12	235±10	232±9	235±10	238±11	239±26	273±49	317±51	312±45	322±65	261±48	234±16

Appendix B44. Table showing return values of ensemble-average wind speeds of hindcast and forecast scenarios, including lower and higher 95 percent confidence intervals, at the Palmyra location.

[Years: Hindcast = 1976–2005; RCP mid = 2026–2045; RCP end = 2081–2100. Wind speeds are in meters per second]

Scenario	Hindcast			RCP4.5 - mid			RCP8.5 - mid			RCP4.5 - end			RCP8.5 - end		
	Low	R_v	High	Low	R_v	High	Low	R_v	High	Low	R_v	High	Low	R_v	High
2-year	14.40	15.43	17.07	13.95	14.98	16.91	13.84	14.78	16.45	14.07	15.21	17.39	13.63	14.09	14.79
5-year	15.17	16.96	20.11	14.48	16.32	20.30	14.22	15.68	18.60	14.61	16.64	21.14	13.88	14.57	15.69
10-year	15.75	18.28	23.10	14.88	17.53	23.96	14.45	16.35	20.49	15.02	17.92	25.20	14.04	14.90	16.38
20-year	16.33	19.75	26.86	15.28	18.94	28.95	14.65	17.01	22.67	15.41	19.40	30.75	14.17	15.21	17.08
50-year	17.09	21.96	33.32	15.80	21.16	38.42	14.88	17.87	26.02	15.93	21.73	41.31	14.32	15.58	18.03
100-year	17.66	23.87	39.67	16.19	23.17	48.64	15.02	18.51	28.99	16.31	23.81	52.73	14.41	15.83	18.76

Appendix B45. Table showing Rose Atoll monthly means and mean of the top 5 percent for wind speed and mean wind direction.

[Years: Hindcast = 1976–2005; RCP mid = 2026–2045; RCP end = 2081–2100. Wind directions are "coming from"]

Month	Jan	Feb	Mar	Apr	May	Jun	July	Aug	Sep	Oct	Nov	Dec
Mean Wind Speed (m/s)												
Hindcast	5.2±2.9	4.9±2.8	5.1±2.8	5.4±2.7	6.3±2.9	6.9±2.7	6.9±2.7	7.1±2.7	7.0±2.7	6.7±2.7	6.0±2.8	5.3±2.6
RCP4.5 - mid	5.3±2.8	5.1±2.8	5.3±2.7	5.5±2.7	6.5±2.9	7.0±2.7	7.0±2.7	7.1±2.6	7.3±2.7	7.0±2.7	6.2±2.9	5.3±2.6
RCP8.5 - mid	5.3±2.8	5.1±2.7	5.1±2.9	5.5±2.8	6.3±2.8	6.7±2.7	6.9±2.7	7.0±2.7	7.2±2.6	7.0±2.7	6.0±2.7	5.4±3.0
RCP4.5 - end	5.3±2.7	5.2±2.7	4.8±2.7	5.4±2.8	6.6±2.9	7.2±2.6	6.9±2.7	7.2±2.6	7.3±2.6	6.9±2.7	6.1±2.7	5.5±2.8
RCP8.5 - end	5.5±2.7	5.3±2.9	5.2±2.7	5.2±2.6	6.2±2.8	7.0±2.8	7.0±2.7	7.3±2.6	7.3±2.6	7.0±2.6	6.0±2.6	5.4±2.5
Top 5 percent Wind Speed (m/s)												
Hindcast	13.2±2.6	12.5±2.9	12.2±2.2	11.6±1.3	12.9±1.6	12.9±1.6	12.6±1.1	12.8±1.1	12.5±1.1	12.5±1.2	12.4±1.3	11.8±2.0
RCP4.5 - mid	12.6±2.4	12.6±2.8	11.8±2.1	11.9±1.5	12.6±1.4	12.6±1.0	12.5±0.8	12.4±1.0	12.8±1.0	12.5±0.8	12.6±1.5	11.6±1.7
RCP8.5 - mid	12.4±2.5	12.3±2.3	12.8±2.9	12.2±1.5	12.4±1.0	12.3±1.2	12.8±1.4	12.7±1.0	12.6±0.8	12.5±1.0	12.0±1.5	13.5±2.7
RCP4.5 - end	12.2±2.2	12.0±2.3	11.9±2.4	12.3±2.2	12.9±1.5	12.6±1.1	12.7±1.1	12.5±1.0	12.6±1.0	12.6±1.1	11.9±1.3	12.5±2.2
RCP8.5 - end	12.7±2.9	13.2±2.5	12.5±2.7	11.3±1.7	12.7±1.7	13.0±1.2	12.6±0.9	12.9±1.0	12.6±1.0	12.1±0.7	11.7±1.2	11.4±1.4
Mean Wind Direction (°)												
Hindcast	242±80	222±94	233±99	280±69	284±53	285±42	285±43	283±39	285±38	284±39	280±51	267±65
RCP4.5 - mid	244±76	217±92	221±10	283±72	286±48	284±42	284±43	284±38	285±34	285±37	283±49	270±66
RCP8.5 - mid	250±68	223±92	240±10	284±70	287±49	286±44	283±43	286±41	284±36	283±36	279±48	264±69
RCP4.5 - end	252±73	222±90	233±10	278±73	286±48	283±39	284±43	285±37	285±33	284±35	280±47	267±62
RCP8.5 - end	253±66	234±88	235±95	278±69	283±49	285±40	285±39	285±34	285±31	283±34	277±43	269±54
Top 5 percent Wind Direction (°)												
Hindcast	208±87	179±90	188±92	289±57	292±34	295±31	295±24	292±24	293±28	296±24	288±40	275±65
RCP4.5 - mid	195±78	169±68	162±85	294±55	294±32	290±32	296±23	297±22	294±23	294±20	289±40	281±57
RCP8.5 - mid	226±72	152±78	180±10	296±46	294±33	295±33	293±31	298±23	295±21	293±25	284±33	279±59
RCP4.5 - end	229±84	171±92	167±83	267±74	297±32	295±25	297±26	296±22	298±18	297±17	292±32	284±52
RCP8.5 - end	233±85	160±89	171±79	285±61	290±40	297±25	297±23	298±24	296±19	294±16	288±33	286±37

Appendix B46. Table showing return values of ensemble-average wind speeds of hindcast and forecast scenarios, including lower and higher 95 percent confidence intervals, at the Rose Atoll location.

[Years: Hindcast = 1976–2005; RCP mid = 2026–2045; RCP end = 2081–2100. Wind speeds are in meters per second]

Scenario	Hindcast			RCP4.5 - mid			RCP8.5 - mid			RCP4.5 - end			RCP8.5 - end		
	Low	R_v	High	Low	R_v	High	Low	R_v	High	Low	R_v	High	Low	R_v	High
2-year	18.65	20.55	23.72	18.11	20.16	23.75	18.97	21.22	25.02	17.60	20.34	26.35	18.34	20.72	25.21
5-year	19.76	22.95	28.88	18.98	22.21	28.61	19.91	23.31	29.68	18.46	23.17	35.74	19.16	22.91	31.03
10-year	20.54	24.91	33.80	19.54	23.77	32.99	20.48	24.80	33.57	19.05	25.65	46.14	19.68	24.57	36.39
20-year	21.28	27.01	39.79	20.03	25.35	38.09	20.96	26.22	37.78	19.59	28.44	60.62	20.12	26.25	42.76
50-year	22.18	30.01	49.78	20.58	27.46	46.14	21.47	27.99	43.91	20.24	32.70	88.84	20.61	28.47	53.04
100-year	22.82	32.47	59.29	20.94	29.06	53.39	21.78	29.25	49.02	20.68	36.41	120.09	20.91	30.16	62.51

Appendix B47. Table showing Howland monthly means and mean of the top 5 percent for wind speed and mean wind direction.

[Years: Hindcast = 1976–2005; RCP mid = 2026–2045; RCP end = 2081–2100. Wind directions are "coming from"]

Month	Jan	Feb	Mar	Apr	May	Jun	July	Aug	Sep	Oct	Nov	Dec
Mean Wind Speed (m/s)												
Hindcast	5.7±1.9	5.9±1.7	5.5±1.6	5.1±1.6	4.8±1.8	5.2±1.9	6.0±1.8	6.1±1.8	6.0±1.9	5.5±1.9	5.3±2.0	5.3±2.1
RCP4.5 - mid	5.6±2.0	5.9±1.7	5.5±1.7	5.2±1.7	4.8±1.8	5.1±1.9	6.0±1.9	6.1±1.8	6.0±1.8	5.6±2.0	5.1±2.1	5.2±2.0
RCP8.5 - mid	5.8±1.9	6.0±1.7	5.5±1.7	5.0±1.6	4.6±1.7	5.1±1.9	6.0±1.9	6.1±1.8	6.0±1.8	5.6±1.9	5.4±2.0	5.4±2.0
RCP4.5 - end	5.8±1.9	5.9±1.8	5.6±1.7	5.0±1.7	4.8±1.8	5.2±1.9	5.9±1.9	6.1±1.8	6.0±1.8	5.6±1.9	5.3±2.0	5.4±2.2
RCP8.5 - end	5.8±1.8	6.0±1.7	5.6±1.7	5.1±1.8	4.9±1.8	5.2±1.9	6.2±2.0	6.5±1.9	6.3±1.8	5.9±1.9	5.5±1.8	5.5±1.9
Top 5 percent Wind Speed (m/s)												
Hindcast	9.6±0.9	9.5±0.8	8.7±0.6	8.2±0.8	8.6±1.1	8.9±0.8	9.3±0.8	9.4±0.6	9.4±0.7	9.2±0.8	9.4±1.1	9.8±1.4
RCP4.5 - mid	9.5±0.7	9.5±0.8	9.0±0.9	8.3±0.6	8.4±0.9	8.8±0.6	9.5±0.6	9.7±0.6	9.6±1.2	9.4±0.6	9.3±1.3	9.1±0.7
RCP8.5 - mid	9.5±0.6	9.6±0.8	8.8±0.6	8.2±0.6	7.9±0.6	8.9±0.7	9.6±0.7	9.6±0.8	9.5±0.7	9.2±0.7	9.6±1.1	9.4±1.2
RCP4.5 - end	9.7±1.0	9.5±0.7	8.8±0.6	8.1±0.5	8.4±0.9	9.1±0.8	9.6±1.0	9.5±0.7	9.4±0.7	9.4±0.7	9.5±1.3	10.1±1.3
RCP8.5 - end	9.5±0.8	9.3±0.7	8.9±0.8	8.5±0.7	8.5±1.4	9.0±0.8	9.7±0.7	9.7±0.6	9.5±0.7	9.6±1.5	8.9±0.6	9.2±0.8
Mean Wind Direction (°)												
Hindcast	256±33	254±28	258±29	268±33	275±38	278±36	279±28	280±27	280±32	280±35	277±41	268±37
RCP4.5 - mid	258±32	254±34	255±35	265±35	272±40	275±37	278±31	278±26	279±27	278±32	277±38	268±36
RCP8.5 - mid	258±32	255±28	258±30	266±31	272±36	276±34	277±29	279±27	279±31	279±37	277±40	266±37
RCP4.5 - end	255±33	253±29	254±31	264±33	270±42	274±37	276±30	279±30	279±32	279±38	276±41	266±39
RCP8.5 - end	258±31	254±25	258±29	263±33	268±37	271±35	277±35	278±31	280±31	280±34	277±34	268±31
Top 5 percent Wind Direction (°)												
Hindcast	234±40	232±30	238±27	260±31	282±53	286±35	283±28	280±17	279±23	276±36	284±72	258±56
RCP4.5 - mid	251±28	235±48	235±41	260±34	282±49	284±30	281±22	277±12	280±27	275±19	280±43	264±29
RCP8.5 - mid	238±30	235±25	241±23	262±31	279±24	281±22	278±17	279±21	279±18	277±33	284±72	240±55
RCP4.5 - end	232±35	229±26	235±26	260±23	273±54	283±40	281±29	279±28	277±31	276±40	284±68	247±66
RCP8.5 - end	239±31	236±26	243±21	260±33	272±53	276±30	277±32	274±21	276±39	277±46	273±32	254±36

Appendix B48. Table showing return values of ensemble-average wind speeds of hindcast and forecast scenarios, including lower and higher 95 percent confidence intervals, at the Howland location.

[Years: Hindcast = 1976–2005; RCP mid = 2026–2045; RCP end = 2081–2100. Wind speeds are in meters per second]

Scenario	Hindcast			RCP4.5 - mid			RCP8.5 - mid			RCP4.5 - end			RCP8.5 - end		
	Low	R_v	High	Low	R_v	High	Low	R_v	High	Low	R_v	High	Low	R_v	High
2-year	12.32	13.36	15.21	12.22	13.15	14.77	11.93	12.83	14.64	12.63	13.84	16.07	12.09	13.17	15.36
5-year	12.93	14.81	18.74	12.78	14.43	17.70	12.32	13.95	17.82	13.15	15.16	19.40	12.54	14.48	19.19
10-year	13.39	16.16	22.60	13.21	15.58	20.77	12.62	14.98	21.41	13.51	16.24	22.66	12.88	15.69	23.52
20-year	13.87	17.75	27.94	13.64	16.90	24.85	12.91	16.19	26.49	13.84	17.39	26.74	13.21	17.11	29.69
50-year	14.51	20.32	38.23	14.22	18.98	32.35	13.29	18.14	36.57	14.23	19.04	33.76	13.64	19.40	41.98
100-year	15.01	22.68	49.51	14.66	20.84	40.20	13.57	19.93	47.95	14.49	20.40	40.63	13.96	21.51	55.91

Appendix B49. Table showing Jarvis monthly means and mean of the top 5 percent for wind speed and mean wind direction.

[Years: Hindcast = 1976–2005; RCP mid = 2026–2045; RCP end = 2081–2100. Wind directions are "coming from"]

Month	Jan	Feb	Mar	Apr	May	Jun	July	Aug	Sep	Oct	Nov	Dec
Mean Wind Speed (m/s)												
Hindcast	6.3±1.9	6.3±1.7	6.0±1.6	5.7±1.7	5.5±1.7	6.1±1.8	6.7±1.8	6.7±1.7	6.5±1.7	6.2±1.7	6.0±1.8	6.0±1.9
RCP4.5 - mid	6.1±1.9	6.0±1.8	5.8±1.7	5.6±1.7	5.3±1.9	6.0±1.8	6.7±1.8	6.7±1.6	6.4±1.5	6.0±1.7	5.9±1.8	5.9±1.8
RCP8.5 - mid	6.3±1.8	6.2±1.7	5.8±1.7	5.5±1.7	5.3±1.7	6.0±1.8	6.7±1.8	6.6±1.7	6.4±1.7	6.1±1.7	5.8±1.8	5.8±1.9
RCP4.5 - end	6.2±1.8	6.1±1.7	5.8±1.7	5.5±1.8	5.3±1.7	6.0±1.8	6.6±1.7	6.7±1.7	6.5±1.6	6.2±1.7	5.8±1.8	5.8±1.9
RCP8.5 - end	6.2±1.6	6.2±1.6	5.8±1.7	5.4±1.7	5.3±1.7	6.0±1.8	6.8±1.9	6.8±1.7	6.4±1.6	6.2±1.6	6.0±1.7	6.0±1.7
Top 5 percent Wind Speed (m/s)												
Hindcast	10.1±1.0	9.6±0.8	9.1±0.7	9.0±1.0	8.8±0.7	9.4±0.7	9.7±0.5	9.8±0.5	9.5±0.6	9.4±0.5	10.0±1.7	9.8±0.7
RCP4.5 - mid	9.6±0.7	9.4±0.8	8.9±0.6	8.7±0.6	8.9±1.0	9.5±0.7	9.8±0.6	9.6±0.5	9.0±0.4	9.2±0.6	9.6±0.7	9.7±0.8
RCP8.5 - mid	9.7±0.7	9.3±0.8	8.9±0.8	8.6±0.7	8.6±0.7	9.4±0.6	9.9±0.8	9.5±0.6	9.3±0.6	9.2±0.6	9.4±0.6	9.5±0.7
RCP4.5 - end	9.8±0.8	9.5±0.7	9.2±1.0	8.8±0.7	8.6±0.7	9.5±0.8	9.6±0.5	9.7±0.6	9.2±0.6	9.3±1.0	9.4±0.7	9.7±0.8
RCP8.5 - end	9.4±0.9	9.4±0.8	8.7±0.5	8.5±0.6	8.6±0.8	9.5±0.7	9.9±0.5	9.7±0.5	9.1±0.6	9.2±0.6	9.3±0.5	9.4±0.6
Mean Wind Direction (°)												
Hindcast	259±29	255±28	258±27	261±26	263±27	266±24	268±23	270±21	270±21	270±22	270±28	265±28
RCP4.5 - mid	261±24	258±29	257±33	257±34	259±34	265±23	267±21	269±20	270±21	269±22	269±25	266±22
RCP8.5 - mid	259±31	256±31	256±30	258±30	262±28	264±23	268±22	269±21	270±20	270±23	269±27	265±30
RCP4.5 - end	259±33	256±29	256±29	257±30	260±31	265±24	268±24	271±23	271±23	271±26	269±30	265±30
RCP8.5 - end	259±26	256±27	256±27	257±28	259±29	264±23	270±23	271±20	272±21	271±26	272±26	267±27
Top 5 percent Wind Direction (°)												
Hindcast	252±40	251±33	255±29	261±30	266±18	266±15	271±16	273±16	271±17	269±15	269±50	261±30
RCP4.5 - mid	260±26	256±33	258±39	263±29	266±33	268±13	268±12	268±14	270±14	268±16	266±26	262±15
RCP8.5 - mid	252±38	250±37	251±28	261±37	267±20	265±10	268±11	269±13	271±13	269±15	267±17	259±30
RCP4.5 - end	251±44	246±32	249±41	257±25	264±26	266±11	268±11	269±17	270±17	268±34	271±56	262±28
RCP8.5 - end	244±38	240±32	252±22	262±16	266±19	264±12	267±11	270±14	269±14	270±30	270±13	262±25

Appendix B50. Table showing return values of ensemble-average wind speeds of hindcast and forecast scenarios, including lower and higher 95 percent confidence intervals, at the Jarvis location.

[Years: Hindcast = 1976–2005; RCP mid = 2026–2045; RCP end = 2081–2100. Wind speeds are in meters per second]

Scenario	Hindcast			RCP4.5 - mid			RCP8.5 - mid			RCP4.5 - end			RCP8.5 - end		
	Low	R_v	High	Low	R_v	High	Low	R_v	High	Low	R_v	High	Low	R_v	High
2-year	12.25	13.09	14.64	11.93	12.75	14.49	11.92	12.58	13.71	12.09	12.84	14.24	11.75	12.41	13.66
5-year	12.81	14.47	18.08	12.21	13.60	17.16	12.21	13.25	15.23	12.40	13.62	16.23	12.04	13.15	15.58
10-year	13.29	15.89	22.28	12.39	14.33	20.06	12.40	13.75	16.58	12.60	14.24	18.14	12.23	13.77	17.53
20-year	13.81	17.72	28.65	12.56	15.15	24.00	12.57	14.26	18.13	12.78	14.90	20.51	12.42	14.45	20.05
50-year	14.60	21.00	42.39	12.76	16.38	31.50	12.76	14.93	20.52	12.99	15.81	24.49	12.64	15.44	24.53
100-year	15.27	24.35	59.17	12.90	17.44	39.61	12.88	15.43	22.64	13.13	16.55	28.33	12.79	16.28	29.06

Appendix C. Monthly Trends in Wave Height

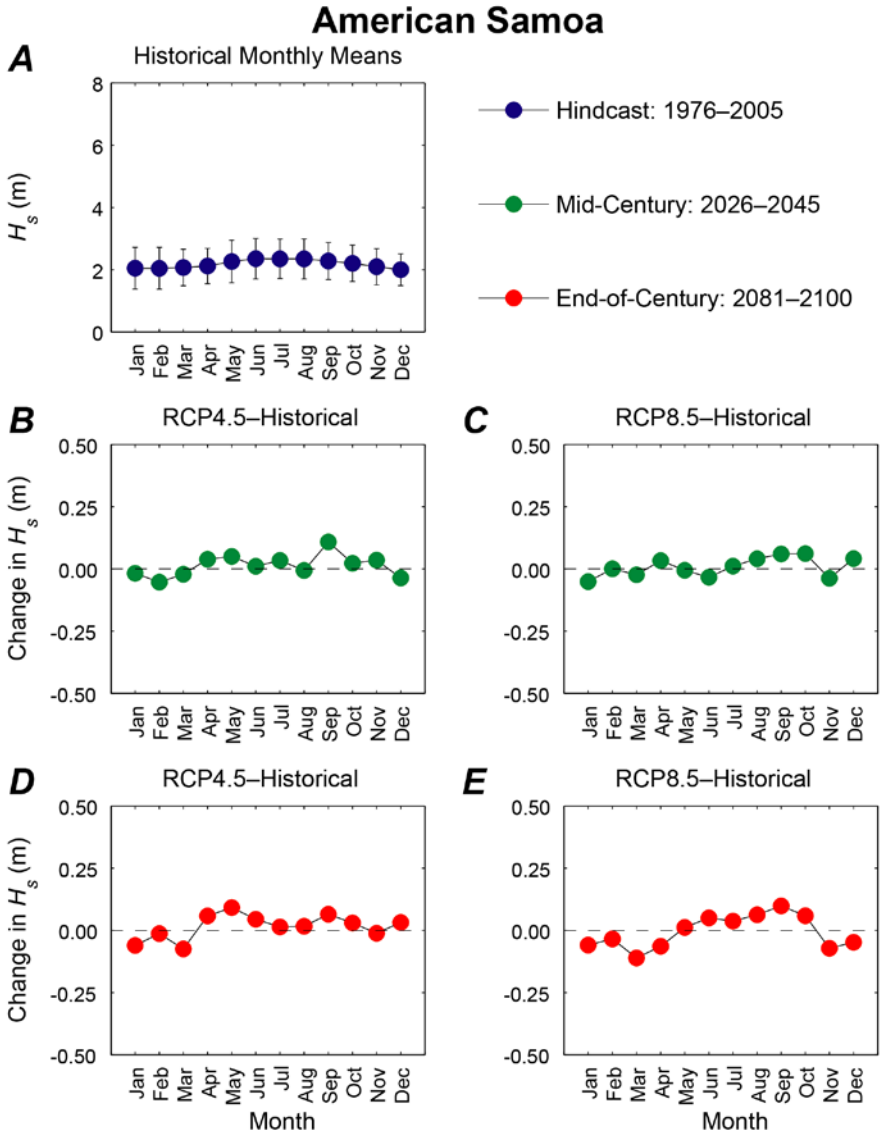

Appendix C1. Plots showing trends in monthly mean significant wave height (H_s), in meters, at the American Samoa location. *A.* Hindcasted (1976–2005) mean significant wave heights by month with associated error bars. *B.* Plot of the change in mean 2026–2045 significant wave heights for the RCP4.5 scenario from hindcasted monthly significant wave height means. *C.* Plot of the change in mean 2026–2045 significant wave heights for the RCP8.5 scenario from hindcasted monthly significant wave height means. *D.* Plot of the change in mean 2081–2100 significant wave heights for the RCP4.5 scenario from hindcasted monthly significant wave height means. *E.* Plot of the change in mean 2081–2100 significant wave heights for the RCP8.5 scenario from hindcasted monthly significant wave height means.

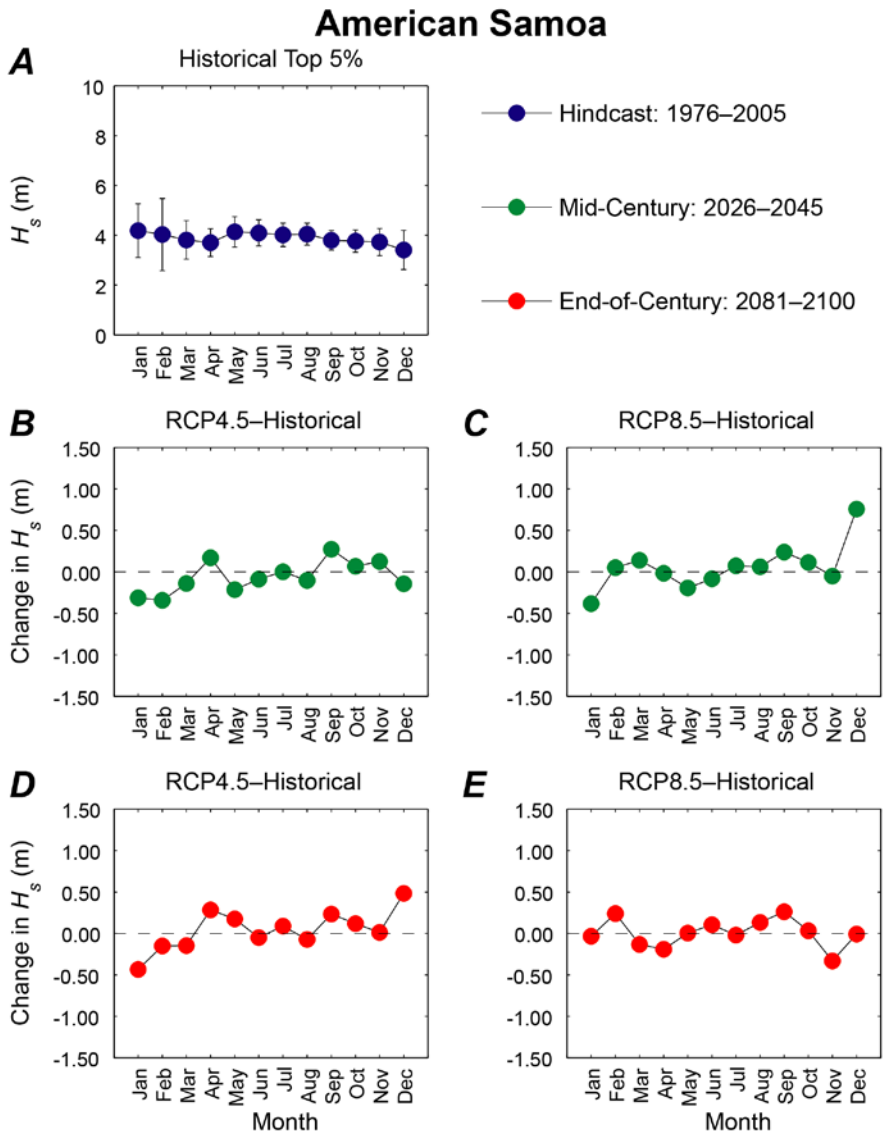

Appendix C2. Plots showing trends in monthly mean of the top 5 percent of significant wave heights (H_S), in meters, at the American Samoa location. *A.* Hindcasted (1976–2005) mean of the top 5 percent of significant wave heights by month with associated error bars. *B.* Plot of the change in mean of the top 5 percent of 2026–2045 significant wave heights for the RCP4.5 scenario from hindcasted top 5 percent of monthly significant wave height means. *C.* Plot of the change in mean of the top 5 percent of 2026–2045 significant wave heights for the RCP8.5 scenario from hindcasted top 5 percent of monthly significant wave height means. *D.* Plot of the change in mean of the top 5 percent of 2081–2100 significant wave heights for the RCP4.5 scenario from hindcasted top 5 percent of monthly significant wave height means. *E.* Plot of the change in mean of the top 5 percent of 2081–2100 significant wave heights for the RCP8.5 scenario from hindcasted top 5 percent of monthly significant wave height means.

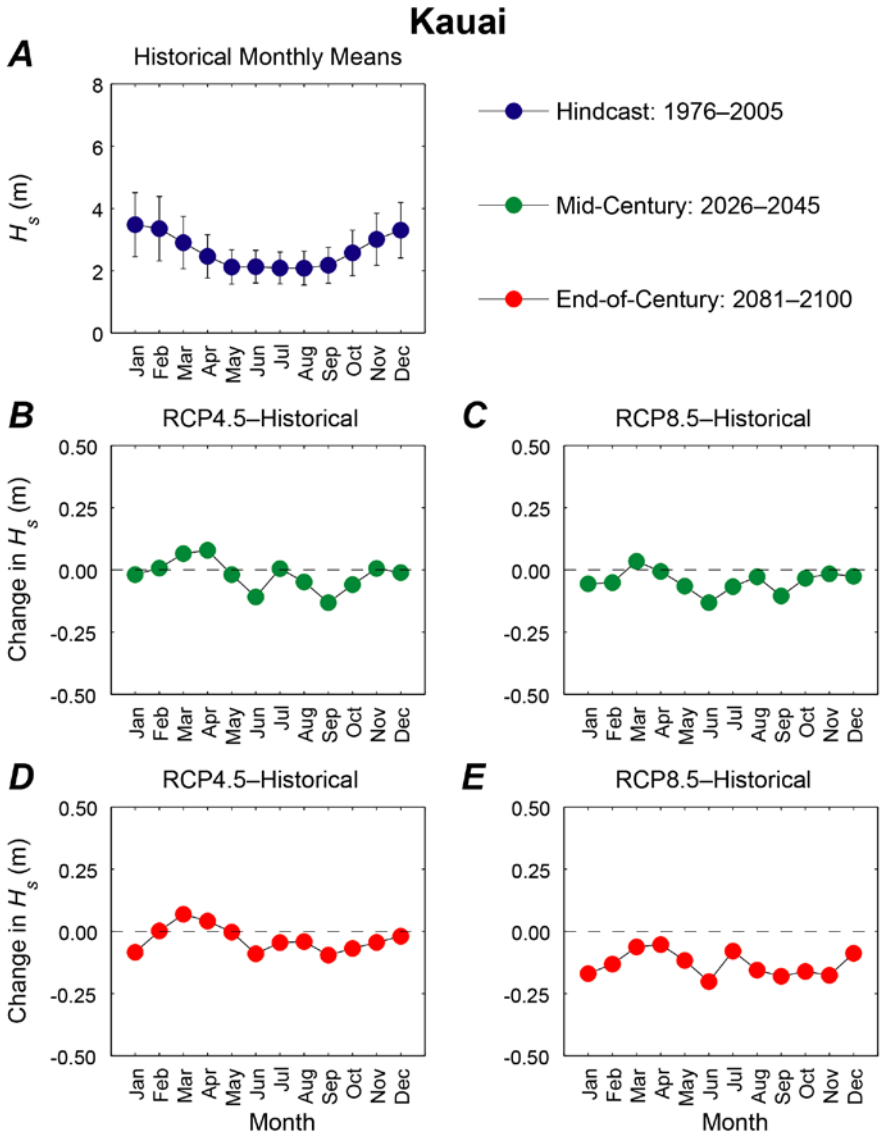

Appendix C3. Plots showing trends in monthly mean significant wave height (H_s), in meters, at the Kauai location. *A.* Hindcasted (1976–2005) mean significant wave heights by month with associated error bars. *B.* Plot of the change in mean 2026–2045 significant wave heights for the RCP4.5 scenario from hindcasted monthly significant wave height means. *C.* Plot of the change in mean 2026–2045 significant wave heights for the RCP8.5 scenario from hindcasted monthly significant wave height means. *D.* Plot of the change in mean 2081–2100 significant wave heights for the RCP4.5 scenario from hindcasted monthly significant wave height means. *E.* Plot of the change in mean 2081–2100 significant wave heights for the RCP8.5 scenario from hindcasted monthly significant wave height means.

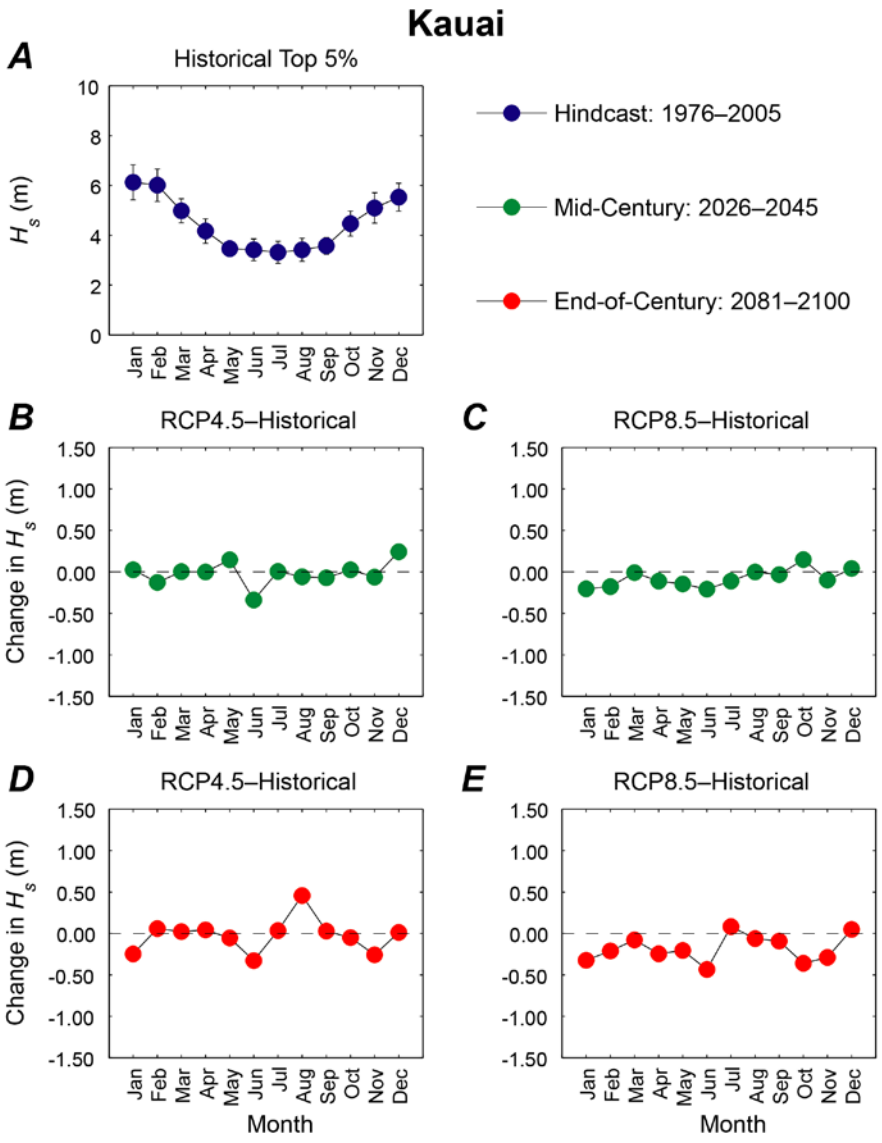

Appendix C4. Plots showing trends in monthly mean of the top 5 percent of significant wave heights (H_S), in meters, at the Kauai location. *A.* Hindcasted (1976–2005) mean of the top 5 percent of significant wave heights by month with associated error bars. *B.* Plot of the change in mean of the top 5 percent of 2026–2045 significant wave heights for the RCP4.5 scenario from hindcasted top 5 percent of monthly significant wave height means. *C.* Plot of the change in mean of the top 5 percent of 2026–2045 significant wave heights for the RCP8.5 scenario from hindcasted top 5 percent of monthly significant wave height means. *D.* Plot of the change in mean of the top 5 percent of 2081–2100 significant wave heights for the RCP4.5 scenario from hindcasted top 5 percent of monthly significant wave height means. *E.* Plot of the change in mean of the top 5 percent of 2081–2100 significant wave heights for the RCP8.5 scenario from hindcasted top 5 percent of monthly significant wave height means.

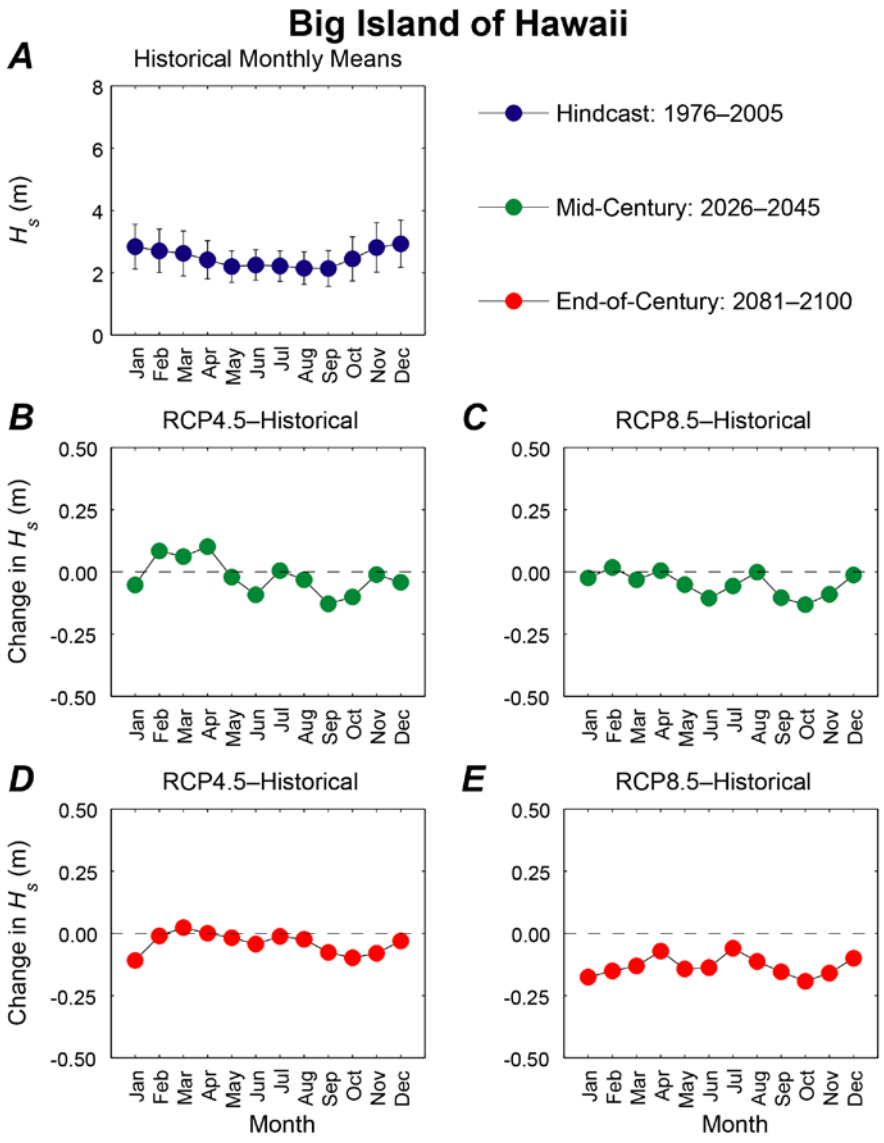

Appendix C5. Plots showing trends in monthly mean significant wave height (H_s), in meters, at the Big Island of Hawaii location. *A.* Hindcasted (1976–2005) mean significant wave heights by month with associated error bars. *B.* Plot of the change in mean 2026–2045 significant wave heights for the RCP4.5 scenario from hindcasted monthly significant wave height means. *C.* Plot of the change in mean 2026–2045 significant wave heights for the RCP8.5 scenario from hindcasted monthly significant wave height means. *D.* Plot of the change in mean 2081–2100 significant wave heights for the RCP4.5 scenario from hindcasted monthly significant wave height means. *E.* Plot of the change in mean 2081–2100 significant wave heights for the RCP8.5 scenario from hindcasted monthly significant wave height means.

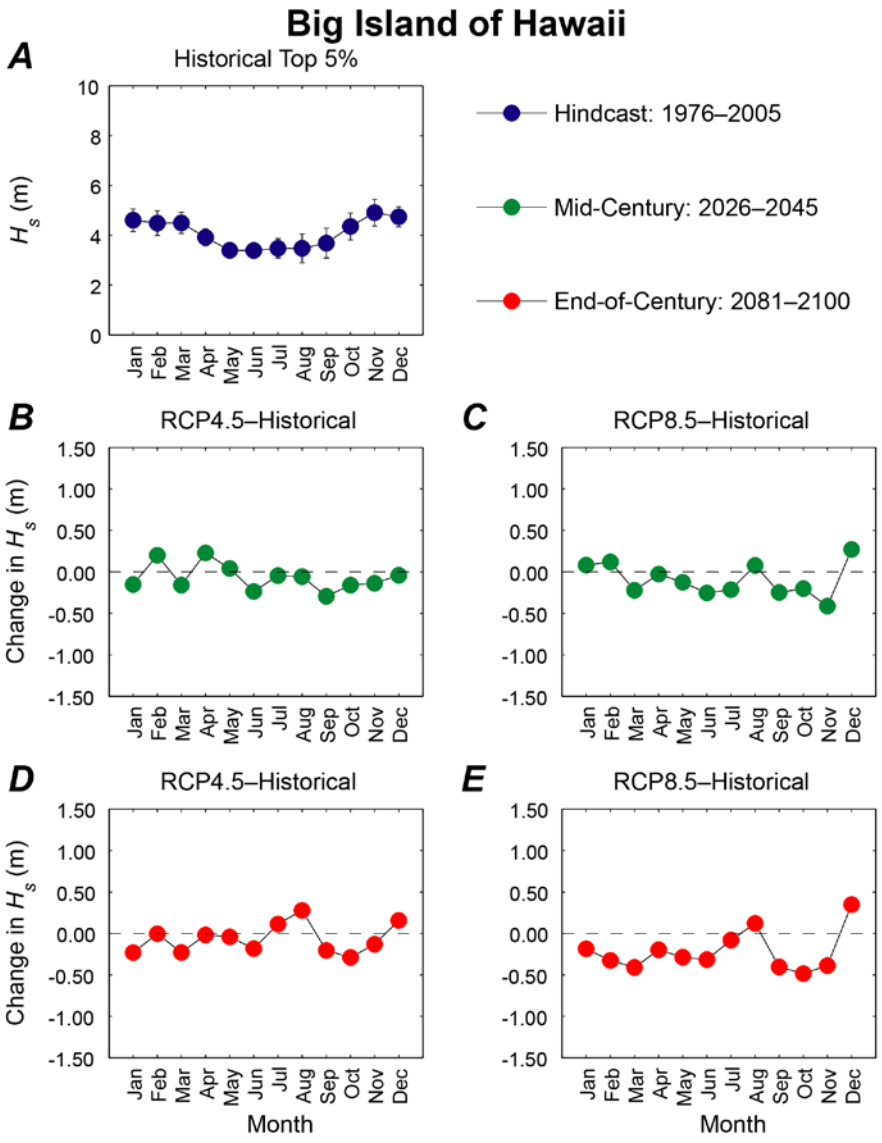

Appendix C6. Plots showing trends in monthly mean of the top 5 percent of significant wave heights (H_S), in meters, at the Big Island of Hawaii location. *A.* Hindcasted (1976–2005) mean of the top 5 percent of significant wave heights by month with associated error bars. *B.* Plot of the change in mean of the top 5 percent of 2026–2045 significant wave heights for the RCP4.5 scenario from hindcasted top 5 percent of monthly significant wave height means. *C.* Plot of the change in mean of the top 5 percent of 2026–2045 significant wave heights for the RCP8.5 scenario from hindcasted top 5 percent of monthly significant wave height means. *D.* Plot of the change in mean of the top 5 percent of 2081–2100 significant wave heights for the RCP4.5 scenario from hindcasted top 5 percent of monthly significant wave height means. *E.* Plot of the change in mean of the top 5 percent of 2081–2100 significant wave heights for the RCP8.5 scenario from hindcasted top 5 percent of monthly significant wave height means.

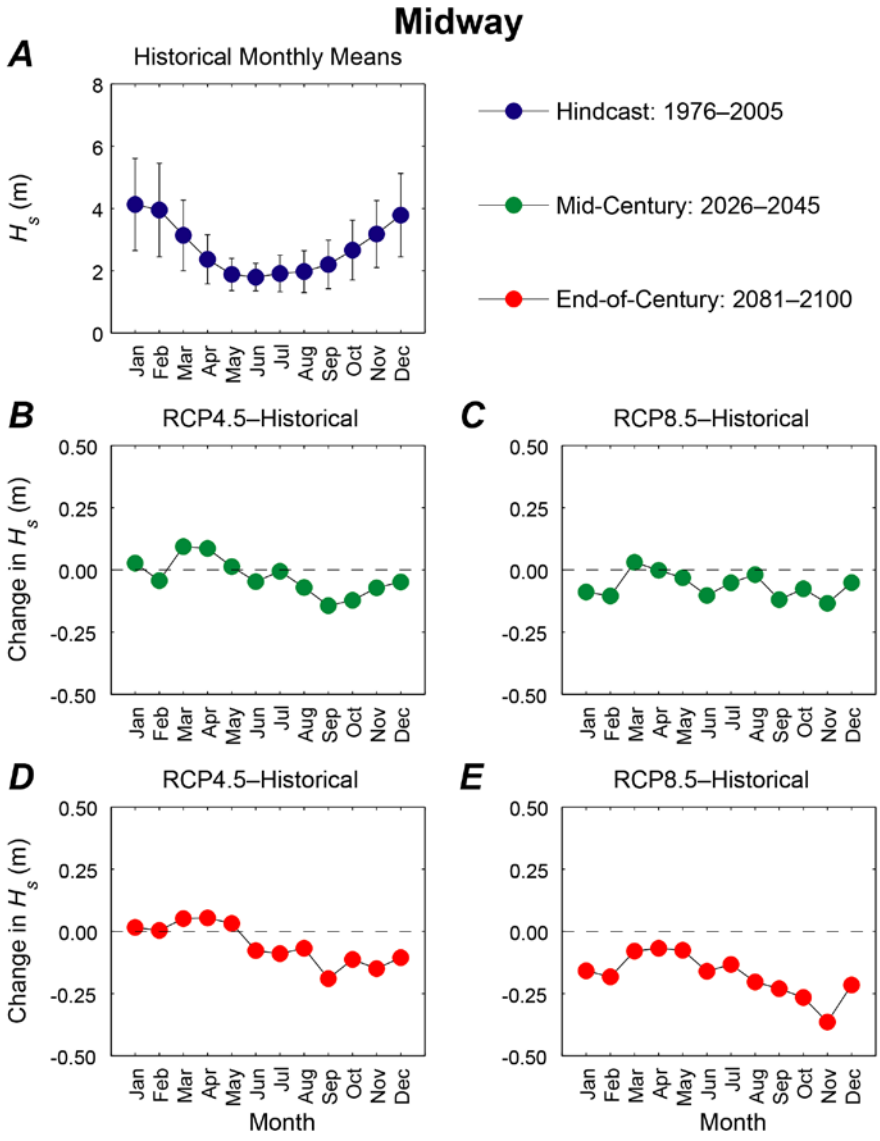

Appendix C7. Plots showing trends in monthly mean significant wave height (H_s), in meters, at the Midway location. *A.* Hindcasted (1976–2005) mean significant wave heights by month with associated error bars. *B.* Plot of the change in mean 2026–2045 significant wave heights for the RCP4.5 scenario from hindcasted monthly significant wave height means. *C.* Plot of the change in mean 2026–2045 significant wave heights for the RCP8.5 scenario from hindcasted monthly significant wave height means. *D.* Plot of the change in mean 2081–2100 significant wave heights for the RCP4.5 scenario from hindcasted monthly significant wave height means. *E.* Plot of the change in mean 2081–2100 significant wave heights for the RCP8.5 scenario from hindcasted monthly significant wave height means.

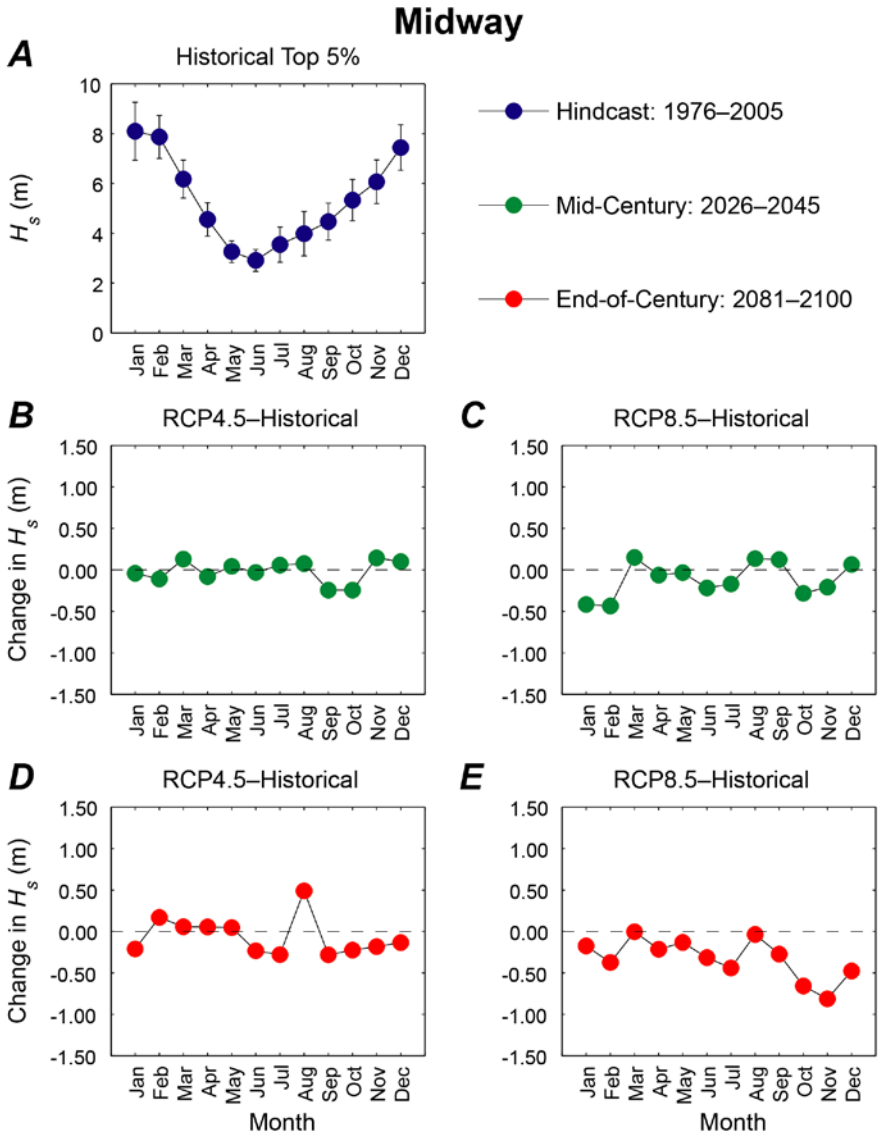

Appendix C8. Plots showing trends in monthly mean of the top 5 percent of significant wave heights (H_S), in meters, at the Midway location. *A.* Hindcasted (1976–2005) mean of the top 5 percent of significant wave heights by month with associated error bars. *B.* Plot of the change in mean of the top 5 percent of 2026–2045 significant wave heights for the RCP4.5 scenario from hindcasted top 5 percent of monthly significant wave height means. *C.* Plot of the change in mean of the top 5 percent of 2026–2045 significant wave heights for the RCP8.5 scenario from hindcasted top 5 percent of monthly significant wave height means. *D.* Plot of the change in mean of the top 5 percent of 2081–2100 significant wave heights for the RCP4.5 scenario from hindcasted top 5 percent of monthly significant wave height means. *E.* Plot of the change in mean of the top 5 percent of 2081–2100 significant wave heights for the RCP8.5 scenario from hindcasted top 5 percent of monthly significant wave height means.

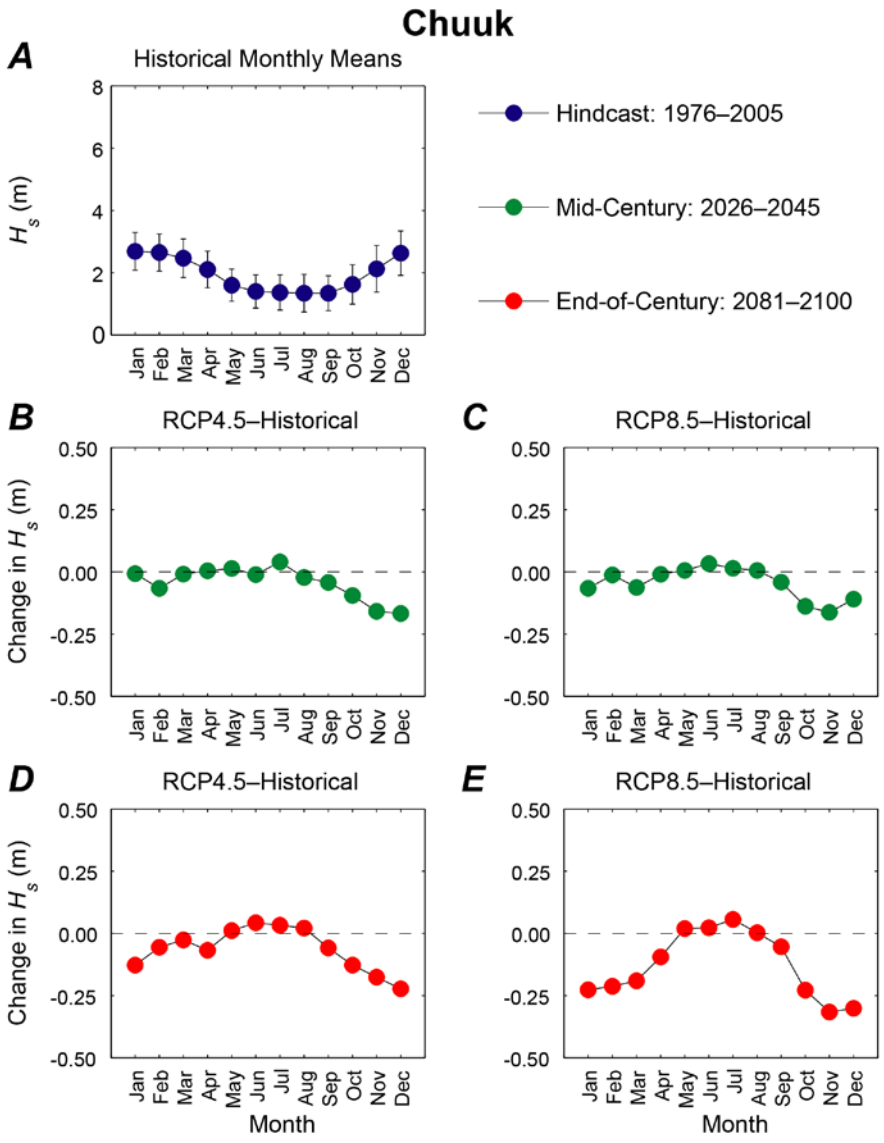

Appendix C9. Plots showing trends in monthly mean significant wave height (H_s), in meters, at the Chuuk location. *A.* Hindcasted (1976–2005) mean significant wave heights by month with associated error bars. *B.* Plot of the change in mean 2026–2045 significant wave heights for the RCP4.5 scenario from hindcasted monthly significant wave height means. *C.* Plot of the change in mean 2026–2045 significant wave heights for the RCP8.5 scenario from hindcasted monthly significant wave height means. *D.* Plot of the change in mean 2081–2100 significant wave heights for the RCP4.5 scenario from hindcasted monthly significant wave height means. *E.* Plot of the change in mean 2081–2100 significant wave heights for the RCP8.5 scenario from hindcasted monthly significant wave height means.

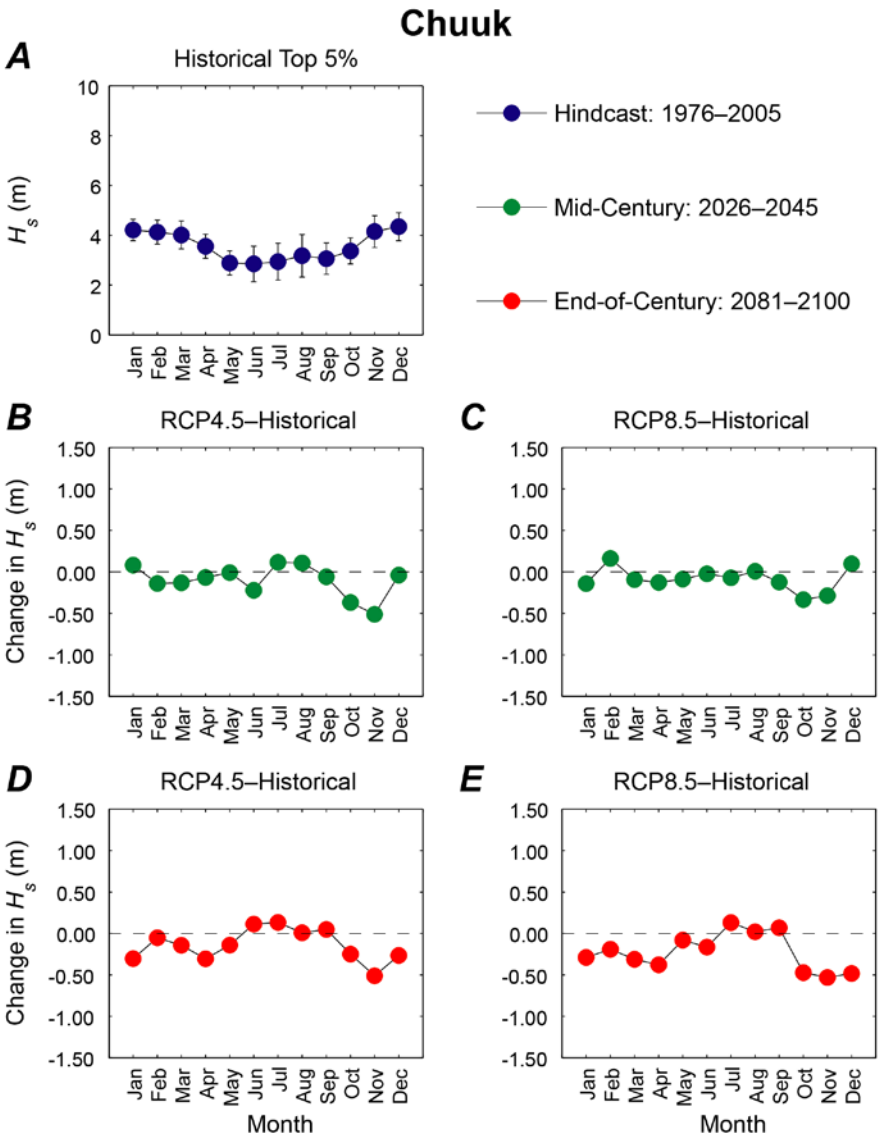

Appendix C10. Plots showing trends in monthly mean of the top 5 percent of significant wave heights (H_S), in meters, at the Chuuk location. *A.* Hindcasted (1976–2005) mean of the top 5 percent of significant wave heights by month with associated error bars. *B.* Plot of the change in mean of the top 5 percent of 2026–2045 significant wave heights for the RCP4.5 scenario from hindcasted top 5 percent of monthly significant wave height means. *C.* Plot of the change in mean of the top 5 percent of 2026–2045 significant wave heights for the RCP8.5 scenario from hindcasted top 5 percent of monthly significant wave height means. *D.* Plot of the change in mean of the top 5 percent of 2081–2100 significant wave heights for the RCP4.5 scenario from hindcasted top 5 percent of monthly significant wave height means. *E.* Plot of the change in mean of the top 5 percent of 2081–2100 significant wave heights for the RCP8.5 scenario from hindcasted top 5 percent of monthly significant wave height means.

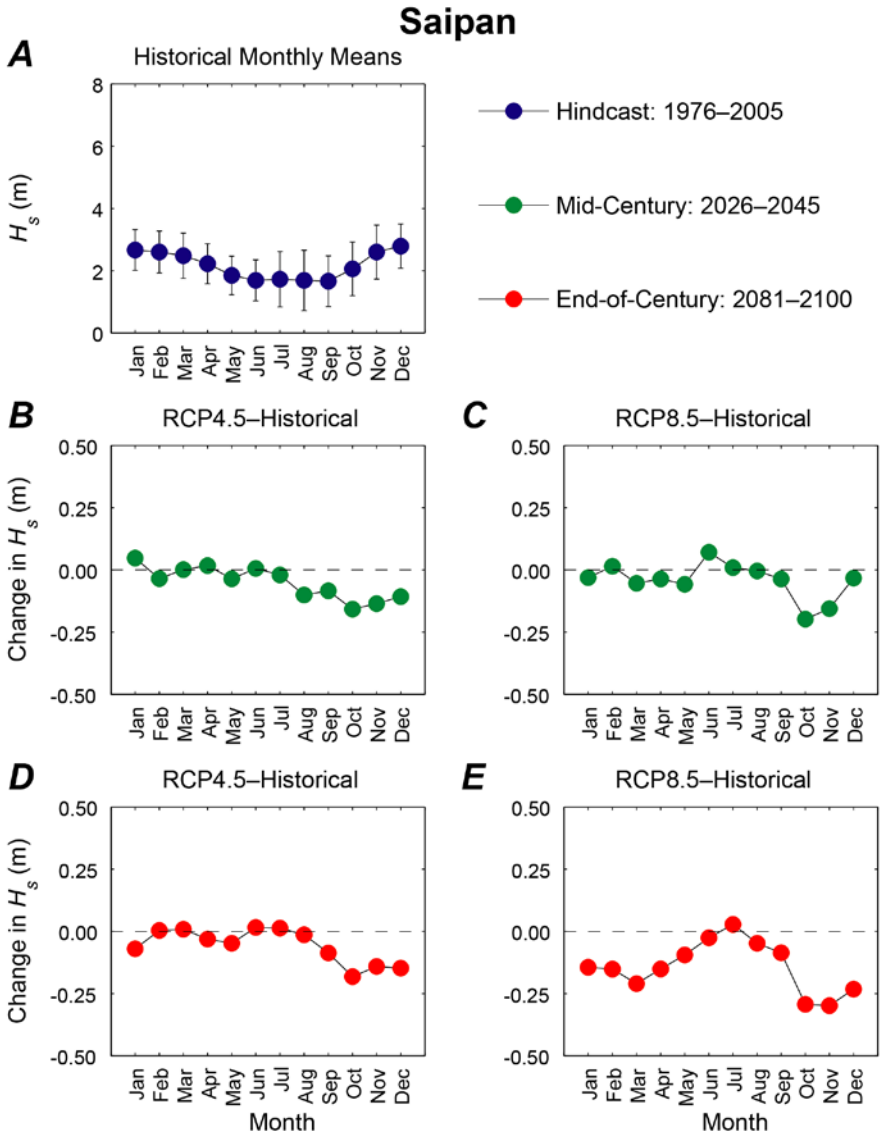

Appendix C11. Plots showing trends in monthly mean significant wave height (H_s), in meters, at the Saipan location. *A.* Hindcasted (1976–2005) mean significant wave heights by month with associated error bars. *B.* Plot of the change in mean 2026–2045 significant wave heights for the RCP4.5 scenario from hindcasted monthly significant wave height means. *C.* Plot of the change in mean 2026–2045 significant wave heights for the RCP8.5 scenario from hindcasted monthly significant wave height means. *D.* Plot of the change in mean 2081–2100 significant wave heights for the RCP4.5 scenario from hindcasted monthly significant wave height means. *E.* Plot of the change in mean 2081–2100 significant wave heights for the RCP8.5 scenario from hindcasted monthly significant wave height means.

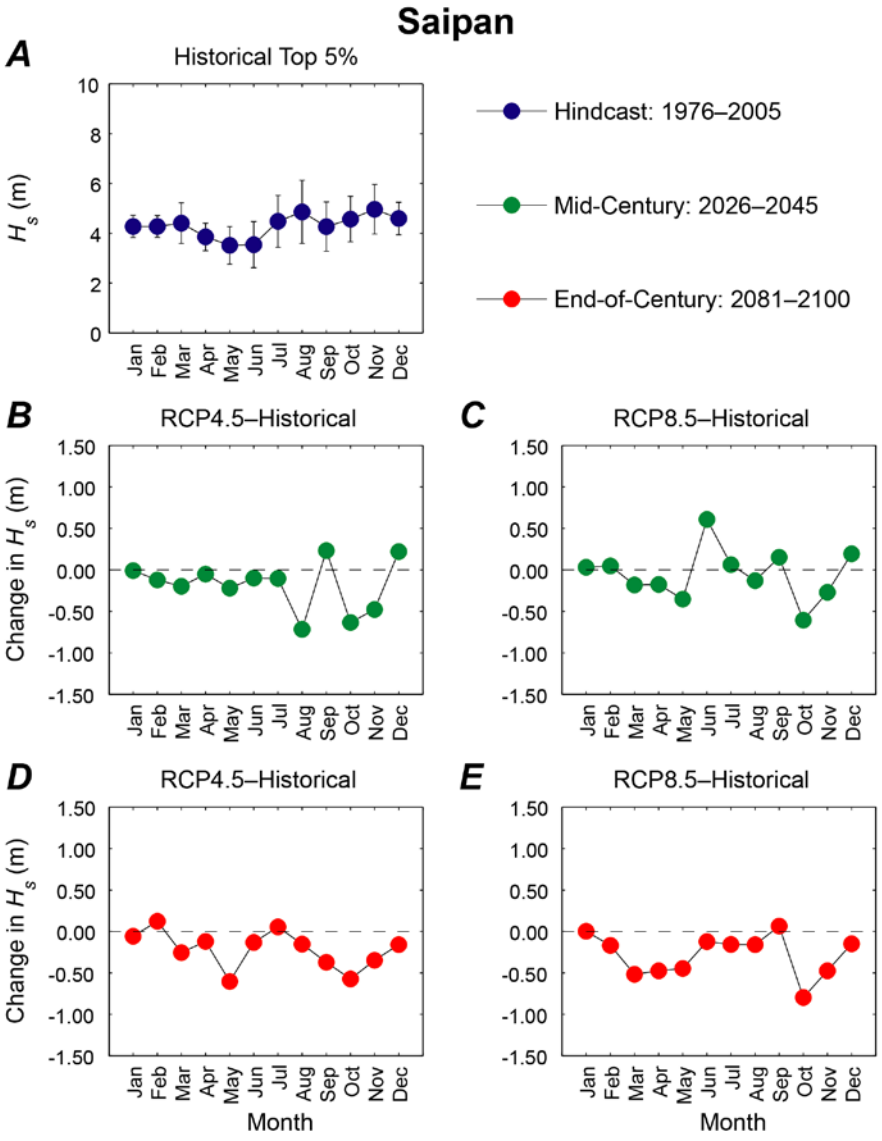

Appendix C12. Plots showing trends in monthly mean of the top 5 percent of significant wave heights (H_S), in meters, at the Saipan location. *A.* Hindcasted (1976–2005) mean of the top 5 percent of significant wave heights by month with associated error bars. *B.* Plot of the change in mean of the top 5 percent of 2026–2045 significant wave heights for the RCP4.5 scenario from hindcasted top 5 percent of monthly significant wave height means. *C.* Plot of the change in mean of the top 5 percent of 2026–2045 significant wave heights for the RCP8.5 scenario from hindcasted top 5 percent of monthly significant wave height means. *D.* Plot of the change in mean of the top 5 percent of 2081–2100 significant wave heights for the RCP4.5 scenario from hindcasted top 5 percent of monthly significant wave height means. *E.* Plot of the change in mean of the top 5 percent of 2081–2100 significant wave heights for the RCP8.5 scenario from hindcasted top 5 percent of monthly significant wave height means.

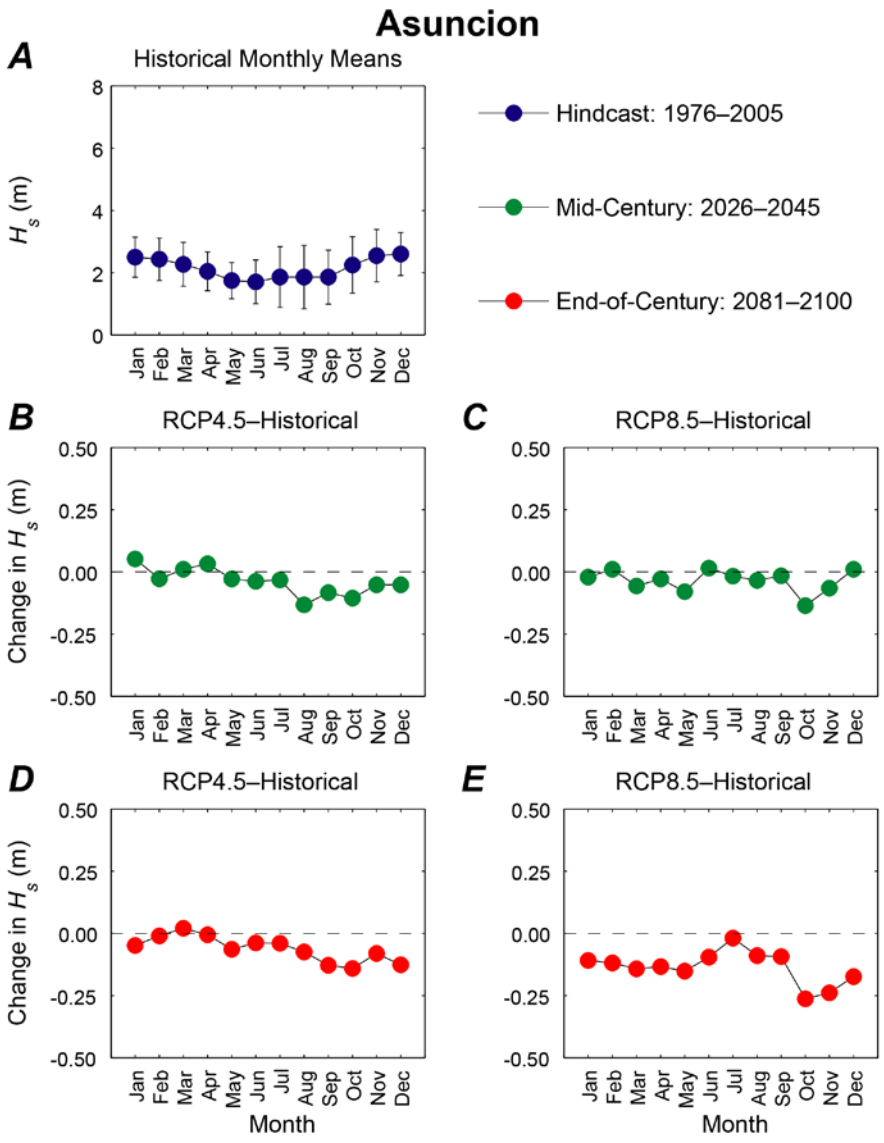

Appendix C13. Plots showing trends in monthly mean significant wave height (H_s), in meters, at the Asuncion location. *A.* Hindcasted (1976–2005) mean significant wave heights by month with associated error bars. *B.* Plot of the change in mean 2026–2045 significant wave heights for the RCP4.5 scenario from hindcasted monthly significant wave height means. *C.* Plot of the change in mean 2026–2045 significant wave heights for the RCP8.5 scenario from hindcasted monthly significant wave height means. *D.* Plot of the change in mean 2081–2100 significant wave heights for the RCP4.5 scenario from hindcasted monthly significant wave height means. *E.* Plot of the change in mean 2081–2100 significant wave heights for the RCP8.5 scenario from hindcasted monthly significant wave height means.

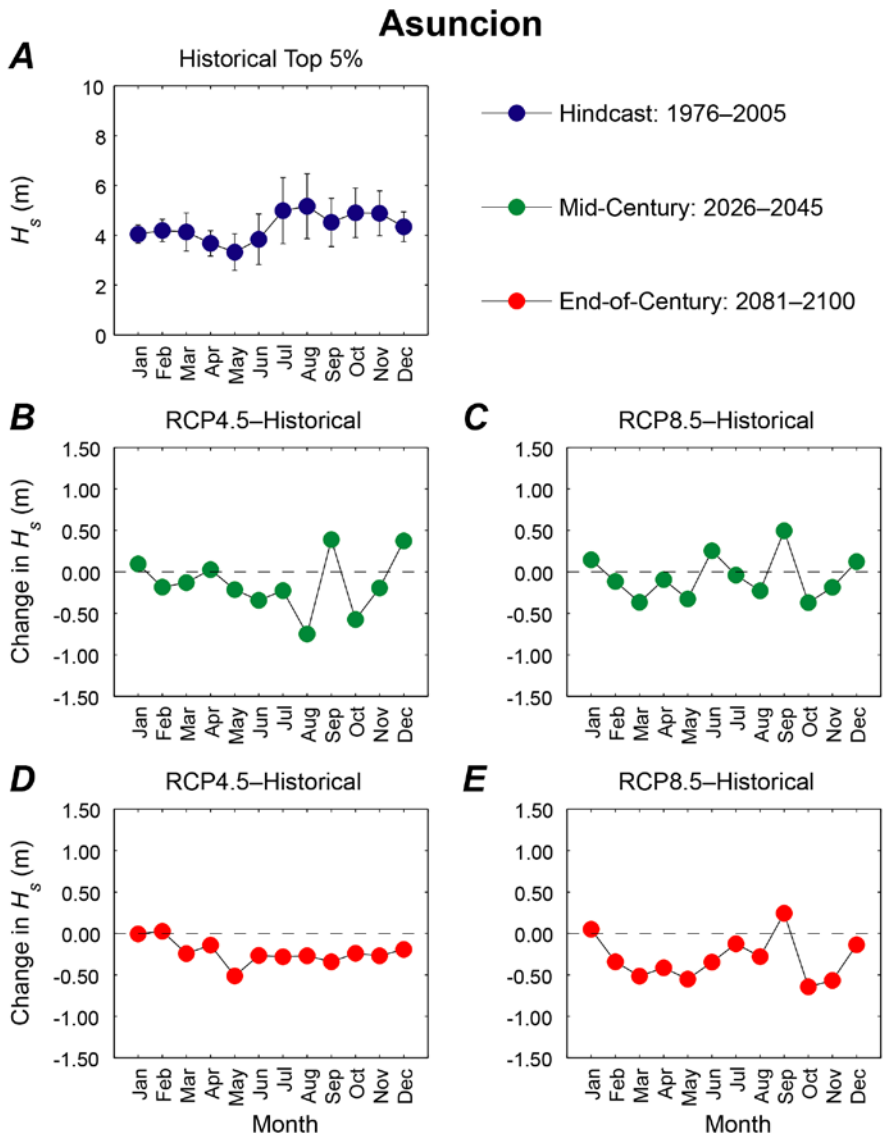

Appendix C14. Plots showing trends in monthly mean of the top 5 percent of significant wave heights (H_S), in meters, at the Asuncion location. *A.* Hindcasted (1976–2005) mean of the top 5 percent of significant wave heights by month with associated error bars. *B.* Plot of the change in mean of the top 5 percent of 2026–2045 significant wave heights for the RCP4.5 scenario from hindcasted top 5 percent of monthly significant wave height means. *C.* Plot of the change in mean of the top 5 percent of 2026–2045 significant wave heights for the RCP8.5 scenario from hindcasted top 5 percent of monthly significant wave height means. *D.* Plot of the change in mean of the top 5 percent of 2081–2100 significant wave heights for the RCP4.5 scenario from hindcasted top 5 percent of monthly significant wave height means. *E.* Plot of the change in mean of the top 5 percent of 2081–2100 significant wave heights for the RCP8.5 scenario from hindcasted top 5 percent of monthly significant wave height means.

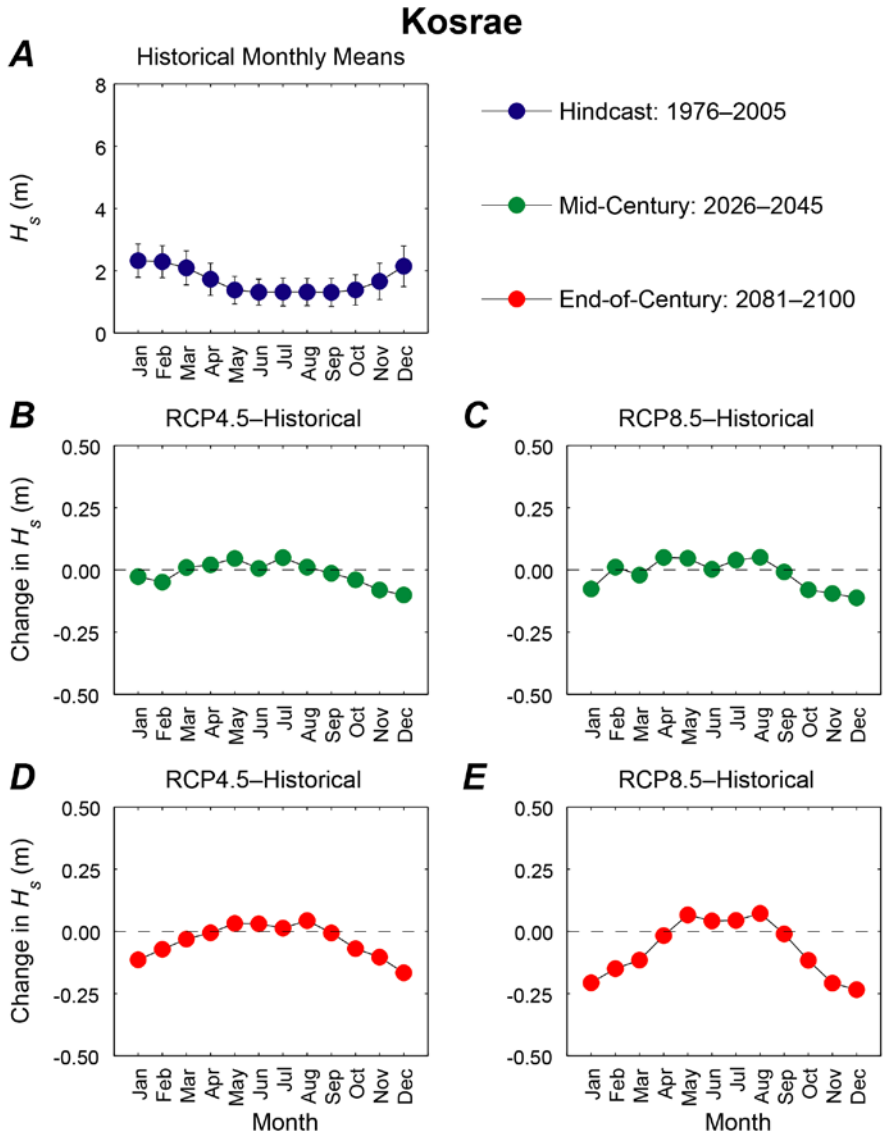

Appendix C15. Plots showing trends in monthly mean significant wave height (H_s), in meters, at the Kosrae location. *A.* Hindcasted (1976–2005) mean significant wave heights by month with associated error bars. *B.* Plot of the change in mean 2026–2045 significant wave heights for the RCP4.5 scenario from hindcasted monthly significant wave height means. *C.* Plot of the change in mean 2026–2045 significant wave heights for the RCP8.5 scenario from hindcasted monthly significant wave height means. *D.* Plot of the change in mean 2081–2100 significant wave heights for the RCP4.5 scenario from hindcasted monthly significant wave height means. *E.* Plot of the change in mean 2081–2100 significant wave heights for the RCP8.5 scenario from hindcasted monthly significant wave height means.

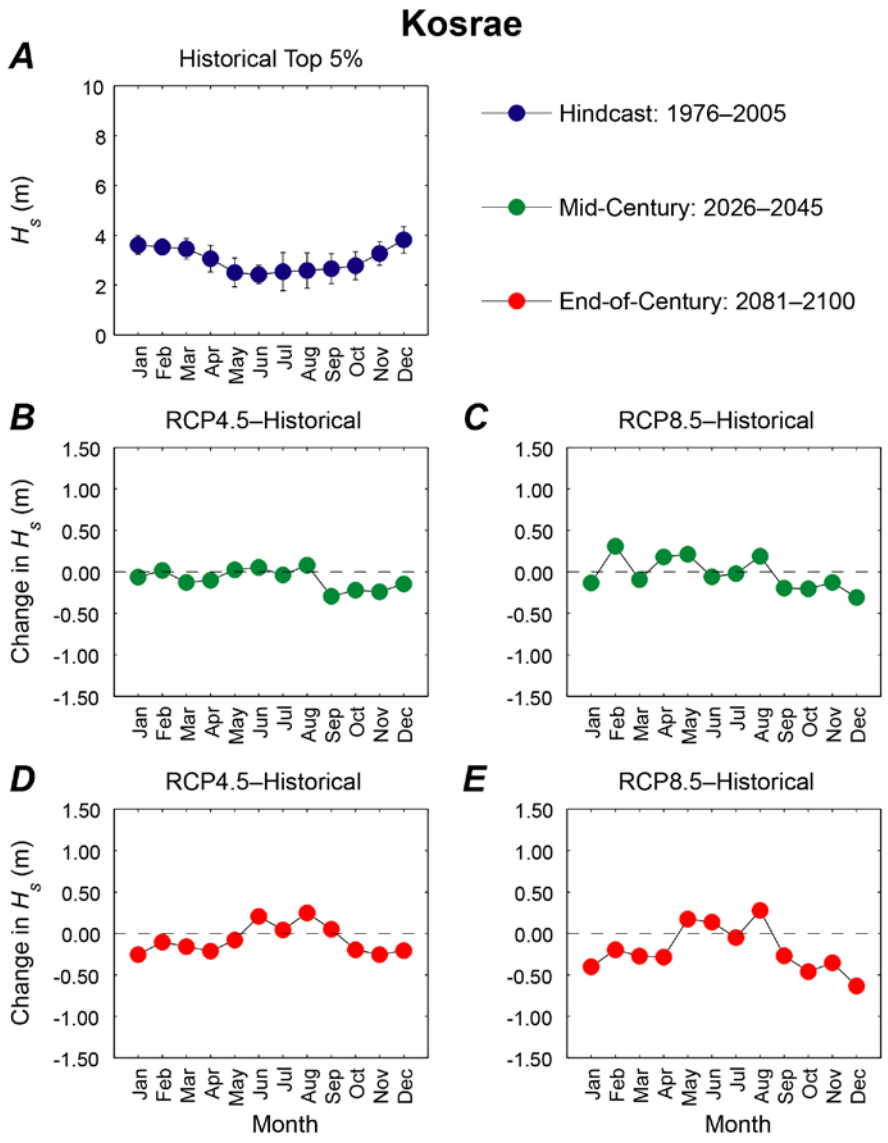

Appendix C16. Plots showing trends in monthly mean of the top 5 percent of significant wave heights (H_S), in meters, at the Kosrae location. *A.* Hindcasted (1976–2005) mean of the top 5 percent of significant wave heights by month with associated error bars. *B.* Plot of the change in mean of the top 5 percent of 2026–2045 significant wave heights for the RCP4.5 scenario from hindcasted top 5 percent of monthly significant wave height means. *C.* Plot of the change in mean of the top 5 percent of 2026–2045 significant wave heights for the RCP8.5 scenario from hindcasted top 5 percent of monthly significant wave height means. *D.* Plot of the change in mean of the top 5 percent of 2081–2100 significant wave heights for the RCP4.5 scenario from hindcasted top 5 percent of monthly significant wave height means. *E.* Plot of the change in mean of the top 5 percent of 2081–2100 significant wave heights for the RCP8.5 scenario from hindcasted top 5 percent of monthly significant wave height means.

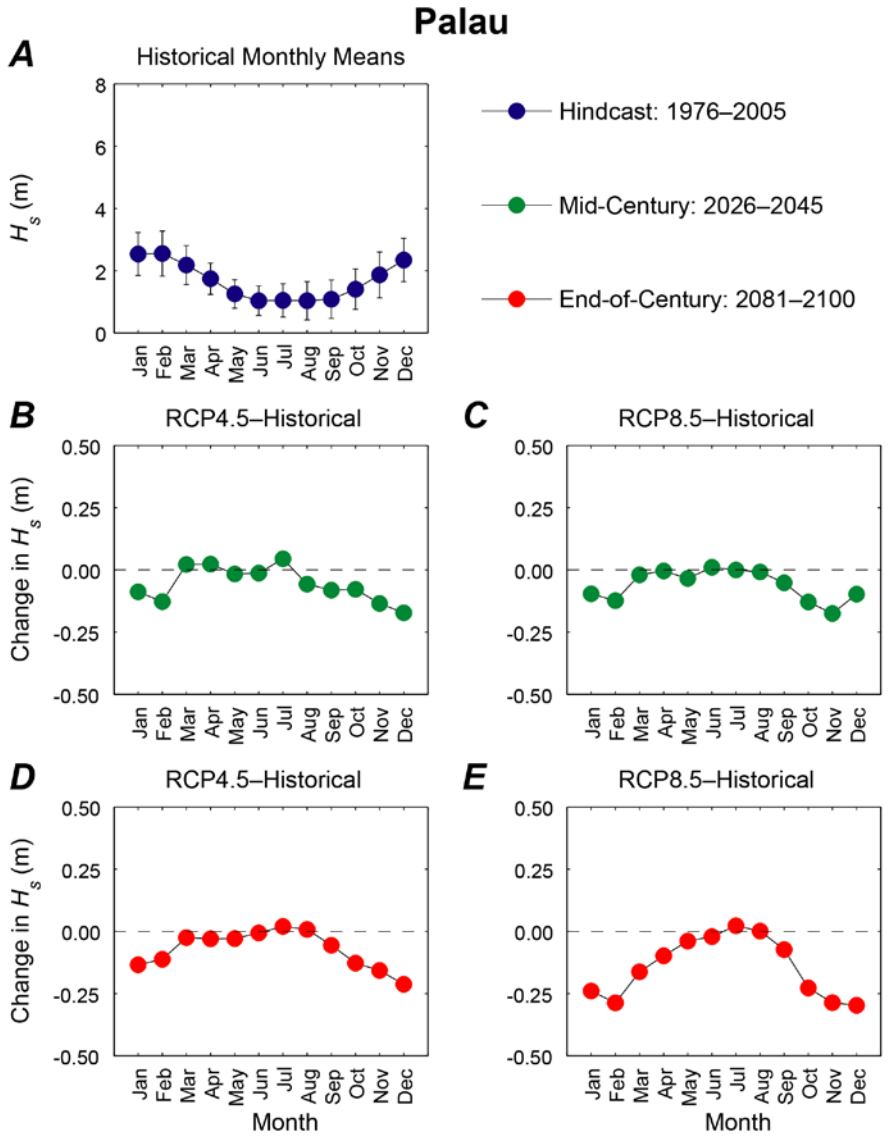

Appendix C17. Plots showing trends in monthly mean significant wave height (H_s), in meters, at the Palau location. *A.* Hindcasted (1976–2005) mean significant wave heights by month with associated error bars. *B.* Plot of the change in mean 2026–2045 significant wave heights for the RCP4.5 scenario from hindcasted monthly significant wave height means. *C.* Plot of the change in mean 2026–2045 significant wave heights for the RCP8.5 scenario from hindcasted monthly significant wave height means. *D.* Plot of the change in mean 2081–2100 significant wave heights for the RCP4.5 scenario from hindcasted monthly significant wave height means. *E.* Plot of the change in mean 2081–2100 significant wave heights for the RCP8.5 scenario from hindcasted monthly significant wave height means.

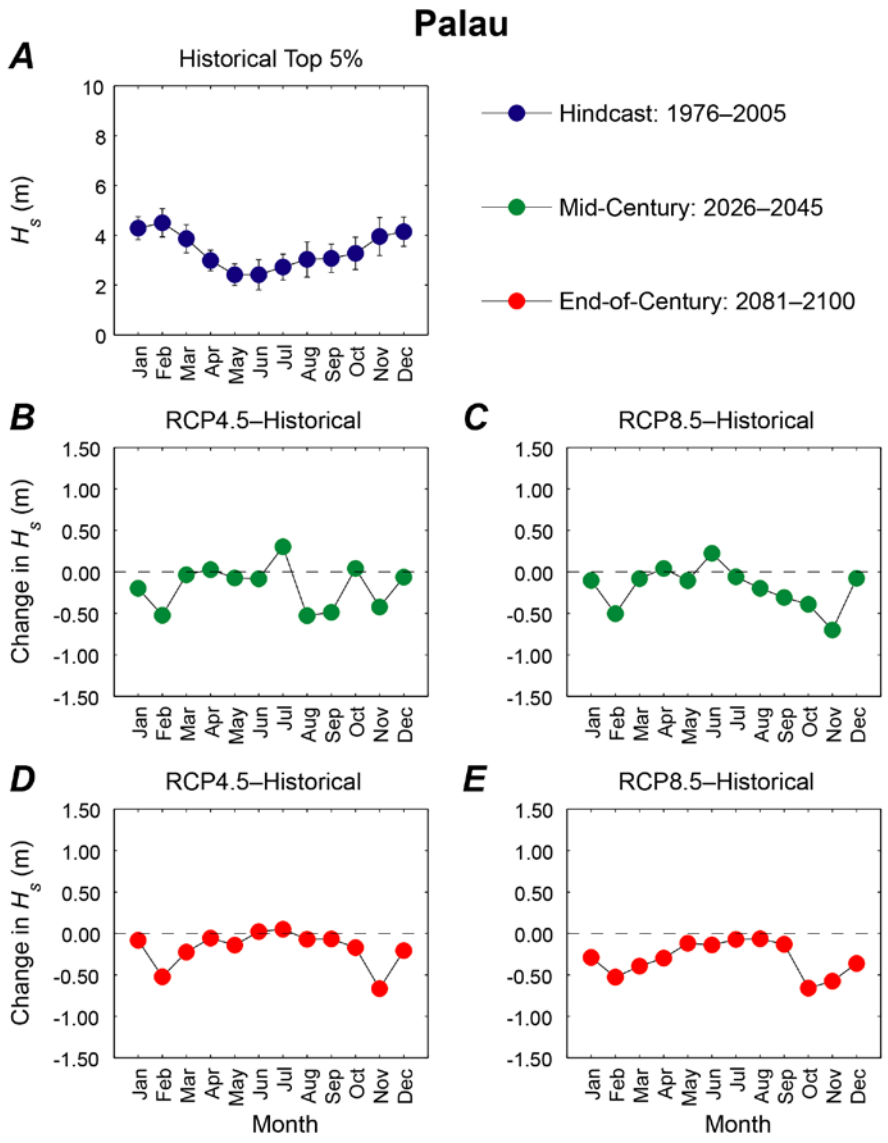

Appendix C18. Plots showing trends in monthly mean of the top 5 percent of significant wave heights (H_S), in meters, at the Palau location. *A.* Hindcasted (1976–2005) mean of the top 5 percent of significant wave heights by month with associated error bars. *B.* Plot of the change in mean of the top 5 percent of 2026–2045 significant wave heights for the RCP4.5 scenario from hindcasted top 5 percent of monthly significant wave height means. *C.* Plot of the change in mean of the top 5 percent of 2026–2045 significant wave heights for the RCP8.5 scenario from hindcasted top 5 percent of monthly significant wave height means. *D.* Plot of the change in mean of the top 5 percent of 2081–2100 significant wave heights for the RCP4.5 scenario from hindcasted top 5 percent of monthly significant wave height means. *E.* Plot of the change in mean of the top 5 percent of 2081–2100 significant wave heights for the RCP8.5 scenario from hindcasted top 5 percent of monthly significant wave height means.

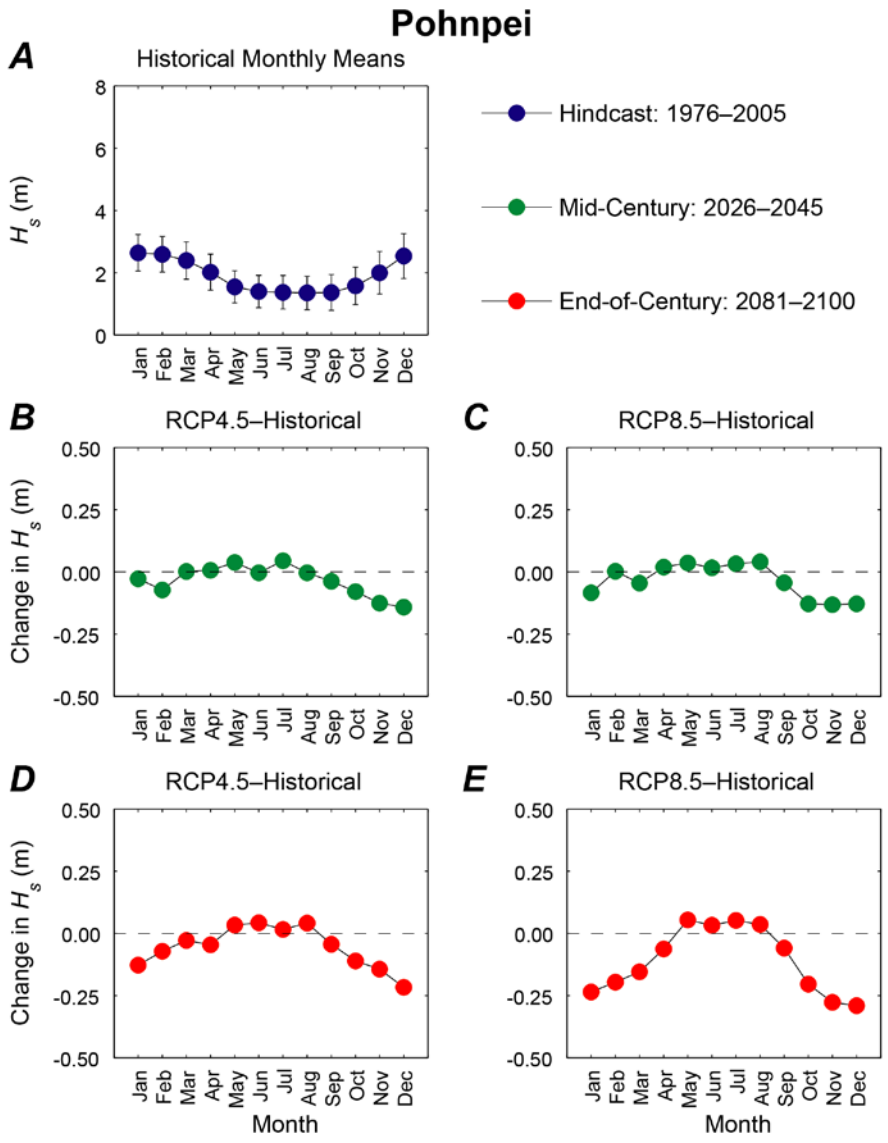

Appendix C19. Plots showing trends in monthly mean significant wave height (H_s), in meters, at the Pohnpei location. *A.* Hindcasted (1976–2005) mean significant wave heights by month with associated error bars. *B.* Plot of the change in mean 2026–2045 significant wave heights for the RCP4.5 scenario from hindcasted monthly significant wave height means. *C.* Plot of the change in mean 2026–2045 significant wave heights for the RCP8.5 scenario from hindcasted monthly significant wave height means. *D.* Plot of the change in mean 2081–2100 significant wave heights for the RCP4.5 scenario from hindcasted monthly significant wave height means. *E.* Plot of the change in mean 2081–2100 significant wave heights for the RCP8.5 scenario from hindcasted monthly significant wave height means.

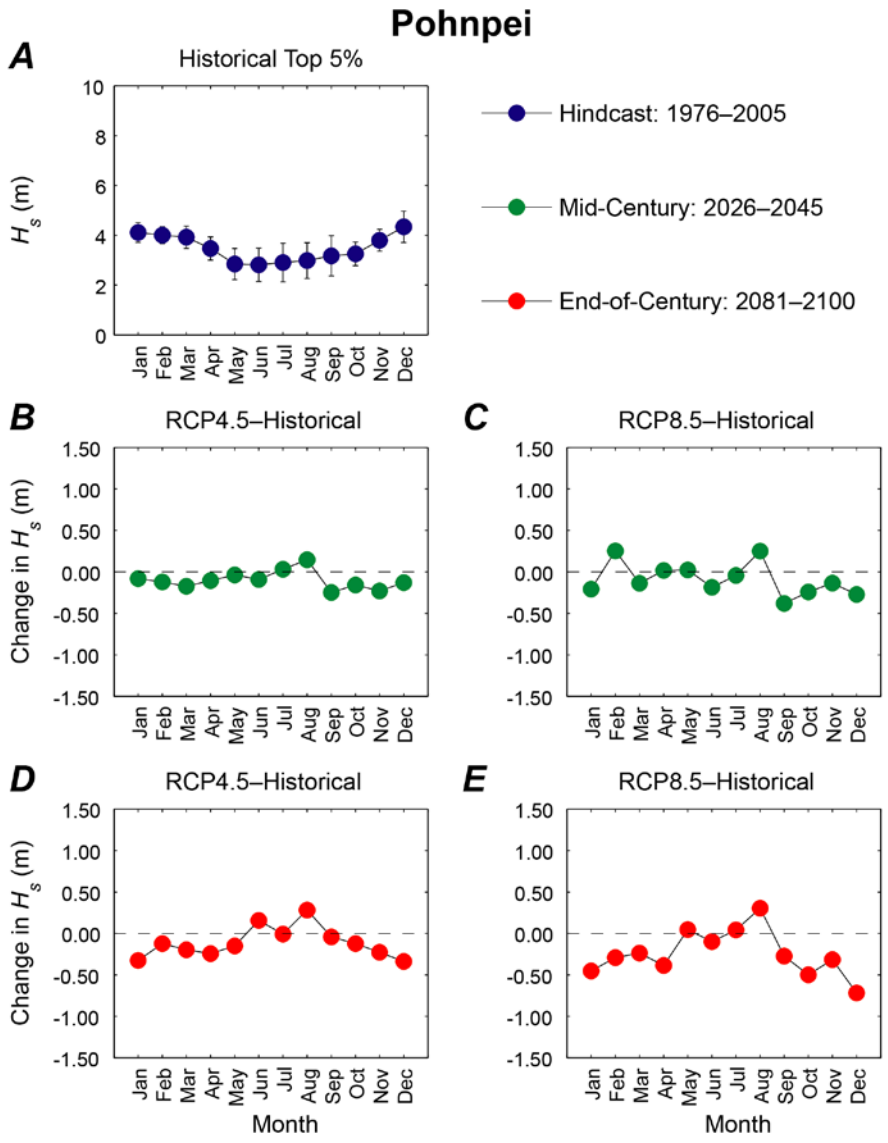

Appendix C20. Plots showing trends in monthly mean of the top 5 percent of significant wave heights (H_S), in meters, at the Pohnpei location. *A.* Hindcasted (1976–2005) mean of the top 5 percent of significant wave heights by month with associated error bars. *B.* Plot of the change in mean of the top 5 percent of 2026–2045 significant wave heights for the RCP4.5 scenario from hindcasted top 5 percent of monthly significant wave height means. *C.* Plot of the change in mean of the top 5 percent of 2026–2045 significant wave heights for the RCP8.5 scenario from hindcasted top 5 percent of monthly significant wave height means. *D.* Plot of the change in mean of the top 5 percent of 2081–2100 significant wave heights for the RCP4.5 scenario from hindcasted top 5 percent of monthly significant wave height means. *E.* Plot of the change in mean of the top 5 percent of 2081–2100 significant wave heights for the RCP8.5 scenario from hindcasted top 5 percent of monthly significant wave height means.

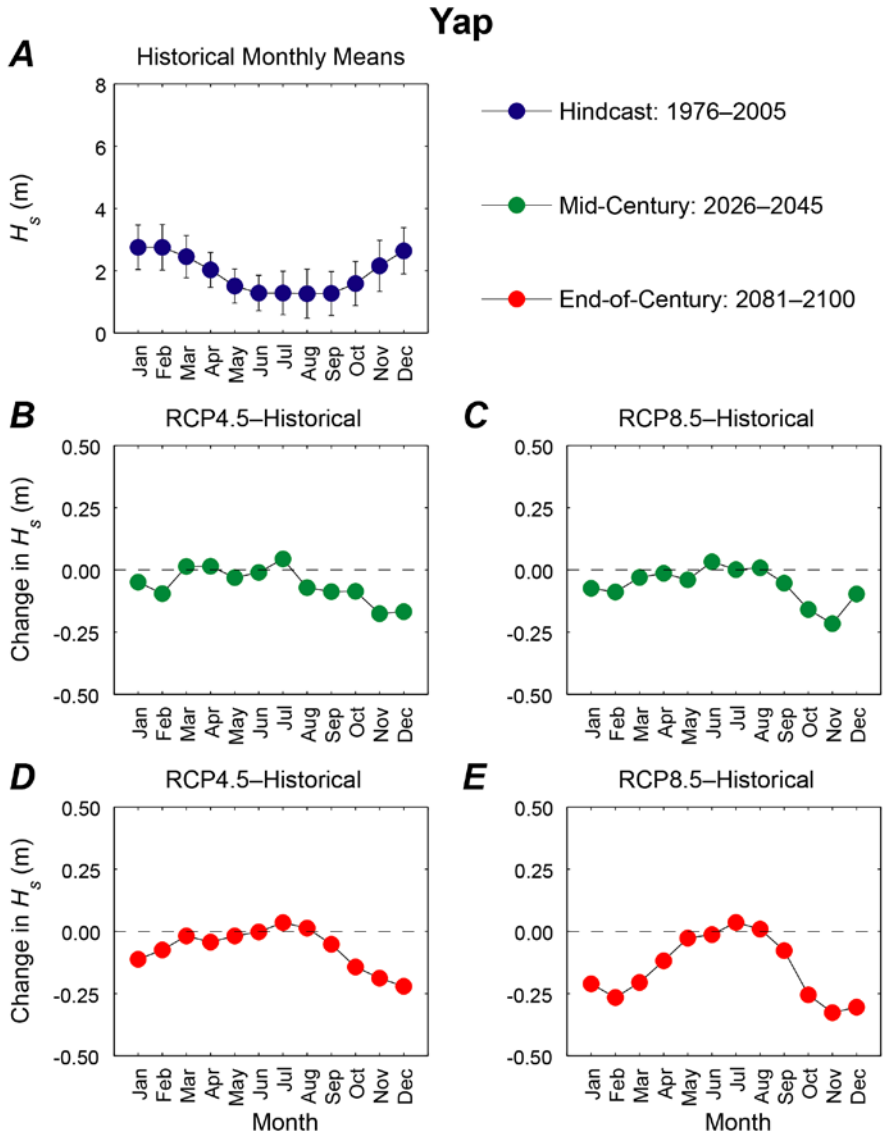

Appendix C21. Plots showing trends in monthly mean significant wave height (H_s), in meters, at the Yap location. *A.* Hindcasted (1976–2005) mean significant wave heights by month with associated error bars. *B.* Plot of the change in mean 2026–2045 significant wave heights for the RCP4.5 scenario from hindcasted monthly significant wave height means. *C.* Plot of the change in mean 2026–2045 significant wave heights for the RCP8.5 scenario from hindcasted monthly significant wave height means. *D.* Plot of the change in mean 2081–2100 significant wave heights for the RCP4.5 scenario from hindcasted monthly significant wave height means. *E.* Plot of the change in mean 2081–2100 significant wave heights for the RCP8.5 scenario from hindcasted monthly significant wave height means.

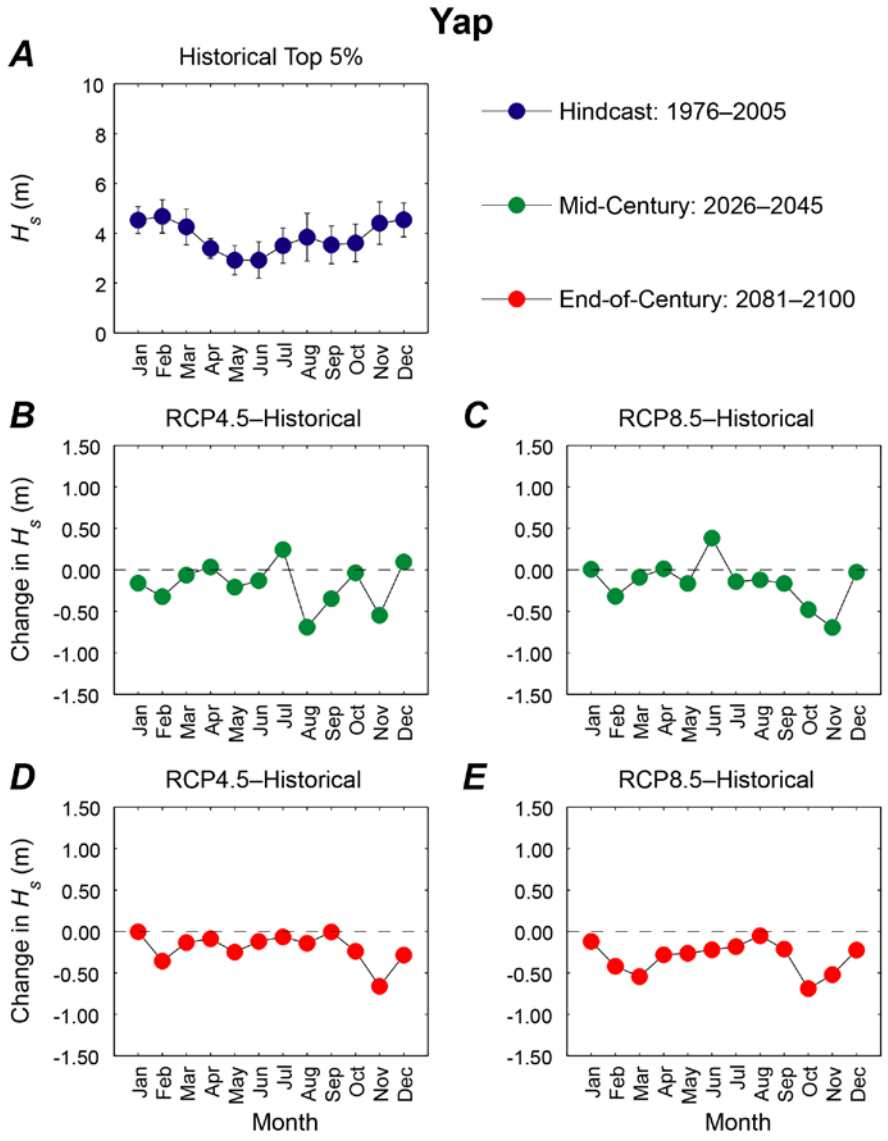

Appendix C22. Plots showing trends in monthly mean of the top 5 percent of significant wave heights (H_S), in meters, at the Yap location. *A.* Hindcasted (1976–2005) mean of the top 5 percent of significant wave heights by month with associated error bars. *B.* Plot of the change in mean of the top 5 percent of 2026–2045 significant wave heights for the RCP4.5 scenario from hindcasted top 5 percent of monthly significant wave height means. *C.* Plot of the change in mean of the top 5 percent of 2026–2045 significant wave heights for the RCP8.5 scenario from hindcasted top 5 percent of monthly significant wave height means. *D.* Plot of the change in mean of the top 5 percent of 2081–2100 significant wave heights for the RCP4.5 scenario from hindcasted top 5 percent of monthly significant wave height means. *E.* Plot of the change in mean of the top 5 percent of 2081–2100 significant wave heights for the RCP8.5 scenario from hindcasted top 5 percent of monthly significant wave height means.

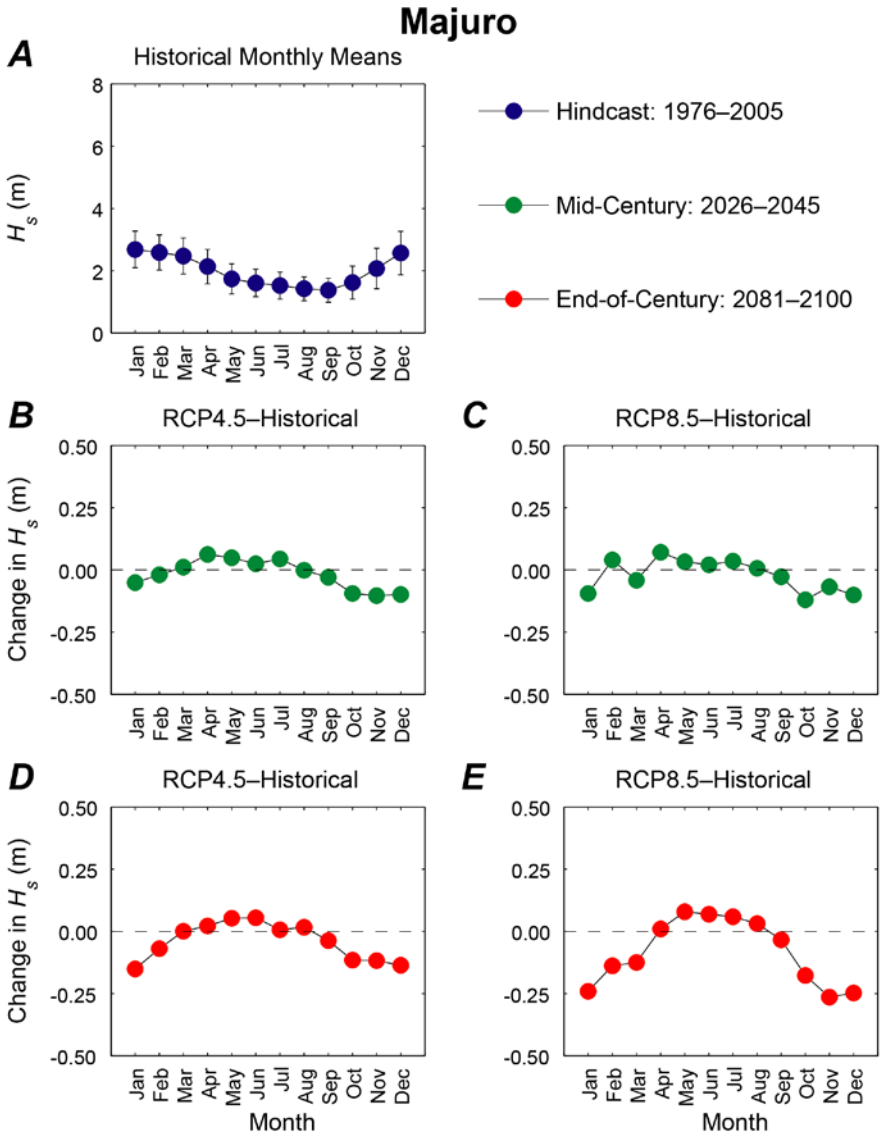

Appendix C23. Plots showing trends in monthly mean significant wave height (H_s), in meters, at the Majuro location. *A.* Hindcasted (1976–2005) mean significant wave heights by month with associated error bars. *B.* Plot of the change in mean 2026–2045 significant wave heights for the RCP4.5 scenario from hindcasted monthly significant wave height means. *C.* Plot of the change in mean 2026–2045 significant wave heights for the RCP8.5 scenario from hindcasted monthly significant wave height means. *D.* Plot of the change in mean 2081–2100 significant wave heights for the RCP4.5 scenario from hindcasted monthly significant wave height means. *E.* Plot of the change in mean 2081–2100 significant wave heights for the RCP8.5 scenario from hindcasted monthly significant wave height means.

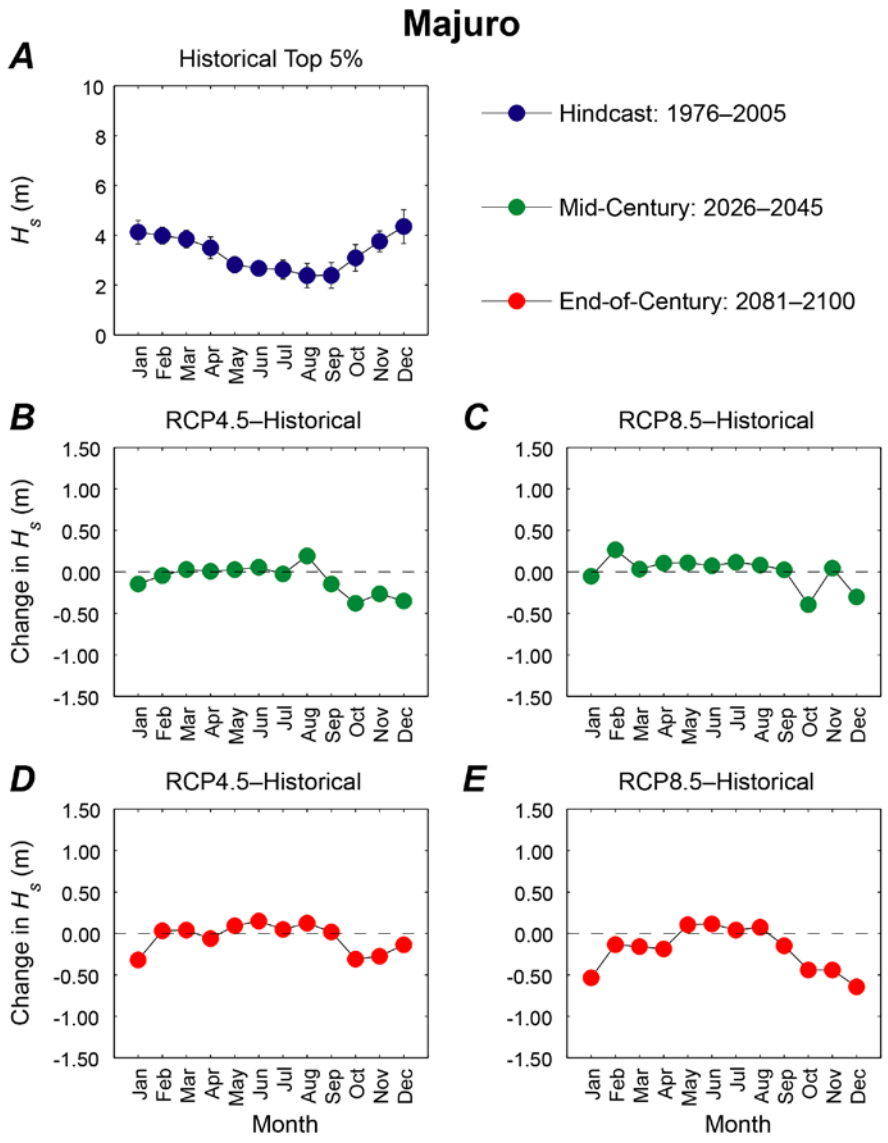

Appendix C24. Plots showing trends in monthly mean of the top 5 percent of significant wave heights (H_S), in meters, at the Majuro location. *A.* Hindcasted (1976–2005) mean of the top 5 percent of significant wave heights by month with associated error bars. *B.* Plot of the change in mean of the top 5 percent of 2026–2045 significant wave heights for the RCP4.5 scenario from hindcasted top 5 percent of monthly significant wave height means. *C.* Plot of the change in mean of the top 5 percent of 2026–2045 significant wave heights for the RCP8.5 scenario from hindcasted top 5 percent of monthly significant wave height means. *D.* Plot of the change in mean of the top 5 percent of 2081–2100 significant wave heights for the RCP4.5 scenario from hindcasted top 5 percent of monthly significant wave height means. *E.* Plot of the change in mean of the top 5 percent of 2081–2100 significant wave heights for the RCP8.5 scenario from hindcasted top 5 percent of monthly significant wave height means.

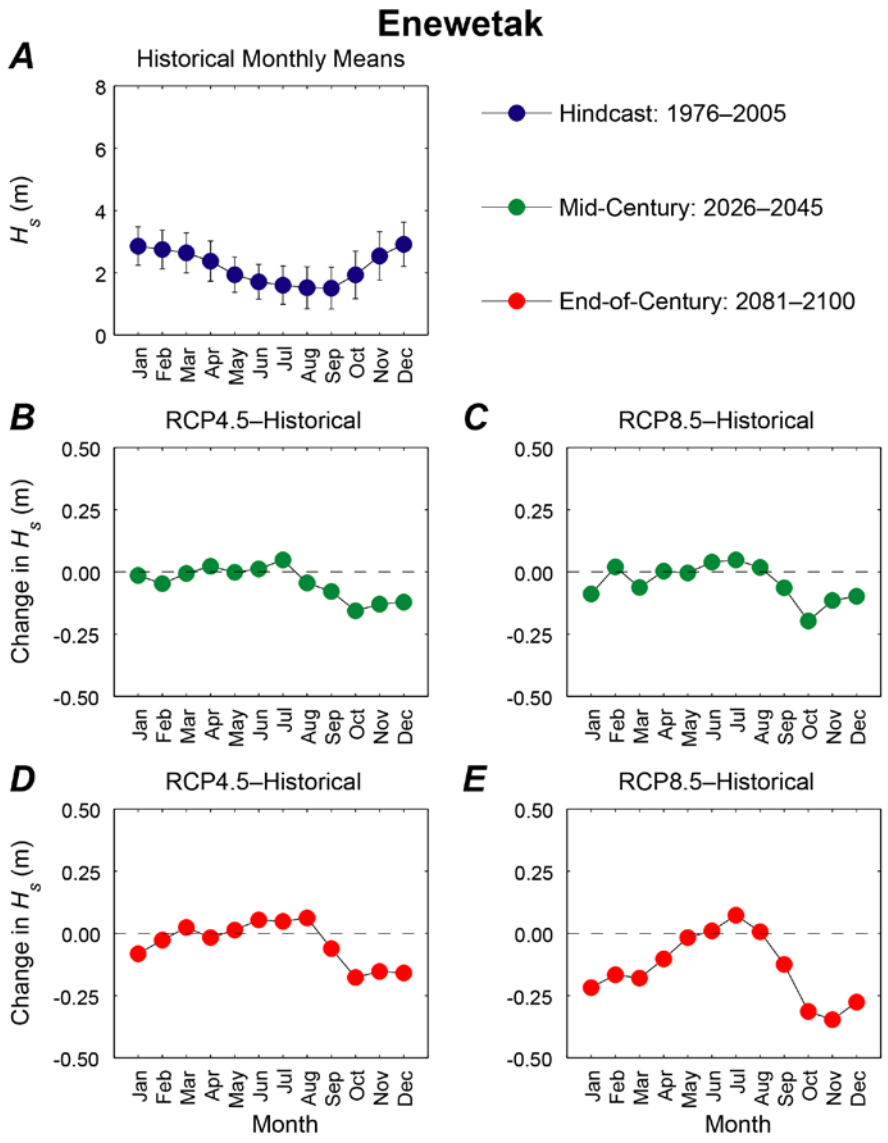

Appendix C25. Plots showing trends in monthly mean significant wave height (H_s), in meters, at the Enewetak location. *A.* Hindcasted (1976–2005) mean significant wave heights by month with associated error bars. *B.* Plot of the change in mean 2026–2045 significant wave heights for the RCP4.5 scenario from hindcasted monthly significant wave height means. *C.* Plot of the change in mean 2026–2045 significant wave heights for the RCP8.5 scenario from hindcasted monthly significant wave height means. *D.* Plot of the change in mean 2081–2100 significant wave heights for the RCP4.5 scenario from hindcasted monthly significant wave height means. *E.* Plot of the change in mean 2081–2100 significant wave heights for the RCP8.5 scenario from hindcasted monthly significant wave height means.

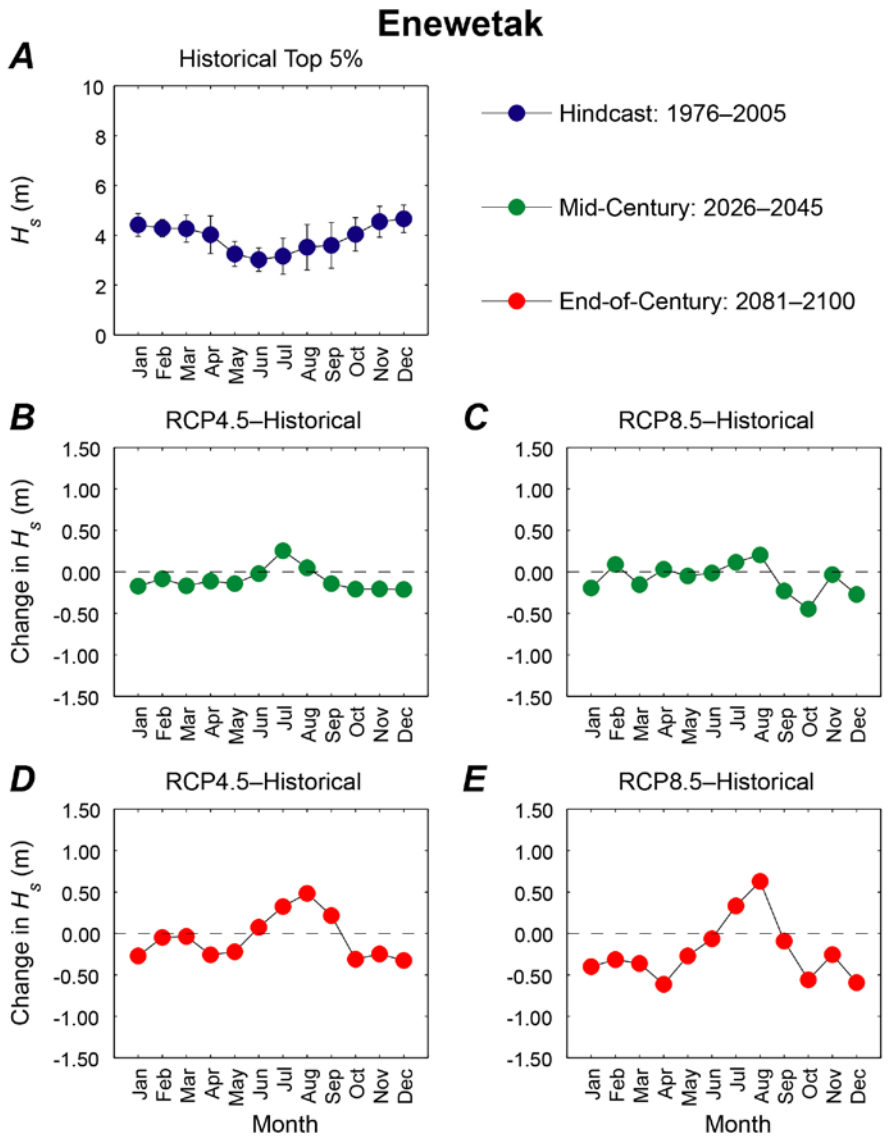

Appendix C26. Plots showing trends in monthly mean of the top 5 percent of significant wave heights (H_S), in meters, at the Enewetak location. *A.* Hindcasted (1976–2005) mean of the top 5 percent of significant wave heights by month with associated error bars. *B.* Plot of the change in mean of the top 5 percent of 2026–2045 significant wave heights for the RCP4.5 scenario from hindcasted top 5 percent of monthly significant wave height means. *C.* Plot of the change in mean of the top 5 percent of 2026–2045 significant wave heights for the RCP8.5 scenario from hindcasted top 5 percent of monthly significant wave height means. *D.* Plot of the change in mean of the top 5 percent of 2081–2100 significant wave heights for the RCP4.5 scenario from hindcasted top 5 percent of monthly significant wave height means. *E.* Plot of the change in mean of the top 5 percent of 2081–2100 significant wave heights for the RCP8.5 scenario from hindcasted top 5 percent of monthly significant wave height means.

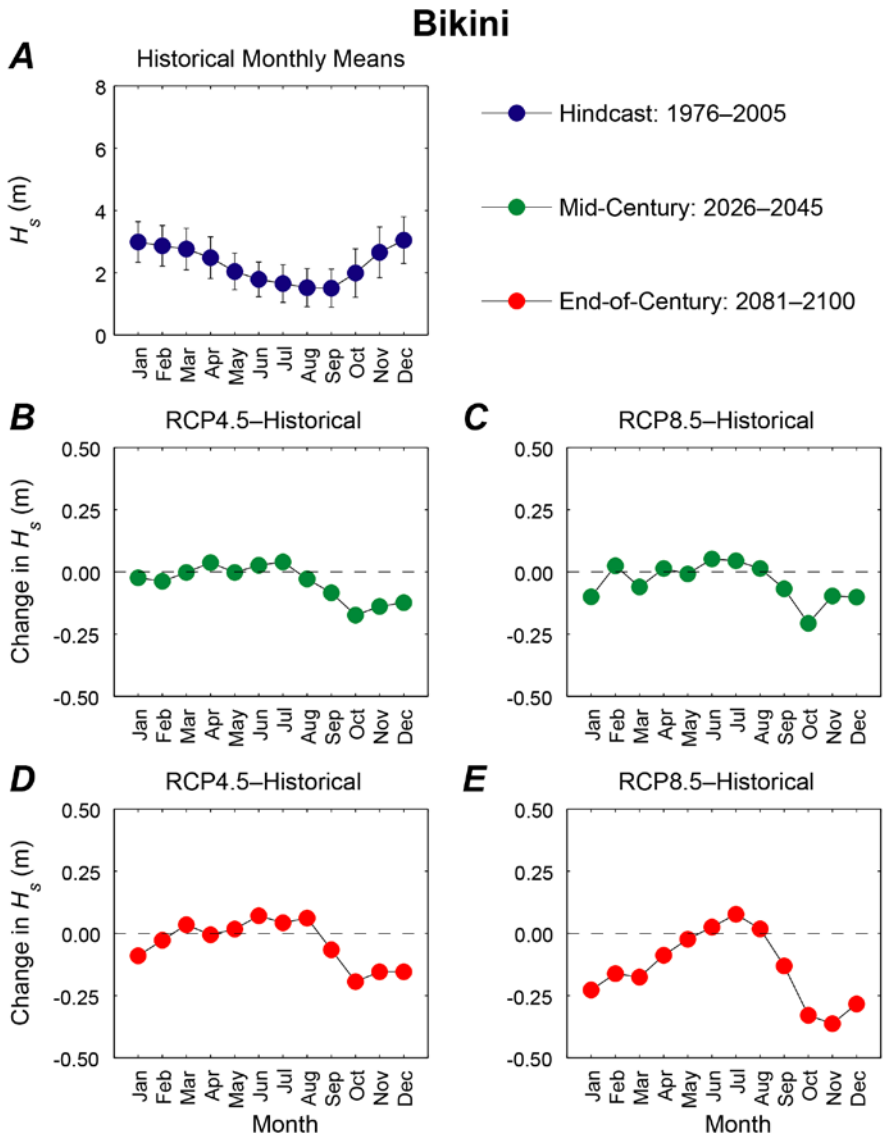

Appendix C27. Plots showing trends in monthly mean significant wave height (H_s), in meters, at the Bikini location. *A.* Hindcasted (1976–2005) mean significant wave heights by month with associated error bars. *B.* Plot of the change in mean 2026–2045 significant wave heights for the RCP4.5 scenario from hindcasted monthly significant wave height means. *C.* Plot of the change in mean 2026–2045 significant wave heights for the RCP8.5 scenario from hindcasted monthly significant wave height means. *D.* Plot of the change in mean 2081–2100 significant wave heights for the RCP4.5 scenario from hindcasted monthly significant wave height means. *E.* Plot of the change in mean 2081–2100 significant wave heights for the RCP8.5 scenario from hindcasted monthly significant wave height means.

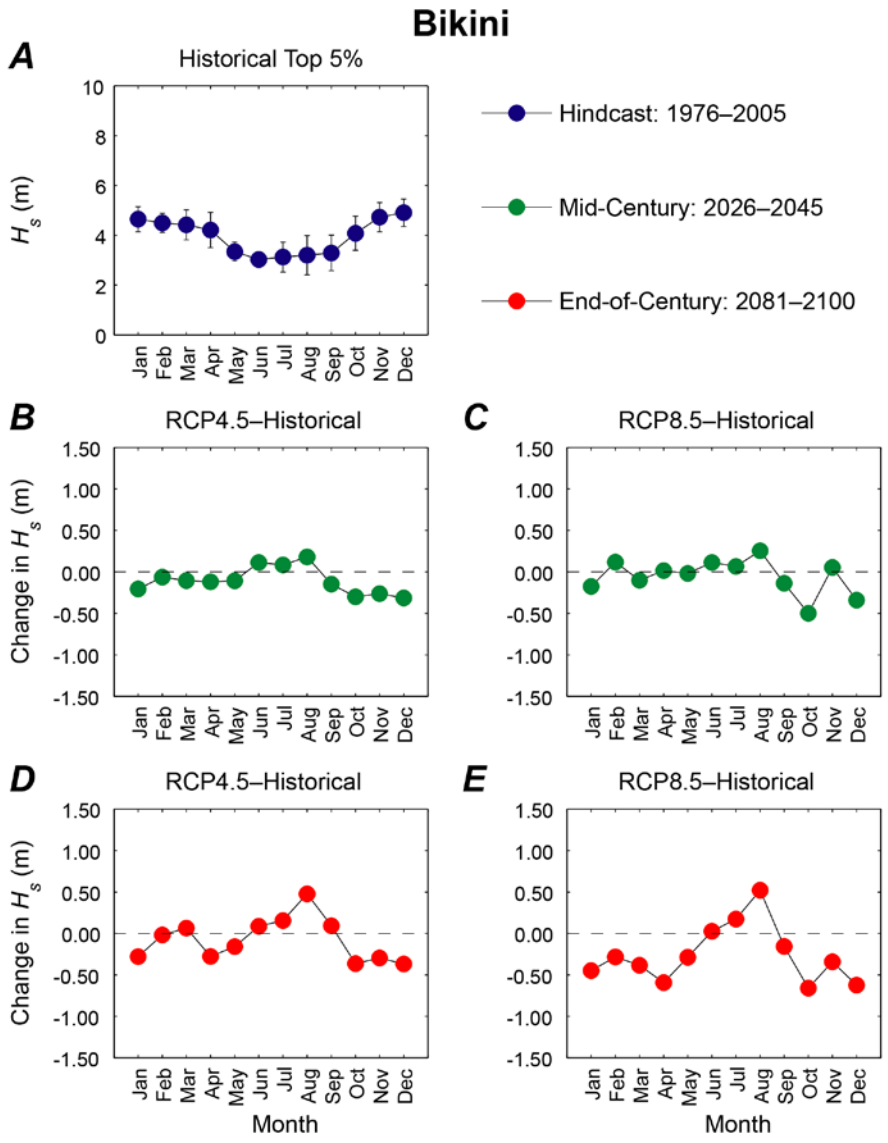

Appendix C28. Plots showing trends in monthly mean of the top 5 percent of significant wave heights (H_S), in meters, at the Bikini location. *A.* Hindcasted (1976–2005) mean of the top 5 percent of significant wave heights by month with associated error bars. *B.* Plot of the change in mean of the top 5 percent of 2026–2045 significant wave heights for the RCP4.5 scenario from hindcasted top 5 percent of monthly significant wave height means. *C.* Plot of the change in mean of the top 5 percent of 2026–2045 significant wave heights for the RCP8.5 scenario from hindcasted top 5 percent of monthly significant wave height means. *D.* Plot of the change in mean of the top 5 percent of 2081–2100 significant wave heights for the RCP4.5 scenario from hindcasted top 5 percent of monthly significant wave height means. *E.* Plot of the change in mean of the top 5 percent of 2081–2100 significant wave heights for the RCP8.5 scenario from hindcasted top 5 percent of monthly significant wave height means.

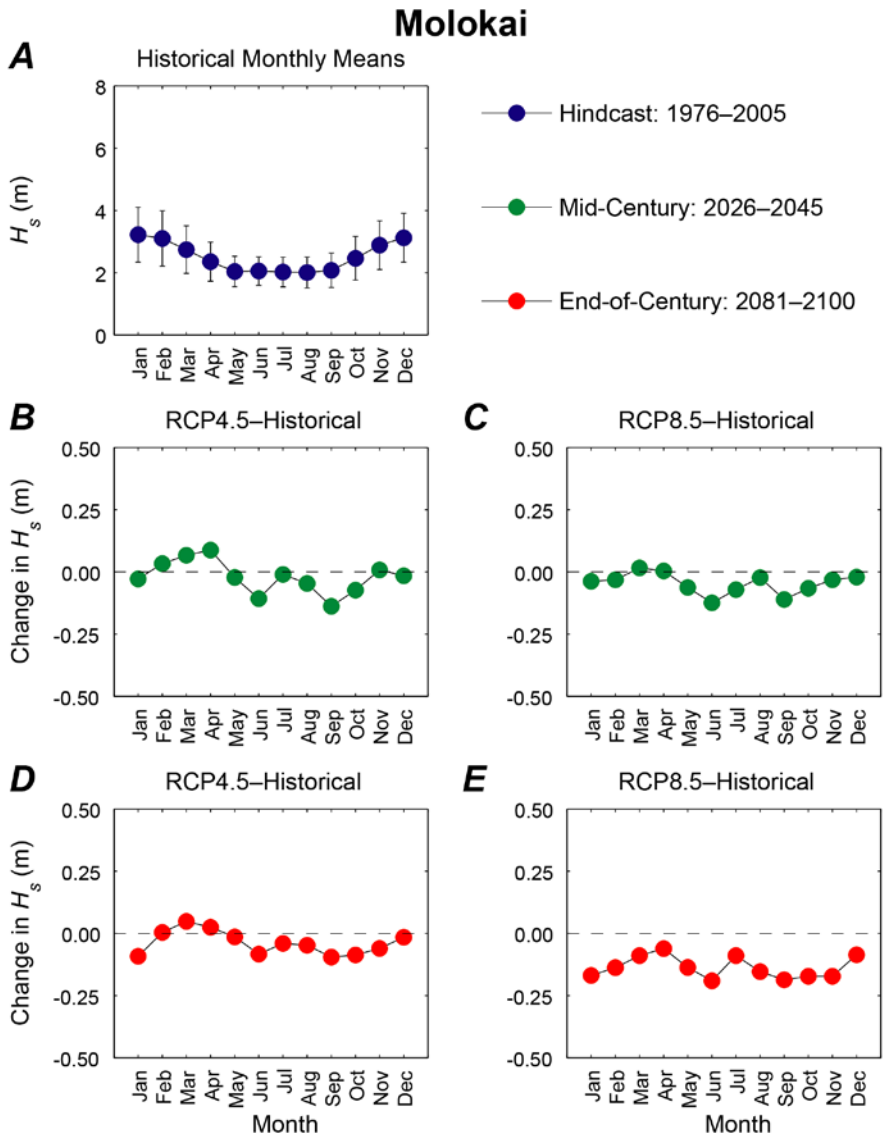

Appendix C29. Plots showing trends in monthly mean significant wave height (H_s), in meters, at the Molokai location. *A.* Hindcasted (1976–2005) mean significant wave heights by month with associated error bars. *B.* Plot of the change in mean 2026–2045 significant wave heights for the RCP4.5 scenario from hindcasted monthly significant wave height means. *C.* Plot of the change in mean 2026–2045 significant wave heights for the RCP8.5 scenario from hindcasted monthly significant wave height means. *D.* Plot of the change in mean 2081–2100 significant wave heights for the RCP4.5 scenario from hindcasted monthly significant wave height means. *E.* Plot of the change in mean 2081–2100 significant wave heights for the RCP8.5 scenario from hindcasted monthly significant wave height means.

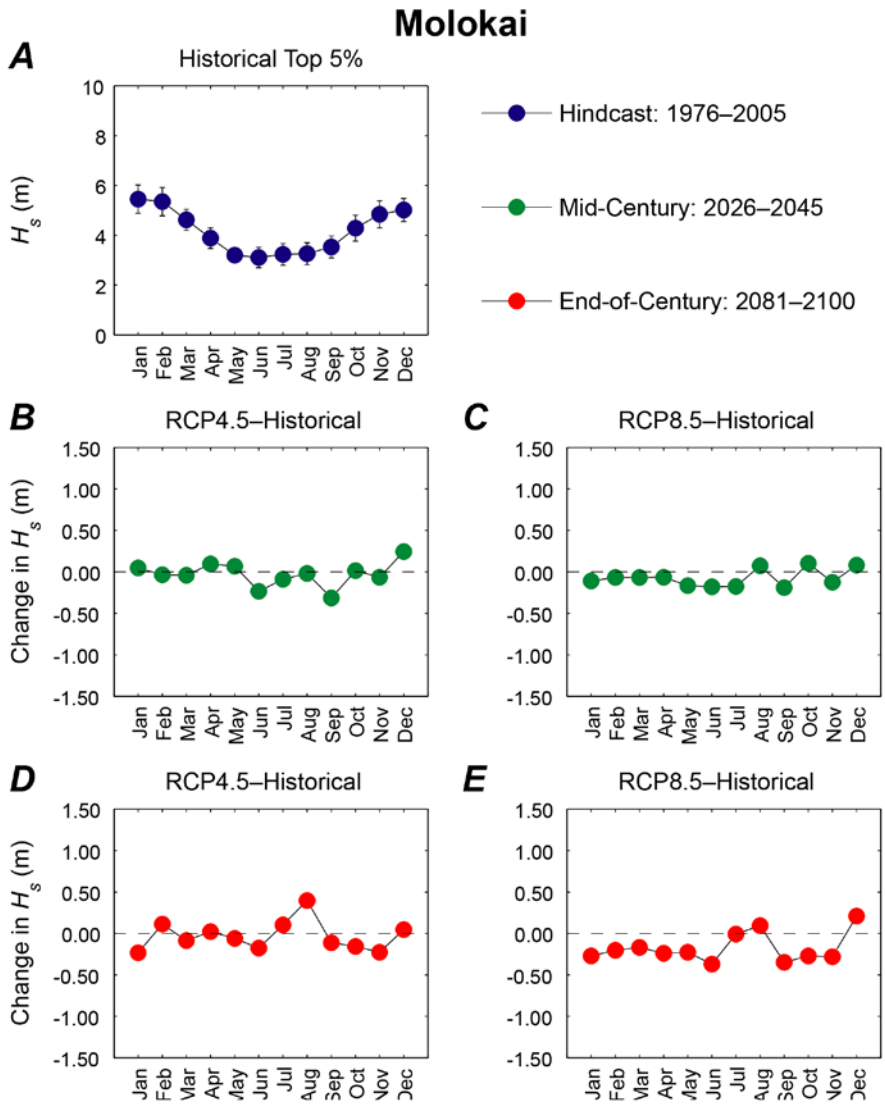

Appendix C30. Plots showing trends in monthly mean of the top 5 percent of significant wave heights (H_S), in meters, at the Molokai location. *A.* Hindcasted (1976–2005) mean of the top 5 percent of significant wave heights by month with associated error bars. *B.* Plot of the change in mean of the top 5 percent of 2026–2045 significant wave heights for the RCP4.5 scenario from hindcasted top 5 percent of monthly significant wave height means. *C.* Plot of the change in mean of the top 5 percent of 2026–2045 significant wave heights for the RCP8.5 scenario from hindcasted top 5 percent of monthly significant wave height means. *D.* Plot of the change in mean of the top 5 percent of 2081–2100 significant wave heights for the RCP4.5 scenario from hindcasted top 5 percent of monthly significant wave height means. *E.* Plot of the change in mean of the top 5 percent of 2081–2100 significant wave heights for the RCP8.5 scenario from hindcasted top 5 percent of monthly significant wave height means.

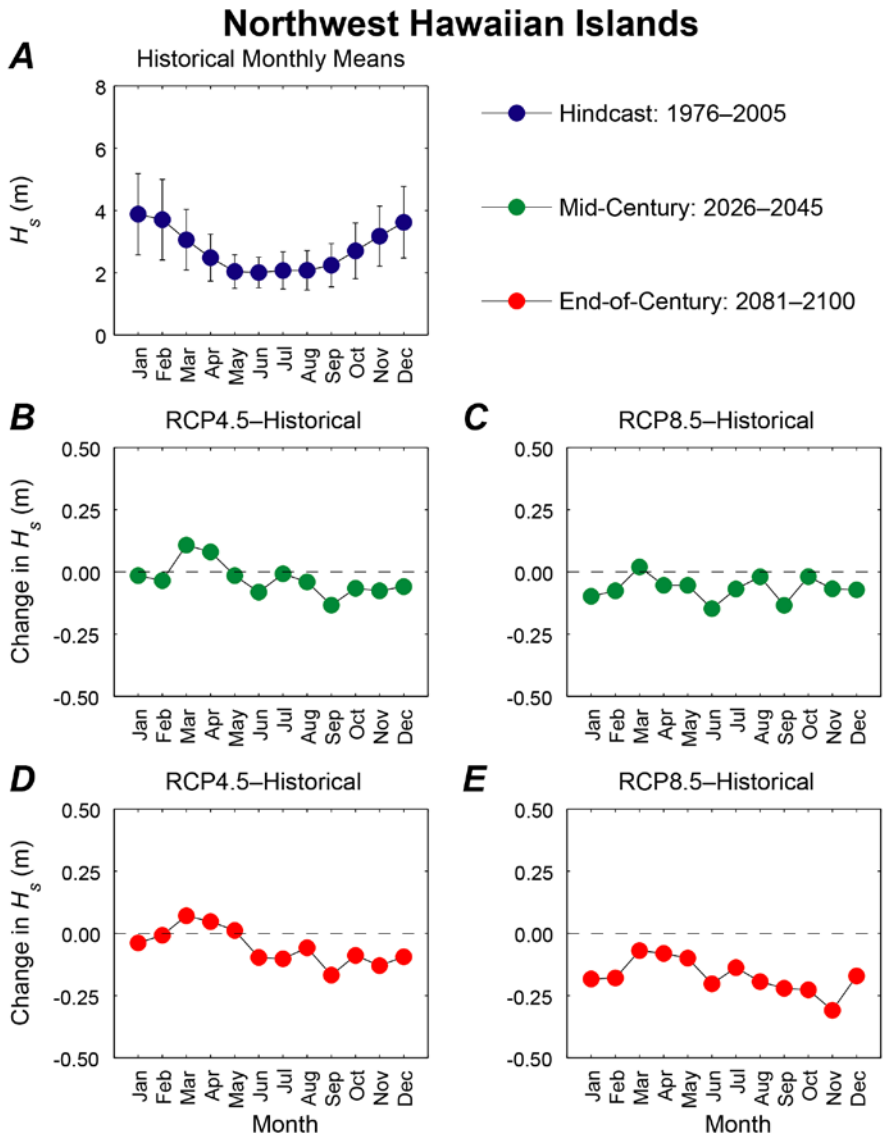

Appendix C31. Plots showing trends in monthly mean significant wave height (H_s), in meters, at the Northwest Hawaiian Islands location. *A.* Hindcasted (1976–2005) mean significant wave heights by month with associated error bars. *B.* Plot of the change in mean 2026–2045 significant wave heights for the RCP4.5 scenario from hindcasted monthly significant wave height means. *C.* Plot of the change in mean 2026–2045 significant wave heights for the RCP8.5 scenario from hindcasted monthly significant wave height means. *D.* Plot of the change in mean 2081–2100 significant wave heights for the RCP4.5 scenario from hindcasted monthly significant wave height means. *E.* Plot of the change in mean 2081–2100 significant wave heights for the RCP8.5 scenario from hindcasted monthly significant wave height means.

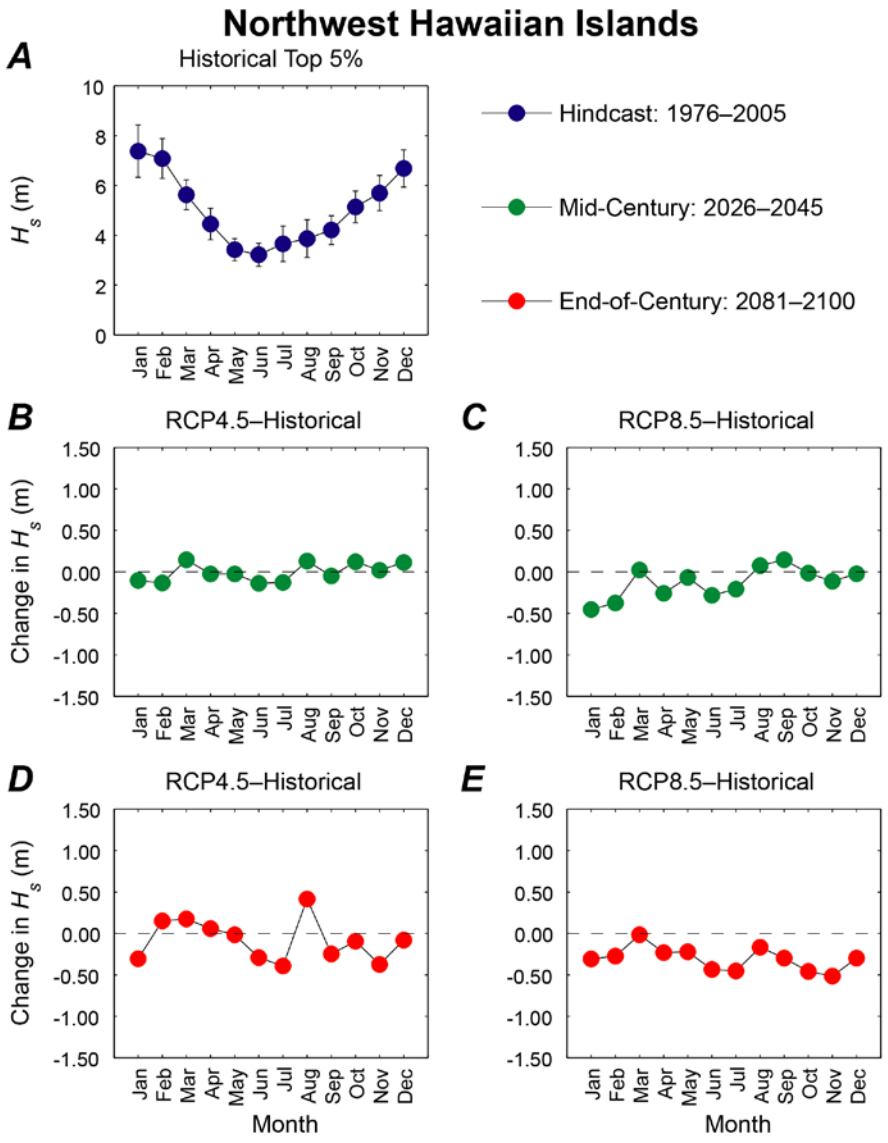

Appendix C32. Plots showing trends in monthly mean of the top 5 percent of significant wave heights (H_S), in meters, at the Northwest Hawaiian Islands location. *A.* Hindcasted (1976–2005) mean of the top 5 percent of significant wave heights by month with associated error bars. *B.* Plot of the change in mean of the top 5 percent of 2026–2045 significant wave heights for the RCP4.5 scenario from hindcasted top 5 percent of monthly significant wave height means. *C.* Plot of the change in mean of the top 5 percent of 2026–2045 significant wave heights for the RCP8.5 scenario from hindcasted top 5 percent of monthly significant wave height means. *D.* Plot of the change in mean of the top 5 percent of 2081–2100 significant wave heights for the RCP4.5 scenario from hindcasted top 5 percent of monthly significant wave height means. *E.* Plot of the change in mean of the top 5 percent of 2081–2100 significant wave heights for the RCP8.5 scenario from hindcasted top 5 percent of monthly significant wave height means.

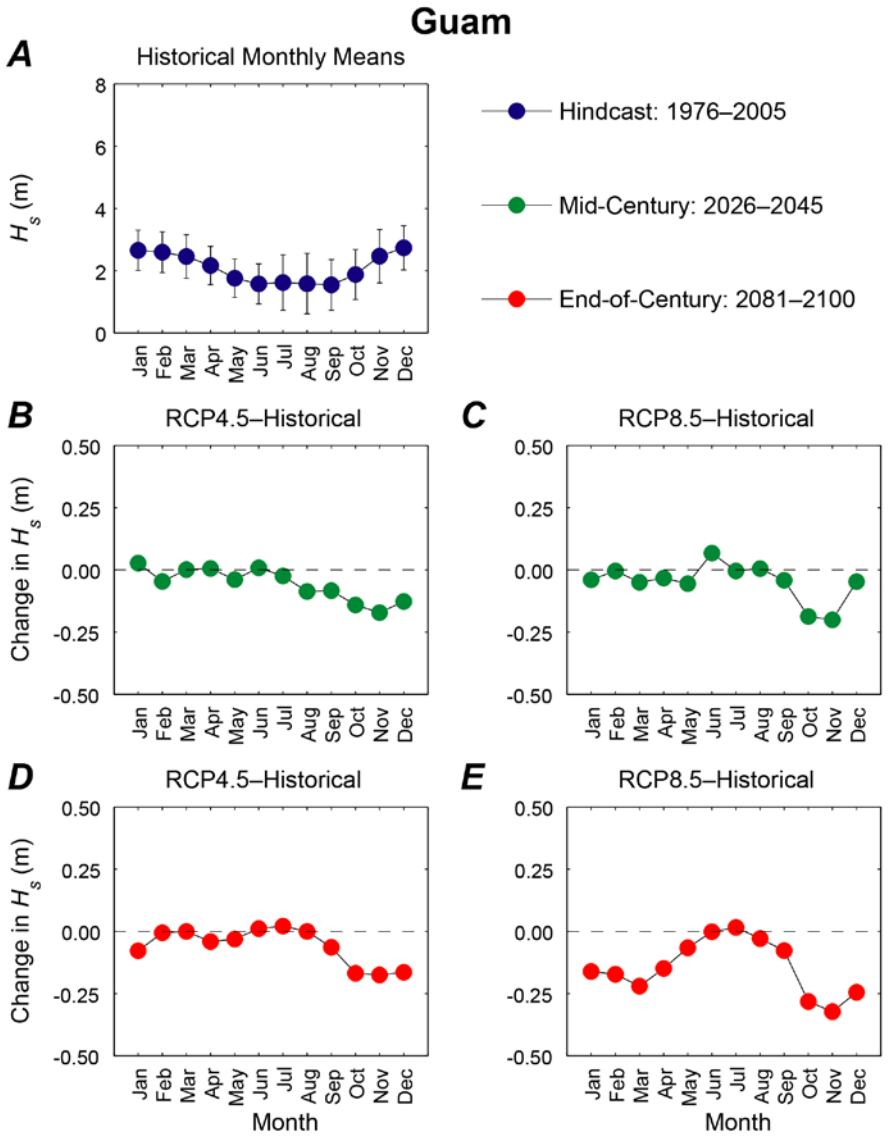

Appendix C33. Plots showing trends in monthly mean significant wave height (H_s), in meters, at the Guam location. *A.* Hindcasted (1976–2005) mean significant wave heights by month with associated error bars. *B.* Plot of the change in mean 2026–2045 significant wave heights for the RCP4.5 scenario from hindcasted monthly significant wave height means. *C.* Plot of the change in mean 2026–2045 significant wave heights for the RCP8.5 scenario from hindcasted monthly significant wave height means. *D.* Plot of the change in mean 2081–2100 significant wave heights for the RCP4.5 scenario from hindcasted monthly significant wave height means. *E.* Plot of the change in mean 2081–2100 significant wave heights for the RCP8.5 scenario from hindcasted monthly significant wave height means.

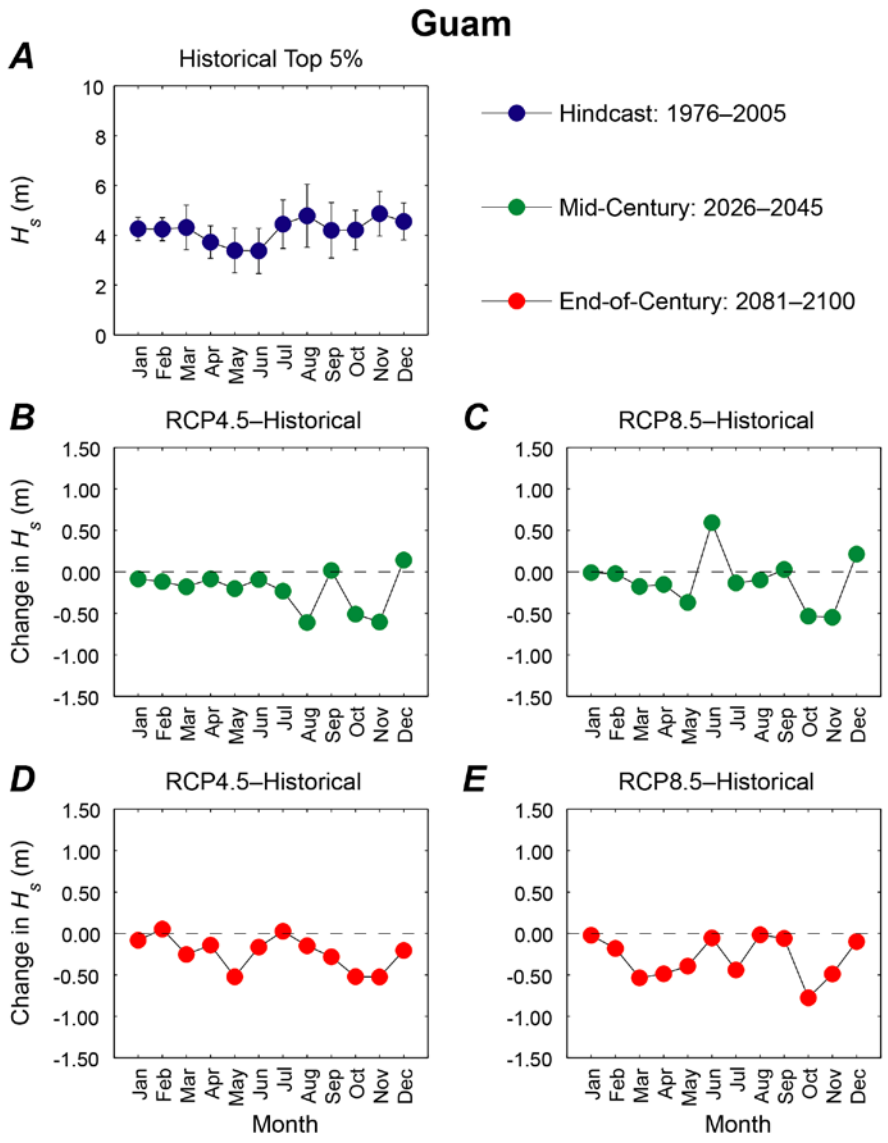

Appendix C34. Plots showing trends in monthly mean of the top 5 percent of significant wave heights (H_S), in meters, at the Guam location. *A.* Hindcasted (1976–2005) mean of the top 5 percent of significant wave heights by month with associated error bars. *B.* Plot of the change in mean of the top 5 percent of 2026–2045 significant wave heights for the RCP4.5 scenario from hindcasted top 5 percent of monthly significant wave height means. *C.* Plot of the change in mean of the top 5 percent of 2026–2045 significant wave heights for the RCP8.5 scenario from hindcasted top 5 percent of monthly significant wave height means. *D.* Plot of the change in mean of the top 5 percent of 2081–2100 significant wave heights for the RCP4.5 scenario from hindcasted top 5 percent of monthly significant wave height means. *E.* Plot of the change in mean of the top 5 percent of 2081–2100 significant wave heights for the RCP8.5 scenario from hindcasted top 5 percent of monthly significant wave height means.

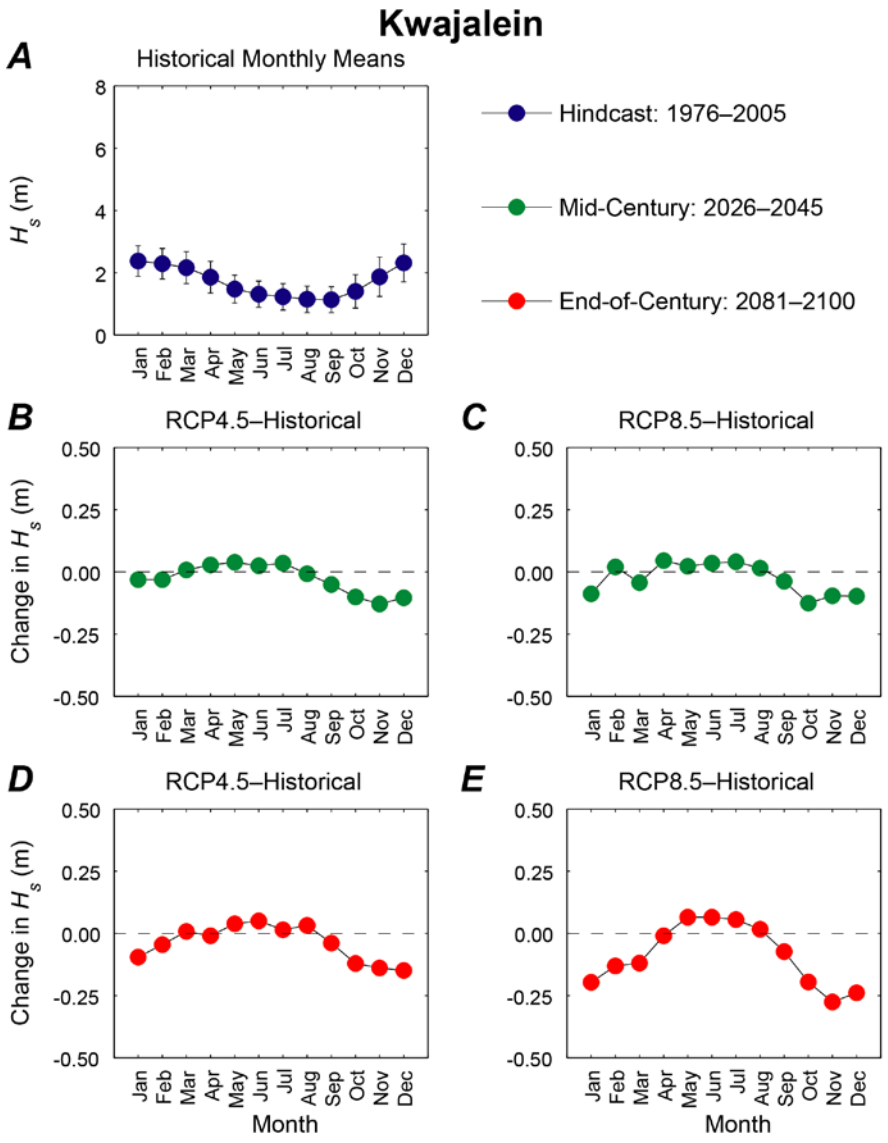

Appendix C35. Plots showing trends in monthly mean significant wave height (H_s), in meters, at the Kwajalein location. *A.* Hindcasted (1976–2005) mean significant wave heights by month with associated error bars. *B.* Plot of the change in mean 2026–2045 significant wave heights for the RCP4.5 scenario from hindcasted monthly significant wave height means. *C.* Plot of the change in mean 2026–2045 significant wave heights for the RCP8.5 scenario from hindcasted monthly significant wave height means. *D.* Plot of the change in mean 2081–2100 significant wave heights for the RCP4.5 scenario from hindcasted monthly significant wave height means. *E.* Plot of the change in mean 2081–2100 significant wave heights for the RCP8.5 scenario from hindcasted monthly significant wave height means.

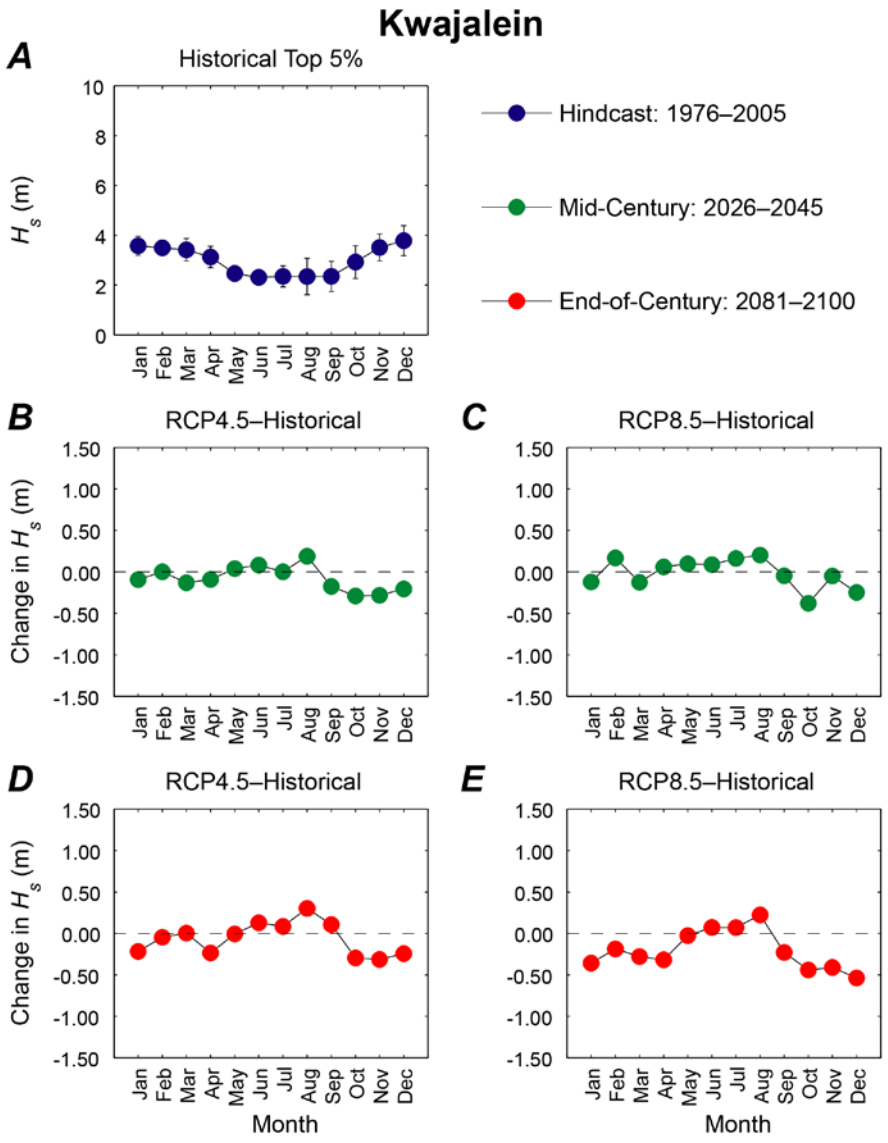

Appendix C36. Plots showing trends in monthly mean of the top 5 percent of significant wave heights (H_S), in meters, at the Kwajalein location. *A.* Hindcasted (1976–2005) mean of the top 5 percent of significant wave heights by month with associated error bars. *B.* Plot of the change in mean of the top 5 percent of 2026–2045 significant wave heights for the RCP4.5 scenario from hindcasted top 5 percent of monthly significant wave height means. *C.* Plot of the change in mean of the top 5 percent of 2026–2045 significant wave heights for the RCP8.5 scenario from hindcasted top 5 percent of monthly significant wave height means. *D.* Plot of the change in mean of the top 5 percent of 2081–2100 significant wave heights for the RCP4.5 scenario from hindcasted top 5 percent of monthly significant wave height means. *E.* Plot of the change in mean of the top 5 percent of 2081–2100 significant wave heights for the RCP8.5 scenario from hindcasted top 5 percent of monthly significant wave height means.

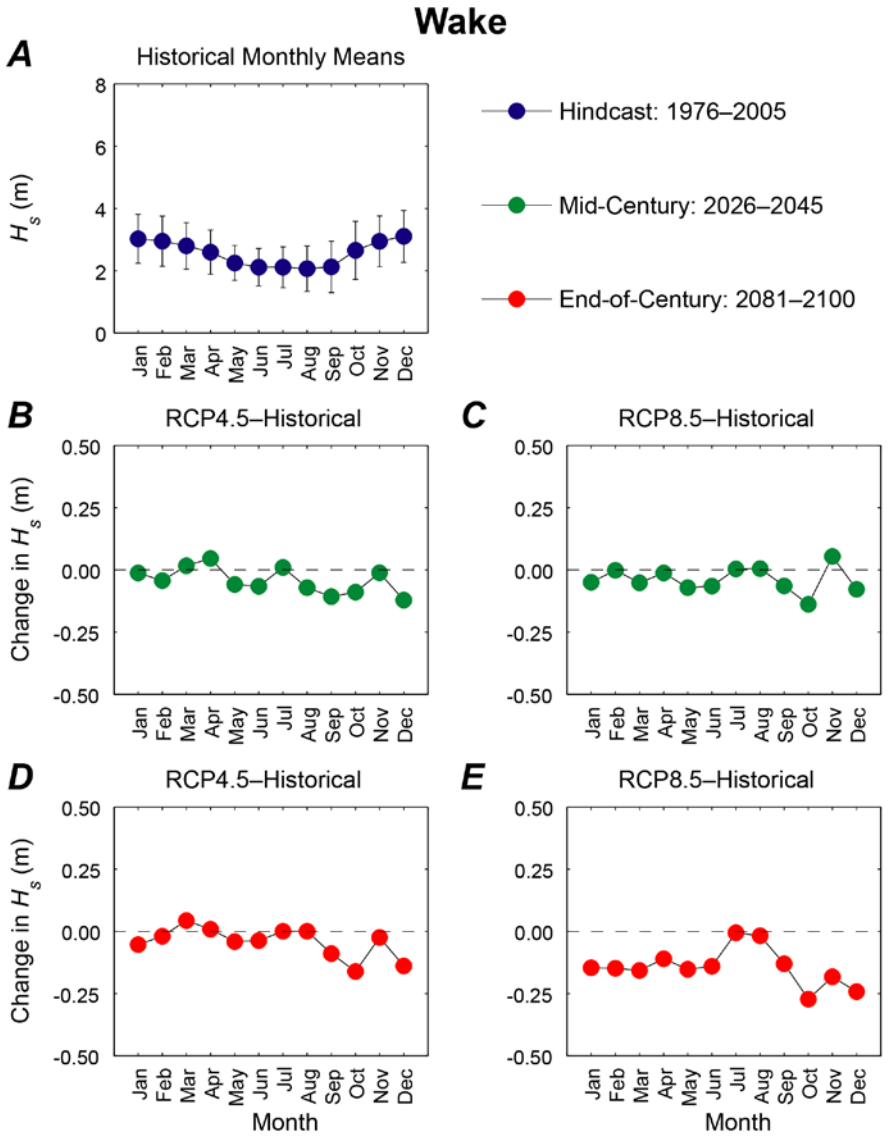

Appendix C37. Plots showing trends in monthly mean significant wave height (H_s), in meters, at the Wake location. *A.* Hindcasted (1976–2005) mean significant wave heights by month with associated error bars. *B.* Plot of the change in mean 2026–2045 significant wave heights for the RCP4.5 scenario from hindcasted monthly significant wave height means. *C.* Plot of the change in mean 2026–2045 significant wave heights for the RCP8.5 scenario from hindcasted monthly significant wave height means. *D.* Plot of the change in mean 2081–2100 significant wave heights for the RCP4.5 scenario from hindcasted monthly significant wave height means. *E.* Plot of the change in mean 2081–2100 significant wave heights for the RCP8.5 scenario from hindcasted monthly significant wave height means.

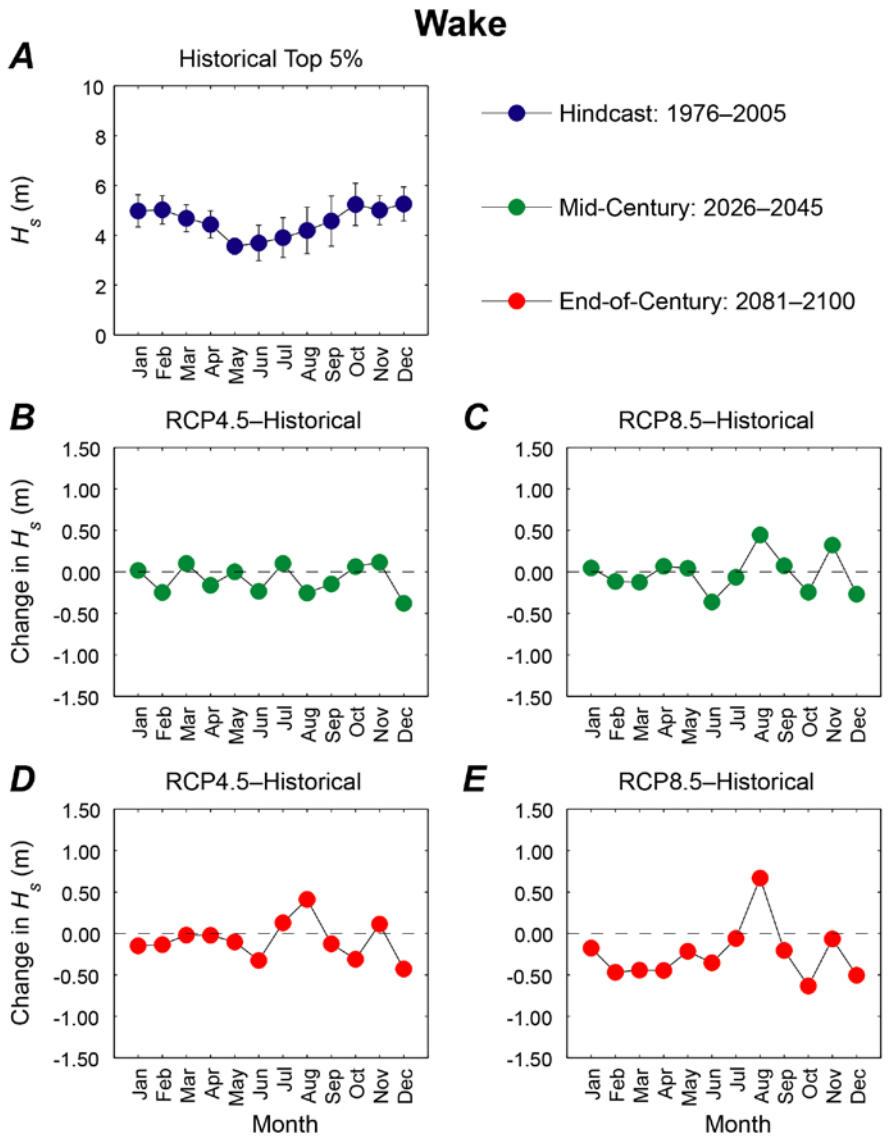

Appendix C38. Plots showing trends in monthly mean of the top 5 percent of significant wave heights (H_S), in meters, at the Wake location. *A.* Hindcasted (1976–2005) mean of the top 5 percent of significant wave heights by month with associated error bars. *B.* Plot of the change in mean of the top 5 percent of 2026–2045 significant wave heights for the RCP4.5 scenario from hindcasted top 5 percent of monthly significant wave height means. *C.* Plot of the change in mean of the top 5 percent of 2026–2045 significant wave heights for the RCP8.5 scenario from hindcasted top 5 percent of monthly significant wave height means. *D.* Plot of the change in mean of the top 5 percent of 2081–2100 significant wave heights for the RCP4.5 scenario from hindcasted top 5 percent of monthly significant wave height means. *E.* Plot of the change in mean of the top 5 percent of 2081–2100 significant wave heights for the RCP8.5 scenario from hindcasted top 5 percent of monthly significant wave height means.

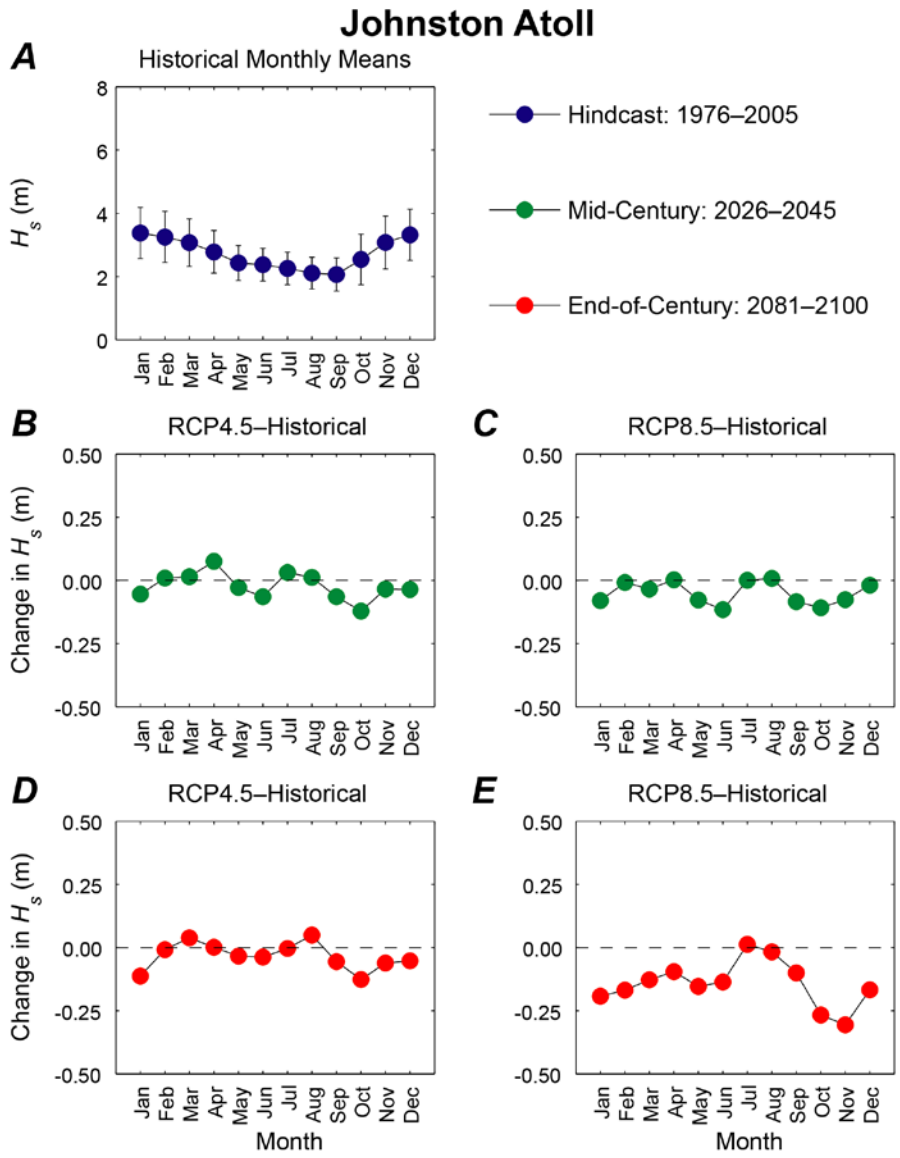

Appendix C39. Plots showing trends in monthly mean significant wave height (H_s), in meters, at the Johnston Atoll location. *A.* Hindcasted (1976–2005) mean significant wave heights by month with associated error bars. *B.* Plot of the change in mean 2026–2045 significant wave heights for the RCP4.5 scenario from hindcasted monthly significant wave height means. *C.* Plot of the change in mean 2026–2045 significant wave heights for the RCP8.5 scenario from hindcasted monthly significant wave height means. *D.* Plot of the change in mean 2081–2100 significant wave heights for the RCP4.5 scenario from hindcasted monthly significant wave height means. *E.* Plot of the change in mean 2081–2100 significant wave heights for the RCP8.5 scenario from hindcasted monthly significant wave height means.

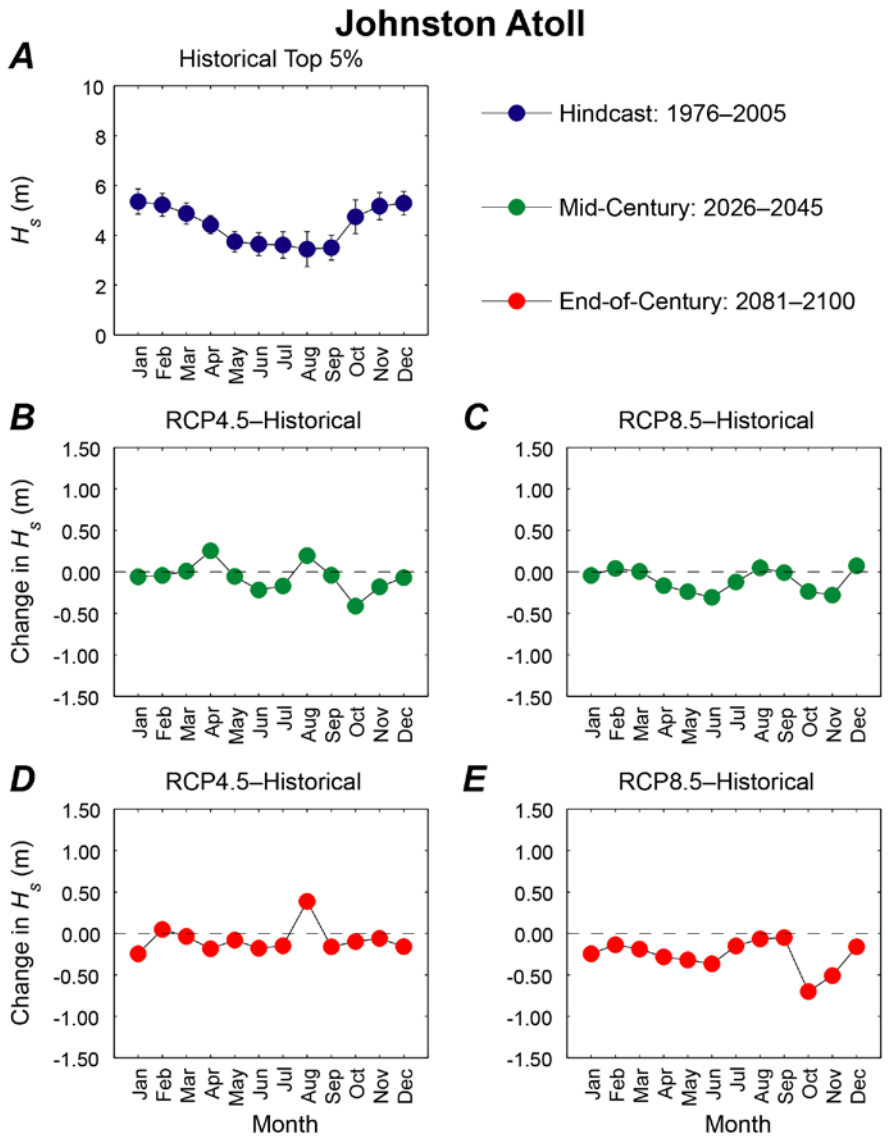

Appendix C40. Plots showing trends in monthly mean of the top 5 percent of significant wave heights (H_S), in meters, at the Johnston Atoll location. *A.* Hindcasted (1976–2005) mean of the top 5 percent of significant wave heights by month with associated error bars. *B.* Plot of the change in mean of the top 5 percent of 2026–2045 significant wave heights for the RCP4.5 scenario from hindcasted top 5 percent of monthly significant wave height means. *C.* Plot of the change in mean of the top 5 percent of 2026–2045 significant wave heights for the RCP8.5 scenario from hindcasted top 5 percent of monthly significant wave height means. *D.* Plot of the change in mean of the top 5 percent of 2081–2100 significant wave heights for the RCP4.5 scenario from hindcasted top 5 percent of monthly significant wave height means. *E.* Plot of the change in mean of the top 5 percent of 2081–2100 significant wave heights for the RCP8.5 scenario from hindcasted top 5 percent of monthly significant wave height means.

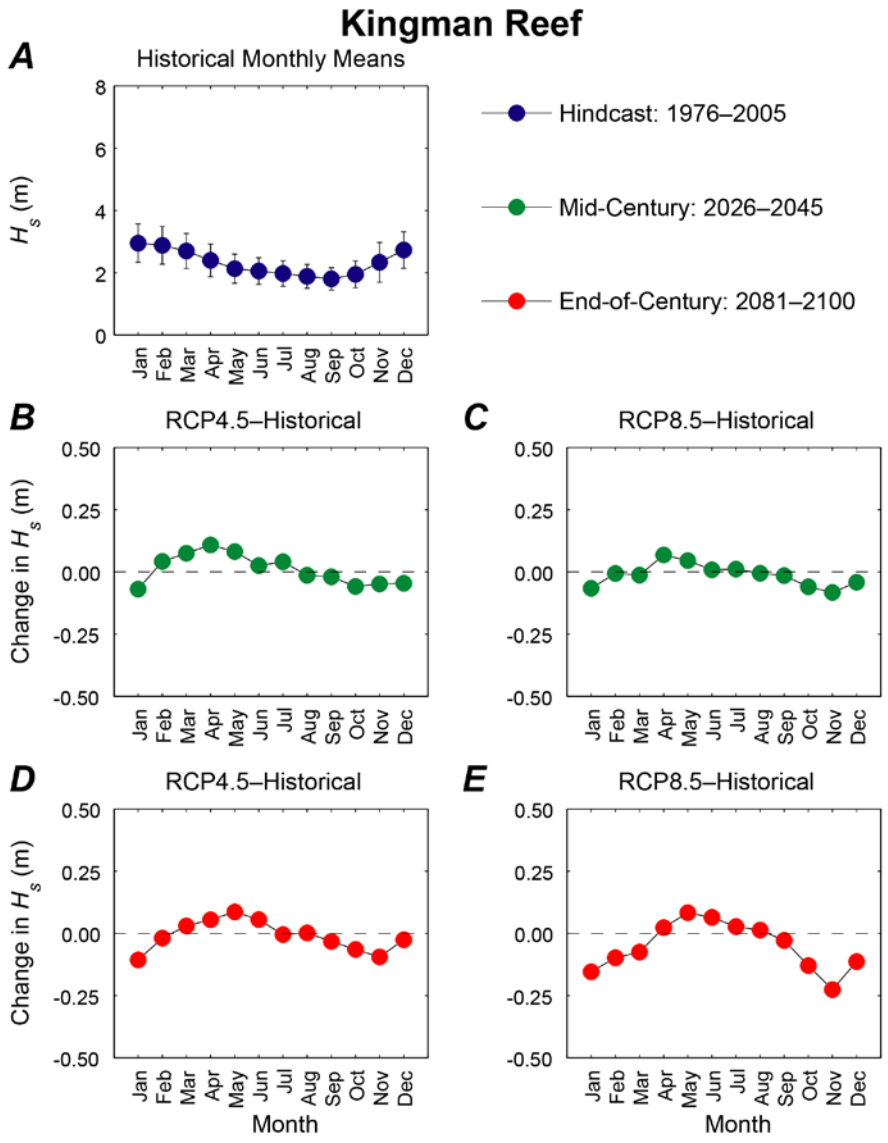

Appendix C41. Plots showing trends in monthly mean significant wave height (H_s), in meters, at the Kingman Reef location. *A.* Hindcasted (1976–2005) mean significant wave heights by month with associated error bars. *B.* Plot of the change in mean 2026–2045 significant wave heights for the RCP4.5 scenario from hindcasted monthly significant wave height means. *C.* Plot of the change in mean 2026–2045 significant wave heights for the RCP8.5 scenario from hindcasted monthly significant wave height means. *D.* Plot of the change in mean 2081–2100 significant wave heights for the RCP4.5 scenario from hindcasted monthly significant wave height means. *E.* Plot of the change in mean 2081–2100 significant wave heights for the RCP8.5 scenario from hindcasted monthly significant wave height means.

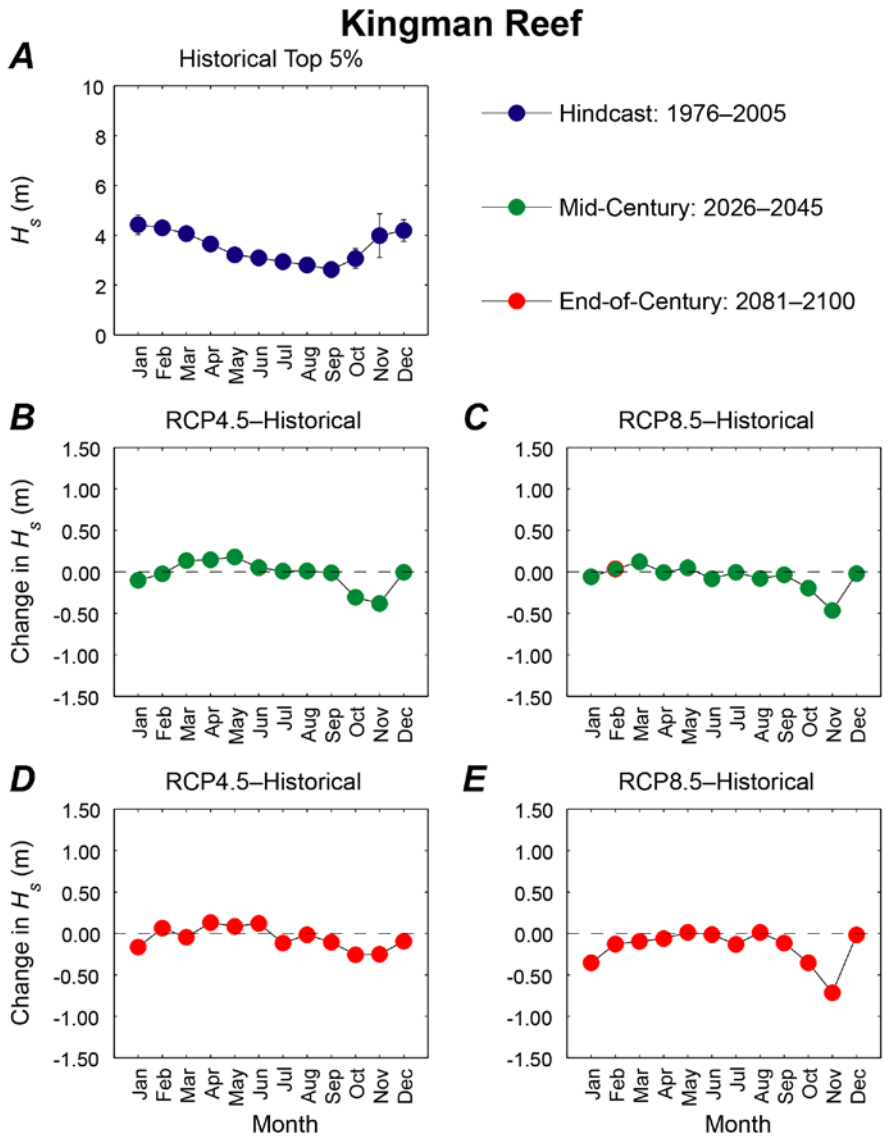

Appendix C42. Plots showing trends in monthly mean of the top 5 percent of significant wave heights (H_S), in meters, at the Kingman Reef location. *A.* Hindcasted (1976–2005) mean of the top 5 percent of significant wave heights by month with associated error bars. *B.* Plot of the change in mean of the top 5 percent of 2026–2045 significant wave heights for the RCP4.5 scenario from hindcasted top 5 percent of monthly significant wave height means. *C.* Plot of the change in mean of the top 5 percent of 2026–2045 significant wave heights for the RCP8.5 scenario from hindcasted top 5 percent of monthly significant wave height means. *D.* Plot of the change in mean of the top 5 percent of 2081–2100 significant wave heights for the RCP4.5 scenario from hindcasted top 5 percent of monthly significant wave height means. *E.* Plot of the change in mean of the top 5 percent of 2081–2100 significant wave heights for the RCP8.5 scenario from hindcasted top 5 percent of monthly significant wave height means.

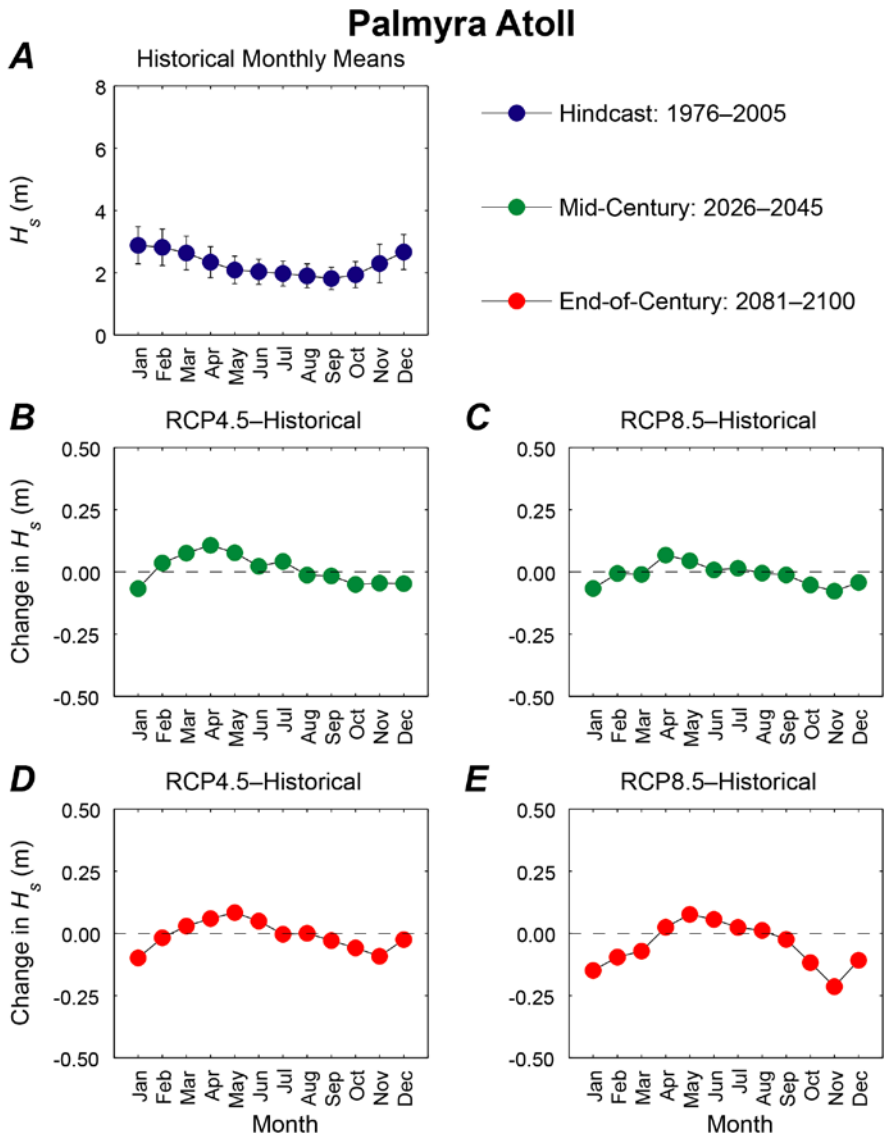

Appendix C43. Plots showing trends in monthly mean significant wave height (H_s), in meters, at the Palmyra Atoll location. *A.* Hindcasted (1976–2005) mean significant wave heights by month with associated error bars. *B.* Plot of the change in mean 2026–2045 significant wave heights for the RCP4.5 scenario from hindcasted monthly significant wave height means. *C.* Plot of the change in mean 2026–2045 significant wave heights for the RCP8.5 scenario from hindcasted monthly significant wave height means. *D.* Plot of the change in mean 2081–2100 significant wave heights for the RCP4.5 scenario from hindcasted monthly significant wave height means. *E.* Plot of the change in mean 2081–2100 significant wave heights for the RCP8.5 scenario from hindcasted monthly significant wave height means.

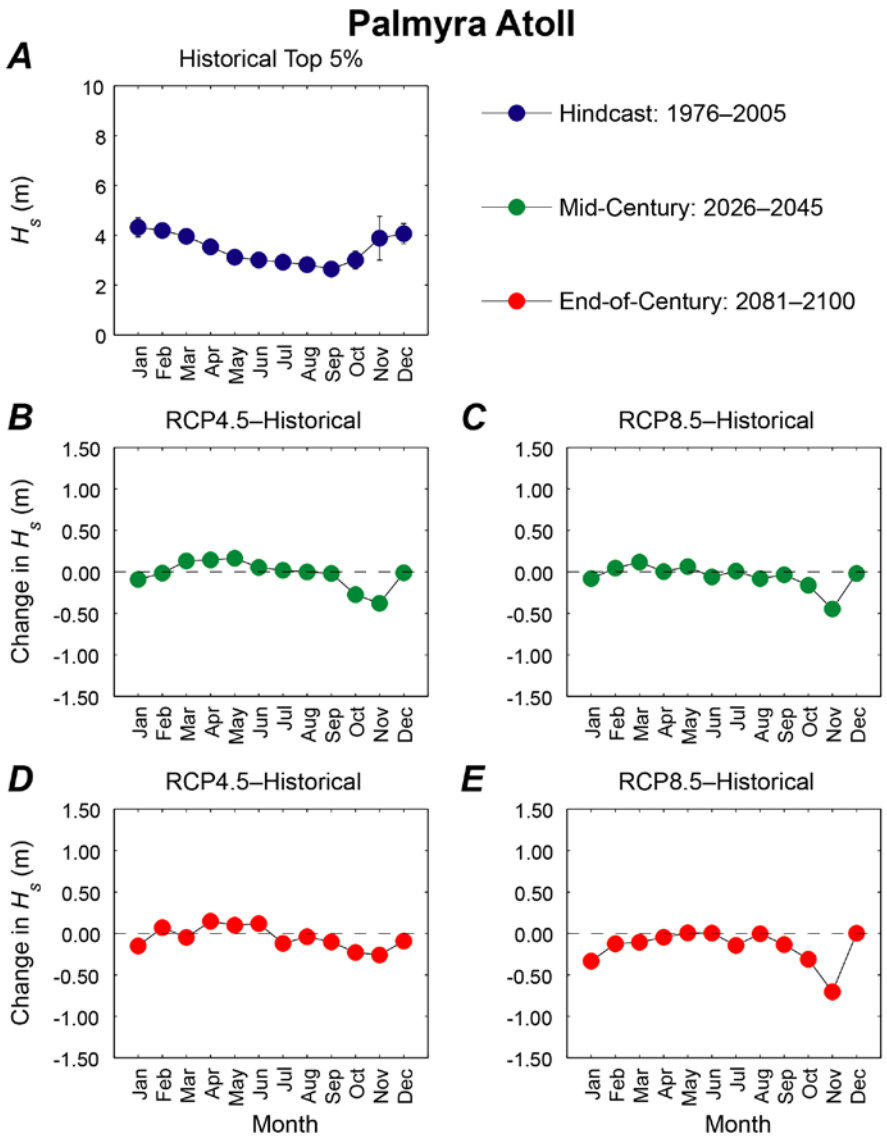

Appendix C44. Plots showing trends in monthly mean of the top 5 percent of significant wave heights (H_S), in meters, at the Palmyra Atoll location. *A.* Hindcasted (1976–2005) mean of the top 5 percent of significant wave heights by month with associated error bars. *B.* Plot of the change in mean of the top 5 percent of 2026–2045 significant wave heights for the RCP4.5 scenario from hindcasted top 5 percent of monthly significant wave height means. *C.* Plot of the change in mean of the top 5 percent of 2026–2045 significant wave heights for the RCP8.5 scenario from hindcasted top 5 percent of monthly significant wave height means. *D.* Plot of the change in mean of the top 5 percent of 2081–2100 significant wave heights for the RCP4.5 scenario from hindcasted top 5 percent of monthly significant wave height means. *E.* Plot of the change in mean of the top 5 percent of 2081–2100 significant wave heights for the RCP8.5 scenario from hindcasted top 5 percent of monthly significant wave height means.

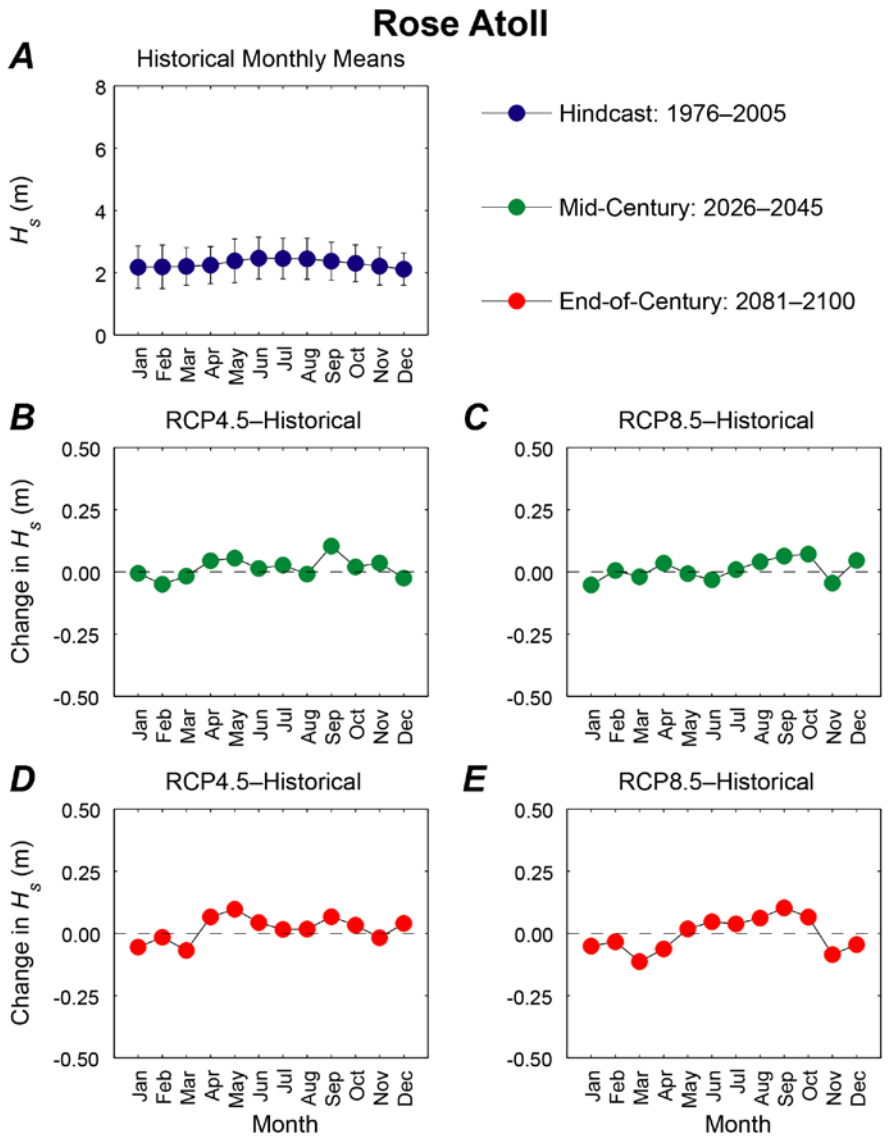

Appendix C45. Plots showing trends in monthly mean significant wave height (H_s), in meters, at the Rose Atoll location. *A.* Hindcasted (1976–2005) mean significant wave heights by month with associated error bars. *B.* Plot of the change in mean 2026–2045 significant wave heights for the RCP4.5 scenario from hindcasted monthly significant wave height means. *C.* Plot of the change in mean 2026–2045 significant wave heights for the RCP8.5 scenario from hindcasted monthly significant wave height means. *D.* Plot of the change in mean 2081–2100 significant wave heights for the RCP4.5 scenario from hindcasted monthly significant wave height means. *E.* Plot of the change in mean 2081–2100 significant wave heights for the RCP8.5 scenario from hindcasted monthly significant wave height means.

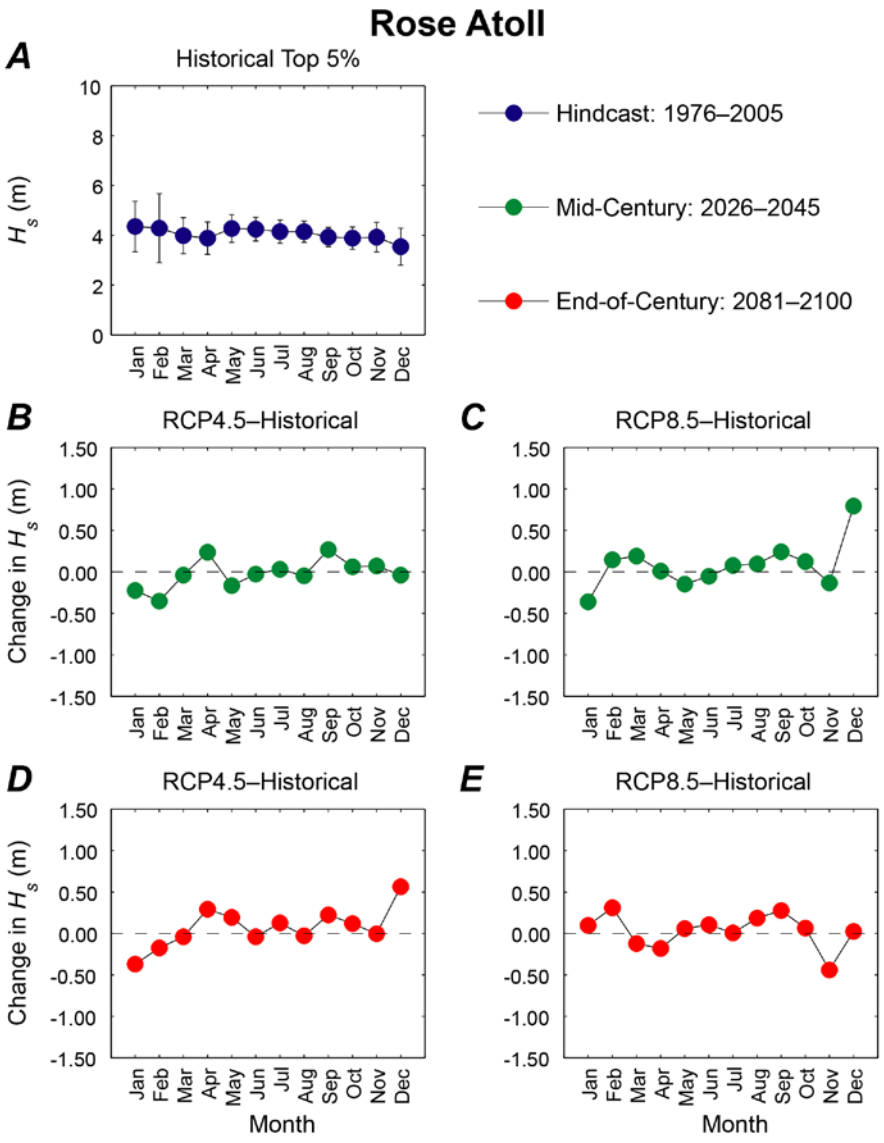

Appendix C46. Plots showing trends in monthly mean of the top 5 percent of significant wave heights (H_S), in meters, at the Rose Atoll location. *A.* Hindcasted (1976–2005) mean of the top 5 percent of significant wave heights by month with associated error bars. *B.* Plot of the change in mean of the top 5 percent of 2026–2045 significant wave heights for the RCP4.5 scenario from hindcasted top 5 percent of monthly significant wave height means. *C.* Plot of the change in mean of the top 5 percent of 2026–2045 significant wave heights for the RCP8.5 scenario from hindcasted top 5 percent of monthly significant wave height means. *D.* Plot of the change in mean of the top 5 percent of 2081–2100 significant wave heights for the RCP4.5 scenario from hindcasted top 5 percent of monthly significant wave height means. *E.* Plot of the change in mean of the top 5 percent of 2081–2100 significant wave heights for the RCP8.5 scenario from hindcasted top 5 percent of monthly significant wave height means.

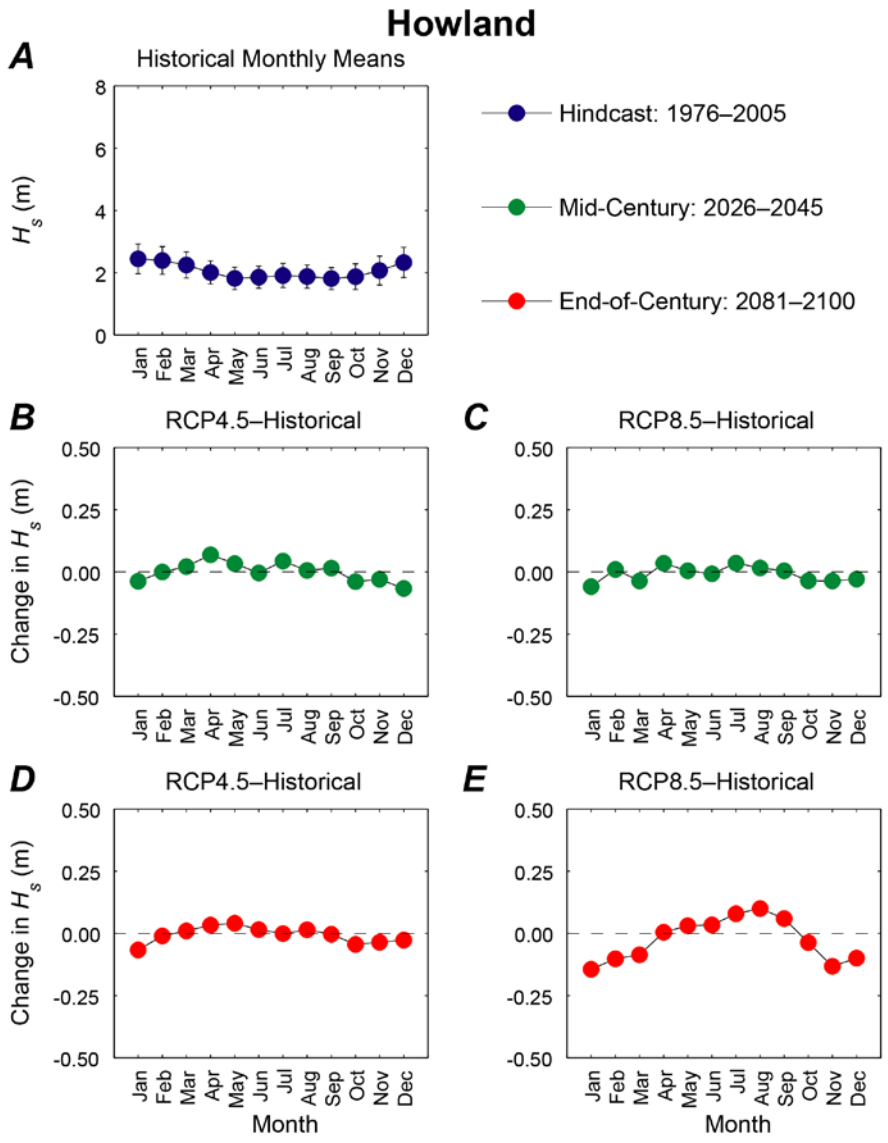

Appendix C47. Plots showing trends in monthly mean significant wave height (H_s), in meters, at the Howland location. *A.* Hindcasted (1976–2005) mean significant wave heights by month with associated error bars. *B.* Plot of the change in mean 2026–2045 significant wave heights for the RCP4.5 scenario from hindcasted monthly significant wave height means. *C.* Plot of the change in mean 2026–2045 significant wave heights for the RCP8.5 scenario from hindcasted monthly significant wave height means. *D.* Plot of the change in mean 2081–2100 significant wave heights for the RCP4.5 scenario from hindcasted monthly significant wave height means. *E.* Plot of the change in mean 2081–2100 significant wave heights for the RCP8.5 scenario from hindcasted monthly significant wave height means.

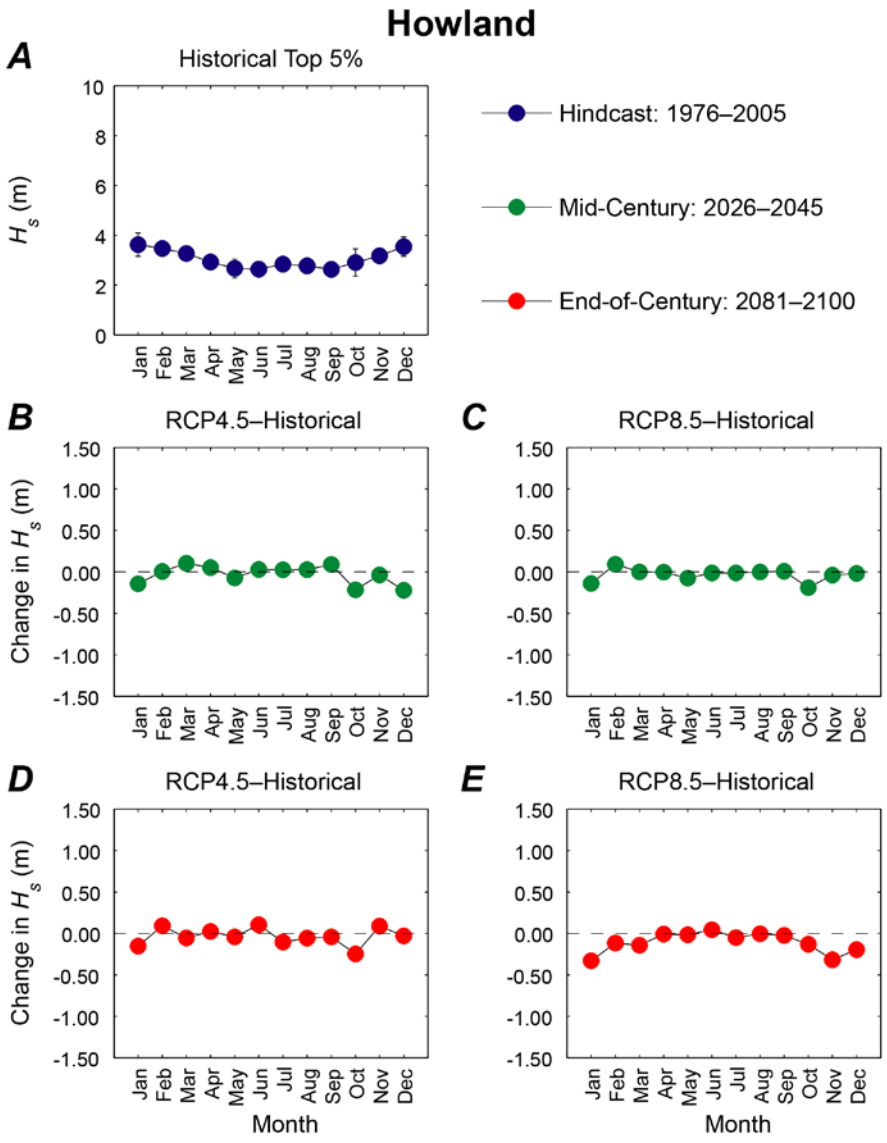

Appendix C48. Plots showing trends in monthly mean of the top 5 percent of significant wave heights (H_S), in meters, at the Howland location. *A.* Hindcasted (1976–2005) mean of the top 5 percent of significant wave heights by month with associated error bars. *B.* Plot of the change in mean of the top 5 percent of 2026–2045 significant wave heights for the RCP4.5 scenario from hindcasted top 5 percent of monthly significant wave height means. *C.* Plot of the change in mean of the top 5 percent of 2026–2045 significant wave heights for the RCP8.5 scenario from hindcasted top 5 percent of monthly significant wave height means. *D.* Plot of the change in mean of the top 5 percent of 2081–2100 significant wave heights for the RCP4.5 scenario from hindcasted top 5 percent of monthly significant wave height means. *E.* Plot of the change in mean of the top 5 percent of 2081–2100 significant wave heights for the RCP8.5 scenario from hindcasted top 5 percent of monthly significant wave height means.

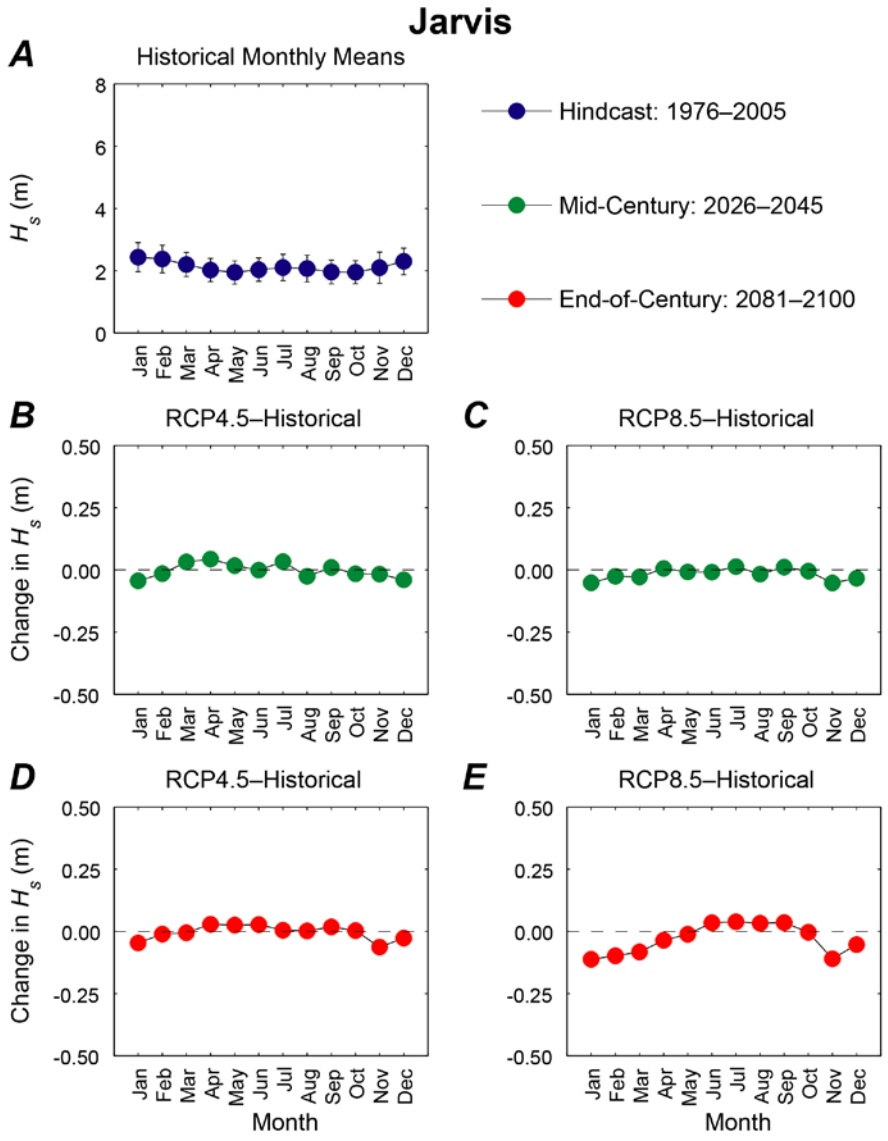

Appendix C49. Plots showing trends in monthly mean significant wave height (H_s), in meters, at the Jarvis location. *A.* Hindcasted (1976–2005) mean significant wave heights by month with associated error bars. *B.* Plot of the change in mean 2026–2045 significant wave heights for the RCP4.5 scenario from hindcasted monthly significant wave height means. *C.* Plot of the change in mean 2026–2045 significant wave heights for the RCP8.5 scenario from hindcasted monthly significant wave height means. *D.* Plot of the change in mean 2081–2100 significant wave heights for the RCP4.5 scenario from hindcasted monthly significant wave height means. *E.* Plot of the change in mean 2081–2100 significant wave heights for the RCP8.5 scenario from hindcasted monthly significant wave height means.

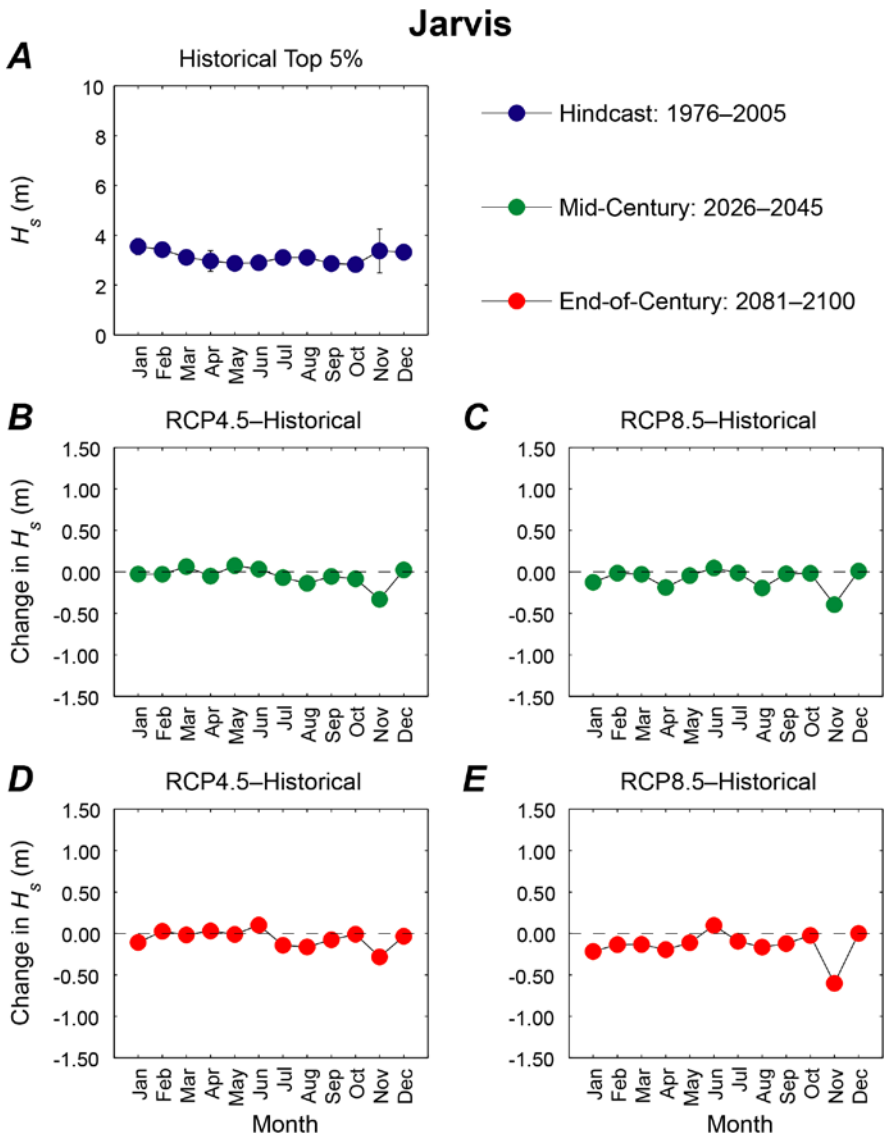

Appendix C50. Plots showing trends in monthly mean of the top 5 percent of significant wave heights (H_S), in meters, at the Jarvis location. *A.* Hindcasted (1976–2005) mean of the top 5 percent of significant wave heights by month with associated error bars. *B.* Plot of the change in mean of the top 5 percent of 2026–2045 significant wave heights for the RCP4.5 scenario from hindcasted top 5 percent of monthly significant wave height means. *C.* Plot of the change in mean of the top 5 percent of 2026–2045 significant wave heights for the RCP8.5 scenario from hindcasted top 5 percent of monthly significant wave height means. *D.* Plot of the change in mean of the top 5 percent of 2081–2100 significant wave heights for the RCP4.5 scenario from hindcasted top 5 percent of monthly significant wave height means. *E.* Plot of the change in mean of the top 5 percent of 2081–2100 significant wave heights for the RCP8.5 scenario from hindcasted top 5 percent of monthly significant wave height means.

Appendix D. Monthly Trends in Wind Speeds

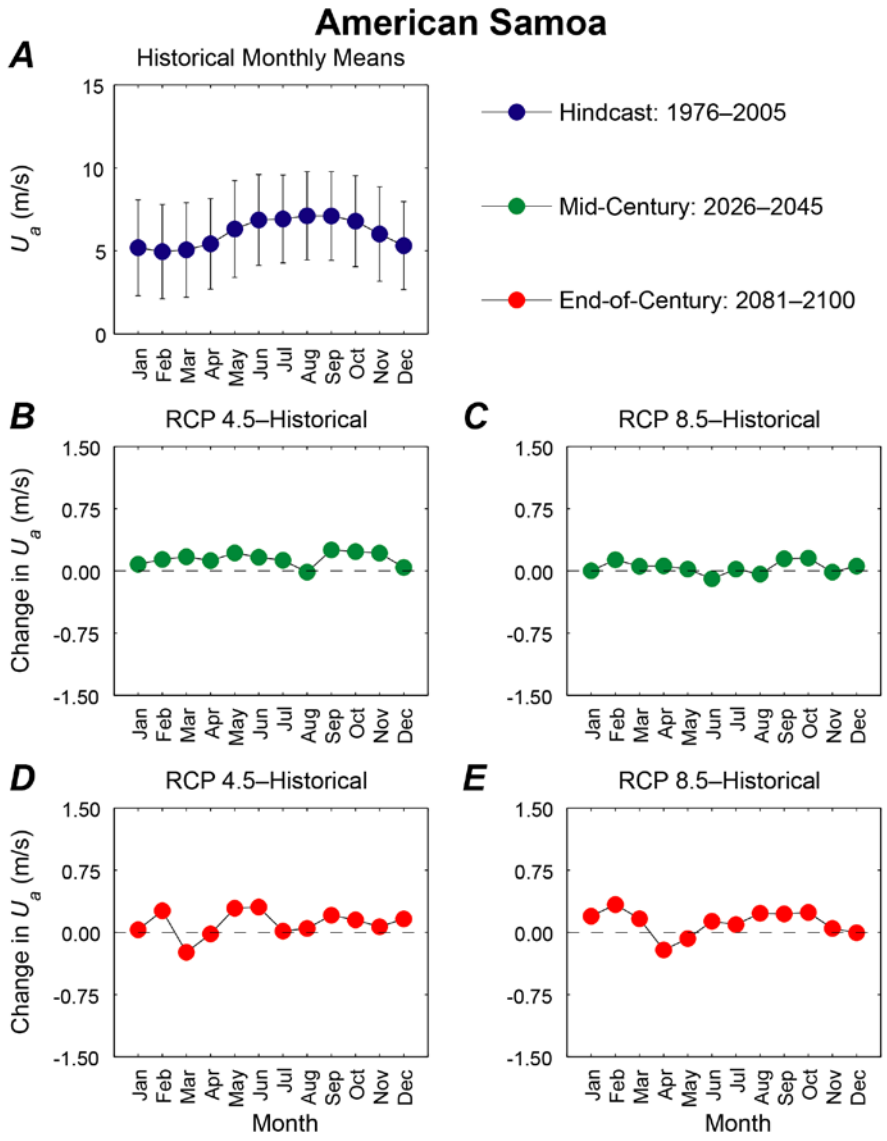

Appendix D1. Plots showing trends in monthly mean wind speed, in meters per second, at the American Samoa location. *A.* Hindcasted (1976–2005) mean wind speeds by month with associated error bars. *B.* Plot of the change in mean 2026–2045 wind speeds for the RCP4.5 scenario from hindcasted monthly wind speed means. *C.* Plot of the change in mean 2026–2045 wind speeds for the RCP8.5 scenario from hindcasted monthly wind speed means. *D.* Plot of the change in mean 2081–2100 wind speeds for the RCP4.5 scenario from hindcasted monthly wind speed means. *E.* Plot of the change in mean 2081–2100 wind speeds for the RCP8.5 scenario from hindcasted monthly wind speed means.

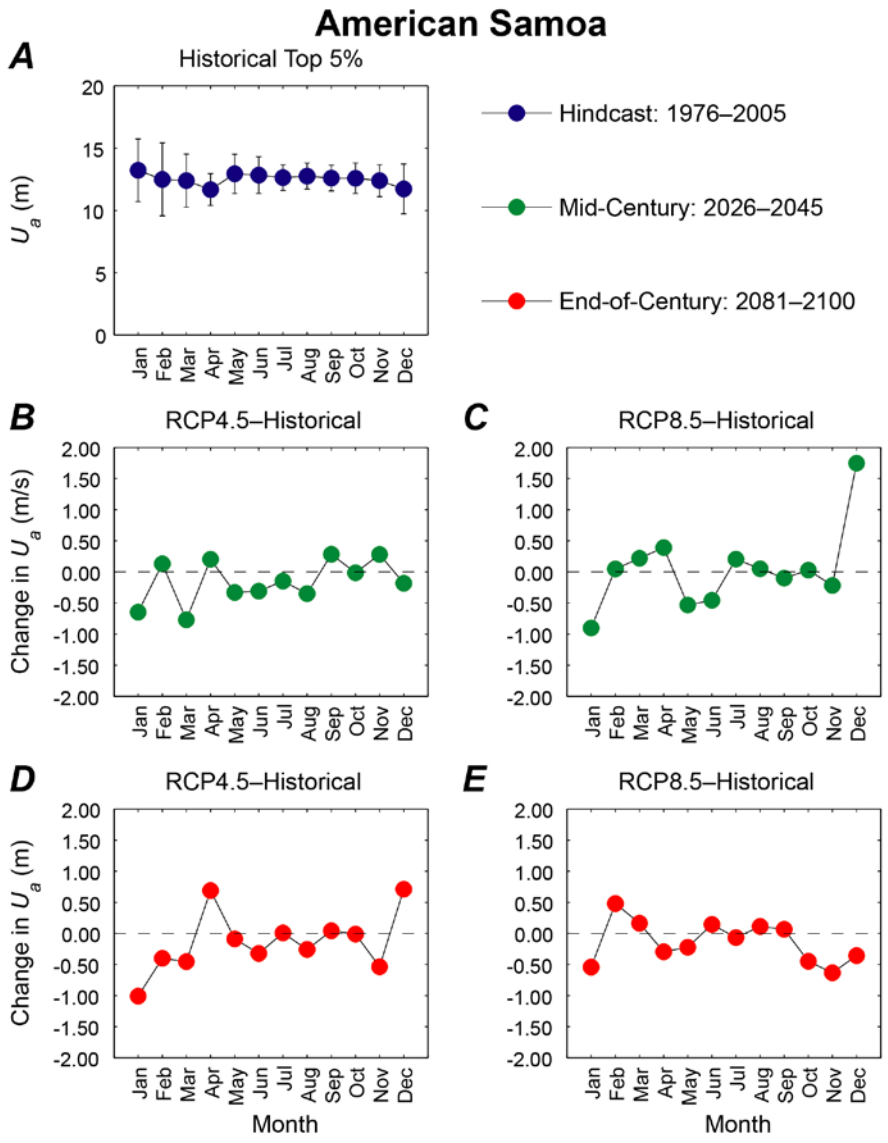

Appendix D2. Plots showing trends in monthly mean of the top 5 percent of wind speeds, in meters, at the American Samoa location. *A.* Hindcasted (1976–2005) mean of the top 5 percent of wind speeds by month with associated error bars. *B.* Plot of the change in mean of the top 5 percent of 2026–2045 wind speeds for the RCP4.5 scenario from hindcasted top 5 percent of monthly wind speed means. *C.* Plot of the change in mean of the top 5 percent of 2026–2045 wind speeds for the RCP8.5 scenario from hindcasted top 5 percent of monthly wind speed means. *D.* Plot of the change in mean of the top 5 percent of 2081–2100 wind speeds for the RCP4.5 scenario from hindcasted top 5 percent of monthly wind speed means. *E.* Plot of the change in mean of the top 5 percent of 2081–2100 wind speeds for the RCP8.5 scenario from hindcasted top 5 percent of monthly wind speed means.

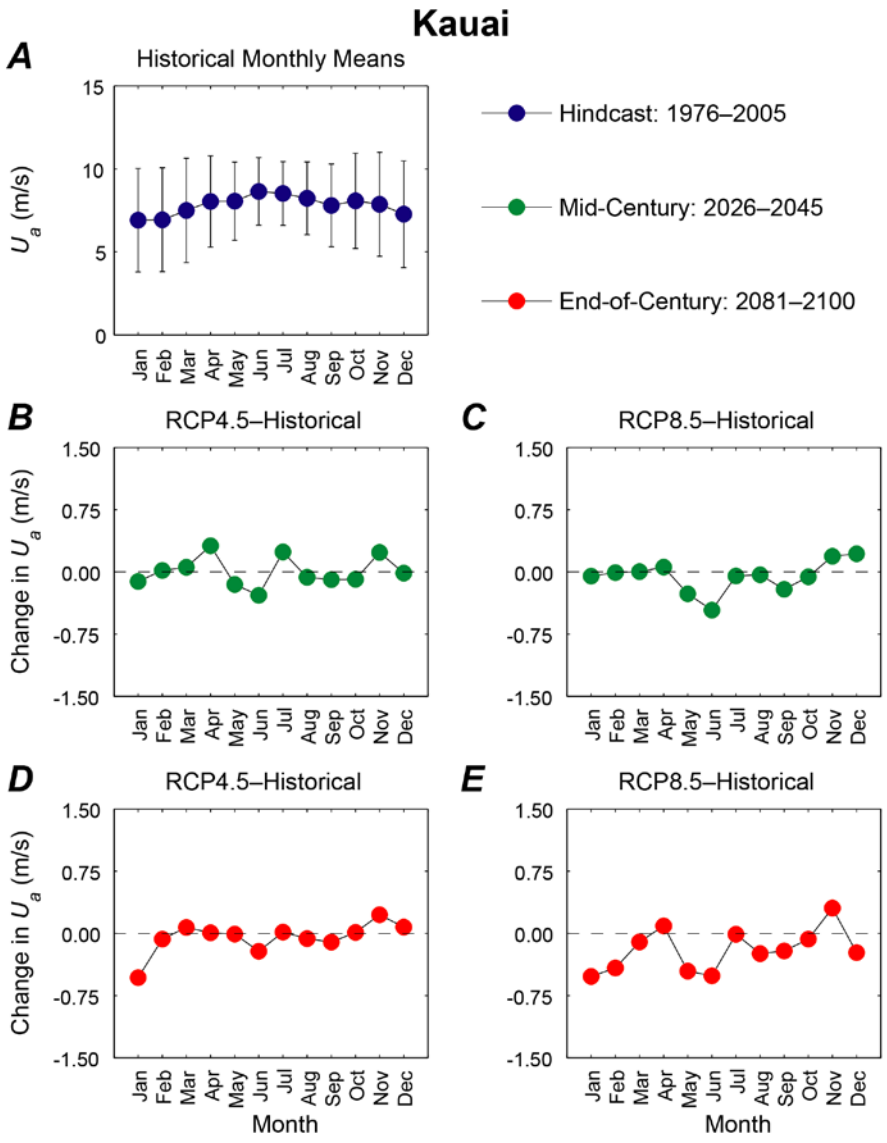

Appendix D3. Plots showing trends in monthly mean wind speed, in meters per second, at the Kauai location. *A.* Hindcasted (1976–2005) mean wind speeds by month with associated error bars. *B.* Plot of the change in mean 2026–2045 wind speeds for the RCP4.5 scenario from hindcasted monthly wind speed means. *C.* Plot of the change in mean 2026–2045 wind speeds for the RCP8.5 scenario from hindcasted monthly wind speed means. *D.* Plot of the change in mean 2081–2100 wind speeds for the RCP4.5 scenario from hindcasted monthly wind speed means. *E.* Plot of the change in mean 2081–2100 wind speeds for the RCP8.5 scenario from hindcasted monthly wind speed means.

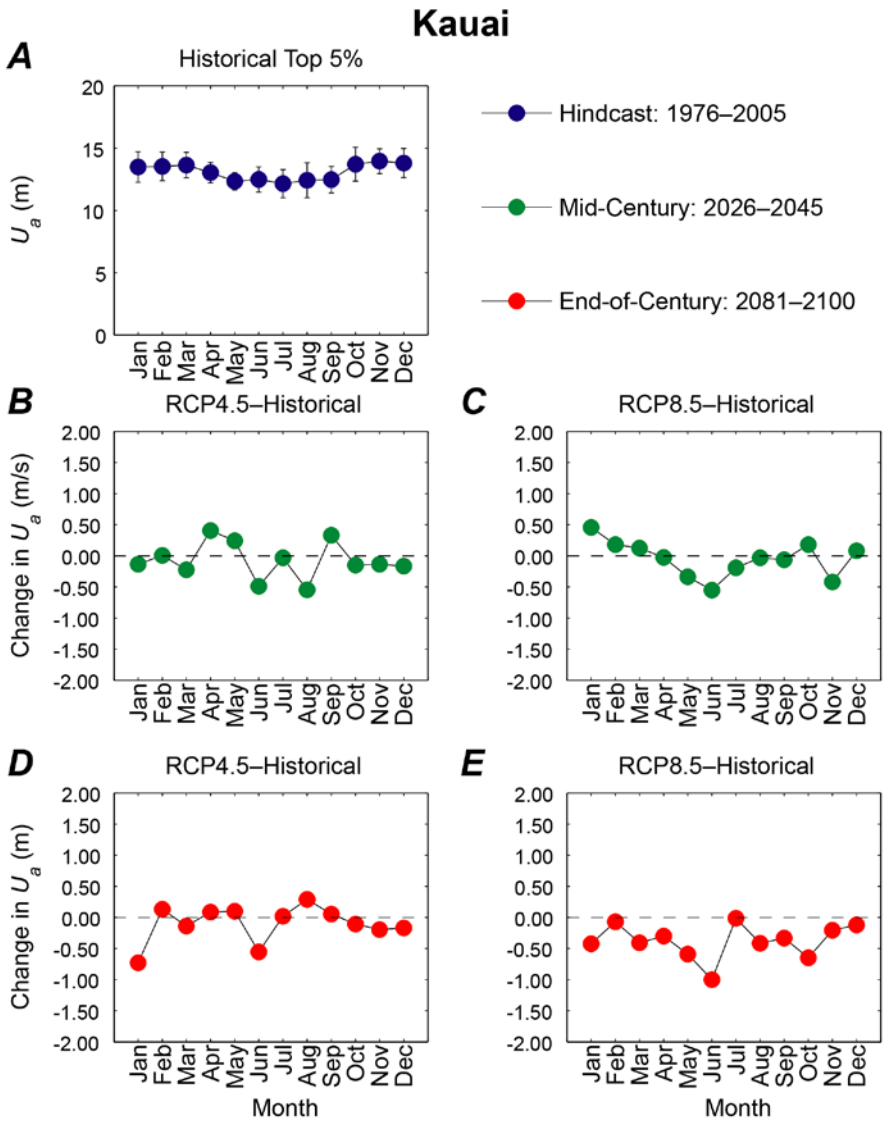

Appendix D4. Plots showing trends in monthly mean of the top 5 percent of wind speeds, in meters, at the Kauai location. *A.* Hindcasted (1976–2005) mean of the top 5 percent of wind speeds by month with associated error bars. *B.* Plot of the change in mean of the top 5 percent of 2026–2045 wind speeds for the RCP4.5 scenario from hindcasted top 5 percent of monthly wind speed means. *C.* Plot of the change in mean of the top 5 percent of 2026–2045 wind speeds for the RCP8.5 scenario from hindcasted top 5 percent of monthly wind speed means. *D.* Plot of the change in mean of the top 5 percent of 2081–2100 wind speeds for the RCP4.5 scenario from hindcasted top 5 percent of monthly wind speed means. *E.* Plot of the change in mean of the top 5 percent of 2081–2100 wind speeds for the RCP8.5 scenario from hindcasted top 5 percent of monthly wind speed means.

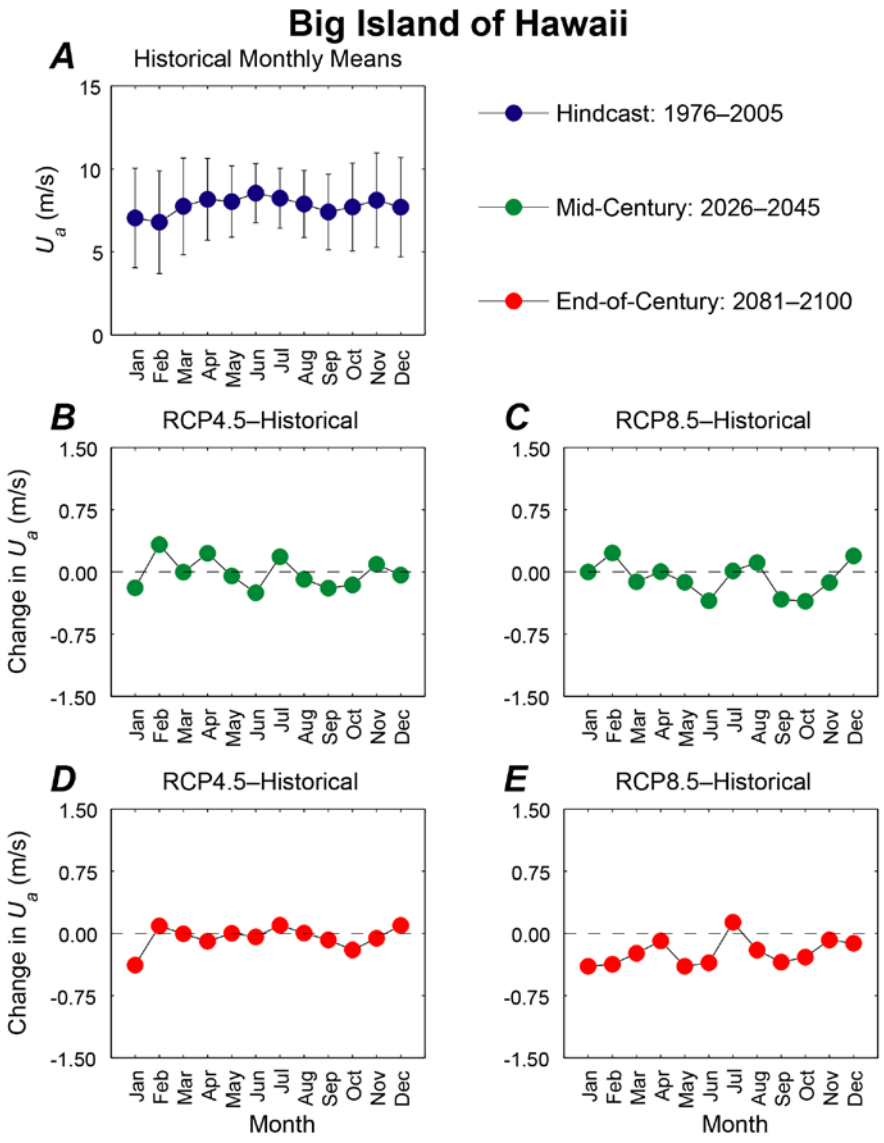

Appendix D5. Plots showing trends in monthly mean wind speed, in meters per second, at the Big Island of Hawaii location. *A.* Hindcasted (1976–2005) mean wind speeds by month with associated error bars. *B.* Plot of the change in mean 2026–2045 wind speeds for the RCP4.5 scenario from hindcasted monthly wind speed means. *C.* Plot of the change in mean 2026–2045 wind speeds for the RCP8.5 scenario from hindcasted monthly wind speed means. *D.* Plot of the change in mean 2081–2100 wind speeds for the RCP4.5 scenario from hindcasted monthly wind speed means. *E.* Plot of the change in mean 2081–2100 wind speeds for the RCP8.5 scenario from hindcasted monthly wind speed means.

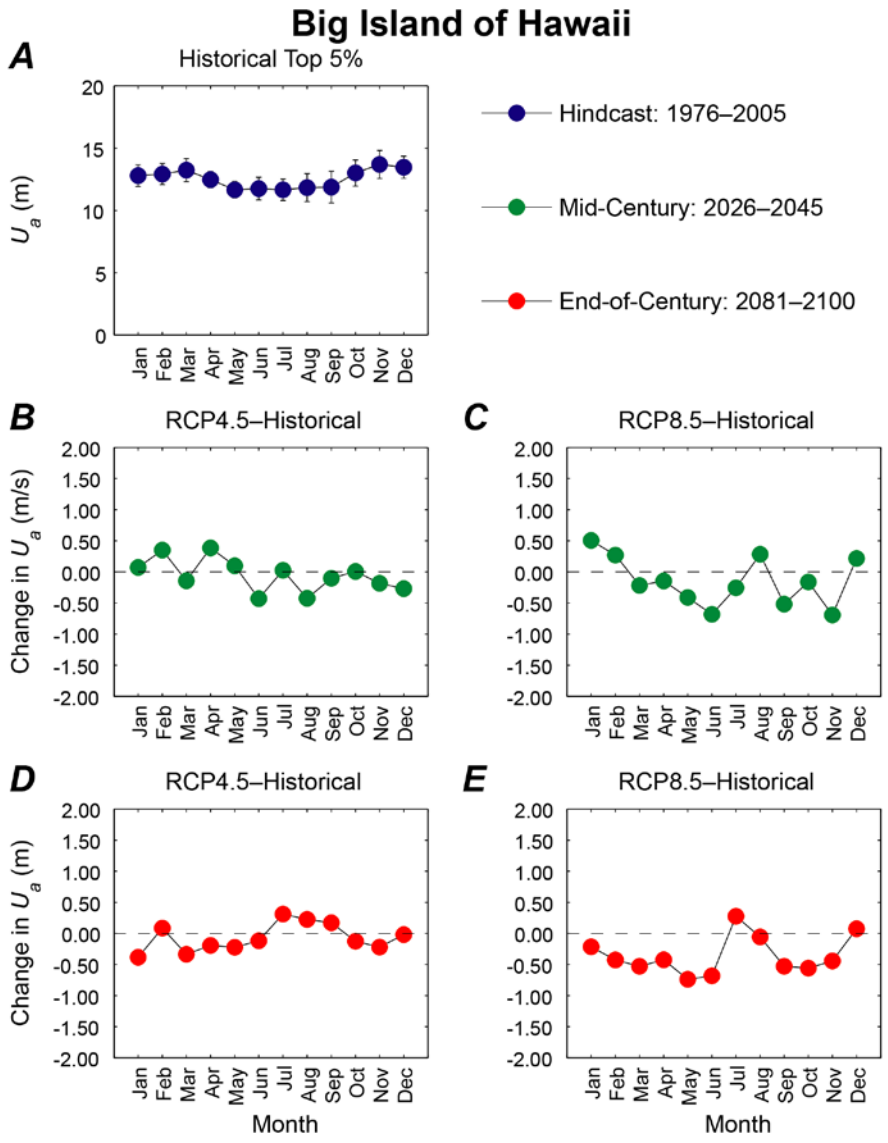

Appendix D6. Plots showing trends in monthly mean of the top 5 percent of wind speeds, in meters, at the Big Island of Hawaii location. *A.* Hindcasted (1976–2005) mean of the top 5 percent of wind speeds by month with associated error bars. *B.* Plot of the change in mean of the top 5 percent of 2026–2045 wind speeds for the RCP4.5 scenario from hindcasted top 5 percent of monthly wind speed means. *C.* Plot of the change in mean of the top 5 percent of 2026–2045 wind speeds for the RCP8.5 scenario from hindcasted top 5 percent of monthly wind speed means. *D.* Plot of the change in mean of the top 5 percent of 2081–2100 wind speeds for the RCP4.5 scenario from hindcasted top 5 percent of monthly wind speed means. *E.* Plot of the change in mean of the top 5 percent of 2081–2100 wind speeds for the RCP8.5 scenario from hindcasted top 5 percent of monthly wind speed means.

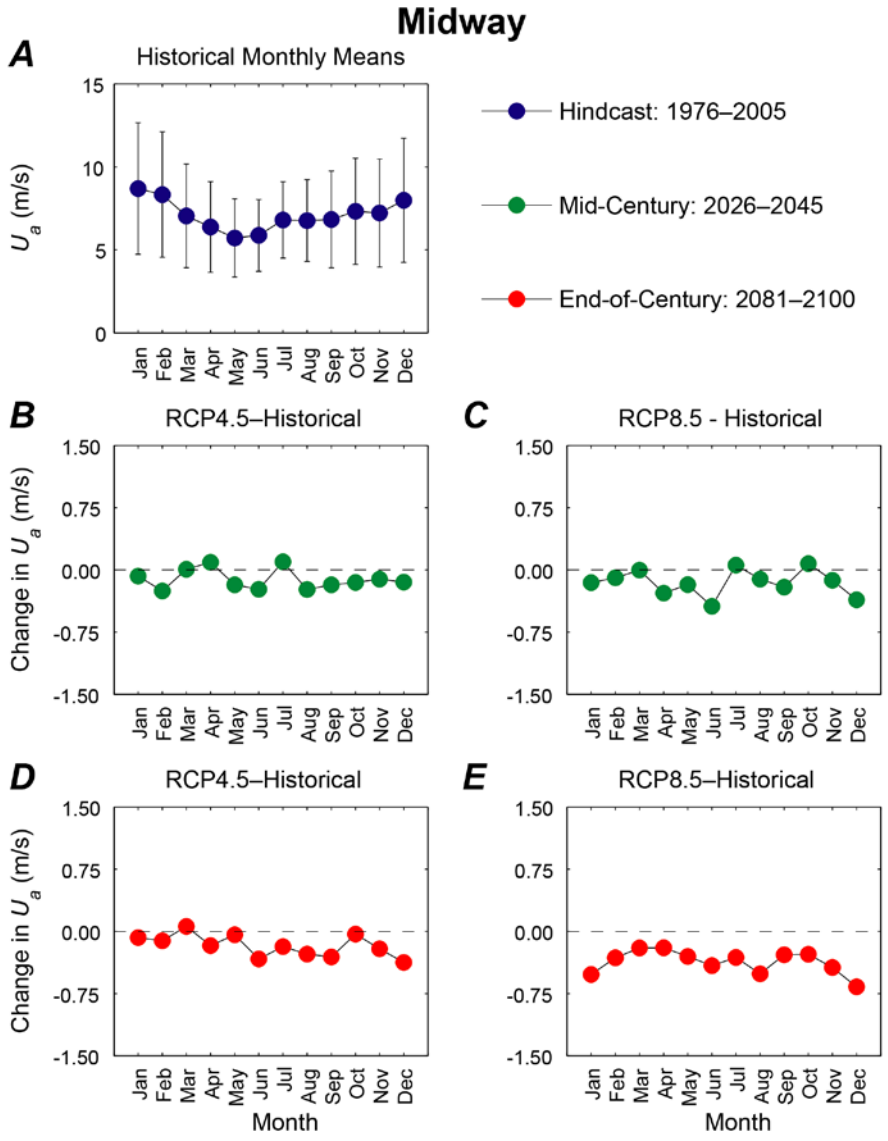

Appendix D7. Plots showing trends in monthly mean wind speed, in meters per second, at the Midway location. *A.* Hindcasted (1976–2005) mean wind speeds by month with associated error bars. *B.* Plot of the change in mean 2026–2045 wind speeds for the RCP4.5 scenario from hindcasted monthly wind speed means. *C.* Plot of the change in mean 2026–2045 wind speeds for the RCP8.5 scenario from hindcasted monthly wind speed means. *D.* Plot of the change in mean 2081–2100 wind speeds for the RCP4.5 scenario from hindcasted monthly wind speed means. *E.* Plot of the change in mean 2081–2100 wind speeds for the RCP8.5 scenario from hindcasted monthly wind speed means.

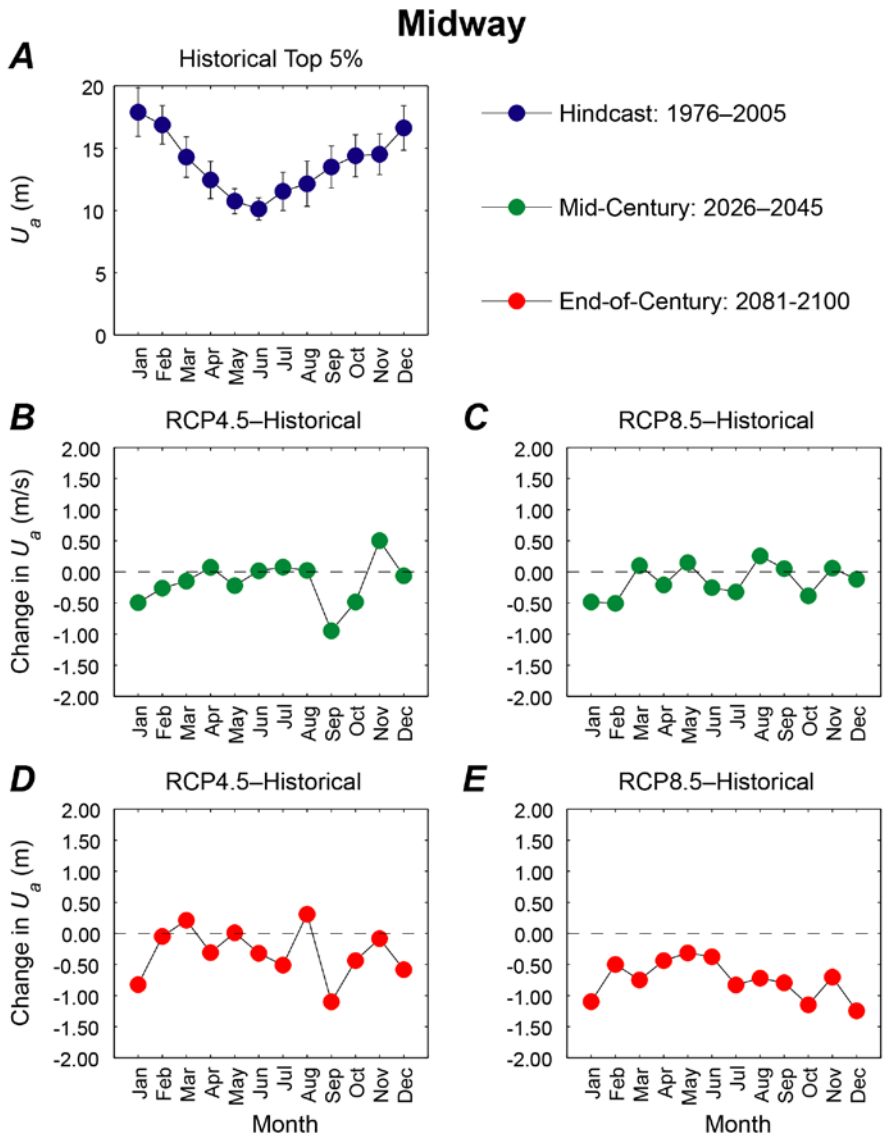

Appendix D8. Plots showing trends in monthly mean of the top 5 percent of wind speeds, in meters, at the Midway location. *A.* Hindcasted (1976–2005) mean of the top 5 percent of wind speeds by month with associated error bars. *B.* Plot of the change in mean of the top 5 percent of 2026–2045 wind speeds for the RCP4.5 scenario from hindcasted top 5 percent of monthly wind speed means. *C.* Plot of the change in mean of the top 5 percent of 2026–2045 wind speeds for the RCP8.5 scenario from hindcasted top 5 percent of monthly wind speed means. *D.* Plot of the change in mean of the top 5 percent of 2081–2100 wind speeds for the RCP4.5 scenario from hindcasted top 5 percent of monthly wind speed means. *E.* Plot of the change in mean of the top 5 percent of 2081–2100 wind speeds for the RCP8.5 scenario from hindcasted top 5 percent of monthly wind speed means.

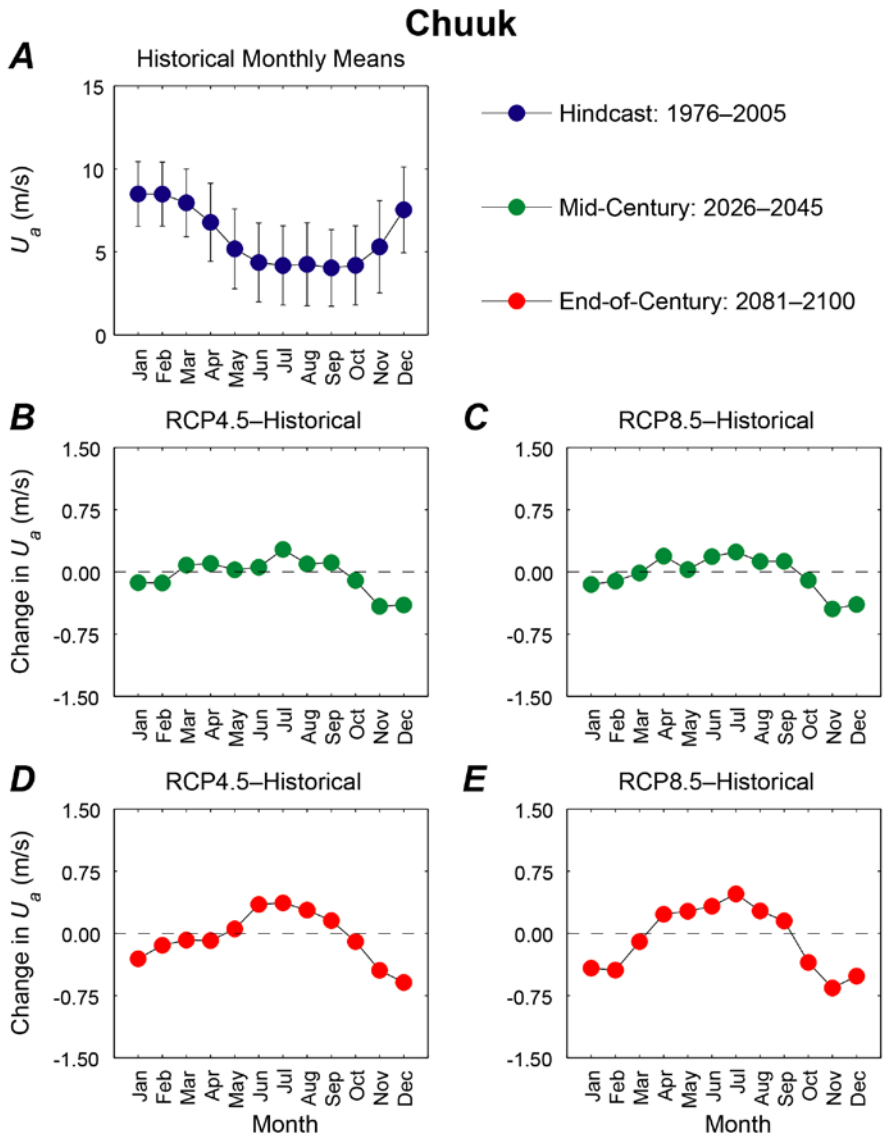

Appendix D9. Plots showing trends in monthly mean wind speed, in meters per second, at the Chuuk location. *A.* Hindcasted (1976–2005) mean wind speeds by month with associated error bars. *B.* Plot of the change in mean 2026–2045 wind speeds for the RCP4.5 scenario from hindcasted monthly wind speed means. *C.* Plot of the change in mean 2026–2045 wind speeds for the RCP8.5 scenario from hindcasted monthly wind speed means. *D.* Plot of the change in mean 2081–2100 wind speeds for the RCP4.5 scenario from hindcasted monthly wind speed means. *E.* Plot of the change in mean 2081–2100 wind speeds for the RCP8.5 scenario from hindcasted monthly wind speed means.

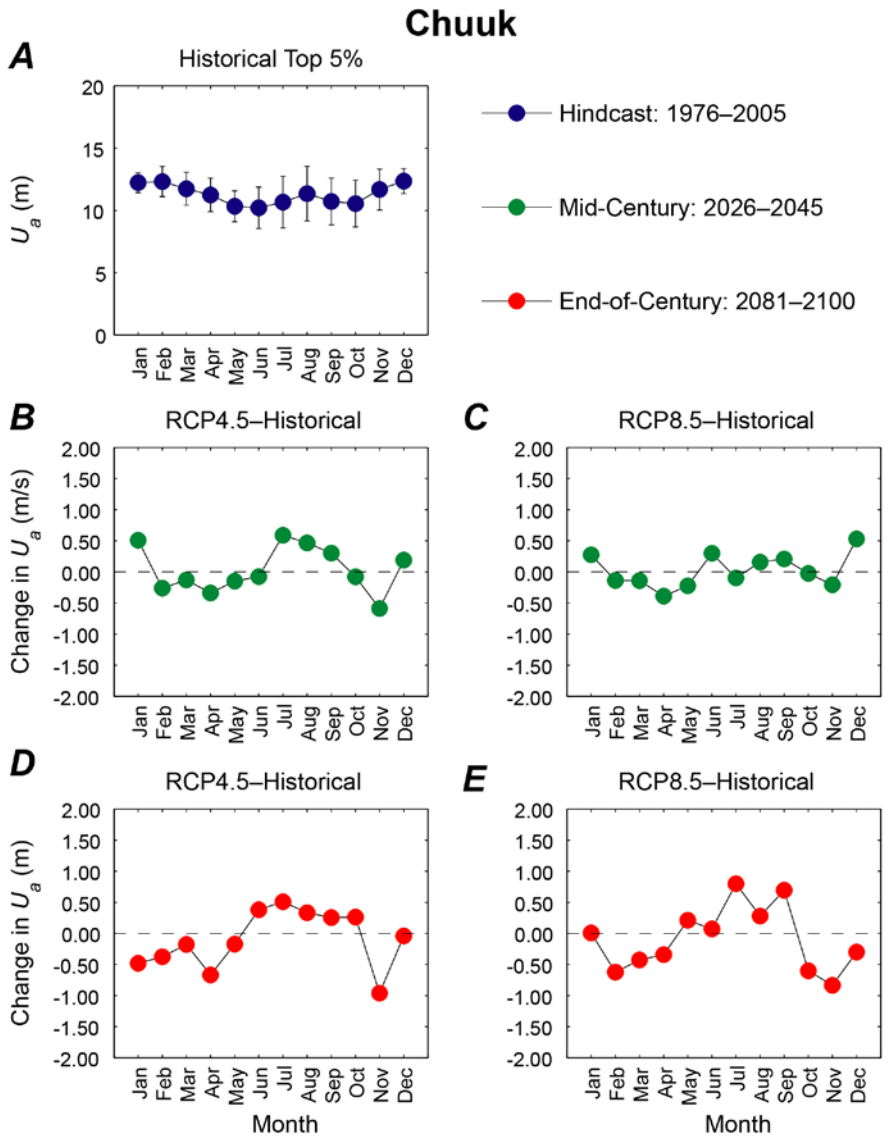

Appendix D10. Plots showing trends in monthly mean of the top 5 percent of wind speeds, in meters, at the Chuuk location. *A.* Hindcasted (1976–2005) mean of the top 5 percent of wind speeds by month with associated error bars. *B.* Plot of the change in mean of the top 5 percent of 2026–2045 wind speeds for the RCP4.5 scenario from hindcasted top 5 percent of monthly wind speed means. *C.* Plot of the change in mean of the top 5 percent of 2026–2045 wind speeds for the RCP8.5 scenario from hindcasted top 5 percent of monthly wind speed means. *D.* Plot of the change in mean of the top 5 percent of 2081–2100 wind speeds for the RCP4.5 scenario from hindcasted top 5 percent of monthly wind speed means. *E.* Plot of the change in mean of the top 5 percent of 2081–2100 wind speeds for the RCP8.5 scenario from hindcasted top 5 percent of monthly wind speed means.

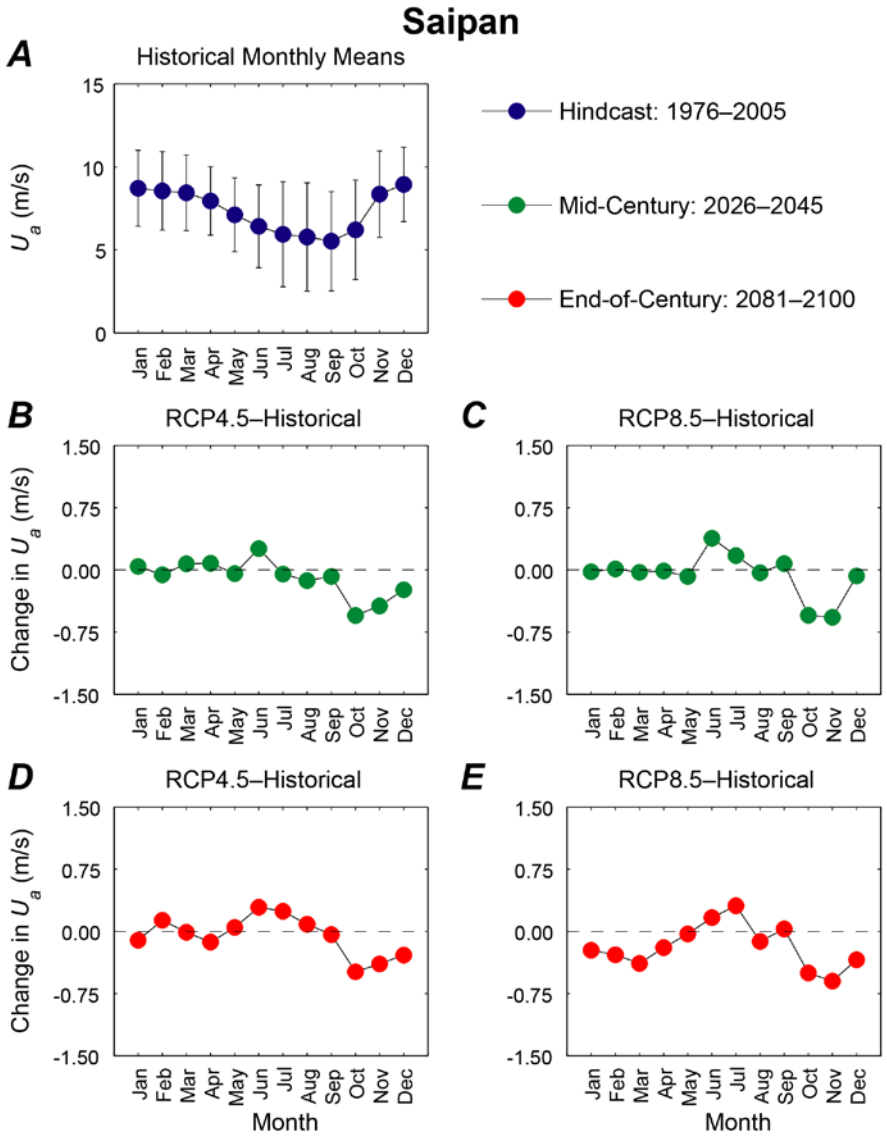

Appendix D11. Plots showing trends in monthly mean wind speed, in meters per second, at the Saipan location. *A.* Hindcasted (1976–2005) mean wind speeds by month with associated error bars. *B.* Plot of the change in mean 2026–2045 wind speeds for the RCP4.5 scenario from hindcasted monthly wind speed means. *C.* Plot of the change in mean 2026–2045 wind speeds for the RCP8.5 scenario from hindcasted monthly wind speed means. *D.* Plot of the change in mean 2081–2100 wind speeds for the RCP4.5 scenario from hindcasted monthly wind speed means. *E.* Plot of the change in mean 2081–2100 wind speeds for the RCP8.5 scenario from hindcasted monthly wind speed means.

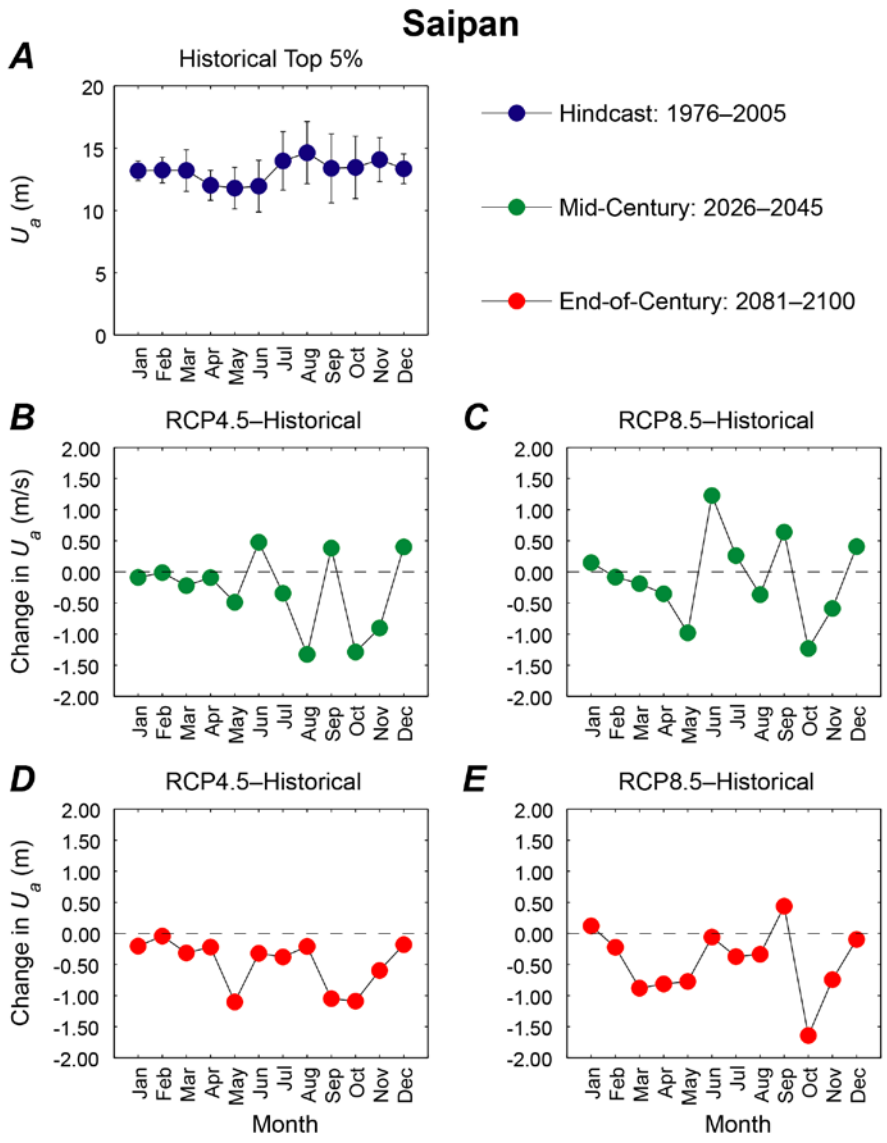

Appendix D12. Plots showing trends in monthly mean of the top 5 percent of wind speeds, in meters, at the Saipan location. *A.* Hindcasted (1976–2005) mean of the top 5 percent of wind speeds by month with associated error bars. *B.* Plot of the change in mean of the top 5 percent of 2026–2045 wind speeds for the RCP4.5 scenario from hindcasted top 5 percent of monthly wind speed means. *C.* Plot of the change in mean of the top 5 percent of 2026–2045 wind speeds for the RCP8.5 scenario from hindcasted top 5 percent of monthly wind speed means. *D.* Plot of the change in mean of the top 5 percent of 2081–2100 wind speeds for the RCP4.5 scenario from hindcasted top 5 percent of monthly wind speed means. *E.* Plot of the change in mean of the top 5 percent of 2081–2100 wind speeds for the RCP8.5 scenario from hindcasted top 5 percent of monthly wind speed means.

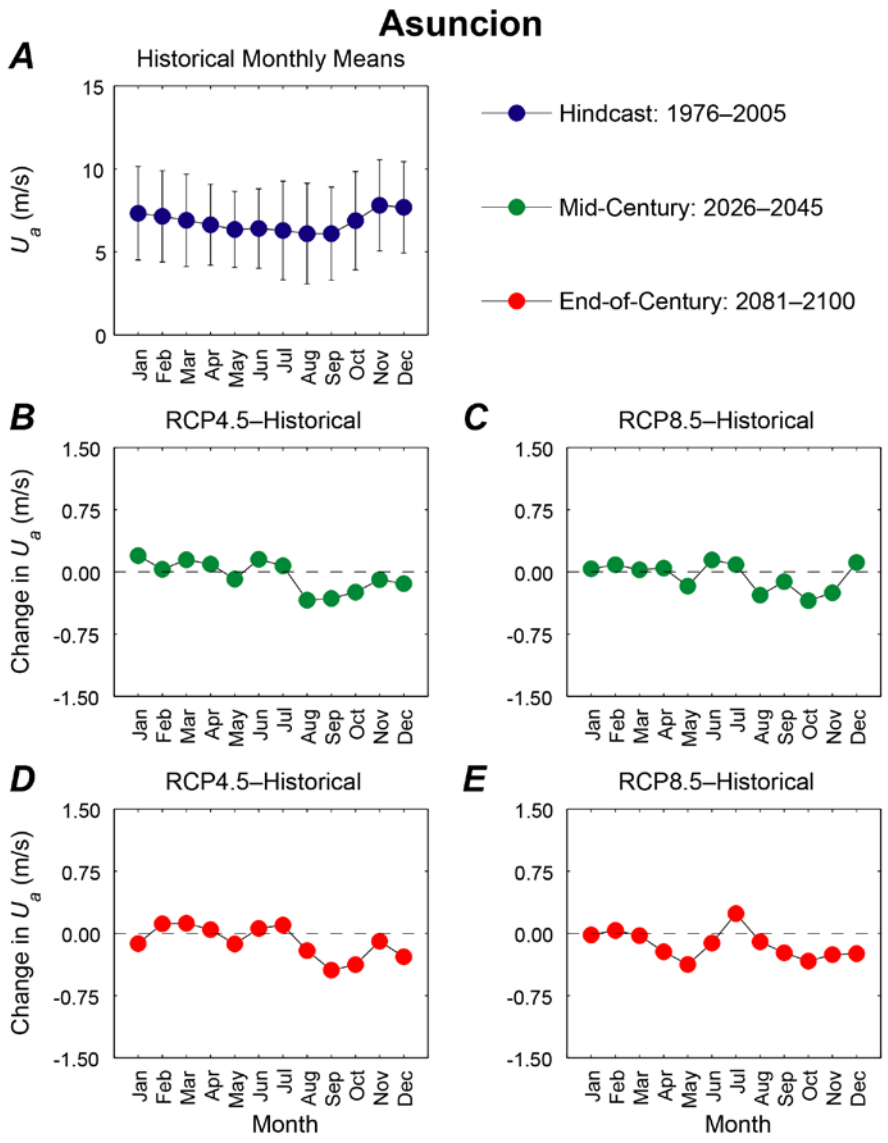

Appendix D13. Plots showing trends in monthly mean wind speed, in meters per second, at the Asuncion location. *A.* Hindcasted (1976–2005) mean wind speeds by month with associated error bars. *B.* Plot of the change in mean 2026–2045 wind speeds for the RCP4.5 scenario from hindcasted monthly wind speed means. *C.* Plot of the change in mean 2026–2045 wind speeds for the RCP8.5 scenario from hindcasted monthly wind speed means. *D.* Plot of the change in mean 2081–2100 wind speeds for the RCP4.5 scenario from hindcasted monthly wind speed means. *E.* Plot of the change in mean 2081–2100 wind speeds for the RCP8.5 scenario from hindcasted monthly wind speed means.

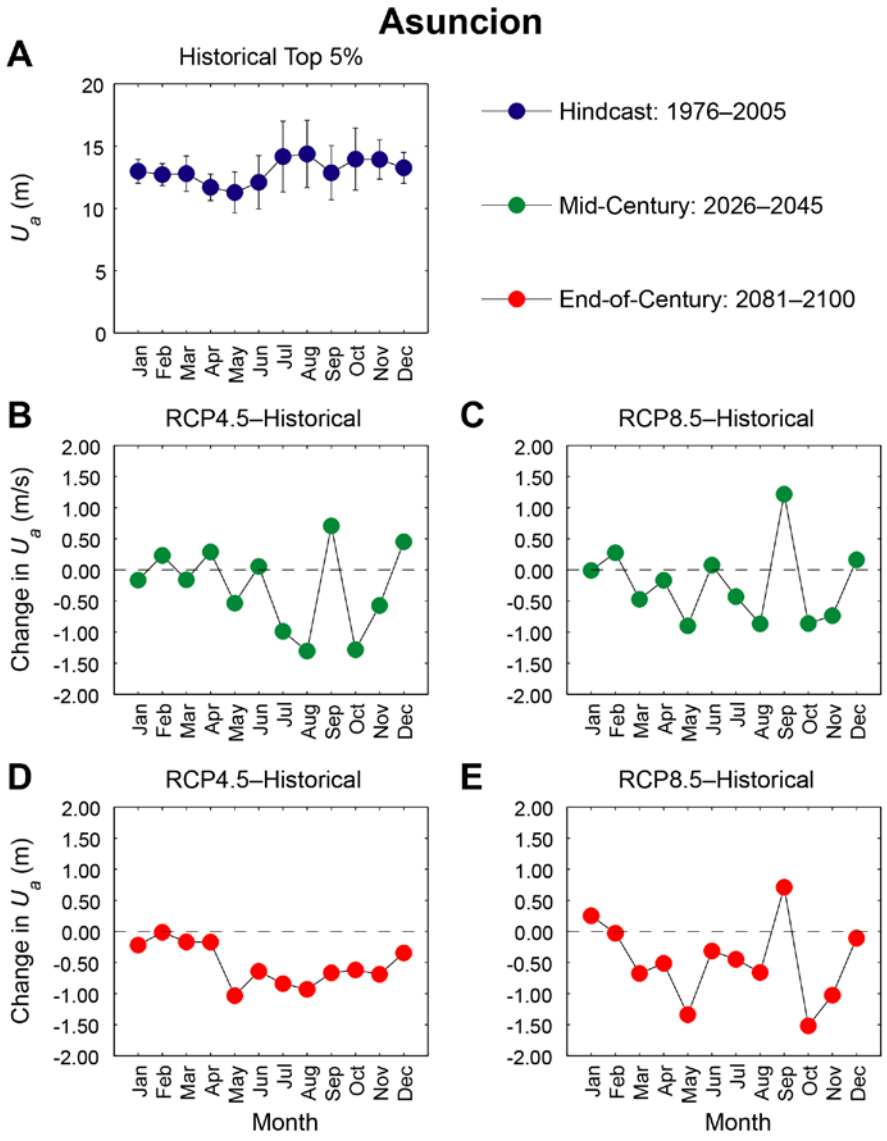

Appendix D14. Plots showing trends in monthly mean of the top 5 percent of wind speeds, in meters, at the Asuncion location. *A.* Hindcasted (1976–2005) mean of the top 5 percent of wind speeds by month with associated error bars. *B.* Plot of the change in mean of the top 5 percent of 2026–2045 wind speeds for the RCP4.5 scenario from hindcasted top 5 percent of monthly wind speed means. *C.* Plot of the change in mean of the top 5 percent of 2026–2045 wind speeds for the RCP8.5 scenario from hindcasted top 5 percent of monthly wind speed means. *D.* Plot of the change in mean of the top 5 percent of 2081–2100 wind speeds for the RCP4.5 scenario from hindcasted top 5 percent of monthly wind speed means. *E.* Plot of the change in mean of the top 5 percent of 2081–2100 wind speeds for the RCP8.5 scenario from hindcasted top 5 percent of monthly wind speed means.

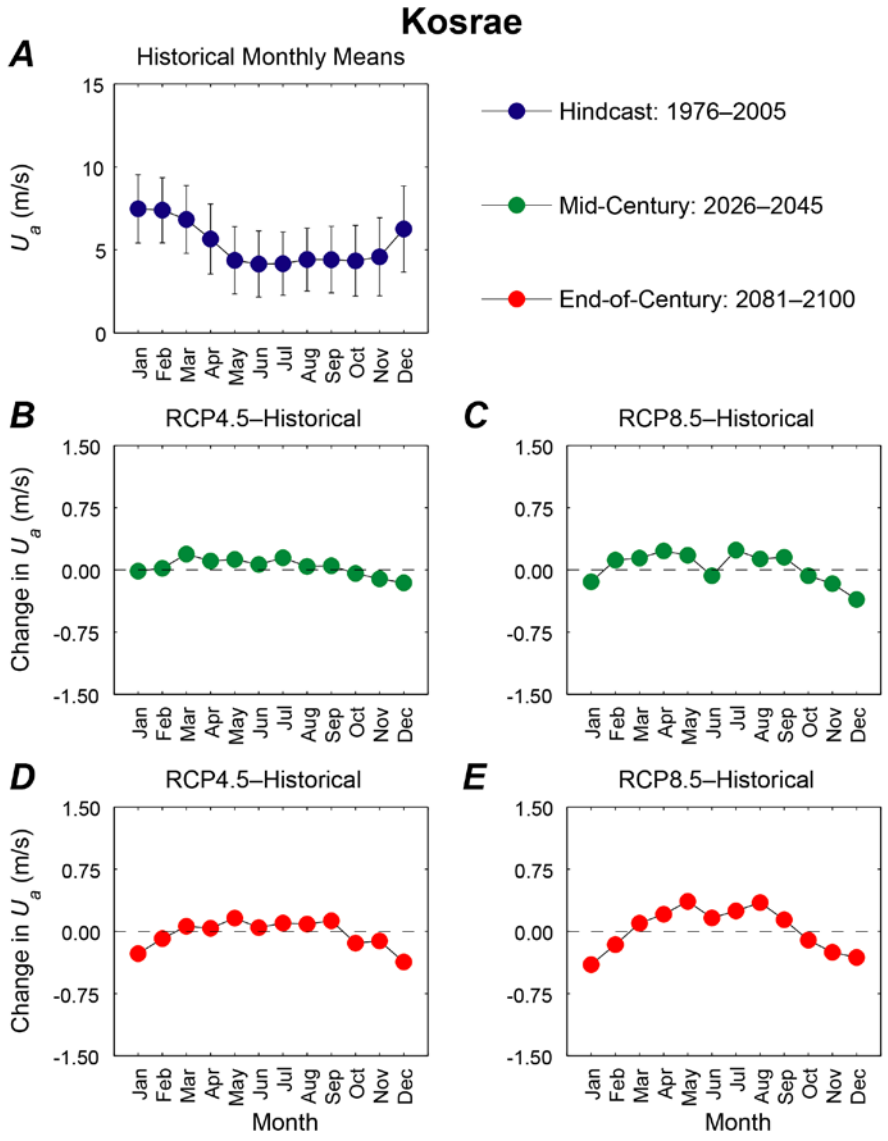

Appendix D15. Plots showing trends in monthly mean wind speed, in meters per second, at the Kosrae location. *A.* Hindcasted (1976–2005) mean wind speeds by month with associated error bars. *B.* Plot of the change in mean 2026–2045 wind speeds for the RCP4.5 scenario from hindcasted monthly wind speed means. *C.* Plot of the change in mean 2026–2045 wind speeds for the RCP8.5 scenario from hindcasted monthly wind speed means. *D.* Plot of the change in mean 2081–2100 wind speeds for the RCP4.5 scenario from hindcasted monthly wind speed means. *E.* Plot of the change in mean 2081–2100 wind speeds for the RCP8.5 scenario from hindcasted monthly wind speed means.

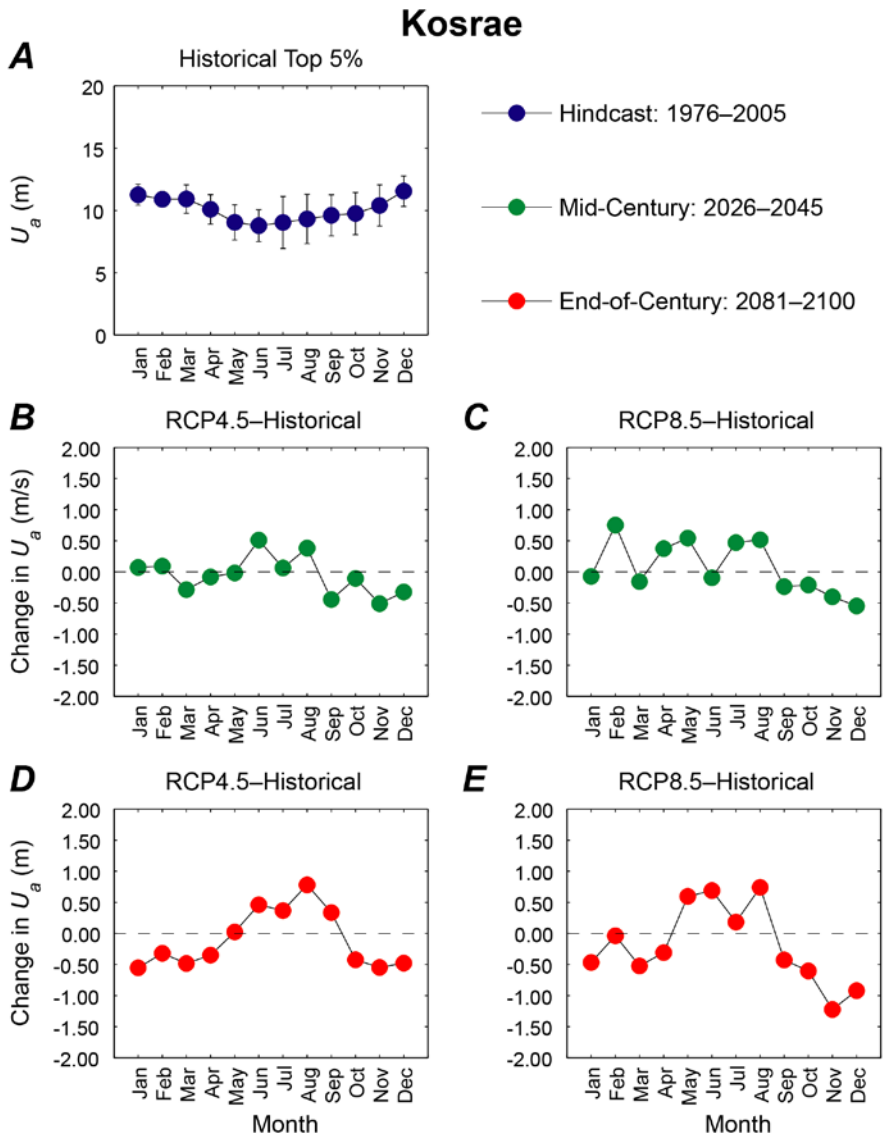

Appendix D16. Plots showing trends in monthly mean of the top 5 percent of wind speeds, in meters, at the Kosrae location. *A.* Hindcasted (1976–2005) mean of the top 5 percent of wind speeds by month with associated error bars. *B.* Plot of the change in mean of the top 5 percent of 2026–2045 wind speeds for the RCP4.5 scenario from hindcasted top 5 percent of monthly wind speed means. *C.* Plot of the change in mean of the top 5 percent of 2026–2045 wind speeds for the RCP8.5 scenario from hindcasted top 5 percent of monthly wind speed means. *D.* Plot of the change in mean of the top 5 percent of 2081–2100 wind speeds for the RCP4.5 scenario from hindcasted top 5 percent of monthly wind speed means. *E.* Plot of the change in mean of the top 5 percent of 2081–2100 wind speeds for the RCP8.5 scenario from hindcasted top 5 percent of monthly wind speed means.

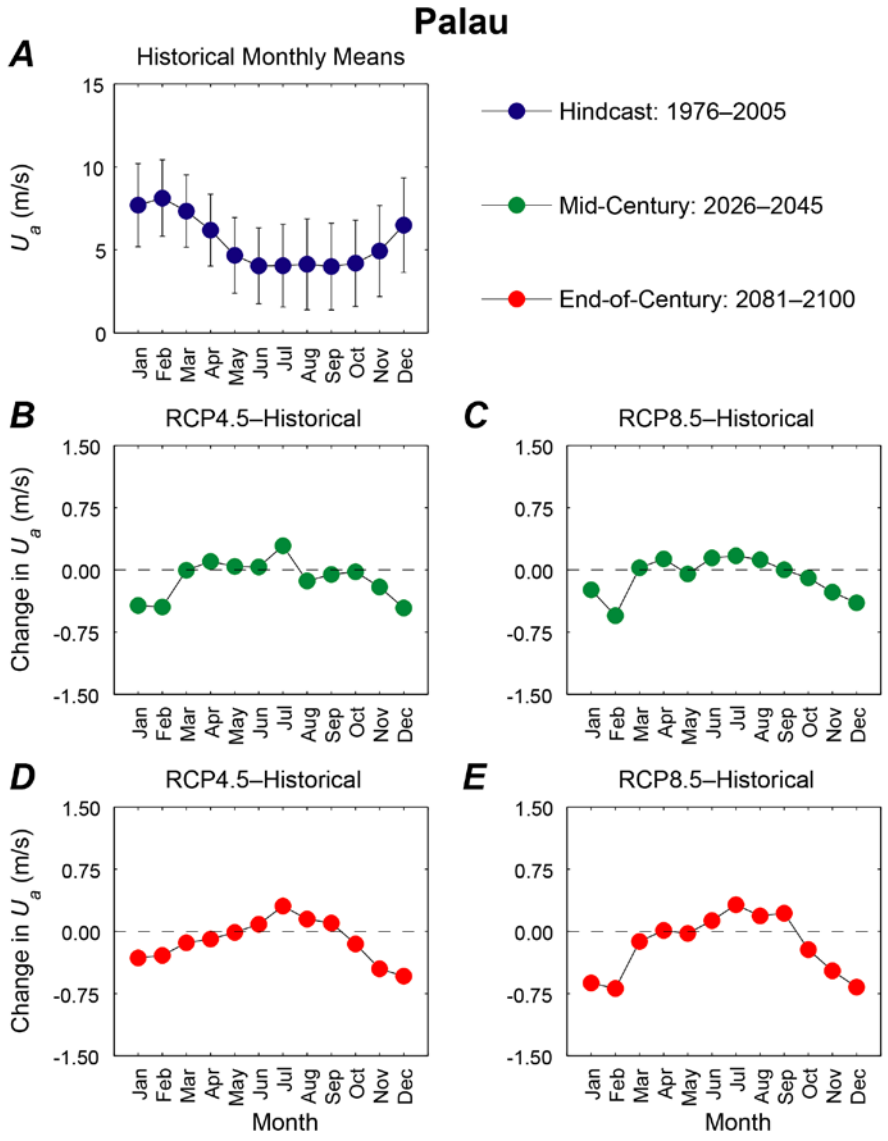

Appendix D17. Plots showing trends in monthly mean wind speed, in meters per second, at the Palau location. *A.* Hindcasted (1976–2005) mean wind speeds by month with associated error bars. *B.* Plot of the change in mean 2026–2045 wind speeds for the RCP4.5 scenario from hindcasted monthly wind speed means. *C.* Plot of the change in mean 2026–2045 wind speeds for the RCP8.5 scenario from hindcasted monthly wind speed means. *D.* Plot of the change in mean 2081–2100 wind speeds for the RCP4.5 scenario from hindcasted monthly wind speed means. *E.* Plot of the change in mean 2081–2100 wind speeds for the RCP8.5 scenario from hindcasted monthly wind speed means.

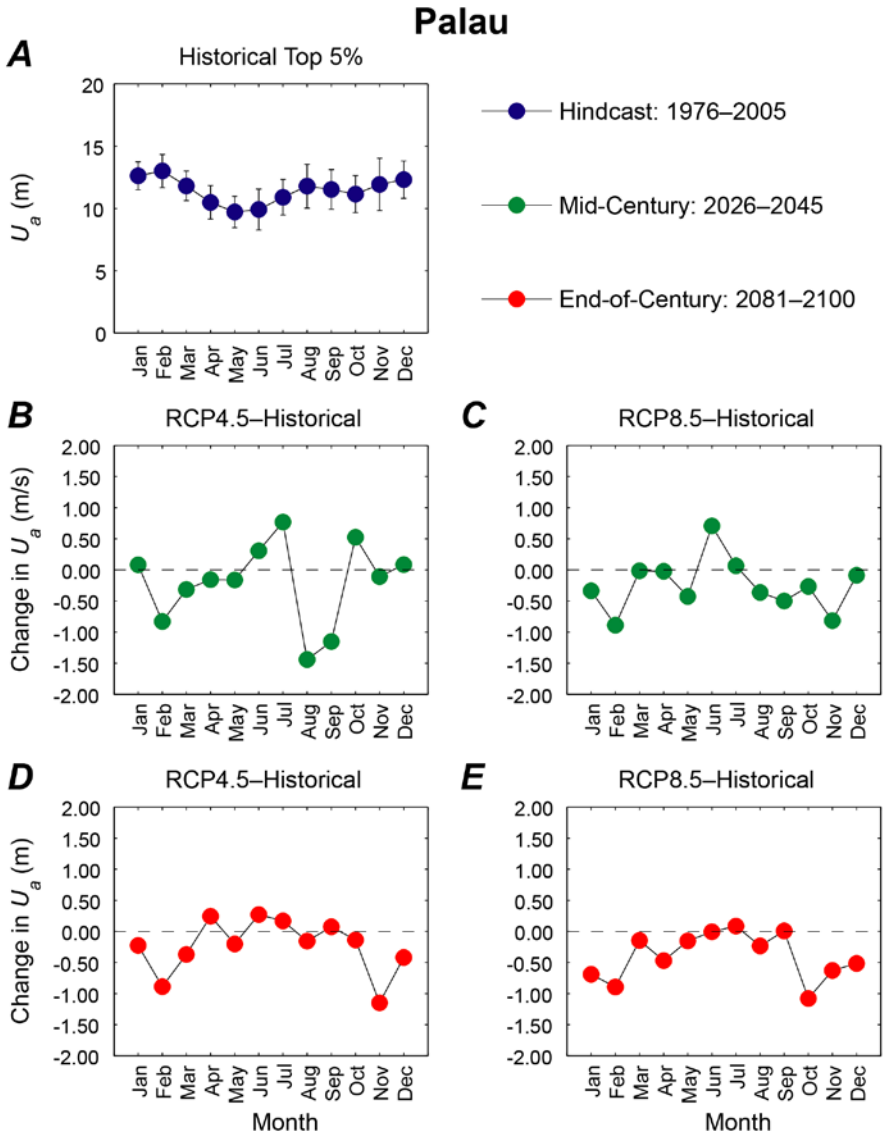

Appendix D18. Plots showing trends in monthly mean of the top 5 percent of wind speeds, in meters, at the Palau location. *A.* Hindcasted (1976–2005) mean of the top 5 percent of wind speeds by month with associated error bars. *B.* Plot of the change in mean of the top 5 percent of 2026–2045 wind speeds for the RCP4.5 scenario from hindcasted top 5 percent of monthly wind speed means. *C.* Plot of the change in mean of the top 5 percent of 2026–2045 wind speeds for the RCP8.5 scenario from hindcasted top 5 percent of monthly wind speed means. *D.* Plot of the change in mean of the top 5 percent of 2081–2100 wind speeds for the RCP4.5 scenario from hindcasted top 5 percent of monthly wind speed means. *E.* Plot of the change in mean of the top 5 percent of 2081–2100 wind speeds for the RCP8.5 scenario from hindcasted top 5 percent of monthly wind speed means.

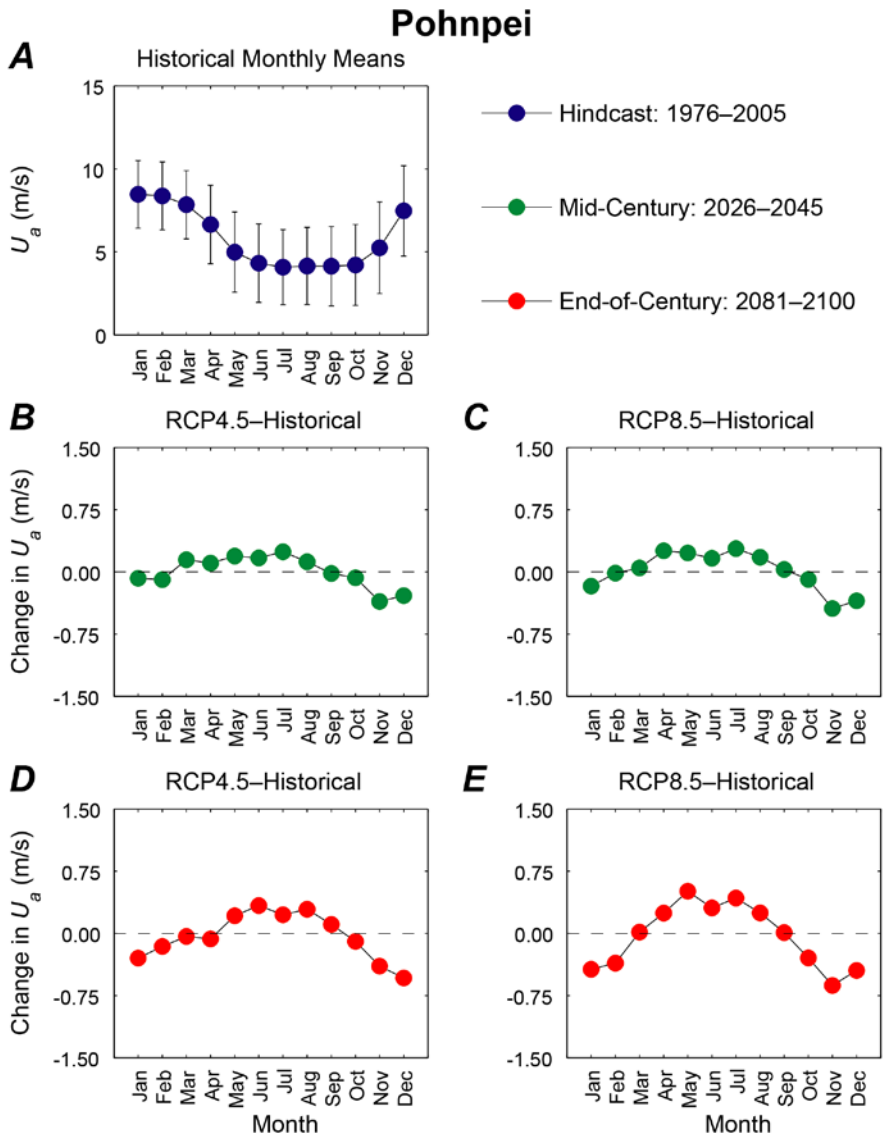

Appendix D19. Plots showing trends in monthly mean wind speed, in meters per second, at the Pohnpei location. *A.* Hindcasted (1976–2005) mean wind speeds by month with associated error bars. *B.* Plot of the change in mean 2026–2045 wind speeds for the RCP4.5 scenario from hindcasted monthly wind speed means. *C.* Plot of the change in mean 2026–2045 wind speeds for the RCP8.5 scenario from hindcasted monthly wind speed means. *D.* Plot of the change in mean 2081–2100 wind speeds for the RCP4.5 scenario from hindcasted monthly wind speed means. *E.* Plot of the change in mean 2081–2100 wind speeds for the RCP8.5 scenario from hindcasted monthly wind speed means.

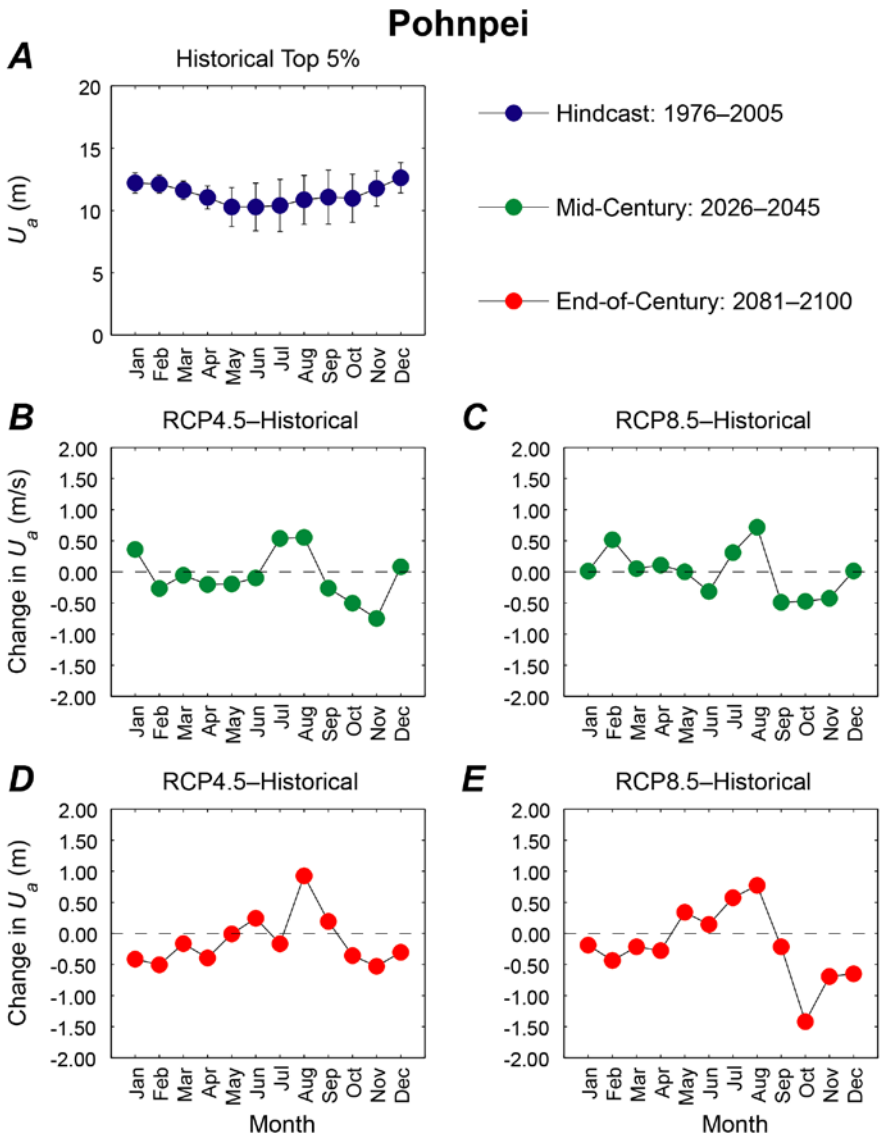

Appendix D20. Plots showing trends in monthly mean of the top 5 percent of wind speeds, in meters, at the Pohnpei location. *A.* Hindcasted (1976–2005) mean of the top 5 percent of wind speeds by month with associated error bars. *B.* Plot of the change in mean of the top 5 percent of 2026–2045 wind speeds for the RCP4.5 scenario from hindcasted top 5 percent of monthly wind speed means. *C.* Plot of the change in mean of the top 5 percent of 2026–2045 wind speeds for the RCP8.5 scenario from hindcasted top 5 percent of monthly wind speed means. *D.* Plot of the change in mean of the top 5 percent of 2081–2100 wind speeds for the RCP4.5 scenario from hindcasted top 5 percent of monthly wind speed means. *E.* Plot of the change in mean of the top 5 percent of 2081–2100 wind speeds for the RCP8.5 scenario from hindcasted top 5 percent of monthly wind speed means.

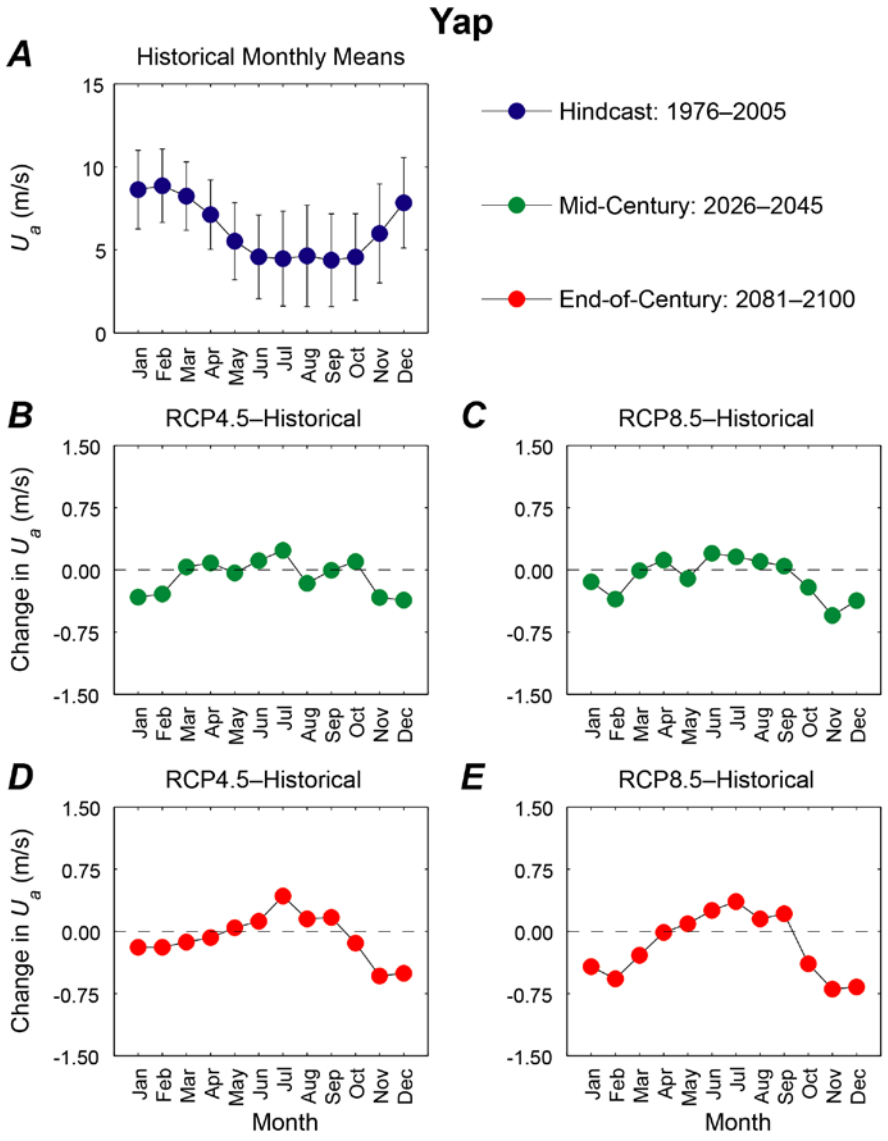

Appendix D21. Plots showing trends in monthly mean wind speed, in meters per second, at the Yap location. *A.* Hindcasted (1976–2005) mean wind speeds by month with associated error bars. *B.* Plot of the change in mean 2026–2045 wind speeds for the RCP4.5 scenario from hindcasted monthly wind speed means. *C.* Plot of the change in mean 2026–2045 wind speeds for the RCP8.5 scenario from hindcasted monthly wind speed means. *D.* Plot of the change in mean 2081–2100 wind speeds for the RCP4.5 scenario from hindcasted monthly wind speed means. *E.* Plot of the change in mean 2081–2100 wind speeds for the RCP8.5 scenario from hindcasted monthly wind speed means.

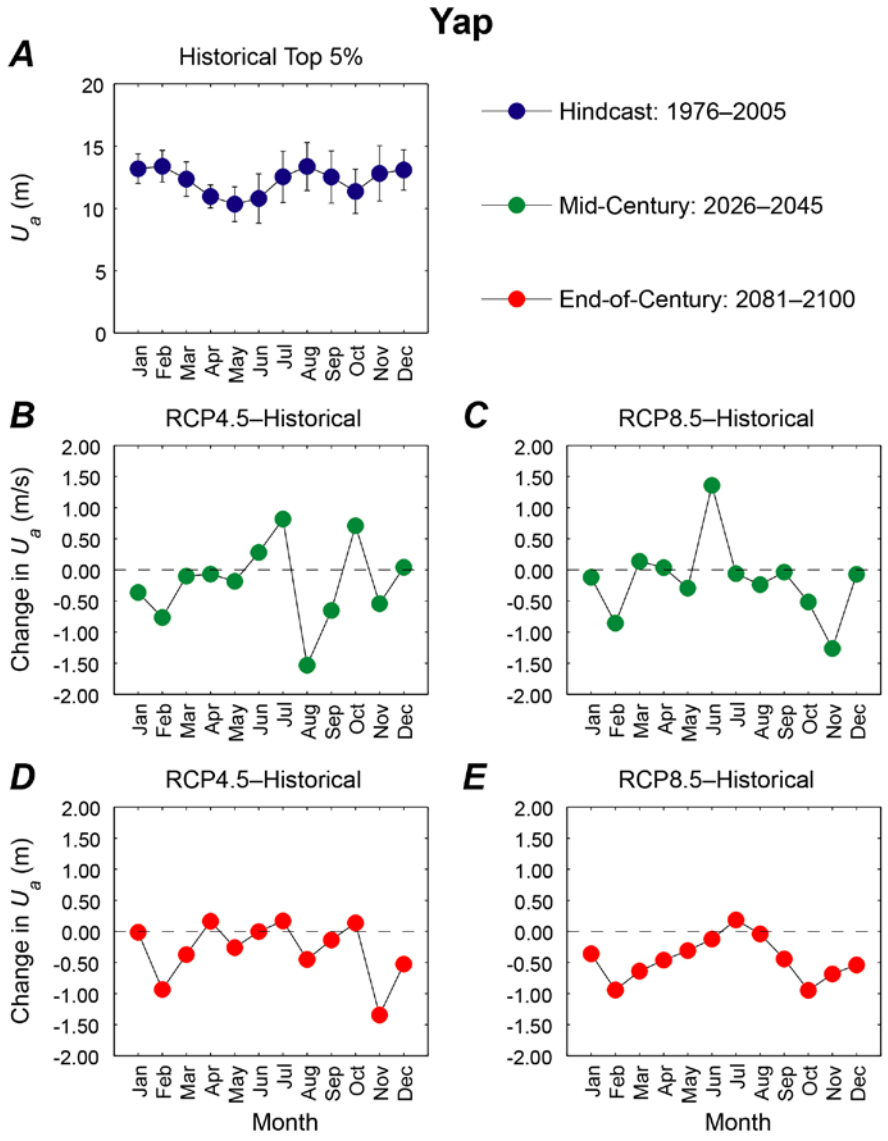

Appendix D22. Plots showing trends in monthly mean of the top 5 percent of wind speeds, in meters, at the Yap location. *A.* Hindcasted (1976–2005) mean of the top 5 percent of wind speeds by month with associated error bars. *B.* Plot of the change in mean of the top 5 percent of 2026–2045 wind speeds for the RCP4.5 scenario from hindcasted top 5 percent of monthly wind speed means. *C.* Plot of the change in mean of the top 5 percent of 2026–2045 wind speeds for the RCP8.5 scenario from hindcasted top 5 percent of monthly wind speed means. *D.* Plot of the change in mean of the top 5 percent of 2081–2100 wind speeds for the RCP4.5 scenario from hindcasted top 5 percent of monthly wind speed means. *E.* Plot of the change in mean of the top 5 percent of 2081–2100 wind speeds for the RCP8.5 scenario from hindcasted top 5 percent of monthly wind speed means.

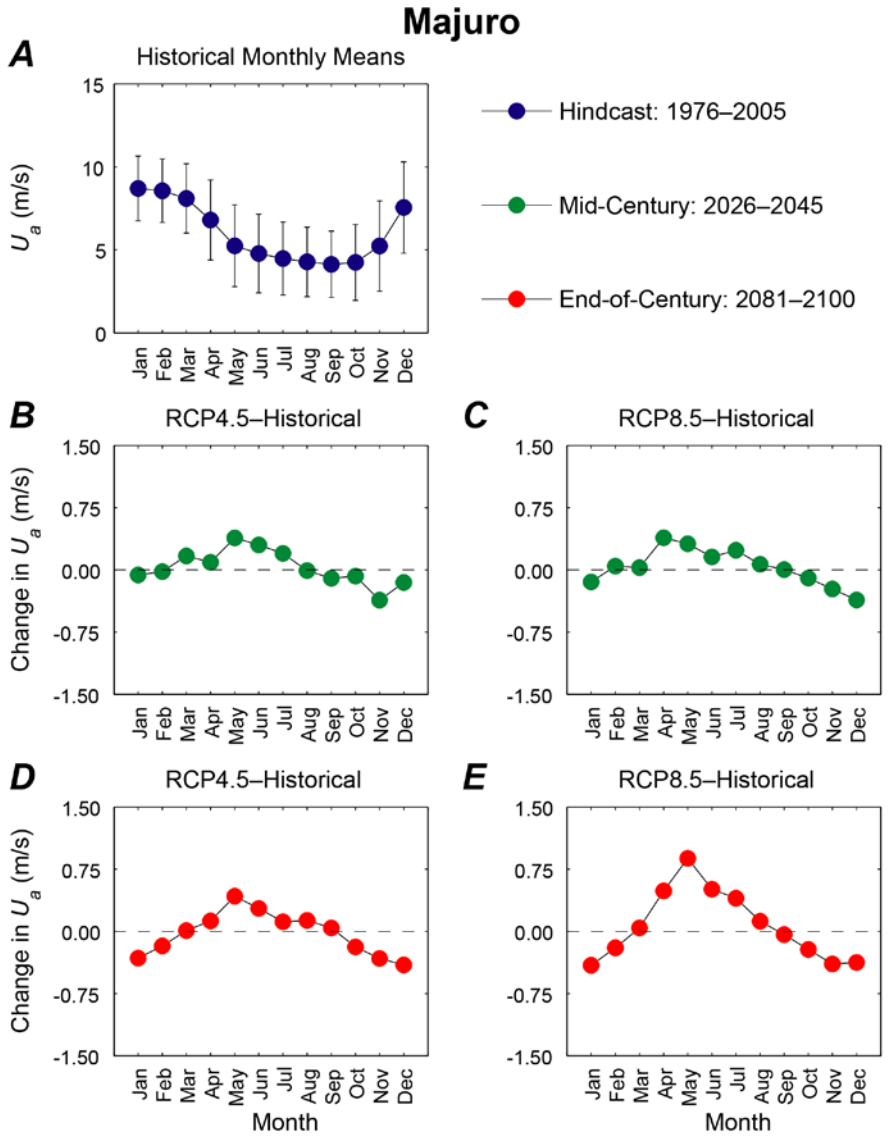

Appendix D23. Plots showing trends in monthly mean wind speed, in meters per second, at the Majuro location. *A.* Hindcasted (1976–2005) mean wind speeds by month with associated error bars. *B.* Plot of the change in mean 2026–2045 wind speeds for the RCP4.5 scenario from hindcasted monthly wind speed means. *C.* Plot of the change in mean 2026–2045 wind speeds for the RCP8.5 scenario from hindcasted monthly wind speed means. *D.* Plot of the change in mean 2081–2100 wind speeds for the RCP4.5 scenario from hindcasted monthly wind speed means. *E.* Plot of the change in mean 2081–2100 wind speeds for the RCP8.5 scenario from hindcasted monthly wind speed means.

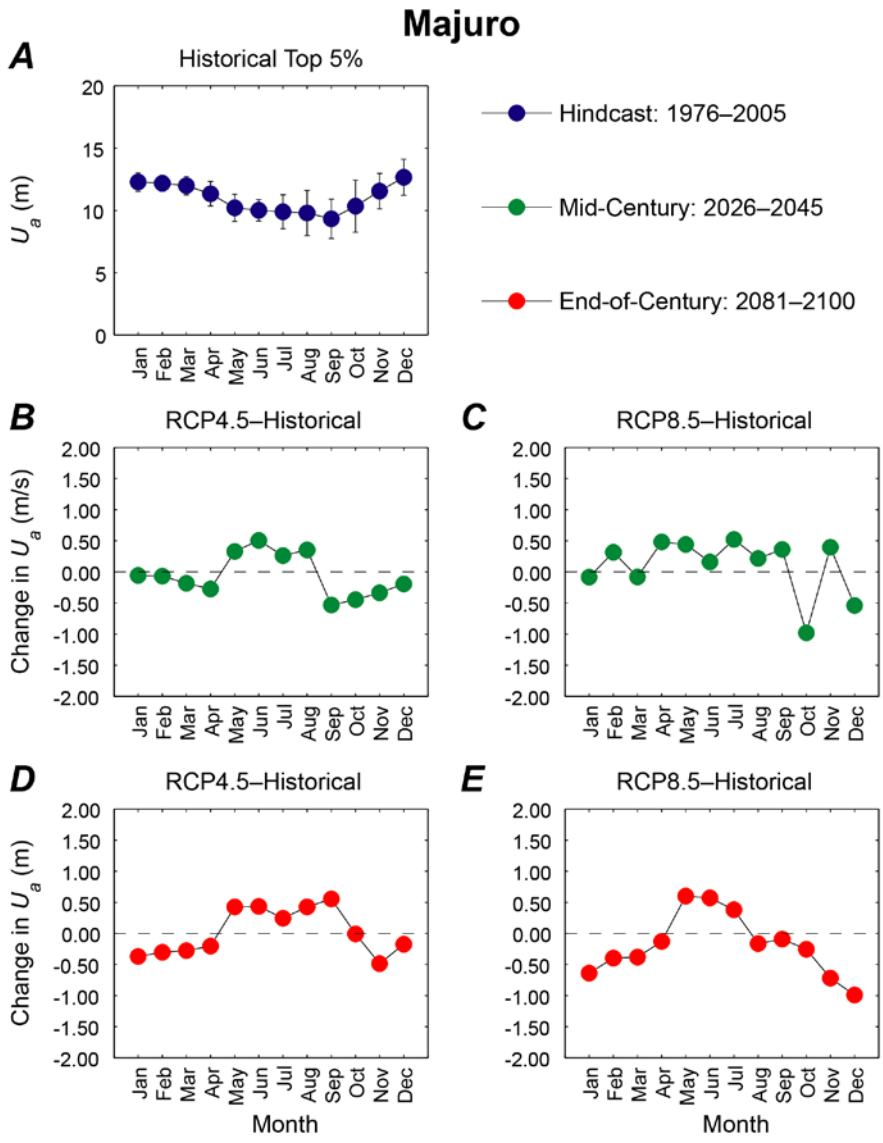

Appendix D24. Plots showing trends in monthly mean of the top 5 percent of wind speeds, in meters, at the Majuro location. *A.* Hindcasted (1976–2005) mean of the top 5 percent of wind speeds by month with associated error bars. *B.* Plot of the change in mean of the top 5 percent of 2026–2045 wind speeds for the RCP4.5 scenario from hindcasted top 5 percent of monthly wind speed means. *C.* Plot of the change in mean of the top 5 percent of 2026–2045 wind speeds for the RCP8.5 scenario from hindcasted top 5 percent of monthly wind speed means. *D.* Plot of the change in mean of the top 5 percent of 2081–2100 wind speeds for the RCP4.5 scenario from hindcasted top 5 percent of monthly wind speed means. *E.* Plot of the change in mean of the top 5 percent of 2081–2100 wind speeds for the RCP8.5 scenario from hindcasted top 5 percent of monthly wind speed means.

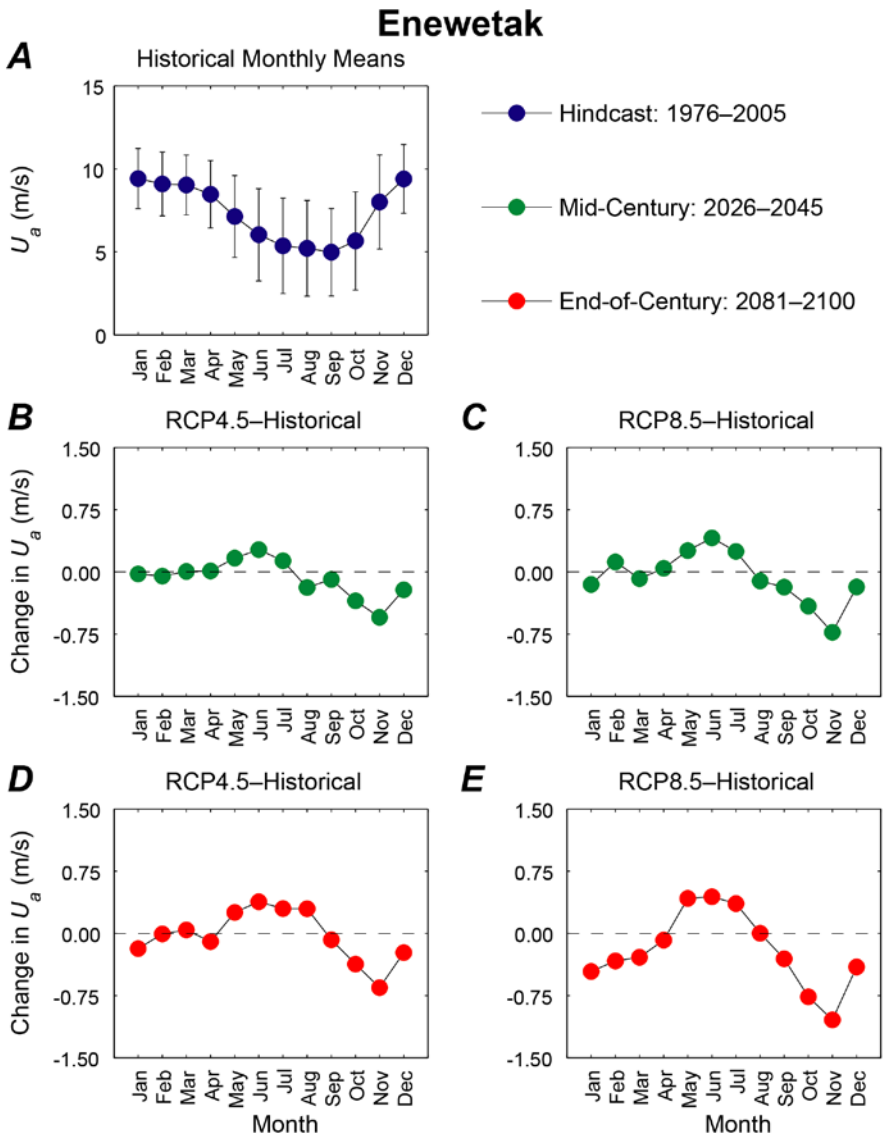

Appendix D25. Plots showing trends in monthly mean wind speed, in meters per second, at the Enewetak location. *A.* Hindcasted (1976–2005) mean wind speeds by month with associated error bars. *B.* Plot of the change in mean 2026–2045 wind speeds for the RCP4.5 scenario from hindcasted monthly wind speed means. *C.* Plot of the change in mean 2026–2045 wind speeds for the RCP8.5 scenario from hindcasted monthly wind speed means. *D.* Plot of the change in mean 2081–2100 wind speeds for the RCP4.5 scenario from hindcasted monthly wind speed means. *E.* Plot of the change in mean 2081–2100 wind speeds for the RCP8.5 scenario from hindcasted monthly wind speed means.

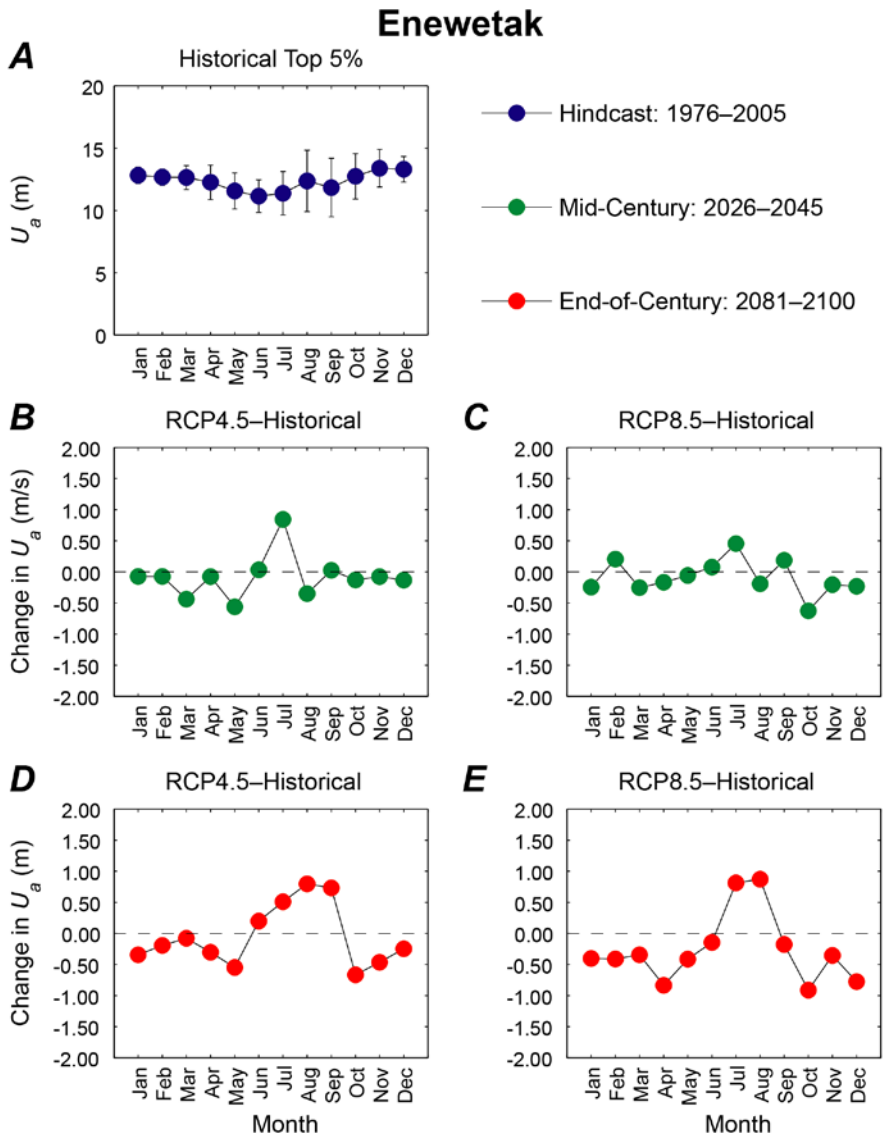

Appendix D26. Plots showing trends in monthly mean of the top 5 percent of wind speeds, in meters, at the Enewetak location. *A.* Hindcasted (1976–2005) mean of the top 5 percent of wind speeds by month with associated error bars. *B.* Plot of the change in mean of the top 5 percent of 2026–2045 wind speeds for the RCP4.5 scenario from hindcasted top 5 percent of monthly wind speed means. *C.* Plot of the change in mean of the top 5 percent of 2026–2045 wind speeds for the RCP8.5 scenario from hindcasted top 5 percent of monthly wind speed means. *D.* Plot of the change in mean of the top 5 percent of 2081–2100 wind speeds for the RCP4.5 scenario from hindcasted top 5 percent of monthly wind speed means. *E.* Plot of the change in mean of the top 5 percent of 2081–2100 wind speeds for the RCP8.5 scenario from hindcasted top 5 percent of monthly wind speed means.

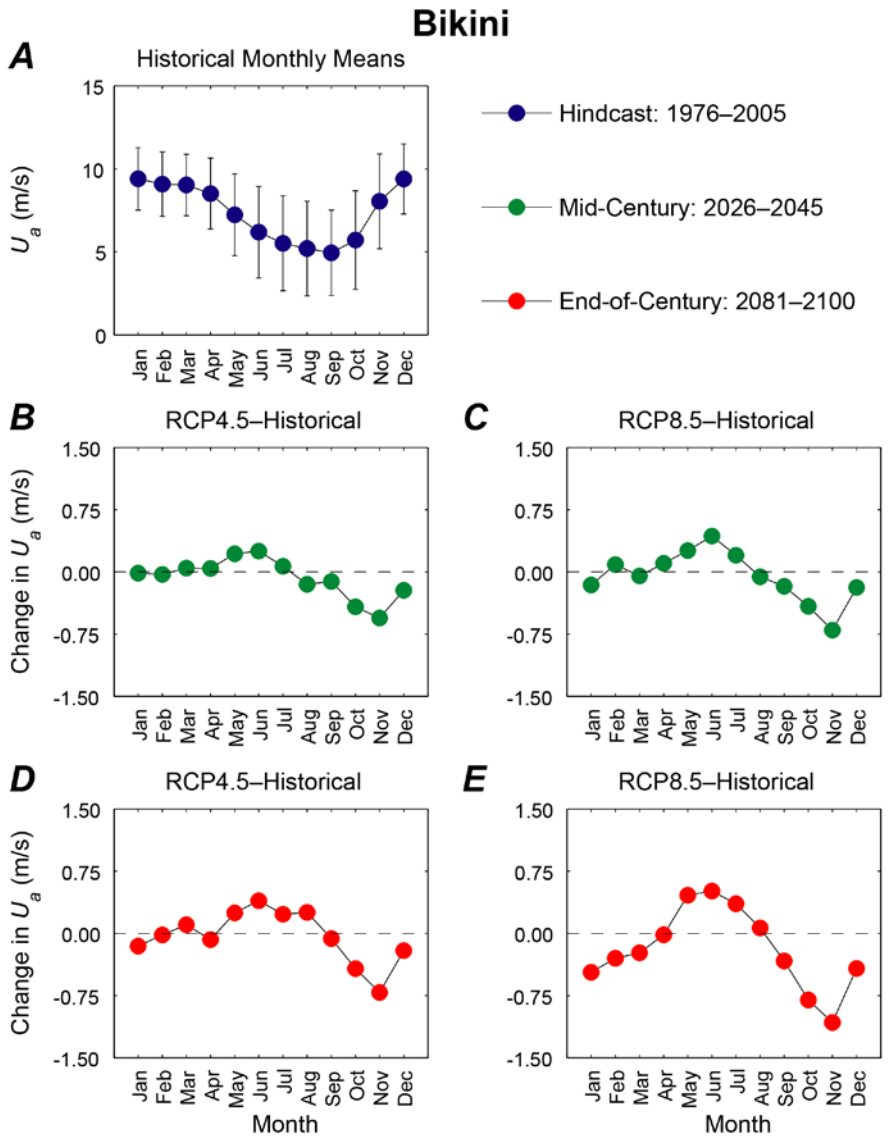

Appendix D27. Plots showing trends in monthly mean wind speed, in meters per second, at the Bikini location. *A.* Hindcasted (1976–2005) mean wind speeds by month with associated error bars. *B.* Plot of the change in mean 2026–2045 wind speeds for the RCP4.5 scenario from hindcasted monthly wind speed means. *C.* Plot of the change in mean 2026–2045 wind speeds for the RCP8.5 scenario from hindcasted monthly wind speed means. *D.* Plot of the change in mean 2081–2100 wind speeds for the RCP4.5 scenario from hindcasted monthly wind speed means. *E.* Plot of the change in mean 2081–2100 wind speeds for the RCP8.5 scenario from hindcasted monthly wind speed means.

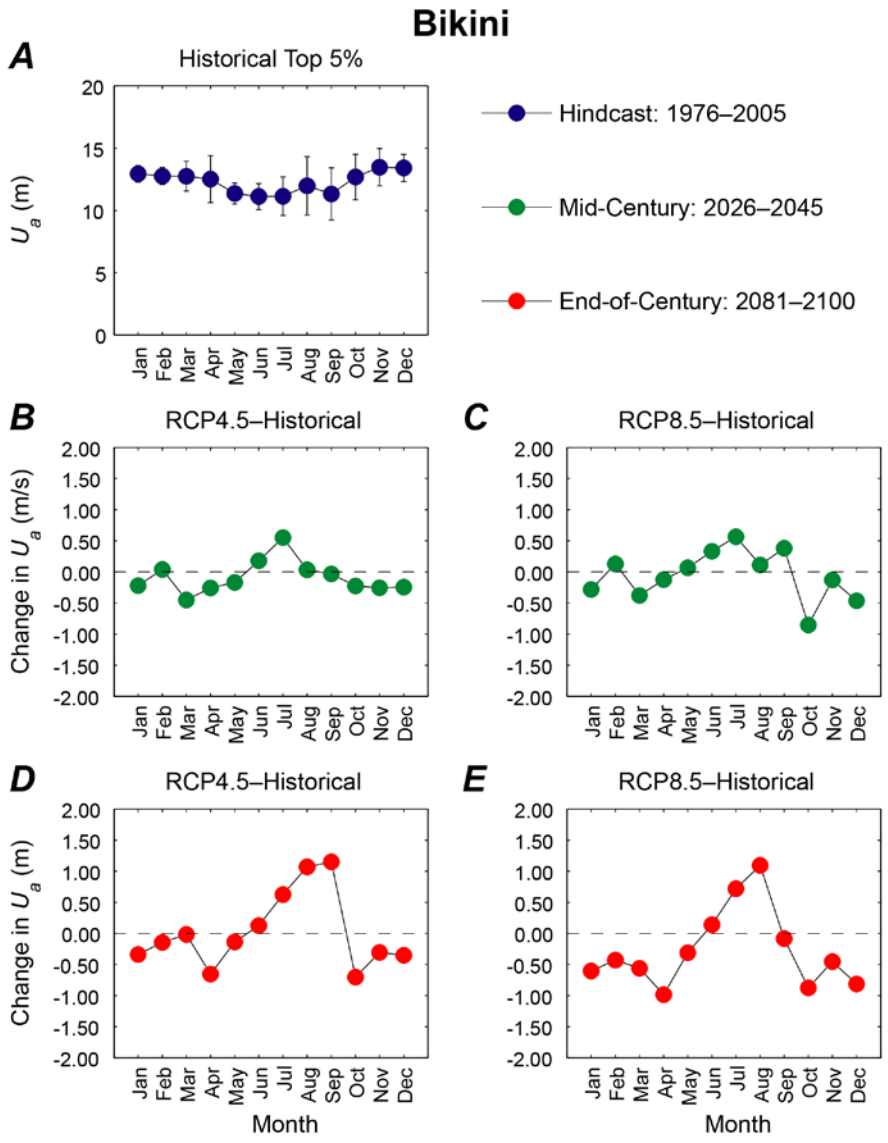

Appendix D28. Plots showing trends in monthly mean of the top 5 percent of wind speeds, in meters, at the Bikini location. *A.* Hindcasted (1976–2005) mean of the top 5 percent of wind speeds by month with associated error bars. *B.* Plot of the change in mean of the top 5 percent of 2026–2045 wind speeds for the RCP4.5 scenario from hindcasted top 5 percent of monthly wind speed means. *C.* Plot of the change in mean of the top 5 percent of 2026–2045 wind speeds for the RCP8.5 scenario from hindcasted top 5 percent of monthly wind speed means. *D.* Plot of the change in mean of the top 5 percent of 2081–2100 wind speeds for the RCP4.5 scenario from hindcasted top 5 percent of monthly wind speed means. *E.* Plot of the change in mean of the top 5 percent of 2081–2100 wind speeds for the RCP8.5 scenario from hindcasted top 5 percent of monthly wind speed means.

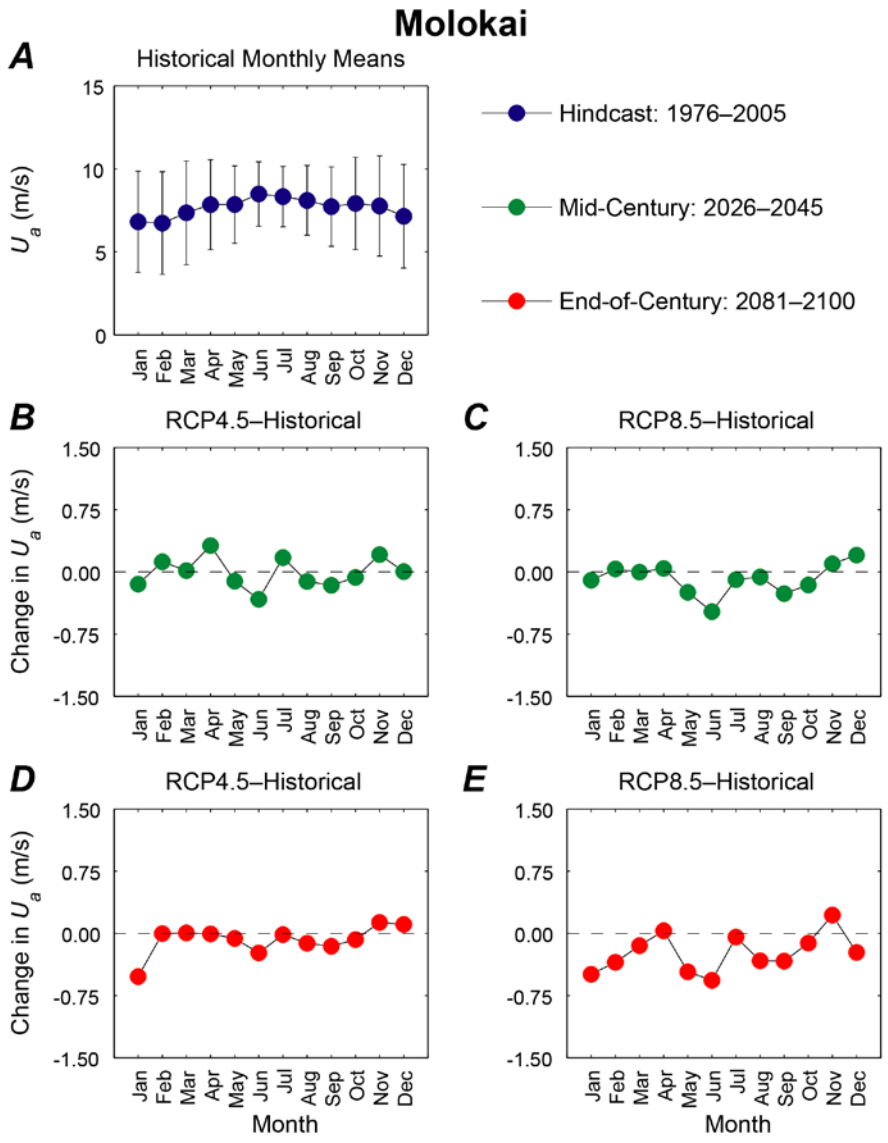

Appendix D29. Plots showing trends in monthly mean wind speed, in meters per second, at the Molokai location. *A.* Hindcasted (1976–2005) mean wind speeds by month with associated error bars. *B.* Plot of the change in mean 2026–2045 wind speeds for the RCP4.5 scenario from hindcasted monthly wind speed means. *C.* Plot of the change in mean 2026–2045 wind speeds for the RCP8.5 scenario from hindcasted monthly wind speed means. *D.* Plot of the change in mean 2081–2100 wind speeds for the RCP4.5 scenario from hindcasted monthly wind speed means. *E.* Plot of the change in mean 2081–2100 wind speeds for the RCP8.5 scenario from hindcasted monthly wind speed means.

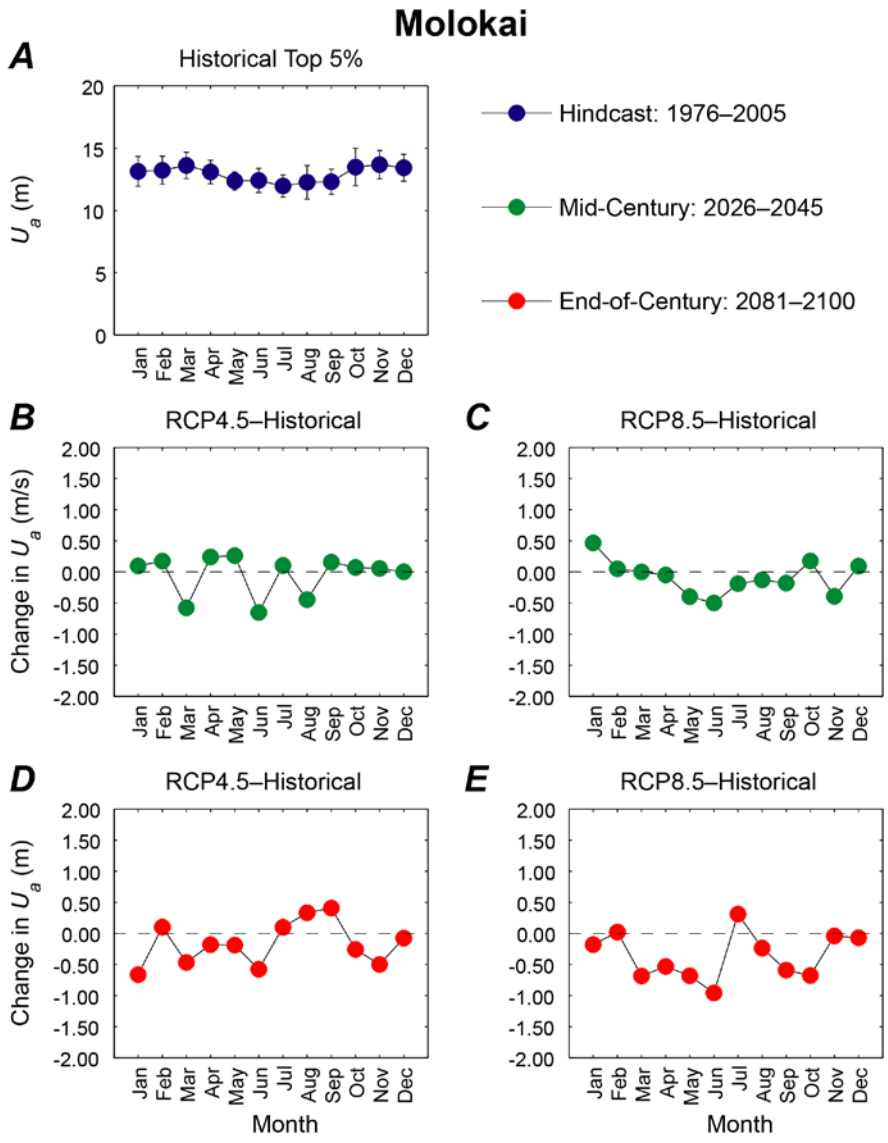

Appendix D30. Plots showing trends in monthly mean of the top 5 percent of wind speeds, in meters, at the Molokai location. *A.* Hindcasted (1976–2005) mean of the top 5 percent of wind speeds by month with associated error bars. *B.* Plot of the change in mean of the top 5 percent of 2026–2045 wind speeds for the RCP4.5 scenario from hindcasted top 5 percent of monthly wind speed means. *C.* Plot of the change in mean of the top 5 percent of 2026–2045 wind speeds for the RCP8.5 scenario from hindcasted top 5 percent of monthly wind speed means. *D.* Plot of the change in mean of the top 5 percent of 2081–2100 wind speeds for the RCP4.5 scenario from hindcasted top 5 percent of monthly wind speed means. *E.* Plot of the change in mean of the top 5 percent of 2081–2100 wind speeds for the RCP8.5 scenario from hindcasted top 5 percent of monthly wind speed means.

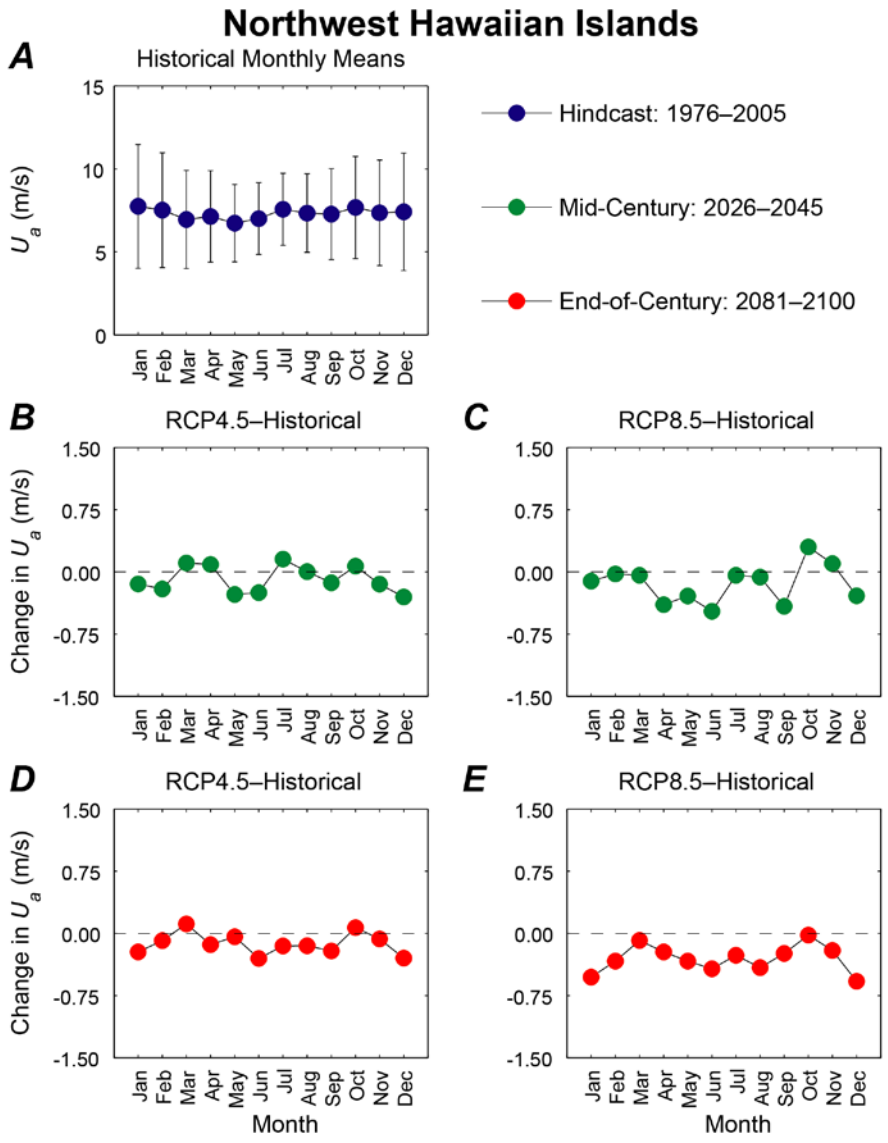

Appendix D31. Plots showing trends in monthly mean wind speed, in meters per second, at the Northwest Hawaiian Islands location. *A.* Hindcasted (1976–2005) mean wind speeds by month with associated error bars. *B.* Plot of the change in mean 2026–2045 wind speeds for the RCP4.5 scenario from hindcasted monthly wind speed means. *C.* Plot of the change in mean 2026–2045 wind speeds for the RCP8.5 scenario from hindcasted monthly wind speed means. *D.* Plot of the change in mean 2081–2100 wind speeds for the RCP4.5 scenario from hindcasted monthly wind speed means. *E.* Plot of the change in mean 2081–2100 wind speeds for the RCP8.5 scenario from hindcasted monthly wind speed means.

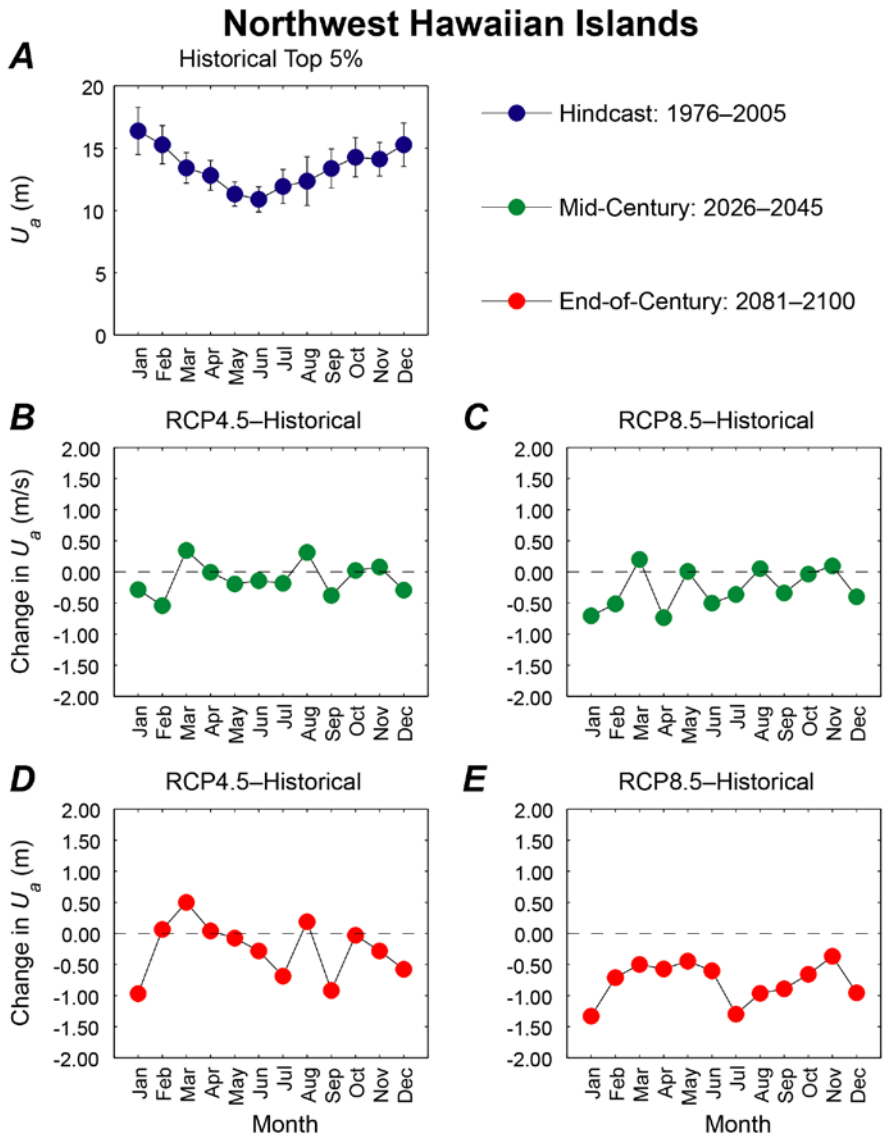

Appendix D32. Plots showing trends in monthly mean of the top 5 percent of wind speeds, in meters, at the Northwest Hawaiian Islands location. *A.* Hindcasted (1976–2005) mean of the top 5 percent of wind speeds by month with associated error bars. *B.* Plot of the change in mean of the top 5 percent of 2026–2045 wind speeds for the RCP4.5 scenario from hindcasted top 5 percent of monthly wind speed means. *C.* Plot of the change in mean of the top 5 percent of 2026–2045 wind speeds for the RCP8.5 scenario from hindcasted top 5 percent of monthly wind speed means. *D.* Plot of the change in mean of the top 5 percent of 2081–2100 wind speeds for the RCP4.5 scenario from hindcasted top 5 percent of monthly wind speed means. *E.* Plot of the change in mean of the top 5 percent of 2081–2100 wind speeds for the RCP8.5 scenario from hindcasted top 5 percent of monthly wind speed means.

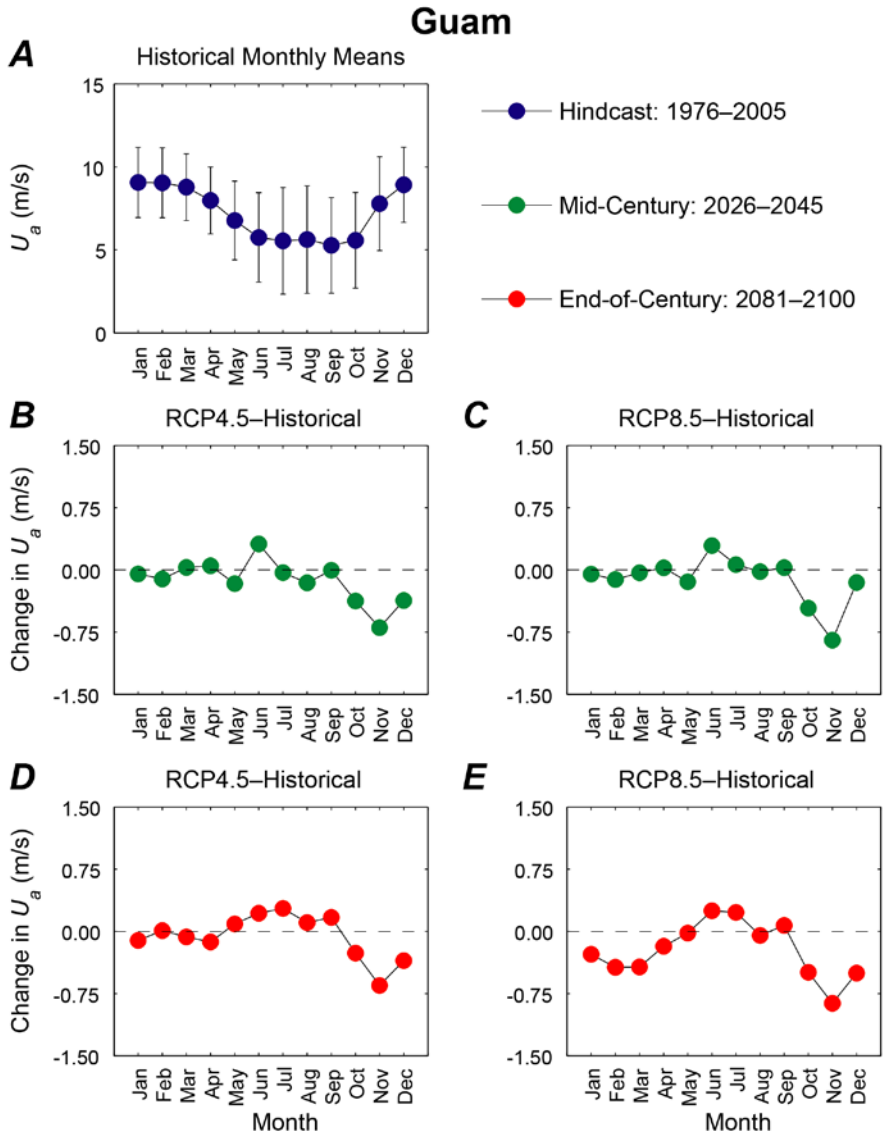

Appendix D33. Plots showing trends in monthly mean wind speed, in meters per second, at the Guam location. *A.* Hindcasted (1976–2005) mean wind speeds by month with associated error bars. *B.* Plot of the change in mean 2026–2045 wind speeds for the RCP4.5 scenario from hindcasted monthly wind speed means. *C.* Plot of the change in mean 2026–2045 wind speeds for the RCP8.5 scenario from hindcasted monthly wind speed means. *D.* Plot of the change in mean 2081–2100 wind speeds for the RCP4.5 scenario from hindcasted monthly wind speed means. *E.* Plot of the change in mean 2081–2100 wind speeds for the RCP8.5 scenario from hindcasted monthly wind speed means.

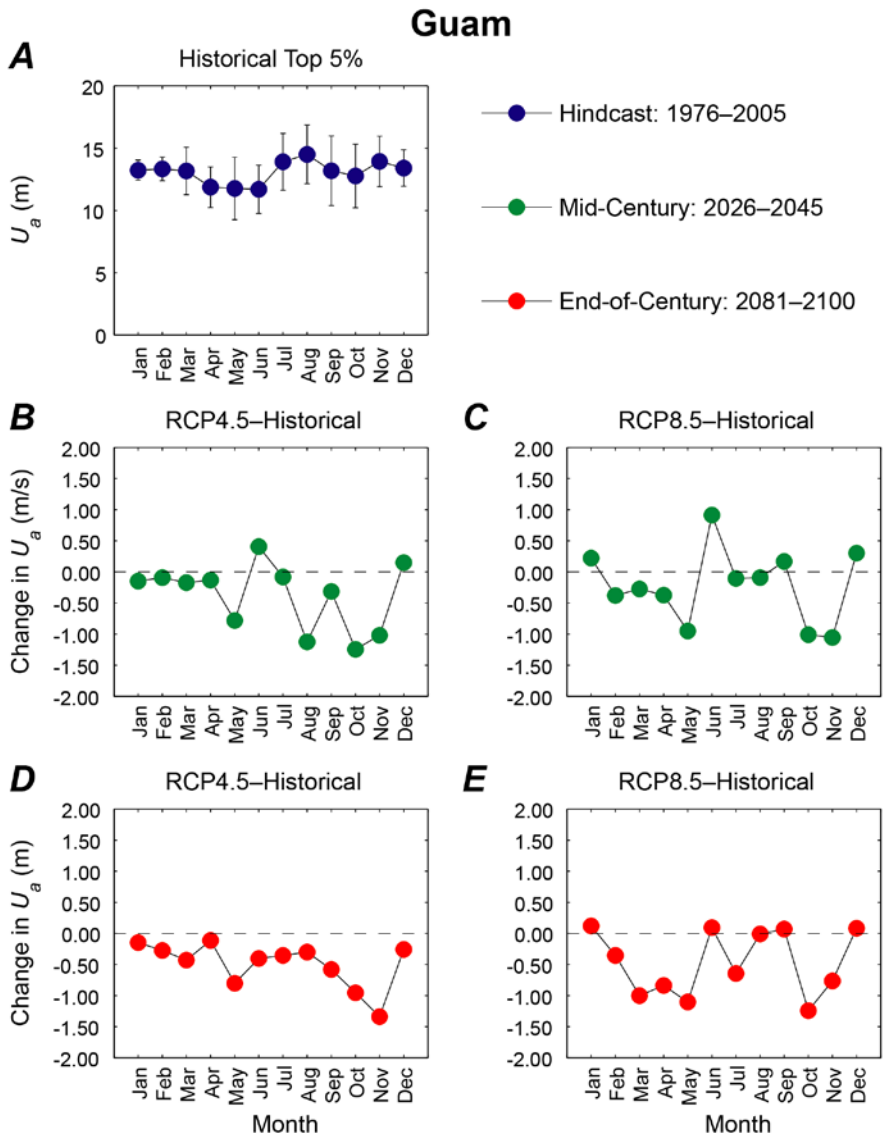

Appendix D34. Plots showing trends in monthly mean of the top 5 percent of wind speeds, in meters, at the Guam location. *A.* Hindcasted (1976–2005) mean of the top 5 percent of wind speeds by month with associated error bars. *B.* Plot of the change in mean of the top 5 percent of 2026–2045 wind speeds for the RCP4.5 scenario from hindcasted top 5 percent of monthly wind speed means. *C.* Plot of the change in mean of the top 5 percent of 2026–2045 wind speeds for the RCP8.5 scenario from hindcasted top 5 percent of monthly wind speed means. *D.* Plot of the change in mean of the top 5 percent of 2081–2100 wind speeds for the RCP4.5 scenario from hindcasted top 5 percent of monthly wind speed means. *E.* Plot of the change in mean of the top 5 percent of 2081–2100 wind speeds for the RCP8.5 scenario from hindcasted top 5 percent of monthly wind speed means.

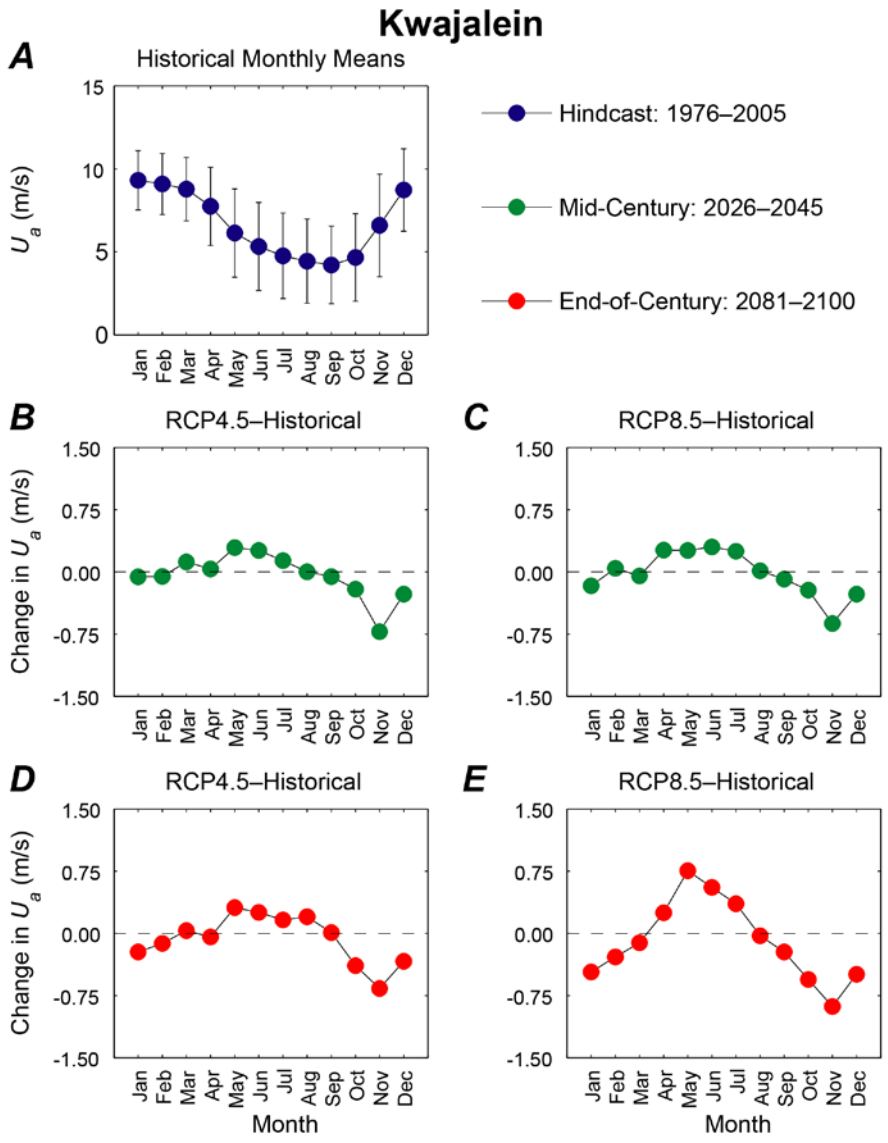

Appendix D35. Plots showing trends in monthly mean wind speed, in meters per second, at the Kwajalein location. *A.* Hindcasted (1976–2005) mean wind speeds by month with associated error bars. *B.* Plot of the change in mean 2026–2045 wind speeds for the RCP4.5 scenario from hindcasted monthly wind speed means. *C.* Plot of the change in mean 2026–2045 wind speeds for the RCP8.5 scenario from hindcasted monthly wind speed means. *D.* Plot of the change in mean 2081–2100 wind speeds for the RCP4.5 scenario from hindcasted monthly wind speed means. *E.* Plot of the change in mean 2081–2100 wind speeds for the RCP8.5 scenario from hindcasted monthly wind speed means.

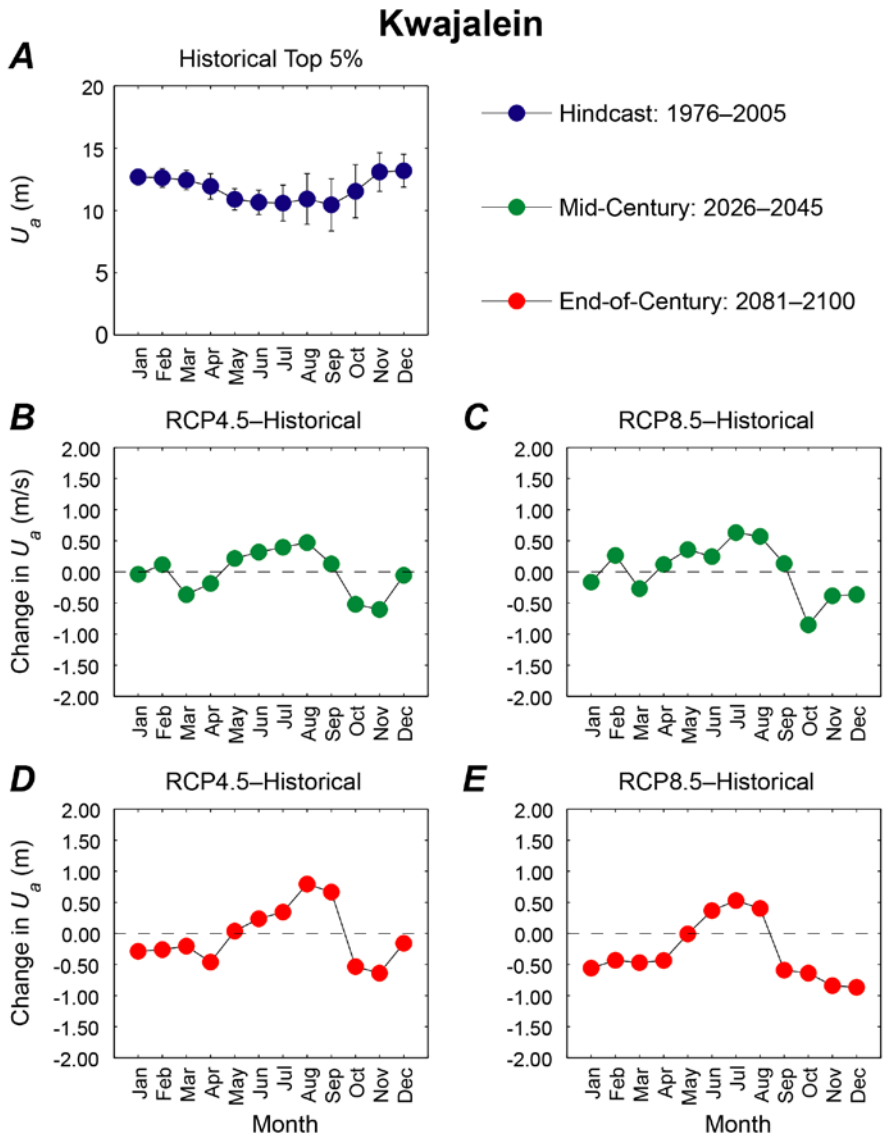

Appendix D36. Plots showing trends in monthly mean of the top 5 percent of wind speeds, in meters, at the Kwajalein location. *A.* Hindcasted (1976–2005) mean of the top 5 percent of wind speeds by month with associated error bars. *B.* Plot of the change in mean of the top 5 percent of 2026–2045 wind speeds for the RCP4.5 scenario from hindcasted top 5 percent of monthly wind speed means. *C.* Plot of the change in mean of the top 5 percent of 2026–2045 wind speeds for the RCP8.5 scenario from hindcasted top 5 percent of monthly wind speed means. *D.* Plot of the change in mean of the top 5 percent of 2081–2100 wind speeds for the RCP4.5 scenario from hindcasted top 5 percent of monthly wind speed means. *E.* Plot of the change in mean of the top 5 percent of 2081–2100 wind speeds for the RCP8.5 scenario from hindcasted top 5 percent of monthly wind speed means.

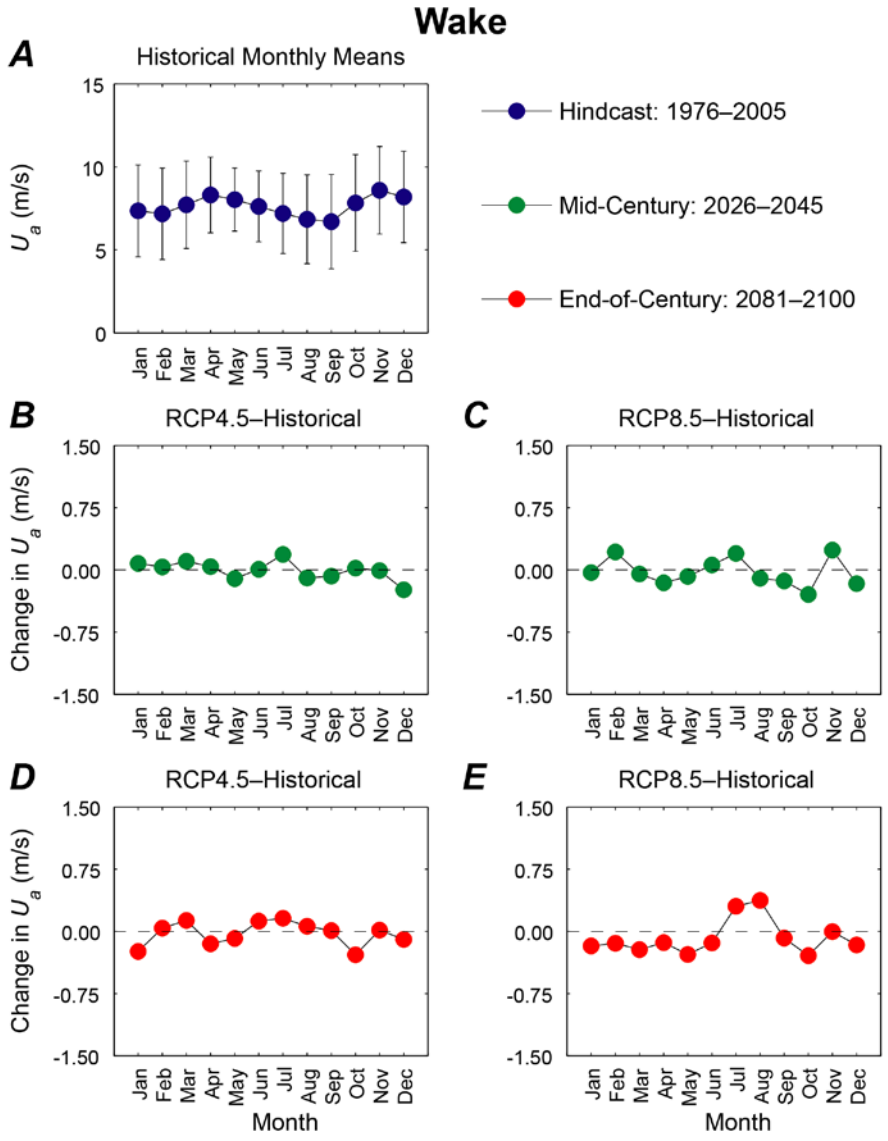

Appendix D37. Plots showing trends in monthly mean wind speed, in meters per second, at the Wake location. *A.* Hindcasted (1976–2005) mean wind speeds by month with associated error bars. *B.* Plot of the change in mean 2026–2045 wind speeds for the RCP4.5 scenario from hindcasted monthly wind speed means. *C.* Plot of the change in mean 2026–2045 wind speeds for the RCP8.5 scenario from hindcasted monthly wind speed means. *D.* Plot of the change in mean 2081–2100 wind speeds for the RCP4.5 scenario from hindcasted monthly wind speed means. *E.* Plot of the change in mean 2081–2100 wind speeds for the RCP8.5 scenario from hindcasted monthly wind speed means.

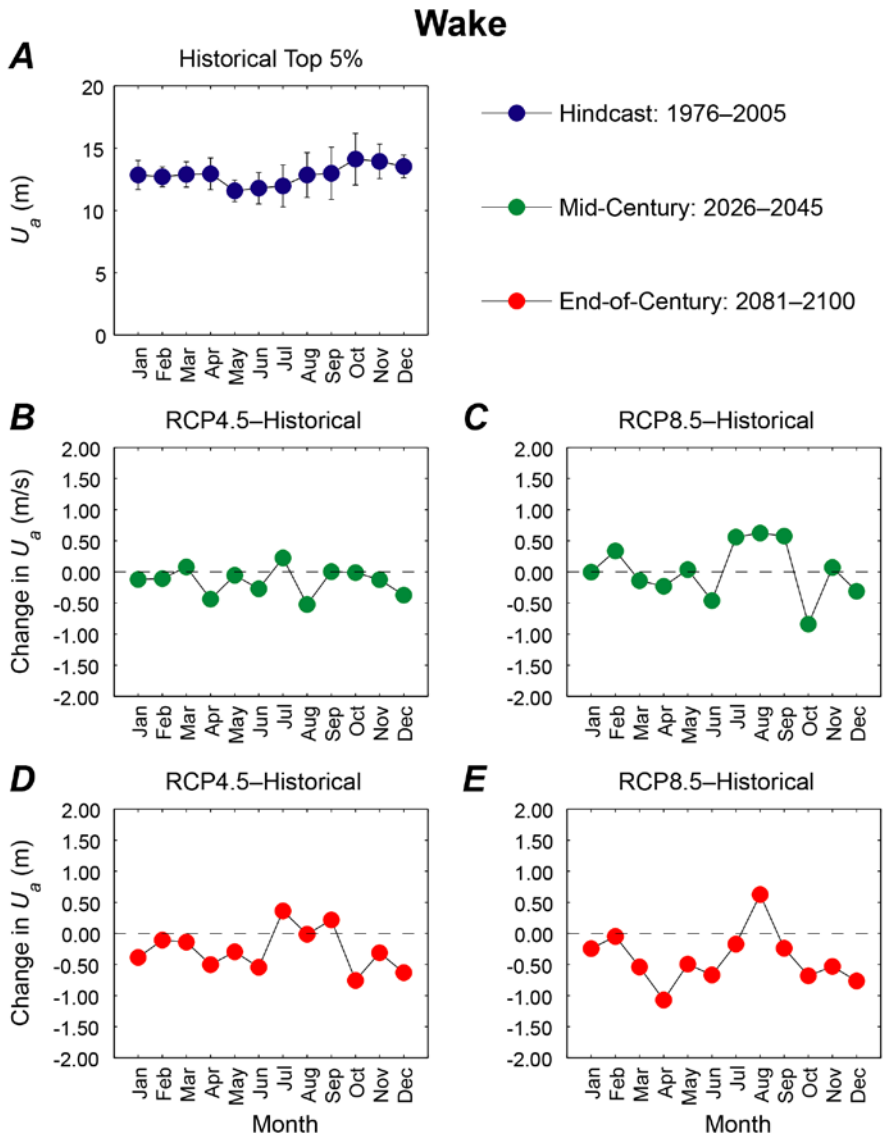

Appendix D38. Plots showing trends in monthly mean of the top 5 percent of wind speeds, in meters, at the Wake location. *A.* Hindcasted (1976–2005) mean of the top 5 percent of wind speeds by month with associated error bars. *B.* Plot of the change in mean of the top 5 percent of 2026–2045 wind speeds for the RCP4.5 scenario from hindcasted top 5 percent of monthly wind speed means. *C.* Plot of the change in mean of the top 5 percent of 2026–2045 wind speeds for the RCP8.5 scenario from hindcasted top 5 percent of monthly wind speed means. *D.* Plot of the change in mean of the top 5 percent of 2081–2100 wind speeds for the RCP4.5 scenario from hindcasted top 5 percent of monthly wind speed means. *E.* Plot of the change in mean of the top 5 percent of 2081–2100 wind speeds for the RCP8.5 scenario from hindcasted top 5 percent of monthly wind speed means.

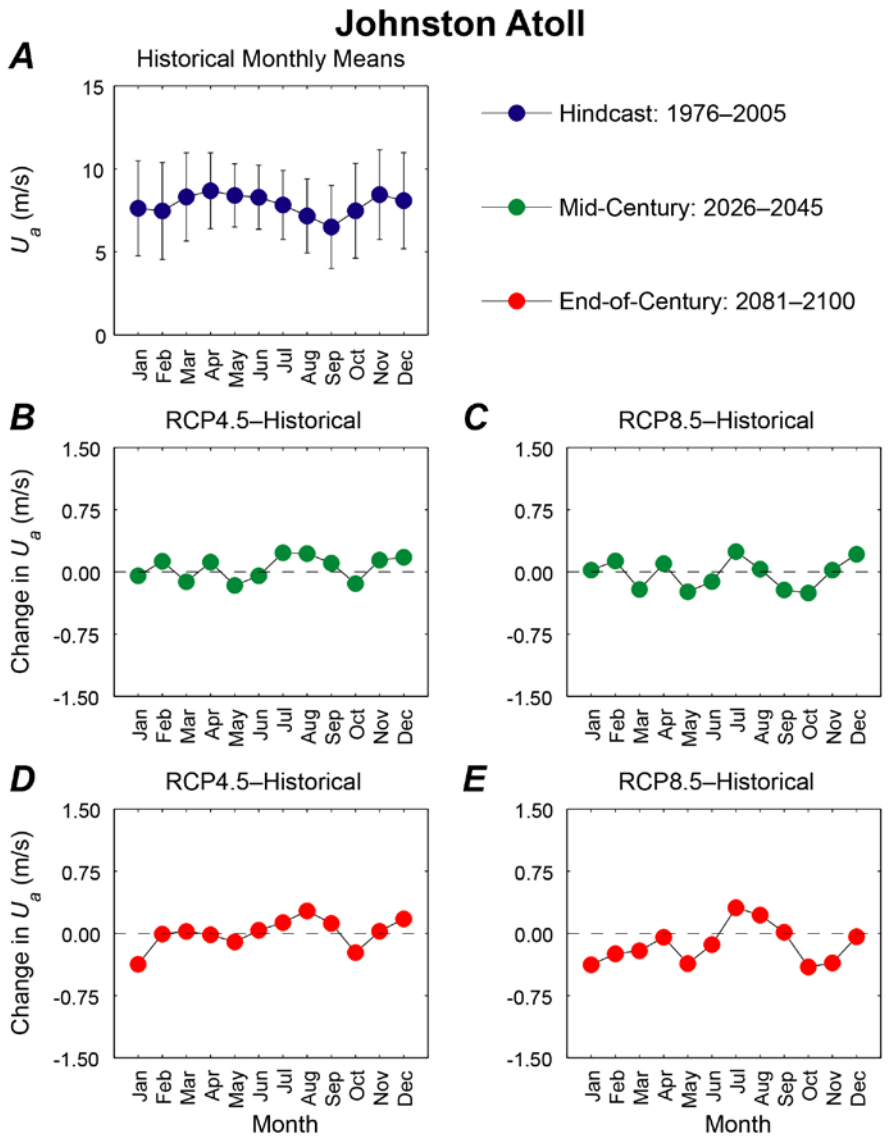

Appendix D39. Plots showing trends in monthly mean wind speed, in meters per second, at the Johnston Atoll location. *A.* Hindcasted (1976–2005) mean wind speeds by month with associated error bars. *B.* Plot of the change in mean 2026–2045 wind speeds for the RCP4.5 scenario from hindcasted monthly wind speed means. *C.* Plot of the change in mean 2026–2045 wind speeds for the RCP8.5 scenario from hindcasted monthly wind speed means. *D.* Plot of the change in mean 2081–2100 wind speeds for the RCP4.5 scenario from hindcasted monthly wind speed means. *E.* Plot of the change in mean 2081–2100 wind speeds for the RCP8.5 scenario from hindcasted monthly wind speed means.

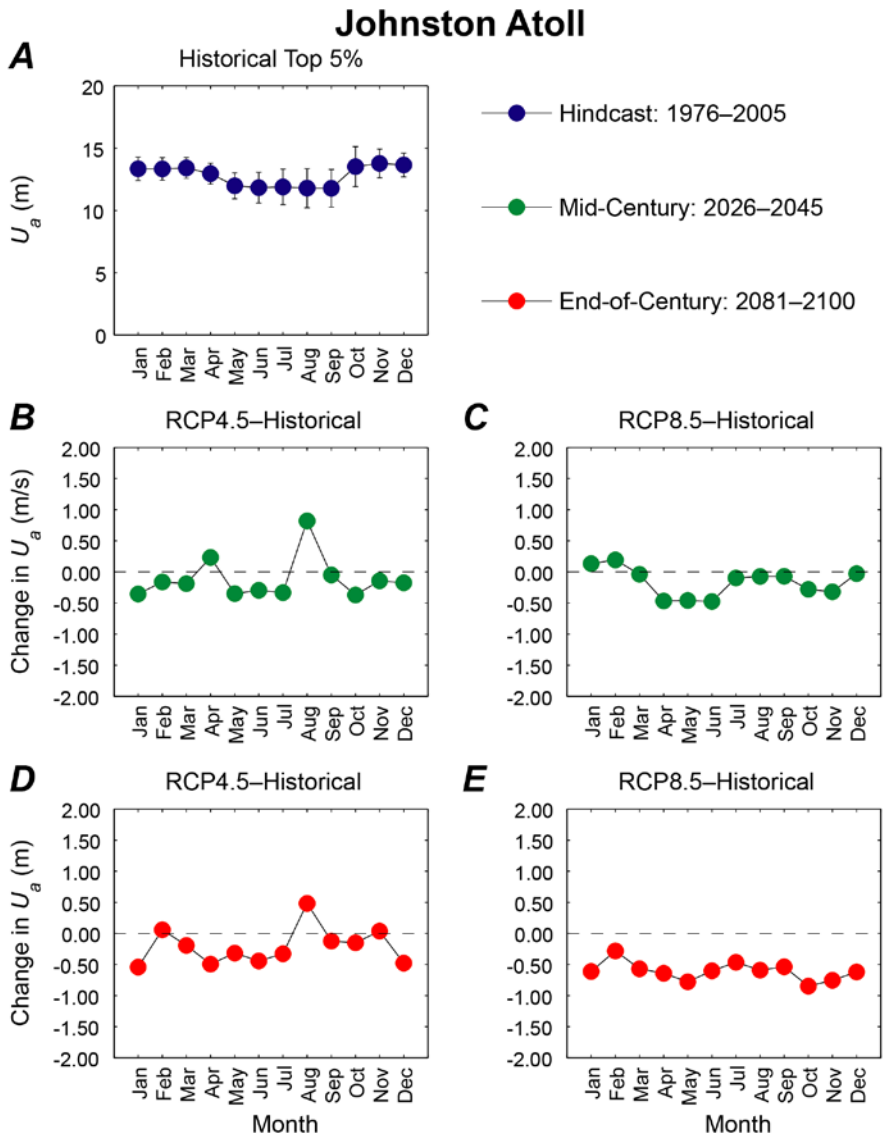

Appendix D40. Plots showing trends in monthly mean of the top 5 percent of wind speeds, in meters, at the Johnston Atoll location. *A.* Hindcasted (1976–2005) mean of the top 5 percent of wind speeds by month with associated error bars. *B.* Plot of the change in mean of the top 5 percent of 2026–2045 wind speeds for the RCP4.5 scenario from hindcasted top 5 percent of monthly wind speed means. *C.* Plot of the change in mean of the top 5 percent of 2026–2045 wind speeds for the RCP8.5 scenario from hindcasted top 5 percent of monthly wind speed means. *D.* Plot of the change in mean of the top 5 percent of 2081–2100 wind speeds for the RCP4.5 scenario from hindcasted top 5 percent of monthly wind speed means. *E.* Plot of the change in mean of the top 5 percent of 2081–2100 wind speeds for the RCP8.5 scenario from hindcasted top 5 percent of monthly wind speed means.

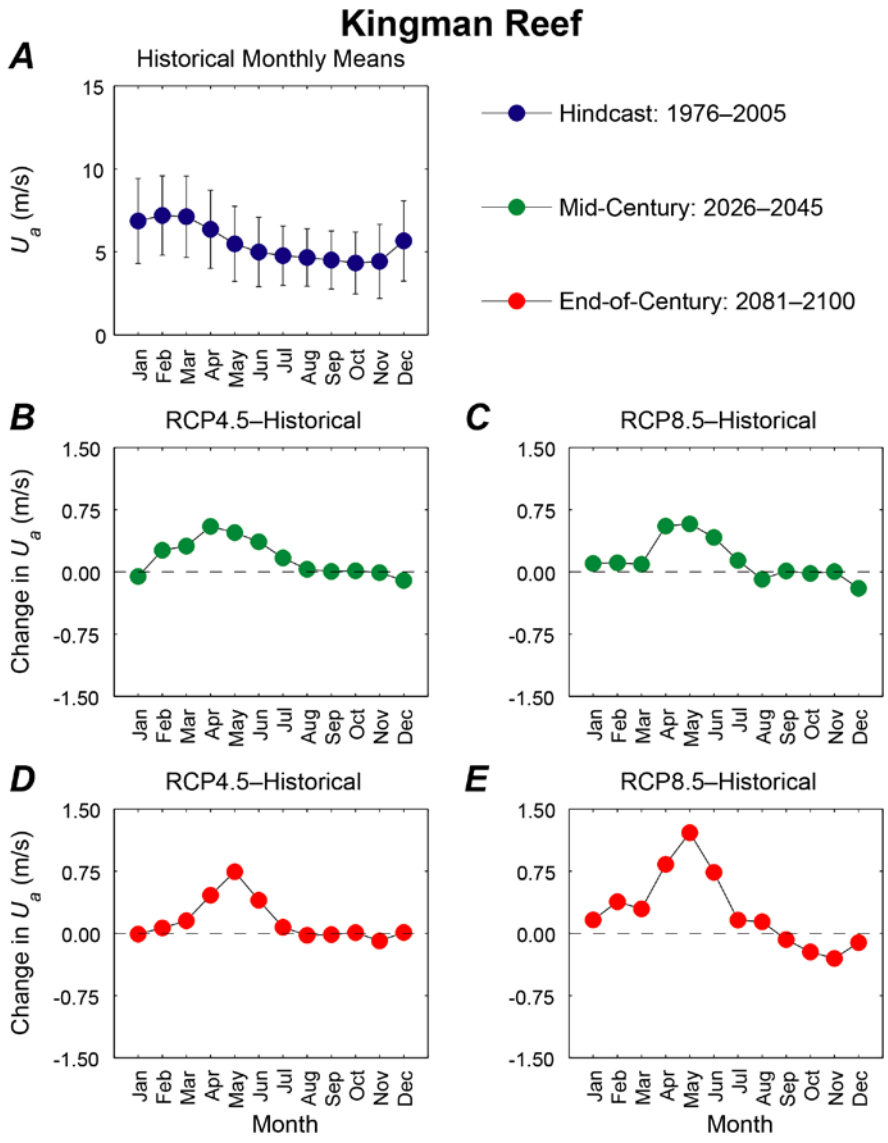

Appendix D41. Plots showing trends in monthly mean wind speed, in meters per second, at the Kingman Reef location. *A.* Hindcasted (1976–2005) mean wind speeds by month with associated error bars. *B.* Plot of the change in mean 2026–2045 wind speeds for the RCP4.5 scenario from hindcasted monthly wind speed means. *C.* Plot of the change in mean 2026–2045 wind speeds for the RCP8.5 scenario from hindcasted monthly wind speed means. *D.* Plot of the change in mean 2081–2100 wind speeds for the RCP4.5 scenario from hindcasted monthly wind speed means. *E.* Plot of the change in mean 2081–2100 wind speeds for the RCP8.5 scenario from hindcasted monthly wind speed means.

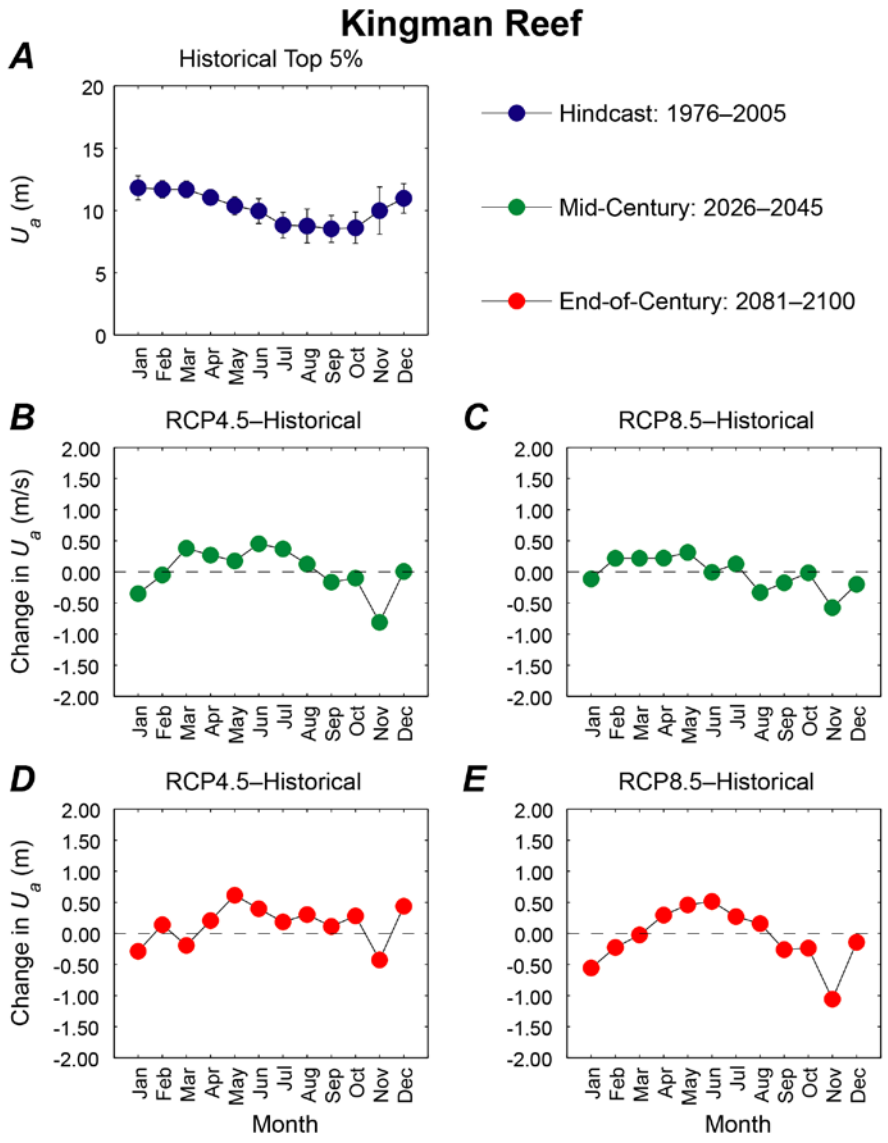

Appendix D42. Plots showing trends in monthly mean of the top 5 percent of wind speeds, in meters, at the Kingman Reef location. *A.* Hindcasted (1976–2005) mean of the top 5 percent of wind speeds by month with associated error bars. *B.* Plot of the change in mean of the top 5 percent of 2026–2045 wind speeds for the RCP4.5 scenario from hindcasted top 5 percent of monthly wind speed means. *C.* Plot of the change in mean of the top 5 percent of 2026–2045 wind speeds for the RCP8.5 scenario from hindcasted top 5 percent of monthly wind speed means. *D.* Plot of the change in mean of the top 5 percent of 2081–2100 wind speeds for the RCP4.5 scenario from hindcasted top 5 percent of monthly wind speed means. *E.* Plot of the change in mean of the top 5 percent of 2081–2100 wind speeds for the RCP8.5 scenario from hindcasted top 5 percent of monthly wind speed means.

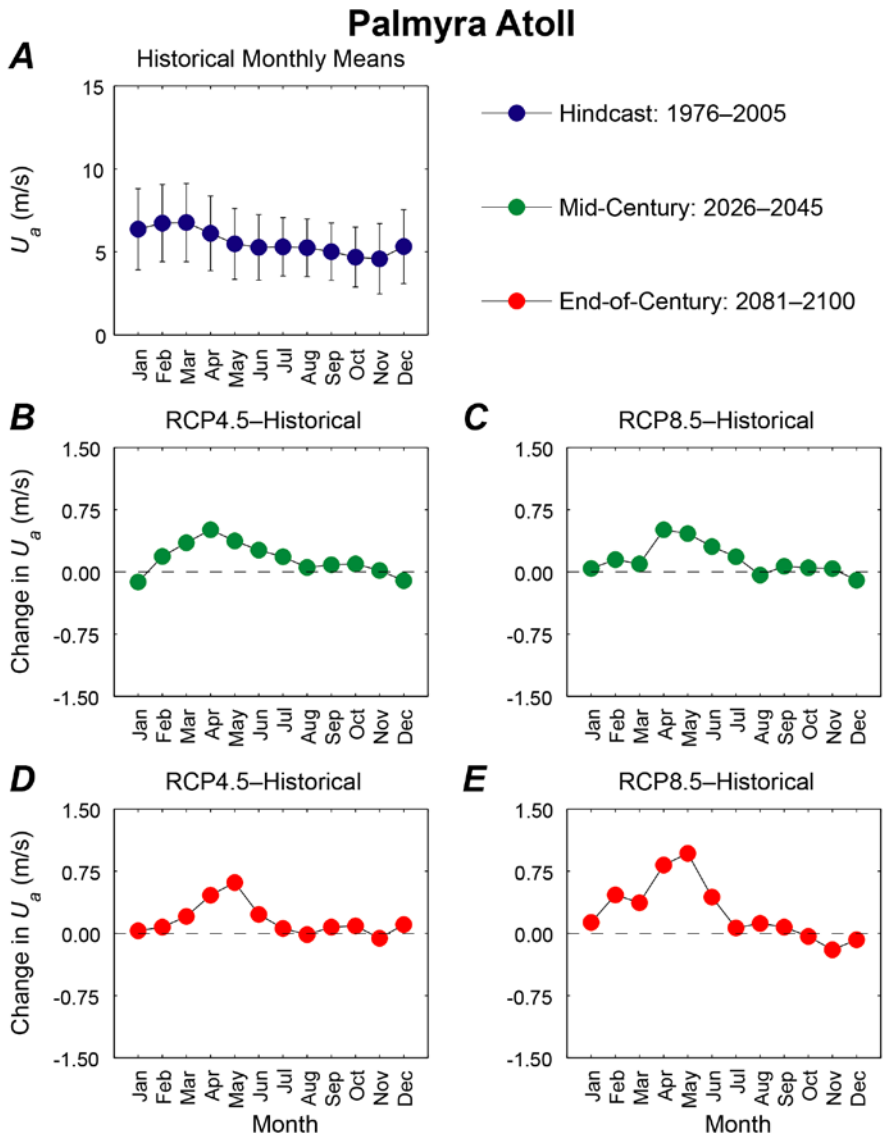

Appendix D43. Plots showing trends in monthly mean wind speed, in meters per second, at the Palmyra Atoll location. *A.* Hindcasted (1976–2005) mean wind speeds by month with associated error bars. *B.* Plot of the change in mean 2026–2045 wind speeds for the RCP4.5 scenario from hindcasted monthly wind speed means. *C.* Plot of the change in mean 2026–2045 wind speeds for the RCP8.5 scenario from hindcasted monthly wind speed means. *D.* Plot of the change in mean 2081–2100 wind speeds for the RCP4.5 scenario from hindcasted monthly wind speed means. *E.* Plot of the change in mean 2081–2100 wind speeds for the RCP8.5 scenario from hindcasted monthly wind speed means.

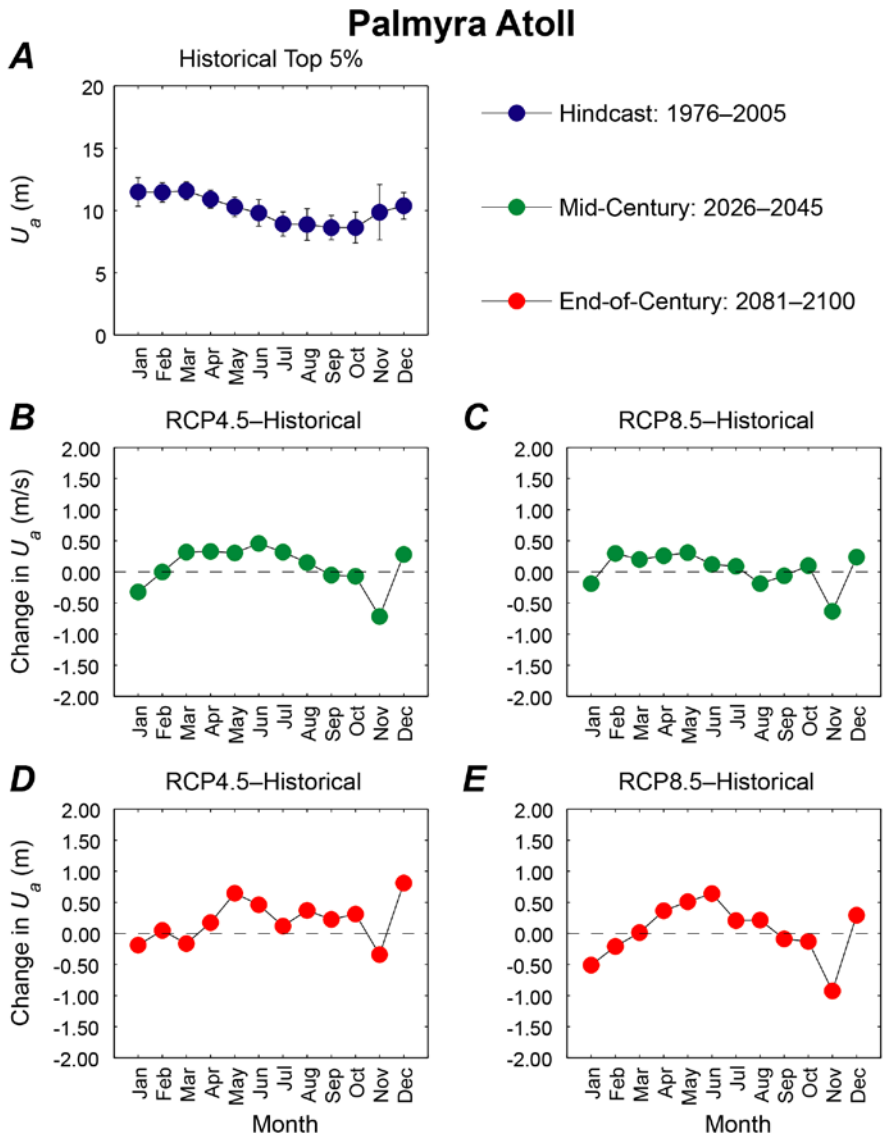

Appendix D44. Plots showing trends in monthly mean of the top 5 percent of wind speeds, in meters, at the Palmyra Atoll location. *A.* Hindcasted (1976–2005) mean of the top 5 percent of wind speeds by month with associated error bars. *B.* Plot of the change in mean of the top 5 percent of 2026–2045 wind speeds for the RCP4.5 scenario from hindcasted top 5 percent of monthly wind speed means. *C.* Plot of the change in mean of the top 5 percent of 2026–2045 wind speeds for the RCP8.5 scenario from hindcasted top 5 percent of monthly wind speed means. *D.* Plot of the change in mean of the top 5 percent of 2081–2100 wind speeds for the RCP4.5 scenario from hindcasted top 5 percent of monthly wind speed means. *E.* Plot of the change in mean of the top 5 percent of 2081–2100 wind speeds for the RCP8.5 scenario from hindcasted top 5 percent of monthly wind speed means.

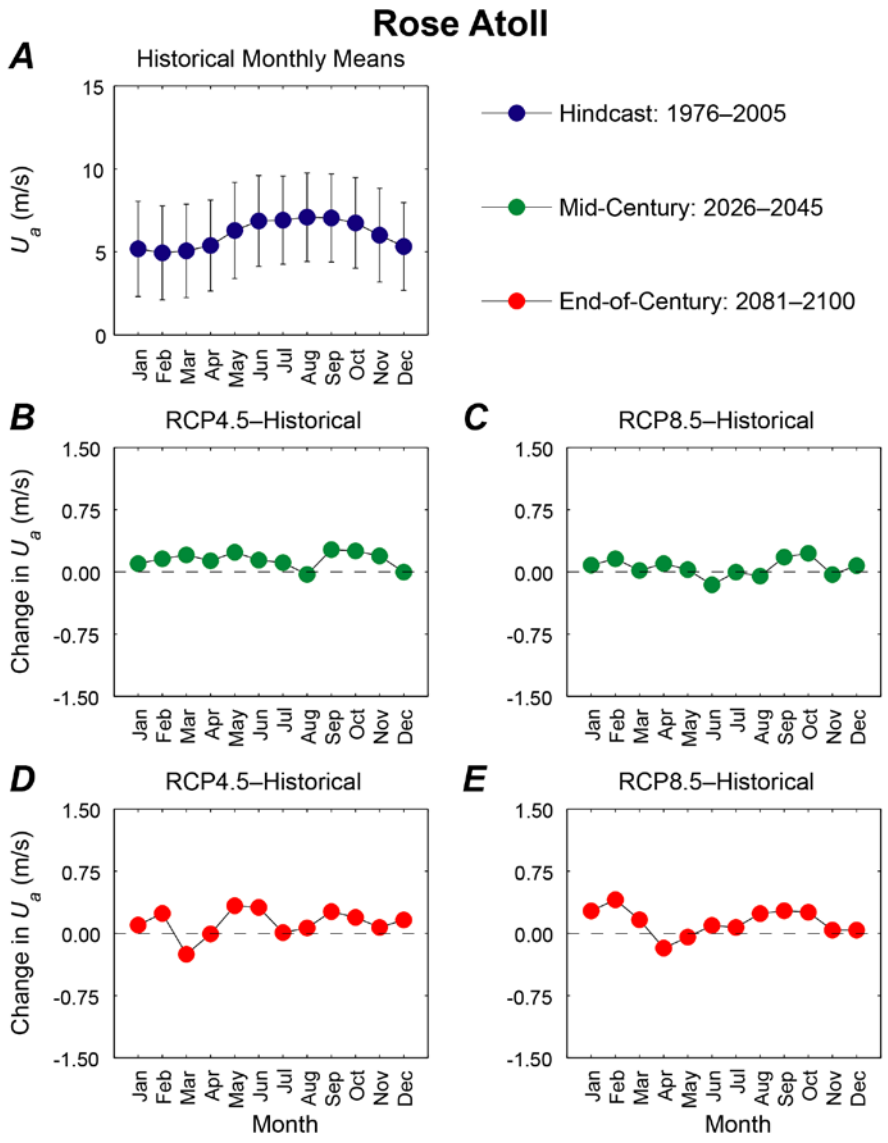

Appendix D45. Plots showing trends in monthly mean wind speed, in meters per second, at the Rose Atoll location. *A.* Hindcasted (1976–2005) mean wind speeds by month with associated error bars. *B.* Plot of the change in mean 2026–2045 wind speeds for the RCP4.5 scenario from hindcasted monthly wind speed means. *C.* Plot of the change in mean 2026–2045 wind speeds for the RCP8.5 scenario from hindcasted monthly wind speed means. *D.* Plot of the change in mean 2081–2100 wind speeds for the RCP4.5 scenario from hindcasted monthly wind speed means. *E.* Plot of the change in mean 2081–2100 wind speeds for the RCP8.5 scenario from hindcasted monthly wind speed means.

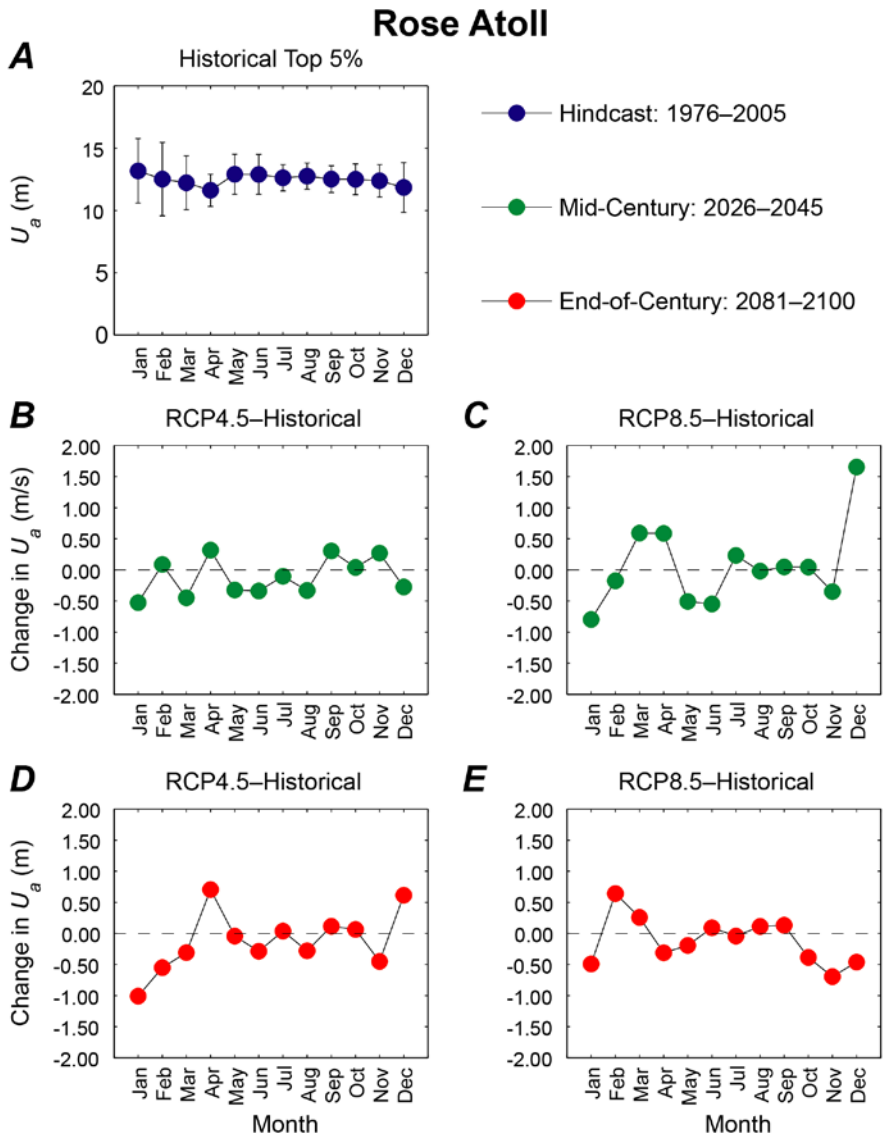

Appendix D46. Plots showing trends in monthly mean of the top 5 percent of wind speeds, in meters, at the Rose Atoll location. *A.* Hindcasted (1976–2005) mean of the top 5 percent of wind speeds by month with associated error bars. *B.* Plot of the change in mean of the top 5 percent of 2026–2045 wind speeds for the RCP4.5 scenario from hindcasted top 5 percent of monthly wind speed means. *C.* Plot of the change in mean of the top 5 percent of 2026–2045 wind speeds for the RCP8.5 scenario from hindcasted top 5 percent of monthly wind speed means. *D.* Plot of the change in mean of the top 5 percent of 2081–2100 wind speeds for the RCP4.5 scenario from hindcasted top 5 percent of monthly wind speed means. *E.* Plot of the change in mean of the top 5 percent of 2081–2100 wind speeds for the RCP8.5 scenario from hindcasted top 5 percent of monthly wind speed means.

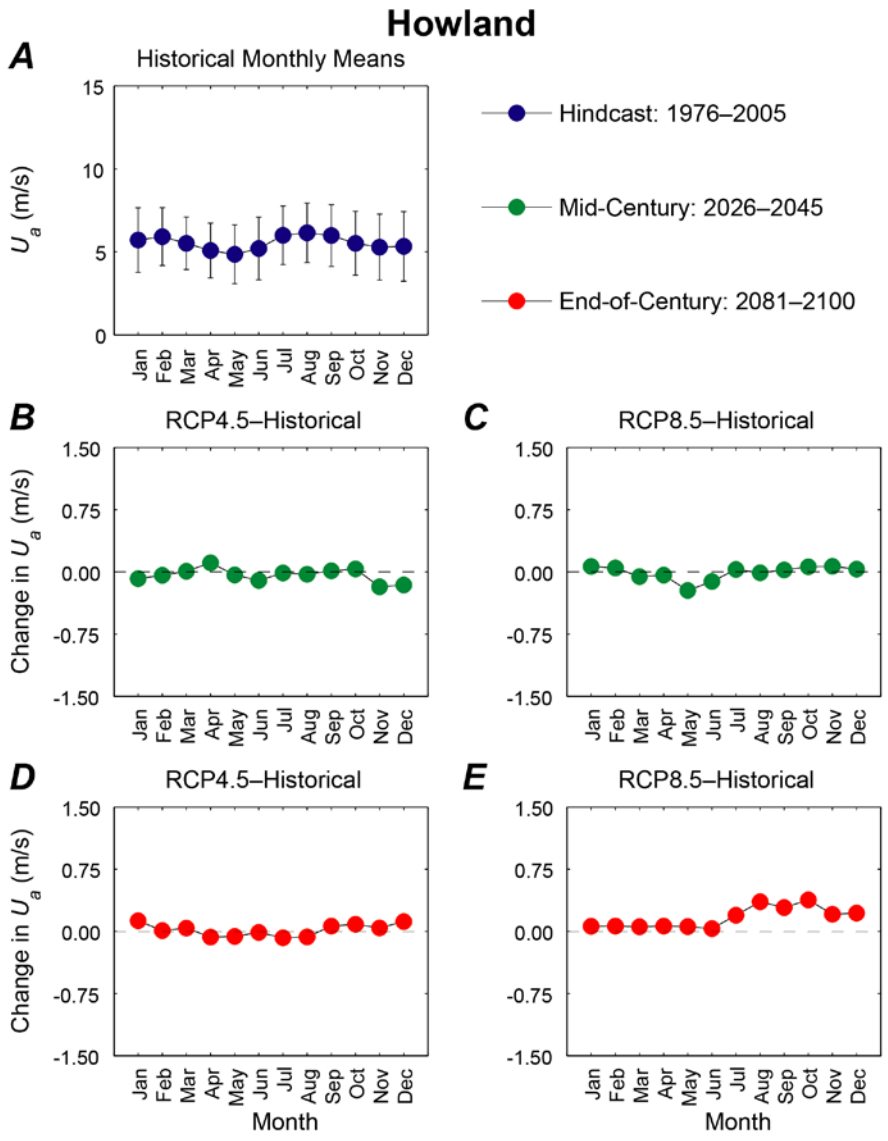

Appendix D47. Plots showing trends in monthly mean wind speed, in meters per second, at the Howland location. *A.* Hindcasted (1976–2005) mean wind speeds by month with associated error bars. *B.* Plot of the change in mean 2026–2045 wind speeds for the RCP4.5 scenario from hindcasted monthly wind speed means. *C.* Plot of the change in mean 2026–2045 wind speeds for the RCP8.5 scenario from hindcasted monthly wind speed means. *D.* Plot of the change in mean 2081–2100 wind speeds for the RCP4.5 scenario from hindcasted monthly wind speed means. *E.* Plot of the change in mean 2081–2100 wind speeds for the RCP8.5 scenario from hindcasted monthly wind speed means.

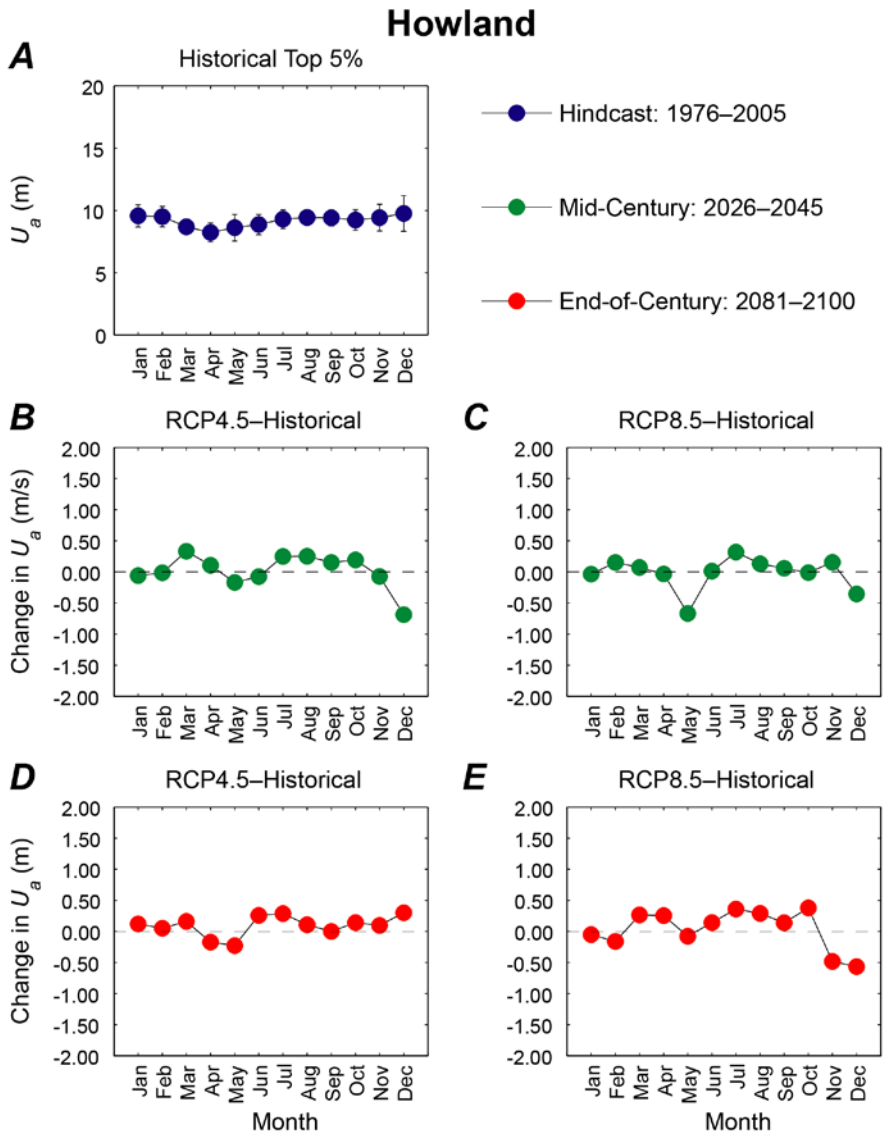

Appendix D48. Plots showing trends in monthly mean of the top 5 percent of wind speeds, in meters, at the Howland location. *A.* Hindcasted (1976–2005) mean of the top 5 percent of wind speeds by month with associated error bars. *B.* Plot of the change in mean of the top 5 percent of 2026–2045 wind speeds for the RCP4.5 scenario from hindcasted top 5 percent of monthly wind speed means. *C.* Plot of the change in mean of the top 5 percent of 2026–2045 wind speeds for the RCP8.5 scenario from hindcasted top 5 percent of monthly wind speed means. *D.* Plot of the change in mean of the top 5 percent of 2081–2100 wind speeds for the RCP4.5 scenario from hindcasted top 5 percent of monthly wind speed means. *E.* Plot of the change in mean of the top 5 percent of 2081–2100 wind speeds for the RCP8.5 scenario from hindcasted top 5 percent of monthly wind speed means.

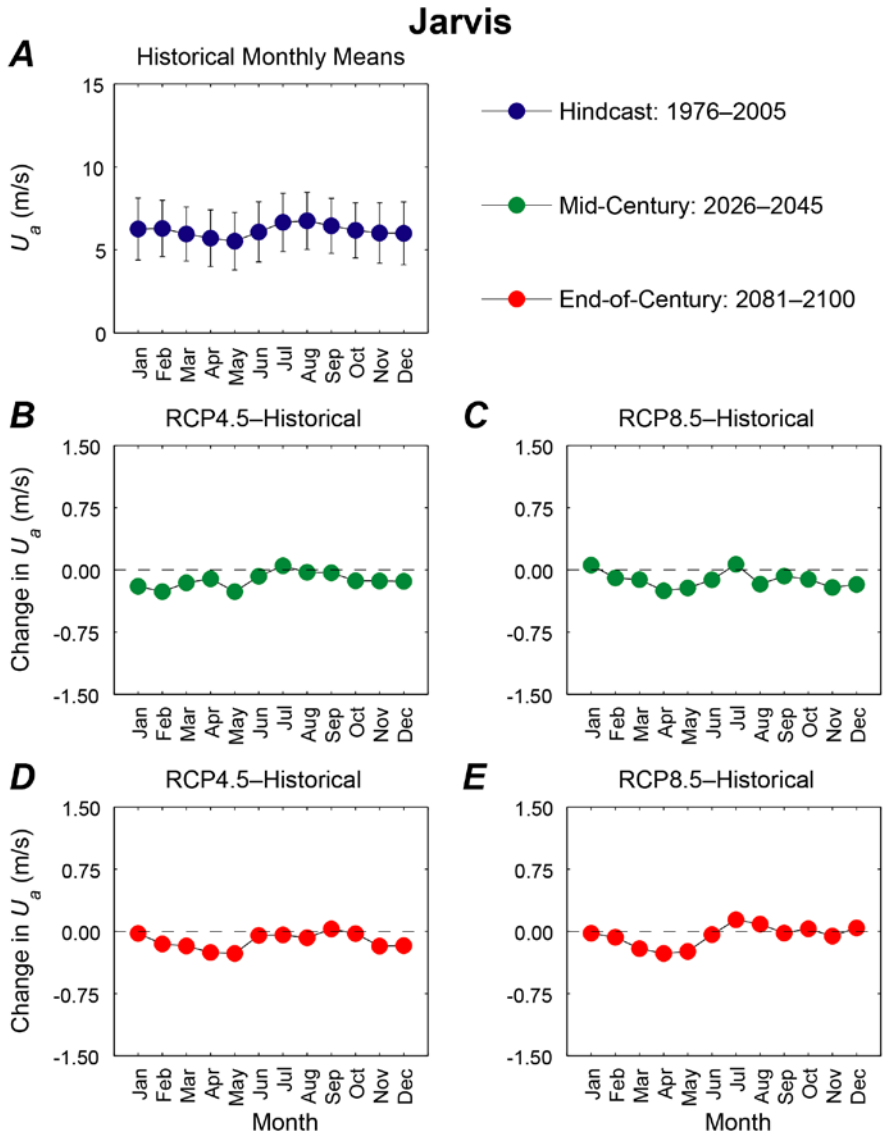

Appendix D49. Plots showing trends in monthly mean wind speed, in meters per second, at the Jarvis location. *A.* Hindcasted (1976–2005) mean wind speeds by month with associated error bars. *B.* Plot of the change in mean 2026–2045 wind speeds for the RCP4.5 scenario from hindcasted monthly wind speed means. *C.* Plot of the change in mean 2026–2045 wind speeds for the RCP8.5 scenario from hindcasted monthly wind speed means. *D.* Plot of the change in mean 2081–2100 wind speeds for the RCP4.5 scenario from hindcasted monthly wind speed means. *E.* Plot of the change in mean 2081–2100 wind speeds for the RCP8.5 scenario from hindcasted monthly wind speed means.

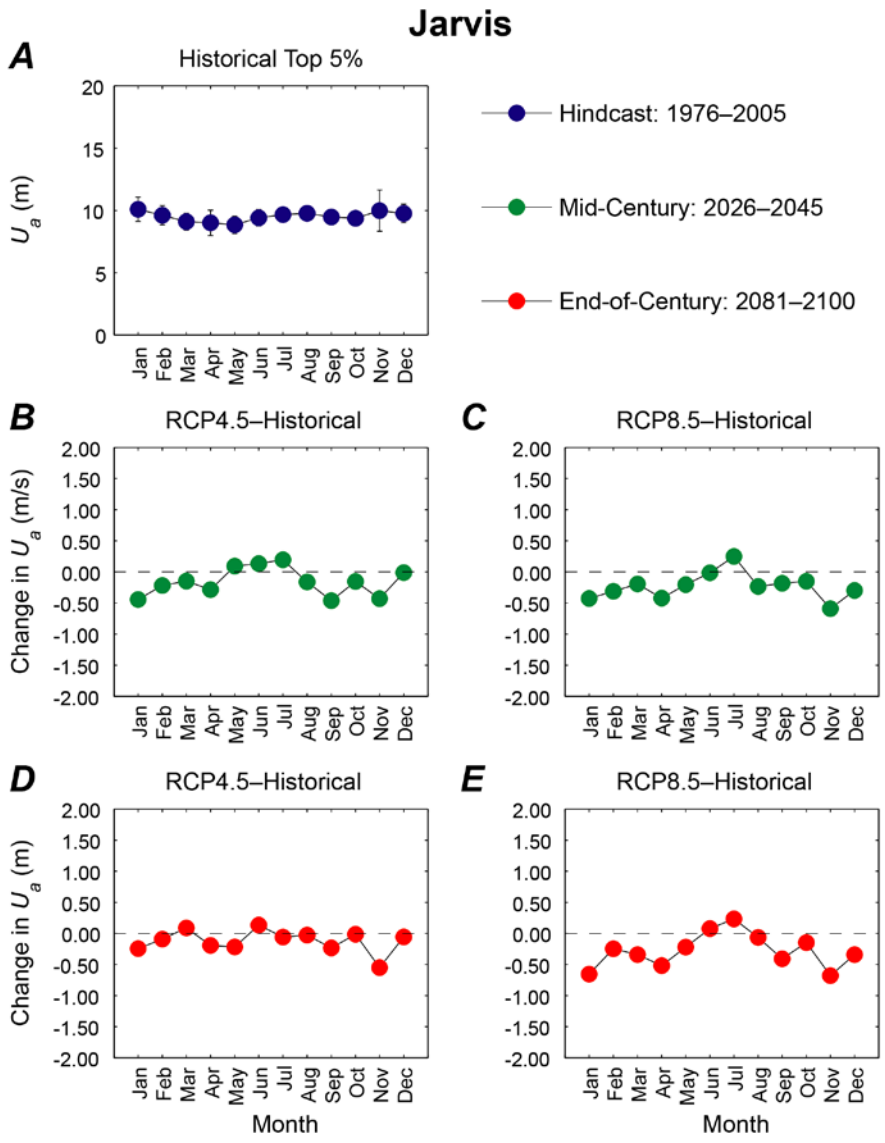

Appendix D50. Plots showing trends in monthly mean of the top 5 percent of wind speeds, in meters, at the Jarvis location. *A.* Hindcasted (1976–2005) mean of the top 5 percent of wind speeds by month with associated error bars. *B.* Plot of the change in mean of the top 5 percent of 2026–2045 wind speeds for the RCP4.5 scenario from hindcasted top 5 percent of monthly wind speed means. *C.* Plot of the change in mean of the top 5 percent of 2026–2045 wind speeds for the RCP8.5 scenario from hindcasted top 5 percent of monthly wind speed means. *D.* Plot of the change in mean of the top 5 percent of 2081–2100 wind speeds for the RCP4.5 scenario from hindcasted top 5 percent of monthly wind speed means. *E.* Plot of the change in mean of the top 5 percent of 2081–2100 wind speeds for the RCP8.5 scenario from hindcasted top 5 percent of monthly wind speed means.